ResearchOnline@JCU

JAMES COOK UNIVERSITY AUSTRALIA

This file is part of the following work:

Halim, Md Abdul (2025) ***New divalent and trivalent lanthanoid complexes from lanthanoid pseudo-Grignard reagents and exploration into their reaction chemistry.*** **PhD Thesis, James Cook University.**

Access to this file is available from:

https://doi.org/10.25903/zmrd%2Dwx25

Copyright © 2025 Md Abdul Halim

The author has certified to JCU that they have made a reasonable effort to gain permission and acknowledge the owners of any third party copyright material included in this document. If you believe that this is not the case, please email researchonline@jcu.edu.au

Title

New divalent and trivalent lanthanoid complexes from lanthanoid pseudo-Grignard reagents and exploration into their reaction chemistry

New divalent and trivalent lanthanoid complexes from lanthanoid pseudo-Grignard reagents and exploration into their reaction chemistry

A thesis submitted for the degree of

Doctor of Philosophy

By

Md Abdul Halim

M.Sc. (KUET) & B. Sc. (JUST)

Bangladesh

Discipline of Chemistry

College of Science and Engineering

James Cook University

Townsville, Australia

February 2025



Dedication

This little effort is dedicated to my adoring little angel Ariba

Declaration

To the best of my knowledge, this thesis is my original work, and contains no material previously published or written by another person, nor any material accepted for the award of any other degree or diploma at any university or other institution, except where proper reference is made in the text.

Md Abdul Halim
Discipline of Chemistry
James Cook University
Townsville, Australia
February 2025

Acknowledgement

Alhamdulillah for everything. Firstly, I would like to thank the Almighty for granting me the strength and perseverance to complete this study while being far from my homeland. After that, I would like to express my deepest gratitude to my supervisor Prof. Peter Junk for your exceptional support and guidance throughout my PhD journey. It has been a great privilege and honor to be a part of your research group, especially working in a field that was entirely new to me. Thank you, Peter, for helping me navigate the frustrations that encountered along the way. You have been not only an outstanding supervisor but also a mentor and guardian to me.

I would like to extend my sincere thanks to Prof. Glen Deacon for his insightful counsel and assistance when I encountered challenges in my research, particularly for his editorial help with my scientific writing. I am also deeply grateful to my secondary supervisor, Dr Murray Davies, for always being there whenever I needed support, and helping me with the administrative tasks.

I am deeply indebted to Dr Zhifang Guo for always being a steadfast source of support, acting as a sister, friend, and mentor. It has been a pleasure to work with you and I am incredibly grateful for all your help with reactions and crystal analysis (crystallography, NMR, IR). Coming from an engineering background, air-sensitive chemistry was entirely new to me. You not only trained me in the art of air-sensitive chemistry but also provided valuable advice over the years. A big thanks, should also goes to the entire Junkies group, notably Vidushi, Ramees, Ameen, Naveena, Angus, T2 and T-bone, as well as my office buddies Mele, Jayson and Kal for all the fun times, support, and encouragement. I would like to extend my gratuity to the technical team in the chemistry lab–Dr Winnie Lee, Shiyoh Nobile, Dr Dana Roberts, Joan Zapiter–for their unwavering support. Many thanks Dr Mark Robertson for assisting me with the NMR challenges. I also appreciate Saffa's contributions for doing some preliminary work on this chemistry.

I would like to appreciate and acknowledge for the support, I received from the Bangladeshi community in Townsville. A special thanks to Rezaul Miazi bhai and Rahat Ara bhabi for helping me in settling down in Townsville back in 2021. I am also like to thank the Bangladeshi brothers, Rizvee, Ashraful, Mizan for their tremendous support and the fun times we shared over the years. Furthermore, a sincere thanks to Elius bhai, Anwarul Islam bhai, Zahirul islam bhai, Babu bhai, Barkatul Islam bhai, Aurup Faisal bhai, Mazibar Rahman bhai, Onti, Sadman,

Siam, Faisal, Nahian, Ferdous for all the fun times and delicious foods, you guys are amazing–thank you.

I would like to thank James Cook University for supporting me with the James Cook University Postgraduate Research Scholarship (JCUPRS) award and the Australian Research Council (ARC) for funding our research project. Additionally, I am grateful to Jashore University of Science and Technology (JUST) for granting my study leave during this period.

I would like to express my sincere gratitude from the bottom of my heart to my family, especially, my Mother (MA), you sacrifice a lot in the last 3.5 years, and I am forever grateful for your unwavering support and trust in me. I am also thankful to all my siblings and their kids for their constant love and support. A special thanks to my elder sister and her husband for their immense support throughout the time. I would like to extend my heartful thanks to my new family (in-laws), especially younger sister Arin Kabir, for her encouragement and support over the years.

Last but not least, to my lovely wife Muftarin Kabir–I am truly blessed to have you in my life. Thank you for your love and support over the past five years. I deeply appreciate your patience and understanding as I navigated the stresses and frustrations of my PhD journey. You were here in Townsville for only seven months, and I wish you could have been here for the entirety of this journey!

To all my friends and well-wishers, thank you.

Statement of the contribution of others

Outside of the personal contributions outlined in the acknowledgements, there have been several contributions in direct support of this thesis:

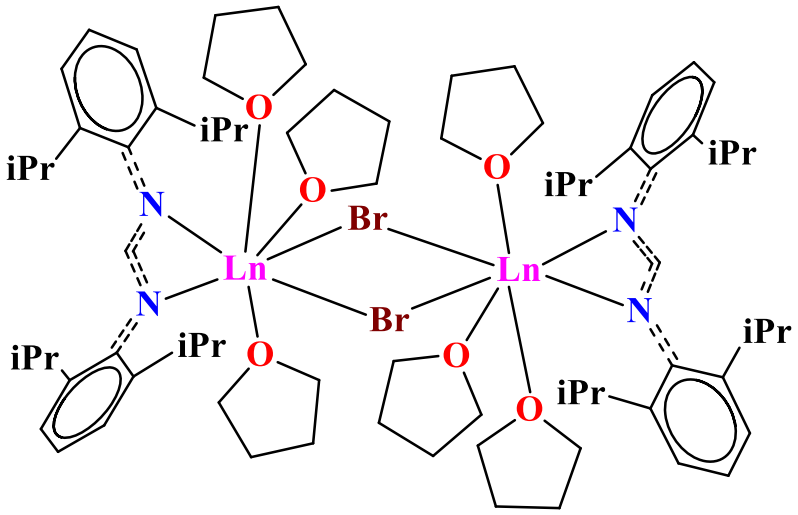
Nature of Assistance	**Contribution**	**Names of the Co-Contributors**
Intellectual Support	Proposal writing, data analysis and editorial assistance	Prof. Peter Junk Prof. Glen Deacon Dr. Murray Davies
Data Collection	X-ray diffraction data from crystals, solving and refining of crystal structures	Dr. Zhifang Guo
Financial Support	Fee offset/waiver and stipend (through JCUPRS fellowship)	James Cook University
	Research costs (through ARC Discovery Project grants)	Australian Research Council
	Travel grants for attending conference (through CRT Project Grant)	College of Science and Engineering

Abstract

This thesis examines the synthesis and spectroscopic characterisation of pseudo-Grignard complexes from the reactivity of pseudo-Grignard reagents with N-donor (formamidines and pyrazoles) ligands (Chapter two and chapter three) and O-donor (4-^{t}Bu-Phenol) ligand (Chapter four). Additionally, it explores an alternative synthesis of pseudo-Grignard complexes involving lanthanoid metal, iodine, and corresponding ligands (Chapter five).

Chapter 1 begins withs an overview of rare earth chemistry, including the abundance, isolation, characteristics, and applications of rare earth elements. It also provides a brief discussion on the formation of rare earth amidinate and pyrazolato complexes, along with the common methods used for synthesising rare earth complexes. The chapter concludes with an introduction to the formation methods of pseudo-Grignard reagents and their subsequent reactivity.

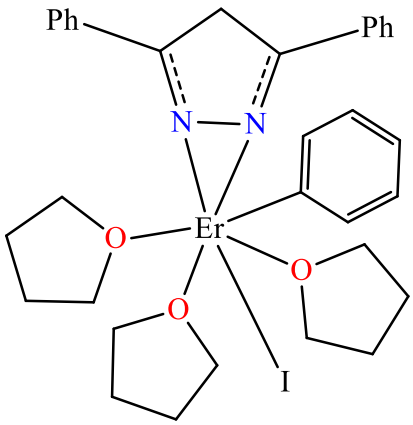
Chapter 2 explores the oxidative addition of phenyl bromide (PhBr) to lanthanoid metal (Sm and Eu) as a synthetic route for preparing various pseudo-Grignard complexes involving 2,6-^{i}Pr$_2$-Phenyl formamidine (DippFormH) and 3,5-diphenyl pyrazole (Ph$_2$pzH). A key finding is the formation of a seven coordinate divalent dimer, [Sm(DippForm)Br(thf)$_3$]$_2$·6thf complex, which is isostructural with the corresponding europium complex.



Ln = Sm, Eu

In contrast, the reaction with Ph_2pzH led only to Schlenk equilibrium redistribution products, specially $[Ln(Ph_2pz)_n(solv)_p]\cdot q(solv)$ (Ln = Sm, n = 3, p = 3, q = 3, solv = thf; p = 2, q = 1, solv = dme; Ln = Eu, n = 2, p = 4, q = 0, solv = thf). Comparatively, less reactive Sm, when react with the oxidant, phenyl iodine (PhI) and then with DippFormH or Ph_2pzH yielded the expected seven coordinated Sm(III) $[Sm(L)I_2(thf)_3]$ (L = DippForm, Ph_2pz) complexes. Similar reactivity was observed with $H_2NPhLnI(thf)_n$ (Ln = Eu, Yb) instead of $PhLnI(thf)_n$ pseudo-Grignard reagents, leading the formation of Ln(II) $[Ln(DippForm)I(thf)_n]\cdot thf$ (Ln = Eu, n = 4; Yb, n = 3) and $[Yb(Ph_2pz)I(thf)_4]$ complexes.

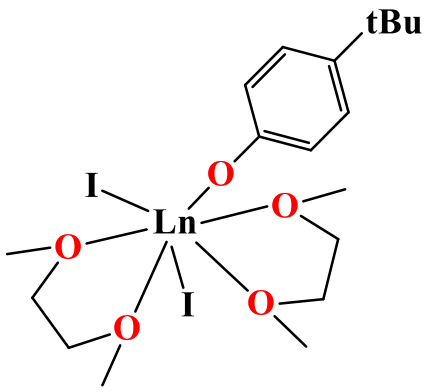
Chapter 3 discusses the synthesis and spectroscopic characterisation of a series of lanthanoid (III) pseudo-Grignard complexes. The protolysis reaction between $Ph_pLnI_{(3-p)}(thf)_n$ (p = 1 or 2; Ln = La, Ce, Nd, Er and Lu) and Ph_2pzH resulted to the formation of trivalent Ln(III) $[Ln(Ph_2pz)I_2(thf)_n]$ (Ln = La, Ce, Nd, n = 4; Ln = Er, Lu, n = 3) complexes. A key findings from the erbium reaction was the isolation of the seven coordinate second product $[Er(Ph_2pz)(Ph)I(thf)_3]\cdot thf$. When thf was replaced with acetonitrile, nine coordinated Schlenk equilibrium products $[Ln(Ph_2pz)_3(CH_3CN)_3]\cdot 2CH_3CN$ (Ln = Nd, Gd) were isolated, instead of the targeted $[Ln(Ph_2pz)I_2(CH_3CN)_n]$ complexes.



Similar reactivity was observed when pyrazole (Ph_2pzH) was replaced by formamidine (DippFormH or XylFormH) leading to the formation of seven coordinated $[Ln(RForm)I_2(thf)_3]$ (Ln = La, Nd, Er; R = 2,6-^{i}Pr$_2$, 2,6-Me$_2$) complexes.

Chapter 4 outlines the trapping capacity of trivalent pseudo-Grignard reagents, $Ph_pLnI_{(3-p)}(thf)_n$ (p = 1 or 2; Ln = La, Ce, Nd, Ho, Gd and Lu), with O-donor ligands; 4-tert-butylphenol (4-^{t}Bu-PhOH), leading to the isolation of seven coordinate diiodo pseudo-Grignard [Ln(4-^{t}Bu-

PhO)I_2(dme)$_2$]·0.5dme (Ln = Ce, Nd, Lu) complexes. Reactions involving Gd and Ho yielded powders of composition [Ln(4-tBu-PhO)I2(dme)2]·0.5dme (Gd and Ho 4). Heating the complex obtained in the reaction involving La yielded [La_2(μ-OPh-4^{t}Bu)$_2$(OCH_3)I_2(dme)$_4$]I^-·2dme instead of the expected [La(4^{t}Bu-O-Ph)I_2(dme)$_2$]·0.5dme complex, a product obtained by the C-O bond scission of dme. The reaction of PhYbI(thf)$_n$ with benzophenone (Ph_2CO) resulted in the formation of a low five (5) coordinate [Yb(Ph_3CO)$_3$(thf)$_2$] complex. Further studies on the reactivity of [Yb(Ph_2pz)I(thf)$_4$] Grignard complex with O-donor ligands KO^{t}Bu and (KMe)Ph(NMe_2) revealed that the equilibrium redistribution product [Yb(Ph_2pz)$_2$(thf)$_4$] was isolated in both cases.



Chapter 5 presents an alternative synthesis of pseudo-Grignard reagents from lanthanoid metal, I_2 using supporting ligands such as ^{t}Bu$_2$pzH and PhMepzH. This synthetic approach has already been proven effective for trapping of a wide range of [Ln(L)I_2(solv)$_n$] and/or [Ln(L)$_2$I(solv)$_n$] (L = Formamidinato) complexes. The direct reaction of lanthanoid metals (Ln = La, Ce, Nd, Tb, Er and Lu) with I_2 and ^{t}Bu$_2$pzH/PhMepzH resulted in the formation of both diiodo [Ln(pz)I_2(thf)$_n$] (pz = ^{t}Bu$_2$pz/PhMepz; n = 3 or 4) and monoiodo [Ln(^{t}Bu$_2$pz)$_2$I(thf)$_2$] (Ln = Er, Lu) pseudo-Grignard complexes.

Overall, this thesis makes a significant contribution to the field of pseudo-Grignard chemistry. It demonstrates that formamidinate and pyrazolato ligands can form stable and structurally intriguing pseudo-Grignard complexes with both the divalent (Sm, Eu, Yb) and the trivalent (La, Ce, Nd, Tb, Gd, Er, Lu) lanthanoid metals. Furthermore, lanthanoid pseudo-Grignard reagents exhibit a strong ability to trap O-donor phenolate ligands.

Abbreviations

Å	Angstrom unit, 10^{-10}m
ArO	Aryloxide
Cp	Cyclopentadienyl ($C_5H_5^-$)
CN	Coordination number
°C	Degree Celsius
C_6D_6	Deuterated benzene
CH_3CN	Acetonitrile
DippFormH	*N,N′*-Bis(2,6-diisopropylphenyl)formamidine
DME	1,2-Dimethoxyethane
Dpp^-	2,6-Ph_2-$C_6H_3^-$
EtFormH	*N,N′*-bis(2,6-diethylphenyl)formamidine
EDTA	Ethylenediaminetetraacetic acid
Et	Ethyl
Et_2O	Diethyl ether
ESMS	Electrospray Mass Spectrometry
h	Hour
^{i}Pr	Isopropyl
IR	Infrared
IUPAC	International Union of Pure and Applied Chemistry
Ln	Lanthanoid
Me	Methyl
m. p.	Melting point
MeO	Methoxy
Mes*	2,4,6-tri-tert-butylphenyl
min	minute
NMR	Nuclear Magnetic Resonance

NIR	Near-infrared
Ph	Phenyl
pzH	Pyrazole
ppm	Parts per million
rt	Room temperature
RE	Rare earth
REEs	Rare earth element
RTP	Redox transmetallation/protolysis
RT	Redox transmetallation
SMMs	Single molecule magnets
^{t}Bu	*tert*-Butyl
THF	Tetrahydrofuran
XylFormH	*N,N′*-bis(2,6-dimethylphenyl)formamidine

Table of Contents

Title	i
Dedication	iii
Declaration	iv
Acknowledgement	v
Abstract	viii
Abbreviations	xi

Chapter 1: Introduction to the general features of the organometallic chemistry of rare earth metals	01
1.1 Rare earth elements	02
1.1.1 General features	02
1.1.2 Abundance of the lanthanoid metals	03

	1.1.3 Isolation of the lanthanoid metals	04
	1.1.4 Properties of the lanthanoid metals	06
	1.1.5 Rare earth organometallic compounds	09
	1.1.6 Application of the lanthanoid metals and their compounds	09
1.2	Complex formation of the lanthanoid metals	10
	1.2.1 Amidinate complexes of rare earth	12
	1.2.2 Pyrazolato complexes of rare earth	15
1.3	Chemistry of rare earth	17
1.4	Pseudo-Grignard reagents	20
1.5	Current Study	23
1.6	References	25

Chapter 2: Reaction of Ln(II) pseudo Grignard reagents with formamidines and pyrazoles		35
2.1	Introduction	36
	2.1.1 Synthesis of divalent pseudo-Grignard reagents using Grignard type reactions	36
	2.1.2 Synthesis of lanthanoid (Sm, Eu and Yb) pseudo-Grignard reagents from common synthetic approaches	41
2.2	Current Study	47
2.3	Results and Discussion	48
	2.3.1 Synthesis and spectroscopic characterisation	48
	2.3.1.1 The reaction of lanthanoid (Sm and Eu) pseudo-Grignard reagents (PhLnBr) with DippFormH	48
	2.3.1.2 The reaction of lanthanoid (Sm and Eu) pseudo-Grignard reagents (PhLnBr) with Ph_2pzH	51
	2.3.1.3 The reaction of samarium (Sm) pseudo-Grignard reagents (PhSmI) with DippFormH and Ph_2pzH	54

2.3.1.4 Synthesis of lanthanoid (Eu and Yb) pseudo-Grignard compounds (reported) from the reaction of lanthanoid (Eu and Yb) metals with $C_6H_4NH_2I$ and DippFormH or Ph_2pzH 58

2.3.2 X-ray Crystal Structures 62

2.3.2.1 $[Ln(DippForm)Br(thf)_3]_2 \cdot 6thf$ (Sm **2.1**, Eu **2.2**) 62

2.3.2.2 $[Sm(Ph_2pz)_3(dme)_2]$ (**2.3b**) 65

2.3.2.3 $[Sm(DippForm)I_2(thf)_3]$ (**2.5**) 67

2.3.2.4 $[Sm(Ph_2pz)I_2(thf)_3]$ (**2.6**) 69

2.3.3 Discussion 71

2.4 Conclusion and Future Outlook 73

2.5 Experimental 74

2.5.1 General Aspects 74

2.5.2 Synthesis of Ln (II) pseudo-Grignard compounds 74

2.5.2.1 The reaction of lanthanoid (Sm and Eu) pseudo-Grignard reagents (PhLnBr) with DippFormH 74

2.5.2.2 The reaction of lanthanoid (Sm and Eu) pseudo-Grignard reagents (PhLnBr) with Ph_2pzH 75

2.5.2.3 The reaction of samarium (Sm) pseudo-Grignard reagents (PhSmI) with DippFormH and Ph_2pzH 77

2.5.2.4 Synthesis of lanthanoid (Eu and Yb) pseudo-Grignard compounds (reported) from the reaction of lanthanoid (Eu and Yb) metals with $C_6H_4NH_2I$ and DippFormH or Ph_2pzH 78

2.6 X-ray crystal data 80

2.7 References 82

Chapter 3: Reaction of Ln(III) pseudo Grignard reagents with formamidines and pyrazoles 87

3.1 Introduction 88

3.1.1 Synthesis of trivalent pseudo-Grignard complexes 89

3.2	Current Study	96
3.3	Results and Discussion	97
	3.3.1 Synthesis and spectroscopic characterisation	97
	3.3.1.1 The reaction of lanthanoid (La, Ce, Nd, Er and Lu) pseudo-Grignard reagents with Ph_2pzH	97
	3.3.1.2 The reaction of lanthanoid (Nd and Gd) pseudo-Grignard reagents with Ph_2pzH in acetonitrile (CH_3CN)	101
	3.3.1.3 The reaction of lanthanoid (La, Nd and Er) pseudo-Grignard reagents with formamidine (DippFormH and XylFormH)	103
	3.3.1.4 The reaction of neodymium pseudo-Grignard reagents with Ph_2pzH	108
	3.3.2 X-ray Crystal Structures	109
	3.3.2.1 $[Ln(Ph_2pz)I_2(thf)_4]$ (La **3.1**, Ce **3.2** and Nd **3.3**)	109
	3.3.2.2 $[Er(Ph_2pz)(Ph)I(thf)_3]$ (**3.4a**), $[Er(Ph_2pz)I_2(thf)_3]$ (**3.4**)	111
	3.3.2.3 $[Lu(Ph_2pz)I_2(thf)_3]$ (**3.5**)	114
	3.3.2.4 $[Ln(Ph_2pz)_3(CH_3CN)_3]\cdot 2CH_3CN$ (Nd **3.6**, Gd **3.7**)	116
	3.3.2.5 $[Er(DippForm)I_2(thf)_3]\cdot thf$ (**3.9**)	119
	3.3.2.6 $[Ln(XylForm)I_2(thf)_3]\cdot 2thf$ (La **3.10**, Er **3.12**)	121
	3.3.2.7 $[Nd(Ph_2pz)Br_2(thf)_{3.5}]$ (**3.13**)	123
	3.3.3 Discussion	125
3.4	Conclusion and Future Outlook	128
3.5	Experimental	129
	2.5.1 General Aspects	129
	3.5.2 Synthesis of Ln (III) pseudo-Grignard complexes	129
	3.5.2.1 Synthesis of lanthanoid(III) pyrazolato pseudo-Grignard compounds	129
	3.5.2.2 Synthesis of lanthanoid(III) formamidinato pseudo-Grignard compounds	133
	3.5.3 Synthesis of lanthanoid(III) dibromo pyrazolato compounds	135
3.6	X-ray crystal data	136

3.7	References	139

Chapter 4: Reactivity of Ln(II) and Ln(III) Grignard reagents with organic molecules		144
4.1	Introduction	145
	4.1.1 Synthesis of lanthanoid phenolate complexes	145
4.2	Current Study	149
4.3	Results and Discussion	149
	4.3.1 Synthesis and spectroscopic characterisation	149
	4.3.1.1 The reaction of lanthanoid (La, Ce, Nd, Gd, Ho and Lu) pseudo-Grignard reagents with 4-tertbutyl phenol	149
	4.3.1.2 Reactivity of ytterbium pseudo-Grignard reagents with O/N-donor ligands	154
	4.3.2 X-ray Crystal Structures	157
	4.3.2.1 [Ln(4-^{t}Bu-PhO)I_2(dme)$_2$]·0.5dme (**4.1** Ce, **4.2** Nd and **4.3** Lu)	157
	4.3.2.2 [(La(4-^{t}Bu-PhO)I(dme)$_2$)$_2$(OCH_3)I)]·2dme (**4.6**)	160
	4.3.2.3 [Yb($OCPh_3$)$_3$(thf)$_2$] (**4.7a**)	162
	4.3.2.4 [Yb_2I_2(μ-O)(μ-I)(thf)$_5$]·thf (**4.7b**)	163
	4.3.2.5 [Yb(Ph_2pz)$_2$(thf)$_4$] (**4.8**)	165
	4.3.3 Discussion	166
4.4	Conclusion and Future Outlook	168
4.5	Experimental	168
	4.5.1 General aspects	168
	4.5.2 Synthesis of lanthanoid (III) phenolate complexes	168
	4.5.3 Explored the reactivity of ytterbium pseudo-Grignard reagents	172
4.6	X-ray crystal data	173
4.7	References	175

Chapter 5: Alternative synthesis of pseudo-Grignard reagents from lanthanoid metal, I_2 and supporting ligands 179

5.1 Introduction 180

5.1.1 Preparation of pseudo-Grignard reagents using some alternative synthetic methods 181

5.2 Current study 185

5.3 Results and Discussion. 186

5.3.1 Synthesis and spectroscopic characterisation 186

5.3.1.1 Synthesis of di-iodo lanthanoid pyrazolato complexes from corresponding metals, I_2 and ^{t}Bu$_2$pzH ligands 186

5.3.1.2 Synthesis of iodo lanthanoid di-pyrazolato complexes from corresponding metals, I_2 and ^{t}Bu$_2$pzH ligands 189

5.3.1.3 Synthesis of lanthanoid di-iodo pyrazolato complexes from corresponding metals, I_2 and PhMepzH ligands 191

5.3.2 X-ray Crystal Structures 197

5.3.2.1 [Ln(^{t}Bu$_2$pz)I$_2$(thf)$_4$] (La **5.1**, Ce **5.2** and Nd **5.3**) 197

5.3.2.2 [Ln(^{t}Bu$_2$pz)$_2$I(thf)$_2$] (Er **5.4**, Lu **5.5**) 199

5.3.2.3 [Ln(PhMepz)I$_2$(thf)$_4$] (La **5.6**, Ce **5.7**, Nd **5.8**) 201

5.3.2.4 [Tb(PhMepz)I$_2$(thf)$_3$]·thf (Tb **5.9**) 204

5.3.3 Discussion 206

5.4 Conclusion and Future Outlook 208

5.5 Experimental 209

5.5.1 General aspects 209

5.5.2 Synthesis of pyrazolato lanthanoid complexes 209

5.6 X-ray crystal data 213

5.7 References 216

Chapter 6: Conclusions	220
References	223

Appendix 1: General aspects	225
Appendix 2: List of Publications	226

List of Tables

Chapter 1: Introduction to the general features of the organometallic chemistry of rare earth metals		01
1.1	Shows the separation time and discoverer of lanthanoid metals	03
1.2	The natural occurrence of lanthanoids in the earth's crust and their percentages on ores	04
1.3	Electronic configuration of lanthanoid metals	07
1.4	The standard redox potentials of lanthanoid metals	08

Chapter 2: Reaction of Ln(II) pseudo Grignard reagents with formamidines and pyrazoles		35
2.1	Summary of alkali metal based pseudo-Grignard complexes formed from Grignard reaction ($RMX(thf)_n$) with ligands	40
2.2	Chemical shifts in ^{1}H-NMR spectra of complexes **2.1** - **2.10** in C_6D_6	61
2.3	A comparison of selected bond lengths (Å) of **2.1** and **2.2** with similar complexes	64
2.4	Selected bond lengths of compounds (**2.1** and **2.6**)	64
2.5	Selected bond angles of compounds (**2.1** and **2.2**)	65
2.6	A comparison of selected bond lengths (Å) of **2.3b** with similar complexes	66
2.7	Selected bond lengths and bond angles of compound (**2.3b**)	67
2.8	A comparison of selected bond lengths (Å) of **2.5** with similar complexes	68

2.9	A comparison of selected bond lengths (Å) of **2.6** with similar complexes	70
2.10	Selected bond lengths and angles of compounds (**2.5** (n = 13) and **2.6** (n = 8))	70

Chapter 3: Reaction of Ln(III) pseudo Grignard reagents with formamidines and pyrazoles		87
3.1	A summary of trivalent lanthanoid metal based pseudo-Grignard complexes using various synthetic procedures	94
3.2	A comparison of the selected average bond lengths (Å) for compounds **3.1**-**3.3** with similar compounds	111
3.3	A comparison of the selected bond lengths (Å) of compounds **3.4**, **3.4a** and **3.5** with similar compounds	115
3.4	Selected bond lengths and angles of compounds (**3.1-3.5**)	115
3.5	A comparison of the selected bond lengths (Å) of compounds **3.6** and **3.7** with similar compounds	118
3.6	Selected bond lengths and angles of compounds (**3.6** and **3.7**)	119
3.7	A comparison of selected bond lengths (Å) of compound **3.9** with similar complexes	120
3.8	A comparison of selected bond lengths (Å) of compounds **3.10** and **3.12** with similar complexes	122
3.9	Selected bond lengths and angles of compounds (**3.9**, **3.10** and **3.12**)	122
3.10	Selected bond lengths and angles of compounds (**3.13**)	124

Chapter 4: Reactivity of Ln(II) and Ln(III) Grignard reagents with organic molecules		145
4.1	A comparison of the selected average bond lengths (Å) with similar compounds	160
4.2	Selected bond lengths and angles of compounds (**4.1**-**4.3**)	160
4.3	Selected bond lengths and angles of the compound (**4.6**)	162
4.4	Selected bond lengths and angles of the compound (**4.7a**)	163
4.5	Selected bond lengths and angles of the compound (**4.7b**)	165

4.6	Selected bond lengths and angles of the compound (**4.8**)	166

Chapter 5: Alternative synthesis of pseudo-Grignard reagents from lanthanoid metal, I_2 and supporting ligands		179
5.1	Chemical shifts in ^{1}H-NMR spectra of complexes **5.1** - **5.10** in C_6D_6	196
5.2	A comparison of selected bond lengths (Å) with similar complexes	198
5.3	Selected bond lengths for complexes (**5.1** - **5.3**)	199
5.4	Selected bond angles for complexes (**5.1** - **5.3**)	199
5.5	A comparison of selected bond lengths (Å) with similar complexes	201
5.6	Selected bond lengths and angles for complexes (**5.3** and **5.4**)	201
5.7	A comparison of selected bond lengths (Å) with similar complexes	203
5.8	A comparison of selected bond lengths (Å) with similar complexes	205
5.9	Selected bond lengths for complexes (**5.6** - **5.9**)	205
5.10	Selected bond angles for complexes (**5.6** - **5.9**)	206

Chapter 1

Introduction to the general features of the organometallic chemistry of rare earth metals

Chapter 1

1.1 Rare earth elements

Rare earth elements, also referred to as rare earth metals, are relatively abundant in the Earth's crust.[1] However, due to their geochemical properties, they are typically dispersed and not concentrated enough to form easily mineable deposits, which makes their extraction challenging. The elements from lanthanum to samarium as classified as light rare earth elements (LREEs) along with scandium and yttrium, while europium to lutetium is considered heavy rare earth elements (HREEs).

1.1.1 General features

The International Union of Pure and Applied Chemistry (IUPAC) recognizes 17 elements as rare earth elements (REEs). These include the lanthanoids, which range from lanthanum to lutetium (atomic numbers 57-71), as well as scandium (Z = 21) and yttrium (Z = 39).[2, 3] Due to their chemical similarities among lanthanoids, their extraction and separation are notoriously difficult.[4] The history of lanthanoids dates back to 1787, when Karl Arrhenius, driven by his scientific curiosity, discovered a dark mineral stone, which he named ytterbite after the Swedish town of Ytterby where he found it.[5, 6] In 1794, Gadolin identified a new element from ytterbite, calling it "ytterearth", which was the first attempt to detect REEs.[6] By 1797, Ekeberg had isolated a new element called yttria.[7] Subsequent chemical studies of yttria revealed that it contained the oxides of several rare earth elements, including yttrium, terbium, erbium, ytterbium, scandium, holmium, thulium, gadolinium, dysprosium, and lutetium.[8] In 1803, Klaproth discovered another mineral, which he named ceria.[7, 9] Research later showed that ceria contained the oxides of cerium, lanthanum, praseodymium, neodymium, samarium, and europium.[8]

Most free lanthanoid atoms exhibit the electronic configuration of $[Xe]4f^n5d^06s^2$, except for lanthanum, cerium, gadolinium, and lutetium.[10] The "f" orbitals of lanthanoids play a crucial role in determining their physicochemical properties.[8] The covalent bonds formed in lanthanoid complexes do not adopt fixed coordination geometries, but are non-directional, making these complexes predominantly ionic in nature.[11] Due to the relatively large size of lanthanoids, the most common coordination numbers in rare earth complexes are 8 and 9.[12] Lanthanoids also possess 5d and 6s atomic orbitals, which contribute to their metallic behavior (accordance with physical characteristics) through significant overlap with 4f orbitals.[8] A key challenge in coordination chemistry is achieving stable divalent lanthanides,

[11] because the +3 oxidation state is the most common among lanthanoids, some exhibit other oxidation states (+2 and +4) due to the stability conferred by unfilled, partially filled or fully filled orbitals.[13]

Table 1.1: Shows the separation time and discoverer of lanthanoid metals.[10, 14]

Elements	Year of Separation	Discoverer
Lanthanum (La)	1839	Mosander
Cerium (Ce)	1839	Mosander
Praseodymium (Pr)	1885	Von Welsback
Neodymium (Nd)	1885	Von Welsback
Promethium (Pm)	1947	Marinsky, Glendenin, Coryell
Samarium (Sm)	1879	De Boisbaudran
Europium (Eu)	1901	Demarcay
Gadolinium (Gd)	1880	Marignac
Terbium (Tb)	1843	Mosander
Dysprosium (Dy)	1886	Boisbaudran
Holmium (Ho)	1879	Cleve
Erbium (Er)	1843	Mosander
Thulium (Tm)	1879	Cleve
Ytterbium (Yb)	1878	Marignac
Lutetium (Lu)	1907	Urbain, Von welsback, James

1.1.2 Abundance of the lanthanoid metals

Promethium is the only lanthanoid metal that cannot be found in the Earth's crust, while all others lanthanoids are naturally occurring. The most stable isotope of promethium, ^{147}Pm, is produced through the fission of uranium.[7, 15-16] Lanthanoids are generally found in rare minerals, [7] with cerium being the most abundant in the Earth's crust (66 ppm), surpassing the abundance of common metals such as cobalt and lead. In contrast, thulium is the least abundant lanthanoid (0.5 ppm), with levels similar to those of silver and mercury.[16,17]

Lanthanoids are present in approximately 100 different minerals, with monazite (Ln, Th)PO_4, bastnasite ($LnFCO_3$), and xenotime (Y, Ln)PO_4 being the most common sources. Light lanthanoids are primarily found in monazite and bastnasite ores, while heavier lanthanoids

are most abundant in xenotime.[18] Commercially, monazite deposits are limited and can be found in the USA, Brazil, Australia, India, South Africa, Malaysia, and Sri Lanka. Bastnaesite is also found in various parts of Europe and Africa, but only a few commercial deposits exist, in the USA, and China.[8,9]

Table 1.2: The natural occurrence of lanthanoids in the Earth's crust and their percentages on ores.[18, 19]

Metals	**La**	**Ce**	**Pr**	**Nd**	**Pm**	**Sm**	**Eu**	**Gd**	**Tb**	**Dy**	**Ho**	**Er**	**Tm**	**Yb**	**Lu**
Occurrence (ppm)	35	66	9.1	40	0	7	2.1	6.1	1.2	4.5	1.3	3.5	0.5	3.1	0.8
Monazite (%)	20	43	4.5	16	0	3	0.1	1.5	0.05	0.6	0.05	0.2	0.02	0.1	0.02
Bastnasite (%)	33.2	49.1	4.3	12	0	0.8	0.12	0.17	***160***	***310***	***50***	***35***	***8***	***6***	***1***
Xenotime (%)	0.5	5	0.7	2.2	0	1.9	0.2	4	1	8.6	2	5.4	0.9	6.2	0.4

Bold italic represents ppm.

1.1.3 Isolation of the lanthanoid metals

A typical chemical process is often employed to extract lanthanoids from their ores, with the choice of digestive chemicals depending on the ore type. For example, hydrochloric acid is used for treating silicate minerals, while hydrofluoric acid is applied to euxenite.[20] Monazite ores are commonly used to isolate heavier lanthanoids, whereas bastnasite is preferred for extracting lighter lanthanoids.

Monazite ore is treated with a few drops of concentrated sulfuric acid (H_2SO_4) at 210°C, forming a gray sludge. Upon treatment with cold water, unreacted monazite sand (SiO_2, TiO_2, $ZnSiO_4$) and other impurities are separated by flotation (separates solid particles from a liquid suspension). The filtrate, containing ions such as Ln^{3+}, Th^{4+}, H_3O^+, HSO_4^- and $H_2PO_4^-$ is neutralized, leading to the precipitation of thorium (IV) and lanthanoid phosphates. Thorium phosphate ($ThPO_4$) is formed from the phosphate present in the ore. The lanthanoid and phosphate ions remaining in the filtrate are treated with a base or acid, resulting in the separation of lanthanoid hydroxides or oxalates. [18, 21]

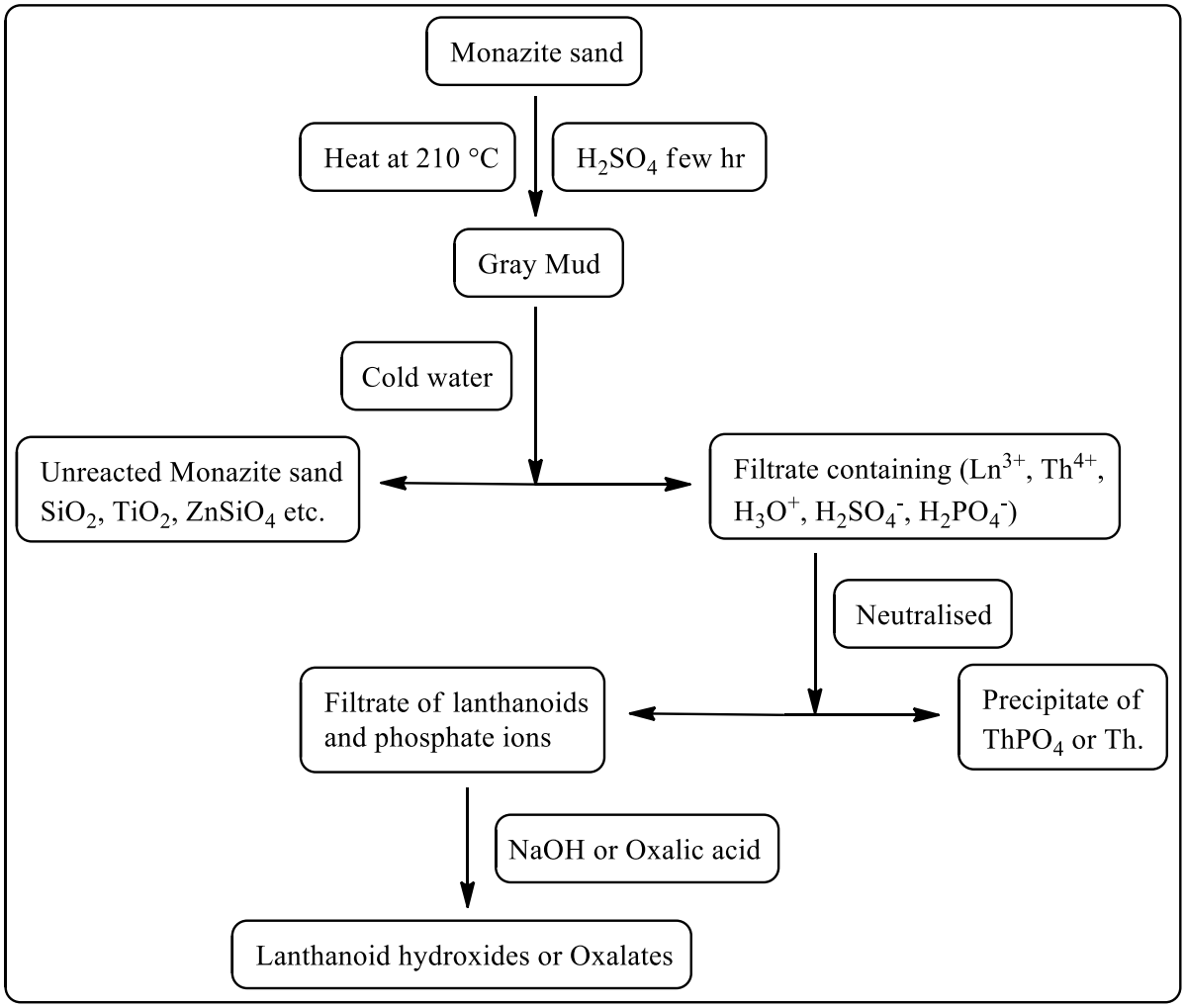


Figure 1.1: Isolation of lanthanoid metals from monazite.[22]

Concentrated bastnasite ore is treated with 10% hydrochloric acid (HCl) to remove calcium carbonate, yielding a mixture containing 70% lanthanoid(III) oxides. After oxidizing these oxides, the cerium content is converted to Ce(IV). The residue is then treated with HCl to extract a mixture of Ln(III) chlorides and CeO_2(s) is precipitated and separated.[18, 21]

For the separation of lanthanoids, ion-exchange and solvent extraction methods are the most widely used techniques.[21] Due to the similar properties and ionic size of the lanthanoids, individual separation is challenging.[21] Cation exchange resins are commonly employed to separate lanthanoid mixtures, with ethylenediaminetetraacetic acid (EDTA) used as a complexing agent to elute the remaining mixture. Heavier lanthanoids are eluted faster as they form stronger complexes with EDTA. A long column is typically used to achieve complete separation.[8, 19] In commercial solvent extraction process, complexing agents such as tributyl phosphate or 2-ethylhexyl phosphoric acid are employed.[8]

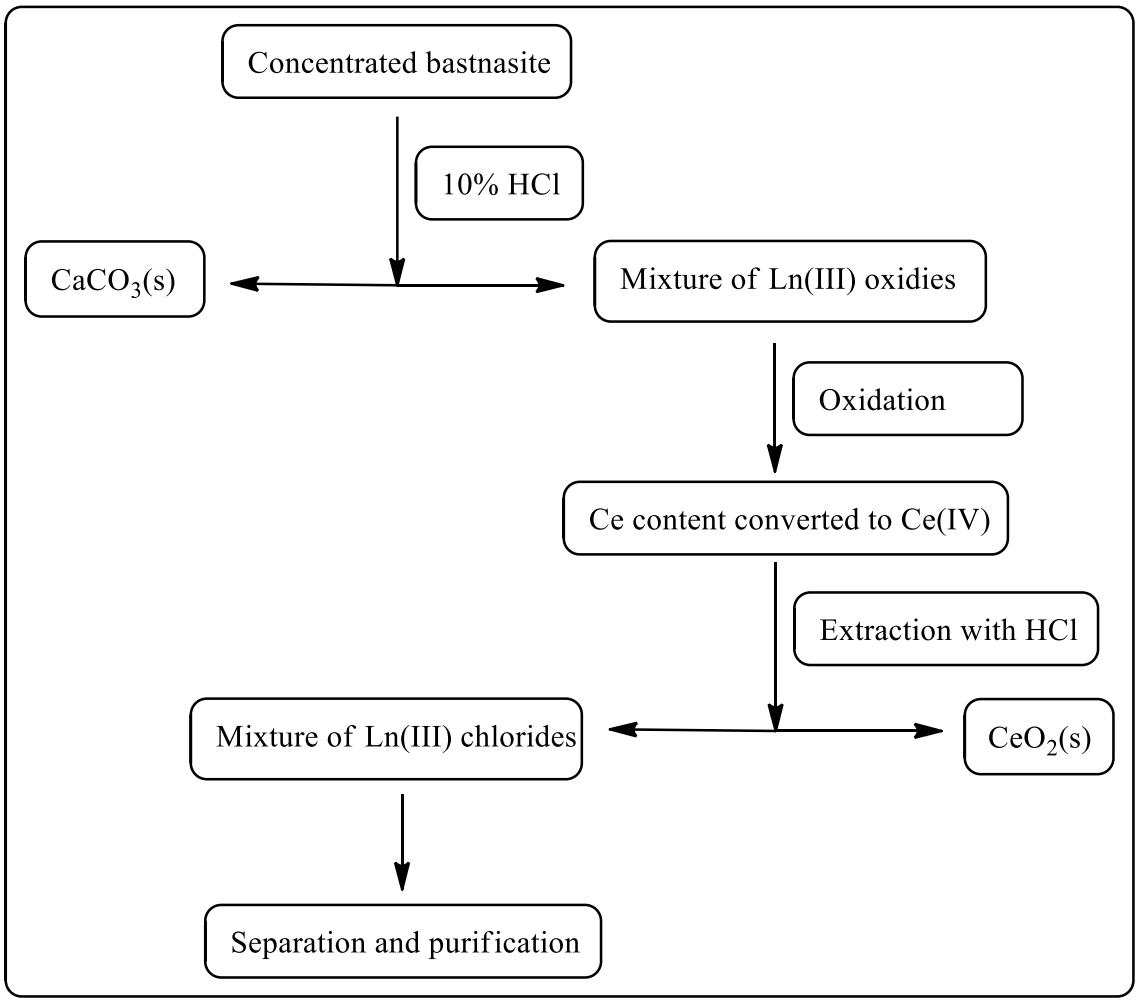


Figure 1.2: Isolation of lanthanoid metals from bastnasite.[23]

1.1.4 Properties of the lanthanoid metals

Electron transfer has facilitated many significant reduction reactions in organic chemistry, [24] with lanthanoids recently playing a significant role in this field. Historically, the earliest application of lanthanoids was Eu(II), which has long been used as a simple one-electron reductant in aqueous redox chemistry.[25, 26] Lanthanoids are highly electropositive, with the +3 oxidation state being the most stable state. However, certain 4f electronic configurations also can give rise to +4 (e.g., Ce, Tb) and +2 (e.g., Eu, Yb) ions.[9, 27] Samarium exhibits versatility by participating in both one (SmI_2) and two-electron processes, expanding the applications of SmI_2.[28] Ce(IV) is also widely used as one-electron oxidant.[29]

The divalent lanthanoid salts, known for their strong reducing properties, have become increasingly important. In earlier studies, the divalent state was considered accessible only to europium (f^7 configuration; half-filled shell), ytterbium (f^{14}; filled shell), and samarium (f^6;

approaches a half-filled shell), which are called as 'classical' divalent metal ions. The electronic configurations and oxidation states of lanthanoid metals are presented in table **1.3**.

Table 1.3: Electronic configuration of lanthanoid metals.[30, 31, 31(a)]

Name	**Symbol**	**Electronic Configuration**	
		Ln^0	Known oxidation State **Common**; Unusual
Lanthanum	La	$5d^16s^2$	**III**; 0, II
Cerium	Ce	$4f^15d^16s^2$	**III, IV**; II
Praseodymium	Pr	$4f^36s^2$	**III, IV**; 0, II
Neodymium	Nd	$4f^46s^2$	**III**; 0, II
Promethium	Pm	$4f^56s^2$	**III**
Samarium	Sm	$4f^66s^2$	**II, III**; 0
Europium	Eu	$4f^76s^2$	**II, III**
Gadolinium	Gd	$4f^75d^16s^2$	**III**; 0, II
Terbium	Tb	$4f^96s^2$	**III, IV**; 0, II
Dysprosium	Dy	$4f^{10}6s^2$	**III**; 0, II
Holmium	Ho	$4f^{11}6s^2$	**III**; 0, II
Erbium	Er	$4f^{12}6s^2$	**III**; 0, II
Thulium	Tm	$4f^{13}6s^2$	**III**; II
Ytterbium	Yb	$4f^{14}6s^2$	**II, III**
Lutetium	Lu	$4f^{14}5d^16s^2$	**III**; 0, II

The reduction of pyridine carboxylic acids using Eu(II), as demonstrated by Vrachnou and Katakis in 1975, represents one of the earliest efforts in this field.[32] In this study, the europium ion formed complexes with nicotinic, isonicotinic, N-methyl isonicotinic, and picolinic acids, involving a metal to ligand charge transfer process. Ytterbium in ammonia proved to be a convenient alternative to traditional alkali metals in Birch-type reductions, facilitating the reduction of α,β-unsaturated ketones to saturated ketones, the conversion of alkynes to *trans* alkenes, and the reduction of aromatic systems to 1,4-dihydroaromatics.[33]

The preparation of divalent europium salts is relatively straightforward compared to other divalent lanthanoid salts, which often require more than one step or unconventional techniques. However, these europium salts are less reactive toward various organic

reagents.[34] Among the 'classical' divalent lanthanoids, ytterbium(II) and samarium(II) possess higher reducing power compared to europium(II), as indicated by their standard reduction potentials; Eu^{2+}/Eu^{3+} = -0.43, Yb^{2+}/Yb^{3+} = -1.15, and Sm^{2+}/Sm^{3+} = -1.55 V.[25, 26] The standard redox potentials for trivalent lanthanoid metals are listed in table **1.4**.

Table 1.4: The standard redox potentials of lanthanoid metals, [35, 36] * = estimated, † = in THF. ⟶

Name	E^0 **(V) for** $RE^{3+}+e^- \rightarrow RE^{2+}$	E^0 **(V) for** $RE^{4+}+e^- \rightarrow RE^{3+}$	E^0 **(V) for** $RE^{3+}+3e^- \rightarrow RE$
Lanthanum	-3.1*	–	-2.37
Cerium	-3.2*	1.70	-2.34
Praseodymium	-2.7*	3.4*	-2.35
Neodymium	-2.6†	4.6*	-2.32
Promethium	-2.6*	4.9*	-2.29
Samarium	-1.55	5.28	-2.30
Europium	-0.34	6.4*	-1.99
Gadolinium	-3.9*	7.9*	-2.29
Terbium	-3.7*	3.3*	-2.30
Dysprosium	-2.5†	5.0*	-2.29
Holmium	-2.9*	6.2*	-2.33
Erbium	-3.1*	6.1*	-2.31
Thulium	-2.3†	6.1*	-2.31
Ytterbium	-1.05	7.1*	-2.22
Lutetium	–	8.5*	-2.30

The availability of the lanthanoid di-iodides $[LnI_2(thf)_n]$ and other halide compounds, which are thermally stable solids for Sm, Eu, and Yb has opened new avenues for the synthesis of organic derivatives.[37] While these compounds are not organic themselves, they play a vital role in reduction chemistry, offering potential as precursors for a new class of reagents suitable for organic synthesis. Consequently, classical divalent lanthanoids have established a significant presence in organometallic chemistry.

1.1.5 Rare earth organometallic compounds

In 1902, the first rare earth (RE) organometallic compound was reported with the synthesis of trimethyl cerium.[38] The field progressed significantly in 1954 when Birmingham and Wilkinson synthesised the first π-bonded lanthanoid tris(cyclopentadienyl) complexes, (Cp_3Ln) (Ln = Sc, Y, La, Ce, Pr, Nd, Sm, Gd; Cp = η^5- cyclopentadienyl).[39] In 1968, Hart and Saran introduced the first σ–bond organometallic RE complex [$Sc(C_6H_5)_3$].[38] Later Ln-C sigma bond [$Lu(Ar)_4$] compound reported by Cotton *et. al* 1972.[38a]

Recently, lanthanoid metal complexes with neutral O- and N-donor ligands have attracted considerable research interest due to their unique steric and electronic properties.[40] The most widely used synthetic methods for lanthanoid organometallic complexes include σ bond metathesis, protolysis reactions, and increasingly, redox trans-metallation/protolysis reactions.[38] Using these common synthesis process Eaborn *et. al* 1994 and 1996 introduced divalent silylamide complexes. [40a, 40b] In review Zimmermann *et. al* 2010 introduced a wide range of homoleptic rare-earth metal complexes containing Ln−C σ-bonds [40c] while Mortis et. al 2024 discussed organic synthesis process of rare earth metal alkyl and aryl compounds [40d] and Ortu 2022 discussed the methodologies for synthetic chemistry of rare earth starting materials. [40e]

1.1.6 Application of the lanthanoid metals and their compounds

Rare earth elements (REEs) have garnered significant attention for their diverse characteristics, leading to numerous medical and industrial applications. In the 1960s, lanthanoid(III) ion complexes were found to exhibit various pharmacological properties, including anticoagulant, anti-inflammatory, antibacterial, anti-allergic, and anti-cancer activities, as well as being effective in treating burns.[41] Additionally, lanthanoid compounds have demonstrated antitumor, antivirus, and antifungal activity.[42, 43] Their coordination complexes show anti-thrombosis effects and are crucial in cancer diagnosis and therapy, as well as serving as next generation drugs for treating neoplastic diseases.[44]

Lanthanoid ions such as Nd(III), Sm(III) or Yb(III) ions emit in the Near-infrared (NIR) range and are utilized for in vivo for luminescence imaging, allowing for deep tissue penetration in animals.[45] Calcium ions (Ca^{2+}) can be substituted by lanthanoid ions in certain enzymes and tissues, which may increase cell apoptosis and affect bone integrity along with cell signaling, confirming the role of rare earth elements in biological process.[44] Due to their

low toxicity, these metal complexes are preferred for bio-imaging applications. Their uses have expanded to include light-emitting diodes, catalysts, lasers, magnetics materials, and MRI contrast agents.[46]

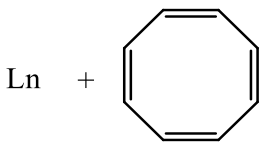
In industrial applications, REEs are used in the production of catalysts, ceramics, alloys, and electronics.[4] Key applications include petrogenetic indicators, petroleum-cracking catalysts, luminescent solar concentrators, and tracing the movement of water masses in oceans.[47-54] Recently, the use of lanthanoids has increased in electronic devices such as computers and smartphones, as well as phosphors for lighting and displays.[55]

Specific applications include rare earth magnets (e.g., $Fe_{14}Nd_2B$ with added Pr and Dy), which are widely used in electric and hybrids cars, wind turbines for renewable energy generation and computers. Cerium ceramics are produced on a large scale to support exhaust emission catalysts, while lanthanoids are also employed in precision military guidance systems, luminesce applications in safety equipment, and medicinal uses. Additionally, they are incorporated in metal-organic compounds for artificial rubber production.[56] In agriculture, they are used to enhance crop production in China, and as animal feedstock supplements in Switzerland.[57, 58] Their environmentally benign nature encourages their use as 'green' corrosion inhibitors to replace toxic metal chromates.[59]

1.2 Complex formation of the lanthanoid metals

Ln(II) complexes

Ytterbium and europium made significant contributions to organometallic chemistry in early 1964, preceding the involvement of Samarium. Both metals can be dissolved in liquid ammonia, allowing for access to their divalent chemistry.[60] Lanthanoid compounds can be isolated using bulky cyclopentadienyl ligands, with lanthanoids typically exhibiting their normal oxidation states of +2.[61] Europium and ytterbium react with cyclopentadiene and cyclooctatetraene to produce cyclopentadienyl and cyclooctatetraenide complexes (**eqn. 1.1**).[62, 63]



$$Ln + \xrightarrow{NH_3} [Ln(C_8H_8)]_n$$

$$Eu + C_5H_6 \xrightarrow{NH_3} (C_5H_5)_2Eu(NH_3) + C_5H_8$$

Equation 1.1: Complexes of cyclopentadienyl and cyclo-octa tetraenyl of lanthanoid (Ln = Yb, Eu).

The later development of divalent samarium chemistry can be attributed to several factors. First, samarium is a larger and more powerful reductant, making it challenging to handle experimentally. Additionally, samarium forms stable metal complexes due to steric saturation within its coordination sphere. The growth of divalent samarium chemistry in the organometallic field was further hindered by a lack of suitable starting material and its insolubility in liquid ammonia.[64]

Divalent halide products of the lanthanoids can be classified as conventional salts or derived from Ln(III) "electrides". Conventional salts include YbI_2, EuI_2, and SmI_2, while the Ln(III) electride salts consists of LaI_2, CeI_2, and GdI_2. Soluble iodide complexes can also be formed with ethers, such as TmI_2(di-methoxy-ethane)$_3$.[65]

The development of organo-lanthanide chemistry intensified with the introduction of cyclopentadienyl complexes and alternative ligand sets, highlighting samarium as the preferred choice among the 14 lanthanides due to its reactivity and strong reducing power.[66] However, several challenges hindered the advancement of samarium in divalent reduction chemistry. Many reactions mediated by Sm^{2+} did not yield fully defined products, obtaining clear NMR spectra proved difficult, as both Sm^{2+} and Sm^{3+} are paramagnetic. Consequently, X-ray crystallography became essential for the identifying reaction products (crystals), but this wasn't feasible in all cases. Typically, such issues in lanthanide chemistry problems could be addressed through size optimization. Unfortunately, this approach was not viable in reductive chemistry, as europium and ytterbium were the only other divalent ions available at that time and their reduction potentials and reactivities were significantly lower than those of samarium.[67]

Although these limitations restrict divalent reductive lanthanide chemistry, researchers continue to explore this field, viewing it as a promising area of study. A significant breakthrough was the discovery of new molecular divalent oxidation states of thulium, dysprosium, and neodymium by Evans, Bochkarev, and co-workers. While some reports of molecular divalent lanthanide complexes involving metals other than samarium, ytterbium, and europium appeared in the literature during the 1960s and 1970s, [68] their existence could not be confirmed due to the lack of adequate X-ray data. In solution chemistry, solid-state

methods produced divalent lanthanide ions for all the metals, although molecular chemistry for these species had not yet been reported.[69]

Ln(III) complexes

Most trivalent lanthanides exist as ionic salts. These trivalent ions readily accept oxygen-donor ligands to form stable complexes and their coordination has recently extended to include nitrogen-donor ligands. In aqueous solutions, larger lanthanide ions typically form 9-coordinate complexes, represented as $[Ln(H_2O)_9]^{3+}$, while smaller ions form 8-coordinate complexes, denoted as $[Ln(H_2O)_8]^{3+}$. The second coordination sphere of the later lanthanides generally contains more water molecules.[70]

Ln(IV) complexes

Cerium(IV) is particularly notable as it is a valuable oxidizing agent, with ceric ammonium nitrate being a prime example. The stability of Ce(IV) is attributed to its empty f shell, while other tetravalent lanthanides are typically unstable, with stable compounds primarily limited to the oxides and fluorides of Pr(IV) and Tb(IV). Recently, however, complexes of Tb(IV) [71-73] and Pr(IV) [74] have been reported in the literature.

1.2.1 Amidinate complexes of rare earth

As two electron donors, amidines ($N = C(R^1) - NR^3R^4$) can form amido groups ($R^2N = C(R^1) - NR^3$) by displacing R^4 which can be achieved through treatment with a strong base when R^4=H (hydrogen).[75] Gerhardt is recognized as the pioneer of amidines (**Fig. 1.3**). In 1858 he synthesized amidines from aniline and N-phenylbenzimidyl chloride.[76] Deprotonated amidinate (**Fig. 1.5**) act as anionic ligands, which can be easily modified both electronically and sterically to form stable metal complexes.[79] In chemistry and material sciences, the complexes of amidinate have multipurpose applications like as; synthesis of non-cyclopentadienyl organolanthanide, amidinate and guanidinate complexes.[40, 80-82]

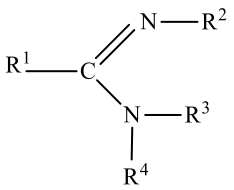
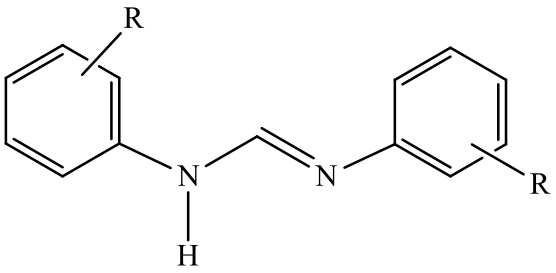


Figure 1.3: The common structure of amidine.[76]

When R^1 = H, the compound is called formamidine. [75] **Fig. 1.4**, shows some common forms of formamidine.



R = 2,6-F; 2,3,4,5-F; 2-F; o-Me; p-Me; m-Me; 2,6-Me; 2,6-Et;2,6-^{i}Pr; 2,4,6-Me; 2,6-Ph

Figure 1.4: N, N′-Bis(aryl) formamidine.[77]

Considering the number and changing the substituents amidines are divided into five general forms (**Fig. 1.5**).[78]

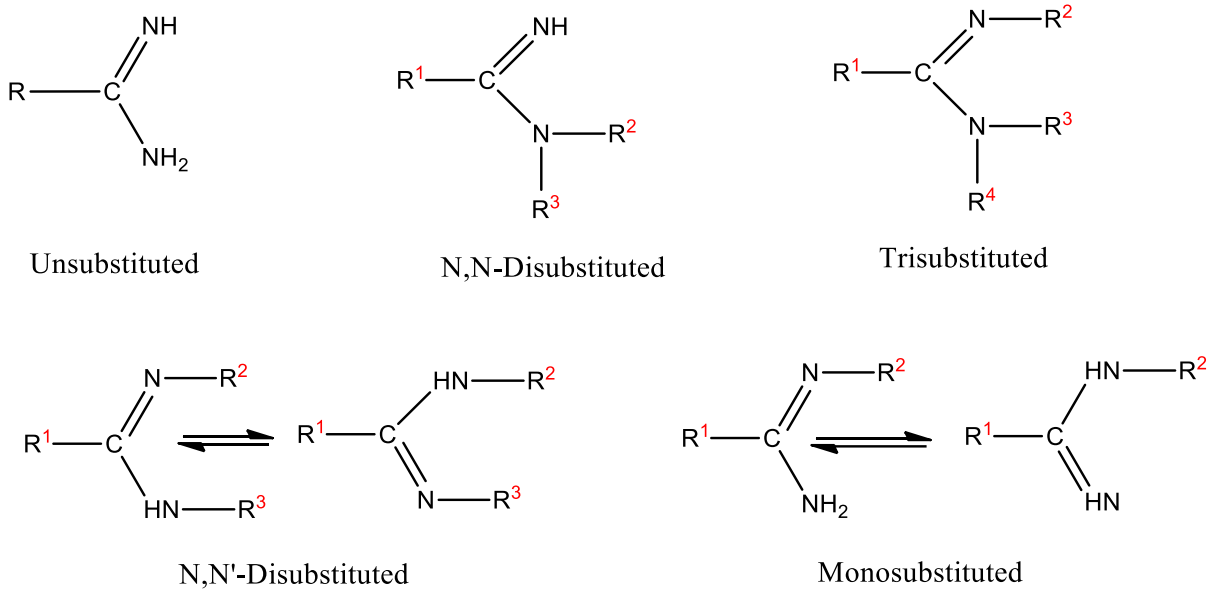


Figure 1.5: Common types of the amidine.

The ligands of N, N′-diarylformamidinate have greater simplicity in their formation compared with their guanidinate and amidinate analogues. The synthesis of formamidines, is straightforward for the availability of various anilines with differing electronic and steric effects has facilitated their widespread use.

Among the amidinate ligands, N, N′-diarylformamidinate $[((ArN)_2CH)^-, (ArForm^-)]$, is notable for its extensive range of applications, including catalytic activity in the Tishchenko reaction.[83] In recent years, N, N′-diarylformamidinate ligands have demonstrated significant

coordination flexibility within the family of organo-amide based ligands.[84, 85] Additionally, formamidines function as anionic ligands that support low valent compounds. Rare earth metals often have N donor atoms attached to ligands, enhancing their steric bulk and electronic properties.[86] By using distinct formamidines with various rare earth metals, a range of metal-organic complexes with different coordination numbers can be synthesised. N, N′-diarylformamidinate ligands can bind to metal centers through multiple modes, (**Fig. 1.6**) resulting a wide variety of complex activities with metals.[87, 88]

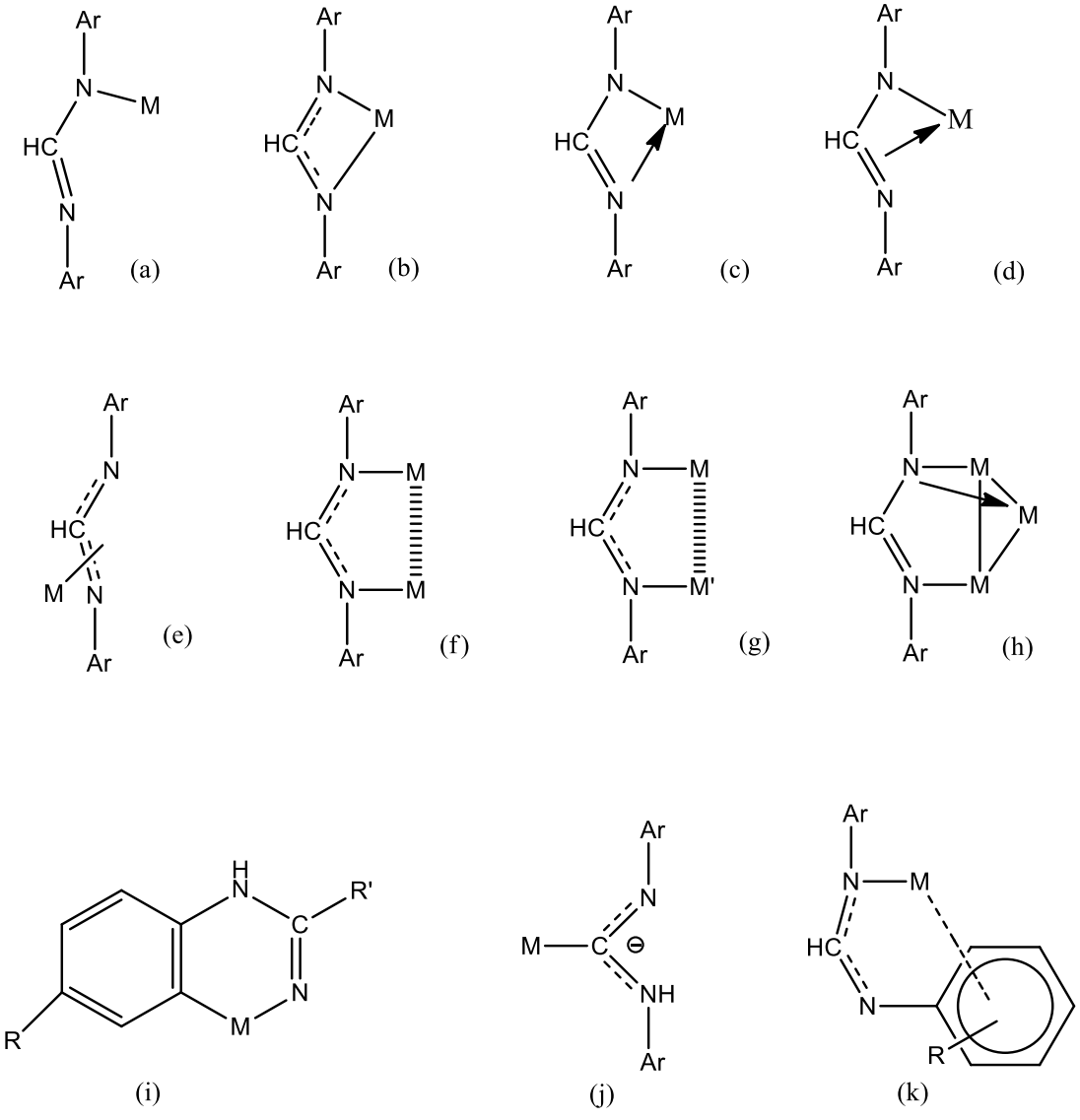


Figure 1.6: Shows the possible bonding modes for N, N′-diarylformamidinate ligands; (a) monodentate, (b-d) chelate, (e) η^3-allyl, (f, g) bridging, (h) capping, (i) ortho-metallation, (j) C-bonded, and (k) η^6 bonding.[75] From these bonding modes, in the chemistry of RE formamidinate the most common one is symmetric chelation (b).

1.2.2 Pyrazolato complexes of rare earth

The heterocyclic organic compound with the molecular formula $C_3H_4N_2$ is known as pyrazole consisting of three carbon atoms and two nitrogen atoms. At 25 °C, the pKb of pyrazole is 11.5, indicating that it functions as a weak base.[89] Pyrazole features have a C_3N_2 ring with adjacent nitrogen atoms.[90] German Chemist Ludwig Knorr in the year 1883, first time used the term pyrazole.[91] Subsequently, in 1898, German chemist Hans von Pechmann established a method for synthesising pyrazole from acetylene and diazomethane.[92]

Pyrazoles can be prepared by using a variety of alkyl, aryl, or other substituents on the carbon atoms of the ring (**Fig. 1.7**).[93] The derivatives of pyrazoles and even pyrazole itself are not freely commercially available. Substitution of carbon *C*3 and *C*5, the carbon atoms adjacent to the two N atoms is relatively simple, and these ligands have a steric effect on the environment around the N-donors to which metal ions can be co-ordinated.

1H-pyrazoles and derivatives have an N-H group at *N*1 and N-donor at *N*2, acting as Lewis's acid pyrrolic and Lewis basic pyridine.[93] These pyrazole derivatives typically bonded in kappa 1 fashion with metal ions at *N*2, leaving the N-H group for interacting with anions or other hydrogen bond acceptors.[94, 95] The pyrazolato ions have *N*1 and *N*2 lone pairs (end-on) and π-system (side-on). Again, the pyrazole (ring) ligands have the property of di-topic nature and coordinative flexibility. They have very flexible bonding arrangements in coordination chemistry.[93]

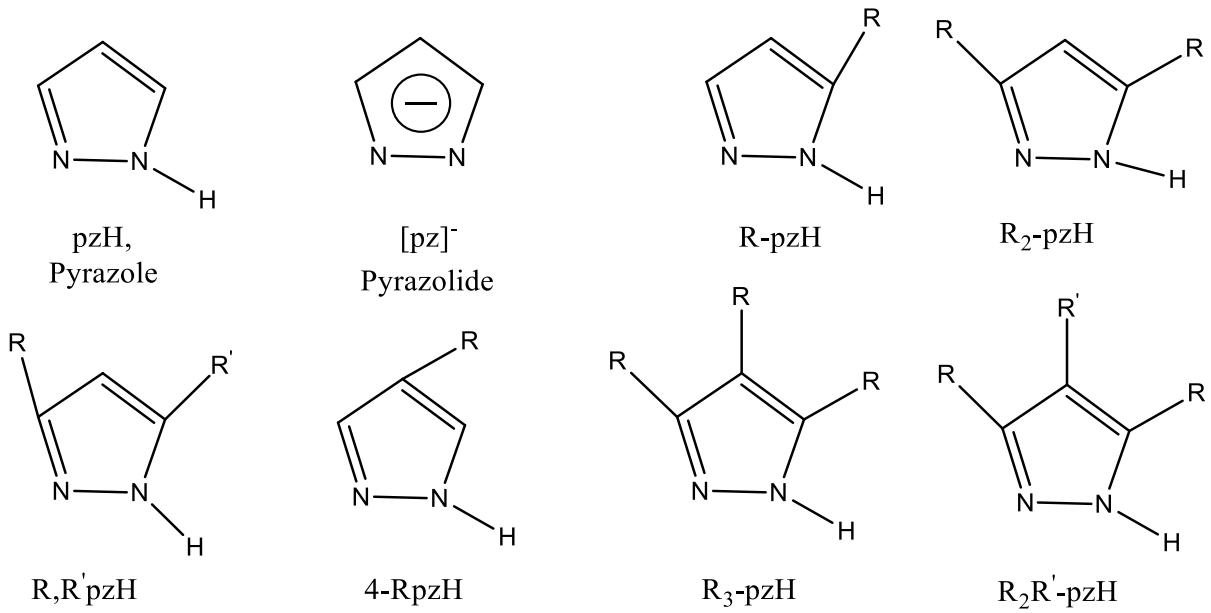


Figure 1.7: Different C substituted derivatives of pyrazole.[93]

The pKa of the protonated version of pyrazole (**eqn. 1.2**) in water is 14.2 and in base is 2.5 (**eqn. 1.3**).[96, 97]

$$pzH \rightleftharpoons pz^- + H^+ \qquad (1.2)$$

$$H_2pz^+ \rightleftharpoons Hpz + H^+ \qquad (1.3)$$

The acidic effect of pyrazole is weaker than aliphatic alcohols. But the basicity of pyridine or simple aromatic amines is higher than pyrazole. Pyrazole is a good π-acceptor but a little bit weaker donor ligand than pyridine.[98] For alkylation or arylation, the pK value of the pyrazole ring can change maximum ± 2. Again, the pKa value of pyrazole changes by influencing electro-withdrawing substitutes.[96, 97] Both solution and solid-state 1H-pyrazoles show tautomeric equilibria (**Fig. 1.8**).[99] ^{13}C NMR spectroscopy is usually used for distinguishing these two unsymmetrical tautomers.[100, 101]

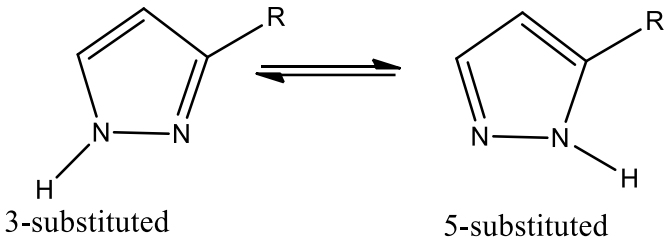
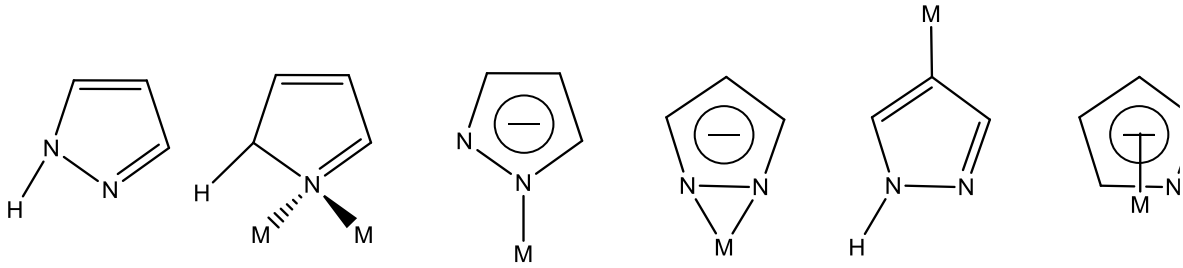


Figure 1.8: Tautomeric equilibrium of 1H-pyrazole.[99]

Fig. 1.9 represents different co-ordination modes of pyrazoles and pyrazolide anions with lanthanoid metals.



k^1 k^1:k^1-μ k^1 k^2 k^1C η^5

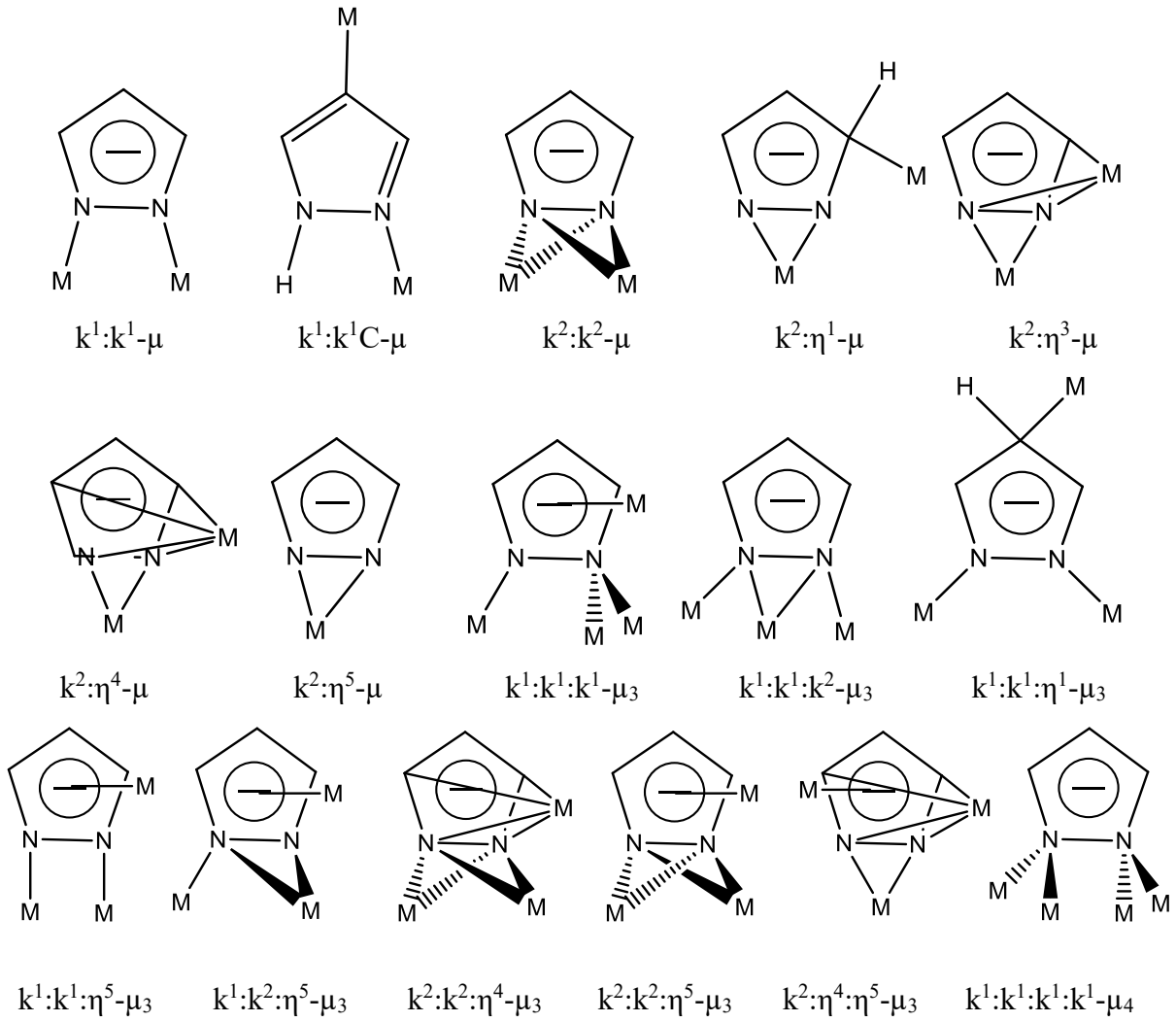


Figure 1.9: Different co-ordination modes of pyrazoles and pyrazolide anions.[93]

1.3 Chemistry of rare earth metals

Lanthanoid complexes can be synthesized by using different methods. Some common synthetic pathways for the preparation of rare earth complexes are discussed here.

(i) Salt elimination reaction

Salt elimination reaction, also known as metathesis, involves the reaction between a rare earth halide and an alkali metal-ligand complex (**eqn. 1.4**).[102, 103]

$$LnX_n + nML \longrightarrow [LnL_n] + nMX$$

M = alkali metal

L = anionic ligand

X = halide

n = 2,3

Equation 1.4: The salt elimination reaction in the synthesis of lanthanoid complexes.

The solubility of solvent-free LnX_n is low, so the choice of alkali metal salt and lanthanoid halide is crucial. Isolation of the desired product (LnL_n) can be difficult leading to low yields and unwanted side products (LnL_nX).[104, 105]

(ii) Protolysis reactions

Protolysis reactions involve the reaction of a lanthanoid precursor (LnR_n) with a protic ligand (LH).[106, 107] This reaction can be performed in non-coordinating solvents (**eqn. 1.5**).

$$Ln(R)_n + nLH \longrightarrow [LnL_n] + nRH$$

R = usually $N(SiMe_3)_2$, $N(SiHMe_2)_2$ or C_6F_5

L = ligand (CH_2SiMe_3, benzyls), n = 2, 3

Equation 1.5: Protolysis reactions in the synthesis of lanthanoid complexes.

Both homoleptic and heteroleptic lanthanoid complexes can be synthesized using this route. The two major drawbacks of this reaction are (i) high air and moisture sensitivity of most reagents and the chance of decomposition, (ii) a metathesis process is required for the preparation of alkyls or amide lanthanoid precursors.[108]

(iii) Redox transmetallation reactions

The preparation of lanthanoid complexes from lanthanoid metal and metal-based ligand is called redox transmetallation reaction (**eqn. 1.6**).[109]

$$mLn + nML_m \longrightarrow m[LnL_n] + nM$$

L = anionic ligand

n = 2,3

m = 1-4

M = Hg, Bi, Sn, $SnMe_3$

Equation 1.6: Redox transmetallation reactions in the synthesis of lanthanoid complexes.

(iv) Direct metallation reactions

Direct metallation reactions are another metal-based reaction that involves the direct reaction between lanthanoid metals and ligands, eliminating H_2 in the process (**eqn. 1.7**).[110-112]

$$Ln + nLH \xrightarrow[T]{Hg} [Ln(L)_n] + n/2H_2$$

L = Ligand, T = temperature

n = 2, 3

Equation 1.7: Direct metallation reaction synthesis of lanthanoid complexes.

The main drawbacks of this process are the use of mercury or chloride of mercury (to activate the surface of metals) can hamper the reaction, [113, 114] both reactants and products should be thermally stable, need high pressure (maximum 15 atm) in Carius tubes.[106, 115, 116]

(v) Redox transmetallation/protolysis (RTP) reaction

The most successful and useable methods for the synthesis of bis $[Ln(L)_2(thf)_2]$ (**eqn. 1.8, i**) and tris $[Ln(L)_3(thf)_m]$ (**eqn. 1.8, ii**) lanthanoid complexes is redox transmetallation/protolysis (RTP). RTP reaction involves the one-pot reaction among lanthanoid metals, bis-pentafluorophenylmercury or tris-pentafluorophenylbismuth and LH in thf.[117-120]

$$Ln + Hg(C_6F_5)_2 + 2LH \xrightarrow[rt]{thf} [Ln(L)_2(thf)_2] + Hg + 2C_6F_5H \qquad \textbf{(i)}$$

LH = Formamidine; Pyrazole

Ln = Yb; Eu; Sm

rt = Room Temperature

$$xLn + yM(C_6F_5)_z + yzLH \xrightarrow[rt]{thf} x[Ln(L)_3(thf)_m] + yM + yzC_6F_5H \qquad \textbf{(ii)}$$

M = Hg; (x=2; y=3; z=2; m=varies)

M = Bi;(x=1; y=1; z=3; m=varies)

LH = Formamidine; Pyrazole

Ln = La; Ce: Nd: Sm; Gd; Tb: Dy; Ho; Er; Tm: Yb; Lu

rt = Room Temperature

Equation 1.8: Redox transmetallation/protolysis (RTP) reactions in the synthesis of lanthanoid complexes.

(vi) Direct reactions

Direct reactions are easy to isolate, having good yield for a wide variety of formamidinatoiodidolanthanoid (III) complexes. This one-pot reaction involves the desired

free metals and iodine with corresponding formamidine (DFFormH or DippFormH) in appropriate ratios.[121]

$$2Ln(xs) + I_2 + 4DFFormH \xrightarrow{thf} 2[Ln(DFForm)_2(thf)_2I] + 2H_2 \quad \textbf{(i)}$$

$$Ln(xs) + I_2 + FormH \xrightarrow{thf} [Ln(Form)(thf)_3I_2] + 1/2H_2 \quad \textbf{(ii)}$$

FormH = DFFormH or DippFormH

Equation 1.9: Direct reactions involving lanthanides.

1.4 Pseudo-Grignard reagents

Victor Grignard received the Nobel Prize (1912) in Chemistry for the synthesis of organomagnesium compounds, mainly organomagnesium halides [$RMg(solv)_nX$] (R = Me, Et, Ph; X = Cl, Br, I; solv = thf, Et_2O, n = number) (**eqn. 1.10**).[122, 123]

$$Mg + RX \xrightarrow[0\ °C]{solv} [RMg(solv)_nX]$$

R = Me, Et, Ph. X = Cl, Br, I

Solv = thf, Et_2O

Equation 1.10: Grignard reagent preparation.

Pseudo-Grignard reagents of organoiodides with lanthanoids to synthesize [$RLn(thf)_nI$] were introduced by Evans et al. in 1971 (**eqn. 1.11**).[124]

$$Ln + RI \xrightarrow[-20\ °C]{thf} RLn(thf)_nI$$

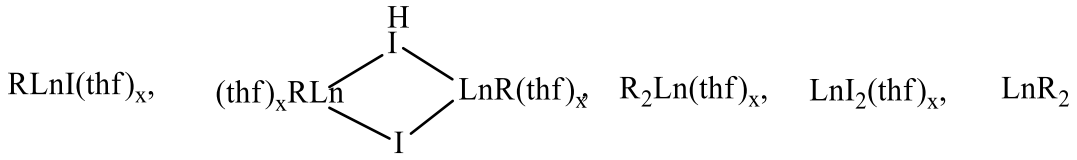
Ln = Sm, Eu, Yb. R = Me, Et, Ph

Equation 1.11: Pseudo Grignard reagent preparation.

Typical pseudo-Grignard reagents have general formula [$RLn(solv)_nX$] (Ln = Sm, Eu and Yb; R = Me, Et, Ph; X = Cl, Br, I; solv = thf, Et_2O), [125, 126] and have similar reactivity towards acids and electrophiles compared to the Mg-based reagents, leading to the reasons why organic and inorganic transformations received practical attention. Considering these reasons, Grignard analogous [$RLn(solv)_nX$] formulated from organolanthanoid halides can be called as pseudo-Grignard reagents.[127, 128] In contemporary times many organolanthanoids (both +2 and +3 oxidation states) with the ligands of cyclopentadienyl and non-cyclopentadienyl have been synthesized.[82,129-136] Pseudo-Grignard reagents [$RLn(thf)_nI$] can

be synthesized by the oxidative addition of organoiodides RI to Ln^0 (Ln = Sm, Eu and Yb, R = Me, Et, Ph) (**eqn. 1.11**).[124, 136]

Previous magnetic susceptibility studies of pseudo-Grignard reagents show that by varing the ratios of Ln: I (Ln = Sm, Eu, Yb) in the reaction (**eqn. 1.12**), we can get a mixture of di-valent and tri-valent complexes. Divalent Lns are the major components in these reactions, though the composition can vary, the amount of divalent Ln is the highest in the case of for example Eu^{2+} (99%), whilst more of the Ln(III) species are formed when using other divalent Lns, such as Yb^{3+} (15%) and Sm^{3+} (50%).[124] The solution of pseudo-Grignard reagents (**eqn. 1.12**) may have the below five different divalent species, where Ln = Yb, Eu, R = 2,6-Ph_2-C_6H_3 and x = number of solvent molecules.[137]



For Yb the Schlenk equilibrium was proved using ^{171}Yb NMR. The chemical shifts of ^{171}Yb NMR spectra detected that, [YbDpp(thf)$_n$I], [Yb(Dpp)$_2$(thf)$_2$], [Yb(thf)$_4$I$_2$] (Dpp = 2,6-Ph_2-C_6H_3) are the major three complexes in the solution (**eqn. 1.12**).[137]

$$2[Yb(Dpp)(thf)_nI] \rightleftharpoons [Yb(Dpp)_2(thf)_2] + [YbI_2(thf)_4]$$

Dpp = 2,6-Ph_2-C_6H_3

Equation 1.12: The Schlenk equilibrium of Yb Grignard reagents.

The major drawback is that the characterization and structural information of these intermediates [YbDpp(thf)$_n$I], [Yb(Dpp)$_2$(thf)$_2$] are very limited.[138, 139] At the end of last century, from the reaction of ytterbium metal and bulky silylated iodoalkyl group in thf, it was possible to isolate the pseudo-Grignard complex [Yb{C(SiMe$_3$)$_2$(SiMe$_2$R)}I(Et$_2$O)]$_2$ (R = Me, MeO, CH=CH$_2$) (**eqn. 1.13**).[140, 141]

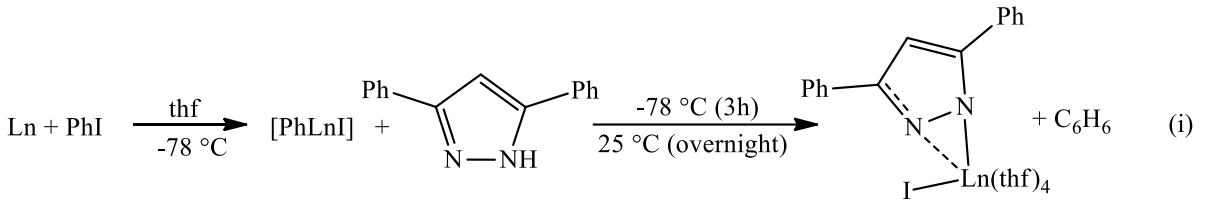
$$2Yb + 2\{C(SiMe_3)_2(SiMe_2R)I\} \xrightarrow[16\ h]{Et_2O} [Yb\{C(SiMe_3)_2(SiMe_2R)\}(Et_2O)I]_2$$

R =CH=CH$_2$, MeO, Me

Equation 1.13: Isolation of [Yb{C(SiMe$_3$)$_2$(SiMe$_2$R)}I(Et$_2$O)]$_2$ pseudo-Grignard complex.

A few years ago, Deacon and co-workers reported a new direction for pseudo-Grignard reaction, using Eu and Yb as lanthanoid metals, pyrazoles (Ph$_2$pzH) as ligand, also added PhI in thf and isolate [Ln(Ph$_2$pz)(thf)$_4$I] complexes. They sonicated the metal powders with PhI,

at a low temperature (-78 °C), then another three (3) hours after the addition of ligands and overnight room temperature (**eqn. 1.14, i**).[142] Recently, Ali and co-workers followed the same procedure and produced some new pseudo-Grignard reagents from lanthanoid metals (Eu, Yb), PhI and formamidines in thf (**eqn. 1.14, ii**).[143]



LH = DippFormH, XylFormH, MesFormH

Ln = Eu, Yb

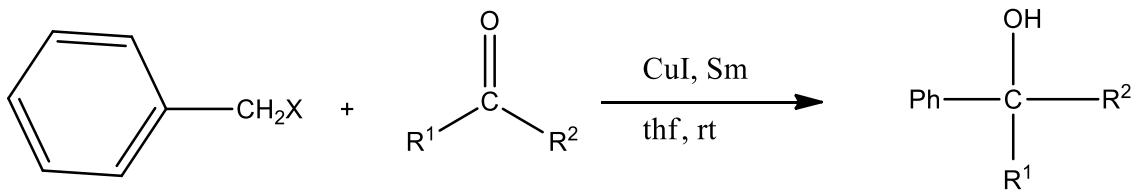
Equation 1.14: Reactivity of pseudo-Grignard lanthanide reagents and preparation of heteroleptic lanthanoid complexes.

The oxidative addition reaction was effectively applied for some tri-valent lanthanoids by Dolgoplosk, et. al., [144] for synthesizing pseudo-Grignard complexes $[(Ph_3C)_2LnCl]$ or $[(Ph_3C)LnCl_2]$ (Ln = Pr^{3+}, Nd^{3+}, Gd^{3+} and Ho^{3+}) (**eqn. 1.15**).

$$2Ln + 3Ph_3CCl \longrightarrow [(Ph_3C)_2LnCl] + [(Ph_3C)LnCl_2]$$

Equation 1.15: Preparation of trivalent pseudo-Grignard complexes.

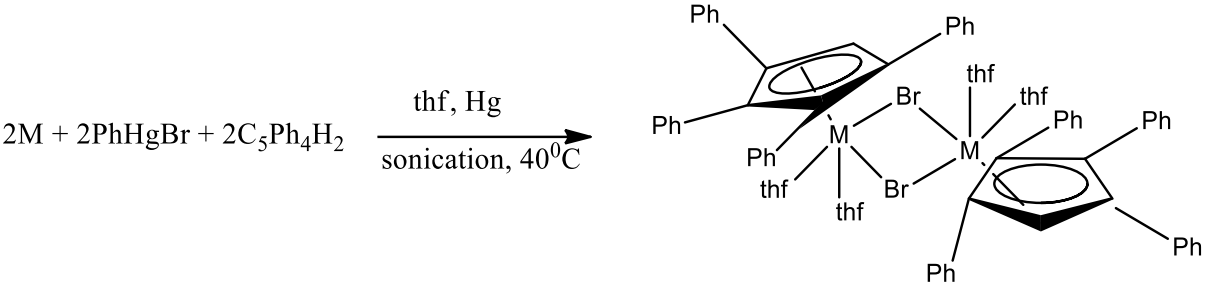
Involving samarium based organo-samarium intermediates new Grignard-type were performed by using varied carbonyl compounds (aldehydes, ketones, esters, acid anhydrides, acyl chlorides, epoxides and formamides) and aromatic/aliphatic halides (Cl, Br, or I) with Sm and CuI in thf as a catalyst (**eqn. 1.16**).[145]



X = Cl, Br, or I, R^1-CO-R^2 = varied carbonyl compounds (aldehydes, ketones, esters, acid anhydrides, acyl chlorides, epoxides and formamides)

Equation 1.16: Samarium based organo-samarium intermediate; Grignard-type addition reaction.

Two five coordinate pseudo-Grignard complexes $[M(C_5Ph_4H)(\mu\text{-}Br)(thf)_2]_2$ (M = Ca, Yb) were reported by Deacon and co-workers by reacting the desired metal, $C_5Ph_4H_2$ and PhHgBr in thf.[146]



Equation 1.17: Preparation of Ca and Yb pseudo-Grignard complexes.

1.5 Current study

Complexes of various divalent and trivalent lanthanides have found diverse applications in fields such as medicine, biology, telecommunications, and process industries, consistently yielding promising results. Recently, their use in trapping novel anionic ligands has garnered significant attention. Lanthanoid pseudo-Grignard reagents, a recent development in organometallic chemistry, have proven effective in capturing these anionic ligands. Within a short period, they have successfully trapped a variety of N-donor ligands, though this has been reported only for Yb and Eu so far. This intriguing area remains ripe for further exploration.

Chapter 2 focuses on our ability to trap lanthanoid pseudo-Grignard reagents "Ln(R)X" (Ln = Sm, Eu and Yb) using various formamidines and pyrazoles. This synthetic approach has already proven effective for trapping a wide range of $[Yb(L)I(solv)_n]$ (L = formamidinato or pyrazolato) compounds. However, these approaches have not yet been explored for Sm, where the Ln(II) state is less stable, or for systems for which Ln(III) is dominant. Initially, we explored the reaction between $PhLnBr(thf)_n$ (Ln = Sm, Eu) with DippFormH/Ph_2pzH yielding some exciting results. Furthermore, we have investigated the reaction capabilities of $PhSmI(thf)_n$ with pro-ligands DippFormH and Ph_2pzH, leading to the isolation of Sm(III) pseudo-Grignard complexes. In the final part of this chapter, we sought various oxidants with similar reactivity toward Ln(II) to isolate Ln(II) pseudo-Grignard complexes.

Chapter 3 aims to expand the study of trivalent pseudo-Grignard reagents, $Ph_pLnI_{(3-p)}(thf)_n$ (p = 1 or 2; Ln = La, Ce, Nd, Er and Lu), formed from the reaction between the lanthanoid metals and organic halide (PhI). The protolysis reaction between $Ph_pLnI_{(3-p)}(thf)_n$ and Ph_2pzH resulted in the synthesis of a series of trivalent Ln(III) pseudo-Grignard complexes. Notably, for Er, we were able to isolate an intermediate $[Er(Ph_2pz)(Ph)I(thf)_3]\cdot thf$ complex. When the solvent thf was replaced with acetonitrile, two Schlenk equilibria products were isolated; $[Ln(Ph_2pz)_3(CH_3CN)_3]\cdot 2CH_3CN$ (Ln = Nd, Gd). Additionally, when using formamidine Pro-ligands, we obtained the expected diiodo pseudo-Grignard $[Ln(Form)I_2(thf)_3]$ (Ln = Nd, Er; Form = DippForm, XylForm) complexes. This synthetic pathway also demonstrated the trapping capacity of $Ph_pNdBr_{(3-p)}(thf)_n$ (p = 1 or 2) Grignard reagent.

Chapter 4 is a brief section focused on exploring the trapping capacity of trivalent pseudo-Grignard reagents, $Ph_pLnI_{(3-p)}(thf)_n$ (p = 1 or 2; Ln = La, Ce, Nd, Gd, Ho and Lu), with O-donor ligands. In chapters **2** and chapter **3**, we discussed the trapping capacity of pseudo-Grignard reagents with N-donor ligands. Here, the reaction of O-donor ligand (4^tBu-C_6H_4OH) and $Ph_pLnI_{(3-p)}(thf)_n$ in dme solvent led to the isolation of diiodo pseudo-Grignard $[Ln(4^tBu\text{-}O\text{-}Ph)I_2(dme)_2]\cdot 0.5dme$ (Ce, Nd, Lu) complexes. Additionally, we investigate the reactivity of "PhYbI" with benzophenone (Ph_2CO). We also attempted to further investigate the reactivity of $[Yb(Ph_2pz)I(thf)_4]$ Grignard complex with O-donor KO^tBu and N-donor $(KMe)Ph(NMe_2)$ ligands. However, in both cases, the Schlenk equilibrium product $[Yb(Ph_2pz)_2(thf)_4]$ was obtained.

Chapter 5 presents an alternative synthesis of pseudo-Grignard reagents from Ln(III) metal, I_2 using supporting ligands such as $^tBu_2pzH$ and PhMepzH. This synthetic approach has already been proven effective for trapping of a wide range of $[Ln(L)I_2(solv)_n]$ and/or $[Ln(L)_2I(solv)_n]$ (L = Formamidinato) complexes. The direct reaction of lanthanoid metals (Ln = La, Ce, Nd, Tb, Er and Lu) with I_2 and $^tBu_2pzH$/PhMepzH resulted in the formation of both diiodo $[Ln(pz)I_2(thf)_n]$ (pz = $^tBu_2pz$/PhMepz) and monoiodo $[Ln(^tBu_2pz)_2I(thf)_2]$ (Ln = Er, Lu) pseudo-Grignard complexes.

1.6 References

1. The **1985** International Union of Pure and Applied Chemistry "Red Book" (p. 45).

2. N. G. Connelly, T. Damhus, R. M. Hartshorn and A. T. Hutton, Nomenclature of Inorganic Chemistry, RSC Press: Cambridge, **2005**.

3. S. R. Taylor and S. M. McLennan, Distribution of the Lanthanides in the Earth's Crust, CRC Press: New York, **2003**, 40, 1-38.

4. C. K. Gupta and N. Krishnamurthy, Extractive Metallurgy of Rare Earths, CRC Press: Boca Raton, FL, **2005**.

5. C. H. Evan, Biochemistry of the Lanthanides, Plenum Press: New York, **1990**.

6. E. Greinacher, History of Rare Earth Applications, Rare Earth Market Today, In Industrial Applications of Rare Earth Elements, ACS Symposium Series: **1981**, 164, 3-17.

7. T. Moeller, The Chemistry of the Lanthanides. Reinhold Publishing Corporation: New York, Chapman, and Hall: London, **1963**.

8. N. Kaltsoyannis and P. Scott, The f Elements. Oxford Science Publications: Oxford, **1999**.

9. N. E. Topp, The Chemistry of the Rare-earth Elements, Elsevier Publishing Company: Amsterdam, London, New York, **1965**.

10. N. N. Greenwood, and A. Earnshaw, Chemistry of the Elements, 2nd edition. Butterworth- Heinemann: Oxford, **1997**.

11. V. I. Spitsyn and L. I. Martynenko, Coordination Chemistry of Rare Earth Elements, Izd, MGU: Moscow, **1973**.

12. F. A. Cotton, G. Wilkinson, C. A. Murillo and M. Bochmann, Advanced Inorganic Chemistry, 6th edition, John Wiley and Sons Inc: New York, **1999**.

13. W. T. Carnal, The Absorption and Fluorescence Spectra of Rare Earth Ions in Solution, In Handbook on the Physics and Chemistry of Rare Earths, K. A. Gschneidner, L. Eyring, Eds. Elsevier, North-Holland Publishing: Amsterdam, **1979**, 3, 171-208.

14. E. J. Wheelwright, Promethium Technology. American Nuclear Society: Illinois, **1973**.

15. B. T. Kiboum, A Lanthanide Lanthology, Part II, M-Z, Molycorp Inc., New York, **1994**.

16. T. Imamoto, in Lanthanides in Organic Synthesis, eds. A. R. Katritsky, O. Meth- Cohn and C. W. Rees, Academic Press, London, **1994**.

17. B. T. Kiboum, A Lanthanide Lanthology, Part I, A-L, Molycorp Inc., New York, **1993**.

18. S. Cotton, Lanthanide and Actinide Chemistry. John Wiley and Sons Ltd: Chichester, **2006**.

19. S. Cotton, Lanthanide and Actinide. MacMillan Education Ltd: London, **1991**.

20. T. Moeller, The Chemistry of the Lanthanides. Reinhold Publishing Corporation: New York, Chapman and Hall: London, **1963**.

21. C. E. Housecroft and A. G. Sharpe, Inorganic Chemistry, Pearson Education Ltd., London, **2005**.

22. https://qsstudy.com/extract-lanthanides-monazite-sand.

23. M. E. Hossain, PhD thesis, James Cook University, **2017**.

24. H. Taube and E. S. Gould, Acc. Chem. Res., **1969**, 2(11), 321-329.

25. P. K. Thamburaj and E. S. Gould, Inorg. Chem., **1975**, 14(1), 15-17.

26. J. Doyle and A. G. Sykes, J. Chem. Soc. A, **1968**, 2836-2839.

27. S. Cotton, Lanthanides and actinides, First ed., Macmillan Education Ltd: London, **1991**.

28. G. A. Molander and C. R. Harris, Chem. Rev., **1996**, 96(1), 307-338.

29. V. Nair, L. Balagopal, R. Rajan and J. Mathew, Acc. Chem. Res., **2004**, 37 (1), 21-30.

30. M. Halka and B. Nordstrom, Lanthanides and Actinides, Facts on File, **2011**.

31. J. C. Bailar, H. J. Emeleus, R. Nyholm and A. F. Trotman-Dickenson, Comprehensive inorganic chemistry, **1973**, 31(a). A. C. Boggiano, C. M. studvick, S. R. Chowdhury, J. E. Niklas, H. Tateyama, H. Wu, J. E. Leisen, F. Kleemiss, B. Vlaisavjevich, I. A. Popov and H. S. L. Pierre, Chem. Rxiv., **2024**, Doi:10.26434/chemrxiv-2024-cb3z.

32. E. Vrachnou-Astra and D. Katakis, J. Am. Chem. Soc., **1975**, 97(19), 5357-5363.

33. J. D. White and G. L. Larson, J. Org. Chem., **1978**, 43(23), 4555-4556.

34. P. Girard, J. L. Namy and H. B. Kagan, J. Am. Chem. Soc., **1980**, 102(8), 2693-2698.

35. S. Cotton, Lanthanide and actinide chemistry, John Wiley & Sons, **2007**.

36. T. D. Tilley, R. A. Andersen and A. Zalkin, Inorg. Chem., **1984**, 23(15), 2271-2276.

37. K. Izod and Angew. Chem. Int. Ed., **2002**, 41(5), 743-744.

38. D. A. Atwood, The Rare Earth Elements, Fundamentals and Applications. John Wiley and Sons Ltd: West Sussex, **2012**, 38(a) S. A. Cotton, F. A. Hart, M. B. Hursthouse and A. J. Welch, J. Chem. Soc., Chem. Commun., **1972**, 1225-1226.

39. G. Wilkinson and J. M. Birmingham, J. Am. Chem. Soc., **1954**, 76(23), 6210-6210.

40. F. T. Edelman, Chem. Soc. Rev., **2012**, 41, 7657-7672, (40a) C. Eaborn, P. B. Hitchcock, K. Izod, Z.-R. Lu, and J. D. Smith, Organometallics, **1996**, 15, 4783-4790, (40b) C. Eaborn, P.B. Hitchcock, K. Izod and J. D. Smith, J. Am. Chem. Soc., **1994**, 116, 26, 12071-12072, (40c) M. Zimmermann and R. Anwander, Chem. Rev., **2010**, 110(10), 6194-6259, (40d) A. Mortis and R. Anwander, Eur. J. Inorg. Chem., **2024**, 27, e202400127, (40e) F. Ortu, Chem. Rev., **2022**, 122(6), 6040-6116.

41. Q. L. Guan, Y. H. Xing, J. Liu, W. J. Wei, X. Wang and F. Y. Bai, J. Inorg. Biochem., **2013**, 128, 57-67.

42. A. M. Ajlouni, Q. Abu-Salem, Z. A. Taha, A. K. Hijazi and W. A. Momani, J. Rare Earths, **2016**, 34(10), 986-993.

43. K. Das, S. Nandi, S. Mondal, T. Askun, Z. Cantürk, P. Celikboyun, C. Massera, E. Garribba, A. Datta, C. Sinha and T. Akitsu, New J. Chem., **2015**, 39, 1101-1114.

44. M. T. Kaczmarek, M. Zabiszak, M. Nowak and R. Jastrzab, Coord. Chem. Rev., **2018**, 370, 42-54.

45. T. Zhang, X. Zhu, W. K. Wong, H. L. Tam and W. Y. Wong, Chem. Eur. J., **2013**, 19(2), 739-748.

46. R. J. Crutchley, Coord. Chem. Rev., **2014**, 1, 273-274.

47. Y. Nozaki. D. Lerche, D. S. Alibi and M. Tsutsumi. Dissolved indium and rare earth elements in three Japanese rivers and Tokyo Bay: Evidence for anthropogenic Gd and In, Geochim. Cosmochim. Acta, **2000**, 64, 3975-3982.

48. I. Olmez, E. R. Sholkovitz, D. Hermann and R. P. Eganhouse, Environ. Sci. Technol., **1991**, 25, 310-316.

49. S. E. Humphris, M. A. Morrison and R. N. Thompson, Chem. Geol., **1978**, 23, 125-137.

50. P. Jakes and J. Gill, Earth Planet. Sci. Lett., **1970**, 9, 17-28.

51. G. N. Hanson, Annu. Rev. Earth Planet. Sci., **1980**, 8, 371-406.

52. D. J. Piepgras and G. J. Wasserburg, Geochim. Cosmochim. Acta., **1987**, 51, 1257-1271.

53. D. McKenzie and R. K. O'Nions, J. Petrol., **1991**, 32(5), 1021-1091.

54. B. C. Rowan, L. R. Wilson and B. S., Richards, IEEE J. Sel. Top. Quantum Electron., **2008**, 14(5), 1312–1322.

55. V. Gonzalez, D. A. L. Vignati, C. Leyval and L. Giamberini, Environ. Int., **2014**, 71, 148-157.

56. S. Cotton, Lanthanide and Actinide Chemistry, John Wiley & Sons, Chichester, **2006**; (b) Rare Earth Coordination Chemistry, Fundamentals and Applications, C. Huang Ed., Chichester, **2010**.

57. K. Redling, Doctoral Thesis, LMU, Muenchen, **2006**.

58. M. L. He, U. Wehr and W. A. Rambeck, J. An. Physiol. & An. Nut., **2010**, 94, 86-92.

59. M. Forsyth, M. Seter, B. Hinton, G. B. Deacon and P. C. Junk, Aust. J. Chem., **2011**, 64, 812-819.

60. S. Salot and J. C. Warf, J. Am. Chem. Soc., **1968**, 90(7), 1932-1933.

61. W. J. Evans, Organometallics, **2016**, 35(18), 3088-3100.

62. E. O. Fischer and D. C. H. Fischer, Angew. Chem. Int. Ed., **1964**, 3(2), 132.

63. R. G.Hayes and J. L. Thomas, J. Am. Chem. Soc., **1969**, 91(24), 6876.

64. W. J. Evans, Coord. Chem. Rev., **2000**, 206-207, 263-283.

65. F. Nief, Dalton trans., **2010**, 39(29), 6589-6598.

66. W. J. Evans, J. Organomet. Chem., **2002**, 652, 61-68.

67. W. J. Evans, Inorg. Chem., **2007**, 46(9), 3435-3449.

68. M. Wedler, A. Recknagel and F. T. Edelmann, J. Organomet. Chem., **1990**, 395, C26-29.

69. G. Meyer and H. J. Meyer, Chem. Mater., **1992**, 4(6), 1157-1168.

70. J. Burgess, Metal ions in solution, New York: Ellis Horwood, **1978**, ISBN: 9780853120278.

71. C. T. Palumbo, I. Zivkovic, R. Scopelliti and M. Mazzanti, J. Am. Chem. Soc., **2019**, 141(25), 9827-9831.

72. N. T. Rice, I. A. Popov, D. R. Russo, J. Bacsa, E. R. Batista, P. Yang, J. Telser and H. S. La Pierre, J. Am. Chem. Soc., **2019**, 141(33), 13222-13233.

73. A. R. Willauer, C. T. Palumbo, R. Scopelliti, I. Zivkovic, I. Douair, L. Maron and M. Mazzanti, Angew. Chem. Int. Ed., **2020**, 59(9), 3549-3553.

74. A. R. Willauer, C. T. Palumbo, I. Zivkovic, F. F. Tirani, I. Douair, L. Maron and M. Mazzanti, J. Am. Chem. Soc., **2020**, 142(12), 5538-5542.

75. J. Barker and M. Kilner, Coord. Chem. Rev., **1994**, 133, 219-300.

76. R. M. Roberts, J. Org. Chem., **1949**, 14(2), 277-284.

77. Z. Guo, R. Huo, Y. Q. Tan, V. Blair, G. B. Deacon and P. C. Junk, Coord. Chem. Rev., **2020**, 415, 213-232.

78. S. Patai, The Chemistry of Amidines and Imidates, John Wiley and Sons: London, New York, Sydney and Toronto, **1975**.

79. F.T. Edelmann, Advances of Organometallic Chemistry, Hill A.; Fink M. J. (Editors), 61, Elsevier Science, **2013**, 55-374.

80. F. T. Edelmann, Chem. Soc. Rev., **2009**, 38, 2253-2268.

81. F.T. Edelmann, Advances of Organometallic Chemistry, Hill A.; Fink M. J. (Editors), 57, Elsevier Science, **2008**, 183.

82. F. T. Edelmann, D. M. Freckmann and H. Schumann, Chem. Rev., **2002**, 102(6), 1851-1896.

83. A. Zuyls, P. W. Roesky, G. B. Deacon, K. Konstas, P. C. Junk, Eur. J. Org. Chem., **2008**, 4, 693-697.

84. M. L. Cole and P. C. Junk, New J. Chem., **2005**, 29, 135-140.

85. M. L. Cole, G. B. Deacon, C. M. Forsyth, K. Konstas and P. C. Junk, Dalton trans., **2006**, 27, 3360-3367.

86. G. B. Deacon, P. C. Junk, L. K. Macreadie and D. Werner, Eur. J. Inorg. Chem., **2014**, 30, 5240-5250.

87. D. I. Arnold, F. A. Cotton, J. H. Matonic and C. A. Murillo, Polyhedron, **1997**, 16(11), 1837-1841.

88. D. B. Mitzi and K. Liang, J. Solid State Chem., **1997**, 134(2), 376-381.

89. "Dissociation constants of organic acids and bases" (PDF). Archived (PDF) from the original on 12 July **2017**.

90. T. Eicher and S. Hauptmann, The Chemistry of Heterocycles: Structure, Reactions, Syntheses, and Applications (2nd edition **2003**), Wiley-VCH. ISBN 3-527-30720-6.

91. L. Knorr, Eur. J. Inorg. Chem., **1883**, 16(2), 2597-2599.

92. H. V. Pechmann, Eur. J. Inorg. Chem., **1898**, 31(3), 2950-2951.

93. M. A. Halcrow, Dalton trans., **2009**, 12, 2059-2073.

94. J. P´erez and L. Riera, Chem. Commun., **2008**, 533-543.

95. J. P´erez and L. Riera, Chem. Soc. Rev., **2008**, 37, 2658-2667.

96. A. L. Llamas-Saiz, C. Foces-Foces, F. H. Cano, P. Jim´enez, J. Laynez, W. Meutermans, J. Elguero, H.-H. Limbach and F. Aguilar-Parrilla, Acta Crystallogr., **1994**, B50, 746-762.

97. J. Catalan, R. M. Claramunt, J. Elguero, J. Laynez, M. Menendez, F. Anvia, J. H. Quian, M. Taagepera and R. W. Taft, J. Am. Chem. Soc., **1988**, 110(13), 4105-4111.

98. S. S. Fielder, M. C. Osborne, A. B. P. Lever and W. J. Pietro, J. Am. Chem. Soc., **1995**, 117(26), 6990-6993.

99. R. M. Claramunt, C. Lopez, M. D. S. Maria and D. Sanz, Elguero, Prog. Nucl. Magn. Reson. Spectrosc., **2006**, 49(3-4), 169-206.

100. R. Faure, E.-J. Vincent, A. Rousseau, R. M. Claramunt and J. Elguero, Can. J. Chem., **1988**, 66(5), 1141-1146.

101. C. Lopez, R. M. Claramunt, S. Trofimenko and J. Elguero, Can. J. Chem., **1993**, 71(5), 678-684.

102. M. N. Bochkarev, L. N. Zakharov and G. S. Kalinina, Organoderivatives of rare earth elements, Kluwer Academic Publishers Dordrecht, **1995**.

103. S. Cotton, In Comprehensive Coordination Chemistry II, edition, Pergamon, Oxford, **2003**, 93-188.

104. K. Izod, S. T. Liddle and W. Clegg, Inorg. Chem., **2004**, 43(1), 214-218.

105. R. C. Mehrotra, P. N. Kapoor and J. M. Batwara, Coord. Chem. Rev., **1980**, 31, 67-91.

106. G. B. Deacon, C. M. Forsyth and S. Nickel, J. Organomet. Chem., **2002**, 647, 50-60.

107. R. Anwander, Lanthanides: Chemistry and Use in Organic Synthesis, Springer, **1999**, 1-61.

108. L. Barton, J. Am. Chem. Soc., **1997**, 119(49), 12028-12028.

109. L. N. Bochkarev, T. A. Stepantseva, L. N. Zakharov, G. K. Fukin, A. I. Yanovsky and Y. T. Struchkov, J. Organomet. Chem., **1995**, 14, 2127-2129.

110. G. Meyer, D. Naumann and L. Wesemann, Inorganic Chemistry Highlights, Wiley, **2002**

111. G. B. Deacon, A. Gitlits, P. W. Roesky, M. R. Bürgstein, K. C. Lim, B. W. Skelton and A. H., White, Chem. Eur. J., **2001**, 7(1), 127-138.

112. K. Müller-Buschbaum, Z. Anorg. Allg. Chem., **2005**, 631, 811-828.

113. T. J. Boyle and L. A. M. Ottley, Chem. Rev., **2008**, 108(6), 1896-1917.

114. J. N. Spencer and A. F. Voigt, J. Phys. Chem., **1968**, 72(2), 464-470.

115. G. B. Deacon and D. G. Vince, J. Organomet. Chem., **1976**, 112, C1-C2.

116. G. B. Deacon, A. J. Koplick, W. D. Raverty and D. G. Vince, J. Organomet. Chem., **1979**, 182, 121-141.

117. M. L. Cole, G. B. Deacon, C. M. Forsyth, P. C. Junk, K. Konstas and J. Wang, Chem. Eur. J., **2007**, 13(29), 8092-8110.

118. M. L. Cole and P. C. Junk, Chem. Commun., **2005**, 21, 2695-2697.

119. M. L. Cole, G. B. Deacon, C. M. Forsyth, P. C. Junk, K. Konstas, J. Wang, H. Bittig and D. Werner, Chem. Eur. J., **2013**, 19(4), 1410-1420.

120. Z. Guo, V. Blair, G. B. Deacon and P. C. Junk, Chem. Eur. J., **2018**, 24, 17464-17474.

121. Z. Guo V. L. Blair, G. B. Deacon and P. C. Junk, Chem. Commun., **2021**, 57, 11513-11516.

122. F. Bickelhaupt, J. Organomet. Chem., **1994**, 475, 1-14.

123. F. A. Carey and R. J. Sundberg, Advanced Organic Chemistry, Reactions and Synthesis, Part B. 4th ed. Plenum Publishers: New York, **2001**.

124. D. F. Evans, G. V. Fazakerley and R. F. Phillips, J. Chem. Soc. A, **1971**, 1931-1934.

125. O. P. Syutkina, L. F. Rybakova, E. S. Petrov and I. P. Beletskaya, J. Organomet. Chem., **1985**, 280, C67-C69.

126. E. S. Petrov, D. M. Roitershtein and L. F. Rybakova, J. Organomet. Chem., **2002**, 647, 21-27.

127. Z. Hou, Y. Fujiwara, T. Jintoku, N. Mine, K. Yokoo and H. Taniguchi, J. Org. Chem., **1987**, 52(16), 3524-3528.

128. T. Fukagawa, Y. Fujiwara, K. Yokoo and H. Taniguchi, Chem. Lett., **1981**, 1771-1774.

129. M. Deng, Y. Yao, Q. Shen, Y. Zhang, J. Lang and Y. Zhou, J. Organomet. Chem., **2003**, 681, 174-179.

130. W. J. Evans, J. Organomet. Chem., **2002**, 647, 2-11.

131. Z. Hou and Y. Wakatsuki, J. Organomet. Chem., **2002**, 647, 61-70.

132. W. J. Evans, G. Zucchi and J. W. Ziller, J. Am. Chem. Soc., **2003**, 125(1), 10-11.

133. P. N. Hazin, C. Lakshminarayan, L. S. Brinen, J. L. Knee, J. W. Bruno, W. E. Streib and K. Folting, Inorg. Chem., **1988**, 27(8), 1393-1400.

134. W. J. Evans, N. T. Allen and J. W. Ziller, Angew. Chem. Int. Ed., **2002**, 41(2), 359-361.

135. H. J. Heeres, J. Renkema, M. Booij, A. Meetsma and J. H. Teuben, Organometallics, **1988**, 7(12), 2495-2502.

136. P. L. Watson, Chem. Commun., **1980**, 652-653.

137. G. Heckmann and M. Niemeyer, J. Am. Chem. Soc., **2000**, 122(17), 4227-4228.

138. M. N. Bochkarev, L. N. Zakharov and G. S. Kalinina, Organoderivatives of Rare Earth Elements. Kluwer Academic: Dordrecht, **1995**.

139. S. A. Cotton, Coord. Chem. Rev., **1997**, 160, 93-127.

140. C. Eaborn, P. B. Hitchcock, K. Izod and J. D. Smith, J. Am. Chem. Soc., **1994**, 116(26), 12071-12072.

141. C. Eaborn, P. B. Hitchcock, K. Izod, Z. Lu and J. D. Smith, Organometallics, **1996**, 15(22), 4783-4790.

142. M. Wiecko, G. B. Deacon and P. C. Junk, Chem. Commun., **2010**, 46(28), 5076-5078.

143. S. H. Ali, G. B. Deacon, P. C. Junk, S. Hamidi, M. Wiecko and J. Wang, Chem. Eur. J., **2018**, 24, 230-242.

144. B. A. Dolgoplosk, E. I. Tinyakova, I. N. Markevich, T. V. Soboleva, G. M. Chernenko, O. K. Sharaev and V. A. Yakovlev, J. Organomet. Chem., **1983**, 255, 71-79.

145. S. Xiao, C. Liu, B. Song, L. Wang, Y. Qi and Y. Liu, Chem. Commun., **2021**, 57, 6169-6172.

146. G. B. Deacon, F. Jaroschik, P. C. Junk and R. P. Kelly, Organometallics, **2015**, 34(11), 2369-2377.

Chapter 2

Reaction of Ln(II) pseudo Grignard reagents with formamidines and pyrazoles

Chapter 2

2.1 Introduction

Grignard reagents have tremendous application in organic and organometallic chemistry, due to their case of formation, structure, and reactivity.[1] Di-valent lanthanoid metals (Sm, Eu and Yb) can be used in place of magnesium for producing pseudo-Grignard reagents, which have similar reactivity towards different organic molecules (halides, ketones, aldehydes etc). These types of reagents have significant diversity in organometallic chemistry. Recently, their application in trapping novel anionic ligands has been attracting researchers.

2.1.1 Synthesis of divalent pseudo-Grignard reagents using Grignard type reactions

Organomagnesium halides [$RMg(solv)_nX$] (R = Me, Et, Ph; X = Cl, Br, I; solv = thf, Et_2O, n = number) (**eqn. 2.1**) can be easily synthesised from the direct reaction between Mg with alkyl or arial halide.[1, 2]

$$\mathbf{Mg + RX \xrightarrow[0\ ^\circ C]{solv} [RMg(solv)_nX]}$$

R = Ph, Et, Me; X = Cl, Br, I

Solv = Et_2O, thf

Equation 2.1: Preparation of magnesium-based Grignard reagent.

Evans et al. in 1971 introduced lanthanoid pseudo-Grignard reagents [$RLn(thf)_nI$] (Ln = Sm, Eu and Yb) of organoiodides, from the oxidation reaction (**eqn. 2.2**).[3]

$$\mathbf{Ln + RI \xrightarrow[-20\ ^\circ C]{thf} RLn(thf)_nI}$$

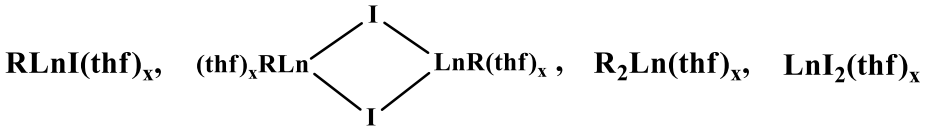
Ln = Sm, Eu, Yb. R = Ph, Et, Me

Equation 2.2: Preparation of lanthanoid pseudo-Grignard reagent.

Structural composition and reactivity of pseudo-Grignard reagents [$RLn(solv)_nX$] (Ln = Sm, Eu and Yb; R = Me, Et, Ph; X = Cl, Br, I; solv = thf, Et_2O, n = number) towards acids and electrophiles are very similar with the classical Grignard reagents [$RMg(solv)_nX$] (solv = thf, Et_2O, n = number), [4, 5] leading to the reasons why organic and inorganic transformations received practical attention.[6, 7] In contemporary times many organolanthanoids (+2 oxidation states) with cyclopentadienyl and non-cyclopentadienyl have been synthesised.[8-16]

Magnetic susceptibility shows the ratios of Ln : I (Ln = Sm, Eu, Yb) in the reaction (**eqn. 2.2**), we can get a mixture of di-valent and tri-valent complexes, where Eu^{2+} (99%), Yb^{2+} (85%) and

somewhat less for Sm^{2+} (50%).[3] The solution of pseudo-Grignard reagents (**eqn. 2.2**) may have the below five (4) different divalent species (depends on the solubility of the compounds, nature of the solvents and halides also the size of the R groups), where Ln = Yb, Eu, R = 2,6-Ph_2-C_6H_3 and x = number of solvent molecules.[17]



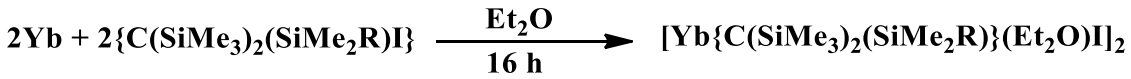
In a more recent study, for Yb the Schlenk equilibrium was proved using ^{171}Yb NMR. The chemical shifts of ^{171}Yb NMR spectra detected that, [YbDpp(thf)$_n$I], [Yb(Dpp)$_2$(thf)$_2$], [Yb(thf)$_4$I$_2$] (Dpp = 2,6-Ph_2-C_6H_3) are the major three complexes in the solution (**eqn. 2.3**).[17] The ^{171}Yb NMR spectra of [YbDpp(thf)$_n$I] in THF-d$_8$ solution shows a main signal at 677 ppm, 927 and 457 ppm for compound [Yb(Dpp)$_2$(thf)$_2$] and [Yb(thf)$_4$I$_2$] respectively. [17] It's very the characterization these intermediates [YbDpp(thf)$_n$I], [Yb(Dpp)$_2$(thf)$_2$].[18, 19]



Dpp = 2,6-Ph_2-C_6H_3

Equation 2.3: The Schlenk equilibrium of Yb Grignard reagents.

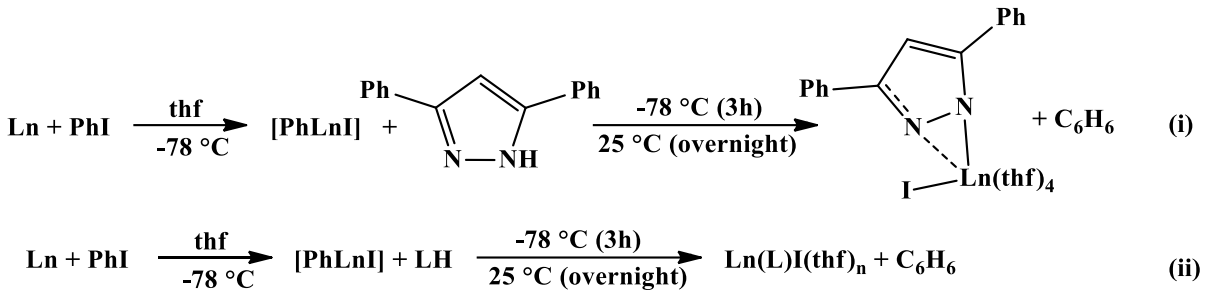
Ytterbium metal react with bulky silylated iodoalkyl group in thf, isolated the new pseudo-Grignard complex [Yb{C(SiMe$_3$)$_2$(SiMe$_2$R)}I(Et$_2$O)]$_2$ (R = Me, MeO, CH=CH$_2$) (**eqn. 2.4)** with good crystalline yield (65% to 85%).[20, 21]



R =CH=CH$_2$, MeO, Me

Equation 2.4: Isolation of [Yb{C(SiMe$_3$)$_2$(SiMe$_2$R)}I(Et$_2$O)]$_2$ pseudo-Grignard complex.

Breakthrough came in lanthanoid Grignard chemistry when Deacon and co-workers reported a new route to isolate pseudo-Grignard reagents. They sonicated the lanthanoid (Eu, Yb) metal powders with PhI, at a low temperature (-78 °C), after the formation of PhLnI(thf)$_n$ they added Ph_2pzH ligand and stirred overnight at room temperature (**eqn. 2.5, i**).[22] Later, Ali and co-workers followed the same procedure and produced some new pseudo-Grignard reagents from lanthanoid (Eu, Yb) formamidinato complexes (**eqn. 2.5, ii**).[23]

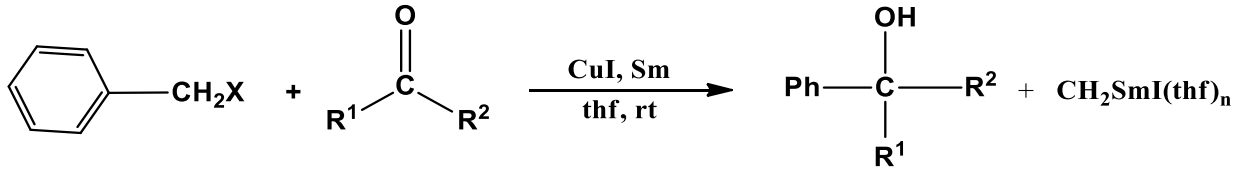


LH = DippFormH, XylFormH, MesFormH

Ln = Eu, Yb

Equation 2.5: Preparation of divalent pseudo-Grignard complexes.

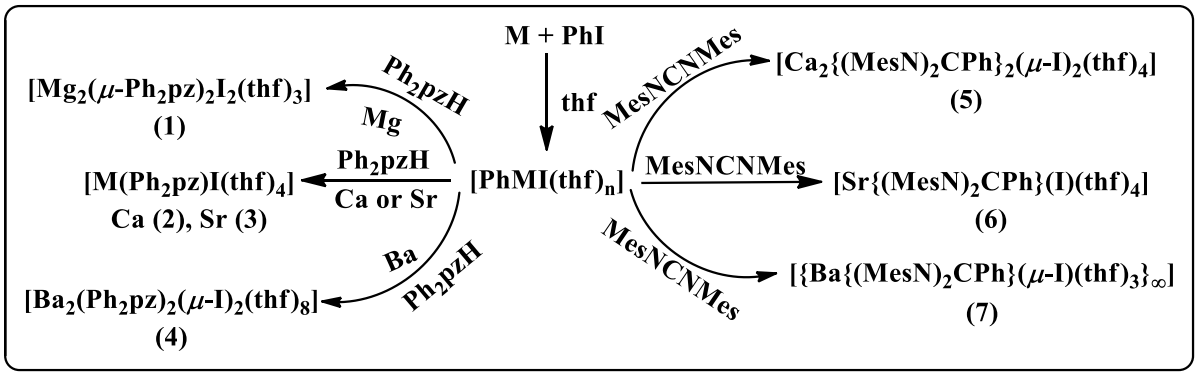
Samarium based pseudo-Grignard Grignard compounds ($CH_2SmI(thf)_n$) can be isolated from the reaction of $PhCH_2X$ (X = Cl, Br, or I) with varied carbonyl compounds (aldehydes, ketones, esters, acid anhydrides, acyl chlorides, epoxides and formamides) in presence of Sm and CuI as catalyst in thf (**eqn. 2.6**).[24]



X = Cl, Br, or I, R^1-CO-R^2 = varied carbonyl compounds (aldehydes, ketones, esters, acid anhydrides, acyl chlorides, epoxides and formamides)

Equation 2.6: Samarium based Grignard-type addition reactions.

In Grignard chemistry, some heavy Grignard complexes have been synthesised using heavy alkaline earth metals. The products isolated from these reactions are summarized in **Table 2.1**.[25] The Grignard reagents [$PhMI(thf)_n$] (M = Mg, Ca, Sr and Ba) were treated with ligands (3,5-diphenyl pyrazole (Ph_2pzH) and dimestylcarbodiimide (MesNCNMes)) (**Scheme 2.1**), which resulted the formation of dimeric [$Mg_2(\mu$-$Ph_2pz)_2I_2(thf)_3$] (**1**), [$Ba_2(Ph_2pz)_2(\mu$-$I)_2(thf)_8$] (**4**), [$Ca_2\{(MesN)_2CPh\}_2(\mu$-$I)_2(thf)_4$] (**5**), monomeric [$M(Ph_2pz)I(thf)_4$] (M = Ca **2**, M = Sr **3**), [$Sr\{(MesN)_2CPh\}I(thf)_4$] (**6**), and polymeric [$\{Ba\{(MesN)_2CPh\}(\mu$-I) $(thf)_3\}_\infty$] (**7**) complexes.[25]



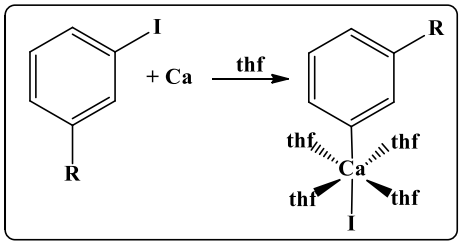
Scheme 2.1: Preparation of alkaline earth pseudo-Grignard complexes using Grignard reaction. M = Mg, Ca, Sr and Ba; Mg react at room temperature; Ca need preactivated using 2 mol % I_2; Ca, Sr and Ba react at -78 °C; reaction time after adding ligand is 16 h.[25]

Three similar types of magnesium based complexes{[Mg(MesC(N*i*Pr)$_2$)(μ-Br)(Et$_2$O)]$_2$ (**8**), {[Mg(MesC(NDipp)$_2$)(μ-Br)(Et$_2$O)]$_2$ (**9**), {[Mg(MesC(NMes)$_2$)(μ-Br)(Et$_2$O)]$_2$ (**10**)} were synthesised from the equimolar mixture between MesMgBr and the desired ligand (RNCNR) (R = *i*Pr, Dipp, Mes) after stirring for 18 h at room temperature in Et$_2$O (**eqn. 2.7**).[26]

$$\mathbf{MesMgBr + RNCNR \xrightarrow[18\ h,\ rt]{Et_2O} [Mg(RNC(Mes)NR)Br(Et_2O)]_2}$$

Equation 2.7: Preparation of magnesium pseudo-Grignard complexes (R = *i*Pr, Dipp and Mes).[26]

Calcium based monomeric Grignard reagents [(R-C$_6$H$_4$)CaI(thf)$_4$] (Me (**11**), F (**12**), Cl (**13**), Br (**14**), and I (**15**)) were synthesised from the reaction between finely divided calcium metal with the required derivatives of iodobenzene at -20 °C (**Scheme 2.2**).



Scheme 2.2: Preparation of calcium Grignard reagents (R = Me, F, Cl, Br, I).[27]

The resulting mixture was allowed to warm at 0 °C with continuous stirring for 1 h, and then room temperature for another 5 h. The resulting crystals were obtained after the extraction of solid residue with thf.[27]

Table 2.1: Summary of alkali earth metal based pseudo-Grignard complexes formed from Grignard reaction ($RMX(thf)_n$) with ligands.

Ligands	Products	Nuclearity	Ref.
Ph_2pzH	$[Mg_2(\mu\text{-}Ph_2pz)_2I_2(thf)_3]$(**1**)	dimer	[25]
Ph_2pzH	$[M(Ph_2pz)I(thf)_4]$ (M = Ca **2**, Sr **3**)	monomer	[25]
Ph_2pzH	$[Ba_2(Ph_2pz)_2(\mu\text{-}I)_2(thf)_8]$(**4**)	dimer	[25]
$(Mes)_2NCN$	$[Ca_2\{(MesN)_2CPh\}_2(\mu\text{-}I)_2(thf)_4]$ (**5**)	dimer	[25]
$(Mes)_2NCN$	$[Sr\{(MesN)_2CPh\}I(thf)_4]$ (**6**)	monomer	[25]
$(Mes)_2NCN$	$[\{Ba\{(MesN)_2CPh\}(\mu\text{-}I)\ (thf)_3\}_\infty]$ (**7**)	1-D polymer	[25]
$(i\text{Pr})_2NCN$	$\{[Mg(MesC(N i\text{Pr})_2)(\mu\text{-}Br)(Et_2O)]_2$ (**8**)	dimer	[26]
$(Dipp)_2NCN$	$\{[Mg(MesC(NDipp)_2)(\mu\text{-}Br)(Et_2O)]_2$ (**9**)	dimer	[26]
$(Mes)_2NCN$	$\{[Mg(MesC(NMes)_2)(\mu\text{-}Br)(Et_2O)]_2$ (**10**)$\}$	dimer	[26]
$Ca(thf)_n$	$[(R'\text{-}C_6H_4)CaI(thf)_4]$(R′ = Me (**11**), F (**12**), Cl (**13**), Br (**14**), I (**15**))	monomer	[27]

R = Ph, X = I (**1**-**7**, and **11**-**15**); R = Mes, X = Br (**8**-**10**)

[Ca(*i*Pr-NC(Ph)N-*i*Pr)I(thf)$_3$] complex can be synthesised by using a two-step reaction sequences. Firstly, reaction of PhLi with *N,N*-diisopropyl carbodiimide for the formation of [PhC(N*i*Pr)$_2$Li]. Secondly, suspension of CaI_2 in thf was stirred for a period of 3 days with [PhC(N*i*Pr)$_2$Li], and after extracting with toluene colourless crystals was obtained (**eqn. 2.8**).[28]

$$\textbf{\textit{i}Pr-NCN-\textit{i}Pr + PhLi + CaI}_2 \xrightarrow[\textbf{-LiI}]{\textbf{thf}} \textbf{[Ca(\textit{i}Pr-NC(Ph)N-\textit{i}Pr)I(thf)}_3\textbf{]}$$

Equation 2.8: Preparation of a calcium pseudo-Grignard reagent from metathesis reaction.[28]

A mixture of equimolar Priso-K (Priso = $i\text{Pr}_2$N-C(N-Dipp)$_2$) and $CaI_2(thf)_4$ yielded [Ca(Priso)(μ-I)(thf)]$_2$ after crystallisation from toluene at -20 °C.[29]

2.1.2 Synthesis of lanthanoid (Sm, Eu and Yb) pseudo-Grignard reagents from common synthetic approaches

Lanthanoid pseudo-Grignard reagents are quite new in organometallics for trapping different anionic ligands. Literature shows, a wide range of reactions (RTP, C-X activation (Cl, F, Br, I), oxidation, reactivity of lanthanoid complexes and direct reaction) were used to synthesise lanthanoid pseudo-Grignard complexes.[30-43] Most of the time it is very difficult to isolate pseudo-Grignard complexes using these methods. Pseudo-Grignard reaction is a very good alternative of these common methods for synthesising pseudo-Grignard complexes. The main reason behind this, within a short period, they can easily trap a variety of anionic ligands. In this section, we will discuss the common synthesis processes used for isolating pseudo-Grignard complexes and later of this chapter, we will also discuss the lanthanoid pseudo-Grignard reaction we used for isolating pseudo- Grignard complexes.

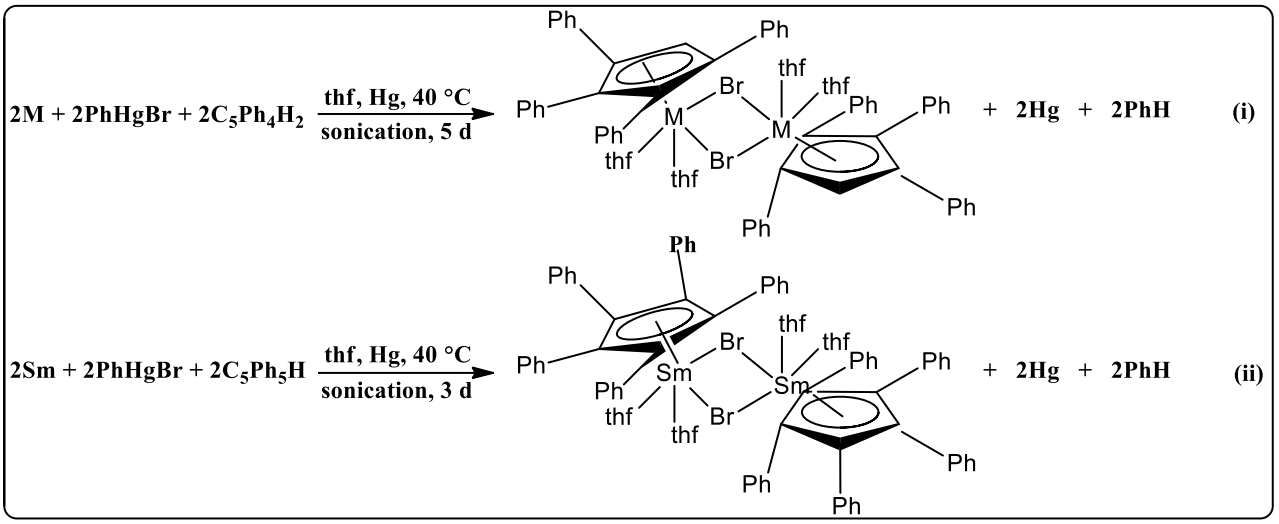
RTP reaction for synthesising pseudo-Grignard complexes

A trivalent pseudo-Grignard complex for samarium ([Sm(DippForm)$_2$F(thf)]) [30] was synthesised by Cole *et. al.* in **2007** from an RTP reaction where the presumed divalent samarium intermediate compound reacted with the organofluoride reagent in a C-F activation process (**eqn. 2.9**).

$$\mathbf{Sm + Hg(C_6F_5)_2 + 2DippFormH} \xrightarrow[\text{thf}]{\text{rt}} \mathbf{[Sm(DippForm)_2F(thf)]}$$

Equation 2.9: Trivalent samarium pseudo-Grignard complex preparation using an RTP reaction.[30]

Three rare (Ca, Yb and Sm) dimeric pseudo-Grignard complexes [M(C_5Ph_4H)(μ-Br)(thf)$_2$]$_2$ (M = Ca, Yb) and [Sm(C_5Ph_5)(μ-Br)(thf)$_2$]$_2$ were synthesised from RTP reactions using the relevant metal, $C_5Ph_4H_2$ and PhHgBr in thf after sonication (Ca and Yb: 5 d; Sm: 3 d) at 40 °C (activated by using 1 drop of mercury 2%). All the crystals have a M_2Br_2 core.[31, 32]

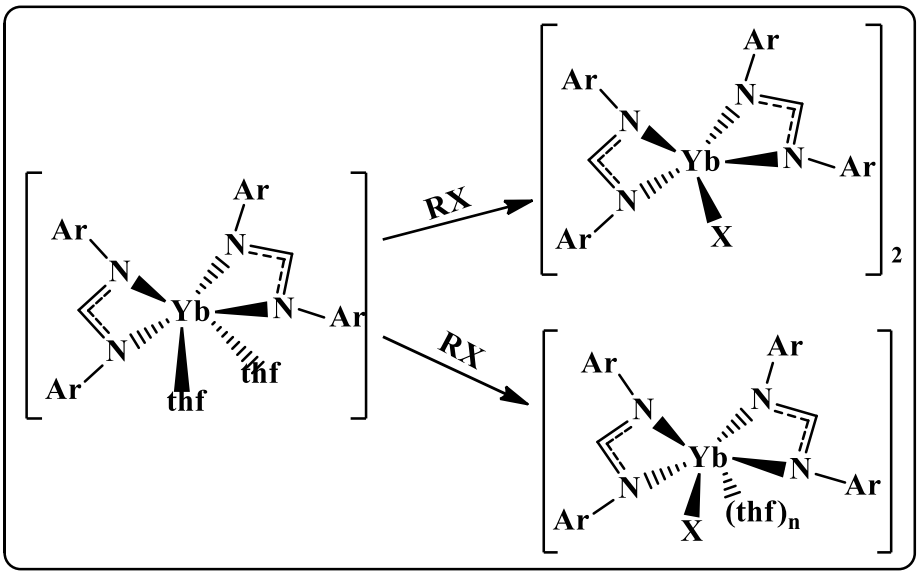


Scheme 2.3: Preparation of M = Ca, Yb and Sm dimeric pseudo-Grignard complexes.[31,32]

C-X (X = F, Cl) activation reaction for synthesising pseudo-Grignard complexes

C-F/Cl activation reaction by highly reactive Yb compounds can produce ytterbium pseudo-Grignard complexes. Perfluorodecalin ($C_{10}F_{18}$) reacts with [Yb(EtForm)$_2$(thf)$_2$] to produce [{Yb(EtForm)$_2$(μ_2-F)}$_2$], with [Yb(o-PhPh)$_2$(thf)$_2$]·2thf to produce [{Yb(o-PhPhForm)$_2$(μ-F)}$_2$], while hexachloroethane (C_2Cl_6) reacts with [Yb(o-PhPh)$_2$(thf)$_2$]·2thf producing [{Yb(o-PhPhForm)$_2$Cl(thf)$_2$]·2thf, and 1,2-dichloroethane ($C_2H_4Cl_2$) provides [Yb(DippForm)$_2$Cl(thf)]·thf after reaction with [Yb(DippForm)$_2$(thf)$_2$]·2thf.[33]

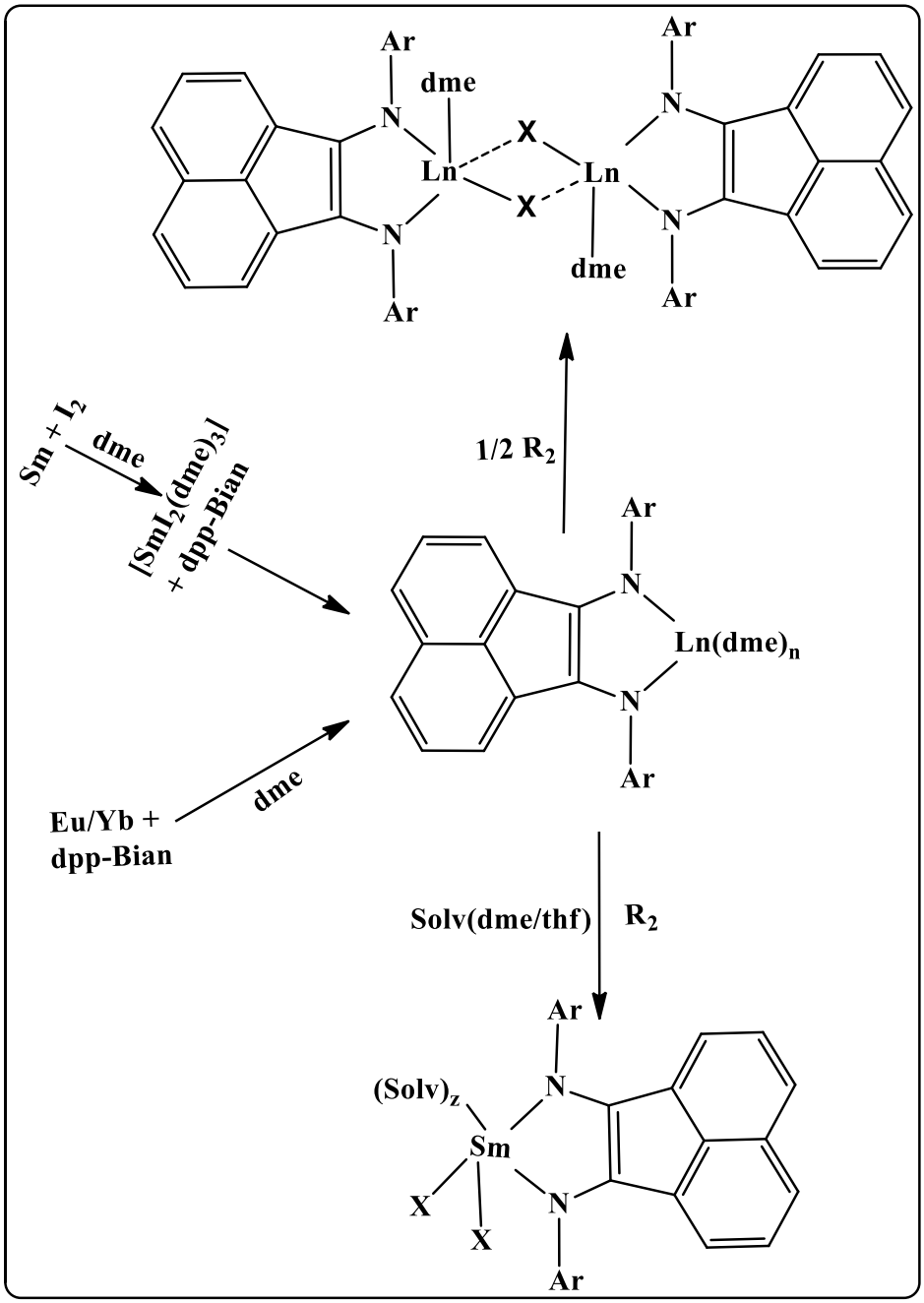
Divalent ytterbium formamidinates [Yb(Form)$_2$(thf)$_2$] (Form = [RNCHNR]; R = 2,6-Et$_2$C$_6$H$_3$, 2-PhC$_6$H$_4$, 2,6-*i*Pr$_2$C$_6$H$_3$) react with different oxidants (perfluorodecalin, hexachloroethane, 1,2-dichloroethane and 2,3,4,5-tetrafluorobenzene) and undergo C-X activation yielding [Yb(EtForm)$_2$F]$_2$, [Yb(o-PhPhForm)$_2$F]$_2$, [Yb(o-PhPhForm)$_2$Cl(thf)$_2$], [Yb(DippForm)$_2$Cl(thf)] and [Yb(DippForm)$_2$Br(thf)] complexes respectively (**Scheme 2.4**). The first two complexes are six coordinate fluoride-bridged dimers, where the metal atom is oriented by two chelating formamidinato ligands and two bridged fluorine atoms, while other three are monomeric complexes with two chelating ligands and one terminal chloride/bromide ligand.[33]



Scheme 2.4: Synthesis of ytterbium pseudo-Grignard complexes from the reactivity of divalent ytterbium complexes; Ar = 2,6-$Et_2C_6H_3$, RX = $C_{10}F_{18}$; Ar = 2-PhC_6H_4, RX = $C_{10}F_{18}$); Ar = 2-PhC_6H_4, RX = C_2Cl_6; Ar = 2,6-*i*$Pr_2C_6H_3$, RX = 1,2-$Cl_2C_2H_4$; Ar = 2,6-*i*$Pr_2C_6H_3$, RX = o-$HBrC_6F_4$).[33]

Oxidation reaction for synthesising pseudo-Grignard complexes

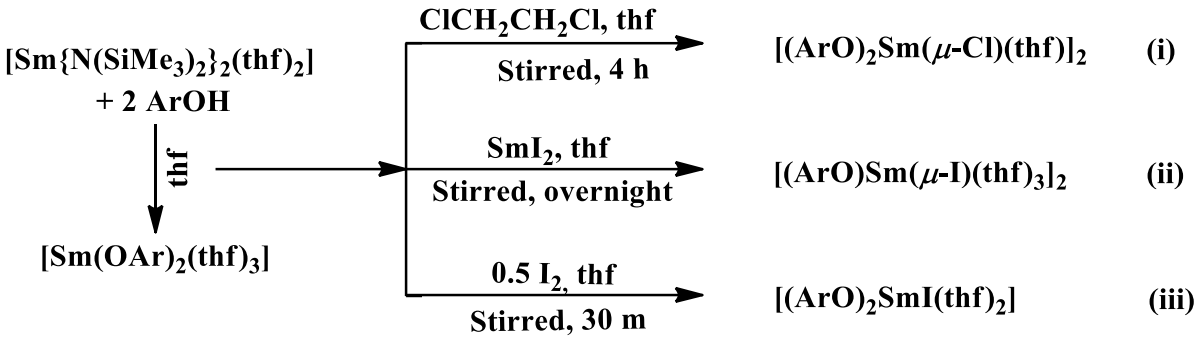
Interesting reaction pathways were introduced [34-36] for the synthesis of dimeric [(dpp-Bian)Ln(dme)$_n$X]$_2$ (Ln = Sm, Eu and Yb; X = Cl or I or Br) and trivalent [(dpp-Bian)SmX$_2$(Solv)$_z$] (X = I or Br) pseudo-Grignard complexes {[(dpp-Bian)SmBr(dme)]$_2$, [(dpp-Bian)Eu(dme)(μ-Br)]$_2$, [(dpp-Bian)Eu(dme)(μ-Cl)]$_2$ and [(dpp-Bian)Yb(dme)(μ-Br)]$_2$ (**Scheme 2.5**). The oxidants (R_2 = Ph(Br)CHCH(Br)Ph or Ph_3SnCl or I_2) are crucial for this reaction: 0.5 mol equivalent produce dimeric divalent complexes, whereas equimolar amounts produce trivalent samarium complexes. The Ln^{II} derivatives are centrosymmetric dimers formed from the monomers where the inversion centre is in the middle of the two metal atoms.[34-36] In the case of the Sm^{III} derivatives [(dpp-Bian)SmBr$_2$(dme)] and [(dpp-Bian)SmI$_2$(thf)$_2$] synthesised in the use of different solvents.[34]



Scheme 2.5: Preparation of Lanthanoid divalent (Sm, Eu and Yb) and trivalent (Sm) pseudo-Grignard complexes {R_2 = Ph(Br)CHCH(Br)Ph or Ph_3SnCl or I_2; Solv = dme or thf; X = Br or Cl or I; n = 2 for Eu and Yb, n = 3 for Sm; z = 1 for dme and 2 for thf; dpp-Bian = 1,2-Bis[(2,6-diisopropylphenyl)imino]acenaphthene; Ar = 2,6-diisopropylphenyl}.[34-36]

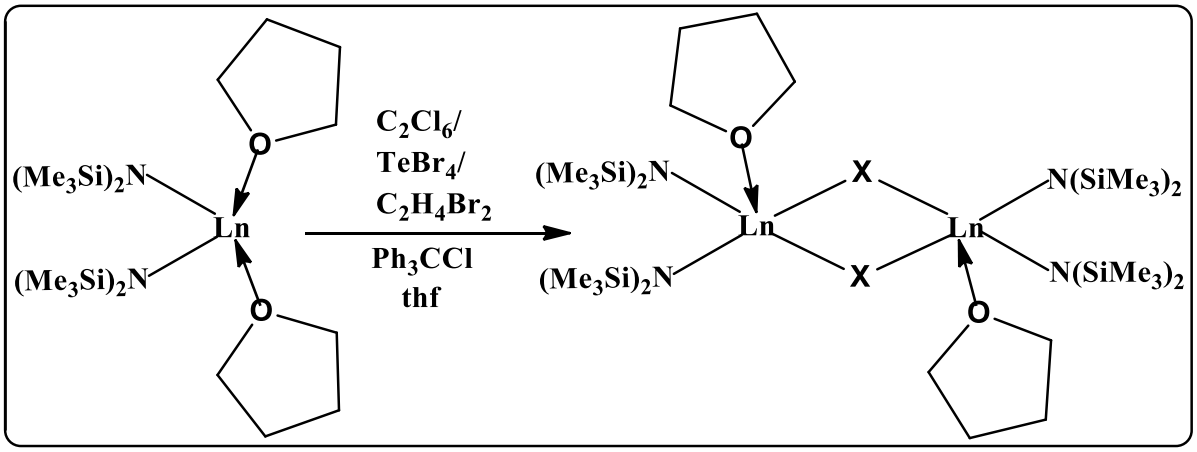
The mixture of $[Sm(OAr)_2(thf)_3]$ and oxidant ($C_2H_4Cl_2$ (**eqn. i**), SmI_2 (**eqn. ii**) and I_2 (**eqn. iii**)) stirred (4 h (**eqn. i**), overnight (**eqn. ii**) and 30 m (**eqn. iii**)) in thf at room temperature produced complexes; $[(ArO)_2Sm(\mu\text{-}Cl)(thf)]_2$, $[(ArO)Sm(\mu\text{-}I)(thf)_3]_2$ and $[(ArO)_2SmI(thf)_2]$. Complex

$[(ArO)Sm(\mu\text{-}I)(thf)_3]_2$ is dimeric where Sm^{II} adopts a Sm···I(3.534(2) Å) interaction, where the other two complexes are both monomeric Sm^{III}.[37]



Equation 2.10: Samarium aryloxide complexes preparation from the reactivity of $[Sm(OAr)_2(thf)_3]$; Ar = $C_6H_2Bu^t_2$-2,6-Me-4.[37]

Treatment of $[Ln\{N(SiMe_3)_2\}(thf)_2]$ with one equivalent of oxidants (C_2Cl_6, $TeBr_4/C_2H_4Br_2$, Ph_3CCl) in thf gave three ($[Sm\{N(SiMe_3)_2\}_2(\mu\text{-}Cl)(thf)]_2$, $[Sm\{N(SiMe_3)_2\}_2(\mu\text{-}Br)(thf)]_2$ and $[Eu\{N(SiMe_3)_2\}_2(\mu\text{-}Cl)(thf)]_2$) dimeric pseudo-Grignard complexes respectively. The samarium products (chlorination and bromination) have the same μ_2-bridging arrangement.[38]



Scheme 2.6: Synthesis of dimeric pseudo-Grignard reagents from the halogenation reaction.[38]

Reactivity reaction of lanthanoid complexes for synthesising pseudo-Grignard complexes

Another samarium trivalent pseudo-Grignard complex $[Sm(DippForm)Br_2(thf)_3]$ was synthesised in 2013 [39] from Sm metal powder, $Hg(2\text{-}BrC_6F_4)_2$ and DippFormH at room temperature (stirred overnight). A range of Sm complexes were obtained from the reactivity of $[Sm(DippForm)_2(thf)_2]$ (green solution) with the solution of *tert*-butyl chloride, 1,2-

dibromoethane and iodine in toluene producing [Sm(DippForm)$_2$Cl(thf)], [Sm(DippForm)$_2$Br(thf)] and [Sm(DippForm)$_2$I(thf)] respectively.[39]

$$C_2H_4Br_2 + [Sm(DippForm)_2(thf)_2] \xrightarrow[\text{toluene}]{\text{stirred, rt}} [Sm(DippForm)_2Br(thf)]$$

Equation 2.11: Preparation of [Sm(DippForm)$_2$Br(thf)] complex from the reactivity of [Sm(DippForm)$_2$(thf)$_2$].[39]

To understand the reactivity of the product ([Yb(DFForm)$_2$(thf)$_3$]) obtained from an RTP reaction, Deacon *et. al.* [40] observed the oxidation reaction between [Yb(DFForm)$_2$(thf)$_3$] and TiCl$_4$(thf)$_2$/Ph$_3$CCl, and as a result they were able to prepare a new pseudo-Grignard reagent [Yb(DFForm)$_2$Cl(thf)$_2$]. After the formation of the latter pseudo-Grignard reagent from [Yb(DFForm)$_2$(thf)$_3$] there is no change in coordination number (seven). C-F activation is observed when divalent ytterbium formamidinato [Yb(DippForm)$_2$(thf)$_2$] complex was treated with perfluoro benzoquinone (pfb) and the trivalent [Yb(DippForm)$_2$F(thf)] complex was obtained.[41] Three different types of pseudo-Grignard complexes were obtained from the reactivity of [Yb(DippForm)$_2$(tpc-O) (tpc = 2,3,4,5-tetraphenylcyclopentadienone) with [SmI$_2$(thf)$_2$]; first a colourless block of [{SmI({C$_5$Ph$_4$}-O)(thf)$_2$}$_2$]·2thf was formed, and from the solution the light orange [Yb(DippForm)$_2$I(thf)] and colourless blocks [Yb(DippForm)I$_2$(thf)$_3$]·Et$_2$O complexes were isolated.[41]

$$[Yb(Dipporm)_2(tpc\text{-}O)] + SmI_2(thf)_2 \xrightarrow[\text{heat}]{\text{thf}} [\{SmI(\{C_5Ph_4\}\text{-}O)(thf)_2]_2\cdot 2thf + \text{Solution}$$

$$\text{Solution} \xrightarrow[\text{recrystallised}]{Et_2O} [Yb(DippForm)_2I(thf)] + [Yb(DippForm)I_2(thf)_3]\cdot Et_2O$$

Equation 2.12: Synthesis of ytterbium pseudo-Grignard complexes from the reactivity ytterbium complex.[41]

Direct reaction for synthesising pseudo-Grignard complexes

Monoclinic dimer structures for Sm ([(K^1-N,η^6-Piso)Sm(thf)(μ-I)$_2$Sm(K^1-N,η^6-Piso)]) and Yb ([{(K^2-*N*,*N*′-Priso)Yb(μ-I)(thf)}$_2$]) were obtained from the reaction between the relevant metal iodide with potassium priso/piso (Priso$^-$ = [(ArN)$_2$CNPr$^i_2$]$^-$; Piso$^-$ = [(ArN)$_2$CBu^t]$^-$ (Ar = 2,6-diisopropylphenyl)) at -80 °C in THF.[42]

$$YbI_2 + K(Priso) \xrightarrow[-78\ °C]{thf} [\{(k^2\text{-}N,N'\text{-}Priso)Yb(\mu\text{-}I)(thf)\}_2] \quad \textbf{(i)}$$

$$SmI_2 + K(Piso) \xrightarrow[-78\ °C]{thf} [(k^1\text{-}N,\eta^6\text{-}Piso)Sm(thf)(\mu\text{-}I)_2Sm(k^1\text{-}N,\eta^6\text{-}Piso)] \quad \textbf{(ii)}$$

Equation 2.13: Preparation of dimeric lanthanoid (Yb, Sm) pseudo-Grignard complex; $Priso^-$ = $[(ArN)_2CNPr^i_2]^-$; $Piso^-$ = $[(ArN)_2CBu^t]^-$ (Ar = 2,6-diisopropylphenyl).[42]

The divalent dimeric Yb complex $[Yb(DippForm)(\mu\text{-}I)(thf)_2]_2$ was obtained from the reaction of $[Yb(DippForm)_2(\{C_{13}H_8\}\text{-}O)(thf)]$ (maroon solution) with $[SmI_2(thf)_2]$ at room temperature.[43]

$$[Yb(DippForm)_2(\{C_{13}H_8\}\text{-}O)(thf)] + [SmI_2(thf)_2] \xrightarrow{\text{stirred, rt}} [Yb(DippForm)(\mu\text{-}I)(thf)_2]_2 + [Sm_{10}O_4(\{C_{13}H_8\}^-O)_{10}(thf)_{10}]$$

Equation 2.14: Dimeric ytterbium Grignard complex synthesis.[43]

2.2 Current Study

This chapter intends to expand the divalent organolanthanum halide complexes from the reaction between the lanthanoid metals (Ln = Sm, Eu and Yb) organic halide (PhBr, PhI and H_2NPhI) and pro-ligands (formamidines and pyrazoles). This synthetic pathway already proved useful for the trapping of a wide range of $[Yb(L)I(solv)_n]$ (L = formamidinato or pyrazolato) compounds. These approaches have yet to be explored for Sm for which the Ln(II) state is less stable, or for systems for which Ln(III) is dominant.

The protolysis reaction between $PhLnBr(thf)_n$ (Ln = Sm, Eu) and DippFormH produced dinuclear bromide bridged Ln(II) compounds for example $[Sm(DippForm)Br(thf)_3]_2\cdot 6thf$ (**2.1**) and $[Eu(DippForm)Br(thf)_3]_2\cdot 6thf$ (**2.2**); but pro-ligand (Ph_2pzH) produced Sm(III) $[Sm(Ph_2pz)_3(thf)_3]\cdot 3thf$ (**2.3a**), $[Sm(Ph_2pz)_3(dme)_2]\cdot dme$ (**2.3b**) and Eu(II) $[Eu(Ph_2pz)_2(thf)_4]$ (**2.4**).

This study also involved the reaction between $PhLnI(thf)_n$ (Ln = Sm, Yb) and pro-ligands (formamidines and pyrazoles) and produced trivalent $[Sm(DippForm)I_2(thf)_3].thf$ (**2.5**), $[Sm(Ph_2pz)I_2(thf)_3]$ (**2.6**), and divalent $[Yb(EtForm)_2(thf)_2]$ (**2.10**).

For further study we examined the reaction process between $H_2NPhLnI(thf)_n$ (Ln = Eu, Yb) and pro-ligands (formamidines and pyrazoles) and produced Ln(II); $[Eu(DippForm)I(thf)_4]\cdot thf$ (**2.7**), $[Yb(DippForm)I(thf)_3]\cdot thf$ (**2.8**) and $[Yb(Ph_2pz)I(thf)_4]$ (**2.9**).

2.3 Results and Discussion

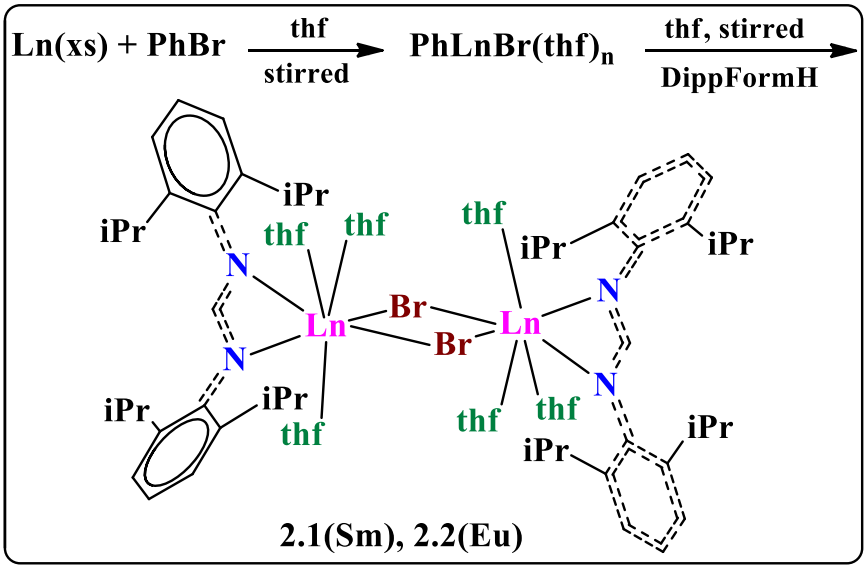
2.3.1 Synthesis and spectroscopic characterisation

2.3.1.1 The reaction of lanthanoid (Sm and Eu) pseudo-Grignard reagents (PhLnBr) with DippFormH

The primary target from the reaction was the synthesise of divalent lanthanoid pseudo-Grignard compounds, especially those of samarium (Sm) and europium (Eu). The reaction was conducted using a 1:1 stoichiometric ratio of PhBr and DippFormH, with an excess lanthanoid (Sm **2.1** and Eu **2.2**) metals filings in thf at 0 °C (Sm) or -78 °C (Eu). For samarium, the mixture was sonicated for 10 min and stirred for 24 h at room temperature, resulting in a light brown solution of [PhSmBr(thf)$_n$]. Subsequently, solid DippFormH (0.368 g, 1.0 mmol) was added and the mixture was stirred at 0 °C for 1 h. After stirring for an additional 24 h at room temperature, a green solution was obtained.

In the case of europium, following sonication for 10 min, a brown solution of [PhEuBr(thf)$_n$] was formed. The mixture was then cooled to -78 °C, solid DippFormH (0.368 g, 1.0 mmol) was added and the mixture was stirred at -78 °C for another 3 h. A brownish-yellow solution developed after further stirring for 24 h at room temperature. Crystallisation from the concentrated solutions resulted the formation of green crystals of **[Sm(DippForm)Br(thf)$_3$]$_2$·6thf** (**2.1**) and yellow crystals of **[Eu(DippForm)Br(thf)$_3$]$_2$·6thf** (**2.2**). Each compound consists of a divalent dimer with a Ln_2Br_2 metal core. The reaction and structural scheme of the compounds are illustrated in **Scheme 2.7**.

Satisfactory ^{1}H NMR spectra were obtained for compound **2.1** (**Fig. 2.1**). in contrast, compound **2.2** (**Fig. 2.2**) exhibited broad features with unsatisfactory integration owing to paramagnetism (Eu^{II}). The NMR spectra of compound **2.1** indicated the loss of 3 THF molecules of crystallisation, which was consistent with the microanalysis results. The methine proton (NC*H*N) resonances for compound **2.1** shifted significantly to lower frequencies (-10.70 ppm), comparable to the paramagnetic compound [Sm(DippForm)$_2$(thf)$_2$] (-14.03 ppm).[44] The CH_2 signals of thf (6 from coordinated and 3 from crystallisation) were observed at δ = 3.23 and 4.99 ppm, while the *i*Pr and CH signals from DippForm appeared at δ = 1.78, and 1.20 ppm.



Scheme 2.7: Synthesis of compounds [Sm(DippForm)Br(thf)$_3$]$_2$·6thf (**2.1**) and [Eu(DippForm)Br(thf)$_3$]$_2$·6thf (**2.2**).

Additionally, the compounds were further characterised by IR spectroscopy and elemental analysis confirmed their bulk purity. The colour of compound **2.1** is associated with a broad visible band at λ_{max} = 588 nm in the UV/vis spectrum (**Fig. 2.3**), which is attributable to an f^6 to f^5d^1 transition.[45]

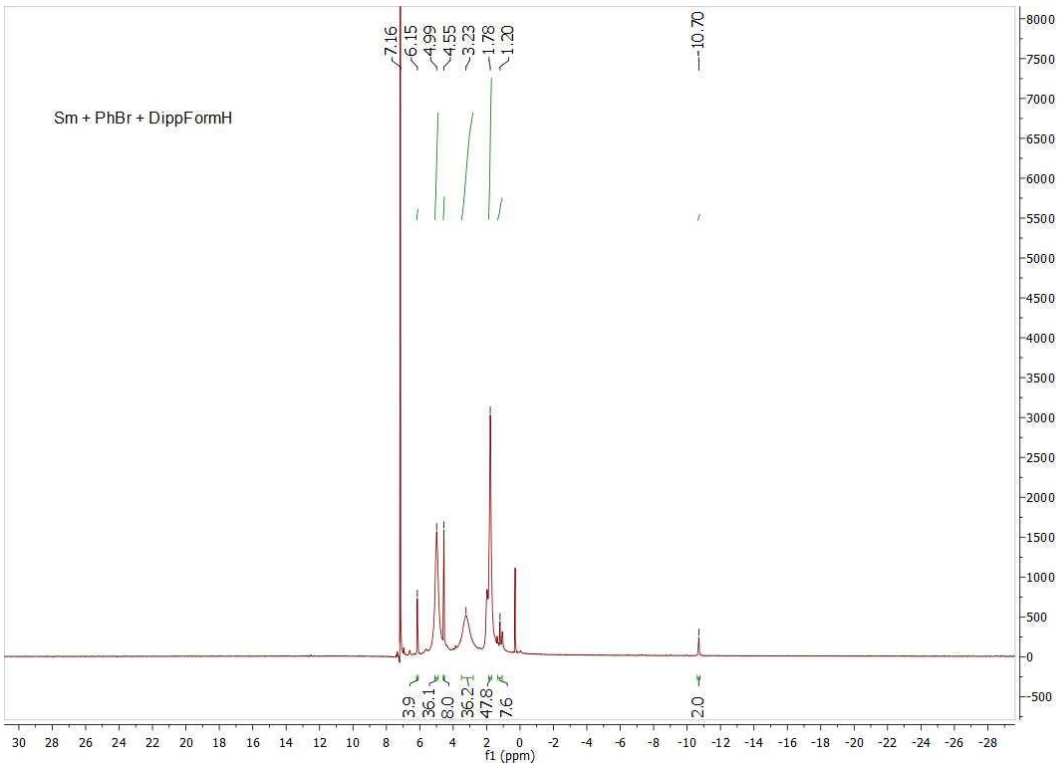


Figure 2.1: ^{1}H NMR spectrum of **[Sm(DippForm)Br(thf)$_3$]$_2$·6thf (2.1)** (loss of 3 thf) in C_6D_6.

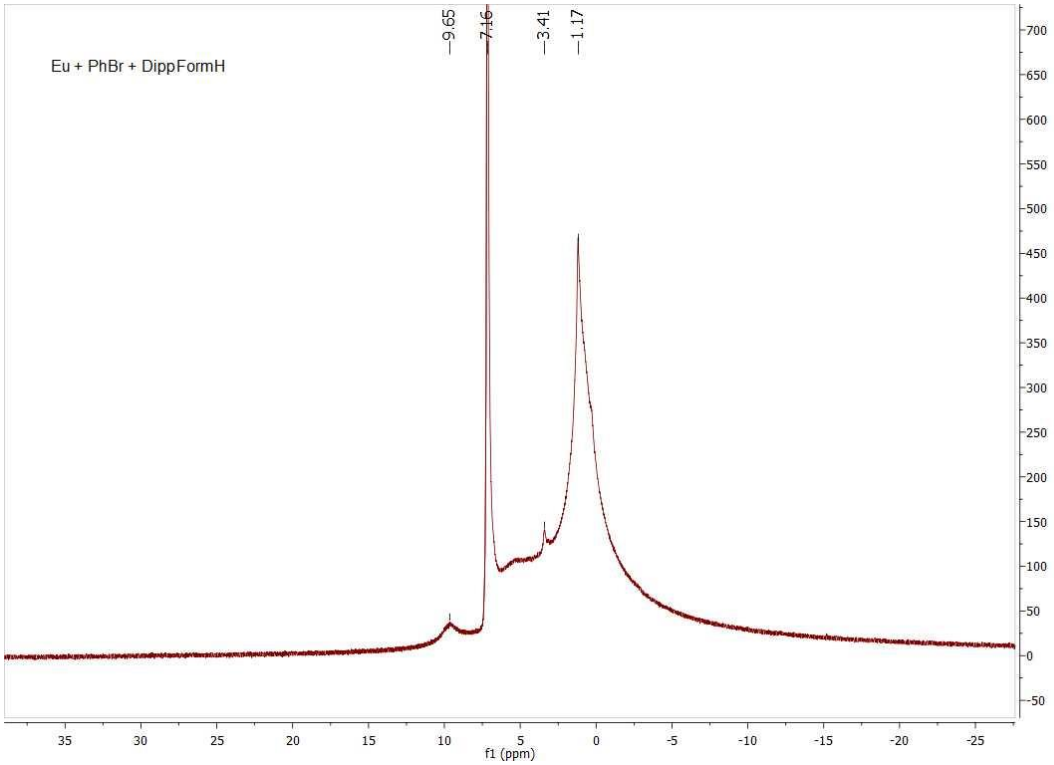


Figure 2.2: ^{1}H NMR spectrum of **[Eu(DippForm)Br(thf)$_3$]$_2$·6thf (2.2)** in C_6D_6.

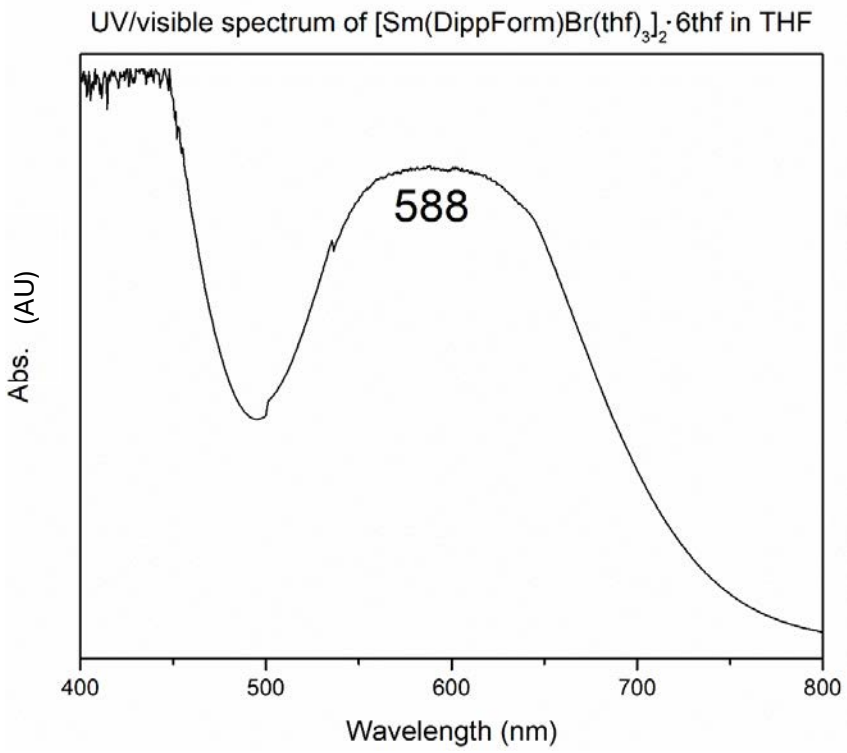
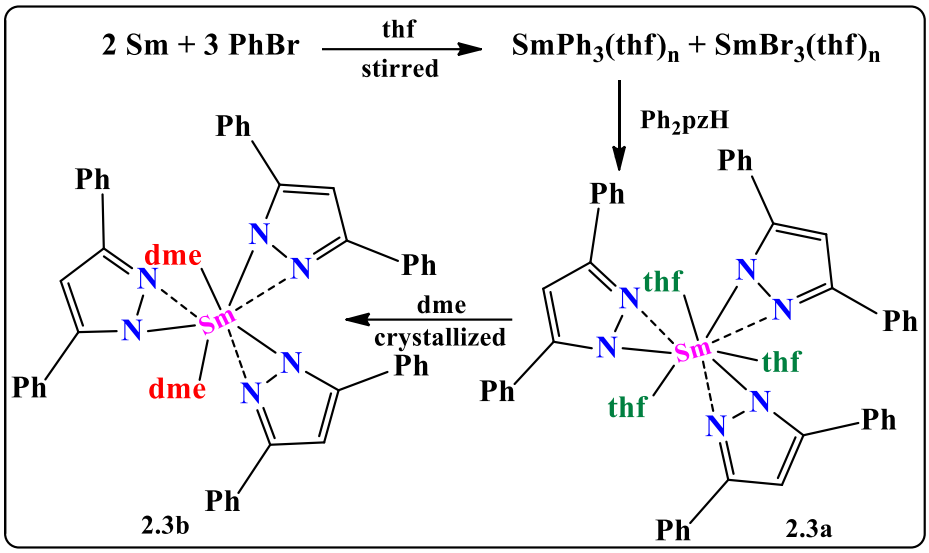


Figure 2.3: UV/visible spectrum of **[Sm(DippForm)Br(thf)$_3$]$_2$·6thf (2.1)** in thf (3.3×10^{-2} molar).

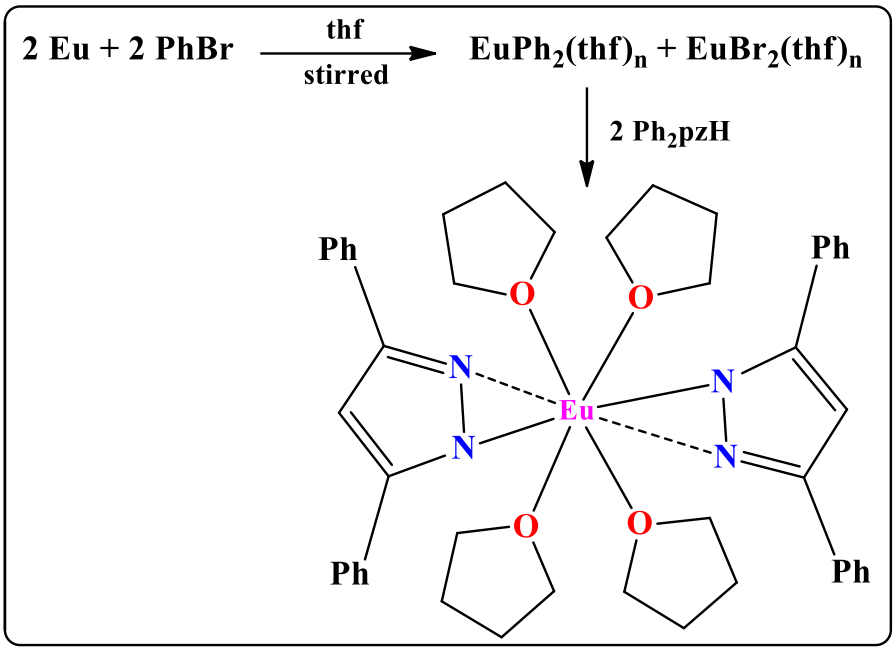
2.3.1.2 The reaction of lanthanoid (Sm and Eu) pseudo-Grignard reagents (PhLnBr) with Ph_2pzH

The primary objective of the reaction was to synthesise divalent lanthanoid pseudo-Grignard compounds, especially those of samarium (Sm) and europium (Eu). The reaction was conducted using a 1:1 stoichiometric ratio of PhBr and Ph_2pzH, with an excess lanthanoid (Sm **2.3 (a, b)** and Eu **2.4**) metals filings in thf at 0 °C for Sm and -78 °C for Eu. For samarium, the mixture was sonicated for 10 min and then stirred for 24 h at room temperature, yielding in a light brown solution of [$SmPh_3(thf)_n$] formed. Solid Ph_2pzH (0.22 g, 1.0 mmol) was subsequently added, and the mixture was stirred at 0 °C for 1 h. After stirring for 24 h at room temperature, a yellowish-brown solution developed.

For europium, after sonication for 10 min, a brown solution of [$EuPh_2(thf)_n$] formed. Following this, the mixture was cooled to -78 °C, and solid Ph_2pzH (0.22 g, 1.0 mmol) was added and the mixture was stirred at -78 °C for another 3 h. A red brown solution developed after further stirring for 24 h at room temperature. Crystallisation from the concentrated solutions resulted in the formation of colourless crystals of **[Sm(Ph_2pz)$_3$(thf)$_3$]·3thf** (**2.3a**) and yellow crystals of **[Eu(Ph_2pz)$_2$(thf)$_4$]** (**2.4**). Additionally, compound **[Sm(Ph_2pz)$_3$(dme)$_2$]·dme** (**2.3b**) was synthesised by crystallising **2.3a** from DME. All three compounds (**2.3a**, **2.3b** and **2.4**) were isolated as products of Schlenk equilibria along with the lanthanoid halide. The reaction and structural schemes for compounds **2.3a** and **2.3b** are presented in **Scheme 2.8**, while compound **2.4** is illustrated in **Scheme 2.9**.



Scheme 2.8: Synthesis of compounds $[Sm(Ph_2pz)_3(thf)_3]\cdot 3thf$ (**2.3a**) and $[Sm(Ph_2pz)_3(dme)_2]\cdot dme$ (**2.3b**).



Scheme 2.9: Synthesis of compound $[Eu(Ph_2pz)_2(thf)_4]$(**2.4**).

Satisfactory ^{1}H NMR spectra were obtained for compounds **2.3a** and **2.3b** (**Fig. 2.4** and **Fig. 2.5**), whereas compound **2.4** (**Fig. 2.6**) showed broad features with unsatisfactory integration due to paramagnetism of Eu(II).

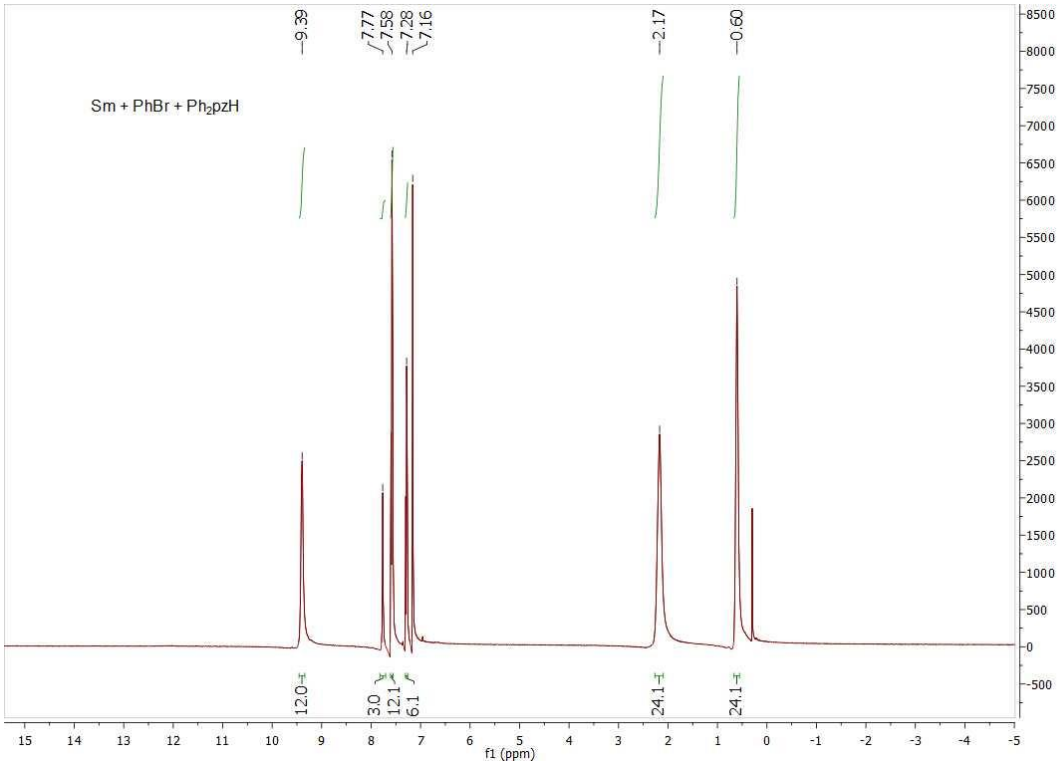


Figure 2.4: ^{1}H NMR spectrum of **[Sm(Ph$_2$pz)$_3$(thf)$_3$].3thf (2.3a)** in C_6D_6.

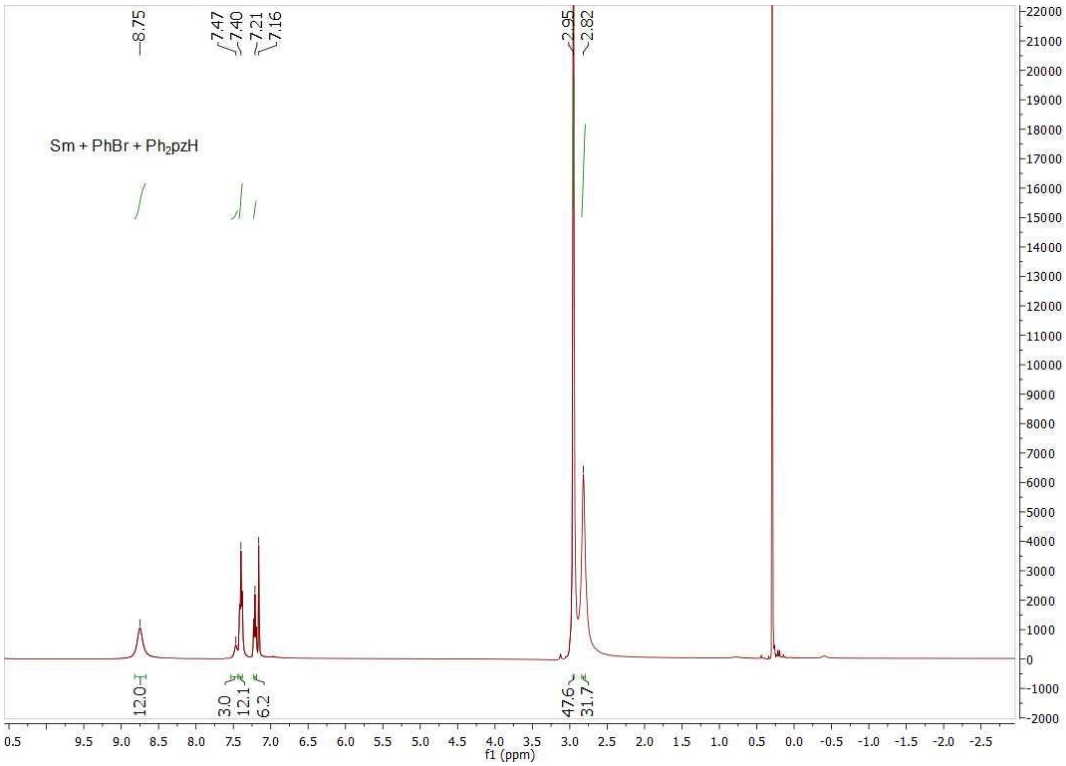


Figure 2.5: ^{1}H NMR spectrum of **[Sm(Ph$_2$pz)$_3$(dme)$_2$]·dme (2.3b)** in C_6D_6.

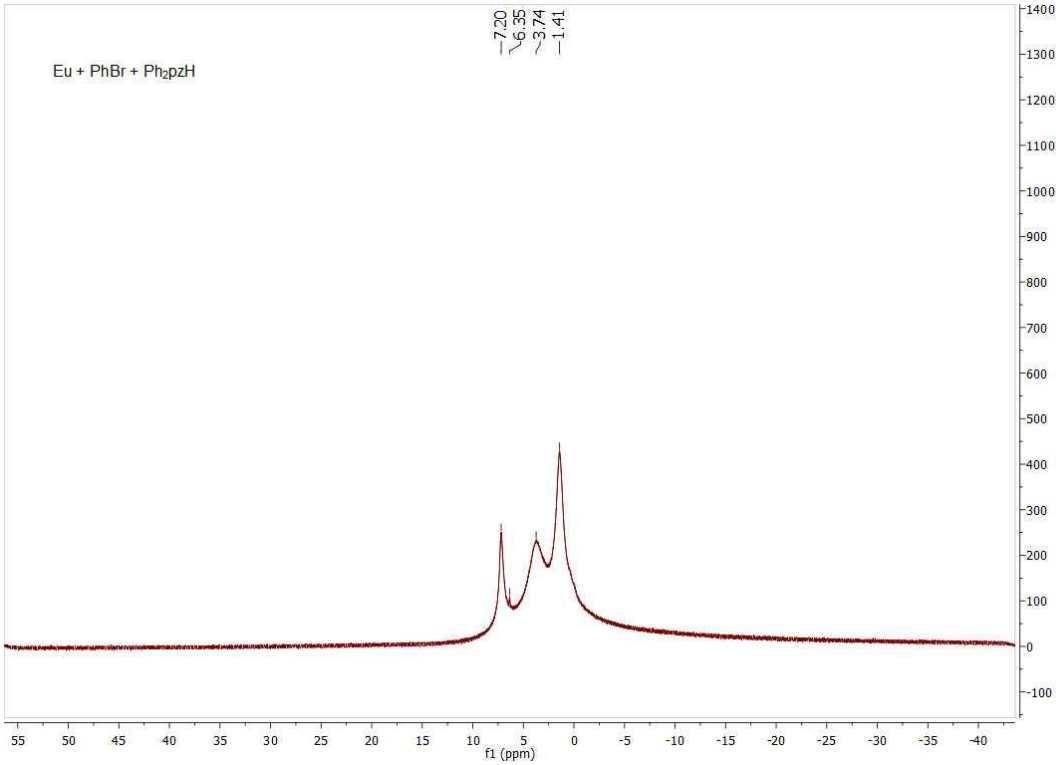


Figure 2.6: ^{1}H NMR spectrum of **[Eu(Ph$_2$pz)$_2$(thf)$_4$]** (**2.4**) in C_6D_6.

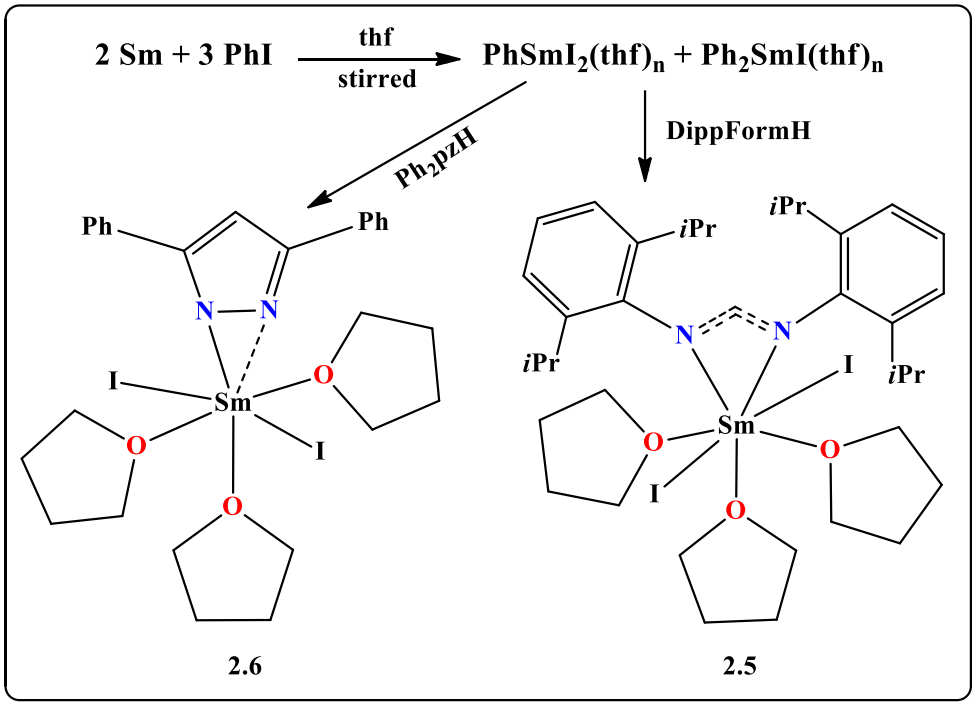
The NMR spectra of compound **2.3b** indicated the presence of excess DME of crystallisation. For compound **2.3a**, the CH-pz resonance shifted to 9.39 ppm, while for **2.3b**, it shifted to 8.75 ppm, compared to the pro- ligand value of 6.63 ppm. In compound **2.3a**, the CH_2 signals from thf were observed at δ = 0.60 and 2.17 ppm, and the CH signals from the phenyl ring were at δ = 7.28, 7.58 and 7.77 ppm. In compound **2.3b**, the CH_3 signals from dme were observed at δ = 2.82 and 2.95 ppm, with the CH signals from the phenyl ring appearing at δ = 7.21, 7.40 and 8.75 ppm. Additionally, the compounds were also characterised by IR spectroscopy and elemental analysis confirmed their bulk purity.

2.3.1.3 The reaction of samarium (Sm) pseudo-Grignard reagents (PhSmI) with DippFormH and Ph$_2$pzH

The primary objective of the reaction was synthesised samarium pseudo-Grignard compounds. The reaction was carried out using a 1:1 stoichiometric ratio of PhI and ligands (DippFormH or Ph$_2$pzH) with an excess lanthanoid metals (Sm **2.5** and **2.6**) filings in thf at 0 °C. The mixture was sonicated for 10 min and then stirred for 24 h at room temperature, resulting in a light brown solution of [PhSmI$_2$(thf)$_n$]. For compound **2.5**, solid DippFormH (0.368 g, 1.0 mmol)

was added and for compound **2.6**, solid Ph_2pzH (0.22 g, 1.0 mmol) was added. The mixtures were stirred at 0 °C for 1 h, and a green solution developed after stirring for 24 h at room temperature.

Crystallisation from the concentrated solutions yielded both yellow crystals of **[Sm(DippForm)I_2(thf)$_3$].thf** (**2.5**) and **[Sm(Ph$_2$pz)I_2(thf)$_3$]** (**2.6**). Both samarium compounds were isolated as trivalent (Sm^{III}) pseudo-Grignard products, with magnetic susceptibility measurement through iodo metric titration indicating a possibility of 50% for Sm^{III}.[3] The reaction and structural scheme for compounds **2.5** and **2.6** are presented in **Scheme 2.10**.



Scheme 2.11: Synthesis of compounds [Sm(DippForm)I_2(thf)$_3$].thf (**2.5**) and [Sm(Ph$_2$pz)I_2(thf)$_3$] (**2.6**).

Satisfactory ^{1}H NMR spectra were obtained for compounds **2.5** (**Fig. 2.7**) and **2.6 Fig. 2.8**). The NMR spectra of compound **2.5** indicated the loss of 2 thf molecules from crystallisation and 1 thf molecule from solvation, which is consistent with the elemental analysis results. In contrast, the NMR spectra of compound **2.6** suggested the presence of an excess of 2 thf molecules from crystallisation, possible due to insufficient drying of the crystals during characterisation.

Compound **2.5**, the methine proton (NC*H*N) resonance shifted significantly to the higher frequencies at 10.57 ppm. The CH_2 signals from thf were observed at δ = 1.41 and 3.63 ppm, while the *i*Pr and CH signals from DippForm appeared at δ = 1.14, and 3.43 ppm. For

compound **2.6**, the CH-pz resonance shifted to 7.80 ppm compared with the pro- ligand value of 6.63 ppm. The CH_2 signals from thf were observed at δ = 1.20 and 3.21 ppm, and the CH signals from the phenyl ring appeared at δ = 7.30, 7.59 and 9.38 ppm. Additionally, the compounds were also confirmed by IR spectroscopy and elemental analysis verified their bulk purity. The colour of (Sm + PhI + Ph_2pzH) solution in thf is associated with visible band at λ_{max} = 558 and λ_{max} = 619 nm in the UV/vis spectrum (**Fig. 2.9**), which is attributable to an f^6 to f^5d^1 transition.[45] This indicated that the Schlenk equilibria products were present in the solution.

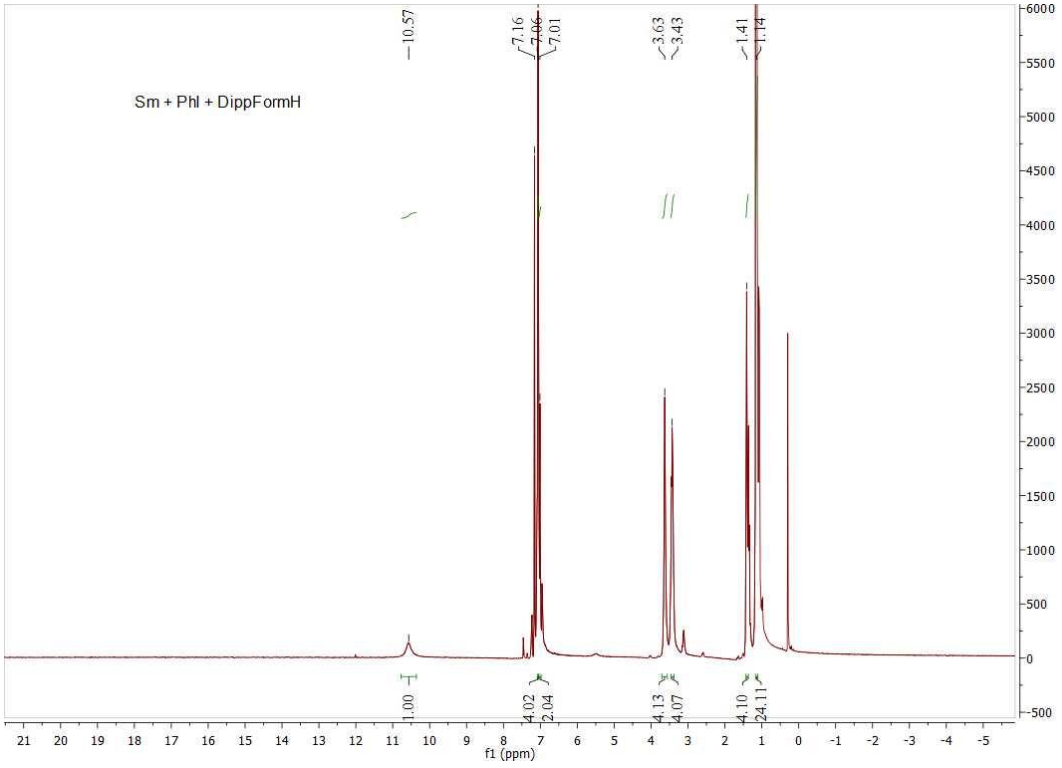


Figure 2.7: ^{1}H NMR spectrum of **[Sm(DippForm)I_2(thf)$_3$].thf (2.5)** in C_6D_6.

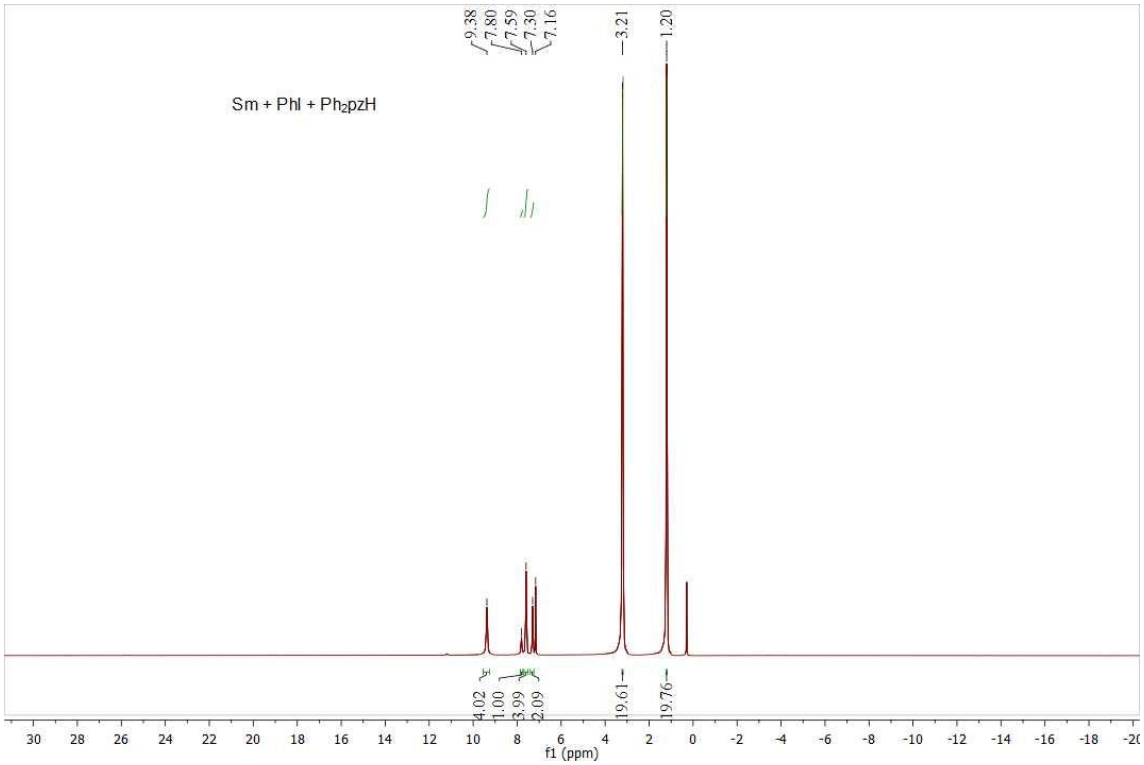


Figure 2.8: ^{1}H NMR spectrum of **[Sm(Ph$_2$pz)I$_2$(thf)$_3$] (2.6)** in C_6D_6.

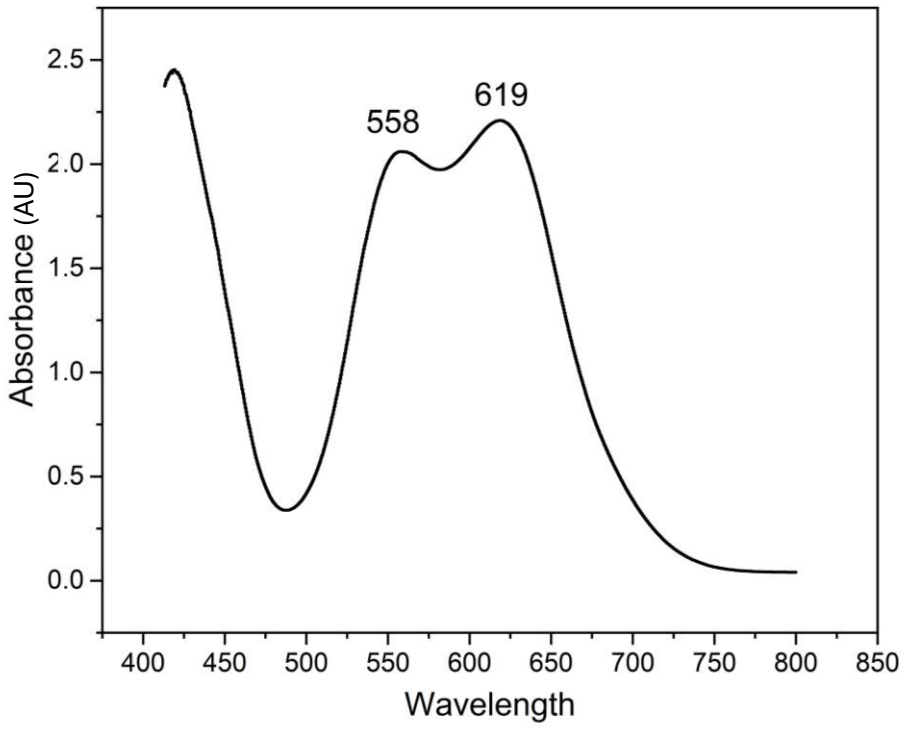
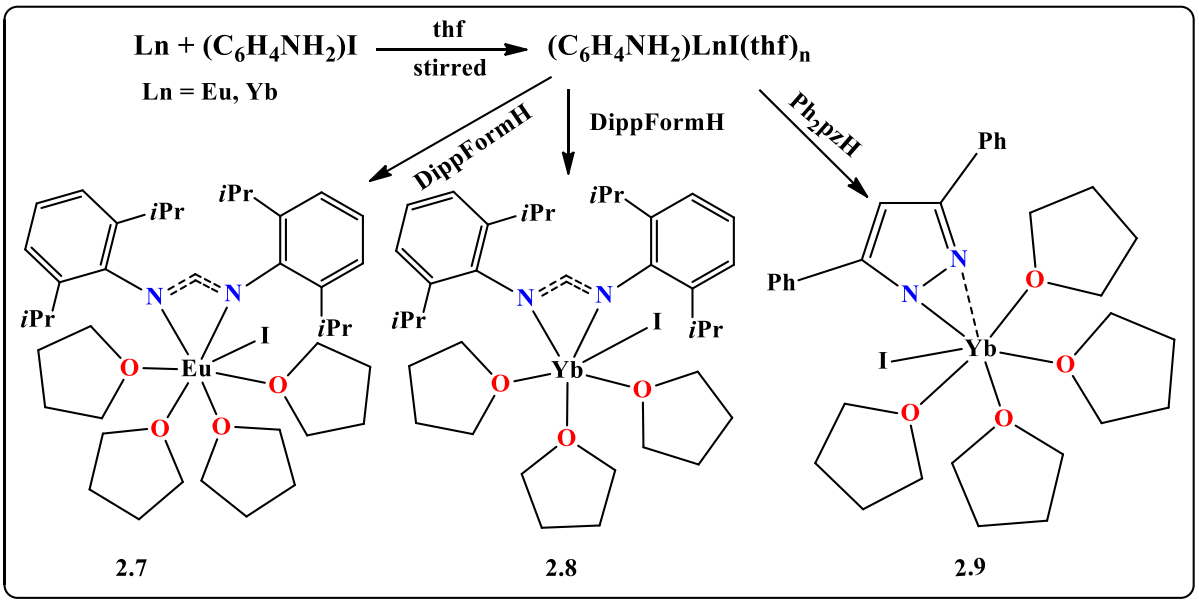


Figure 2.9: UV/visible spectrum of green solution **(Sm + PhI + Ph$_2$pzH)** in thf (6.7×10^{-2} molar).

2.3.1.4 Synthesis of lanthanoid (Eu and Yb) pseudo-Grignard compounds (reported) from the reaction of lanthanoid (Eu and Yb) metals with $C_6H_4NH_2I$ and DippFormH or Ph_2pzH

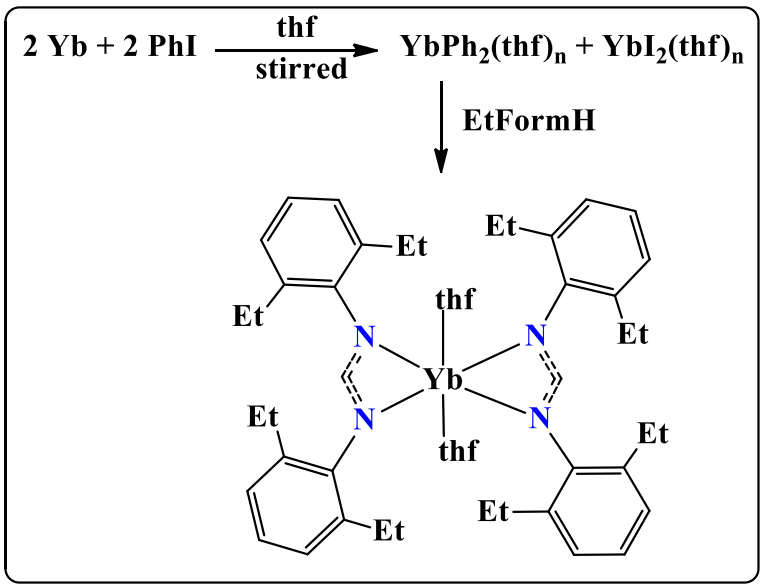
The reactions were conducted using a 1:1 stoichiometric ratio of oxidant ($C_6H_4NH_2I$ or PhI) and ligand (DippFormH or Ph_2pzH), with an excess of lanthanoid (Eu **2.7** and Yb **2.8**; **2.9**) metal filings in thf at 0 °C. The mixture was sonicated for 10 min and stirred for 2 h at room temperature, when a yellow solution of $[(C_6H_4NH_2)EuI(thf)_n]$ and an orange solution of $[(C_6H_4NH_2)YbI(thf)_n]$ formed. For compounds **2.7** and **2.8**, solid DippFormH (0.368 g, 1.0 mmol) was added and for compound **2.9** solid Ph_2pzH (0.22 g, 1.0 mmol) was added. The mixture was stirred at 0 °C for 1 h, leading to the formation of a red-yellow solution for compound **2.7** and a red orange solution for compounds **2.8** and **2.9** after stirring for an additional 24 h at room temperature. Crystallisation from the concentrated solutions yielded yellow crystals of **[Eu(DippForm)I(thf)$_4$]·thf (2.7)**, red crystals of **[Yb(DippForm)I(thf)$_3$]·thf (2.8)** and **[Yb(Ph$_2$pz)I(thf)$_4$] (2.9)**. The reaction and structural schemes for compounds **2.7**, **2.8** and **2.9** are provided in **Scheme 2.11**.



Scheme 2.11: Synthesis of compounds [Eu(DippForm)I(thf)$_4$]·thf (**2.7**), [Yb(DippForm)I(thf)$_3$]·thf (**2.8**) and [Yb(Ph$_2$pz)I(thf)$_4$] (**2.9**).

In a separate reaction, a 1:1 stoichiometric ratio of PhI and EtFormH was used with excess ytterbium metal filings in thf solvent at -78 °C. The mixture was sonicated for 10 min resulting in a red-orange solution of $[PhYbI(thf)_n]$ ($[PhYbI(thf)_n] \leftrightarrow [YbPh_2(thf)_n] + [YbI_2(thf)_n]$). After cooling to -78 °C, solid EtFormH (0.308 g, 1.0 mmol) was added, and the mixture was stirred

for an additional 3 h. A red solution developed after further stirring for 24 h at room temperature. Crystallisation from the concentrated solution yielded red crystals of **[Yb(EtForm)$_2$(thf)$_2$] (2.10)**. The reaction and structural scheme for compound **2.10** are illustrated in **Scheme 2.12**.



Scheme 2.12: Synthesis of compounds **[Yb(EtForm)$_2$(thf)$_2$] (2.10)**.

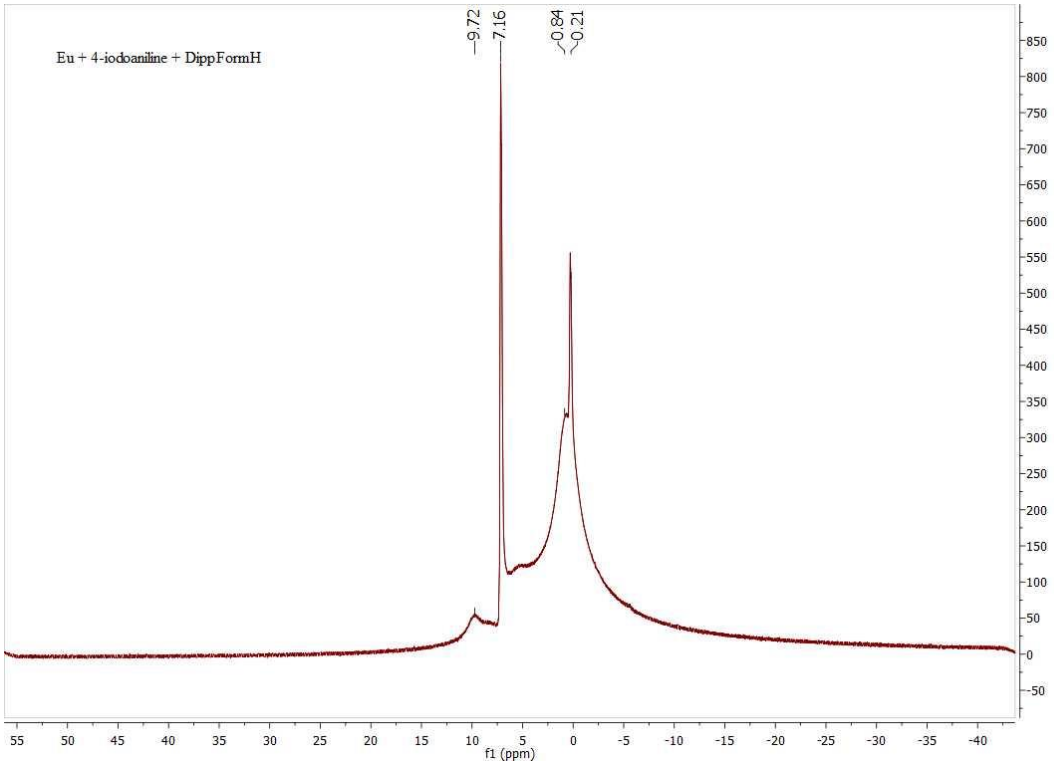


Figure 2.10: ^{1}H NMR spectrum of **[Eu(DippForm)I(thf)$_4$]·thf (2.7)** in C_6D_6.

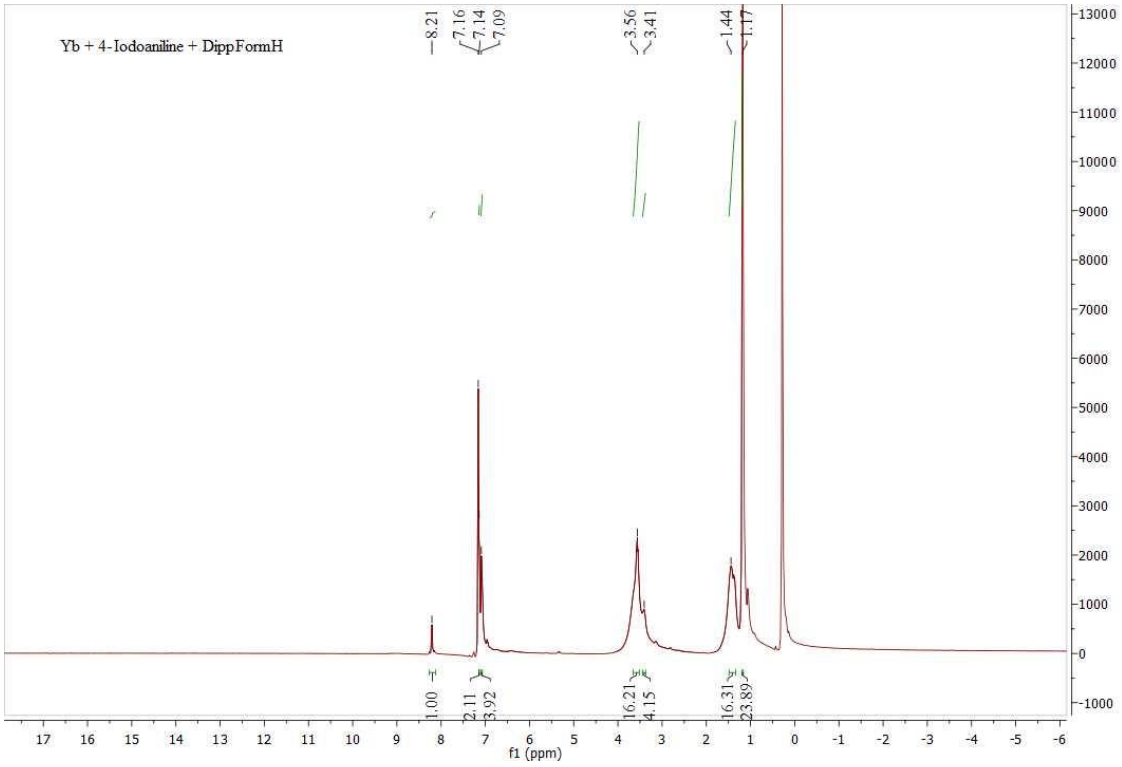


Figure 2.11: ^{1}H NMR spectrum of **[Yb(DippForm)I(thf)$_3$]·thf (2.8)** in C_6D_6.

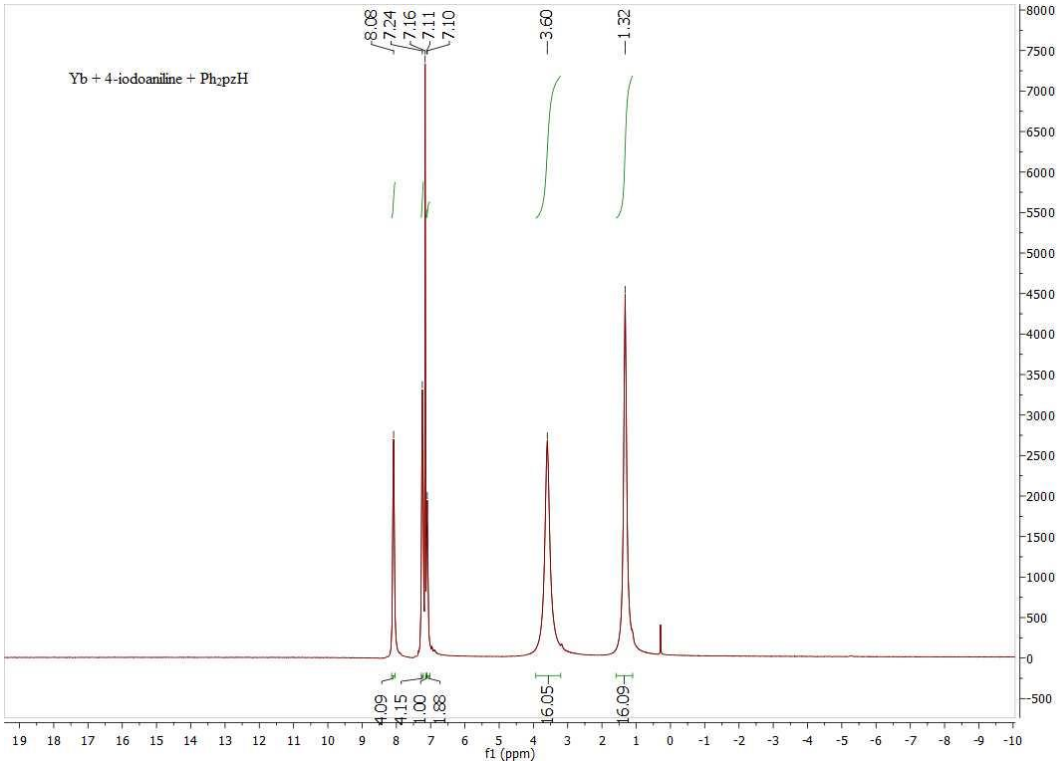


Figure 2.12: ^{1}H NMR spectrum of **[Yb(Ph$_2$pz)I(thf)$_4$] (2.9)** in C_6D_6.

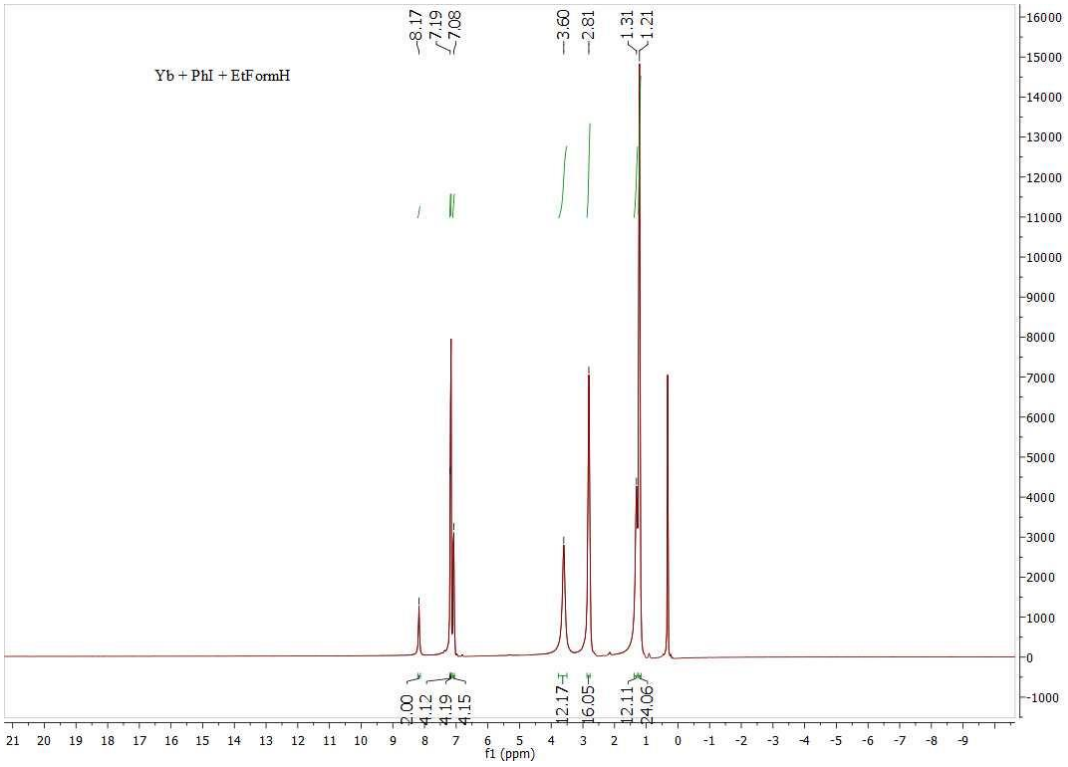


Figure 2.13: ^{1}H NMR spectrum of **[Yb(EtForm)$_2$(thf)$_2$] (2.10)** in C_6D_6.

Satisfactory ^{1}H NMR spectra were obtained for compounds **2.8** to **2.10** (**Fig. 2.11** to **2.13**). The methine proton (NC*H*N) resonances shifted to δ = 8.21 ppm for compound **2.8** and 8.17 ppm for compound **2.10**. In compound **2.8**, the *i*Pr and the CH signals from DippForm appeared at δ = 1.17 and 3.41 ppm, while in compound **2.10** the CH_3 and the CH_2 signals from EtForm were observed at δ = 1.21 and 2.81 ppm, respectively. For compound **2.9** the CH-pz resonance shifted to 7.11 ppm and the CH signals from the phenyl ring appeared at δ = 7.10 and 7.24 ppm. Compound **2.7** (**Fig. 2.10**) exhibited broad features with unsatisfactory integration owing to paramagnetism (Eu^{II}). Additionally, these compounds were further characterized by IR spectroscopy and metal analysis confirmed their bulk purity.

Table 2.2: Chemical shifts in ^{1}H-NMR spectra of complexes **2.1** - **2.10** in C_6D_6.

	Chemical shift (ppm)					
^{1}H-NMR	N(CH)N /CH(pz)	CH (*i*Pr)/ CH_2/ (Et)	CH_3 (*i*Pr)/ (Et)	CH_2 (thf /dme)	OCH_2 (thf)/ OCH_3 (dme)	Ph
[Sm(DippForm)Br(thf)$_3$]$_2$·6thf	-10.70	1.20	1.78	3.23	4.99	4.55, 6.15

$[Sm(Ph_2pz)_3(thf)_3]\cdot 3thf$	7.77			0.60	2.17	7.28, 7.58, 9.39
$[Sm(Ph_2pz)_3(dme)_2]\cdot dme$	7.47			2.82	2.95	7.21, 7.40, 8.75
$[Sm(DippForm)I_2(thf)_3]. thf$	10.57	1.14	3.43	1.41	3.63	7.06, 7.01,
$[Sm(Ph_2pz)I_2(thf)_3]$	7.80			1.20	3.21	7.30, 7.59, 9.38
$[Yb(DippForm)I(thf)_3]\cdot thf$	8.21	1.17	3.41	1.44	3.56	7.09, 7.14
$[Yb(Ph_2pz)I(thf)_4]$	7.11			1.32	3.60	7.10, 7.24, 8.08
$[Yb(EtForm)_2(thf)_2]$	8.17	1.21	2.81	1.31	3.60	7.08, 7.18-7.19

2.3.2 X-ray Crystal Structures

2.3.2.1 $[Ln(DippForm)Br(thf)_3]_2\cdot 6thf$ (Sm **2.1**, Eu **2.2**)

Compounds $[Ln(DippForm)Br(thf)_3]_2\cdot 6thf$ (**2.1, 2.2**) are seven coordinate bromide bridged dimers, featuring one chelating DippForm and three coordinated thf ligands bound to each lanthanoid (Ln) atom. The geometry of seven coordinate compounds **2.1** (Sm^{2+}) and **2.2** (Eu^{2+}) can be described as distorted as pentagonal bipyramid (**Fig. 2.14**). The DippForm ligands are oriented perpendicular to the Ln_2Br_2 plane, with one ligand is *cis* {C(13)-Sm(1)-Br(1) 95.057°, C(13)-Eu(1)-Br(1) 97.708°} to Br1 and *trans* {C(13)-Sm(1)-Br(2) 174.339°, C(13)-Eu(1)-Br(2) 176.919°} to Br2. The average bite angle in compound **2.1** is 51.665(11)° and the Br(1)-Sm-Br(2) is 79.476(18)°. In contrast, in compound **2.2** the average bite angle is 0.01° larger and Br(1)-Ln -Br(2) is 0.26° smaller than that in compound **2.1** (see the **Table 2.5**).

The average Sm-N bond length in $[Sm(DippForm)Br(thf)_3]_2$ **2.1** is 2.639(4) Å, which is longer than the average Sm-N bond length 2.576(3) Å in VI coordinate $[Sm(DippForm)_2(thf)_2]$, [46] consistent with the change in coordination number.[47] The <Sm-Br> bond length in seven coordinate compound **2.1** is 3.0988(7) Å, comparable to the <Sm-Br> bond length of 3.0256(4) Å in the seven coordinate $[Sm(C_5Ph_5)(\mu\text{-}Br)(thf)_2]_2$.[32]

However, it is longer than the reported average Sm-Br bond length of 2.8363(4) Å in seven coordinate $[Sm(DippForm)Br_2(thf)_3]$, [39] which features non-bridging Sm-Br bonds and a Sm(III) oxidation state. Additionally, the average $Sm\text{-}O_{(thf)}$ bond length in **2.1** is 2.629(3) Å, which is very close to the average $Sm\text{-}O_{(thf)}$ bond length of 2.579(2) Å in $[Sm(C_5Ph_5)(\mu\text{-}Br)(thf)_2]_2$, [32] but longer than the average $Sm\text{-}O_{(thf)}$ bond length of 2.479(2) Å in $[Sm(DippForm)Br_2(thf)_3]$, [39] attributed to difference in oxidation states.[47]

For [Eu(DippForm)Br(thf)$_3$]$_2$ (**2.2**) the average bond lengths (Å) of Eu-N 2.631(2), Eu-O$_{(thf)}$ 2.612(2) and Eu-Br 3.05250(6), which are comparable with those of the six coordinate [Eu(DippForm)$_2$(thf)$_2$] (Eu-N 2.595(6), Eu-O$_{(thf)}$ 2.556(5)) [33] and [(dpp-Bian)Eu(dme)(μ-Br)]$_2$ (Eu-Br 3.069(5)) [35] reflecting the expected relationship due to the differences in coordination number.[47]

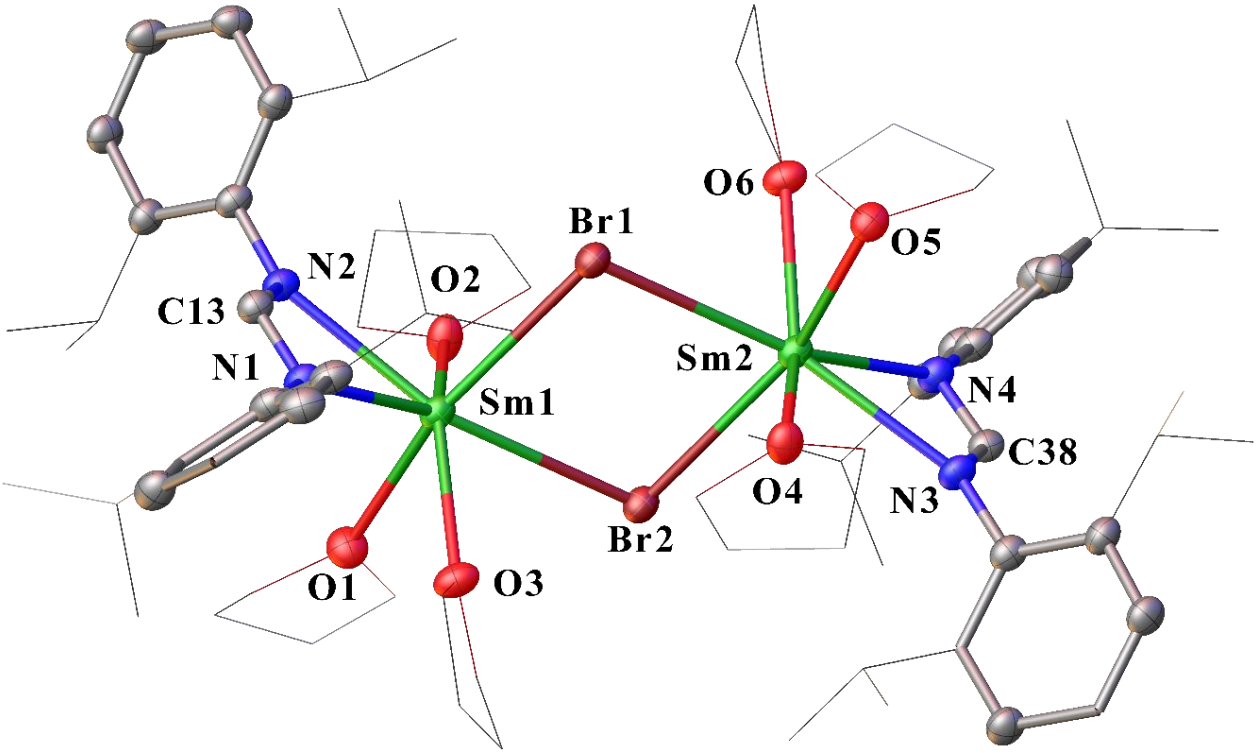


Figure 2.14: X-ray crystal structure of [Sm(DippForm)Br(thf)$_3$]$_2$·6thf (representative of Sm **2.1**, Eu **2.2**). Thermal ellipsoids are set at the 50% probability level. Hydrogen atoms and lattice thf molecules are omitted and coordinated thf molecules and *i*Pr groups are drawn as wireframe for clarity. Selected bond lengths (Å): Sm(1)-N(1) 2.634(4), Sm(1)-N(2) 2.644(4), Sm(1)-Br(1) 3.0260(8), Sm(1)-O(1) 2.580(3), Sm(1)-O(2) 2.591(3), Sm(1)-O(3) 2.650(3); Eu(1)-N(1) 2.625(2), Eu(1)-N(2) 2.635(2), Eu(1)-Br(1) 3.1157(6), Eu(1)-O(1) 2.634(2), Eu(1)-O(2) 2.590(2), Eu(1)-O(3) 2.589(2). More details including parameters for Ln(2), see the **Table 2.4**.

Table 2.3: A comparison of selected bond lengths (Å) of **2.1** and **2.2** with similar complexes.

Compounds	<Ln-N>	<Ln-X>	<Ln-O>	Ref.
[Sm(DippForm)Br(thf)$_3$]$_2$·6thf	2.639(4)	3.099(7)	2.629(3)	Current work
[Sm{N(SiMe$_3$)$_2$}$_2$(μ-Br)(thf)]$_2$	2.261(1)	2.961(2)	2.461(1)	[38]
[Sm{N(SiMe$_3$)$_2$}$_2$(μ-Cl)(thf)]$_2$	2.275(4)	2.789(1)	2.453(5)	[38]
[Sm(DippForm)I(thf)$_4$]	2.620(6)	3.275(10)	2.603(6)	[48]
[Sm(DippForm)$_2$(thf)$_2$]	2.576(3)		2.579(3)	[46]
[Sm(DippForm)$_2$F(thf)]	2.449(3)	2.093(2)	2.457(2)	[46]
[Sm(DippForm)$_2$Br(thf)]	2.437(3)	2.751(5)	2.454(3)	[39]
[Sm(DippForm)$_2$I(thf)]	2.432(15)	2.985(1)	2.454(13)	[39]
[(dpp-Bian)SmBr(dme)]$_2$	2.261(2)	2.481(1)	2.984(8)	[34]
[Eu(DippForm)Br(thf)$_3$]$_2$·6thf	2.631(2)	3.0525(6)	2.612(2)	Current work
[Eu(DippForm)$_2$(thf)$_2$]	2.595(6)		2.556(5)	[33]
[Eu(DippForm)I(thf)$_4$]	2.628(3)	3.263(7)	2.609(3)	[23]
[Eu{N(SiMe$_3$)$_2$}$_2$(μ-Cl)(thf)]$_2$	2.265(3)	2.784(8)	2.454(2)	[38]
[Nd(DippForm)$_2$Br(thf)]	2.461(4)	2.783(6)	2.487(4)	[33]

Table 2.4: Selected bond lengths of compounds (**2.1** and **2.2**).

Bond Lengths(Å)	2.1	2.2	Bond Lengths(Å)	2.1	2.2
Ln(1)-N(1)	2.634(4)	2.625(2)	Ln(2)-N(3)	2.645(4)	2.629(2)
Ln(1)-N(2)	2.644(4)	2.635(2)	Ln(2)-N(4)	2.633(4)	2.636(2)
Ln (1)-Br(1)	3.026(8)	3.116(6)	Ln(2)-Br(1)	3.128(7)	3.011(6)
Ln(1)-Br(2)	3.172(7)	3.034(7)	Ln(2)-Br(2)	3.049(8)	3.161(6)
Ln(1)-O(1)	2.580(3)	2.634(2)	Ln(2)-O(4)	2.600(3)	2.583(2)
Ln(1)-O(2)	2.591(3)	2.590(2)	Ln(2)-O(5)	2.606(3)	2.637(2)
Ln(1)-O(3)	2.650(3)	2.589(2)	Ln(2)-O(6)	2.647(3)	2.637(2)

Table 2.5: Selected bond angles of compounds (**2.1** and **2.2**).

Bond Angles(°)	2.1	2.2	Bond Angles(°)	2.1	2.2
C(13)-Ln(1)-Br(1)	95.057	176.919	C(n)-Ln(2)-Br(1)	177.636	95.083
C(13)-Ln(1)-Br(2)	174.339	97.708	C(n)-Ln(2)-Br(2)	98.121	174.103
C(13)-Ln(1)-O(1)	100.811	100.970	C(n)-Ln(2)-O(4)	101.859	104.124
C(13)-Ln(1)-O(2)	104.107	102.036	C(n)-Ln(2)-O(5)	102.242	100.893
C(13)-Ln(1)-O(3)	102.855	102.070	C(n)-Ln(2)-O(6)	101.047	102.939
O(1)-Ln(1)-O(2)	75.570(11)	77.780(7)	O(4)-Ln(2)-O(5)	74.600(11)	75.190(8)
O(1)-Ln(1)-O(3)	77.670(11)	147.100(7)	O(4)-Ln(2)-O(6)	147.280(10)	144.590(7)
O(2)-Ln(1)-O(3)	144.910(11)	74.690(8)	O(5)-Ln(2)-O(6)	77.940(10)	77.620(8)
N(1)-Ln(1)-N(2)	51.750(11)	51.650(7)	N(3)-Ln(2)-N(4)	51.580(11)	51.710(7)

2.3.2.2 $[Sm(Ph_2pz)_3(dme)_2]$ (**2.3b**)

The trigonal prismatic nine coordinate compound $[Sm(Ph_2pz)_3(dme)_2]$ (**2.3b**) crystallises in the monoclinic space group $P2_1/c$. The metal centre is coordinated to three η^2-Ph_2pz ligands, one chelating dme ligand and one monodentate dme ligand (**Fig. 2.15**). Complex **2.3b** is isomorphous with $[Nd(Ph_2pz)_3(dme)_2]$.[49]

The bond angles between the Ph_2pz ligand centers are closely aligned: C(8)-Sm-C(23) = 110.355°, C(8)-Sm-C(38) = 134.567° and C(23)-Sm-C(38) = 113.207°. The <Sm-N> bond length in $[Sm(Ph_2pz)_3(dme)_2]$ (**2.3b**) is 2.431(3) Å, which is identical to the <Sm-N> bond length of 2.436(4) Å in nine coordinate $[Sm(Ph_2pz)_3(thf)_3]$, [49] and comparable to the <Nd-N> bond length of 2.458(3) Å in nine coordinate $[Nd(Ph_2pz)_3(dme)_2]$.[49] The average $Sm\text{-}O_{(dme)}$ bond length in **2.3b** is 2.529(3) Å, which is close to the reported $<Sm\text{-}O_{(thf)}>$ bond lengths of 2.537(3) Å in $[Sm(Ph_2pz)_3(thf)_3]$, [49] and also comparable to the $<Nd\text{-}O_{(dme)}>$ bond length of 2.553(2) Å in $[Nd(Ph_2pz)_3(dme)_2]$.[49] These bond lengths reflects the similarity between the ionic radii of nine coordinate Sm^{3+} (1.132 Å) and Nd^{3+} (1.163 Å).[47]

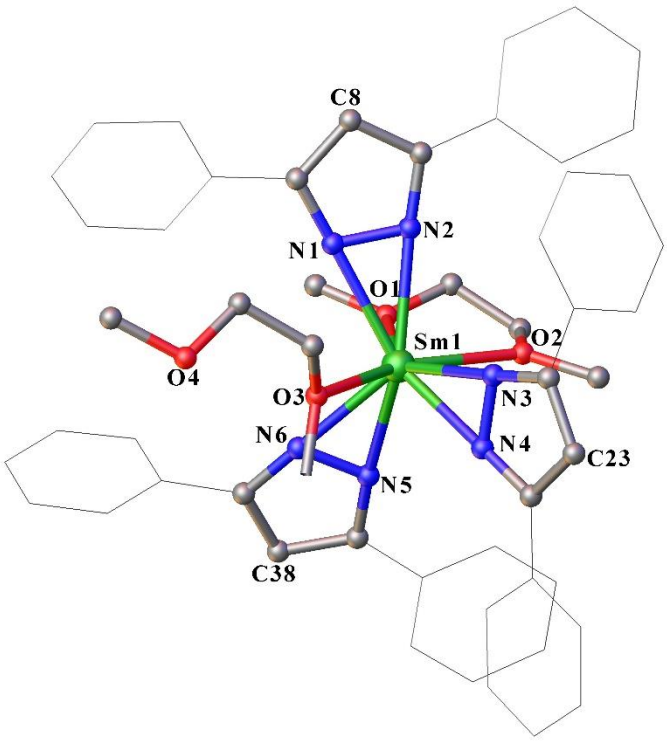


Figure 2.15: X-ray crystal structure of $[Sm(Ph_2pz)_3(dme)_2]\cdot dme$ (**2.3b**). Thermal ellipsoids are set at the 50% probability level. Hydrogen atoms and lattice dme molecules are omitted, phenyl groups are drawn as wireframe for clarity. Selected bond lengths (Å): Sm(1)-N(1) 2.446(3), Sm(1)-N(2) 2.419(3), Sm(1)-N(3) 2.434(3), Sm(1)-N(4) 2.424(3), Sm(1)-N(5) 2.403(3), Sm(1)-N(6) 2.456(3). For more details, see the **Table 2.7**.

Table 2.6: A comparison of selected bond lengths (Å) of **2.3b** with similar complexes.

Compounds	<Ln-N>	<Ln-O>	Ref.
$[Sm(Ph_2pz)_3(dme)_2]\cdot dme$	2.431(3)	2.529(3)	Current work
$[Sm(Ph_2pz)_3(thf)_3]\cdot 3thf$	2.436(4)	2.537(3)	[49]
$[Eu(Ph_2pz)_3(dme)_2]\cdot 2dme$	2.427(3)	2.514(2)	[49]
$[Nd(Ph_2pz)_3(dme)_2]\cdot dme$	2.458(3)	2.553(2)	[49]
$[Sm(Ph_2pz)_2(dme)_2]$	2.547(3)	2.651(6)	[50]
$[Ce(Ph_2pz)_3(thf)_3]$	2.507(3)	2.599(2)	[51]
$[Er(Ph_2pz)_3(dme)_2]$	2.339(7)	2.481(11)	[52]
$[Yb(Ph_2pz)_2(dme)_2]$	2.423(7)	2.530(6)	[50]
$[Sm(ttfpz)_3(thf)_3]\cdot 0.5thf$	2.538(2)	2.569(18)	[53]

Table 2.7: Selected bond lengths and bond angles of compound (**2.3b**).

Bond Lengths(Å)	**2.3(b)**	**Bond Lengths(Å)**	**2.3(b)**
Sm-N(1)	2.448(4)	Sm-N(6)	2.458(3)
Sm-N(2)	2.419(3)	Sm-O(1)	2.533(3)
Sm-N(3)	2.433(3)	Sm-O(2)	2.545(3)
Sm-N(4)	2.423(3)	Sm-O(3)	2.510(3)
Sm-N(5)	2.404(3)		
Bond Angles(°)	**2.3(b)**	**Bond Angles(°)**	**2.3(b)**
C(8)-Sm-O(1)	79.693	C(38)-Sm-O(1)	74.881
C(8)-Sm-O(2)	99.954	C(38)-Sm-O(2)	101.706
C(8)-Sm-O(3)	87.148	C(38)-Sm-O(3)	88.892
C(23)-Sm-O(1)	140.820	C(8)-Sm-C(23)	113.208
C(23)-Sm-O(2)	76.957	C(8)-Sm-C(38)	110.370
C(23)-Sm-O(3)	79.033	C(23)-Sm-C(38)	134.551

2.3.2.3 [Sm(DippForm)I_2(thf)$_3$]·thf (**2.5**)

Compound [Sm(DippForm)I_2(thf)$_3$]·thf (**2.5**) was isolated in the orthorhombic space group *P*bca and is isomorphous with [Nd(DippForm)I_2(thf)$_3$].[54] The geometric structure of the seven coordinate monomeric compound (**2.5**) is distorted pentagonal bipyramid, with the metal centre coordinated to one chelating DippForm ligand, three thf ligands and two *trans* iodide ligands (**Fig. 2.16**).

The bite angle (N(1)-Sm-N(2)) of the compound (**2.5**) is 34.68(19)°, the bite angle is 1.00° shorter than that of the same coordinate erbium compound [Er(DippForm)I_2(thf)$_3$] (56.68(17)°).[48] The I(1)-Sm-I(2) bond angle is 167.130(6)°, and the iodide ligands are positioned *cis* to the DippForm ligand, with (I(1)-Sm-C(13) 95.990(12)° and I(2)-Sm-C(13) 96.860(14)°). The average Sm-N bond length of 2.435(5) Å is ~0.014 Å shorter than (2.449(3)) that in the seven coordinate compound [Sm(DippForm)Br_2(thf)$_3$].[39] The average Sm-I bond length in compound **2.5** is 3.0893(9) Å, which is comparable with 3.043(1) Å in the six coordinate compound [Sm(dpp-Bian)I_2(thf)$_2$] {dpp-Bian = 1,2-bis[(2,6-

diisopropylphenyl)imino]acenaphthene}.[34] Additionally, the <Sm-O> bond length compound **2.5** is 2.472(5) Å, statistically equivalent to the analogous Sm-O interaction (2.479(2) Å) observed in the compound [Sm(DippForm)Br_2(thf)$_3$].[39]

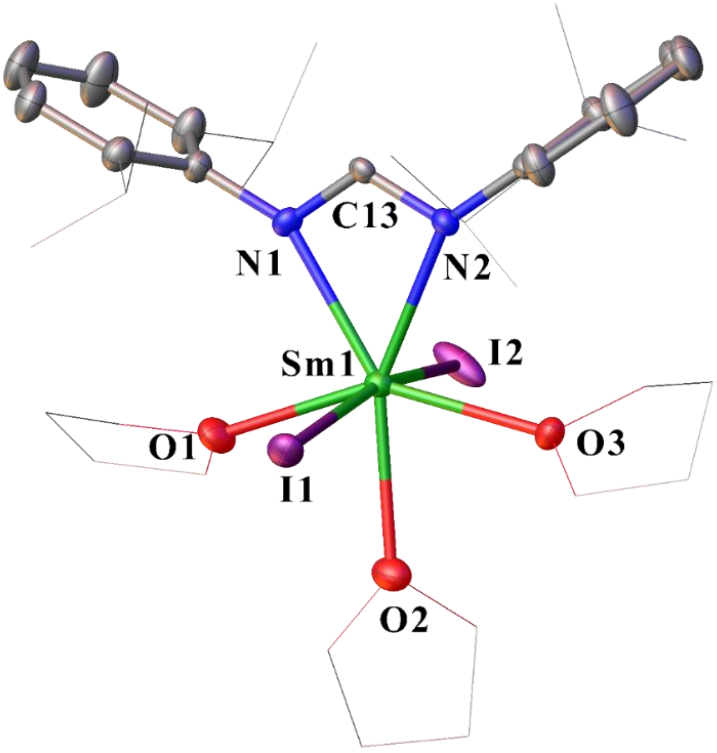


Figure 2.16: X-ray crystal structure of [Sm(DippForm)I_2(thf)$_3$] (**2.5**). Thermal ellipsoids are set at the 50% probability level. Hydrogen atoms are omitted and coordinated thf molecules and *i*Pr groups are drawn as wireframe for clarity. Selected bond lengths (Å): Sm-N(1) 2.439(5), Sm-N(2) 2.431(5), Sm -I(1) 3.0876(6), Sm-I(2) 2.991(11), Sm-O(1) 2.447(5), Sm-O(2) 2.523(6), Sm-O(3) 2.446(5). For more details, see the **Table 2.10**.

Table 2.8: A comparison of selected bond lengths (Å) of **2.5** with similar complexes.

Compounds	<Ln-N>	<Ln-I>	<Ln-O>	Ref.
[Sm(DippForm)I_2(thf)$_3$]	2.435(5)	3.0893(9)	2.472(5)	Current work
[Sm(DippForm)I(thf)$_4$]	2.620(6)	3.275(10)	2.603(6)	[48]
[Sm(DippForm)$_2$I(thf)]	2.432(15)	2.985(1)	2.454(13)	[39]
[Sm(DippForm)$_2$Br(thf)]	2.437(3)	2.751(5)	2.454(3)	[39]
[Sm(DippForm)$_2$(thf)$_2$]	2.576(3)		2.579(3)	[46]

[Sm(DippForm)$_2$F(thf)]	2.449(3)	2.093(2)	2.457(2)	[46]
[CpSmI$_2$(thf)$_3$]		3.1554(6)	2.463(5)	[55]
[Nd(DippForm)I$_2$(thf)$_3$]	2.469(4)	3.1135(4)	2.499(3)	[49]
[Gd(DippForm)I$_2$(thf)$_3$]	2.426(8)	3.0638(9)	2.440(7)	[49]
[Eu(DippForm)I(thf)$_4$]	2.628(3)	3.263(7)	2.609(3)	[23]

2.3.2.4 [Sm(Ph$_2$pz)I$_2$(thf)$_3$] (**2.6**)

The seven coordinate compound [Sm(Ph$_2$pz)I$_2$(thf)$_3$] (**2.6**) was isolated in the monoclinic space group *C2*/c. In this compound, the samarium cation is coordinated to one chelating Ph$_2$pz ligand, two iodide ligands and three thf ligands. The geometric structure of the compound **2.6** is described as pentagonal bipyramid (**Fig. 2.17**). The iodine ligands are *trans* to each other (I(1)-Sm-I(2) 167.650(4)°), while the both iodide ligands are *cis* to the pyrazolato ligand (I(1)-Sm-C(8) 93.167°, I(2)-Sm-C(8) 99.048°).

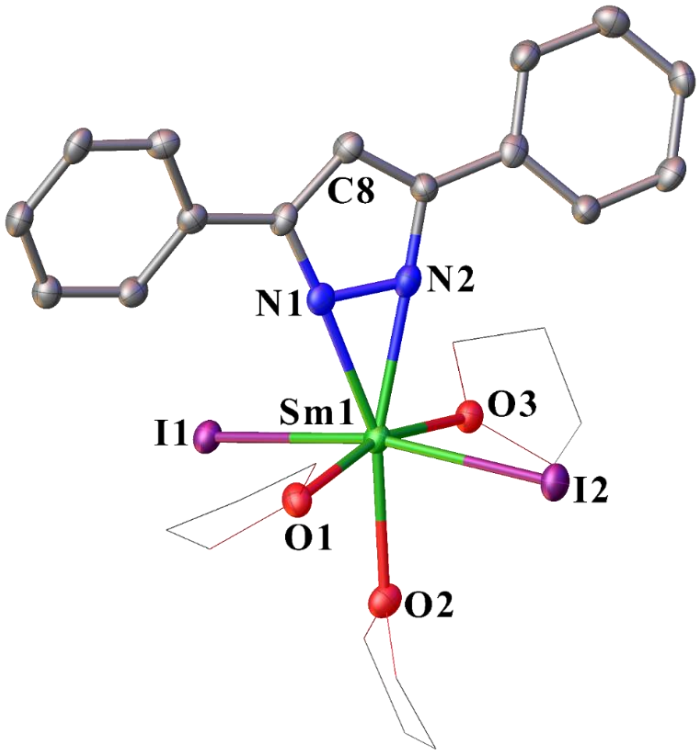


Figure 2.17: X-ray crystal structure of [Sm(Ph$_2$pz)I$_2$(thf)$_3$] (**2.6**). Thermal ellipsoids are set at the 50% probability level. Hydrogen atoms are omitted and coordinated thf molecules are drawn as wireframe for clarity. Selected bond lengths (Å): Sm-N(1) 2.334(11), Sm-N(2)

2.359(12), Sm -I(1) 3.0528(13), Sm-I(2) 3.0979(13), Sm-O(1) 2.399(9), Sm-O(2) 2.464(10), Sm-O(3) 2.402(9). For more details, see the **Table 2.10**.

The bite angle (N(1)-Sm-N(2)) of the compound (**2.6**) is 34.40(4)°, is higher than that of the eight coordinate trivalent neodymium compound [Nd(Ph_2pz)I_2(thf)$_4$] (32.400(3)°).[56] The <Sm-N> bond length in compound **2.6** is 2.346(11) Å, is slightly longer than the <Yb-N> bond length of 2.249(14) Å in [Yb(Ph_2pz)I_2(thf)$_3$].[23] The average Sm-O bond length in the compound **2.6** is 2.422(9) Å, is longer than (2.323(12)) in [Yb(Ph_2pz)I_2(thf)$_3$].[23] The average Sm-I bond length in compound **2.6** is 3.075(13) Å, which is 0.064 Å shorter than (3.139(1)) that in the eight coordinate compound [Sm$Cp^R I_2$](thf)$_3$.[57] These differences can happen due to the different ionic radii of metals (Sm^{3+} 1.160Å, Yb^{3+} 1.065Å) and variations in coordination involving the same oxidation state (Sm^{3+}).[47]

Table 2.9: A comparison of selected bond lengths (Å) of **2.6** with similar complexes.

Compounds	<Ln-N>	<Ln-I>	<Ln-O>	Ref.
[Sm(Ph_2pz)I_2(thf)$_3$]	2.346(11)	3.0754(13)	2.422(9)	Current work
[Nd(Ph_2pz)I_2(thf)$_4$]	2.455(9)	3.167(12)	2.524(8)	[56]
[Lu(Ph_2pz)I_2(thf)$_3$]	2.259(10)	2.9880(14)	2.315(9)	[56]
[Sm(Ph_2pz)$_3$(thf)$_3$]·3thf	2.436(4)		2.537(3)	[48]
[CpSmI_2(thf)$_3$]		3.1554(6)	2.463(5)	[55]
[Yb(Ph_2pz)I_2(thf)$_3$]	2.249(14)	2.9916(13)	2.323(12)	[23]
[Eu(Ph_2pz)I(thf)$_4$]	2.535(17)	3.1983(2)	2.591(8)	[22]
[Yb(Ph_2pz)I(thf)$_4$]	2.433(3)	3.0966(4)	2.477(4)	[22]

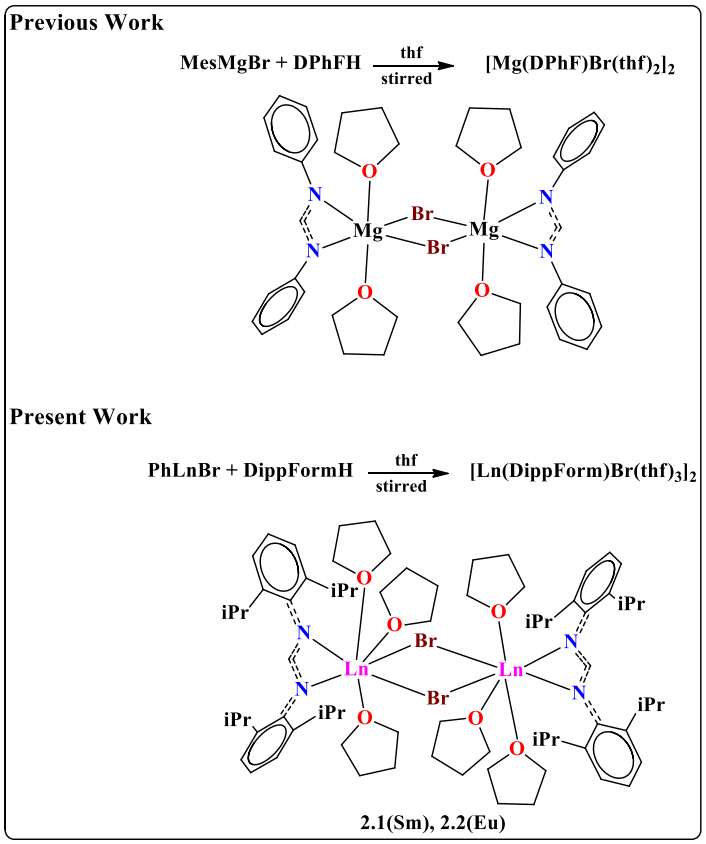
Table 2.10: Selected bond lengths and angles of compounds (**2.5** (n = 13) and **2.6** (n = 8)).

Bond Lengths(Å)	2.5	2.6	Bond Angles(°)	2.5	2.6
Sm-N(1)	2.439(5)	2.334(11)	C(n)-Sm-I(1)	95.99(12)	93.167

Sm-N(2)	2.431(5)	2.359(12)	C(n)-Sm-I(2)	95.50(2)	99.048
Sm -I(1)	3.0876(6)	3.0528(13)	C(n)-Sm-O(1)	105.72(19)	97.389
Sm-I(2)	2.991(11)	3.0979(13)	C(n)-Sm-O(2)	178.89(19)	175.816
Sm-O(1)	2.447(5)	2.399(9)	C(n)-Sm-O(3)	106.36(18)	96.667
Sm-O(2)	2.523(6)	2.464(10)	O(1)-Sm-O(2)	74.00(2)	84.00(3)
Sm-O(3)	2.446(5)	2.402(9)	O(1)-Sm-O(3)	147.90(19)	165.50(3)
			O(2)-Sm-O(3)	73.95(18)	82.20(3)

2.3.3 Discussion

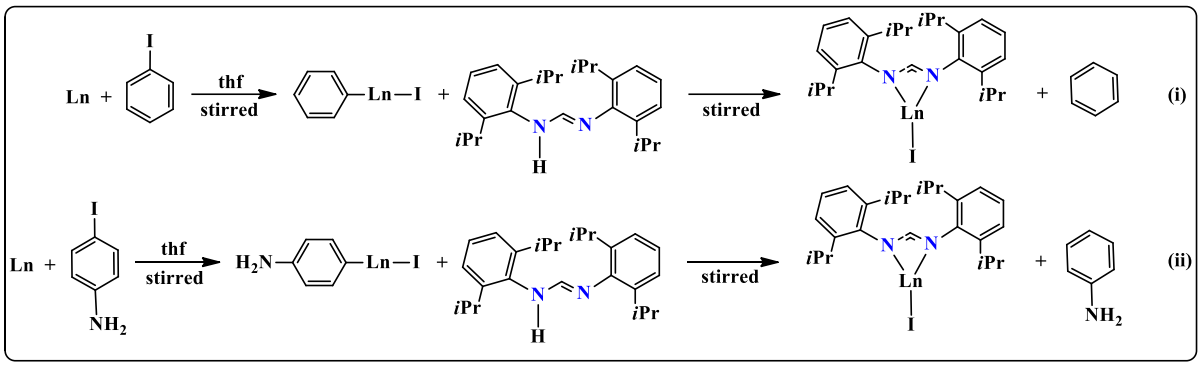
Ln(II) compounds [Ln(DippForm)Br(thf)$_3$]$_2$·6thf (Sm **2.1**, Eu **2.2**) were isolated from the reaction between Ln metals with PhBr and DippFormH. These isostructural compounds exhibits similar crystal structure to the Mg based Grignard compound [Mg(DPhForm)Br(thf)$_2$]$_2$].[58] The bulky DippFormH ligands facilitate to isolation of divalent Sm and Eu in the presence with the PhBr oxidant. A similar compound ([Mg(MesC(N*i*Pr)$_2$)(μ-Br)(Et$_2$O)]$_2$) was synthesised from magnesium (Mg) based Grignard reagents (MesMgBr).[59]



Scheme 2.13: comparable previous research work (Mg based Grignard's) with present work (Ln pseudo-Grignard's).[60]

From the reaction of samarium metal, PhI and DippFormH/Ph_2pzH, we successfully isolated Sm(III) compounds: [Sm(DippForm)I_2(thf)$_3$] (**2.5**) and [Sm(Ph_2pz)I_2(thf)$_3$] (**2.6**). The magnetic susceptibility of samarium Grignard reagent is more likely Sm^{3+}.[3] For compound **2.6**, the change in the reaction colour and the formation of green solution and UV-vis spectra suggested the presence of Sm(II). However, upon removal of the crystals for structural identification, the green colour rapidly transitioned to yellow, indicating (Sm(III)). UV-vis spectroscopy of the reaction solution supported the hypothesis regarding the divalent samarium, suggesting that the compound was [Sm(Ph_2pz)I(thf)$_3$].

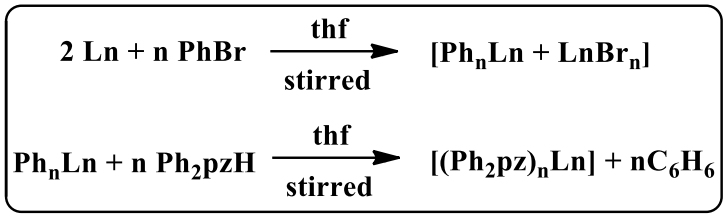
Several divalent pseudo-Grignard compounds ([Eu(DippForm)I(thf)$_4$]·thf (**2.7**), [Yb(DippForm)I(thf)$_3$]·thf (**2.8**), and [Yb(Ph_2pz)I(thf)$_4$] (**2.9**)) were also isolated during reactions with (NH_2)PhI in place of PhI.[22, 23] In this investigation, we aimed to discerm any differences between the H and NH_2 groups attached in the para position (**H**-C_6H_4I and **H_2N**-C_6H_4I) but found no significant distinctions. The colour changes observed for compounds **2.7**-**2.9**, along with additional characterisations (^{1}H-NMR, IR), provided insights into the possible reaction mechanisms, as depicted in **Scheme 2.14**.



Scheme 2.14: Possible reaction mechanism of compounds [Eu(DippForm)I(thf)$_4$]·thf (**2.7**) and [Yb(DippForm)I(thf)$_3$]·thf (**2.8**).

In the reactions involving Ln (Sm, Eu) with PhBr and Ph_2pzH we obtained only schlenk equilibria products: [Sm(Ph_2pz)$_3$(thf)$_3$]·3thf (**2.3a**), [Sm(Ph_2pz)$_3$(dme)$_2$]·dme (**2.3b**), and [Eu(Ph_2pz)$_2$(thf)$_4$] (**2.4**). These compounds are readily accessible due to the diverse Schlenk equilibria products present in solutions of pseudo-Grignard reagents.[17] The lighter molecular weight of the Ph_2pzH ligand compared with DippFormH ligand consistently leads to the formation of [Ln(Ph_2pz)$_n$] compounds. Microanalysis and/or metal analysis confirmed the

accuracy of the crystal structures. Thus, the reaction pathway for these processes can be summarised in **eqn. 2.20**.



Equation 2.20: Possible reaction pathway for the Schlenk equilibria products (Sm: n = 3, Eu; n = 2).

2.4 Conclusion and Future Outlook

The results obtained from the first part of this chapter highlight the rich chemistry of PhLnBr Grignard reagents, which significantly alter the outcomes compared to previous reactions involving PhLnI.[23] Notably, the success observed with samarium is particularly significant. The reaction of Ln^0 metals with PhBr, followed by addition of DippFormH, facilitates the synthesis of the divalent dimeric pseudo-Grignard complexes, $[Ln(DippForm)Br(thf)_3]_2{\cdot}6thf$ (Ln = Sm, Eu) in moderate crystalline yields. These two compounds feature a Ln_2Br_2 bridged dimer core, with $Ln\cdots C_{(backbone)}$ distances of 3.03 Å for **2.1** and 3.02 Å for **2.2** respectively. Using the pro-ligand Ph_2pzH, we obtained nine coordinate trivalent $[Sm(Ph_2pz)_3(thf)_3].3thf$, and $[Sm(Ph_2pz)_3(dme)_2]{\cdot}dme$ complexes, as well as divalent compound $[Eu(Ph_2pz)_2(thf)_4]$ owing to protonation of Schlenk equilibrium products following oxidation in the case of Sm. However, the reaction of Yb with PhBr and Ph_2pzH did not yielded any crystals. These outcomes differ completely from analogous reactions of PhLnI.[22, 23]

In the second phase, we investigate the earlier reaction pathway of PhLnI with widely used Sm metal (new in Grignard chemistry), where $Ln^{(III)}$ is more prevalent. The findings from the reaction yielded trivalent Grignard products ($[Sm(L)I_2(thf)_3]$) (L = DippForm, Ph_2pz). For further study we also isolated some reported structures; $[Eu(DippForm)I(thf)_4]{\cdot}thf$, $[Yb(DippForm)I(thf)_3]{\cdot}thf$ and $[Yb(Ph_2pz)I(thf)_4]$, derived from the reaction of $H_2NPhLnI(thf)_n$ (Ln = Eu, Yb) with pro-ligands (DippFormH and Ph_2pzH). One notable advantage of using H_2NPhI as oxidant, compared to PhI, is the ability to conduct reactions at comparatively higher temperature (room temperature), making the process easier to manage.

Further exploration of PhLnBr reactions could involve other formamidines, such as EtFormH, XylFormH, and MesFormH. The product obtained from the reaction of PhSmI with Ph_2pzH or DippFormH was $Sm^{(III)}$, but the UV-vis spectroscopy of the reaction solution say that UV-vis analysis suggests that a $Sm^{(II)}$ species is also present. Thus, the less dominant $Sm^{(II)}$ species presents a promising area for further investigation.

2.5 Experimental

2.5.1 General Aspects

For general aspects, see Appendix 1.

2.5.2 Synthesis of Ln (II) pseudo-Grignard compounds

This chapter we will focuses on the divalent lanthanoid pseudo-Grignard reagents using phenyl bromide (PhBr), phenyl iodine (PhI) and 4-Iodoaniline ($IC_6H_4NH_2$) as oxidant, here we also used *N,N′*-bis(aryl) formamidines (ArNCHNAr; Ar = 2,6-*i*$Pr_2C_6H_3$, and 2,6-$Et_2C_6H_3$) and pyrazole (Ph_2pzH) as the trapping pro-ligands.

2.5.2.1 The reaction of the lanthanoid (Sm and Eu) pseudo-Grignard reagents (PhLnBr) with DippFormH

Excess amounts of lanthanoid metals powder (1.50 mmol) were suspended in dry THF (15 ml) under N_2, and then the phenyl bromide (0.157 g, 1.0 mmol) were added at desired temperature. The mixture was sonicated for 10 min and stirred at room temperature, after the formation of the pseudo-Grignard reagents, solid pro-ligand (DippFormH) (1.0 mmol) were added at fixed temperature and stirred for another 24 hr. Crystals were obtained after the filtrates were evaporated to the 5 ml volume under a vacuum and kept in the fridge at around -25 °C. Yields were calculated based on the pro-ligand.

$[Sm(DippForm)Br(thf)_3]_2 \cdot 6thf$ (2.1)

Samarium metal powder (0.225 g, 1.5 mmol) was suspended in dry THF (15 ml) under N_2, and then PhBr (0.157 g, 1.0 mmol) was added at 0 °C. The mixture was sonicated for 10 min and stirred for 24 h at room temperature, when a light brown solution formed. Solid DippFormH (0.368 g, 1.0 mmol) was added and the mixture was stirred at 0 °C for 1 h, and the green

solution developed after stirring for 24 h at room temperature. The resulting mixture was filtered and concentrated to 5 ml under vacuum. Green crystals (0.656 g, 64%) were obtained after cooling at -25 °C for 3 days. M.P. 203-205 °C. Elemental analysis: Found: C 55.83, H 7.83, N 2.90; $C_{98}H_{166}Br_2N_4O_{12}Sm_2$ (2052.86 g.mol^{-1}) requires: C 57.34, H 8.15, N 2.73; loss of 3 thf of crystallisation, $C_{86}H_{142}Br_2N_4O_9Sm_2$ (1836.59 g. mol^{-1}) requires: C 56.24, H 7.79, N 3.05. IR (Nujol): 1671s, 15991m, 1529m, 1340w, 1274m, 1198w, 1103w, 1074s, 1014s, 948m, 915m, 857m, 800m, 774w, 755m, 722m, 666w cm^{-1}. ^{1}H NMR (C_6D_6): -10.70(2H, NC(H)N), 1.20(8H, CH), 1.78(48H, CH_3), 3.23(br 36H, thf), 4.55(8H, H(3,5)), 4.99(36H, thf), and 6.15 ppm(4H, H(4)) corresponding to loss of 3 thf of crystallisation. UV: broad peak at λ_{max} = 588nm.

[Eu(DippForm)Br(thf)$_3$]$_2$·6thf (2.2)

Europium metal powder (0.23 g, 1.5 mmol) was suspended in dry THF (15 ml) under N_2, and then PhBr (0.157 g, 1.0 mmol) was added at -78 °C. The mixture was sonicated for 10 min when a brown solution formed. After cooling to -78 °C, solid DippFormH (0.368 g, 1.0 mmol) was added and the mixture was stirred at -78 °C for another 3 h. A brownish-yellow solution developed after further stirring for 24 h at room temperature. The resulting mixture was filtered and concentrated to 5 ml under vacuum. Yellow crystals (0.495 g, 48%) were obtained after cooling at -25 °C for 3 days. M.P. 186-188 °C. Elemental analysis: Found: C 53.54, H 7.08, N 3.65, Eu 20.42: $C_{98}H_{166}Br_2Eu_2N_4O_{12}$ (2056.08 g mol^{-1}) requires: C 57.25, H 8.14, N, 2.72, Eu 14.78: loss of 6 thf of crystallisation and 2 coordinated. $C_{66}H_{102}Br_2Eu_2N_4O_4$ (1479.27 g mol^{-1}) requires: C 53.59, H 6.95, N 3.79, Eu 20.55. IR (Nujol): 1668s, 1589w, 1345w, 1312w, 1261m, 1170m, 1075m, 1010s, 923m, 852w, 771w, 723s, 665w cm^{-1}.

2.5.2.2 The reaction of lanthanoid (Sm and Eu) pseudo-Grignard reagents (PhLnBr) with Ph_2pzH

Excess amounts of lanthanoid metal powder (1.50 mmol) were suspended in dry THF (15 ml) under N_2, and then the phenyl bromide (0.157 g, 1.0 mmol) were added at desired temperature. The mixture was sonicated for 10 min and stirred at room temperature, after the formation of pseudo-Grignard reagents, solid pro-ligand (Ph_2pzH) (1.0 mmol) were added at a specific temperature and stirred for another 24 hr. Crystals were obtained after the filtrates were

evaporated to the 5 ml volume under a vacuum and kept in the fridge at around -25 °C. Yields were calculated based on the pro-ligand.

[Sm(Ph$_2$pz)$_3$(thf)$_3$]·3thf (2.3a)

The synthesis procedure for compound **2.3(a)** was similar as described in **2.1**. Here, solid Ph$_2$pzH (0.22 g, 1.0 mmol) was added and got yellowish brown solution. The resulting mixture was filtered and concentrated to 5 ml under vacuum. Colourless crystals (0.248 g, 60%) were obtained after cooling at -25 °C for 4 days. M. P. 157-159 °C. Metal Analysis: Found: 14.48%; $C_{69}H_{81}N_6O_6Sm$ (1240.75 g.mol^{-1}) requires: Sm,12.12%; loss of three THF of crystallisation, $C_{57}H_{57}N_6O_3Sm$ (1024.46 g.mol^{-1}) requires: Sm,14.68%. IR (Nujol): = 1605s, 1512w, 1340w, 1297m, 1261w, 1229m, 1178m, 1156w, 1073s, 1028s, 971s, 915s, 868s, 842w, 801m, 762s, 724w, 697s, 684m, 665w cm^{-1}. ^{1}H NMR (400.13 MHz, C_6D_6): δ = 0.60 (24H, thf), 2.17(24H, thf), 7.28 (6H, H(4)), 7.58 (12H, H(3,5)), 7.77 (3H, CH-pz), and 9.39 ppm(12H, H(2,6)). For compound **2.3(a)** (triclinic, *P*-1space group) the unit cell is; a = 13.307(3) Å, b = 18.547(4) Å, c = 25.198(5) Å, α = 76.38(3)°, β = 84.83(3)°, γ = 87.37(3)°, V = 6018(2) Å^3, the reported unit cell is; a = 13.343(3) Å, b = 18.579(4) Å, c = 25.270(5) Å, α = 76.58(3)°, β = 85.19(3)°, γ = 87.35(3)°, V = 6070(2) Å^3.[49]

[Sm(Ph$_2$pz)$_3$(dme)$_2$]·dme (2.3b)

Colourless crystals (0.19 g, 53%) from a solution of **2.3(a)** in DME after cooling at -25 °C for 3 days. M. P. 161-163 °C. Elemental analysis: Found: C 63.59, H 5.93, N 7.46, Sm 14.07%; $C_{57}H_{63}SmN_6O_6$ (1078.48 g.mol^{-1}) requires: C 63.48, H 5.89, N 7.79, Sm 13.94%. IR (Nujol): 2722m, 1604s, 1513m, 1422w, 1338w, 1306m, 1283m, 1246m, 1224w, 1193s, 1114m, 1027w, 970s, 913s, 864s, 802m, 757s, 695s, 682w cm^{-1}. ^{1}H NMR (400.13 MHz, C_6D_6): δ = 2.82 (32H, dme), 2.95 (48H, dme), 7.21 (6H, H(4)), 7.40 (12H, H(3,5)), 7.47 (3H, CH-pz), 8.75 ppm(12H, H(2,6)).

[Eu(Ph$_2$pz)$_2$(thf)$_4$] (2.4)

The synthesis procedure for compound **2.4** was similar as described for **2.2**. Here, solid Ph$_2$pzH (0.22 g, 1.0 mmol) was added and a red brown solution formed. The resulting mixture was

filtered and concentrated to 5 ml under vacuum. Yellow crystals (0.273 g, 62%) were obtained after cooling at -25 °C for 5 days. M.P. 224–226 °C. Metal Analysis: Found: Eu 17.64%; $C_{46}H_{54}EuN_4O_4$ (878.89 g.mol^{-1}) requires: Eu 17.29%. IR (Nujol): = 1602s, 1524m,1512w, 1421w, 1295w, 1259w, 1218m, 1178w, 1042s, 999w, 968s, 903s, 791w, 767s, 753s, 702s, 681s, 665w cm^{-1}. For compound **2.4** (triclinic, *P*-1space group) the unit cell is; a= 9.126(18) Å, b= 18.668(4) Å, c= 24.427(5) Å, α= 110.04(3)°, β= 91.64(3)°, γ = 90.22(3)°, V= 3907.5(16) Å^3, the reported unit cell is; a= 9.27(19) Å, b= 18.952(4) Å, c= 24.803(5) Å, 09.99(3)°, β= 91.78(3)°, γ = 90.52(3)°, V= 4092.1(16) Å^3. [61]

2.5.2.3 The reaction of samarium (Sm) pseudo-Grignard reagents (PhSmI) with DippFormH and Ph_2pzH

Excess amounts of samarium metal powder (1.50 mmol) were suspended in dry THF (15 ml) under N_2, and then the phenyl iodine (0.204 g, 1.0 mmol) were added at 0 °C temperature. The mixture was sonicated for 10 min and stirred at room temperature for 24 h, after the formation of Grignard reagent, solid pro-ligands (DippFormH or Ph_2pzH) (1.0 mmol) was added at fixed temperature and stirred for another 24 h. Crystals were obtained after the filtrates were evaporated to the 5 ml volume under a vacuum and kept in the fridge at around -25 °C. Yields were calculated based on the pro-ligands.

[Sm(DippForm)I_2(thf)$_3$]. thf (2.5)

The synthesis procedure for **2.5** was similar as described for **2.1**. Here, PhI was used as oxidant instead of PhBr. Yellow crystals (0.623 g, 59%) were obtained after cooling at -25 °C for 3 days. M. P. 207-209 °C. Elemental analysis: Found: C 41.98, H 5.42, N 3.04, Sm 18.22%; $C_{41}H_{67}I_2N_2SmO_4$ (1056.15 g/mol): requires C 46.63, H 6.39, N 2.63, Sm, 14.24 %. Loss of 3 thf from crystallisation and solvation, $C_{29}H_{43}I_2N_2SmO$ (839.83 g/mol) requires: C 41.47, H 5.16, N 3.34, Sm 17.90%. IR (Nujol ν/cm^{-1}): 1667s, 1586m, 1522s, 1333w, 1296w, 1259w, 1235m, 1188s, 1159w, 1106s, 1074w, 1055w, 1015m, 957m, 934s, 912w, 884m, 824s, 804w, 757s, 728w, 712w, 674s, 608s. ^{1}H NMR (400.13 MHz, C_6D_6): δ = 10.57 (1H, NCHN), 7.06 (4H, H(3,5)), 7.01 (2H, H(4)), 3.63 (4H, thf), 3.43 (4H, CH), 1.41 (4H, thf), and 1.14 ppm(24H, CH_3).

[Sm(Ph$_2$pz)I$_2$(thf)$_3$] (2.6)

The synthesis procedure for compound **2.6** was similar as described for **2.5**. Here, solid Ph$_2$pzH (0.22 g, 1.0 mmol) was added and got a dark green solution. The resulting mixture was filtered and concentrated to 5 ml under vacuum. Yellow crystals (0.596 g, 71%) were obtained after cooling at -25 °C for 7 days. M. P. 122-124 °C. Metal analysis: Found: Sm 15.48%; $C_{27}H_{35}SmI_2N_2O_3$ (839.75, requires: Sm 17.91%; extra 2 thf molecules of crystallisation, $C_{35}H_{51}SmI_2N_2O_5$ (983.96 g.mol^{-1}) requires: Sm 15.28%. IR (Nujol): 1605s, 1512m, 1340w, 1293 w, 1263m, 1220w, 1174m, 1156w, 1069s, 1026m, 971s, 915s, 870s, 803 w, 759s, 696s cm^{-1}. ^{1}H NMR (400.13 MHz, C_6D_6): δ = 1.20 (20H, thf), 3.21(20H, thf), 7.30 (2H, H(4)), 7.59 (4H, H(3,5)), 7.80 (1H, CH-pz), 9.38 ppm(4H, H(2,6)).

2.5.2.4 Synthesis of lanthanoid (Eu and Yb) pseudo-Grignard compounds (reported) from the reaction of lanthanoid (Eu and Yb) metals with $C_6H_4NH_2I$ and DippFormH or Ph$_2$pzH

Excess amounts of lanthanoid (Eu and Yb) metal powder (1.50 mmol) were suspended in dry THF (15 ml) under N_2, and then the 4-iodoaniline (0.219 g, 1.0 mmol) were added at desired temperature. The mixture was sonicated for 10 min and stirred at room temperature, after the formation of Grignard reagent, solid pro-ligands (DippFormH or Ph$_2$pzH) (1.0 mmol) were added at fixed temperature and stirred for another 24 hr. Crystals were obtained after the filtrates were evaporated to the 5 ml volume under and kept in the fridge at around -25 °C. Yields were calculated based on the pro-ligands.

[Eu(DippForm)I(thf)$_4$]·thf (2.7)

Europium metal powder (0.23 g, 1.5 mmol) was suspended in dry THF (15 ml) under N_2, and then the 4-Iodoaniline (0.22 g, 1.0 mmol) was added at 0 °C. The mixture was sonicated for 10 min and stirred for 2 h at room temperature and a yellow solution formed. After cooling to -78 °C, solid DippFormH (0.368 g, 1.0 mmol) was added, and the mixture was stirred for another 3 h. A red-yellow solution developed after stirring for 24 h at room temperature. The resulting mixture was filtered and concentrated to 5 ml under vacuum. Yellow crystals (0.622 g, 62 %) were obtained after cooling at -25 °C for 3 days. M. P. 247–249 °C. Metal Analysis: Found: Eu 15.21%; $C_{45}H_{75}N_2O_5IEu$ (1002.96 g.mol^{-1}) requires: Eu 15.15%. IR (Nujol): 1666s,

1601m, 1589m, 1530s,1500m, 1320m, 1289m, 1259m, 1235w, 1182s, 1160w, 1099s, 1075m, 1034w, 913s, 882w, 821w, 801m, 767m, 755m, 722w, 692w, 665m cm^{-1}. For compound **2.7** (monoclinic, $P2_1/c$ space group) the unit cell is; a= 16.447(3) Å, b= 16.854(3) Å, c= 16.962(3) Å, β= 91.86(3)°, V= 4699.4(16) $Å^3$, the reported unit cell is; a= 16.326(3) Å, b= 16.752(3) Å, c= 17.069(3) Å, β= 91.62(3)° V= 4666.389 $Å^3$.[23]

[Yb(DippForm)I(thf)$_3$]·thf (2.8)

The synthesis procedure for compound **2.8** was similar as described **2.7**. The resulting red solution was filtered and concentrated to 5 ml under vacuum. Red crystals (0.846 g, 89%) were obtained after cooling at -25 °C for 3 days. M. P. 158-160 °C. Metal Analysis: Found: Yb 18.32%; $C_{41}H_{67}N_2O_4IYb$ (951.93 $g.mol^{-1}$) requires: Yb 18.18%. IR (Nujol): 1667s, 1605m, 1595m, 1317m, 1260m, 1236w, 1180s, 1162m, 1095s, 1075m, 1034w, 912s, 884w, 822w, 800m, 770m, 757m, 726w, 690w, 668m cm^{-1}. ^{1}H NMR (400.13 MHz, C_6D_6): δ = 1.17 (24 H, CH_3), 1.44 (16 H, thf), 3.41 (4 H, CH), 3.56 (16 H, thf), 7.09 (4H, H(3,5)), 7.14 (2 H, H(4)), and 8.21 ppm(1H, NCHN). For compound **2.8** (monoclinic, $P2_1/n$ space group) the unit cell is; a= 14.04298(16) Å, b= 19.2629(8) Å, c= 15.9698(7) Å, β= 91.328(2)° V= 4407.56(8) $Å^3$, the reported unit cell is; a= 13.9097(6) Å, b= 19.3883(2) Å, c= 16.192(18) Å, β= 91.235(10)°, V= 4277.8(3) $Å^3$.[23]

[Yb(Ph$_2$pz)I(thf)$_4$] (2.9)

The synthesis procedure for compound **2.9** was similar as described **2.7**. Here, solid Ph_2pzH (0.22g, 1.0 mmol) was added, the resulting red orange solution was filtered and concentrated to 5 ml under vacuum. Red crystals (0.76 g, 94%) were obtained after cooling at -25 °C for 3 days. M. P. 266-268 °C (decomposed). Metal analysis: Found: Yb, 21.56%; $C_{31}H_{43}N_2O_4IYb$ (807.63), requires: Yb 21.43%), IR (Nujol): 1621m, 1601s, 1378s, 1341m, 1292w, 1261m, 1173m, 1155w, 1072w, 968m, 960m, 919w, 872w, 812w, 775w, 689s, 667w cm^{-1}. ^{1}H NMR (400.13 MHz, C6D6): δ = 1.32 (16H, thf), 3.60 (16H, thf), 7.10 (2H, H(4)), 7.11(1H, CH-pz), 7.24 (4H, H(3,5)), and 8.08 ppm(4H, H(2,6)). For compound **2.9** (orthorhombic, *P*mn2 space group) the unit cell is; a= 17.7729(3) Å, b= 8.81177(19) Å, c= 10.2434(2) Å, V= 1605.22(4) $Å^3$, the reported unit cell is; a= 17.6761(8) Å, b= 8.7327(4) Å, c= 10.1877(5) Å, V= 1572.57(13) $Å^3$.[22]

[Yb(EtForm)$_2$(thf)$_2$] (2.10)

Ytterbium metal powder (0.26 g, 1.5 mmol) was suspended in dry THF (15 ml) under N_2, and then the phenyl iodide (0.204 g, 1.0 mmol) was added at -78 °C. The mixture was sonicated for 10 min and a red-orange solution formed. After cooling to -78 °C, solid EtFormH (0.308g, 1.0 mmol) was added and the mixture was stirred for another 3 h. A red solution developed after further stirring for 24 h at room temperature. The resulting mixture was filtered and concentrated to 5 ml under vacuum. Red crystals (0.689g; 74%) were obtained after cooling at -25 °C for 5 days. M.P. 166-168 °C. Metal Analysis: Found: Yb 18.62%, $C_{50}H_{70}N_4O_2Yb$ (932.17 g.mol^{-1}) requires: Yb 18.56%. IR (Nujol): 1667s, 1588m, 1538s, 1289w, 1259w,1235w, 1188m, 1146m, 1073s, 1036w, 959w, 916s, 864w, 827w, 808m, 756m,722w, 639w cm^{-1}. ^{1}H NMR (400.13 MHz, C_6D_6): δ =1.21 (24H, CH_3), 1.31 (12H, thf), 2.81 (16H, CH_2), 3.60 (12H, thf), 7.08 (4H, H(4)), 7.18-7.19 (8H, H(3,5)), and 8.17 ppm(2H; NCHN). For compound **2.10** (triclinic, *P*-1space group) the unit cell is; a= 11.1913(5) Å, b= 11.8455(6) Å, c= 19.6729(6) Å, α= 89.960(3)°, β= 88.836(3)°, γ= 62.248(3)°, V= 2307.412(4) Å^3, the reported unit cell is; a= 11.177(2) Å, b= 11.837(2) Å, c= 19.657(9) Å, α= 89.89(3)°, β= 88.73(3)°, γ= 62.41(3), V= 2304.2(8) Å^3.[33]

2.6 X-ray crystal data

Single crystals coated with viscous hydrocarbon oil were mounted on glass fibres or loops. All complexes (**2.1**-**2.10**) were measured at -173 °C (100 K) at the Australian Synchrotron on the MX1 beamline, data integration was completed using Blue-ice [62] and XDS [63] software programs. Structural solutions were obtained by either direct methods [64] or charge flipping [65] methods and refined using full-matrix least-squares methods against F2 using SHELX2018, [66] in conjunction with the X-Seed [67] or Olex2 [65] graphical user interface. All hydrogen atoms were placed in calculated positions using the riding model. Multiscan were applied for absorption corrections. All CIF files were checked at https://checkcif.iucr.org.

[Sm(DippForm)Br(thf)$_3$]$_2$·6thf (2.1)

$C_{98}H_{166}Br_2N_4O_{12}Sm_2$ (*M* =2052.86 g/mol): monoclinic, space group $P2_1/c$ (no. 14), a = 25.498(5) Å, b = 19.543(4) Å, c = 20.321(4) Å, β = 97.27(3)°, V = 10045(4) Å^3, Z = 4, T = 100(2) K, μ(Synchrotron) = 2.011 mm^{-1}, *Dcalc* = 1.357 g/cm^3, 115242 reflections measured

(1.61° ≤ 2Θ ≤ 50.13°), 17610 unique (R_{int} = 0.0676, R_{sigma} = 0.0354) which were used in all calculations. The final R_1 was 0.0489 (I > 2σ(I)) and wR_2 was 0.1433 (all data).

[Eu(DippForm)Br(thf)$_3$]$_2$·6thf (2.2)

$C_{98}H_{166}Br_2Eu_2N_4O_{12}$ (M =2056.08 g/mol): monoclinic, space group $P2_1/c$ (no. 14), a = 25.420(5) Å, b = 19.530(4) Å, c = 20.300(4) Å, β = 96.91(3)°, V = 10005(4) Å^3, Z = 4, T = 100(2) K, μ(Synchrotron) = 2.099 mm^{-1}, $Dcalc$ = 1.365 g/cm^3, 174528 reflections measured (1.614° ≤ 2Θ ≤ 51.362°), 18883 unique (R_{int} = 0.0432, R_{sigma} = 0.0227) which were used in all calculations. The final R_1 was 0.0376 (I > 2σ(I)) and wR_2 was 0.1086 (all data).

[Sm(Ph$_2$pz)$_3$(dme)$_2$]·dme (2.3b)

$C_{57}H_{63}N_6O_6Sm$ (M =1078.48 g/mol): monoclinic, space group $P2_1/c$ (no. 14), a = 12.393(3) Å, b = 16.007(3) Å, c = 26.785(5) Å, β = 98.26(3)°, V = 5258.4(19) Å^3, Z = 4, T = 100(2) K, μ(Synchrotron) = 1.172 mm^{-1}, $Dcalc$ = 1.362 g/cm^3, 60044 reflections measured (2.972° ≤ 2Θ ≤ 50.054°), 9181 unique (R_{int} = 0.0213, R_{sigma} = 0.0125) which were used in all calculations. The final R_1 was 0.0417 (I > 2σ(I)) and wR_2 was 0.1183 (all data).

[Sm(DippForm)I$_2$(thf)$_3$]·thf (2.5)

$C_{78}H_{126}I_4N_4O_7Sm_2$ (M =2040.12 g/mol): orthorhombic, space group $Pbca$ (no. 61), a = 19.6059(4) Å, b = 18.8573(4) Å, c = 24.1239(4) Å, V = 8919.0(3) Å^3, Z = 4, T = 123(2) K, μ(MoKα) = 2.736 mm^{-1}, $Dcalc$ = 1.519 g/cm^3, 100757 reflections measured (4.978° ≤ 2Θ ≤ 52.742°), 9114 unique (R_{int} = 0.0971, R_{sigma} = 0.0411) which were used in all calculations. The final R_1 was 0.0565 (I > 2σ(I)) and wR_2 was 0.1498 (all data).

[Sm(Ph$_2$pz)I$_2$(thf)$_3$] (2.6)

$C_{27}H_{35}I_2N_2O_3Sm$ (M =839.72 g/mol): monoclinic, space group $C2/c$ (no. 15), a = 15.460(3) Å, b = 11.989(2) Å, c = 31.630(6) Å, β = 97.62(3)°, V = 5811(2) Å^3, Z = 8, T = 100(2) K, μ(Synchrotron) = 4.176 mm^{-1}, $Dcalc$ = 1.920 g/cm^3, 5001 reflections measured (2.598° ≤ 2Θ ≤ 50.122°), 5001 unique (R_{int} = ?, R_{sigma} = 0.0561) which were used in all calculations. The final R_1 was 0.0851 (I > 2σ(I)) and wR_2 was 0.2422 (all data).

2.7 References

[1]. F. Bickelhaupt, J. Organomet. Chem., **1994**, 475, 1-14.

[2]. F. A. Carey and R. J. Sundberg. Advanced Organic Chemistry, Reactions and Synthesis, Part B. 4th ed. Plenum Publishers: New York, **2001**.

[3]. D. F. Evans, G. V. Fazakerley and R. F. Phillips, J. Chem. Soc. A, **1971**, 1931-1934.

[4]. O. P. Syutkina, L. F. Rybakova, E. S. Petrov and I. P. Beletskaya, J. Organomet. Chem., **1985**, 280, C67-C69.

[5]. E. S. Petrov, D. M. Roitershtein and L. F. Rybakova, J. Organomet. Chem., **2002**, 647, 21-27.

[6]. Z. Hou, Y. Fujiwara, T. Jintoku, N. Mine, K. Yokoo and H. Taniguchi, J. Org. Chem., **1987**, 52, 3524-3528.

[7]. T. Fukagawa, Y. Fujiwara, K. Yokoo and H. Taniguchi, Chem. Lett., **1981**, 1771-1774.

[8]. F. T. Edelmann, D. M. Freckmann and H. Schumann, Chem. Rev., **2002**, 102, 1851-1896.

[9]. M. Deng, Y. Yao, Q. Shen, Y. Zhang, J. Lang and Y. Zhou, J. Organomet. Chem., **2003**, 681, 174-179.

[10]. W. J. Evans, J. Organomet. Chem., **2002**, 647, 2-11.

[11]. Z. Hou and Y. Wakatsuki, J. Organomet. Chem., **2002**, 647, 61-70.

[12]. W. J. Evans, G. Zucchi and J. W. Ziller, J. Am. Chem. Soc., **2003**, 125, 10-11.

[13]. P. N. Hazin, C. Lakshminarayan, L. S. Brinen, J. L. Knee, J. W. Bruno, W. E. Streib and K. Folting, Inorg. Chem., **1988**, 27, 1393-1400.

[14]. W. J. Evans, N. T. Allen and J. W. Ziller, Angew. Chem. Int. Ed., **2002**, 41, 359-361.

[15]. H. J. Heeres, J. Renkema, M. Booij, A. Meetsma and J. H. Teuben, Organometallics, **1988**, 7, 2495-2502.

[16]. P. L. Watson, Chem. Commun., **1980**, 652-653.

[17]. G. Heckmann and M. Niemeyer, J. Am. Chem. Soc., **2000**, 122, 4227-4228.

[18]. M. N. Bochkarev, L. N. Zakharov and G. S. Kalinina, Organoderivatives of Rare Earth Elements. Kluwer Academic: Dordrecht, **1995**.

[19]. S. A. Cotton, Coord. Chem. Rev., **1997**, 160, 93-127.

[20]. C. Eaborn, P. B. Hitchcock, K. Izod and J. D. Smith, J. Am. Chem. Soc., **1994**, 116, 12071-12072.

[21]. C. Eaborn, P. B. Hitchcock, K. Izod, Z. Lu and J. D. Smith, Organometallics, **1996**, 15, 4783-4790.

[22]. M. Wiecko, G. B. Deacon and P. C. Junk, Chem. Commun., **2010**, 46, 5076-5078.

[23]. S. H. Ali, G. B. Deacon, P. C. Junk, S. Hamidi, M. Wiecko and J. Wang, Chem. Eur. J., **2018**, 24, 230-242.

[24]. S. Xiao, C. Liu, B. Song, L. Wang, Y. Qi and Y. Liu, Chem. Commun., **2021**, 57, 6169-6172.

[25]. C. N. de Bruin-Dickason, G. B. Deacon, C. Jones, P. C. Junk and M. Wiecko, Eur. J. Inorg. Chem., **2019**, 1030-1038.

[26]. R. Green, A. C. Walker, M. P. Blake and P. Mountford, Polyhedron, **2016**, 116, 64-75.

[27]. M. Kȍhler, J. Langer, H. Gȍrls and M. Westerhausen, Organometallics, **2012**, 31, 8647-8653.

[28]. S. Yadav, V. S. V. S. N. Swamy and R. Gonnade, S. S. Sen, ChemistrySelect, **2016**, 5, 1066-1071.

[29]. C. Glock, C. Loh, H. Görls, S. Krieck and M. Westerhausen, Eur. J. Inorg. Chem., **2013**, 3261-3269.

[30]. M. L. Cole, G. B. Deacon, C. M. Forsyth, P. C. Junk, K. Konstas and J. Wang, Chem. Eur. J., **2007**, 13, 8092-8110.

[31]. G. B. Deacon, F. Jaroschik, P. C. Junk and R. P. Kelly, Organometallics, **2015**, 34, 2369-2377.

[32]. R. P. Kelly, T. D. M. Bell, R. P. Cox, D. P. Daniels, G. B. Deacon, F. Jaroschik, P. C. Junk, X. F. L. Goff, G. Lemercier, A. Martinez, J. Wang and D. Werner, Organometallics, **2015**, 34, 5624-5636.

[33]. M. L. Cole, G. B. Deacon, C. M. Forsyth, P. C. Junk, K. Konstas, J. Wang, H. Bittig and D. Werner, Chem. Eur. J., **2013**, 19, 1410-1420.

[34]. I. L. Fedushkin, O. V. Maslova, M. Hummert and H. Schumann, Inorg. Chem., **2010**, 49, 2901-2910.

[35]. I. L. Fedushkin, A. A. Skatova, D. S. Yambulatov, A. V. Cherkasov and S. V. Demeshkob, Russ. Chem. Bull., Int. Ed., **2015**, 64, 38-43.

[36]. I. L. Fedushkin, O. V. Maslova, E. V. Baranov and A. S. Shavyrin, Inorg. Chem., **2009**, 48, 2355-2357.

[37]. Z. Hou, A. Fujita, T. Yoshimura, A. Jesorka, Y. Zhang, H. Yamazaki and Y. Wakatsuki, Inorg. Chem., **1996**, 35, 7190-7195.

[38]. A. M. Bienfait, B. M. Wolf, K. W. Tӧrnroos and R. Anwander, Inorg. Chem., **2018**, 57, 5204-5212.

[39]. M. L. Cole, G. B. Deacon, P. C. Junk, and J. Wang, Organometallics, **2013**, 32, 1370-1378.

[40]. G. B. Deacon, P. C. Junk and D. Werner, Chem. Eur. J., **2016**, 22, 160-173.

[41]. D. Werner, X. Zhao, S. P. Best, L. Maron, P. C. Junk and G. B. Deacon, Chem. Eur. J., **2017**, 23, 2084-2102.

[42]. D. Heitmann, C. Jones, D. P. Millsa, and A. Stasch, Dalton Trans., **2010**, 39, 1877-1882.

[43]. D. Werner, G. B. Deacon and P. C. Junk, Eur. J. Inorg. Chem., **2018**, 2241-2246.

[44]. M. L. Cole, G. B. Deacon, C. M. Forsyth, P. C. Junk, D. P. Ceron and J. Wang, Dalton Trans., **2010**, 39, 6732-6738.

[45]. M. Karbowiak and A. Urbanowicz, Phys. Rev. B., **2007**, 76, 115-125(1-9).

[46]. M. L. Cole and P. C. Junk, Chem. Commun., **2005**, 2695-2697.

[47]. R. D. Shannon, Acta Crystallogr. Sect. A, **1976**, 32, 751-767.

[48]. Z. Guo, M. A. Halim, V. Blair, G. B. Deacon and P. C. Junk, Chem. Asian J., **2023**, 18, e202300333.

[49]. S. Beaini, G. B. Deacon, M. Hilder, P. C. Junk, and D. R. Turner, Eur. J. Inorg. Chem., **2006**, 3434-3441.

[50]. S. Beaini, G. B. Deacon, E. E. Delbridge, P. C. Junk, B. W. Skelton and A. H. White, Eur. J. Inorg. Chem., **2008**, 4586-4596.

[51]. Z. Guo, J. Luu, V. Blair, G. B. Deacon and P. C. Junk, Eur. J. Inorg. Chem., **2019**, 1018-1029.

[52]. J. E. Cosgriffs, G. B. Deacon, G. D. Fallon, B. M. Gatehouse, H. Schumann, and R. Weimann, Chem. Bcr., **1996**, 129, 953-958.

[53]. G. B. Deacon, P. C. Junk and A. Urbatsch, Eur. J. Inorg. Chem., **2011**, 3592-3600.

[54]. Z. Guo, V. Blair, G. B. Deacon and P. C. Junk, Chem. Commun., **2021**, 57, 11513-11516.

[55]. D. Stellfeldt, G. Meyer, and G. B. Deacon, Z. Anorg. Allg. Chem., **1999**, 625, 1252-1254.

[56]. M. A. Halim, Z. Guo, V. L. Blair, G. B. Deacon, and P. C. Junk, Eur. J. Inorg. Chem., **2024**, e202400672.

[57]. W.-P. Leung, F.-Q. Song, F. Xue, Z.-Y. Zhang and T. C. W. Mak, J. Organomet. Chem., **1999**, 582, 292-300.

[58]. Y.-J. Tsai, M. B. Pastor, W. Lo and Q. Zhao, Inorg. Chim. Acta, **2015**, 434, 85-91.

[59]. A. R. Green, A. C. Walker, M. P. Blake and P. Mountford, Polyhedron, **2016**, 116, 64-75.

[60]. Y. J. Tasi, M. B. Pastor, W. Lo and Q. Zhao, Inorg. Chim. Acta., **2015**, 85–91.

[61]. Z. Guo, V. L. Blair, G. B. Deacon and P. C. Junk, Chem. Eur. J., **2022**, 28, e202103865.

[62]. T. M. McPhillips, S. E. McPhillips, H. J. Chiu, A. E. Cohen, A. M. Deacon, P. J. Ellis, E. Garman, A. Gonzalez, N. K. Sauter, R. P. Phizackerley, S. M. Soltis and J. P. Kuhn, J. Synchrotron Radiat., **2002**, 9, 401-406.

[63]. W. Kabsch, J. Appl. Crystallogr., **1993**, 26, 795.

[64]. G. M. Sheldrick, Acta Crystallogr. Sect. A., **2008**, 64, 112-122.

[65]. O. V. Dolomanov, L. J. Bourhis, R. J. Gildea, J. A. K. Howard and H. Puschmann, J. Appl. Crystallogr., **2009**, 42, 339-341.

[66]. G. M. Sheldrick, Acta Cryst., **2015**, C71, 3-8.

[67]. L. J. Barbour, J. Supramol. Chem., **2001**, 1, 189-191.

Chapter 3

Reactions of Ln(III) pseudo Grignard reagents with formamidines and pyrazoles

Chapter 3

3.1 Introduction

In this section, lanthanoid compounds synthesised from Grignard reagents using trivalent lanthanoid metals will be referred to as trivalent lanthanoid pseudo-Grignard compounds. In a major breakthrough, Evans first showed that ytterbium metal reacts with alkyl and aryl iodides to form "RYbI" species in a manner reminiscent of the formation of Grignard reagents.[1] This was followed up by similar studies with europium and samarium metal.[2] Magnetic susceptibility measurements by the Evans NMR method showed the products were a mixture of divalent and trivalent complexes. Divalent complexes were most prevalent for Ln = Eu and less so for Ln = Yb and considerably less for Ln = Sm {Eu^{2+} (99%), Yb^{2+} (85%) and Sm^{2+} (50%)}.[2] In the case of ytterbium, the highest proportion of Yb^{II} was achieved with 2,6-dimethyliodobenzene.[1] Given the versatility and prevalence of Grignard reagents, it might have been expected that this discovery might have led to a burgeoning chemistry, but in fact, developments have been slow. From the 1980s, Russian workers have sought to examine the scope of their formation, and Japanese workers have developed some organic chemistry, and, from the 1990s, limited structures utilising bulky ligand stabilisation emerged. The reason for the lack of interest is not easily understood, but perhaps cost and accessibility of lanthanoid metals may be a factor. However, groups studying lanthanoid metal reactions have been able to overcome this problem.

We have limited the review to the classic divalent lanthanoid elements Sm, Eu, and Yb, as products of reactions of other Ln metals with organic halides are predominantly trivalent species. Trivalent species of the type $LLnX_2$ would open an enormous Pandora's box. These compounds can be synthesised by using various synthetic ways. The commonly used synthetic methods are redox transmetallation/protolysis (RTP) and metathesis reactions. Beside these two, some other used methods in the literature include redox transmetallation, oxidation, H/F exchange and direct reactions. In the previous chapter, we discussed divalent pseudo-Grignard reactions with various anionic ligands. This section will introduce some of these common synthetic processes for trivalent lanthanoid pseudo-Grignard complexes. Given that trivalent lanthanoid pseudo-Grignard reactions are a novel area in pseudo-Grignard chemistry, this exploration promises to be a significant contribution to the field. Later in this chapter, we will discuss the synthesis of Ln(III) pseudo-Grignard complexes derived from pseudo-Grignard reactions.

3.1.1 Synthesis of trivalent pseudo-Grignard complexes

The pseudo-Grignard reaction with trivalent lanthanoid (Ce, Lu) and organic halides was introduced in the literature in the 1970s, leading to the isolation of pseudo-Grignard reagents involving $La^{3+}$and Ce^{3+} (**eqn. (3.1)**).[2]

$$Ln_{excess} + 3RX \xrightarrow[25\ °C]{thf} "R_2LnX(thf)_n" + "RLnX_2(thf)_n"$$

R = Et, Ph
Ln = La, Ce

Equation 3.1: Preparation of lanthanoid (La, Ce) pseudo-Grignard complexes.[2]

Later, in 1983, Dolgoplosk, *et al*. effectively applied the oxidative addition reaction to several tri-valent lanthanoids, synthesising pseudo-Grignard complexes such as $[(Ph_3C)_2LnCl]$ or $[(Ph_3C)LnCl_2]$ (Ln = Pr^{3+}, Nd^{3+}, Gd^{3+} and Ho^{3+}) (**Scheme 3.1 eqn. (ii, iii)**). The proposed reaction pathway for the formation Ln^{3+} Grignard complexes is illustrated in **Scheme 3.1**.[3]

$$Ln + Ph_3CCl \longrightarrow Ph_3CLnCl \quad (i)$$

$$Ph_3CLnCl + Ph_3CCl \longrightarrow Ph_3CLnCl_2 + Ph_3C^{\bullet} \quad (ii)$$

$$Ph_3CLnCl + 2Ph_3C^{\bullet} \longrightarrow (Ph_3C)_2LnCl + Ph_3C^{\bullet} \quad (iii)$$

Scheme 3.1: Preparation of trivalent pseudo-Grignard reagents.[3]

Subsequently, Deacon *et al.* in **2010** and Ali *et al.* in **2018** explored the pseudo-Grignard reaction primarily for divalent lanthanoids, notably Eu and Yb.[4, 5] The reaction of $PhLnI(thf)_n$ (Ln = Eu and Yb) with the pro-ligand 3,5-diphenylpyrazole (Ph_2pzH) resulted in the isolation of the divalent complex $[Ln(Ph_2pz)I(thf)_4]$ (**Scheme 3.2 eqn.(ii)**).[4]

$$Ln_{(excess)} + PhI \xrightarrow[\text{sonication}]{-78\ °C/thf} "PhLnI(thf)_n" \quad \textbf{(i)}$$

Ln = Eu, Yb

$$"PhLnI(thf)_n" + Ph_2pzH \xrightarrow[RT\ (overnight)]{-78\ °C/thf} [Ln(Ph_2pz)I(thf)_4] + PhH \quad \textbf{(ii)}$$

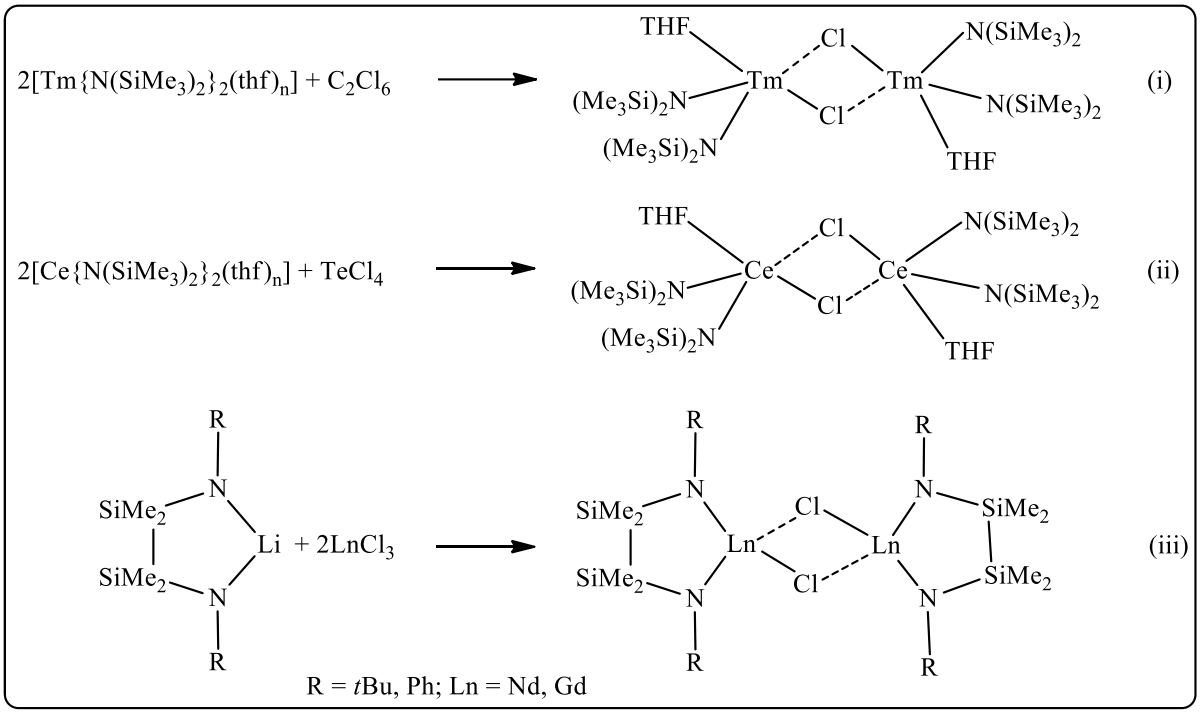
$$"PhLnI(thf)_n" + DippFormH \xrightarrow[RT\ (overnight)]{-78\ °C/thf} [Ln(DippForm)I_n(thf)_3] + PhH \quad \textbf{(iii)}$$

n = 1 or 2

Scheme 3.2: Reported pseudo-Grignard complexes.[4, 5]

However, in reactions involving formamidines, PhYbI produced both Yb^{II} and Yb^{III} complexes. For example *N,N'*-bis(2,6-diisopropylphenyl)formamidine (DippFormH) yielded a mixture of $[Yb^{II}(DippForm)I(thf)_3]$ and $[Yb^{III}(DippForm)I_2(thf)_3]$ (**Scheme 3.2 eqn. (iii)**).[5]

An ubiquitous ligand for isolating lanthanoid complexes is bistrimethylsilylamide. **Scheme 3.3** illustrates the synthesis processes of some bistrimethylsilylamide based lanthanoid pseudo-Grignard complexes.



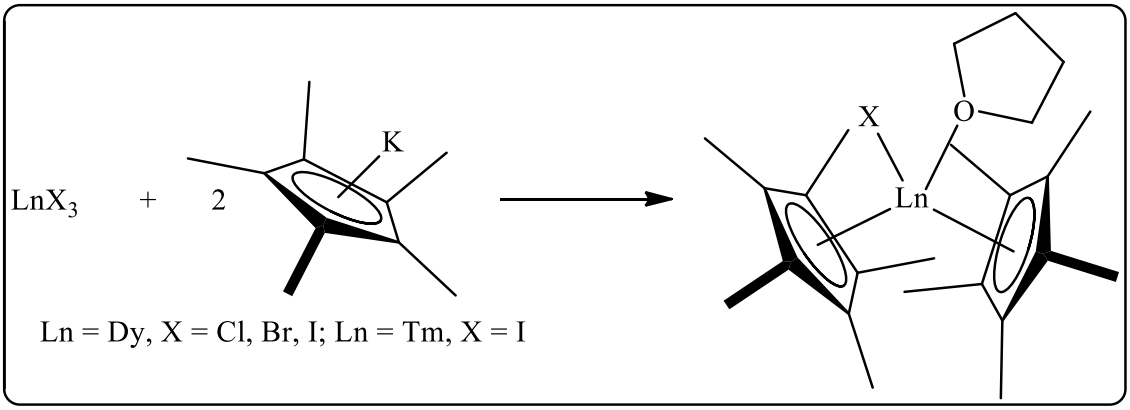
Scheme 3.3: Synthesis of $[Ln\{N(SiMe_3)_2\}_2(\mu\text{-}Cl)(thf)]_2$ (Ln = Tm **1**, Ce **2**) and $[\{Ln\{(R)NSiMe_2\}_2(\mu\text{-}Cl)(thf)\}_2]$ (R = *t*Bu, Ln = Nd **3**, Gd **4**; R = Ph, Ln = Nd **5**, Gd **6**) complexes.[6-8]

Complex $[Tm\{N(SiMe_3)_2\}_2(\mu\text{-}Cl)(thf)]_2$(**1**) was isolated from the halogenation reaction obtained between 2 equiv. of $[Tm\{N(SiMe_3)_2\}_2(thf)_n]$ with 1 equiv. C_2Cl_6 in n-hexane solution (**Scheme 3.3 eqn. (i)**).[6] The isostructural complex $[Ce(N(SiMe_3)_2)_2(\mu\text{-}Cl)(thf)]_2$(**2**) was obtained from the oxidation reaction between $[Ce\{N(SiMe_3)_2\}_2(thf)_n]$ and $TeCl_4$ in thf (**Scheme 3.3 eqn. (ii)**).[7] Both complexes (**1**, **2**) are five coordinated dimers. Similar types of complexes $[\{Ln\{(t\text{-}Bu)NSiMe_2\}_2(\mu\text{-}Cl)(thf)\}_2]$ (Nd **3**, Gd **4**) and $[\{Ln\{(Ph)NSiMe_2\}_2(\mu\text{-}Cl)(thf)\}_2]$ (Nd **5**, Gd **6**) were synthesised using metathesis reaction (**Scheme 3.3 eqn. (iii)**).[8] Complex $[Pr\{N(SiMe_3)_2\}_2Cl(thf)]_2$] (**7**) also resulted from a metathesis reaction.[9]

When $[Ce\{N(SiMe_3)_2\}_2(thf)_n]$ is reacted with $TeBr_4$ the complex $[Ce(N(SiMe_3)_2)Br_2(thf)_3]$ (**8**) is obtained. Interestingly, $TeBr_4$ yielded monomeric complex **8** where $TeCl_4$ yielded dimeric

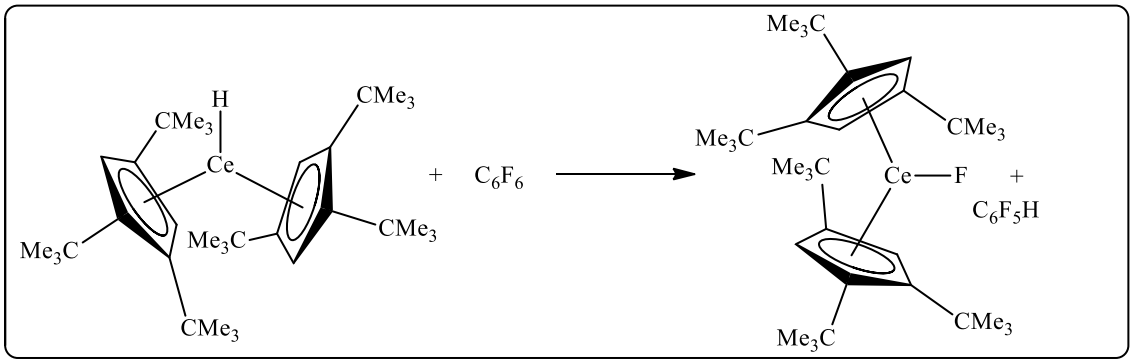
complex **2**.[7] The halogenation reaction between compound $[Tm\{N(SiMe_3)_2\}_2(thf)_n]$ and $C_2H_4I_2$ yielded seven coordinate monomeric complex $[Tm\{N(SiMe_3)_2\}I_2(thf)_3]$ (**9**).[6] Ce(IV) pseudo-Grignard complexes $[Ce(N(SiMe_3)_2)_3X]$(X = F **10**, Cl **11**, Br **12**) were yielded from the oxidation reaction between $[Ce(N(SiMe_3)_2)_3]$ and a corresponding oxidant. Complex $[Ce(N(SiMe_3)_2)_3F]$ (**10**) was yielded from using oxidants ($FcPF_6$, Ph_3CPF_6, $FcBF_4$, Ph_3CBF_4), [10] while oxidant $TeCl_4/PhICl_2$ yielded complex $[Ce(N(SiMe_3)_2)_3Cl]$ (**11**) [11, 12] and PBr_2Ph_3 yielded complex $[Ce(N(SiMe_3)_2)_3Br]$ (**12**).[7] A summary of these complexes is illustrated in table **3.1**.

The metathesis reaction is very effective for isolating corresponding lanthanoid pseudo-Grignard complexes from alkali metal derivatives of cyclopentadienide and lanthanoid chlorides. The reaction between lithium bis(trimethylsilyl)cyclopentadienyl ($Li\{C_5H_3(SiMe_3)_2\}$) and $LnCl_3$ affords $[Ln\{\eta\text{-}(C_5H_3(SiMe_3)_2)\}_2Cl_2]$ (Ln = La **13**, Ce **14**, Pr **15**, Nd **16**, Gd **17**, Tb **18**, Dy **19**, Ho **20**, Er **21**, Tm **22**, Lu **23**) complexes.[13] Ten years later Shen *et al*. 1991 isolated $[Ln(t\text{BuCp})_2Cl]$ (Ln = Pr **24**, Nd **25**, Gd **26**) complexes from the metathesis reaction between sodium *t*-butylcyclopentadienide ($Na\{^tBuC_5H_4\}$) and corresponding lanthanoid chloride ($LnCl_3$) salts.[14] Later at 1998, $[Lu(C_5Me_4{}^iPr)_2Cl(thf)]$(**27**) was isolated from the reaction of $LuCl_3$ with ($Na\{C_5Me_4{}^iPr\}$).[15] Bis-pentamethylcyclopentadienyl ($C_5(Me)_5$)-supported lanthanoid complexes $[Ln(C_5Me_5)_2X(thf)]$ (Ln = Dy, X = Cl **28**, Br **29**, I **30**; Ln = Tm, X = I **31**) were obtained from the reaction between $(C_5(Me)_5)K$ and corresponding LnX_3 salts (**Scheme 3.4**).[16, 17] The reaction of $K(Cp^{ttt})$ (Cp^{ttt} = 1,2,4-tri(tert-butyl)cyclopentadienide) with corresponding $LnCl_3$ salts yielded $[Ln(Cp^{ttt})_2Cl]$ (La **32**, Ce **33**, Dy **34**, Pr **35**, Nd **36**) complexes.[17a, 17b, 17c] A summary of these complexes is illustrated in table **3.1**.



Scheme 3.4: Synthesis of $[Ln(C_5Me_5)_2X(thf)]$ (Ln = Dy, X = Cl **28**, Br **29**, I **30**; Ln = Tm, X = I **31**) complexes.[16, 17]

Besides products obtained from these metathesis reactions, oxidation of Tm(II) [$TmI_2(thf)_2$] yielded the Tm(III) [$Tm(C_5Me_5)_2I(thf)$] (**37**) complex [16] and an H/F exchange reaction between $CeH(Cp')_2$ (Cp′ = 1,3,4-$(Me_3C)_3(C_5H_2)$) and C_6F_6 yielded [$CeCp'_2F$] (**38**) (**Scheme 3.5**).[18] The dichloro neodymium cyclopentadienyl complex [$Nd(\eta^5\text{-}C_5H_5)Cl_2$] (**39**) was synthesised from the metathesis reaction between $NdCl_3$ and NaC_5H_5, [19] but the isostructural complex **39**, [$Ho(\eta^5\text{-}C_5H_5)Cl_2$] (**40**) was obtained from a direct reaction of $HoCl_3$ with 5 equiv. C_5H_6 and 1 equiv. sodium metal.[20]



Scheme 3.5: Synthesis of [$CeCp'_2F$] (**38**) (Cp′ = 1,3,4-$(Me_3C)_3(C_5H_2)$) from an H/F exchange reaction.[18]

Dimeric isostructural complexes [$Ln(Ap)Cl(\mu\text{-}Cl)(thf)_2]_2$ (Nd **41**, Lu **42**) (ApH = {2,6-diisopropylphenyl)-[6-(2,4,6-triisopropylphenyl)pyridin-2-yl]amine}) were yielded from the metathesis reactions between $[ApK]_n$ and the corresponding $LnCl_3$ in thf.[21, 22] Complex [$Lu(Ap)Cl_2(thf)_2$] (**43**) was yielded as a side product with complex **42**.[22] The reaction between Ap*K ({Ap* = (2,6-diisopropylphenyl)-[6-(2,6-dimethylphenyl)pyridin-2-yl]amine} and LnX_3 (X = Br, Cl) in thf yielded the mono halide [$Ln(Ap^*)_2X(thf)$] (X = Br, Ln = La **44**; X = Cl, Ln = Nd **45**, Lu **46**) complexes (**eqn. (3.2)**).[21, 23] A summary of these complexes is illustrated in table **3.1**.

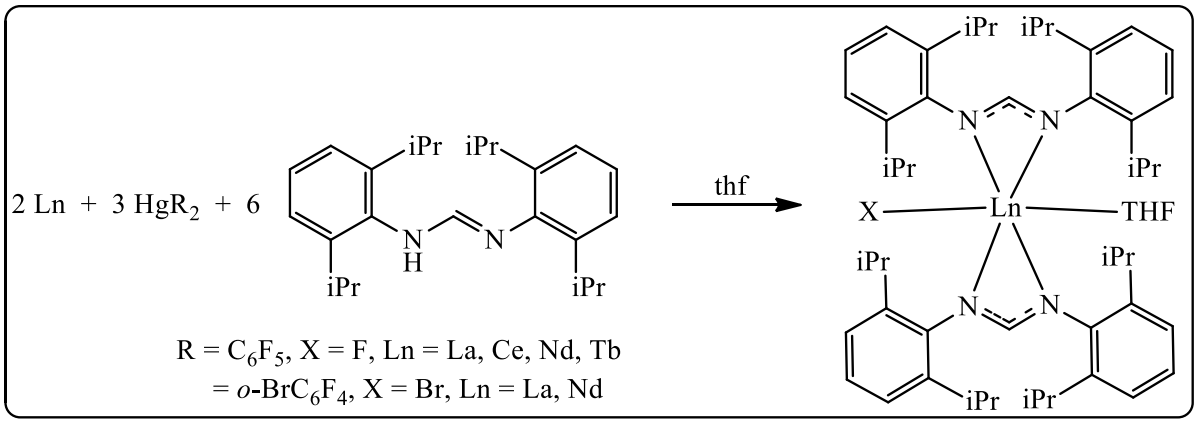
$$LnX_3 + Ap^*K \xrightarrow{thf} [Ln(Ap^*)_2X(thf)]$$

X = Br, Ln = La; X = Cl, Ln = Nd, Lu

Equation 3.2: Synthesis of [$Ln(Ap^*)_2X(thf)$] (X = Br, Ln = La **44**; X = Cl, Ln = Nd **45**, Lu **46**) complexes.[21, 23]

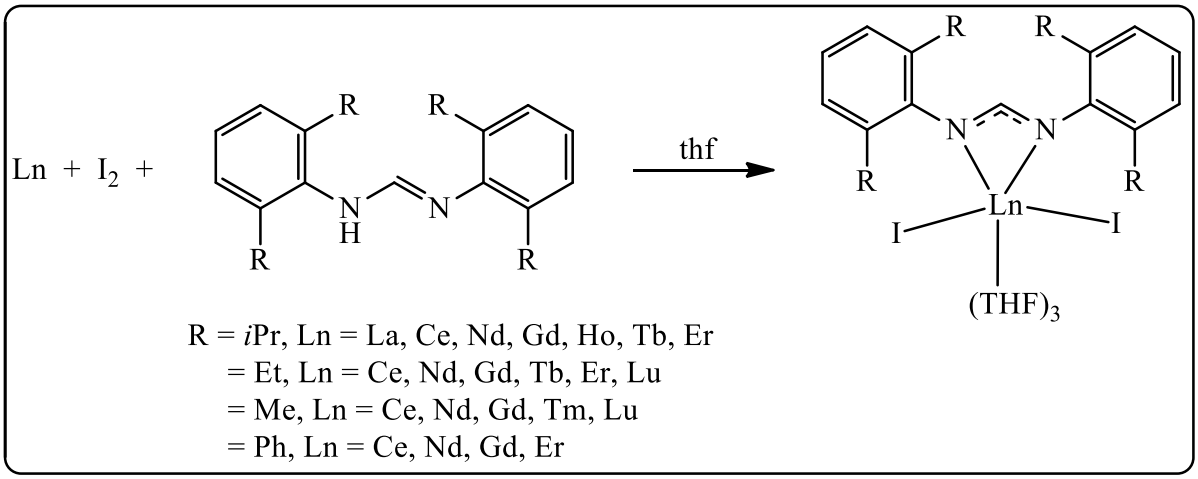
A very important series of trivalent lanthanoid pseudo-Grignard complexes [$Ln(DippForm)_2X(thf)$] (X = F, Ln = La **47**, Ce **48**, Nd **49**, Tm **50**; X = Br, Ln = La **51**, Nd **52**) were synthesised from the redox transmetallation/protolysis reactions between the lanthanoid

metal filings, DippFormH and bis (C_6F_5 or *o*-BrC_6F_4) mercury in THF, accompanied by C-X activation (**Scheme 3.6**). These six-coordinate monomeric complexes (**47-52**) were isomorphous where the X ligand is *cisoid* with the DippForm ligands.[24, 25] The seven coordinate terbium complex [Tb(DippForm)$_2$Cl(thf)$_2$] (**53**) was yielded from the metathesis reaction between [Na(DippForm)(thf)$_3$] and $TbCl_3$ in THF.[26] A summary of these complexes is illustrated in table **3.1**.



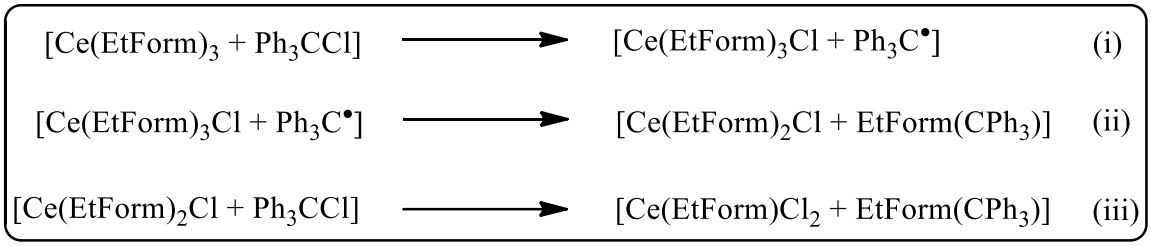
Scheme 3.6: Synthesis of [Ln(DippForm)$_2$X(thf)] (X = F, Ln = La **47**, Ce **48**, Nd **49**, Tm **50**; X = Br, Ln = La **51**, Nd **52**) complexes.[24, 25]

A major breakthrough occurred in lanthanoid pseudo-Grignard chemistry, when Guo *et al*. used a direct reaction between lanthanoid metal, I_2 and a corresponding formamidine and successfully isolated a range of lanthanoid diiodo formamidinato complexes.[27] Later, in 2023 Guo and her coworkers again successfully isolated a family of similar formamidinato complexes using the same direct reaction.[28] The reaction between lanthanoid metal, I_2 and DippFormH (*N*,*N*′-bis(2,6-diisopropylphenyl)formamidine) yielded [Ln(DippForm)I_2(thf)$_3$] (Ln = La **54**, Ce **55**, Nd **56**, Gd **57**, Ho **58**, Tb **59**, Er **60**) complexes. By changing proligand DippFormH with other formamidines they were also effective in isolating [Ln(Form)I_2(thf)$_3$] (Form = EtForm, Ln = Ce **61**, Nd **62**, Gd **63**, Tb **64**, Er **65**, Lu **66**; Form = XylForm, Ln = Ce **67**, Nd **68**, Gd **69**, Tm **70**, Lu **71**; Form = PhForm, Ln = Ce **72**, Nd **73**, Gd **74**, Er **75**) complexes (**Scheme 3.7**).[27, 28] Interestingly all the formamidinatoiodidolanthanoid(III) complexes are seven coordinated monomers, where both iodide ligands are *transoid*. A summary of these complexes is illustrated in table **3.1**.



Scheme 3.7: Synthesis of [Ln(Form)I_2(thf)$_3$] (Form = DippForm, Ln = La **54**, Ce **55**, Nd **56**, Gd **57**, Ho **58**, Tb **59**, Er **60**; Form = EtForm, Ln = Ce **61**, Nd **62**, Gd **63**, Tb **64**, Er **65**, Lu **66**; Form = XylForm, Ln = Ce **67**, Nd **68**, Gd **69**, Tm **70**, Lu **71**; Form = PhForm, Ln = Ce **72**, Nd **73**, Gd **74**, Er **75**) complexes. [27, 28]

[Ce(EtForm)Cl_2(thf)$_3$] (**76**) was isolated from the oxidation reaction of [Ce(EtForm)$_3$] and Ph_3CCl through an interesting reaction pathway. The reaction pathway of the seven coordinated [Ce(EtForm)Cl_2(thf)$_3$] complex is illustrated in **Scheme 3.8**.[29]



Scheme 3.8: The possible reaction pathway for the formation of [Ce(EtForm)Cl_2(thf)$_3$] (**76**).[29]

Table 3.1: A summary of trivalent lanthanoid metal based pseudo-Grignard complexes using various synthetic procedures.

Complexes	Reactions	Ref.
[Tm{N(SiMe$_3$)$_2$}$_2$(μ-Cl)(thf)]$_2$(**1**)	Halogenation	[6]
[Ce(N(SiMe$_3$)$_2$)$_2$(μ-Cl)(thf)]$_2$(**2**)	Redistribution	[7]
[{Ln{(*t*-Bu)NSiMe$_2$}$_2$(μ-Cl)(thf)}$_2$] (Ln = Nd **3**, Gd **4**)	Metathesis	[8]
[{Ln{(Ph)NSiMe$_2$}$_2$(μ-Cl)(thf)}$_2$] (Ln = Nd **5**, Gd **6**)		[8]
[Pr{N(SiMe$_3$)$_2$}$_2$Cl(thf)]$_2$] (**7**)		[9]

$[Ce(N(SiMe_3)_2)Br_2(thf)_3]$ (**8**)	Redistribution	[7]
$Tm\{N(SiMe_3)_2\}I_2(thf)_3]$(**9**)	Salt metathesis	[6]
$[Ce(N(SiMe_3)_2)_3X]$(X = F **10**, Cl **11**, Br **12**)	Oxidation	[7, 10-12]
$[Ln\{\eta\text{-}(C_5H_3(SiMe_3)_2)\}_2Cl_2]$(Ln = La **13**, Ce **14**, Pr **15**, Nd **16**, Gd **17**, Tb **18**, Dy **19**, Ho **20**, Er **21**, Tm **22**, Lu **23**)	Metathesis	[13]
$[Ln(t\text{BuCp})_2Cl]$(Ln = Pr **24**, Nd **25**, Gd **26**)		[14]
$[Lu(C_5Me_4{}^iPr)_2Cl(thf)]$(**27**)		[15]
$[Dy(C_5Me_5)_2X(thf)]$(Ln = Dy, X = Cl **28**, Br **29**, I **30**; Ln = Tm, X = I **31**)		[16, 17]
$[Ln(Cp^{ttt})_2Cl]$(La **32**, Ce **33**, Dy **34**, Pr **35**, Nd **36**)		[17a, 17b, 17c, 30, 31]
$[Tm(C_5Me_5)_2I(thf)]$ (**37**)	Oxidation	[16]
$[CeCp'_2F]$(**38**)	H/F exchange	[18]
$[Nd(\eta^5\text{-}C_5H_5)Cl_2]$(**39**)	Metathesis	[19]
$[Ho(\eta^5\text{-}C_5H_5)Cl_2]$(**40**)	Direct	[20]
$[Ln(Ap)Cl(\mu\text{-}Cl)(thf)_2]_2$(Nd **41**, Lu **42**)	Metathesis	[21, 22]
$[Lu(Ap)Cl_2(thf)_2]$ (**43**)		[22]
$[Ln(Ap^*)_2X(thf)]$(X = Br, Ln = La **44**; X = Cl, Ln = Nd **45**, Lu **46**)		[21, 23]
$[Ln(DippForm)_2F(thf)]$(La **47**, Ce **48**, Nd **49**, Tm **50**)	RTP/C-F	[24, 25]
$[Ln(DippForm)_2Br(thf)]$(La **51**, Nd **53**)	Activation	[26]
$[Tb(DippForm)_2Cl(thf)_2]$(**53**)	Metathesis	[26]
$[Ln(DippForm)I_2(thf)_3]$(La **54**, Ce **55**,Nd **56**, Gd **57**, Ho **58**, Tb **59**, Er **60**)	Direct	[27, 28]
$[Ln(EtForm)I_2(thf)_3]$(Ce **61**, Nd **62**, Gd **63**, Tb **64**, Er **65**, Lu **66**)		[28]
$[Ln(XylForm)I_2(thf)_3]$(Ce **67**, Nd **68**, Gd **69**, Tm **70**, Lu **71**)		[28]
$[Ln(PhForm)I_2(thf)_3]$(Ce **72**, Nd **73**, Gd **74**, Er **75**)		[10]
$[Ce(EtForm)Cl_2(thf)_3]$(**76**)	Oxidation	[29]

In the latter sections of this chapter, we will discuss the synthesis processes of trivalent pseudo-Grignard complexes using N-donor ligands; pyrazole (Ph_2pzH) and formamidines (DippFormH and XylFormH). Firstly we will introduce trivalent Grignard reactions for isolating Ln(III) pseudo-Grignard complexes, where we successfully isolated 14 complexes (among them 12 complexes are new and 2 complexes were isolated previously using direct reaction process) such as; $[Ln(Ph_2pz)I_2(thf)_n]$ (n = 4, Ln = La **3.1**, Ce **3.2**, Nd **3.3**; n = 3, Ln = Er **3.4**, Lu **3.5**), $[Er(Ph_2pz)(Ph)I(thf)_3]\cdot thf$ (**3.4a**), $[Ln(Ph_2pz)_3(CH_3CN)_3]\cdot 2CH_3CN$ (Ln = Nd **3.6**, Gd **3.7**), $[Ln(DippForm)I_2(thf)_3]\cdot nthf$ (n = 1, Ln = Nd **3.8**, n = 0.5, Ln = Er **3.9**), $[Ln(XylForm)I_2(thf)_3]\cdot thf$ (Ln = La **3.10**, Nd **3.11**, Er **3.12**) and $[Nd(Ph_2pz)Br_2(thf)_{3.5}]$ (**3.13**).

3.2 Current Study

This chapter aims to expand the study of trivalent organolanthanum halide complexes formed through the reaction of lanthanoid metals (Ln = La, Ce, Nd, Gd, Er and Lu), with an organic halide (PhI) and pro-ligands (pyrazoles and formamidines). This synthetic pathway has already been successful in trapping a wide range of divalent compounds, but similar approaches for trivalent species, where Ln(III) is predominant, remain unexplored.

The protolysis reaction between $Ph_pLnI_{(3-p)}(thf)_n$ (p = 1 or 2; Ln = La, Ce, Nd, Er and Lu) and Ph_2pzH produced several trivalent (Ln(III)) compounds, including $[La(Ph_2pz)I_2(thf)_4]$ (**3.1**), $[Ce(Ph_2pz)I_2(thf)_4]$ (**3.2**), $[Nd(Ph_2pz)I_2(thf)_4]$ (**3.3**), $[Er(Ph_2pz)(Ph)I(thf)_3]\cdot thf$ (**3.4a**), $[Er(Ph_2pz)I_2(thf)_3]$ (**3.4**) and $[Lu(Ph_2pz)I_2(thf)_3]$ (**3.5**). By replacing THF with acetonitrile as the solvent, we were able to isolate Schlenk equilibria products such as $[Nd(Ph_2pz)_3(CH_3CN)_3]\cdot 2CH_3CN$ (Nd **3.6**) and $[Gd(Ph_2pz)_3(CH_3CN)_3]\cdot 2CH_3CN$ (Gd **3.7**).

This study also involved the reaction of $Ph_pLnI_{(3-p)}(thf)_n$ (p = 1 or 2; Ln = La, Nd and Er) and pro-ligands (formamidines), resulting in the formation of trivalent complexes such as $[Nd(DippForm)I_2(thf)_3]\cdot thf$ (**3.8**), $[Er(DippForm)I_2(thf)_3]\cdot 0.5thf$ (**3.9**), $[La(XylForm)I_2(thf)_3]\cdot thf$ (**3.10**), $[Nd(XylForm)I_2(thf)_3]\cdot thf$ (**3.11**) and $[Er(XylForm)I_2(thf)_3]\cdot thf$ (**3.12**).

For further investigation, we examined the reaction process between $Ph_pNdBr_{(3-p)}(thf)_n$ (p = 1 or 2) and Ph_2pzH, which produced the trivalent neodymium bromide $[Nd(Ph_2pz)Br_2(thf)_{3.5}]$ (**3.13**) compound.

3.3 Results and Discussion

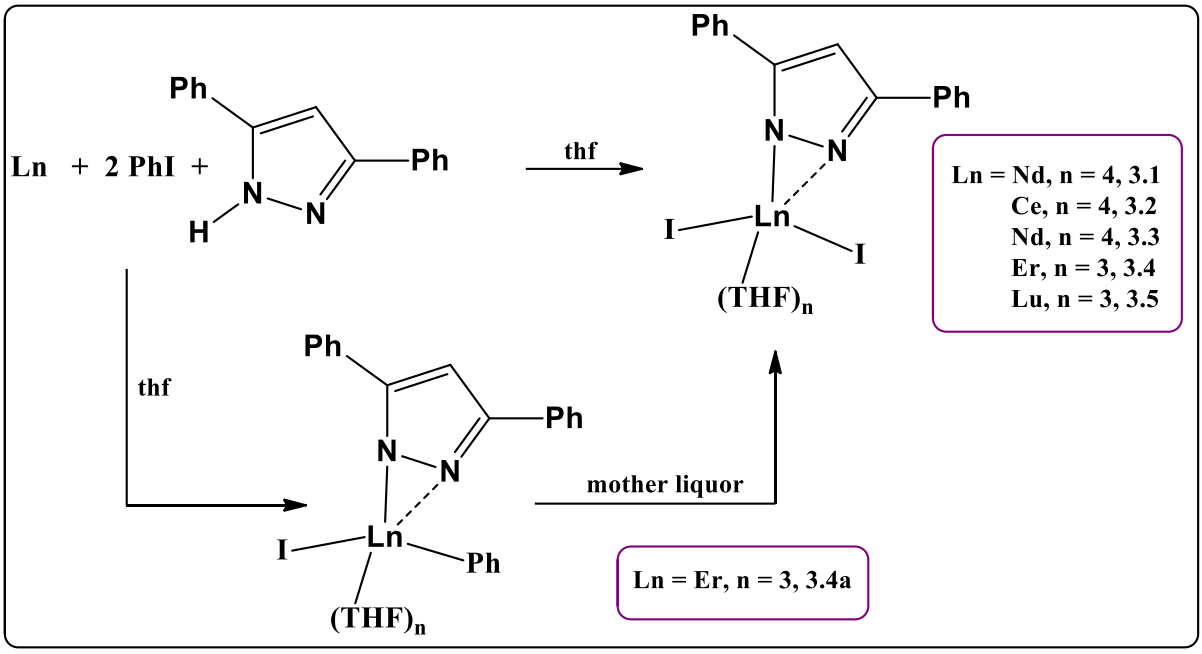
3.3.1 Synthesis and spectroscopic characterisation

3.3.1.1 The reaction of lanthanoid (La, Ce, Nd, Er and Lu) pseudo-Grignard reagents with Ph_2pzH

The primary objective was to synthesise trivalent lanthanoid pseudo-Grignard compounds, specifically those of La, Ce, Nd, Er and Lu. Phenyllanthanoid halides, $Ph_pLnI_{3-p}(thf)_n$ (p = 1 or 2; Ln = La **3.1**, Ce **3.2**, Nd **3.3**, Er **3.4** and Lu **3.5**) were generated *in situ* by reactions of an excess of Ln metal activated with Hg metal with iodobenzene (PhI) in tetrahydrofuran solvent (thf) on sonication and further stirring at room temperature. Experiments were also carried out without Hg activation, observing that La reacts with PhI overnight (~15 h), while Nd requires approximately 36 h to achieve the desired reaction. To increase the yield, the reaction rate and reduce the initiation time, we introduced Hg metal to activate the lanthanoid metals.

The pseudo-Grignard reagent products obtained from these reactions were treated directly with the proligand 3,5-diphenylpyrazole (Ph_2pzH; 0.22g, 1.0 mmol) (mole ratio PhI: Ph_2pzH = 2:1) at 0 °C for 1 h and then at room temperature. The desired coloured solution developed: light yellow for compound **3.1**, brown for compounds **3.2** and **3.5**, brownish blue for compound **3.3** and pink for compound **3.4**. Crystallisation from the concentrated solution yielded colourless crystals of $[La(Ph_2pz)I_2(thf)_4]$ (**3.1**), yellow crystals of $[Ce(Ph_2pz)I_2(thf)_4]$ (**3.2**), purple crystals of $[Nd(Ph_2pz)I_2(thf)_4]$ (**3.3**), pink crystals of both $[Er(Ph_2pz)I_2(thf)_3]$ (**3.4**) and $[Er(Ph_2pz)(Ph)I(thf)_3]\cdot thf$ (**3.4a**) and colourless crystals of $[Lu(Ph_2pz)I_2(thf)_3]$ (**3.5**). The crystalline yield of these complexes varies from 44% to 62%. The reaction and structural schemes for compounds **3.1** to **3.5** are provided in **Scheme 3.9**.

Satisfactory ^1H NMR spectra were obtained for compounds **3.1** (**Fig. 3.1**), **3.2** (**Fig. 3.2**), **3.3** (**Fig. 3.3**) consistent with the results of elemental analysis. The ^1H NMR spectra of compound **3.5** (**Fig. 3.5**) indicated the presence of an additional THF solvent molecule. Compound **3.4** (**Fig. 3.4**) exhibited broad features with unsatisfactory integration owing to paramagnetism (Er^{III}).



Scheme 3.9: Synthesis of compounds [Ln(Ph_2pz)I_2($thf)_4$] (**3.1** La, **3.2** Ce and **3.3** Nd), [Er(Ph_2pz)(Ph)I($thf)_3$]·thf (**3.4a**), [Ln(Ph_2pz)I_2($thf)_3$] (**3.4** Er and **3.5** Lu).

In the ^{1}H NMR spectra, the CH-pz resonances for compound **3.1** appeared at 7.28 ppm, for compound **3.2** at 13.52 ppm, for compound **3.3** at 26.17 ppm, and for compound **3.5** at 7.50 ppm, with the pro- ligand value being at 6.66 ppm. For compound **3.2**, the CH_2 signals of thf were observed at δ = 0.61 and 1.54 ppm, while the CH signals from the phenyl ring appeared at δ = 7.65 to 7.79 ppm and 10.58 ppm. In compound **3.3**, the CH_2 signals of thf were found at δ = 1.26 and 1.74 ppm, while CH signals from the phenyl ring were at δ = 8.45 and 9.38 ppm. For compound **3.5**, the CH_2 signals of thf were observed at δ = 1.31 and 3.67 ppm, while the CH signals from phenyl ring appeared at δ = 7.11, 7.27 and 8.32 ppm. IR spectra showed the presence of the appropriate Ph_2pz ligand. The absence of (N-H) absorption (around 3300-3400 cm^{-1}) in the infrared spectra proved the complete deprotonation of the ligands. Additionally, micro or metal analysis validated their bulk purity; the latter being used when there were issues with elemental analysis. The melting points indicate significant thermal stability of the new Ph_2pz compounds.

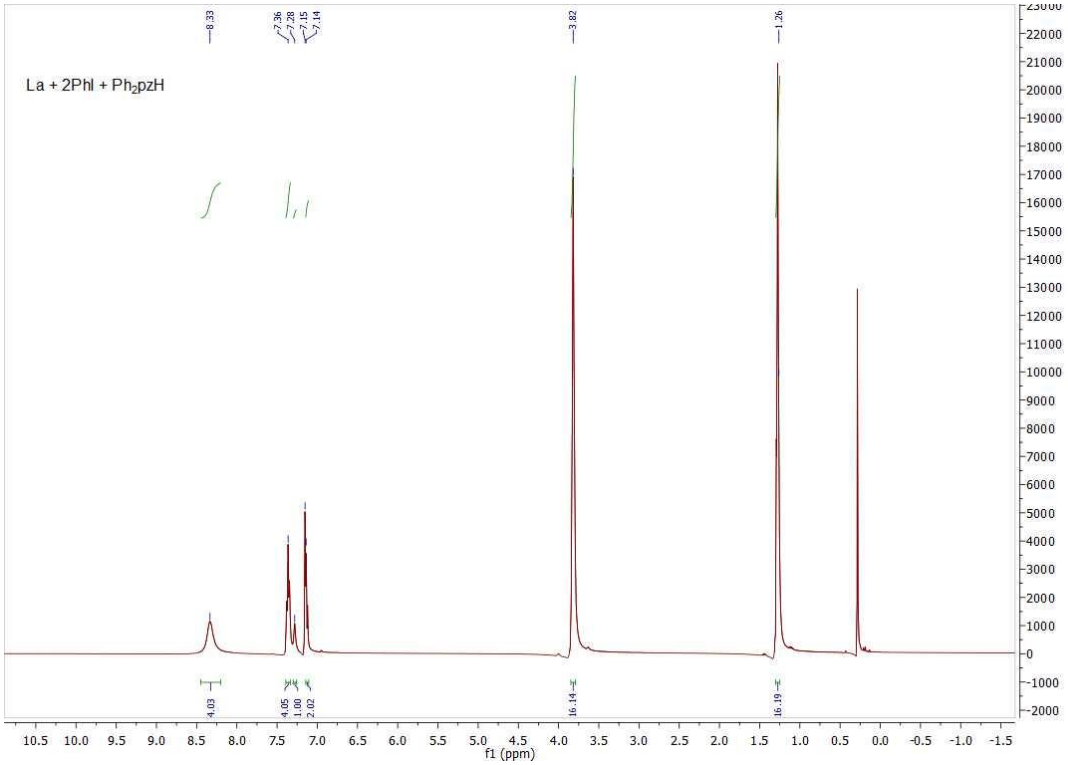


Figure 3.1: ^{1}H NMR spectrum of **[La(Ph$_2$pz)I$_2$(thf)$_4$] (3.1)** in C_6D_6.

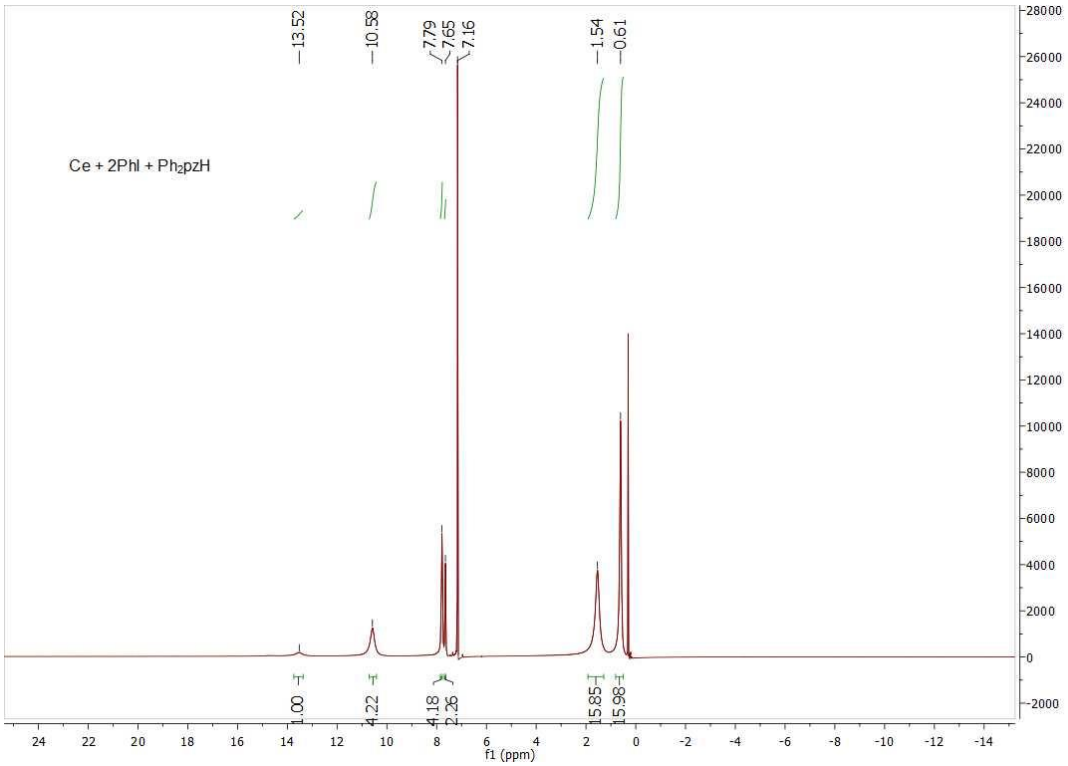


Figure 3.2: ^{1}H NMR spectrum of **[Ce(Ph$_2$pz)I$_2$(thf)$_4$] (3.2)** in C_6D_6.

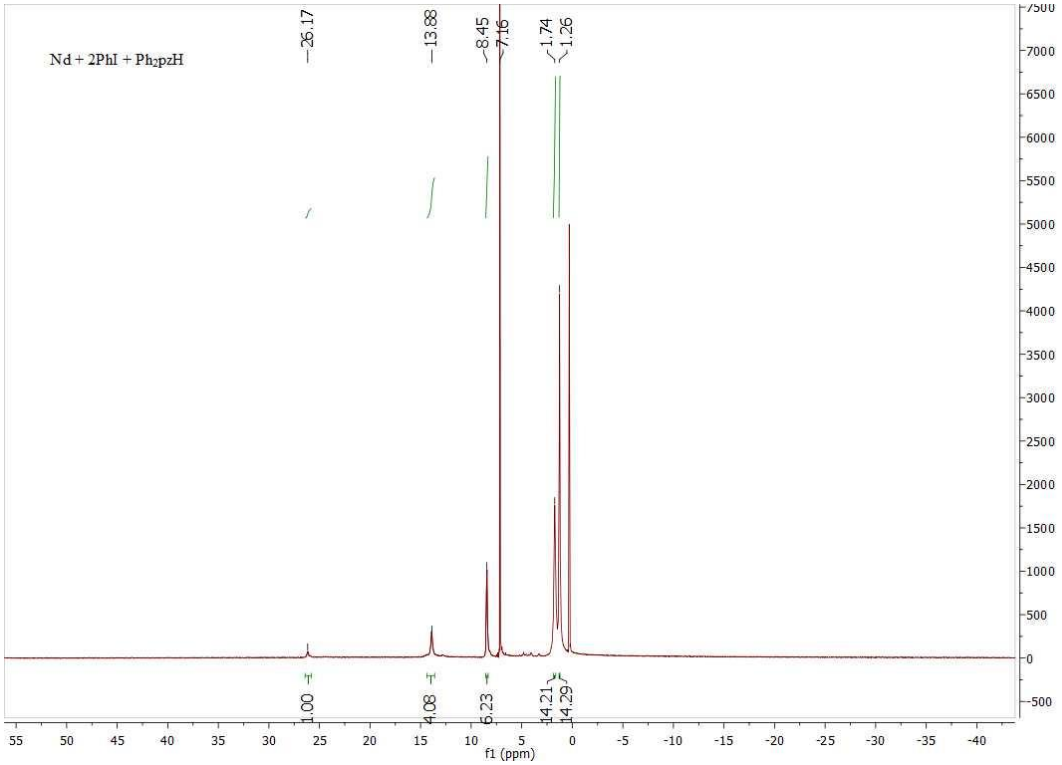


Figure 3.3: ^{1}H NMR spectrum of **[Nd(Ph$_2$pz)I$_2$(thf)$_4$] (3.3)** in C_6D_6.

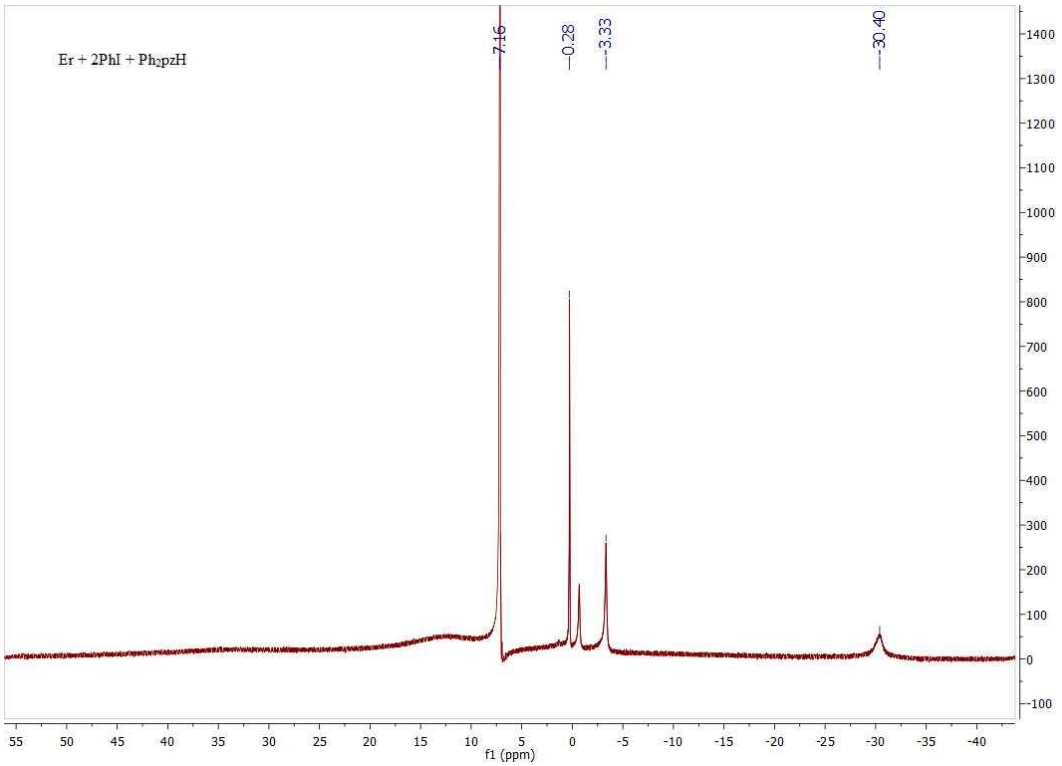


Figure 3.4: ^{1}H NMR spectrum of **[Er(Ph$_2$pz)I$_2$(thf)$_3$]·thf (3.4)** in C_6D_6.

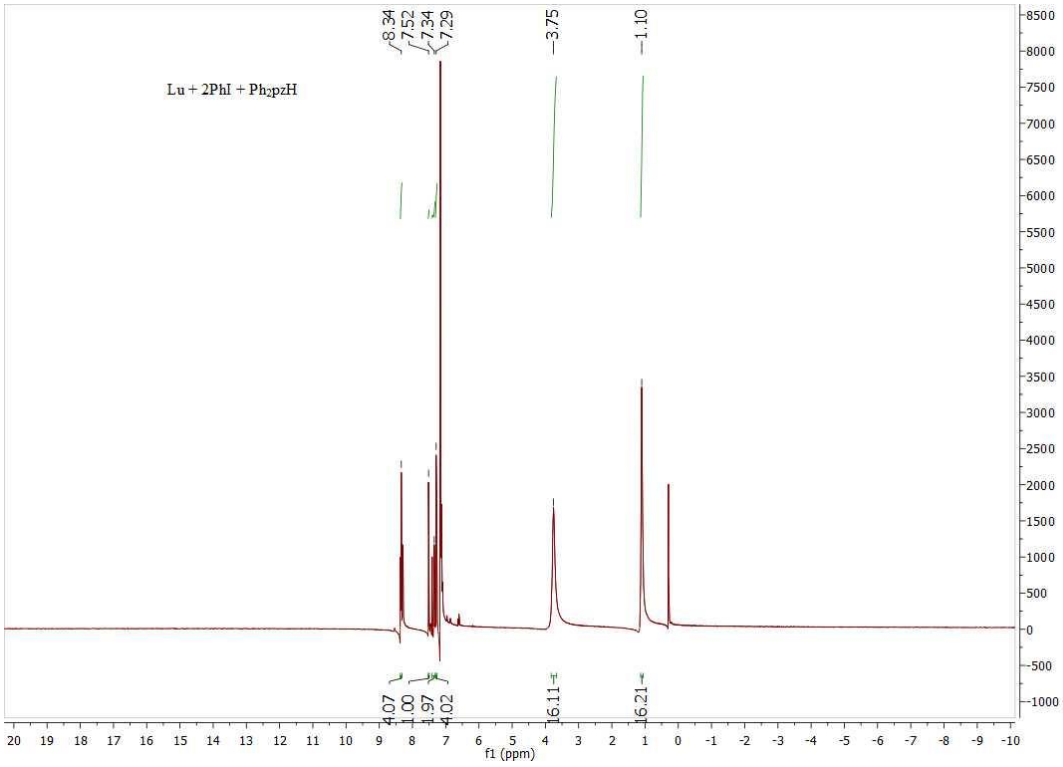
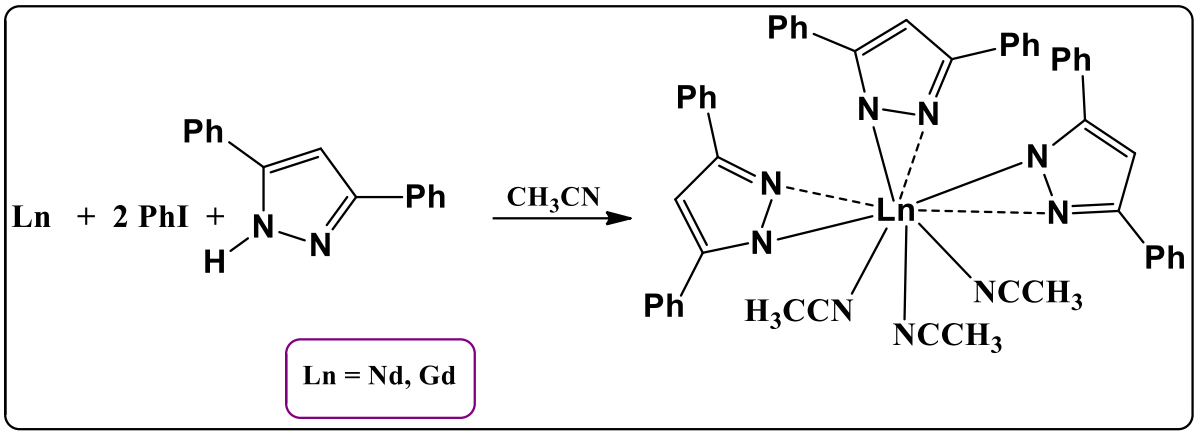


Figure 3.5: ^{1}H NMR spectrum of **[Lu(Ph$_2$pz)I$_2$(thf)$_3$] (3.5)** in C_6D_6.

3.3.1.2 The reaction of lanthanoid (Nd and Gd) pseudo-Grignard reagents with Ph$_2$pzH in acetonitrile (CH$_3$CN)

The primary objective of these reactions was to synthesise trivalent lanthanoid pseudo-Grignard compounds, specifically those of Nd and Gd. The reactions were conducted using a 2:1 stoichiometric ratio of PhI and the proligand Ph$_2$pzH, with an excess of lanthanoid (Nd **3.6** and Gd **3.7**) metal filings in acetonitrile (CH_3CN) at 25 °C. The mixture of lanthanoid metals and PhI was activated with a single drop of Hg, sonicated for 10 m and stirred for 5 to 10 h at room temperature, resulting in a light brown solution of [Ph$_3$Ln(CH_3CN)$_n$].

Solid Ph$_2$pzH (0.22g, 1.0 mmol) was then added to the mixture, which was stirred at 0 °C for 1 h. After stirring for 24 h at room temperature, the desired coloured solution developed: blue for compound **3.6** and pale-yellow for compound **3.7**. Crystallisation from the concentrated solution resulted in the formation of yellow needle crystals of [Nd(Ph$_2$pz)$_3$(CH_3CN)$_3$]·2CH_3CN (Nd **3.6**) and colourless crystals of [Gd(Ph$_2$pz)$_3$(CH_3CN)$_3$]·2CH_3CN (Gd **3.7**). The reaction and structural scheme for compounds **3.6** and **3.7** are provided in **Scheme 3.10**.



Scheme 3.10: Synthesis of compounds $[Nd(Ph_2pz)_3(CH_3CN)_3]\cdot 2CH_3CN$ (Nd **3.6**) and $[Gd(Ph_2pz)_3(CH_3CN)_3]\cdot 2CH_3CN$ (Gd **3.7**).

Satisfactory ^1H NMR spectra were obtained for compound **3.6** (**Fig. 3.6**). The NMR spectrum indicated the loss of one acetonitrile molecule during crystallisation, consistent with the results of metal analysis. Compound **3.7** (**Fig. 3.7**) exhibited broad features with unsatisfactory integration due to paramagnetism of Gd^{3+}. The CH-pz resonances in the ^1H NMR spectrum for compound **3.6** shifted significantly to 16.77 ppm compared to the pro- ligand value of 6.66 ppm. The CH_3 signals from acetonitrile were observed at δ = 1.65 ppm, while the CH signals from phenyl ring appeared at δ = 10.91 and 7.79 ppm. IR spectra showed the presence of the appropriate Ph_2pz ligand.

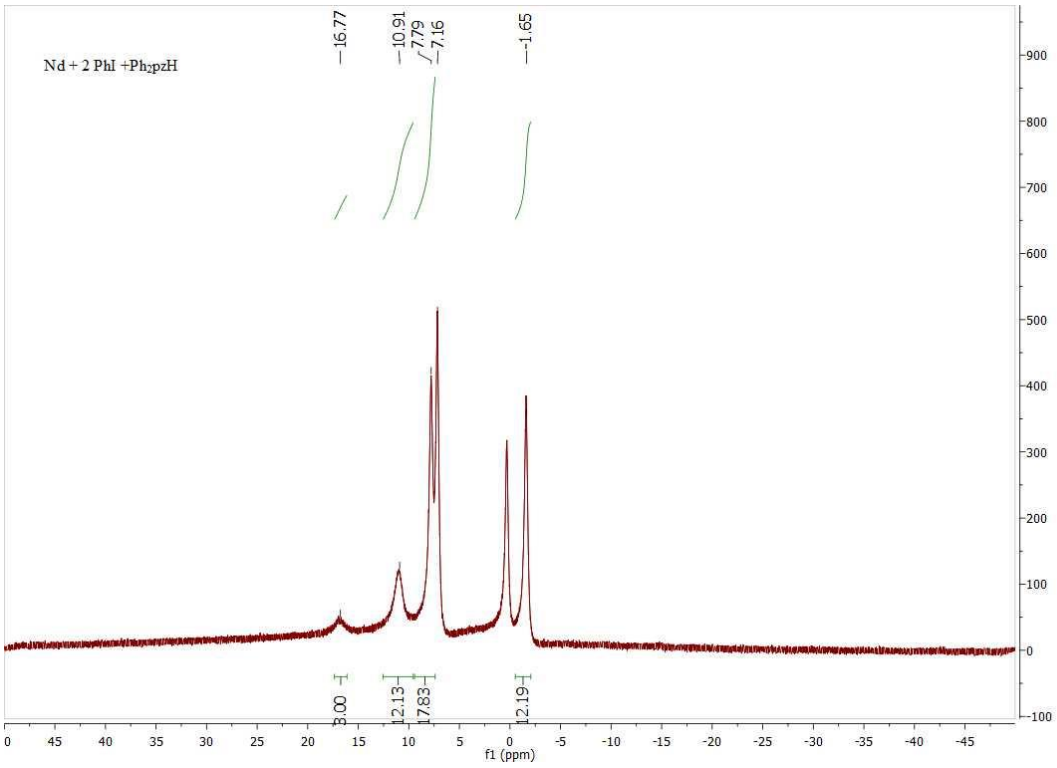


Figure 3.6: ^{1}H NMR spectrum of **[Nd(Ph$_2$pz)$_3$(CH$_3$CN)$_3$]·2CH$_3$CN (3.6)** in C_6D_6.

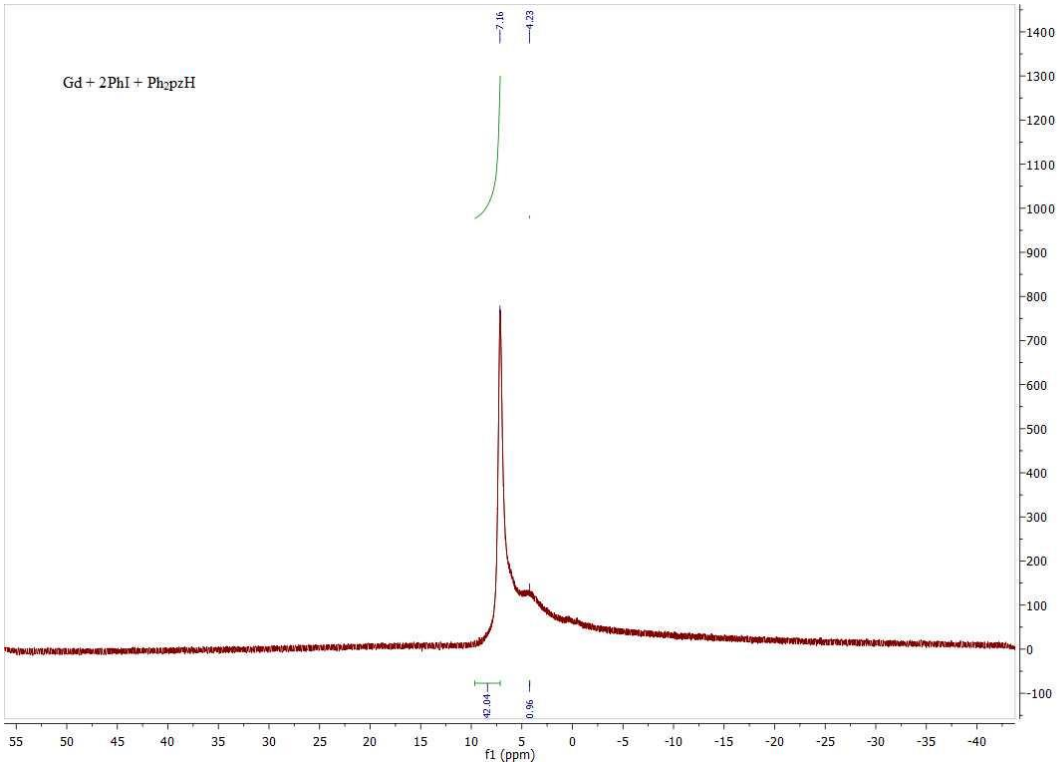


Figure 3.7: ^{1}H NMR spectrum of **[Gd(Ph$_2$pz)$_3$(CH$_3$CN)$_3$]·2CH$_3$CN (3.7)** in C_6D_6.

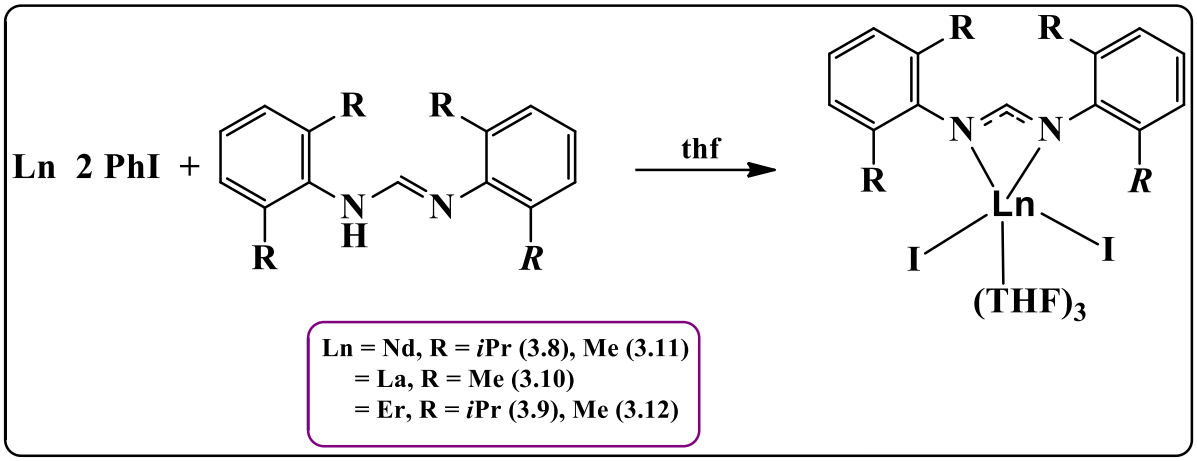
For compounds **3.6** and **3.7**; the absence of (N-H) absorption (around 3300-3400 cm^{-1}) in the infrared spectra proved the complete deprotonation of the ligands. Additionally, metal analysis validated their bulk purity. The melting points indicate significant thermal stability of the new Ph$_2$pz compounds.

3.3.1.3 The reaction of lanthanoid (La, Nd and Er) pseudo-Grignard reagents with formamidines (DippFormH or XylFormH)

The main target of these reactions was to synthesise trivalent lanthanoid pseudo-Grignard compounds, specifically those of La, Nd and Er. The reaction was conducted using a 2:1 stoichiometric ratio of PhI and the proligands DippFormH or XylFormH, with excess of lanthanoid metals filings (Nd (**3.8**, **3.11**), La **3.10** and Er (**3.9**, **3.12**)) in thf at 25 °C. The mixture of lanthanoid metals and PhI was activated with a single drop of Hg, sonicated for 10 m, and then stirred for 5 to10 h at room temperature, resulting in a light brown solution of [Ph$_p$LnI$_{2-p}$(thf)$_n$] (p = 1 or 2).

Solid proligand (DippFormH or XylFormH) (0.5 mmol) were then added to the mixture, which were stirred at 0 °C for 1 h. After stirring for 24 h at room temperature, the desired coloured

solution developed: blue for compounds **3.8** and **3.11**, pink for compounds **3.9** and **3.12** and brown for compound **3.10**. Crystallisation from the concentrated solution resulted in the formation of purple crystals of [Nd(DippForm)I_2(thf)$_3$]·thf (**3.8**), pink crystals of [Er(DippForm)I_2(thf)$_3$]·0.5thf (**3.9**), colourless crystals of [La(XylForm)I_2(thf)$_3$]·thf (**3.10**), blue crystals of [Nd(XylForm)I_2(thf)$_3$]·thf (**3.11**) and pink crystals of [Er(XylForm)I_2(thf)$_3$]·thf (**3.12**). The reaction and structural schemes for compounds **3.8** to **3.12** are illustrated in **Scheme 3.11**.



Scheme 3.11: Synthesis of compounds [Nd(DippForm)I_2(thf)$_3$]·thf (**3.8**), [Er(DippForm)I_2(thf)$_3$]·0.5thf (**3.9**), [La(XylForm)I_2(thf)$_3$]·thf (**3.10**), [Nd(XylForm)I_2(thf)$_3$]·thf (**3.11**) and [Er(XylForm)I_2(thf)$_3$]·thf (**3.12**).

Satisfactory ^{1}H NMR spectra were obtained for compounds **3.8** (**Fig. 3.8**), **3.9** (**Fig. 3.9**) **3.10** (**Fig. 3.10**) and **3.11** (**Fig. 3.11**). The NMR spectra of compounds **3.8** and **3.11** indicated the loss of one THF molecule during crystallisation, consistent with the metal analysis results. Compound **3.12** (**Fig. 3.12**) displayed broad features with unsatisfactory integration owing to paramagnetism of Er^{III}.

In compound **3.8**, the methine proton (NC*H*N) resonances shifted significantly to higher frequencies (30.10 ppm), which is in agreement with the reported resonance (30.04 ppm) for the compound prepared by the direct reaction between Nd, iodine and DippFormH.[27] The CH_2 signals from thf appeared at δ = -2.02 and 3.08 ppm, while the ^{i}Pr signals from DippForm were observed at δ = 1.19 and 4.08 ppm and CH of DippForm is at 1.37 ppm. The CH signals from phenyl ring appeared at δ = 8.43 and 10.10 ppm. For compound **3.9**, the methine proton (NC*H*N) resonances shifted significantly to 3.42 ppm, the CH_2 signals from thf were observed at δ = -6.66 and 5.69 ppm, while the ^{i}Pr signals from DippForm appeared at higher frequencies

at δ = 5.80 ppm and the CH signals of DippForm appaired at δ = -3.51 ppm. The CH signals from the phenyl ring were recorded at δ = 1.21 and 25.24 ppm.

In compound **3.10** the methine proton (NC*H*N) resonances shifted slightly to 7.72 ppm, the CH_2 signals of thf were observed at δ = 1.18 and 3.87 ppm and the CH_3 signals from XylFormH appeared at δ = 2.67 ppm. The CH signals from Ph ring were noted at δ = 6.92 and 7.01 ppm. For compound **3.11** the methine proton (NC*H*N) resonances shifted significantly to higher frequencies at 30.60 ppm, while it is at 25.93 ppm in the reported [Ce(XylForm)I_2(thf)$_3$]·1.5thf.[28] The CH_2 signals from thf were observed at δ = 2.08 ppm, merging with the CH_3 signals from XylFormH at 4.79 ppm. The CH signals from the phenyl ring appeared at δ = 8.34 and 10.10 ppm. Additionally, IR spectra showed the presence of the appropriate DippForm or XylForm ligand. For compounds **3.8-3.12**; the absence of (N-H) absorption (around 3300-3400 cm^{-1}) in the infrared spectra proved the complete deprotonation of the ligands. Micro or metal analysis established bulk purity; the latter being used when there were issues with elemental analysis. The melting points indicate significant thermal stability of the new DippForm/XylForm compounds.

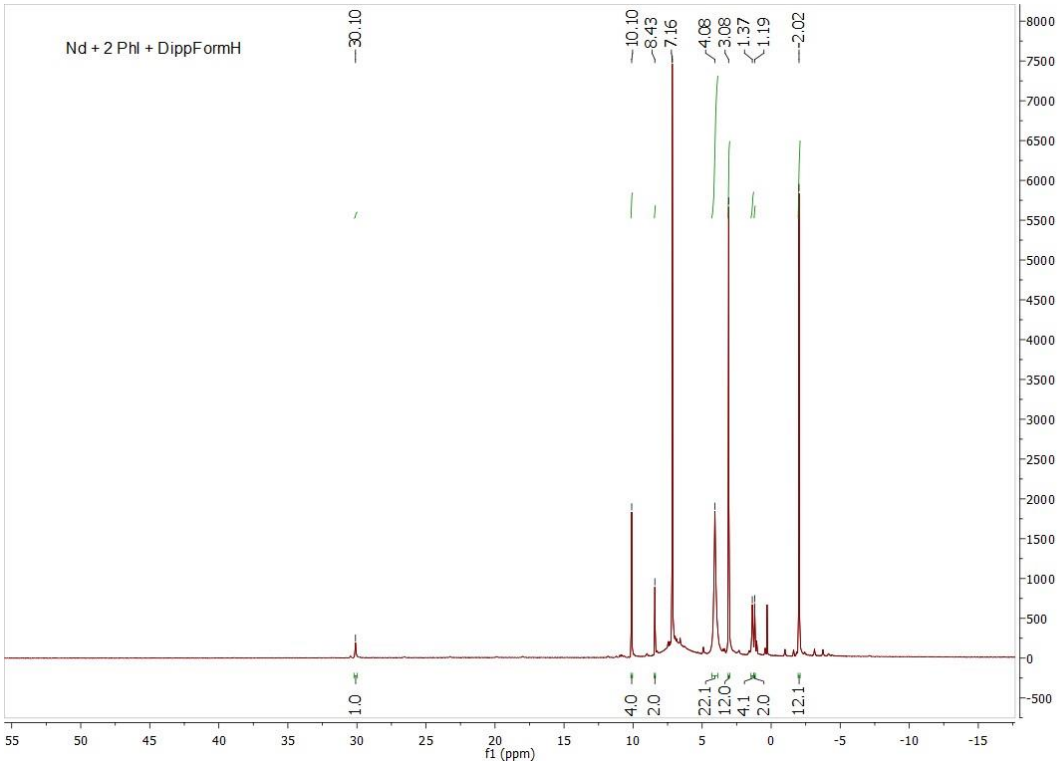


Figure 3.8: ^{1}H NMR spectrum of **[Nd(DippForm)I_2(thf)$_3$]·thf (3.8)** in C_6D_6.

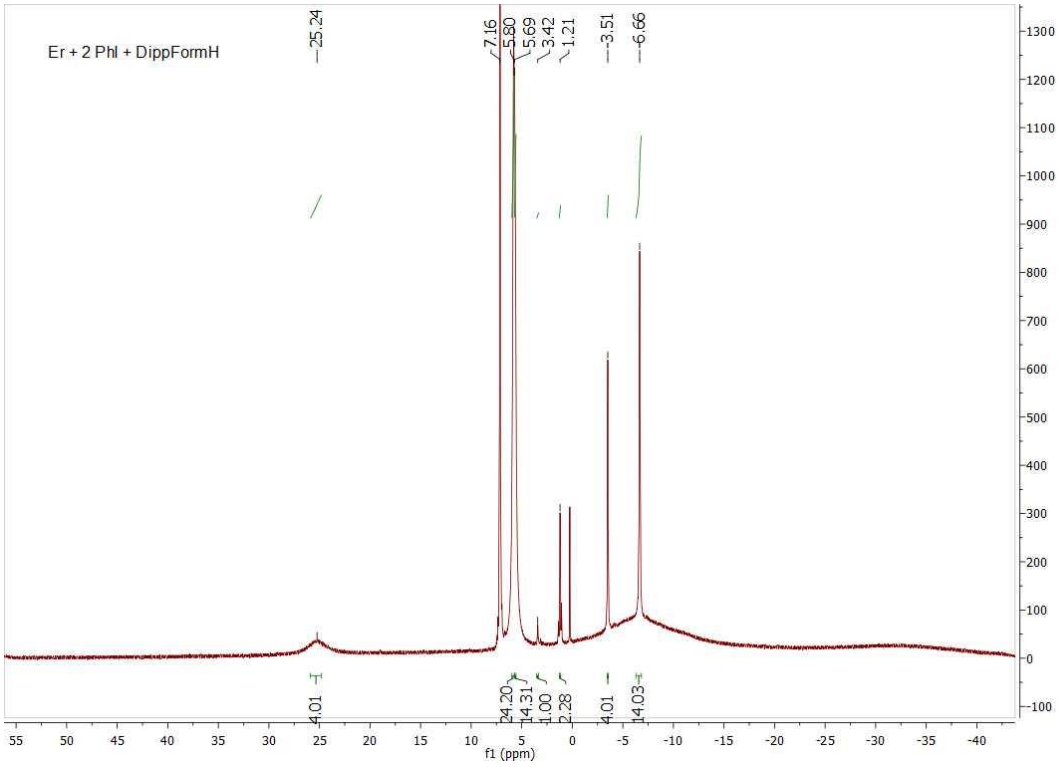


Figure 3.9: ^{1}H NMR spectrum of **[Er(DippForm)I_2(thf)$_3$]·thf (3.9)** in C_6D_6.

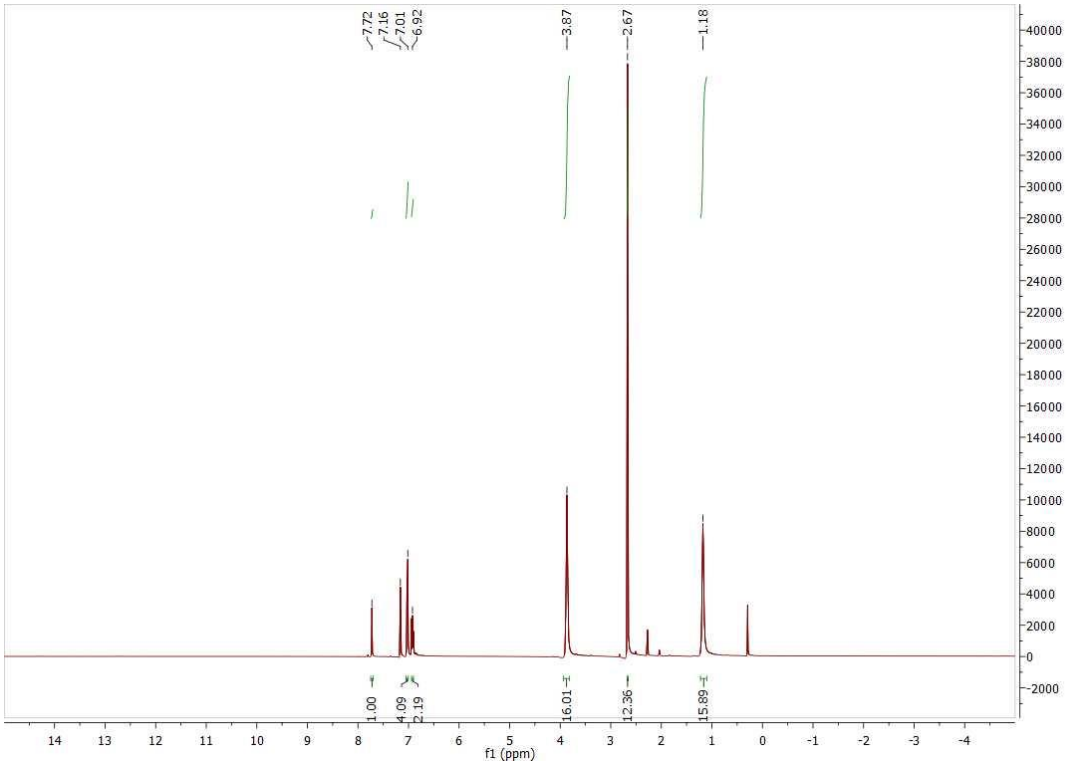


Figure 3.10: ^{1}H NMR spectrum of **[La(XylForm)I_2(thf)$_3$]·thf (3.10)** in C_6D_6.

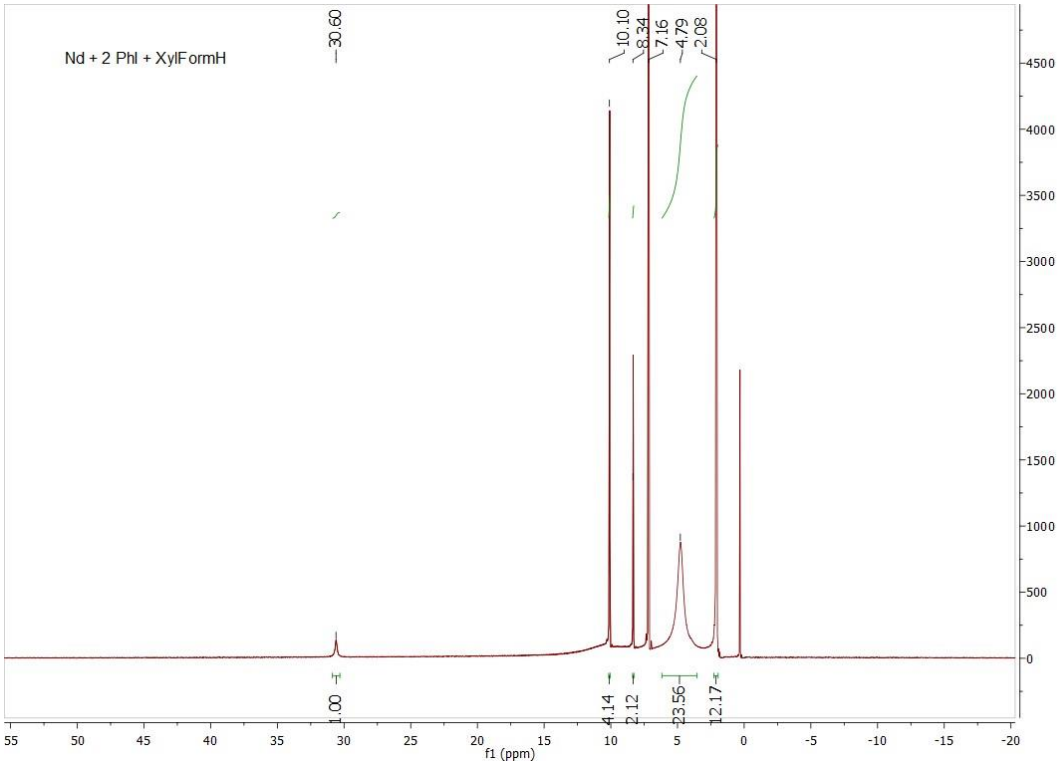


Figure 3.11: ^{1}H NMR spectrum of **[Nd(XylForm)I$_2$(thf)$_3$]·thf (3.11)** in C_6D_6.

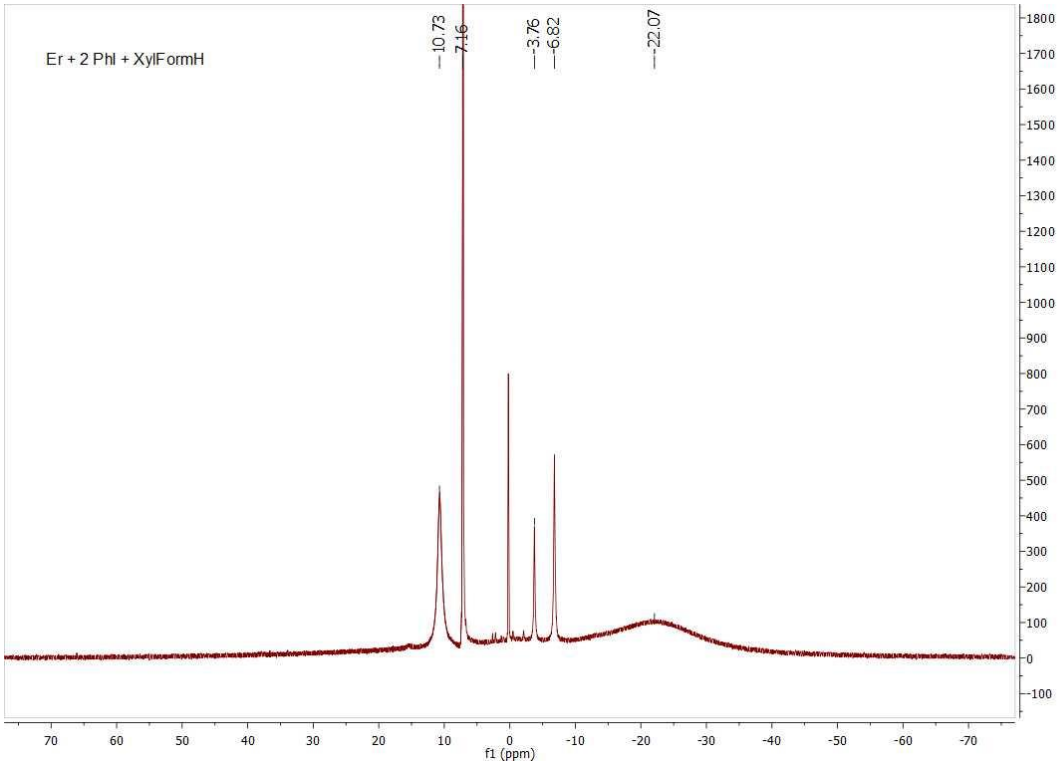
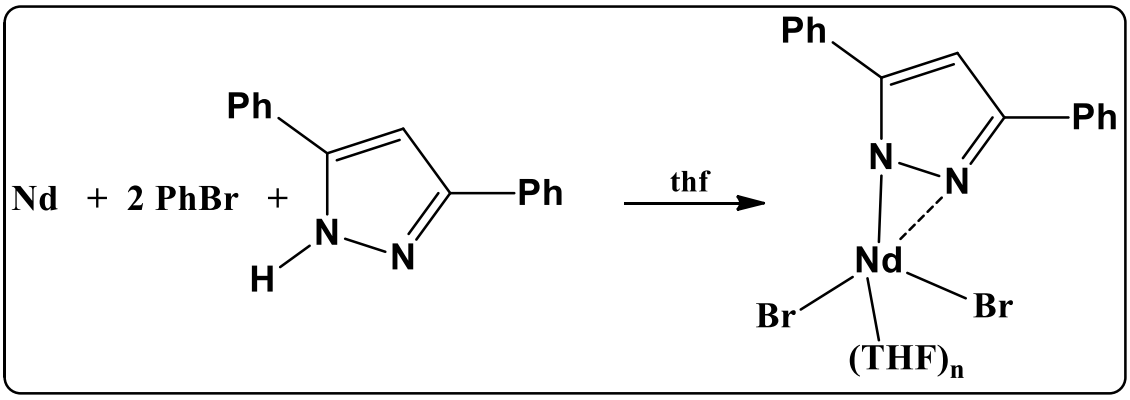


Figure 3.12: ^{1}H NMR spectrum of **[Er(XylForm)I$_2$(thf)$_3$]·thf (3.12)** in C_6D_6.

3.3.1.4 The reaction of neodymium pseudo-Grignard reagents ($PhNdBr_2$) with Ph_2pzH

The main target from this reaction was to synthesise neodymium (Nd) pseudo-Grignard reagent compounds. The reaction was conducted in a 2:1 stoichiometric ratio of PhBr and Ph_2pzH, with excess Nd (**3.13**) metals filings in thf at 25 °C. The mixture of Nd metal and PhBr was activated with one drop of Hg, sonicated for 10 min, and then stirred for 10 h at room temperature, resulting in a light brown solution of $[Ph_pNdBr_{3-p}(thf)_n]$ (p = 1 or 2). Afterward, solid Ph_2pzH (0.22g, 1.0 mmol) was added, and the mixture was stirred at 0 °C for 1 h, yielding a blue coloured solution developed after stirring for 24 h at room temperature. Crystallisation from the concentrated solution produced blue crystals of $[Nd(Ph_2pz)Br_2(thf)_{3.5}]$ (**3.13**). The reaction and structural scheme of the compound **3.13** is illustrated in **Scheme 3.12**.



Scheme 3.12: Synthesis of compounds $[Nd(Ph_2pz)Br_2(thf)_n]$ (**3.13**) (n = 3 or 4).

The ^1H NMR spectra of compound **3.13** (**Fig. 3.13**) indicated the loss of two solvated THF molecules compared with the X-ray crystal structure analysis but was consistent with the results of the metal analysis. The CH-pz resonances in the NMR for compound **3.13** shifted significantly to 20.07 ppm compared to the pro- ligand value of 6.66 ppm. The CH_2 signals from thf were observed at δ = -8.33 and -4.27 ppm, while the CH signals from the phenyl ring appeared at δ = 8.19, 8.38 and 13.85 ppm. Additionally, IR spectra showed the presence of the appropriate Ph_2pz ligand. The absence of (N-H) absorption (around 3300-3400 cm^{-1}) in the infrared spectra proved the complete deprotonation of the ligand. Furthermore, the metal analysis confirmed the bulk purity.

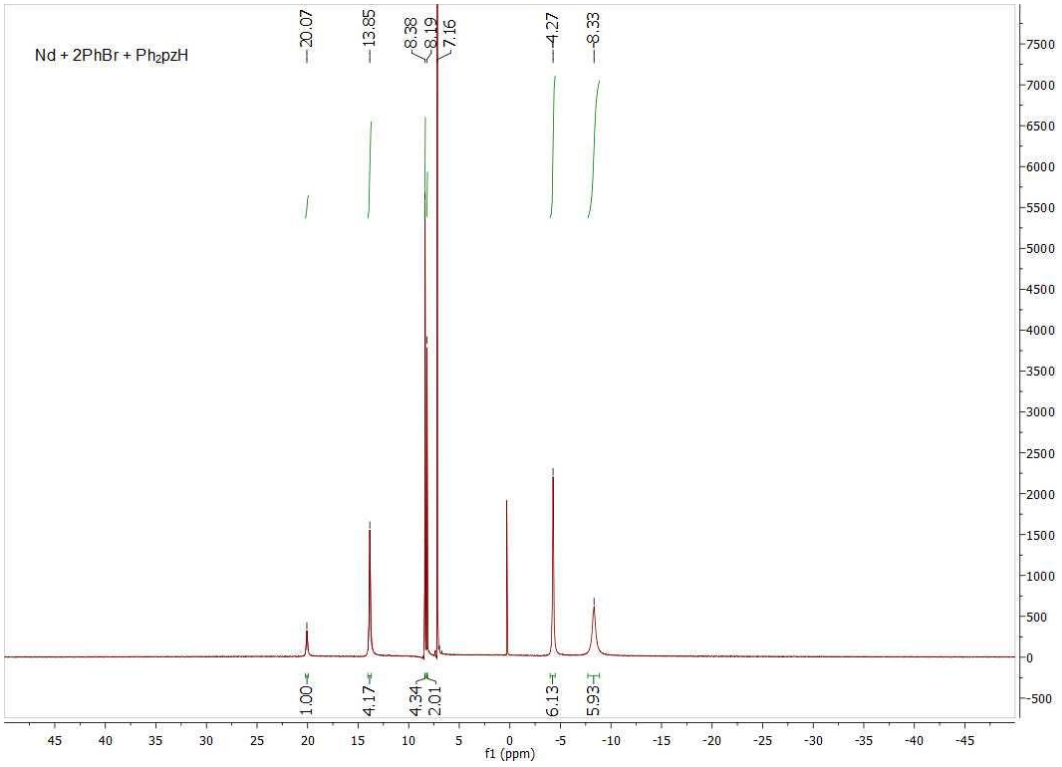


Figure 3.13: ^{1}H NMR spectrum of **[Nd(Ph$_2$pz)Br$_2$(thf)$_{3.5}$] (3.13)** in C_6D_6.

3.3.2 X-ray Crystal Structures

3.3.2.1 [Ln(Ph$_2$pz)I$_2$(thf)$_4$] (La **3.1**, Ce **3.2** and Nd **3.3**)

Isomorphous compounds [Ln(Ph$_2$pz)I$_2$(thf)$_4$] (**3.1**-**3.3**) were isolated in the triclinic space group *P*-1, where two molecules present in each unit cell. The coordination geometry of these monomeric compounds (**3.1**-**3.3**) is characterised as square antiprism, where the eight-coordinate metal centre is coordinated by one η^2-Ph$_2$pz ligand, four thf ligands and two *transoid* iodine ligands (**Fig. 3.14**). The I(1)-Ln-I(2) bond angles are measured at 155.95(5)°, 156.18(8)° and 156.28(3)° for compounds **3.1** to **3.3** respectively. The iodide ligands are *cisoid* to the Ph$_2$pz ligand, with bond angles I(1)-La-C(8) at 100.27° and I(2)-La-C(8) at 103.33°; I(1)-Ce-C(8) 99.23° and I(2)-Ce-C(8) 103.69° and I(1)-Nd-C(8) 100.21° and I(2)-Nd-C(8) 102.89°. The lanthanoid contraction is evident in the average Ln-N bond lengths of the complexes (**3.1** to **3.3**): La-N (2.52)> Ce-N (2.49)> Nd-N (2.45). These three pseudo-Grignard compounds (**3.1**-**3.3**) are the first compounds isolated using Ph$_2$pzH ligand.

The bite angles (N(1)-Ln-N(2)) for these compounds are 31.644(2)°, 31.950(4)° and 32.400(3)° respectively. These bite angles are comparable to the seven coordinate trivalent ytterbium compound [Yb(Ph$_2$pz)I$_2$(thf)$_3$], which has a bite angle of 35.200(4)°.[27] The <La-N> bond

length of 2.521(13) Å is very close to the 2.534(3) Å observed in the nine coordinate compound [La(Ph$_2$pz)$_3$(thf)$_3$], [32] while the average Ce-N bond length of 2.495(2) Å in nine coordinate compound [Ce(Ph$_2$pz)$_3$(thf)$_3$].[32] The average Nd-N bond length of 2.455(9) Å is smaller than that in the seven coordinate compound {2-[Ph$_2$P(O)]C$_6$H$_4$NC(Bu^t)N(2,6-Me$_2$C$_6$H$_3$)}NdI$_2$(thf)$_2$ where the ligand is bulkier.[33] These variations are attributed to the effect of ionic radius and different coordination numbers (eight coordinate La^{3+} 1.16 Å < nine coordinate La^{3+} 1.216 Å, eight coordinate Ce^{3+} 1.143 Å < nine coordinate Ce^{3+} 1.196 Å and eight coordinate Nd^{3+} 1.109 Å > seven coordinate Nd^{3+} 0.983 Å).[34]

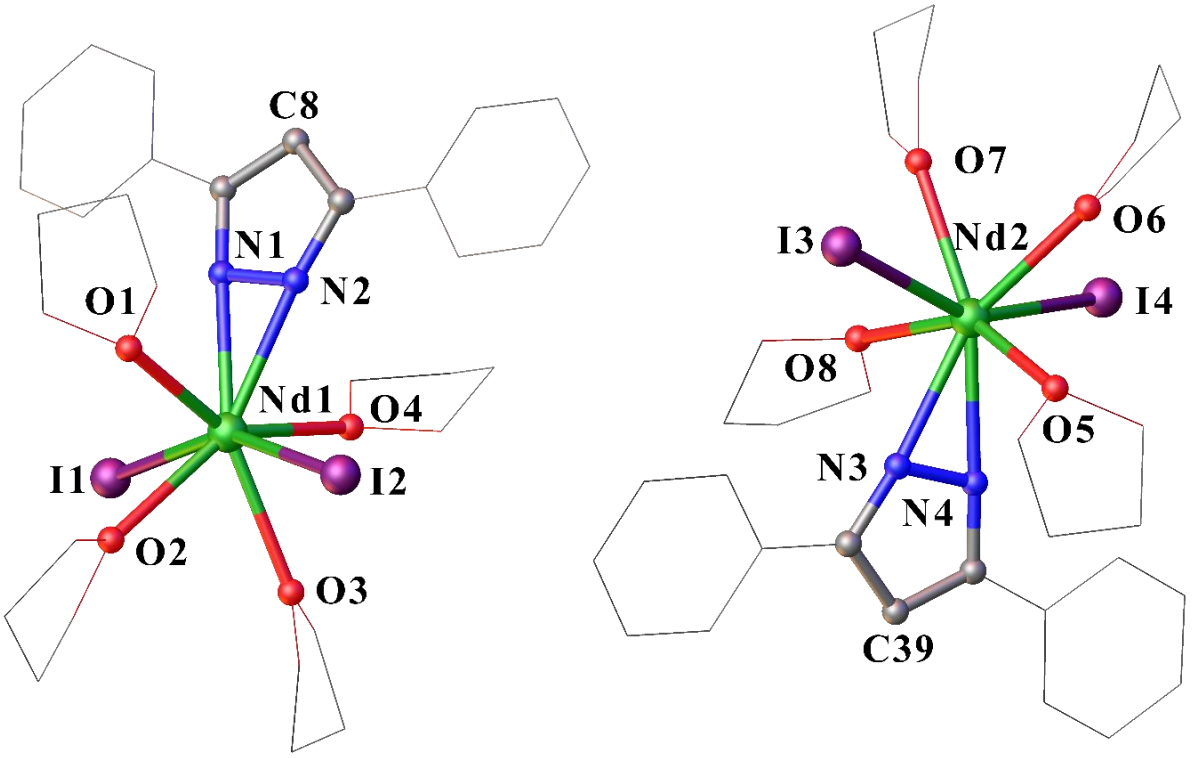


Figure 3.14: Molecular diagram of [Nd(Ph$_2$pz)I$_2$(thf)$_4$] (also representative of La **3.1** and Ce **3.2**). Thermal ellipsoids are set at the 50% probability level. Hydrogen atoms are omitted and coordinated thf molecules and Ph groups are drawn as wireframe for clarity. Selected bond lengths (Å): La(1)-N(1) 2.525(14), La(1)-N(2) 2.516(13), La(1)-N(3) 2.535(12), La(1)-N(4) 2.504(13), La(1)-I(1) 3.213(2), La(1)-I(2) 3.221(3), La(1)-I(3) 3.211(3), La(1)-I(4) 3.205(3); Ce(1)-N(1) 2.50(2), Ce(1)-N(2) 2.49(2), Ce(1)-N(3) 2.50(3), Ce(1)-N(4) 2.48(3), Ce(1)-I(1) 3.198(3), Ce(1)-I(2) 3.201(3), Ce(1)-I(3) 3.200(3), Ce(1)-I(4) 3.184(3); Nd(1)-N(1) 2.458(9), Nd(1)-N(2) 2.451(9), Nd(1)-N(3) 2.449(10), Nd(1)-N(4) 2.467(10), Nd(1)-I(1) 3.161(13), Nd(1)-I(2) 3.169(12), Nd(1)-I(3) 3.149(15), Nd(1)-I(4) 3.165(15). For more details, see the **Table 3.4**. The data for the complexes were not optimal leading to refinement issues and

therefore the crystal structures of **3.1** and **3.2** are reported for connectivity only but does establish proof of concept of synthetic utility.

The average La-I bond length in compound **3.1** is 3.217(3) Å, which is slightly longer than the 3.167(4) Å observed in the seven coordinate compound [La(DippForm)I_2(thf)$_3$].[28] The <Ce-I> bond length in compound **3.2** is 3.199(3) Å, which is 0.054 Å higher than 2.145(13) A° in the seven coordinate compound [Ce(DippForm)I_2(thf)$_3$].[28] In compound **3.3**, the average Nd-I bond length is 3.167(12) Å, comparable to 3.115(4) Å in the seven coordinate compound [Nd(DippForm)I_2(thf)$_3$], [27] consistent with the change in coordination number.[34] The average Ln-O bond length in compounds **3.1** to **3.3** is 2.545(12) Å, 2.556(10) Å, 2.524(8) Å respectively, these are longer than the 2.323(12) Å observed in the seven coordinate compound [Yb(Ph$_2$pz)I_2(thf)$_3$].[5]

Table 3.2: A comparison of the selected average bond lengths (Å) for compounds **3.1**-**3.3** with similar compounds.

Compounds	<Ln-N>	<Ln-I>	<Ln-O>	Ref.
[La(Ph$_2$pz)I_2(thf)$_4$]	2.521(13)	3.217(3)	2.545(12)	Current work
[Ce(Ph$_2$pz)I_2(thf)$_4$]	2.495(2)	3.199(3)	2.556(10)	Current work
[Nd(Ph$_2$pz)I_2(thf)$_4$]	2.455(9)	3.167(12)	2.524(8)	Current work
[La(Ph$_2$pz)$_3$(thf)$_3$]	2.534(3)		2.606(3)	[32]
[Ce(Ph$_2$pz)$_3$(thf)$_3$]	2.491(3)		2.593(2)	[32]
[Nd(Ph$_2$pz)$_3$(thf)$_3$]	2.459(9)		2.534(8)	[35]
[La(DippForm)I_2(thf)$_3$]	2.519(3)	3.167(4)	2.555(3)	[28]
[Ce(DippForm)I_2(thf)$_3$]	2.495(10)	2.145(13)	2.521(9)	[28]
[Nd(DippForm)I_2(thf)$_3$]	2.469(4)	3.115(4)	2.499(3)	[27]
[Yb(Ph$_2$pz)I_2(thf)$_3$]	2.249(14)	2.991(13)	2.323(12)	[5]

3.3.2.2 [Er(Ph$_2$pz)(Ph)I(thf)$_3$]·thf (**3.4a**), [Er(Ph$_2$pz)I_2(thf)$_3$] (**3.4**)

Compound [Er(Ph$_2$pz)(Ph)I(thf)$_3$] (**3.4a**) crystallised in the monoclinic space group $P2_1/c$. The coordination geometry of this monomeric compound is described as pentagonal bipyramid. The seven-coordinate metal centre is coordinated by one η^2-Ph$_2$pz ligand, one phenyl (Ph)

ligand, one iodine ligand and three thf ligands (**Fig. 3.15**). The phenyl (Ph) ring is positioned *cisoid* to both the Ph_2pz (C(21)-Er-C(8) 96.861°) and iodide (C(21)-Er-I(1) 98.309(11)°) ligands. The iodide ligand is *transoid* to the Ph_2pz ligand (I(1)-Er-C(8) bond angle is 164.783°). The bond angles between the iodine and thf molecules vary from 79.420(7)° to 88.760(7)°. The average Er-N bond length of 2.313(3) Å is smaller than for the seven coordinated compound $[Er(DFForm)_2I(thf)_2]$ [27] attributable to the bulkier Form ligand. The Er-I bond length in compound **3.4a** is 3.071(6) Å, which is very close to 3.082(3) Å in six coordinate compound $[Er(CH_2C_6H_5)_2I(thf)_3]$.[36] The average Er-O bond length (2.386(3) Å) in compound **3.4a** is longer with the average Er-O bond length 2.358(2) Å in that compound, [36] with the differences attributed to the effect of ionic radius (seven coordinate Er^{3+} 0.945 Å > six coordinate Er^{3+} 0.89 Å) and differing coordination number.[34]

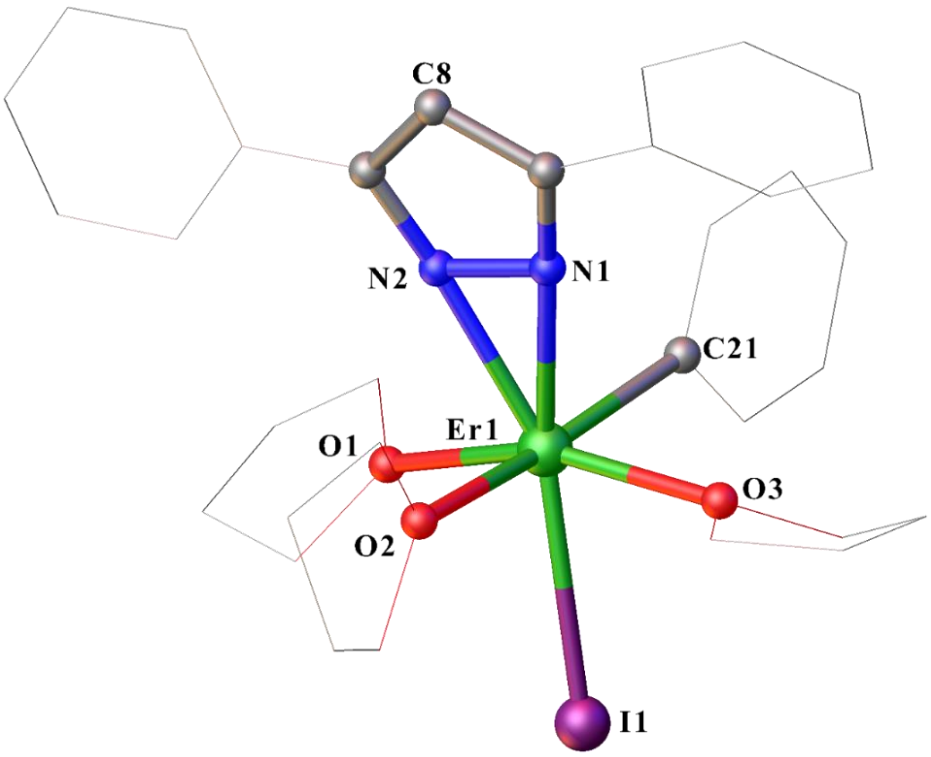


Figure 3.15: Molecular diagram of $[Er(Ph_2pz)(Ph)I(thf)_3]\cdot thf$ (**3.4a**). Hydrogen atoms and lattice thf molecules are omitted and coordinated thf molecules and Ph groups are drawn as wireframe for clarity and thermal ellipsoids are set at the 50% probability level. Selected bond lengths (Å): Er(1)-N(1) 2.309(3), Er(1)-N(2) 2.318(3), Er(1)-C(21) 2.396(4), Er(1)-I(1) 3.0709(6), Er(1)-O(2) 2.459(3). For more details, see the **Table 3.4**.

A second compound $[Er(Ph_2pz)I_2(thf)_3]$ (**3.4**), was isolated from the mother liquor of compound **3.4a** and crystallised in the monoclinic space group *C*2/c. The coordination geometry of this seven-coordinate monomeric compound (**3.4**) is described as pentagonal bipyramid, with the metal centre coordinated to one chelating Ph_2pz ligand, two iodide ligands and three thf ligands (**Fig. 3.15**). The Ph_2pz ligand is positioned *cisoid* to both iodide ligands, with bond angles of C(8)-Er-I(1) 93.004° and C(8)-Er-I(2) 97.784°. The iodide ligands are *transoid* to each other, with an I(1)-Er-I(2) bond angle of 169.066(13)°.

The bond angles between the Ph_2pz and thf molecules are as follows: C(8)-Er-O(1) 98.114°, C(8)-Er-O(2) 99.798° and C(8)-Er-O(3) 176.256°. The average Er-N bond length of 2.270(4) Å is comparable to the 2.267(3) Å found in the five coordinate compound $[Er(L)I_2(thf)]$ (L= ArNC(Me)CHC(Me)NAr; Ar= 2,6-^{i}Pr$_2$-C$_6$H$_3$).[37] The average Er-I bond length in compound **3.4** is 3.008(4) Å, which is greater than the 2.918(4) Å observed in compound $[Er(L)I_2(thf)]$.[37] This difference is attributed to the variations in coordination number.[34]

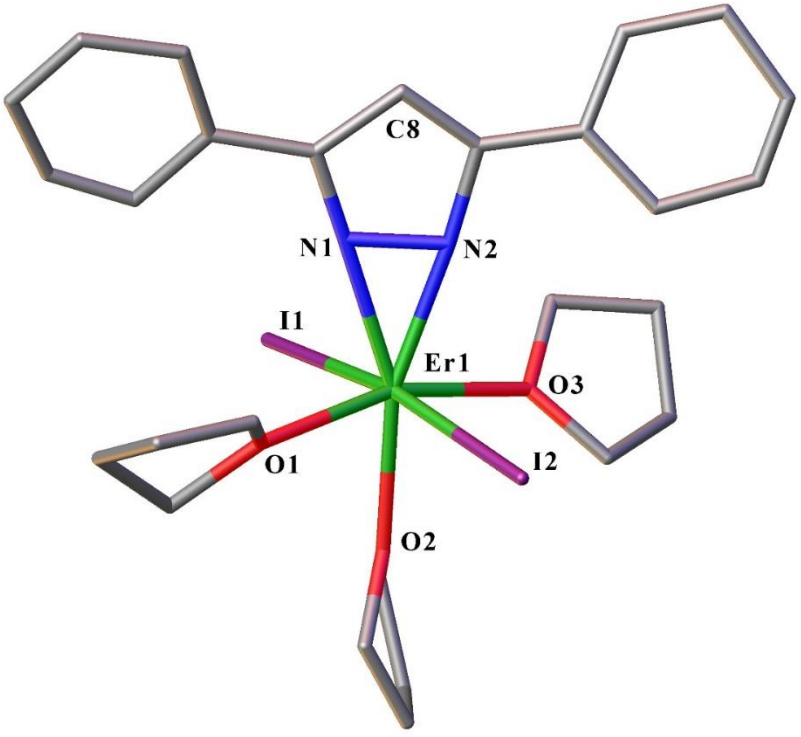


Figure 3.16: Molecular diagram of $[Er(Ph_2pz)I_2(thf)_3]$ (**3.4**) is shown in wireframe. Hydrogen atoms are omitted for clarity. Selected bond lengths (Å): Er(1)-N(1) 2.31(4), Er(1)-N(2) 2.23(5), Er(1)-I(1) 2.997(4), Er(1)-I(2) 3.019(4), Er(1)-O(2) 2.370(3). For more details, see the **Table 3.4**.

3.3.2.3 [Lu(Ph$_2$pz)I$_2$(thf)$_3$] (**3.5**)

The compound [Lu(Ph$_2$pz)I$_2$(thf)$_3$] (**3.5**) was crystallised in the monoclinic space group *C*2/c. In this compound, the lutetium atom is seven coordinated with an η^2-Ph$_2$pz ligand, two iodine atoms and three thf molecules (**Fig. 3.16**). The geometry is described as a distorted pentagonal bipyramid. The two iodine atoms are arranged in a *transoid* arrangement (I(1)-Lu-I(2) 173.750(3)°), while both are *cisoid* to the Ph$_2$pz ligand (I(1)-Lu-C(8) 92.157° and I(2)-Lu-C(8) 93.815°).

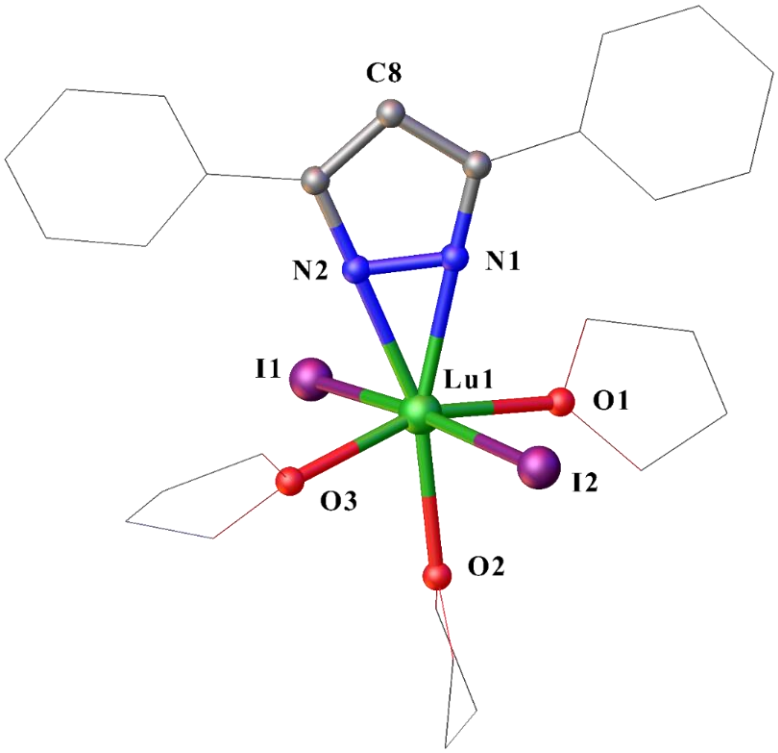


Figure 3.16: Molecular diagram of [Lu(Ph$_2$pz)I$_2$(thf)$_3$] (**3.5**). Hydrogen atoms are omitted and coordinated thf molecules and Ph groups are drawn as wireframe for clarity and thermal ellipsoids are set at the 50% probability level. Selected bond lengths (Å): Lu(1)-N(1) 2.269(10), Lu(1)-N(2) 2.252(11), Lu(1)-I(1) 2.9637(14), Lu(1)-I(2) 3.0123(14), Lu(1)-O(2) 2.361(9). For more details, see the **Table 3.4**.

The Ph$_2$pz ligand and thf O(2) are almost linear (C(8)-Lu-O(2) 177.843°), but the O(1)-Lu-O(3) angle (159.600(3)°) deviates significantly from 180°. The average Lu-N bond length in **3.5** is 2.259(10) Å, is slightly smaller than that (2.301(5) Å) of the six coordinate compound [Lu(Ap)Cl$_2$(thf)$_2$] {ApH = (2,6-diisopropylphenyl)-[6-(2,4,6-triisopropylphenyl)pyridin-2-yl]amine}), [22] with a bulkier bidentate ligand. The <Lu-O> bond length (2.315(9) Å) of

compound **3.5** is close to the average Lu-O bond length of 2.349(2) Å in compound $[Lu(ImN^{Dipp})Cl_2(thf)_3]$ { $ImN^{Dipp}H$ = 1,3-bis(2,6-diisopropylphenyl)imidazolin-2-imine }.[38]

Table 3.3: A comparison of the selected bond lengths (Å) of compounds **3.4**, **3.4a** and **3.5** with similar compounds.

Compounds	<Ln-N>	Ln-I(1)	Ln-I(2)	<Ln-O>	Ref.
$[Er(Ph_2pz)(Ph)I(thf)_3]$	2.313(3)	3.071(6)		2.386(3)	Current work
$[Er(Ph_2pz)I_2(thf)_3]$	2.270(4)	2.997(4)	3.019(4)	2.350(3)	Current work
$[Lu(Ph_2pz)I_2(thf)_3]$	2.259(10)	2.9637(14)	3.0123(14)	2.315(9)	Current work
$[Er(DFForm)_2I(thf)_2]$	2.412(2)	2.988(3)		2.301(17)	[27]
$[Er(CH_2C_6H_5)_2I(thf)_3]$		3.082(3)		2.358(2)	[36]
$[Er(Ph_2pz)_3(py)_2]\cdot 2thf$	2.345(3)				[32]
$[Er(EtForm)I_2(thf)_3]\cdot thf$	2.380(2)	3.0015(18)	3.0021(18)	2.395(17)	[28]
$[Er(DippForm)I_2(thf)_3]$	2.381(2)	3.0107(2)	3.0044(2)	2.468(15)	[28]
$[Lu(Ap)Cl_2(thf)_2]$	2.301(5)			2.2995(4)	[22]
$[Lu(EtForm)I_2(thf)_3]\cdot thf$	2.357(11)	2.9769(2)	2.9754(19)	2.369(17)	[28]
$[Lu(XylForm)I_2(thf)_3]$	2.351(9)	2.984(3)	2.975(9)	2.374(7)	[28]

Table 3.4: Selected bond lengths and angles of compounds (**3.1-3.5**).

Bond lengths (Å)	3.1	3.2	3.3	3.4a	3.4	3.5
Ln-N(1)	2.525(14)	2.50(2)	2.458(9)	2.309(3)	2.31(4)	2.268(10)
Ln-N(2)	2.516(13)	2.49(2)	2.451(9)	2.318(3)	2.23(5)	2.251(11)
N(1)-N(2)	1.375(18)	1.410(4)	1.372(12)	1.377(5)	1.430(6)	1.350(15)
$Ln\text{-}C_{(pz\text{-}centre)}$	4.564	4.513	4.481	4.326	4.299	4.289
Ln-I(1)	3.213(2)	3.198(3)	3.1605(13)	3.0709(6)	2.997(4)	2.9639(14)

Ln-I(2)/C(Ph)	3.221(3)	3.201(3)	3.1686(12)	2.396(4)	3.019(4)	3.0126(14)
Ln-O(1)	2.546(12)	2.52(2)	2.492(8)	2.358(3)	2.33(3)	2.286(9)
Ln-O(2)	2.540(12)	2.593(19)	2.543(8)	2.459(3)	2.37(3)	2.361(9)
Ln-O(3)	2.594(12)	2.568(19)	2.565(7)	2.341(3)	2.35(3)	2.287(9)
Ln-O(4)	2.620(12)	2.55(3)	2.482(8)			
Bond angles (°)	**3.1**	**3.2**	**3.3**	**3.4a**	**3.4**	**3.5**
O(1)-Ln-O(2)	147.4(4)	69.5(7)	70.2(3)	97.23(10)	83.1(12)	79.2(3)
O(1)-Ln-O(3)	141.7(4)	140.0(7)	140.5(2)	79.42(7)	162.1(12)	159.6(3)
O(1)-Ln-O(4)	69.7(4)	148.2(7)	81.48(17)			
O(2)-Ln-O(3)	70.6(4)	73.4(6)	74.9(2)	86.16(10)	79.4(12)	80.7(3)
O(2)-Ln-O(4)	141.1(4)	140.5(7)	141.5(2)			
O(3)-Ln-O(4)	75.3(4)	71.7(7)	69.7(2)			
C(8)-Ln-I(1)	103.009	103.696	100.209	164.784	93.004	93.736
C(8)-Ln-I(2)/C(Ph	100.092	99.289	102.894	96.861	97.784	92.215
I(1)-Ln-I(2)/C(Ph)	155.95(5)	156.18(8)	156.28(3)	98.29(10)	169.06(13)	173.75(3)
C(8)-Ln-O(1)	71.013	70.823	76.941	100.137	98.114	99.418
C(8)-Ln-O(2)	76.545	139.659	145.063	76.034	176.256	177.896
C(8)-Ln-O(3)	144.828	146.723	140.029	99.742	99.798	100.860
C(8)-Ln- O(4)	139.814	77.77	71.351			

3.3.2.4 $[Ln(Ph_2pz)_3(CH_3CN)_3]\cdot 2CH_3CN$ (Nd **3.6**, Gd **3.7**)

Compounds $[Ln(Ph_2pz)_3(CH_3CN)_3]$ (**3.6**, **3.7**) are isomorphous, exhibiting similar crystallographic and molecular parameters, and crystallise in the monoclinic $P2_1/c$ space group and are monomeric (**Fig. 3.17**). The nine coordinate Ln (Nd **3.6**, Gd **3.7**) metal atom is coordinated by three η^2-Ph_2pz ligands, and three CH_3CN ligands. The stereochemistry of these compounds is tricapped trigonal prism. The lanthanoid contraction is observed in the average Ln-N bond lengths <Nd-N> (2.52)> <Gd-N> (2.47).

In compound $[Nd(Ph_2pz)_3(CH_3CN)_3]$ (**3.6**) all Ph_2pz ligands are unsymmetrically η^2-bonded to neodymium, where the N-N bond distance of the Ph_2pz ligands are 1.373(4) Å [N(1)-N(2)], 1.369(4) Å [N(3)-N(4)] and 1.376(4) Å [N(5)-N(6)]. All Ph_2pz ligands are *cisoid* to each other (C(8)-Nd-C(23) 95.529°, C(8)-Nd-C(38) 95.994° and C(23)-Nd-C(38) 98.496°), as the MeCN ligands. Each CH_3CN is *transoid* to a Ph_2pz ligand (C(8)-Nd-N(8) 162.947°, C(23)-Nd-N(9) 161.916°, C(38)-Nd-N(7) 161.316°). The <Nd-N> bond length for Ph_2pz in **3.6** is 2.464(3) Å and is the same (2.467(9) Å) as in nine coordinate compound $[Nd(Ph_2pz)_3(thf)_3]$.[35] The <Nd-N> bond length for CH_3CN in **3.6** is 2.647(3) Å, which is shorter that recently observed in $[Sm\{(Ph_2P(O))_2N\}_3(CH_3CN)_3]$ (2.780(3) Å) [39] and greater than the average Nd-O bond lengths of 2.535(5) Å in $[Nd(Ph_2pz)_3(thf)_3]$ [35] and 2.556(2) Å in $[Nd(Ph_2pz)_3(dme)_2]$.[40]

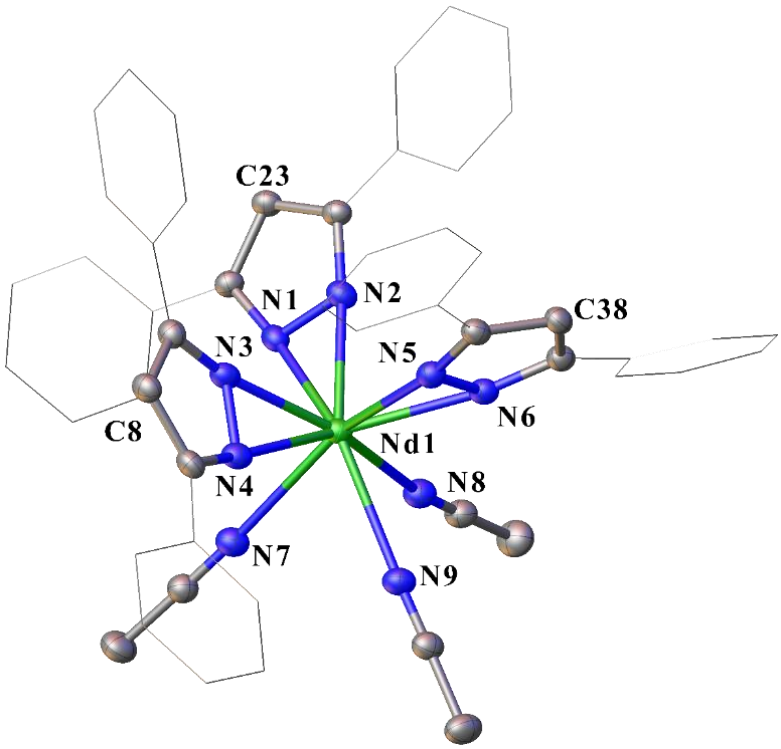


Figure 3.17: Molecular diagram of $[Nd(Ph_2pz)_3(CH_3CN)_3]\cdot 2CH_3CN$ (also representative of Gd **3.7**). Thermal ellipsoids are set at the 50% probability level. Hydrogen atoms and lattice CH_3CN molecules are omitted, and Ph groups are drawn as wireframe for clarity. Selected bond lengths (Å): Nd(1)-N(1) 2.469(3), Nd(1)-N(2) 2.450(3), Nd(1)-N(3) 2.430(3), Nd(1)-N(4) 2.506(3), Nd(1)-N(5) 2.447(3), Nd(1)-N(6) 2.476(3),Nd(1)-N(7) 2.636(3), Nd(1)-N(8) 2.657(4), Nd(1)-N(9) 2.650(3); Gd(1)-N(1) 2.425(2), Gd(1)-N(2) 2.402(2), Gd(1)-N(3) 2.436(2), Gd(1)-N(4) 2.396(2), Gd(1)-N(5) 2.379(2), Gd(1)-N(6) 2.461(2), Gd(1)-N(7) 2.573(2), Gd(1)-N(8) 2.579(2), Gd(1)-N(9) 2.579(2). For more details, see the **Table 3.6**.

Similarly, in compound $[Gd(Ph_2pz)_3(CH_3CN)_3]$ **(3.7)**, all Ph_2pz ligands are unsymmetrically η^2-bonded to gadolinium, where the N-N bond distance of the Ph_2pz ligands are 1.368(3) Å [N(1)-N(2)], 1.374(3) Å [N(3)-N(4)] and 1.371(3) Å [N(5)-N(6)]. All Ph_2pz ligands are also in a *cisoid* arrangement (C(8)-Gd-C(23) 99.113°, C(8)-Gd-C(38) 96.042° and C(23)-Gd-C(38) 96.693°). The bond angles between the MeCN ligand and the axil Ph_2pz ligands deviate significantly from 180° (C(8)-Gd-N(7) 160.982°, C(23)-Gd-N(8) 160.767°, C(38)-Gd-N(9) 162.225°).

The <Gd-N> bond length for Ph_2pz in **3.7** is 2.426(2) Å, which is statistically identical to the 2.464(6) Å observed in the nine coordinate compound $[Nd(Ph_2pz)_3(thf)_3]$.[35] The average Gd-N bond length for CH_3CN in compound **3.7** is 2.574(2) Å, which is shorter than that recently observed in $[Sm\{(Ph_2P(O))_2N\}_3(CH_3CN)_3]$ (2.780(3) Å) [39] and the average Nd-N bond length in compound **3.6** (2.647(3) Å). This phenomenon can be attributed to the differences in ionic radii, with the nine coordinate Gd^{3+} (1.107 Å) being smaller than the nine coordinate Nd^{3+} (1.163 Å).[34]

Table 3.5: A comparison of the selected bond lengths (Å) of compounds **3.6** and **3.7** with similar compounds.

Compounds	<Ln-N> (ligand 1)	<Ln-N> (ligand 2)	<Ln-N> (ligand 3)	<Ln-O> Solv.	Ref.
$[Nd(Ph_2pz)_3(CH_3CN)_3]$	2.459(3)	2.468(3)	2.462(3)	2.651(3)	Current work
$[Gd(Ph_2pz)_3(CH_3CN)_3]$	2.413(2)	2.416(2)	2.421(2)	2.577(2)	Current work
$[Nd(Ph_2pz)_3(thf)_3]$	2.485(8)	2.456(9)	2.439(10)	2.535(5)	[35]
$[Nd(Ph_2pz)_3(dme)_2]$	2.461(3)	2.547(3)	2.457(2)	2.553(2)	[40]
$[Sm\{(Ph_2P(O))_2N\}_3(CH_3CN)_3]$				2.780(3)	[39]
$[Er(Ph_2pz)_3(OPPh_3)_2]$	2.333(12)	2.322(17)	2.378(12)	2.207(9)	[35]
$[Gd(Ph_2pz)_3(Ph_2pzH)_2]$	2.405(2)	2.465(5)	2.383(2)		[41]
$[Dy(Ph_2pz)_3(Py)_2]$	2.373(3)	2.321(3)	2.351(2)	2.500(2)	[32]
$[Eu(tBu_2pz)_3(py)_2]$	2.382(2)	2.418(2)	2.404(2)	2.571(2)	[42]

Table 3.6: Selected bond lengths and angles of compounds (**3.6** and **3.7**).

Bond lengths (Å)	**3.6**	**3.7**	**Bond lengths (Å)**	**3.6**	**3.7**
Ln-N(1)	2.469(3)	2.425(2)	Ln-N(9)	2.650(3)	2.570(2)
Ln-N(2)	2.450(3)	2.402(2)	N(1)-N(2)	1.373(4)	1.368(3)
Ln-N(3)	2.430(3)	2.436(2)	N(3)-N(4)	1.369(4)	1.374(3)
Ln-N(4)	2.506(3)	2.396(2)	N(5)-N(6)	1.376(4)	1.371(3)
Ln-N(5)	2.447(3)	2.379(2)	Ln-$C_{23(pz\text{-}centre)}$	4.466	4.430
Ln-N(6)	2.476(3)	2.461(2)	Ln-$C_{8(pz\text{-}centre)}$	4.489	4.423
Ln-N(7)	2.636(3)	2.573(2)	Ln-$C_{38(pz\text{-}centre)}$	4.482	4.438
Ln-N(8)	2.657(4)	2.579(2)			
Bond angles (°)	**3.6**	**3.7**	**Bond angles (°)**	**3.6**	**3.7**
C(8)-Ln-C(23)	95.529	99.113	N(7)-Ln-N(8)	75.39(10)	74.435
C(8)-Ln-C(38)	95.994	96.039	N(7)-Ln-N(9)	74.67(10)	72.583
C(23)-Ln-C(38)	98.496	96.688	N(8)-Ln-N(9)	72.28(10)	75.324
C(8)-Ln-N(7)	87.728	160.982	C(23)-Ln-N(9)	161.916	99.548
C(8)-Ln-N(8)	162.947	99.265	C(38)-Ln-N(7)	161.316	101.434
C(8)-Ln-N(9)	101.192	88.497	C(38)-Ln-N(8)	99.257	86.966
C(23)-Ln-N(7)	99.360	86.328	C(38)-Ln-N(9)	86.642	162.225
C(23)-Ln-N(8)	89.749	160.767			

3.3.2.5 [Er(DippForm)I_2(thf)$_3$]·0.5thf (**3.9**)

Compound [Er(DippForm)I_2(thf)$_3$]·0.5thf was crystallised in the orthorhombic space group *P*bca and is isomorphous with [Ln(DippForm)I_2(thf)$_3$]0.5thf (where Ln = La, Ce, Nd, Sm, Gd, Dy, Tb, Ho, Tm), but), but the reported [Er(DippForm)I_2(thf)$_3$]·2thf crystallised in the triclinic space group with more solvent of crystallisation.[27, 28] The compound is monomeric, and the geometry of the seven coordinate Er metal is pentagonal bipyramid, with one chelating DippForm ligand, two *transoid* iodide ligands (I(1)-Er-I(2) 165.17(3)°), and three thf ligands (**Fig. 3.18**). The I(1)-Er-I(2) bond angle is 165.170(3)°, with three O atoms from thf and two N atoms occupying the equatorial plane around the Er^{III} ion. The iodide ligands are *cisoid* to

the DippForm ligand [I(1)-Er-C(13) is 96.045° and I(2)-Er-C(13) is 97.466°]. The average Er-N bond length in this compound (2.381(4) Å) is smaller than that of the seven coordinate [Gd(DippForm)I_2(thf)$_3$] (2.426(8) Å). In contrast, the <Er-I> bond length (3.028(10) Å) is shorter than that of the compound [Gd(DippForm)I_2(thf)$_3$] (3.064(9) Å).[27]

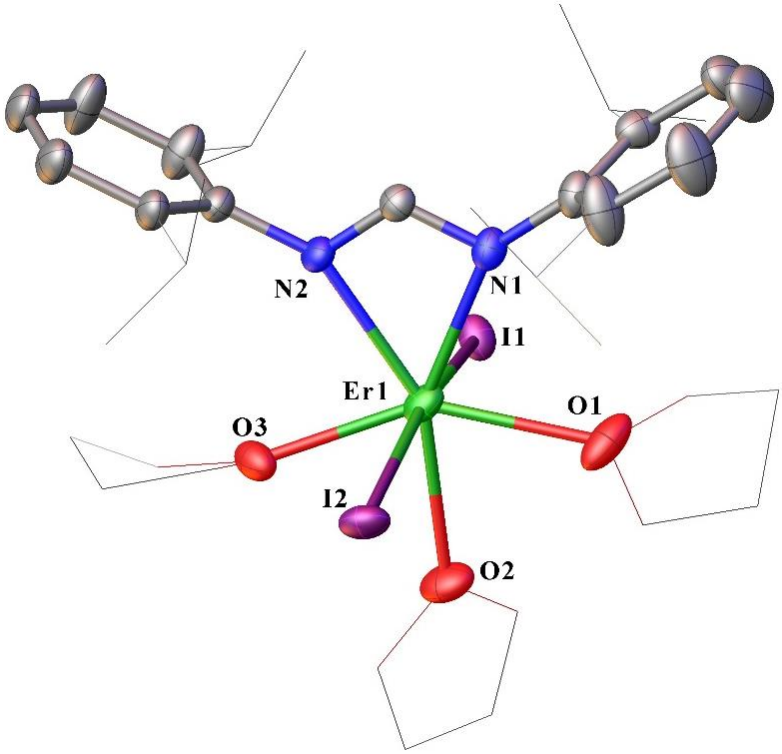


Figure 3.18: Molecular diagram of [Er(DippForm)I_2(thf)$_3$]·0.5thf (**3.9**). Hydrogen atoms and lattice thf molecules are omitted and coordinated thf molecules and *i*Pr groups are drawn as wireframe for clarity and thermal ellipsoids are set to the 50% probability level. Selected bond lengths (Å): Er(1)-N(1) 2.384(5), Er(1)-N(2) 2.378(4), Er(1)-I(1) 3.012(7), Er(1)-I(2) 3.044(12), Er(1)-O(2) 2.470(4). For more details, see the **Table 3.9**.

Table 3.7: A comparison of selected bond lengths (Å) of compound **3.9** with similar complexes.

Compounds	<Ln-N>	<Ln-X>	<Ln-O>	Ref.
[Er(DippForm)I_2(thf)$_3$]·0.5thf	2.313(3)	3.071(6)	2.386(3)	Current work
[Er(DippForm)I_2(thf)$_3$]·2thf	2.381(2)	3.0072(2)	2.468(15)	[28]
[Er(EtForm)I_2(thf)$_3$]·thf	2.380(2)	3.0018(18)	2.395(17)	[28]
[Er(EtForm)I_2(thf)$_3$]	2.367(3)	2.9927(5)	2.382(2)	[28]

[Er(DippForm)$_2$F(thf)]	2.369(2)	2.0368(14)	2.3681(17)	[43]
[Er(DFForm)$_2$I(Py)(thf)]	2.394(7)	3.0358(11)	2.317(5)	[43]

3.3.2.6 [Ln(XylForm)I$_2$(thf)$_3$]·thf (La **3.10**, Er **3.12**)

The isomorphous [Ln(XylForm)I$_2$(thf)$_3$]·thf complexes (La **3.10** and Er **3.12**) were crystallised in the monoclinic space group *C*2/c. The monomeric Ln^{III} compounds **(3.10** and **3.12)** features a seven coordinate, comprising one chelating XylForm ligand, two *transoid* iodide ligands (I(1)-La-I(2) 169.93(4)°, I(1)-Er-I(2) 170.10(2)°) and three thf ligands (**Fig. 3.19**). The geometry of both compounds are described as a distorted pentagonal bipyramid, which is similar to the reported [Ln(ArForm)I$_2$(thf)$_3$] (ArForm = DFForm or DippForm).[27]

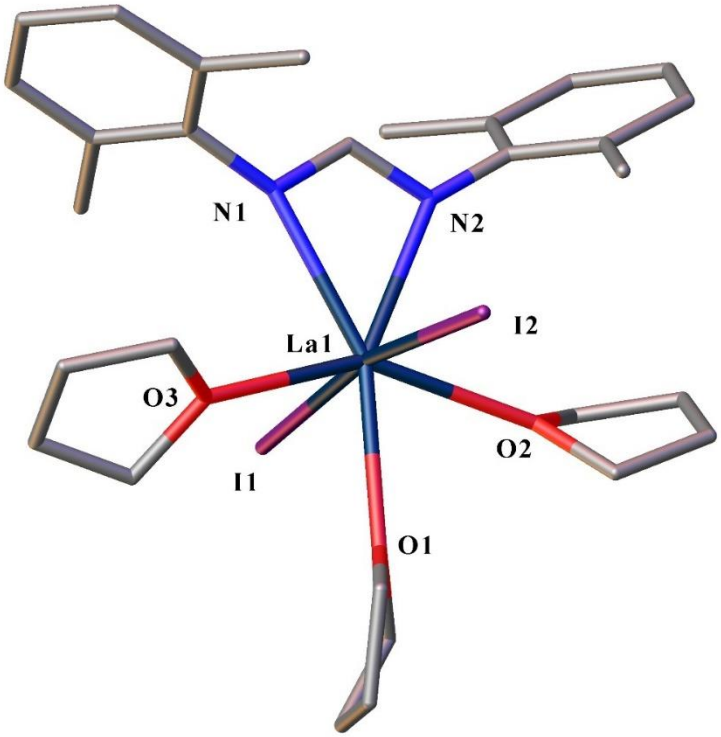


Figure 3.19: Molecular diagram of [La(XylForm)I$_2$(thf)$_3$]·thf (also representative of Er **3.12**) is shown in wireframe. Hydrogen atoms and lattice thf molecules are omitted for clarity. Selected bond lengths (Å): La(1)-N(1) 2.516(5), La(1)-N(2) 2.503(6), La(1)-I(1) 3.1765(6), La(1)-I(2) 3.1475(17), La(1)-O(2) 2.519(4); Er(1)-N(1) 2.354(9), Er(1)-N(2) 2.381(6), Er(1)-I(1) 3.008(8), Er(1)-I(2) 2.996(8), Er(1)-O(2) 2.440(6). For more details, see the **Table 3.9**.

The average bond lengths for compound **3.10** (La-N (2.509(5) Å), La-O (2.536(4) Å), and La-I (3.1577(13) Å)) and Er-N (2.367(7) Å), Er-O (2.394(6) Å), and Er-I 3.002(8) (Å) in

compound **3.12** are consistent with the lanthanoid [Ln(XylForm)$_2$I(thf)$_2$] (Ln = Nd, Gd, Tm, Lu) complexes.[28]

Table 3.8: A comparison of selected bond lengths (Å) of compounds **3.10** and **3.12** with similar complexes.

Compounds	<Ln-N>	<Ln-I>	<Ln-O>	Ref.
[La(XylForm)I$_2$(thf)$_3$]·thf	2.509(5)	3.1577(13)	2.536(4)	Current work
[Er(XylForm)I$_2$(thf)$_3$]·thf	2.367(7)	3.002(8)	2.394(6)	Current work
[Ce(XylForm)I$_2$(thf)$_3$]	2.489(3)	3.141(3)	2.516(2)	[28]
[Tm(XylForm)I$_2$(thf)$_3$]	2.362(10)	2.991(10)	2.380(8)	[28]
[Lu(XylForm)I$_2$(thf)$_3$]	2.351(9)	2.979(7)	2.374(7)	[28]
[Er(EtForm)I$_2$(thf)$_3$]·thf	2.380(2)	3.0018(18)	2.395(17)	[28]
[Lu(EtForm)I$_2$(thf)$_3$]·thf	2.357(11)	2.9761(2)	2.369(17)	[28]
[La(DippForm)I$_2$(thf)$_3$]·2thf	2.519(3)	3.168(4)	2.555(4)	[32]
[Er(DippForm)I$_2$(thf)$_3$]·2thf	2.381(2)	3.0072(2)	2.468(15)	[28]

Table 3.9: Selected bond lengths and angles of compounds (**3.9**, **3.10** and **3.12**).

Bond lengths (Å)	3.9	3.10	3.12
Ln-N(1)	2.384(5)	2.516(5)	2.354(9)
Ln-N(2)	2.378(4)	2.503(6)	2.381(6)
N(1)-N(2)	2.260	2.269	2.268
Ln-C$_{n(pz\text{-}centre)}$	2.767	2.900	2.774
Ln-I(1)	3.012	3.1765(6)	3.0086(8)
Ln-I(2)	3.0436(12)	3.1475(17)	2.9965(8)
Ln-O(1)	2.399(5)	2.586(4)	2.364(6)
Ln-O(2)	2.470(4)	2.519(4)	2.440(6)
Ln-O(3)	2.375(5)	2.504(5)	2.377(5)
Bond angles (°)	**3.9**	**3.10**	**3.12**
O(1)-Ln-O(2)	74.54(19)	73.63(15)	73.10(2)
O(1)-Ln-O(3)	148.051	74.36(15)	146.20(2)

O(2)-Ln-O(3)	73.55(16)	147.91(15)	73.20(2)
C(n)-Ln-I(1)	96.045	96.114	95.34
C(n)-Ln-I(2)	97.466	93.287	94.488
I(1)-Ln-I(2)	166.17(3)	169.93(4)	170.10(2)
C(n)-Ln-O(1)	105.309	178.659	105.757
C(n)-Ln-O(2)	179.64	106.918	178.612
C(n)-Ln-O(3)	106.63	105.046	107.989

3.9 (n = 13), **3.10**, **3.12** (n = 9)

3.3.2.7 $[Nd(Ph_2pz)Br_2(thf)_n]$ (**3.13**; n = 3 or 4)

Compound $[Nd(Ph_2pz)Br_2(thf)_n]$ (**3.13**) was isolated as triclinic space group *P*-1, with four molecules per unit cell. In all four molecules disordered in Br ligands are observed. In molecule one Br(1)-Nd(1)-Br(2) bond angle is 158.290(3)°, while the Br(1)-Nd-Br(2A) bond angle measures 144.000(5)°. All bromide ligands are in a *cis* arrangement relative to the Ph_2pz ligand, with angles of Br(1)-Nd-C(8) 101.390°, Br(2)-Nd-C(8) 100.250° and Br(2A)-Nd-C(8) 107.380°.

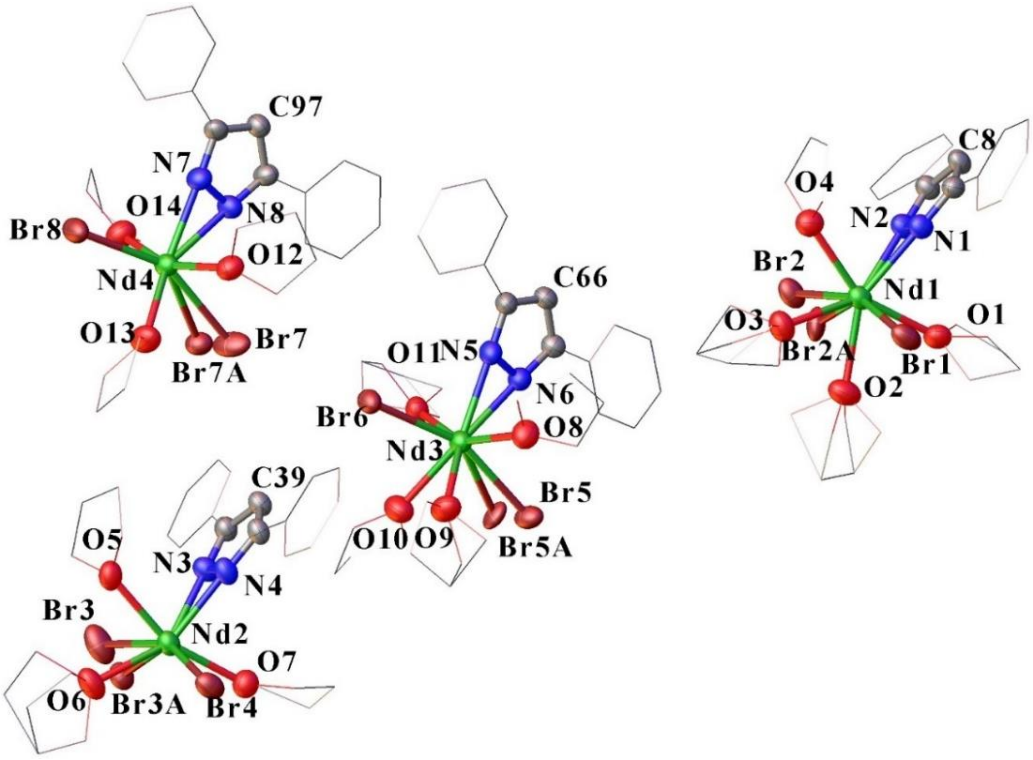


Figure 3.20: X-ray crystal structure of [Nd(Ph_2pz)Br_2(thf)$_n$] (**3.13**). Thermal ellipsoids are set at the 50% probability level. Hydrogen atoms are omitted and coordinated thf molecules and Ph groups are drawn as wireframe for clarity. Selected bond lengths (Å): Nd(1)-N(1) 2.451(6), Nd(1)-N(2) 2.445(6), Nd(1)-Br(1) 2.9048(11), Nd(1)-Br(2) 2.8815(12), Nd(1)-O(2) 2.560(6), Nd(2)-N(3) 2.425(6), Nd(2)-N(4) 2.409(6), Nd(2)-Br(3) 2.9600(7), Nd(2)-Br(4) 2.8475(11), Nd(2)-O(6) 2.496(6), Nd(3)-N(5) 2.452(6), Nd(3)-N(6) 2.438(6), Nd(3)-Br(5) 2.8855(15), Nd(3)-Br(6) 2.9040(12), Nd(3)-O(10) 2.560(6), Nd(4)-N(7) 2.411(6), Nd(4)-N(8) 2.408(6), Nd(4)-Br(7) 2.9300(6), Nd(4)-Br(8) 2.8519(13), Nd(4)-O(13) 2.508(6). For more details, see the **Table 3.10**.

The bond angles between the Ph_2pz and thf ligands are follows: C(8)-Nd-O(1) 76.820°, C(8)-Nd-O(2) 145.010°, C(8)-Nd-O(3) 143.120° and C(8)-Nd-O(4) 75.860°. The <Nd-N> bond length in molecule two is 2.417(6) Å is 0.081 Å shorter than that in the seven coordinate compound [Nd(DFForm)I_2(thf)$_3$].[27] The <Nd-Br> bond length same molecule is 2.9037(9) Å, comparable to the 2.8363(4) Å observed in the seven coordinate compound [Sm(DippForm)Br_2(thf)$_3$].[44] The <Nd-O> bond length of molecule three is 2.477(6) Å in compound **3.13** is shorter that of the six coordinate compound [Ce($NSiMe_3$)Br_2(thf)$_3$] (2.545(3) Å).[7]

Table 3.10: Selected bond lengths and angles of compounds (**3.13**).

Bond lengths (Å)	3.13	Bond angles (°)	3.13	Bond angles (°)	3.13
Nd-N(1)	2.451(6)	O(1)-Nd-O(2)	69.39(19)	Br(1)-Nd-Br(2)	158.29(3)
Nd-N(2)	2.445(6)	O(1)-Nd-O(3)	138.62(18)	Br(1)-Nd-Br(2*)	144.0(5)
Nd-Br(1)	2.9048(11)	O(1)-Nd-O(4)	152.67(18)	C(8)-Nd-O(1)	76.822
Nd-Br(2)	2.8815(12)	O(2)-Nd-O(3)	71.865	C(8)-Nd-O(2)	145.006
Nd-O(1)	2.516(6)	O(2)-Nd-O(4)	137.611	C(8)-Nd-O(3)	143.121
Nd-O(2)	2.560(6)	O(3)-Nd-O(4)	68.174	C(8)-Nd-O(4)	75.86
Nd-O(3)	2.531(6)	C(8)-Nd-Br(1)	101.39	C(8)-Nd-Br(2)	100.258

3.3.3 Discussion

Metathesis reactions have traditionally been employed to synthesise lanthanoid pseudo-Grignard complexes. Recently, a novel direct reaction involving lanthanoid metals, iodine (I_2) and corresponding formamidines has been developed, yielding pseudo-Grignard complexes with good crystalline yields. Most of the reported complexes involve ligands such as formamidinates,[27, 28] bistrimethylsilylamide or cyclopentadienyl and their derivatives.[13-17, 21-23, 30-31] Pyrazole-based Ln(III) pseudo-Grignard complexes are notably rare in Grignard chemistry. For the first time, we introduced Grignard reactions to isolate trivalent Grignard complexes. To enhance the yield, increase reaction rate and reduce initiation time, we incorporated mercury (Hg) metal to activate the lanthanoid metals.

The reaction between lanthanoid (III) metals (La, Ce, Nd, Er and Lu), PhI and Ph_2pzH, facilitated the isolation of Ln(III) complexes, such as ($[Ln(Ph_2pz)I_2(thf)_n]$ (n = 3 or 4) (**3.1-3.5**). Notably, for the Er metal, we were able to isolate a second product $[Er(Ph)(Ph_2pz)I(thf)_3]$ (**3.4a**). Larger atomic redius metals (La, Ce and Nd) yielded eight coordinated complexes, where each unit contains two molecules. In these complexes, the metal center is coordinated by one η^2-Ph_2pz ligand, four thf ligands and two *transoid* iodide ligands. In contrast, the smaller atomic redius metals (Er and Lu) formed seven coordinated complexes, which consist of one η^2-Ph_2pz ligand, two iodine atoms and three thf molecules. The proposed reaction pathway for complexes **3.1**-**3.5** is illustrated in scheme **3.13**. This pathway is compareble to the Ln(II) Grignard reactions involving lanthanoid metals (Eu, Yb), PhI and Ph_2pzH.[4]

$$Ln + 3PhI \xrightarrow{thf} PhLnI_2 + Ph_2LnI$$

$$PhLnI_2 + Ph_2pzH \xrightarrow{thf} [Ln(Ph_2pz)I_2(thf)_n + PhH$$

n = 4, Ln = La, Ce, Nd; n = 3, Ln = Er, Lu

Scheme 3.13: Possible reaction pathway of complexes ($[Ln(Ph_2pz)I_2(thf)_n]$ (n = 3 or 4).

The formation of (**3.4a**) can be attributed to protolysis of Ph_2ErI, the only case where the second product of reaction (3.3) gave rise to an isolable compound.

$$Ph_2ErI + Ph_2pzH \xrightarrow{thf} [ErPh(Ph_2pz)I(thf)_3 + PhH$$

Equation 3.3: Synthesis of $[Er(Ph)(Ph_2pz)I(thf)_3]$ (**3.4a**) complex.

The reaction of lanthanoid metals (Gd and Tb) with PhI and Ph_2pzH results in a brown solution for Gd and a light brown solution for Tb, indicating that the reactions were successful. However, due to difficulties in crystallisation, we were unable to isolate any crystalline products. Despite attempts to concentrate the solution and maintain it at a temperature (-25 °C), all efforts were unsuccessful.

When we replaced the ligand Ph_2pzH with the bulkier DippFormH or XylFormH, the reaction processes remained unaffected, resulting in the isolation of similar types of pseudo-Grignard complexes: $[Ln(DippForm)I_2(thf)_3]\cdot thf$ (**3.8** Nd, **3.9** Er), $[Ln(XylForm)I_2(thf)_3]\cdot thf$ (La **3.10**, Nd **3.11**, Er **3.12**). All the five complexes are seven coordinate, featuring one chelating formamidinate ligand, two *transoid* iodide ligands and three thf ligands. Compounds **3.8** and **3.11** were previously isolated from the direct reaction of Nd metal, I_2 and corresponding ligand.[27, 28] The proposed reaction pathway is the same as described in Scheme **3.13**. The geometry of the five complexes (**3.8**-**3.12**) is a distorted pentagonal bipyramid, similar to the reported $[Ln(ArForm)I_2(thf)_3]$ (ArForm = DFForm or DippForm).[27] In the reaction involving holmium (Ho), PhI and XylFormH, we were unable to isolate any crystalline compounds, instead, we obtained a powder.

Schlenk-type equilibria is very common in pseudo-Grignard reactions. Both the Ln^{II} and Ln^{III} complexes can undertake in different Schlenk-type equilibria, enhancing our understanding of the reaction chemistry. Typically, Ln^{II} undergoes the following Schlenk-type equilibria products.[45]

$$[RLnI]_2 \rightleftharpoons 2\ RLnI \rightleftharpoons R_2Ln + LnI_2$$

Ln^{III} can also participate in extended Schlenk equilibria, as shown in **eqn. 3.3 (i, ii)**).[46]

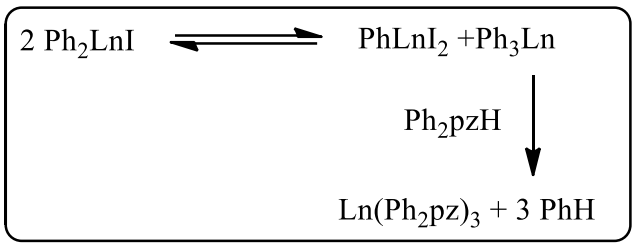
$$2RLnX_2(solv)_n \rightleftharpoons R_2LnX(solv)_n + LnX_3(solv)_n \quad (i)$$

$$2R_2LnX(solv)_n \rightleftharpoons RLnX_2(solv)_n + LnR_3(solv)_n \quad (ii)$$

Equation 3.4: Extended Schlenk equilibria for Ln(III) pseudo-Grignard reagents.[46]

To investigate the effect of solvent on Grignard complexes, we replaced thf with acetonitrile (MeCN), and observed an extension of the Schlenk equilibria. In reactions involving lanthanoid metals (Nd and Gd), PhI and Ph_2pzH in MeCN, we successfully isolated nine coordinate $[Ln(Ph_2pz)_3(CH_3CN)_3]$ (Nd **3.6**, Gd **3.7**) complexes instead of the expected seven coordinate $[Ln(Ph_2pz)I_2(CH_3CN)_3]$. This indicates that the outcomes of protolysis of the in *situ* generated

lanthanoid(III) pseudo-Grignards are solvent dependent. Similar types of complexes for trivalent lanthanoids have previously been obtained through RTP reactions.[35, 47-49] Furthermore, when we conducted the reaction of lutetium (Lu) with PhI and Ph_2pzH in MeCN, we were unable to isolate any crystalline products; instead, we obtained an oily brown solution without any solid. The proposed reaction pathway of complexes **3.6**-**3.7** is illustrated in scheme **3.14**.



Scheme 3.14: Possible reaction pathway of complexes $[Ln(Ph_2pz)_3(CH_3CN)_3]$ (Nd **3.6**, Gd **3.7**).

In chapter two, we were unable to isolate Grignard complexes from the reaction between divalent lanthanoid metals (Sm, Eu), PhBr and Ph_2pzH in thf. Instead, we isolated complexes of the form $[Ln(Ph_2pz)_n]$ (n = 3, Ln = Sm; n = 2, Ln = Eu). This this chapter, we conducted a reaction with neodymium (Nd), PhBr and Ph_2pzH in thf, successfully yielding the complex $[Nd(Ph_2pz)Br_2(thf)_{3.5}]$ (**3.13**), which contains four molecules in one unit. Complex **3.13** exhibits mixed coordination, with two molecules are eight coordinate and the remaining two being seven coordinates. This finding indicates that, Grignard reactions based on PhBr can be effective with trivalent lanthanoid metals.

Overall, in chapter three, we aimed to explore trivalent pseudo-Grignard chemistry and successfully isolated a total of 14 different complexes. However, we are unable to isolate any complexes involving Ho and Tb metals due to crystallisation difficulties. The crystal systems, geometries and coordination numbers suggest that both pyrazoles (Ph_2pzH) and formamidines (DippFormH and XylFormH) react similarly with pseudo-Grignard reagents.

3.4 Conclusion and Future Outlook

The results obtained from this chapter demonstrate that the use of the Ph_nLnI_{3-n} (n = 1 or 2) Grignard reagents effectively trap N-donor ligands such as Ph_2pzH, DippFormH, and XylFormH. The reaction of Ln^0 metals with PhI, followed by the addition of Ph_2pzH, allows for the synthesis of trivalent monomeric pseudo-Grignard complexes, $[Ln(Ph_2pz)I_2(thf)_4]$ (Ln = La, Ce and Nd) and $[Ln(Ph_2pz)I_2(thf)_3]$ (Ln = Er and Lu) yielding good crystalline products. Notably, for the reaction of Er, PhI and Ph_2pzH we successfully isolated the intermediate product $[Er(Ph_2pz)(Ph)I(thf)_3]$.thf alongside the desired compound $[Er(Ph_2pz)I_2(thf)_3]$·thf. By replacing thf with acetonitrile, we obtained Schlenk equilibria products, $[Ln(Ph_2pz)_3(CH_3CN)_3]$·$2CH_3CN$ (Ln = Nd and Gd). However, these were not our target products, promoting us to discontinue this synthetic route.

We further investigated the reaction pathway of Ph_nLnI_{3-n} (n = 1 or 2) with formamidine ligands (DippFormH and XylFormH), and successfully isolated Ln^{III} pseudo-Grignard compounds $[Ln(DippForm)I_2(thf)_3]$·nthf (Ln = Nd, n= 1; Er, n = 0.5) and $[Ln(XylForm)I_2(thf)_3]$·thf (Ln = La, Nd, Er). These findings align with those obtained from direct reactions involving iodine.[27, 28] Additionally, we explored the reaction pathway of Ph_nLnBr_{3-n} (n = 1 or 2, Ln = Nd) with Ph_2pzH and isolated the complex $[Nd(Ph_2pz)Br_2(thf)_z]$.

These findings suggest that the Ln^{III} pseudo-Grignard reactions present a promising avenue for further exploration of N-donor pro-ligands including formamidines (DippFormH, EtFormH, XylFormH, MesFormH) and pyrazoles (Ph_2pzH, $^tBu_2pzH$, PhMepzH), but also a large array of many other amido ligands. Further work could entail using the Grignard reagents in organic syntheses to compare with traditional Mg based Grignard reagents, as well as further functionalisation using metathesis to synthesise highly reactive homoleptic lanthanoid complexes.

3.5 Experimental

2.5.1 General Aspects

For the general aspects see the appendix 1.

3.5.2 Synthesis of Ln (III) pseudo-Grignard complexes

This chapter we will focuses on trivalent lanthanoid pseudo-Grignard using phenyl iodine (PhI) or phenyl bromide (PhBr) as oxidant, here we also used pyrazole (Ph_2pzH) and *N,N*-bis(aryl) formamidines (ArNCHNAr; Ar = 2,6-*i*$Pr_2C_6H_3$, and 2,6-$Me_2C_6H_3$) as trapping ligands. In some reaction we try to replace the solvent thf with acetonitrile.

2.5.2.1 Synthesis of lanthanoid (III) pyrazolato pseudo-Grignard compounds

Ln metals powder (1.5 mmol) was suspended in dry THF/ acetonitrile (CH_3CN) (15ml) under N_2, and then PhI (2.0 mmol) and 1 drop Hg were added at room temperature. The mixture was sonicated for 10 min and stirred for 5 to 12 h at room temperature, when a light brown colour solution formed. Ph_2pzH (1.0 mmol) were added, and the mixture was stirred at 0 °C for 1 h, and a coloured solution developed after stirring for 24 h at room temperature. The resulting mixture was filtered and concentrated to 5 ml under vacuum.

$[La(Ph_2pz)I_2(thf)_4]$ (**3.1**)

Lanthanum metal powder (0.209 g, 1.5 mmol) was suspended in dry THF (15 ml) under N_2, and then PhI (0.408 g, 2.0 mmol) with 1 drop Hg were added at 25 °C. The mixture was sonicated for 10 min and stirred for ~5 h at room temperature, when a light brown colour solution formed. Solid Ph_2pzH (0.22 g, 1.0 mmol) were added, and the mixture was stirred at 0 °C for 1 h, and a light-yellow solution developed after stirring for 24 h at room temperature. The resulting mixture was filtered and concentrated to ~5 ml under vacuum. Colourless crystals (0.396 g, 44%) were obtained after cooling at -25 °C for 5 days. M. P. 128-130 °C. Elemental analysis: Found: C 41.32, H 4.46, N 2.75, La 15.62; $C_{31}H_{43}I_2LaN_2O_4$ (900.38 g/mol) requires: C 41.35, H 4.81, N 3.11, La 15.43. IR (Nujol): 1603s, 1420w, 1400w, 1342w, 1295m, 1261s, 1227w, 1179m, 1152m, 1093w, 1021s, 969s, 962w, 919s, 861s-br, 808m, 766s, 698s cm^{-1}. ^1H NMR (400.13 MHz, C_6D_6): δ = 1.26 (16H, thf), 3.82(16H, thf), 7.14 (2H, H(4)), 7.28 (1H, CH-pz), 7.36 (4H, H(2,6)), 8.33 ppm(4H, H(3,5)).

[Ce(Ph_2pz)I_2(thf)$_4$] (**3.2**)

Cerium metal powder (0.212 g, 1.5 mmol) was suspended in dry THF (15 ml) under N_2, and then PhI (0.408 g, 2.0 mmol) with 1 drop Hg were added at 25 °C. The mixture was sonicated for 10 min and stirred ~8 h at room temperature, when a brown colour solution formed. Solid Ph_2pzH (0.22 g, 1.0 mmol) was added, and the mixture was stirred at 0 °C for 1h, and a yellowish-brown solution developed after stirring for 24 h at room temperature. The resulting mixture was filtered and concentrated to ~5 ml under vacuum. Colourless crystals (0.416 g, 46%) were obtained after cooling at -25 °C for 3 days. M. P. 135-137 °C. Elemental analysis: Found: C 40.87, H 4.53, N 2.91, Ce,15.82; $C_{31}H_{43}I_2N_2CeO_4$ (901.61g/mol) requires: C 41.30, H 4.81, N 3.11, Ce 15.54. IR (Nujol): 1603s, 1508m, 1421w, 1341w, 1295m, 1260s, 1229m, 1179w, 1153m, 1064w, 1022s, 970s, 915s, 866s, 801w, 762s, 696m, 684m cm^{-1}. ^1H NMR (400.13 MHz, C_6D_6): δ = 0.61 (16H, thf), 1.54(16H, thf), 7.65 (2H, H(4)), 7.79 (4H, H(3,5)), 10.58 (4H, H(2,6)), 13.52 ppm(1H, CH-pz).

The data for the complexes were not optimal leading to refinement issues and therefore the crystal structures of **3.1** and **3.2** are reported for connectivity only but does establish proof of concept of synthetic utility.

[Nd(Ph_2pz)I_2(thf)$_4$] (**3.3**)

Neodymium metal powder (0.216 g, 1.5 mmol) was suspended in dry THF (15 ml) under N_2, and then PhI (0.408 g, 2.0 mmol) with 1 drop Hg were added at 25 °C. The mixture was sonicated for 10 min and stirred ~8 h at room temperature, when a light brown solution formed. Solid Ph_2pzH (0.22 g, 1.0 mmol) was added, and the mixture was stirred at 0 °C for 1h, and a brownish blue solution developed after stirring for 24 h at room temperature. The resulting mixture was filtered and concentrated to ~5 ml under vacuum. Purple crystals (0.562 g, 62%) were obtained after cooling at -25 °C for 3 days. M. P. 123-125 °C. Elemental analysis: Found: C 40.03, H 4.42, N 3.23, Nd,16.42; $C_{31}H_{43}I_2N_2NdO_4$ (905.71 g/mol) requires: C 41.11, H 4.79, N 3.09, Nd, 15.93; loss of 0.5 thf of crystallisation $C_{29}H_{39}I_2NdN_2O_{3.5}$ (869.71 g/mol) requires: C 40.04, H 4.51, N 3.22, Nd 16.58. IR (Nujol): 1603s, 1510m, 1419w, 1341m, 1294m, 1261s, 1228w, 1179m, 1153m, 1073w,1023w, 969s, 912s, 807w, 771w, 698s, 686w, 666w cm^{-1}. ^1H NMR (400.13 MHz, C_6D_6): δ = 1.26 (14H, thf), 1.74 (14H, thf), 8.45 (6H, H(2,4,6)), 13.88 (4H, H(3,5)), 26.17 (1H, CH-pz).

[Er(Ph_2pz)(Ph)I($thf)_3$].thf (**3.4a**), [Er(Ph_2pz)I_2($thf)_3$] (**3.4**)

Erbium metal powder (0.251 g, 1.5 mmol) was suspended in dry THF (15 ml) under N_2, and then PhI (0.408 g, 2.0 mmol) with 1 drop Hg were added at 25 °C. The mixture was sonicated for 10 min and stirred ~10 h at room temperature, when a light brown solution formed. Solid Ph_2pzH (0.22g, 1.0 mmol) was added and the mixture was stirred at 0 °C for 1 h, and a pink solution developed after stirring for 24 h at room temperature. The resulting mixture was filtered and concentrated to ~5 ml under vacuum. Pink crystals of (**3.4a**) (0.132 g, 15%) were obtained after for 5 days. M. P. 137-139 °C. Another pink crystal of (**3.4**) (0.427 g, 46%) were obtained for another 3 days from the mother liquor. M. P. 125-127 °C. Elemental analysis (**3.4**): Found: C 35.12, H 3.99, N 3.62, Er 21.42; $C_{27}H_{35}ErI_2N_2O_3$ (856.65 g/mol) requires: C 37.86, H 4.12, N 3.27, Er 19.52; loss of one thf of crystallisation $C_{23}H_{27}ErI_2N_2O_2$ (784.54 g/mol) requires: C 35.21, H 3.47, N 3.57, Er 21.32. IR (Nujol): 1603s, 1508w, 1421m, 1408m, 1342m, 1293w, 1281w, 1261s, 1227m, 1174 s, 1093w, 1073w, 1055m, 1012s, 913w, 857s, 822m, 774w, 763m, 703w cm^{-1}. ^1H NMR (400.13 MHz, C_6D_6): δ = got paramagnetic.

[Lu(Ph_2pz)I_2($thf)_3$] (**3.5**)

Lutetium metal powder (0.262 g, 1.5 mmol) was suspended in dry THF (15 ml) under N_2, and then PhI (0.408 g, 2.0 mmol) with 1 drop Hg were added at 25 °C. The mixture was sonicated for 10 min and stirred for ~12 h at room temperature, when a light brown solution formed. Solid Ph_2pzH (0.22 g, 1.0 mmol) were added, and the mixture was stirred at 0 °C for 1 h, and a brown solution developed after stirring for 24 h at room temperature. The resulting mixture was filtered and concentrated to ~5 ml under vacuum. The colourless crystals (0.41 g, 47%) were obtained for 3 days. M. P. 118-120 °C. Elemental analysis: Found: C 38.97, H 4.07, N 3.10, Lu 20.04; $C_{27}H_{35}I_2LuN_2O_3$ (864.34 g/mol) requires: C 37.52, H 4.08, N 3.24, Lu, 20.24; extra 0.5 thf from solvation $C_{29}H_{39}I_2LuN_2O_{3.5}$ (890.4 g/mol) requires: C 39.40, H 4.44, N 3.16, Lu, 19.65. IR (Nujol): 1604s, 1508w, 1422m, 1410m, 1343m, 1297m, 1281w, 1261w, 1227s, 1189w, 1177w, 1152w, 1095w, 1068w, 1053m, 1022w, 971s, 916s, 857s-br, 769s, 722s cm^{-1}. ^1H NMR (400.13 MHz, C_6D_6): δ = 1.10 (16H, thf), 3.75(16H, thf), 7.29 (4H, H(2,6)), 7.34 (2H, H(4)), 7.52 (1H, CH-pz), 8.34 ppm(4H, H(3,5)), 1 extra thf from solvation.

$[Nd(Ph_2pz)_3(CH_3CN)_3]\cdot 2CH_3CN$ (**3.6**)

Neodymium metal powder (0.216 g, 1.5 mmol) was suspended in dry acetonitrile (CH_3CN) (15 ml) under N_2, and then PhI (0.408 g, 2.0 mmol) with 1 drop Hg were added at 25 °C. The mixture was sonicated for 10 min and stirred ~8 h at room temperature, when a light brown solution formed. Solid Ph_2pzH (0.22 g, 1.0 mmol) was added the mixture was stirred at 0 °C for 1h, and a blue solution developed after stirring for 24 h at room temperature. The yellow needle crystals (0.56 g, 62%) were obtained after cooling at -25 °C for 3 days. M. P. 195-197 °C (decomposed). Metal analysis: Found: Nd 15.48; $C_{55}H_{48}N_{11}Nd$ (1007.28 g/mol) requires: 14.32; loss of 1 CH_3CN of crystallisation requires $C_{53}H_{45}N_{10}Nd$ (966.23 g/mol): Nd 14.93. IR (Nujol): 2297m, 2270m, 2250w, 1603s, 1511w, 1421w, 1364w, 1281w, 1222m, 1159m, 1073w, 1058s, 1027m, 999w, 970s, 929w, 917m, 758s cm^{-1}. ^1H NMR (400.13 MHz, C_6D_6): δ = -1.65 (12H, CH_3CN), 7.79 (18H, H(2,4,6)), 10.91(12H, H(3,5)), 16.77 (3H, CH-pz) corresponding to loss of 3 CH_3CN.

$[Gd(Ph_2pz)_3(CH_3CN)_3]\cdot 2CH_3CN$ (**3.7**)

Gadolinium metal powder (0.235 g, 1.5 mmol) was suspended in dry acetonitrile (CH_3CN) (15 ml) under N_2, and then PhI (0.408 g, 2.0 mmol) with 1 drop Hg were added at 25 °C. The mixture was sonicated for 10 min and stirred ~10 h at room temperature, when a brownish yellow solution formed. Solid Ph_2pzH (0.22 g, 1.0 mmol) was added the mixture was stirred at 0 °C for 1h, and a pale-yellow solution developed after stirring for 24 h at room temperature. The colourless crystals (0.228 g, 22%) were obtained after cooling at -25 °C for 4 days. M. P. 148-150 °C. Metal analysis: Found Gd 16.42; $C_{55}H_{48}N_{11}Gd$ (1020.29 g/mol) requires: Gd, 15.41; loss of 1 CH_3CN of crystallisation, $C_{53}H_{45}N_{10}Gd$ (979.24 g/mol) requires: Gd, 16.06. IR (Nujol): 2299m, 2272m, 2250w, 1603s, 1512w, 1422w, 1367w, 1281w, 1270w, 1222m, 1156m, 1084w, 1073w, 1060s, 1027m, 1000m, 970s, 929w, 917m, 758s cm^{-1}. ^1H NMR (400.13 MHz, C_6D_6): δ = Very broad paramagnetic peak (5.37 ppm to -0.77 ppm).

3.5.2.2 Synthesis of lanthanoid(III) formamidinato pseudo-Grignard compounds

Excess amounts of lanthanoid metals powder (1.50 mmol) were suspended in dry THF (15ml) under N_2, and then phenyl iodide (1.0 mmol) and 1 drop Hg were added at desired temperature. The mixture was sonicated for 10 min and stirred at room temperature until the formation of Grignard reagent, after that, solid formamidine (DippFormH, or XylFormH) (0.5 mmol) were added at 0 °C temperature and stirred for another 24 h. Crystals were obtained after the filtrates were evaporated to ~5 ml volume under a vacuum and kept in the fridge at -25 °C. Yields were calculated based on the formamidine ligand.

[Nd(DippForm)I_2(thf)$_3$]·thf (**3.8**)

Neodymium metal powder (0.216 g, 1.5 mmol) was suspended in dry THF (15 ml) under N_2, and then PhI (0.204 g, 1.0 mmol) with 1 drop Hg were added at 25 °C. The mixture was sonicated for 10 min and stirred ~8 h at room temperature, when a light brown solution formed. Solid DippFormH (0.184 g, 0.5 mmol) was added and the mixture was stirred at 0 °C for 1 h, and a blue solution developed after stirring for 24 h at room temperature. The resulting mixture was filtered and concentrated to ~5 ml under vacuum. Purple crystals (0.386 g, 73.5%) were obtained after cooling at -25 °C for 2 days. M.P. 221-223 °C, reported M. P. 226-228 °C.[31] Metal Analysis: Found: Nd 14.88, $C_{41}H_{67}I_2N_2O_4Nd$ (1050.6 g/mol) requires: Nd 13.74; loss of 1 thf of crystallisation, $C_{37}H_{59}I_2N_2O_3Nd$ (977.92 g/mol) requires: Nd 14.75. IR and ^{1}H NMR consist with the reported one.[27] IR (Nujol): 1667s, 1589w, 1520w, 1319w, 1261m, 1186m, 1099s, 1072s, 1016s, 933w, 915w, 863w, 823w, 801s, 757s, 722m cm^{-1}. ^{1}H NMR (400.13 MHz, C_6D_6): δ = -2.02(m, 12H, thf), 1.37 (m, 6H, CH_3), 3.08 (m, 12H, thf), 4.08 (m, 18H, CH_3), 8.43 (m, 6H, H(3,4,5)), 10.10 (m, 4H, CH), 30.10 ppm (1H, NCHN), corresponding to loss of 1 thf of crystallisation. For compound **3.8** (orthorhombic, *P*bca space group) the unit cell is: a = 19.66 Å, b = 18.90 Å, c = 24.05 Å, V = 8872.6(3) Å^3, the reported unit cell is: a = 19.6958(3) Å, b = 18.9803(3) Å, c = 24.0171(5) Å, V = 8978.4(3) Å^3.[27]

[Er(DippForm)I_2(thf)$_3$]·0.5thf (**3.9**)

Erbium metal powder (0.251 g, 1.5 mmol) was suspended in dry THF (15 ml) under N_2, and then PhI (0.204 g, 1.0 mmol) with 1 drop Hg were added at 25 °C. The mixture was sonicated for 10 min and stirred for ~10 h at room temperature, when a light brown solution formed.

Solid DippFormH (0.184 g, 0.5 mmol) was added and the mixture was stirred at 0 °C for 1 h, and a pink solution developed after stirring for 24 h at room temperature. The resulting mixture was filtered and concentrated to ~5 ml under vacuum. Pink crystals (0.238 g, 46%) were obtained after cooling at -25 °C for 5 days. M.P. 248-250 °C. Elemental analysis: Found: C 45.41, H 6.31, N 2.55, Er 16.34; $C_{39}H_{63}ErI_2N_2O_{3.5}$ (1036.99 g/mol) requires: C 45.17, H 6.12, N 2.70, Er 16.13. IR (Nujol): 1664m, 1593m, 1559w, 1379s, 1360m, 1334w, 1275s, 1195s, 1100m, 1067m, 1018s, 914m, 870s, 805s, 773s, 762m cm^{-1}. ^1H NMR (C_6D_6): δ = -6.66(m, 14H, thf), -3.51(m, 4H, CH), 1.21(t, 2H, H(4)), 3.42(s, 1H, NC(H)N), 5.69 (m, 14H, thf), 5.80(d, 24H, CH_3), and 25.24 ppm(d, 4H, H(3,5)).

[La(XylForm)I_2(thf)$_3$]·thf (**3.10**)

The synthesis procedure for **3.10** was similar as described for **3.1**. Here, solid XylFormH (0.126 g, 0.5 mmol) was added at 0 °C and a brown solution was obtained. The resulting mixture was filtered and concentrated to ~5 ml under vacuum. Colour less crystals (0.196 g, 42%) were obtained after cooling at -25 °C for 5 days. M.P. 212-214 °C. Elemental analysis: Found: C 40.37, H 5.12, N 3.09; $C_{33}H_{51}I_2LaN_2O_4$ (932.46 g/mol) requires: C 42.51, H 5.51, N 3.00, loss of 1 thf of crystallisation $C_{29}H_{43}I_2LaN_2O_3$ (860.38 g/mol) requires: C 40.48, H 5.04, N 3.26. IR (Nujol): 1593m, 1379s, 1342w, 1288s, 1254w, 1206s, 1092s, 1016s, 942s, 918m, 861s, 784s, 773m, 766w, 668m cm^{-1}. ^1H NMR (400.13 MHz, C_6D_6): δ = 1.18 (16H, thf), 2.67 (s, 12H, CH_3), 3.87 (16H, thf), 6.92 (t, 2H, H(4)), 7.07 (d, 4H, H(3,5)), 7.72 ppm(s, 1H, NCHN).

[Nd(XylForm)I_2(thf)$_3$]·thf (**3.11**)

The synthesis procedure for **3.11** was similar as described for **3.8**. Light blue crystals (0.299 g, 69%) were obtained after cooling at -25 °C for 2 days. M.P. 201-203 °C, reported M. P. 202-204 °C.[32] Metal analysis: Nd 17.58, $C_{33}H_{51}I_2N_2NdO_4$ (937.79 g/mol) requires: Nd 16.38; loss of 1.5 thf of crystallisation $C_{27}H_{39}I_2N_2NdO_{2.5}$ (829.69 g/mol) requires: Nd 17.37. IR consist with the reported one.[28] IR (Nujol): 1668m, 1593m, 1525s, 1280s, 1207s, 1070s, 1017s, 942m, 915s, 862s, 774s, 730w cm^{-1}.^1H NMR (400.13 MHz, C_6D_6): δ = 2.08(m, 12H, thf), 4.79 (m, 24H, thf, CH_3), 8.34 (t, 2H, H(4)), 10.10 (d, 4H, H(3,5)), 30.60 ppm(s, 1H, NCHN). For compound **3.11** (orthorhombic, *P*bca space group) the unit cell is a = 19.66(2) Å, b = 18.932(3)

Å, c = 24.052(6) Å, V = 8912.2(3) Å^3, the reported unit cell is a = 19.6958(3) Å, b = 18.9803(3) Å, c = 24.0171(5) Å, V = 8978.4(3) Å^3.[28]

[Er(XylForm)I_2(thf)$_3$]·thf (**3.12**)

The synthesis procedure for **3.12** was similar as described for **3.9**. Here, solid XylFormH (0.126 g, 0.5 mmol) was added at 0 °C and a pink solution was obtained. The resulting mixture was filtered and concentrated to ~5 ml under vacuum. Pink crystals (0.0.296 g, 62%) were obtained after cooling at -25 °C for 4 days. M.P. 182-184 °C. Elemental analysis: Found: C 41.53, H 5.31, N 2.75, Er 17.98; $C_{33}H_{51}ErI_2N_2O_4$ (960.81 g/mol) requires: C 41.25, H 5.35, N 2.75, Er 17.41. IR (Nujol): 1656m, 1594m, 1532s, 1279s, 1210s, 1068s, 1015s, 945m, 917s, 858s, 773s, 734w cm^{-1}. ^{1}H NMR cannot integrate due to paramagnetism obtained peak at 10.73 ppm, -3.69 ppm, -3.76 pm, -6.79 ppm and -22.07 ppm.

3.5.3 Synthesis of lanthanoid(III) dibromo pyrazolato compounds

Excess amounts of neodymium metal powder (1.5 mmol) were suspended in dry THF (15 ml) under N_2, and then PhBr (0.315 g, 2.0 mmol) with one drop Hg was added at 25 °C. The mixture was sonicated for 10 min and stirred for ~10 h at room temperature, when a light brown solution formed. Solid Ph_2pzH (0.22 g, 1.0 mmol) were added at fixed temperature and stirred for 24 h. Crystals were obtained after the filtrates were evaporated to ~5 ml volume under a vacuum and kept in the fridge at around -25 °C. Yields were calculated based on the Ph_2pzH ligand.

[Nd(Ph_2pz)Br_2(thf)$_{3.5}$] (**3.13**)

Neodymium metal powder (0.216 g, 1.5 mmol) was suspended in dry THF (15 ml) under N_2, and then PhBr (0.315 g, 2.0 mmol) with one drop mercury Hg were added at 25 °C. The mixture was sonicated for 10 min and stirred ~10 h at room temperature, when a light brown solution formed. Solid Ph_2pzH (0.22 g, 1.0 mmol) was added the mixture was stirred at 0 °C for 1h, and a brownish blue solution developed after stirring for 24 h at room temperature. The resulting mixture was filtered and concentrated to ~5 ml under vacuum. The blue crystals (0.49 g, 46%) were obtained after cooling at -25 °C for 7 days. M. P. 112-114 °C. Elemental analysis: Found C 66.30, H 5.77, N 5.57, Nd 21.48; $C_{29}H_{39}Br_2N_2NdO_4$ (783.68 g.mol^{-1}) requires: C 44.45, H 5.02, N 3.57, Nd 18.41; loss of 2 thf of crystallisation, $C_{21}H_{23}NdBr_2N_2O_2$ (639.47 g/mol)

requires: C 39.44, H 3.63, N 4.38, Nd 22.56. IR (Nujol): 1604s, 1509w, 1422w, 1340w, 1295m, 1225m, 1179w, 1154w, 1064m, 1026s, 999w, 970s, 915m, 867s, 799w, 761s, 696w, 683w cm^{-1}. ^1H NMR (400.13 MHz, C_6D_6): δ = -8.33 (4H, thf), -4.27 (4H, thf), 8.19 (2H, H(4)), 8.38 (4H, H(3,5)), 13.85 (4H, H(2,6)), 20.07 ppm (H, CH-pz) corresponding to loss of 2 thf molecules of crystallisation.

3.6 X-ray crystal data

Single crystals coated with viscous hydrocarbon oil were mounted on glass fibres or loops. All complexes (**3.1**-**3.13**) were measured -173 °C (100 K) at the Australian Synchrotron on the MX1 beamline, data integration was completed using Blue-ice [50] and XDS [51] software programs. Structural solutions were obtained by either direct methods [52] or charge flipping [53] methods and refined using full-matrix least-squares methods against F2 using SHELX2018, [54] in conjunction with the X-Seed [55] or Olex2 [53] graphical user interface. All hydrogen atoms were placed in calculated positions using the riding model. Multiscan were applied for absorption corrections. All CIF files were checked at https://checkcif.iucr.org.

[La(Ph$_2$pz)I$_2$(thf)$_4$] (**3.1**)

$C_{31}H_{43}I_2LaN_2O_4$, M_r =900.38 g/mol, triclinic, space group *P*-1 (no. 2), a = 8.986(7) Å, b = 18.42(2) Å, c = 20.51(2) Å, α = 99.09(4)°, β = 90.07(3)°, γ = 97.52(3)°, V = 3323(6) Å^3, Z = 4, T = 293(2) K, μ(MoKα) = 3.180 mm^{-1}, *Dcalc* = 1.800 g/cm^3, 232972 reflections measured (4.024° ≤ 2Θ ≤ 56.714°), 16487 unique (R_{int} = 0.0973, R_{sigma} = 0.0425) which were used in all calculations. The final R_1 was 0.1258 (I > 2σ(I)) and wR_2 was 0.2958 (all data).

[Ce(Ph$_2$pz)I$_2$(thf)$_4$] (**3.2**)

$C_{31}H_{43}I_2N_2CeO_4$, M_r =901.61 g/mol, triclinic, space group *P*-1 (no. 2), a = 8.9830(18) Å, b = 18.355(4) Å, c = 20.473(4) Å, α = 81.01(3)°, β = 89.98(3)°, γ = 82.45(3)°, V = 3304.6(12) Å^3, Z = 2, T = 293(2) K, μ(MoKα) = 3.279 mm^{-1}, *Dcalc* = 1.725 g/cm^3, 8224 reflections measured (2.014° ≤ 2Θ ≤ 50.152°), 8224 unique (R_{int} = ?, R_{sigma} = 0.1004) which were used in all calculations. The final R_1 was 0.1195 (I > 2σ(I)) and wR_2 was 0.3756 (all data).

[Nd(Ph$_2$pz)I$_2$(thf)$_4$] (**3.3**)

$C_{31}H_{43}I_2N_2NdO_4$, M_r =905.71 g/mol, triclinic, space group *P*-1 (no. 2), a = 9.0500(18) Å, b = 18.430(4) Å, c = 20.200(4) Å, α = 100.01(3)°, β = 90.11(3)°, γ = 97.38(3)°, V = 3289.4(12) Å^3, Z = 4, T = 100(2) K, μ(Synchrotron) = 3.492 mm^{-1}, *Dcalc* = 1.829 g/cm^3, 11368 reflections measured (2.048° ≤ 2Θ ≤ 50.156°), 11368 unique (R_{int} = ?, R_{sigma} = 0.0530) which were used in all calculations. The final R_1 was 0.0663 (I > 2σ(I)) and wR_2 was 0.1956 (all data).

[Er(Ph$_2$pz)I$_2$(thf)$_3$] (**3.4**)

$C_{27}H_{35}ErI_2N_2O_3$ (M =856.65 g/mol): monoclinic, space group *C*2/c (no. 15), a = 15.367(3) Å, b = 12.038(2) Å, c = 31.263(6) Å, β = 97.88(3)°, V = 5729(2) Å^3, Z = 46, T = 293(2) K, μ(MoKα) = 22.879 mm^{-1}, *Dcalc* = 4.496 g/cm^3, 25862 reflections measured (2.63° ≤ 2Θ ≤ 50.054°), 4891 unique (R_{int} = 0.0840, R_{sigma} = 0.0586) which were used in all calculations. The final R_1 was 0.2009 (I > 2σ(I)) and wR_2 was 0.4724 (all data).

[Er(Ph$_2$pz)(Ph)I(thf)$_3$].thf (**3.4a**)

$C_{37}H_{48}ErIN_2O_4$, M_r =878.93 g/mol, monoclinic, space group *P*2$_1$/c (no. 14), a = 12.630(3) Å, b = 15.690(3) Å, c = 18.140(4) Å, β = 97.05(3)°, V = 3567.5(12) Å^3, Z = 4, T = 100(2) K, μ(MoKα) = 3.258 mm^{-1}, *Dcalc* = 1.636 g/cm^3, 59362 reflections measured (3.25° ≤ 2Θ ≤ 50.054°), 6271 unique (R_{int} = 0.0513, R_{sigma} = 0.0245) which were used in all calculations. The final R_1 was 0.0388 (I > 2σ(I)) and wR_2 was 0.1050 (all data).

[Lu(Ph$_2$pz)I$_2$(thf)$_3$] (**3.5**)

$C_{27}H_{35}I_2LuN_2O_3$, M_r =864.34 g/mol, monoclinic, space group *C*2/c (no. 15), a = 15.448(3) Å, b = 12.313(3) Å, c = 30.499(6) Å, β = 90.03(3)°, V = 5801(2) Å^3, Z = 8, T = 100(2) K, μ(MoKα) = 5.561 mm^{-1}, *Dcalc* = 1.979 g/cm^3, 5070 reflections measured (2.67° ≤ 2Θ ≤ 50.06°), 5070 unique (R_{int} = ?, R_{sigma} = 0.0311) which were used in all calculations. The final R_1 was 0.0818 (I > 2σ(I)) and wR_2 was 0.2553 (all data).

$[Nd(Ph_2pz)_3(CH_3CN)_3]\cdot 2CH_3CN$ (**3.6**)

$C_{55}H_{48}N_{11}Nd$, M_r =1007.28 g/mol, monoclinic, space group $P2_1/c$ (no. 14), a = 10.547(2) Å, b = 31.650(6) Å, c = 14.797(3) Å, β = 100.86(3)°, V = 4851.0(17) Å^3, Z = 4, T = 100(2) K, μ(MoKα) = 1.120 mm^{-1}, *Dcalc* = 1.379 g/cm^3, 57093 reflections measured (2.574° ≤ 2Θ ≤ 51.362°), 8988 unique (R_{int} = 0.0542, R_{sigma} = 0.0323) which were used in all calculations. The final R_1 was 0.0418 (I > 2σ(I)) and wR_2 was 0.1110 (all data).

$[Gd(Ph_2pz)_3(CH_3CN)_3]\cdot 2CH_3CN$ (**3.7**)

$C_{55}H_{48}GdN_{11}$ (M =1020.29 g/mol): monoclinic, space group $P2_1/c$ (no. 14), a = 10.511(2) Å, b = 31.498(6) Å, c = 14.805(3) Å, β = 100.79(3)°, V = 4814.9(17) Å^3, Z = 4, T = ? K, μ(MoKα) = 1.426 mm^{-1}, *Dcalc* = 1.405 g/cm^3, 56439 reflections measured (2.586° ≤ 2Θ ≤ 50.078°), 8221 unique (R_{int} = 0.0455, R_{sigma} = 0.0244) which were used in all calculations. The final R_1 was 0.0271 (I > 2σ(I)) and wR_2 was 0.0675 (all data).

$[Er(DippForm)I_2(thf)_3]\cdot 0.5thf$ (**3.9**)

$C_{39}H_{63}ErI_2N_2O_{3.5}$ (M =1036.97 g/mol): orthorhombic, space group $Pbca$ (no. 61), a = 19.414(4) Å, b = 18.865(4) Å, c = 24.137(5) Å, V = 8840(3) Å^3, Z = 8, T = 100(2) K, μ(MoKα) = 3.330 mm^{-1}, *Dcalc* = 1.558 g/cm^3, 96244 reflections measured (3.374° ≤ 2Θ ≤ 49.998°), 7746 unique (R_{int} = 0.0459, R_{sigma} = 0.0164) which were used in all calculations. The final R_1 was 0.0516 (I > 2σ(I)) and wR_2 was 0.1401 (all data).

$[La(XylForm)I_2(thf)_3]\cdot thf$ (**3.10**)

$C_{33}H_{51}I_2LaN_2O_4$ (M =932.46 g/mol): monoclinic, space group $C2/c$ (no. 15), a = 25.0270(14) Å, b = 13.0035(7) Å, c = 23.6878(11) Å, β = 104.676(2)°, V = 7457.4(7) Å^3, Z = 8, T = 123.0 K, μ(MoKα) = 2.836 mm^{-1}, *Dcalc* = 1.661 g/cm^3, 109461 reflections measured (3.78° ≤ 2Θ ≤ 55.09°), 8572 unique (R_{int} = 0.0537, R_{sigma} = 0.0244) which were used in all calculations. The final R_1 was 0.0500 (I > 2σ(I)) and wR_2 was 0.1140 (all data).

[Er(XylForm)I_2(thf)$_3$]·thf (**3.12**)

$C_{33}H_{51}ErI_2N_2O_4$ (M =960.81 g/mol): monoclinic, space group $C2/c$ (no. 15), a = 24.319(5) Å, b = 13.145(3) Å, c = 23.346(5) Å, β = 104.09(3)°, V = 7238(3) Å^3, Z = 8, T = 100(2) K, μ(MoKα) = 4.061 mm^{-1}, *Dcalc* = 1.763 g/cm^3, 39496 reflections measured (3.454° ≤ 2Θ ≤ 50.068°), 6331 unique (R_{int} = 0.0590, R_{sigma} = 0.0337) which were used in all calculations. The final R_1 was 0.0568 (I > 2σ(I)) and wR_2 was 0.1731 (all data).

[Nd(Ph$_2$pz)Br$_2$(thf)$_{3.5}$] (**3.13**)

$C_{29}H_{38.85}Br_2N_2NdO_{3.5}$, M_r =775.53 g/mol, triclinic, space group P-1 (no. 2), a = 18.440(4) Å, b = 18.640(4) Å, c = 18.900(4) Å, α = 76.78(3)°, β = 89.93(3)°, γ = 75.75(3)°, V = 6119(2) Å^3, Z = 8, T = 100(2) K, μ(MoKα) = 4.342 mm^{-1}, *Dcalc* = 1.684 g/cm^3, 107364 reflections measured (2.218° ≤ 2Θ ≤ 50.054°), 21368 unique (R_{int} = 0.0653, R_{sigma} = 0.0487) which were used in all calculations. The final R_1 was 0.0555 (I > 2σ(I)) and wR_2 was 0.1634 (all data).

3.7 References

[1]. D. F. Evans, G. V. Fazakerley and R. F. Phillips, J. Chem. Soc. D., **1970**, 244-244.

[2]. D. F. Evans, G. V. Fazakerley and R. F. Phillips, J. Chem. Soc. A., **1971**, 1931-1934.

[3]. B. A. Dolgoplosk, E. I. Tinyakova, I. N. Markevich, T. V. Soboleva, G. M. Chernenko, O. K. Sharaev and V. A. Yakovlev, J. Organomet. Chem., **1983**, 71-79.

[4]. M. Wiecko, G. B. Deacon and P. C. Junk, Chem. Commun., **2010**, 46, 5076-5078.

[5]. S. H. Ali, G. B. Deacon, P. C. Junk, S. Hamidi, M. Wiecko and J. Wang, Chem. Eur. J., **2018**, 24, 230-242.

[6]. A. M. Bienfait, B. M. Wolf, K. W. Tӧrnroos and R. Anwander, Inorg. Chem., **2018**, 57, 5204-5212.

[7]. P. B. Hitchcock, A. G. Hulkes and M. F. Lappert, Inorg. Chem., **2004**, 43, 1031-1038.

[8]. S. A. A. Shah, H. Dorn, H.t W. Roesky, P. Lubini and H.-G. Schmidt, Inorg. Chem., **1997**, 36, 1102-1106.

[9]. E. Hemmer, C. Cavelius, V. Huch and S. Mathur, Inorg. Chem., **2015**, 54, 6267-6280.

[10]. U. J. Williams, J. R. Robinson, A. J. Lewis, P. J. Carroll, P. J. Walsh and E. J. Schelter, Inorg. Chem., **2014**, 53, 27-29.

[11]. O. Eisenstein, P. B. Hitchcock, A. G. Hulkes, M. F. Lappert and L. Maron, Chem. Commun., **2001**, 1560-1561.

[12]. P. Dröse, S. Lashkari, J. Gottfriedsen, S. Blaurock, C. G. Hrib, A. R. Crozier, C. Maichle-Mössmer and C. Schädle, J. Am. Chem. Soc., **2010**, 132, 14046-14047.

[13]. M. F. Lappert, A. Singh, J. L. Atwood and W. E. Hunter, J. C. S. Chem. Commun., **1981**, 1190-1191.

[14]. Q. Shen, M. Qi, J. Guan and Y. Lin, J. Organomet. Chem., **1991**, 406, 353-361.

[15]. H. Schumann, M. R. Keitsch, J. Winterfeld, S. Muhle and G. A. Molander, J. Organomet. Chem., **1998**, 559, 181-190.

[16]. I. L. Fedushkin, F. Girgsdies, H. Schumann and M. N. Bochkarev, Eur. J. Inorg. Chem., **2001**, 2405-2410.

[17]. Y.-S. Meng, Y.-Q. Zhang, Z.-M. Wang, B.-W. Wang and S. Gao, Chem. Eur. J., **2016**, 22, 12724-12731, (17a) F. Jaroschik, F. Nief, X.-F. L. Goff, and L. Ricard Organometallics, **2007**, 26, 1123-1125, (17b) C. A. P. Goodwin, D. Reta, F. Ortu, N. F. Chilton and D. P. Mills, J. Am. Chem. Soc., **2017**, 139, 18714-18724, (17c) C. A. P. Goodwin, D. Reta, F. Ortu, J. Liu, N. F. Chilton and D. P. Mills, Chem. Commun., **2018**, 54, 9182-9185.

[18]. L. Maron, E. L. Werkema, L. Perrin, O. Eisenstein and R. A. Andersen, J. Am. Chem. Soc., **2005**, 127, 279-292.

[19]. G. Yang, Y. Fan, Z. Jin, Y. Xing and W. Chen, J. Organomet. Chem., **1987**, 322, 51-63.

[20]. Z. Wu, Z. Xu, X. You, X. Zhou, H. Wang and Y. Yang, Polyhedron, **1993**, 12, 795-800.

[21]. N. M. Scott and R. Kempe, Eur. J. Inorg. Chem., **2005**, 1319-1324.

[22]. S. M. Guillaume, M. Schappacher, N. M. Scott and R. Kempe, J. Polym. Sci., Part A: Polym. Chem., **2007**, 45, 3611-3619.

[23]. S. Qayyum, G. G. Skvortsov, G. K. Fukin, A. A. Trifonov, W. P. Kretschmer, C. Döring and R. Kempe, Eur. J. Inorg. Chem., **2010**, 248-257.

[24]. M. L. Cole, G. B. Deacon, C. M. Forsyth, P. C. Junk, K. Konstas and J. Wang, Chem. Eur. J., **2007**, 13, 8092-8110.

[25]. M. L. Cole, G. B. Deacon, P. C. Junk and K. Konstas, Chem. Commun., **2005**, 1581-1583.

[26]. M. L. Cole, G. B. Deacon, C. M. Forsyth, P. C. Junk, K. Konstas, J. Wang, H. Bittig and D. Werner, Chem. Eur. J., **2013**, 19, 1410-1420.

[27]. Z. Guo, V. L. Blair, G. B. Deacon and P. C. Junk, Chem. Commun., **2021**, 57, 11513-11516.

[28]. Z. Guo, M. A. Halim, V. L. Blair, G. B. Deacon and P. C. Junk, Chem. Asian J., **2023**, 18, e202300333.

[29]. D. Werner, G. B. Deacon, P. C. Junk and R. Anwander, Chem. Eur. J., **2014**, 20, 4426-4438.

[30]. F.-S. Guo, B. M. Day, Y.-C. Chen, M.-L. Tong, A. Mansikkamaki and R. A. Layfield, Angew. Chem. Int. Ed., **2017**, 56, 11445-11449.

[31]. J. Liu, D. Reta, J. A. Cleghorn, Y. X. Yeoh, F. Ortu, C. A. P. Goodwin, N. F. Chilton and D. P. Mills, Chem. Eur. J., **2019**, 25, 7749-7758.

[32]. Z. Guo, J. Luu, V. Blair, G. B. Deacon and P. C. Junk, Eur. J. Inorg. Chem., **2019**, 1018-1029

[33]. A. O. Tolpygin, O. A. Linnikova, T. A. Kovylina, A. V. Cherkasov, G. K. Fukin and A. A. Trifonov, Russ. Chem. Bull., Int. Ed., **2019**, 68, 32-39.

[34]. R. D. Shannon, Acta Crystallogr. Sect. A, **1976**, 32, 751-767.

[35]. J. E. Cosgriff, G. B. Deacon and B. M. Gatehouse, Aust. J. Chem., **1993**, 46, 1881-1896.

[36]. D. P. Mills, A. J. Wooles, J. McMaster, W. Lewis, A. J. Blake and S. T. Liddle, Organometallics, **2009**, 28, 6771-6776.

[37]. K. R. D. Johnson, A. P. Cote and P. G. Hayes, J. Organomet. Chem., **2010**, 695, 2747-2755.

[38]. T. K. Panda, S. Randoll, C. G. Hrib, P. G. Jones, T. Bannenberg and M. Tamm, Chem. Commun., **2007**, 5007-5009.

[39]. S. Rangarajan, O. Beaumont, M. S. Balakrishna, G. B. Deacon and V. L. Blair, Inorganica Chim. Acta., **2024**, 122385.

[40]. S. Beaini, G. B. Deacon, M. Hilder, P. C. Junk and D. R. Turner, Eur. J. Inorg. Chem., **2006**, 3434-3441.

[41]. G. B. Deacon, C. M. Forsyth, A. Gitlits, B. W. Skelton and A. H. White, Dalton Trans., **2004**, 1239-1247.

[42]. Z. Guo, V. L. Blair, G. B. Deacon and P. C. Junk, Chem. Eur. J. **2022**, 28, e202103865.

[43]. Z. Guo, V. L. Blair, G. B. Deacon and P. C. Junk, Dalton Trans., **2020**, 49, 13588-13600.

[44]. M. L. Cole, G. B. Deacon, P. C. Junk and J. Wang, Organometallics, **2013**, 32, 1370-1378.

[45]. G. Heckmann and M. Niemeyer, J. Am. Chem. Soc., **2000**, 122(17), 4227-4228.

[46]. M. A. Halim, Z. Guo, V. L. Blair, G. B. Deacon and P. C. Junk, J. Organomet. Chem., **2024**, 123094.

[47]. J. E. Cosgriff, G. B. Deacon, B. M. Gatehouse, P. R. Lee and H. Schumann, Z. anorg. allg. Chem., **1996**, 622, 1399-1403.

[48]. G. B. Deacon, B. M, Gatehouse, S. Nickel and S. N. Platts, Aust. J. Chem., **1991**, 44, 613-621.

[49]. J. E. Cosgriff, G. B. Deacon, B. M. Gatehouse, H. Hemling and H. Schumann, Aust. J. Chem., **1994**, 47, 1223-1235.

[50]. T. M. McPhillips, S. E. McPhillips, H. J. Chiu, A. E. Cohen, A. M. Deacon, P. J. Ellis, E. Garman, A. Gonzalez, N. K. Sauter, R. P. Phizackerley, S. M. Soltis and J. P. Kuhn, J. Synchrotron Radiat., **2002**, 9, 401-406.

[51]. W. Kabsch, J. Appl. Crystallogr., **1993**, 26, 795.

[52]. G. M. Sheldrick, Acta Crystallogr. Sect. A., **2008**, 64, 112-122.

[53]. O. V. Dolomanov, L. J. Bourhis, R. J. Gildea, J. A. K. Howard and H. Puschmann, J. Appl. Crystallogr., **2009**, 42, 339-341.

[54]. G. M. Sheldrick, Acta Cryst., **2015**, C71, 3-8.

[55]. L. J. Barbour, J. Supramol. Chem., **2001**, 1, 189-191.

Chapter 4

Reactivity of Ln(II) and Ln(III) Grignard reagents with organic molecules

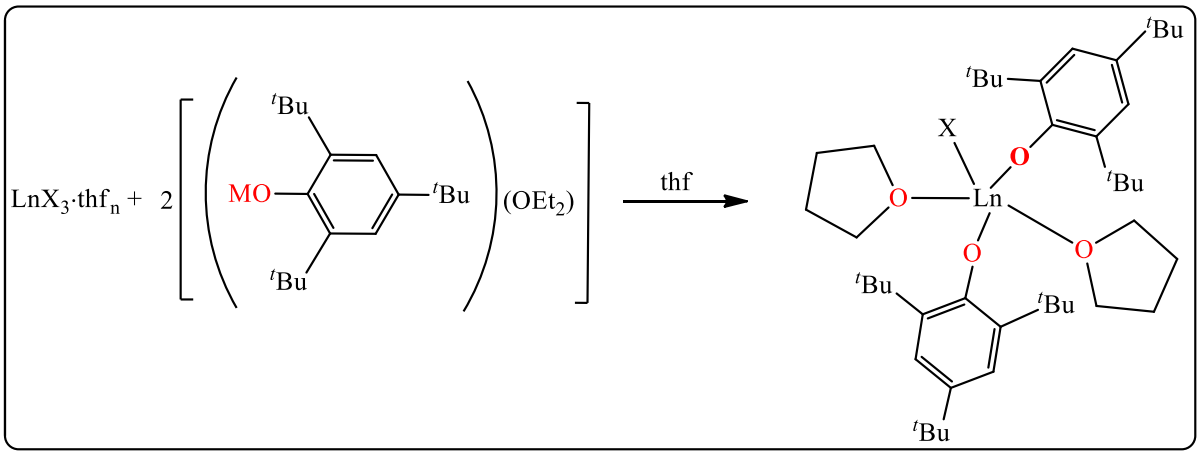
Chapter 4

4.1 Introduction

Phenol is an O-donor organic molecule. Complexes formed between lanthanoid metals and phenol are known as lanthanoid phenolate complexes. Lanthanoid phenolate complexes with Ln-O bonds continue to be of interest in research due to their exceptional performance as single-molecule magnets (SMMs) for quantum computing.[1, 2] Normally, low coordinate lanthanoid complexes are highly promising for high-performance owing to the large magnetic anisotropy of the Ln(III) cations, enhanced by the strong donation of the phenolate ligands along specific magnetic axes and possibility of stabilizing the most magnetic electronic distributions for each lanthanide (e.g. oblate, m_J = 13/2 for Dy^{3+}).[3] Bulky aryloxides are particularly effective in producing low coordinate (3~6) lanthanoid complexes.[4-6] Over the last two decades, phenolate ligand systems have been used to synthesise main group and transition metal coordination complexes, most of them have shown both significant, and selective catalytic activity, [7-16] mainly for synthesizing cyclic esters.[17] Metathesis reactions are commonly employed to synthesise lanthanoid pseudo-Grignard phenolate complexes. In the following section, we will discuss some standard synthesis methods for lanthanoid phenolate complexes.

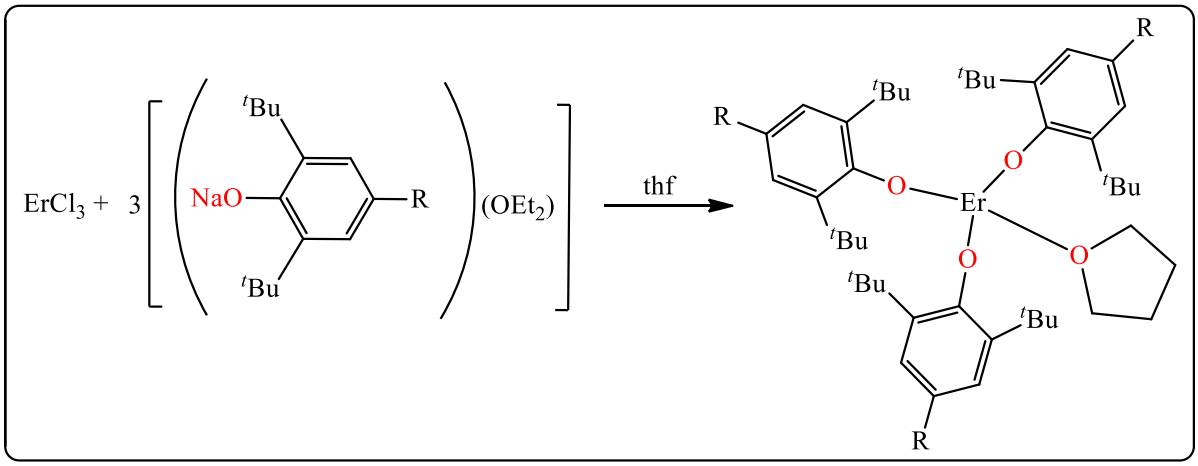
4.1.1 Synthesis of lanthanoid phenolate complexes

The $[Ln(Mes^*O)_2X(thf)_2]$ complexes (Mes* = 2,4,6-tri-tert-butylphenyl) {Ln = Y, Dy, M = Na, X = Cl; M = K, X = Br, I} were prepared directly via metathesis reactions between 2 equivalents of MOMes* and the corresponding metal halide ($LnX_3{\cdot}thf_n$) salts. These complexes exhibit a distorted square pyramidal geometry.[1]



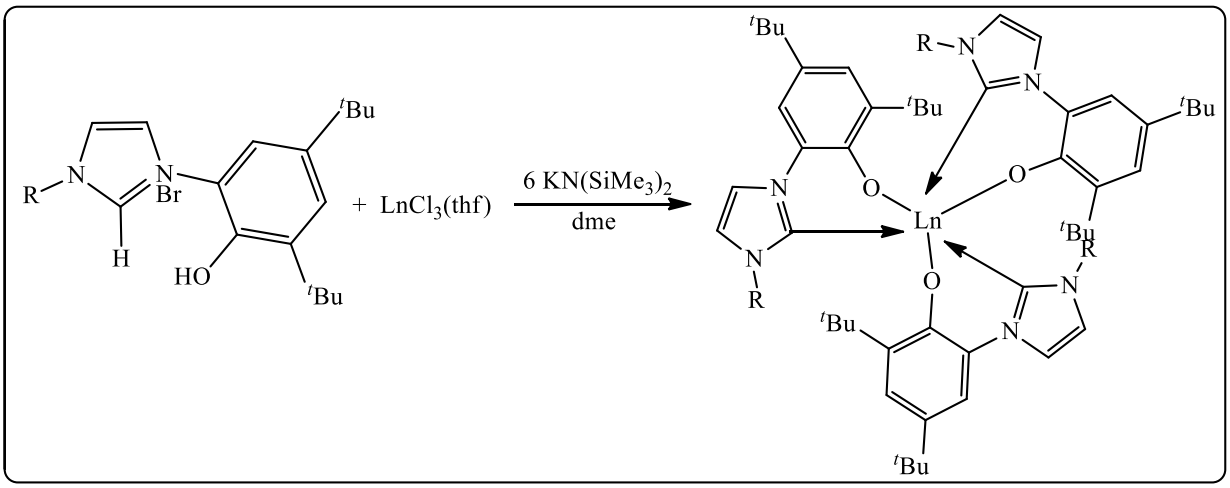
Scheme 4.1: Synthesis of $[Ln(Mes^*O)_2X(thf)_2]$ complexes. Ln = Y, Dy, M = Na, X = Cl; M = K, X = Br, I.[1]

The [Er(2,6-di-^{t}Bu, 4-R-Ph-O)$_3$(thf)] (R = ^{t}Bu, 4-CH$_3$) complexes were synthesised by reacting $ErCl_3$ with [Na(2,6-di-^{t}Bu, 4-R-Ph-O)·Et_2O] in thf at a 1:3 molar ratio at room temperature for 3 d.[2]



Scheme 4.2: Synthesis of [Er(2,6-di-*t*Bu, 4-R-Ph-O)$_3$(thf)] complexes (R = ^{t}Bu, 4-CH$_3$).[2]

Some Ce, Sm and Eu complexes [Ln(2-O-3,5-^{t}Bu$_2$-C_6H_2(1-C{N(CH)$_2$N(R)}))$_3$] (R = ^{i}Pr, ^{t}Bu, Mes; Ln = Ce, Sm, Eu) (**Scheme 4.3**) were isolated from the reaction of 3 equivalents of [*o*-H_2(2-O-3,5-^{t}Bu$_2$-C_6H_2(1-C{N(CH)$_2$N(R)}))Br] with 6 equivalents of KN(SiMe$_3$)$_2$ and 1 equivalent of LnCl$_3$(thf)$_n$. The reaction mixture was initially cooled to -20 °C and stirred for 5 min. Subsequently, LnCl$_3$(thf)$_n$ was added at room temperature and the mixture was stirred for an additional 2 h. The coordination geometry of the resulting complexes [Ln(2-O-3,5-^{t}Bu$_2$-C_6H_2(1-C{N(CH)$_2$N(R)}))$_3$] is pseudo-octahedral.[18]



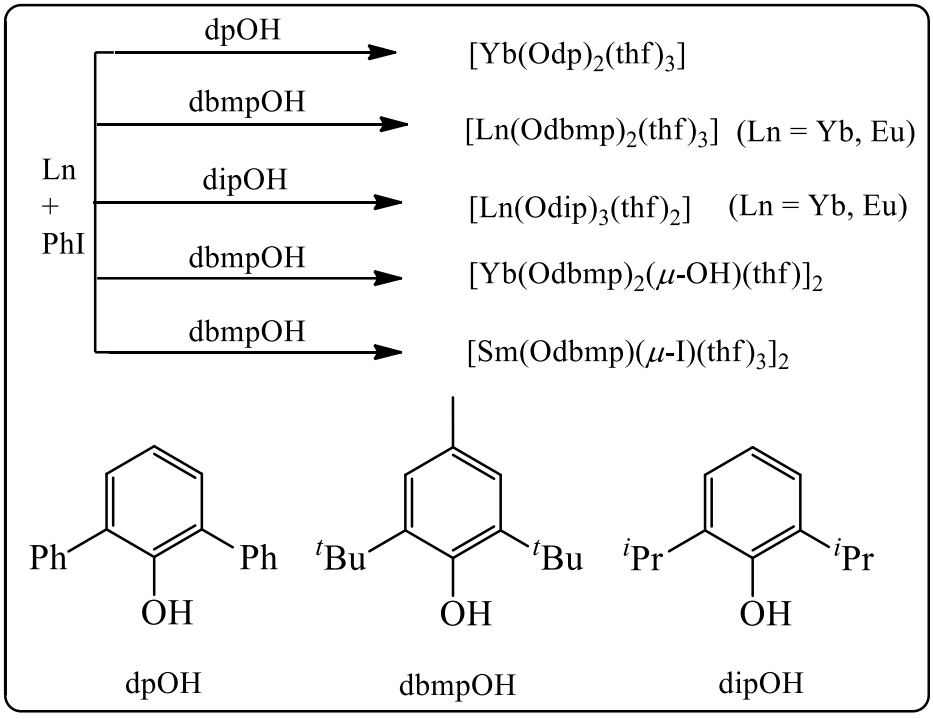
Scheme 4.3: Synthesis of solvent free lanthanoid (III) aryloxide complexes (Ln = Ce, Sm, Eu, R = ^{i}Pr; Ln = Ce, R = ^{t}Bu, Mes).[18]

A series of dimeric ytterbium (III) phenolate complexes $[Yb(OAr)_2F(thf)]_2$, were synthesised by reacting divalent ytterbium aryloxides, $[Yb(OAr)_2(thf)_3]$ (OAr = OC_6H_2-2,6-$^tBu_2$-4-R; R = ^{t}Bu, Me, H), with perfluorodecalin ($C_{10}F_{18}$) at room temperature for 48 h. These complexes feature fluoride bridges and exhibit a five-coordinate dimeric structure.[19]

$$2\ [Yb(OAr)_2(thf)_3] + C_{10}F_{18} \longrightarrow [Yb(OAr)_2F(thf)]_2$$

Equation 4.1: Synthesis of ytterbium aryloxides pseudo-Grignard complexes.[19]

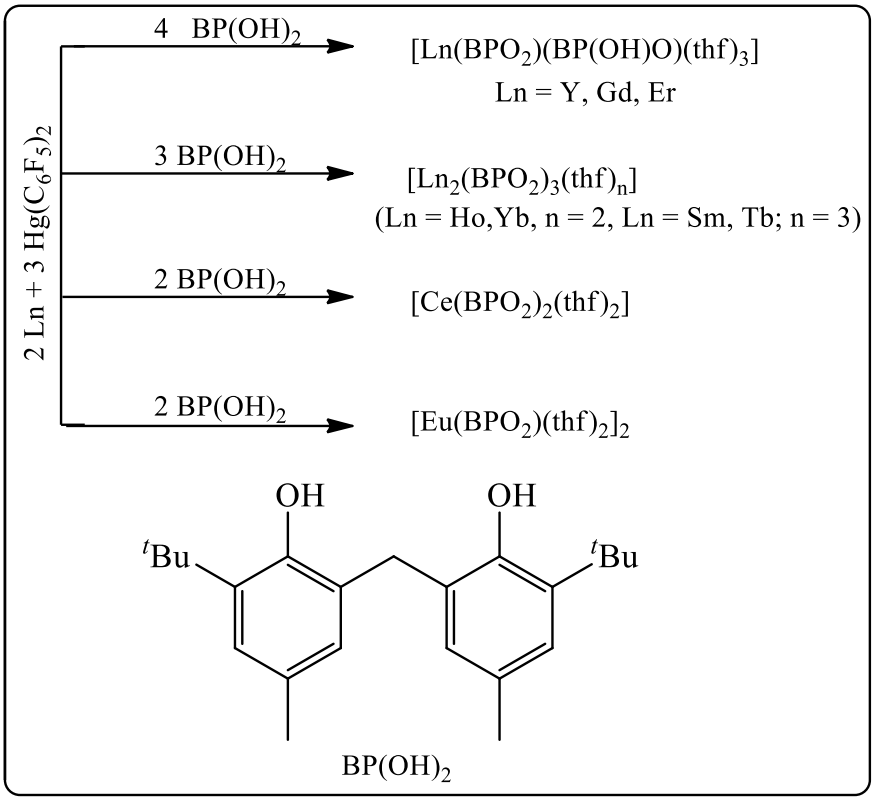
In his undergraduate thesis, Bruin-Dickason synthesised a series of lanthanoid phenolate complexes using the ligands; 2,6-diphenylphenol (dpOH), 2,6-di-tert-butyl-4-methylphenol (dbmpOH), 2,6-di-isopropylphenol (dipOH). The reaction involving lanthanoid metals (Sm, Eu and Yb), PhI and the respective ligands led to the isolation of several complexes: $[Yb(Odp)_2(thf)_3]$, $[Ln(Odbmp)_2(thf)_3]$ (Ln = Eu, Yb), $[Ln(Odip)_3(thf)_2]$ (Ln = Eu, Yb), $[Yb(Odbmp)_2(\mu\text{-OH})(thf)]_2$, and $[Sm(Odbmp)(\mu\text{-I})(thf)_3]_2$, the former three being products of the shift in the Schlenk equilibrium, and the penultimate being a product of hydrolysis.[20] These reactions are illustrated in the Scheme **4.4**.



Scheme 4.4: Synthesis of lanthanoid phenolate complexes from Grignard reaction.[20]

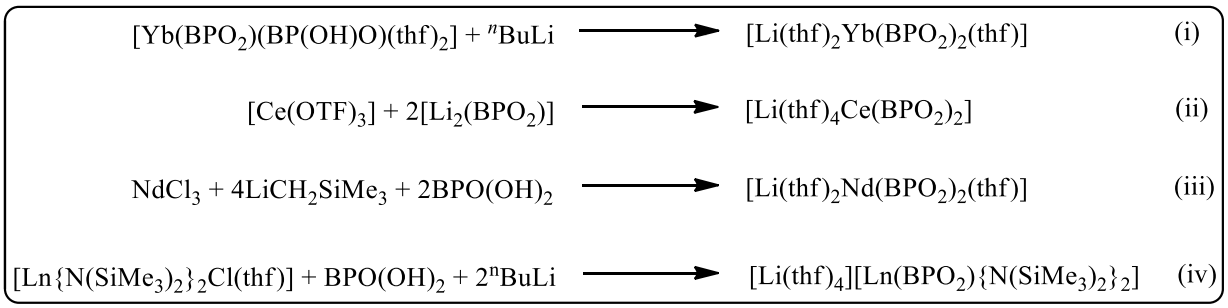
The RTP reaction between the corresponding lanthanoid metal, $Hg(C_6F_5)_2$ and biphenol ($BP(OH)_2$: 2,2′-methylene-bis(6-*tert*-butyl-4-methylphenol)) was employed to synthesise lanthanoid biphenolate complexes, as detailed in the Scheme **4.5**. Trivalent complexes

$[Ln(BPO_2)(BP(OH)O)(thf)_3]$ (Ln = Y, Gd and Er) were obtained by reacting 4 equivalents of $BP(OH)_2$ with 3 equivalents of $Hg(C_6F_5)_2$ and 2 equivalents of the lanthanoid metal. The use of 3 equivalents of the ligand resulted in the formation of bimetallic $[Ln_2(BPO_2)_3(thf)_n]$ (Ln = Ho, Yb, Sm and Tb) complexes, while 2 equivalents led to the synthesis of the tetravalent $[Ce(BPO_2)_2(thf)_2]$ complex and the divalent $[Eu(BPO_2)(thf)_2]$ complex.[21, 22]



Scheme 4.5: Synthesis of lanthanoid biphenolate complexes from RTP reaction.[21, 22]

The synthesis of several heterobimetallic phenolate complexes; $[Li(thf)_2Yb(BPO_2)_2(thf)]$ (**eqn. i**), $[Li(thf)_4Ce(BPO_2)_2]$ (**eqn. ii**), $[Li(thf)_2Nd(BPO_2)_2(thf)]$ (**eqn. iii**) and $[Li(thf)_4][Ln(BPO_2)\{N(SiMe_3)_2\}_2]$ (**eqn. iv**) is illustrated in the Scheme **4.6**. The chemistry of lanthanoid metals in this context have a great scope for further exploration.



Scheme 4.6: Synthesis of heterobimetallic phenolate complexes.[21, 22]

4.2 Current Study

This chapter aims to expand the trapping capacity, of divalent and trivalent lanthanoid pseudo-Grignard reagents, $Ph_pLnI_{(3-p)}(thf)_n$ (p = 1 or 2; Ln = La, Ce, Nd, Gd, Ho and Lu) with O-donor ligands (in this case, 4-^{t}Bu-C_6H_4OH). In chapter **2** and **3**, we have discussed the reactivity of pseudo-Grignard reagents with N-donor ligands, such as formamidines and pyrazoles. Here, the reaction of O-donor ligand, 4-tert-butylphenol (4-^{t}Bu-PhOH) with $Ph_pLnI_{(3-p)}(thf)_n$ in thf and crystallised in dme resulted in the isolation of diiodo pseudo-Grignard complexes **[Ln(4-^{t}Bu-PhO)I_2(dme)$_2$]·0.5dme** (Ce **4.1**, Nd **4.2**, and Lu **4.3**). Reaction involving Gd and Ho yielded powders of composition **[Ln(4-^{t}Bu-PhO)I_2(dme)$_2$]·0.5dme** (Gd **4.4**, and Ho **4.5**). Heating the complex obtained in the reaction involving La resulted in the isolation of **[(La(4-^{t}Bu-PhO)I(dme)$_2$)$_2$(OCH_3)]I·2dme** (**4.6**) a product obtained by the C-O bond scission of dme.

As a further study, we investigated the reactivity of PhYbI with benzophenone (Ph_2CO) that yielded red crystals of **[Yb($OCPh_3$)$_3$(thf)$_2$] (4.7a**) and yellow crystals of **[Yb_2I_2(μ-O)(μ-I)(thf)$_5$]·thf (4.7b)**. Later [Yb(Ph_2pz)I(thf)$_4$] Grignard complexes were treated with O-donor KO^{t}Bu and N-donor (KMe)Ph(NMe_2) ligands. However, in both cases, the Schlenk equilibrium product **[Yb(Ph_2pz)$_2$(thf)$_4$]** (**4.8**) was isolated, instead of the anticipated heteroleptic products [Yb(Ph_2pz)(O^{t}Bu)(thf)$_x$], [Yb(Ph_2pz){(Me)Ph(NMe_2)}(thf)$_x$].

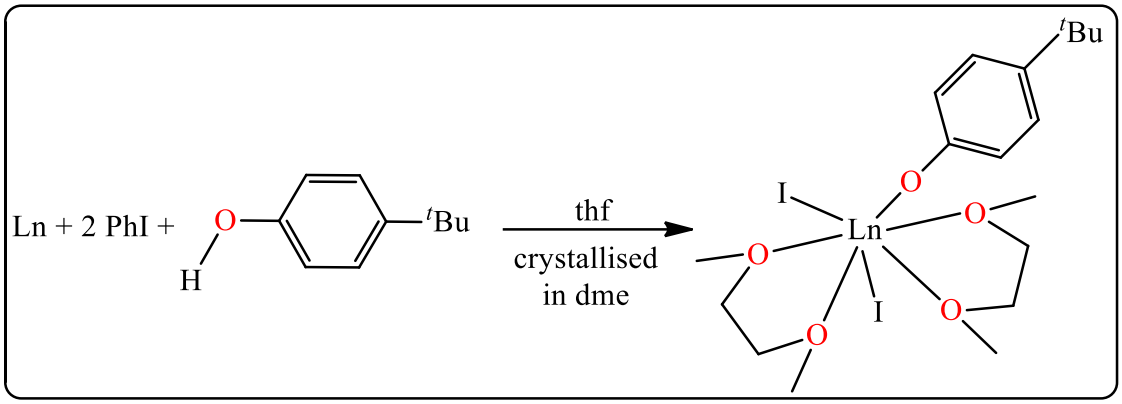
4.3 Results and Discussion

4.3.1 Synthesis and spectroscopic characterisation

4.3.1.1 The reaction of lanthanoid (La, Ce, Nd, Gd, Ho and Lu) pseudo-Grignard reagents with 4-tertbutyl phenol

The goal of this reaction process initial aim was to synthesise trivalent lanthanoid di-iodo phenolate complexes, specifically those of La, Ce, Nd, Gd, Ho and Lu. Phenyllanthanoid halides, $Ph_pLnI_{3-p}(thf)_n$ (p = 1 or 2; Ln = Ce **4.1**, Nd **4.2**, Lu **4.3**, Gd **4.4**, and Ho **4.5**) were generated *in situ* by reactions of an excess of Ln metal activated with Hg metal with iodobenzene (PhI) in tetrahydrofuran (thf) on sonication and further stirring at room temperature. The mixture of lanthanoid metals and PhI was sonicated for 10 min and stirred for 5-12 h at room temperature. After the formation of the Grignard reagent (Ph_nLnI_{n-1}; n = 1 or 2) solid phenol (4-^{t}Bu-PhOH; 1 mmol) was added at room temperature, resulting in coloured solutions (Ce, yellow; Nd, brownish blue, Lu and Gd, brown and Ho brownish yellow) after stirring for ~36 h. Crystallisation from the concentrated solution in dme produced yellow

crystals of **[Ce(4-^{t}Bu-PhO)I_2(dme)$_2$]·0.5dme (4.1)**, blue crystals of **[Nd(4-^{t}Bu-PhO)I_2(dme)$_2$]·0.5dme (4.2)**, colourless crystals of **[Lu(4-^{t}Bu-PhO)I_2(dme)$_2$]·0.5dme (4.3)** and colourless powders of **[Ln(4-^{t}Bu-PhO)I_2(dme)$_2$]·0.5dme** (Gd **4.4**, Ho **4.5)**. These isostructural compounds **(4.1**, **4.2** and **4.3)** are seven coordinate monomers. The reaction and structural scheme of these compounds (**4.1**-**4.5**) is demonstrated in the **Scheme 4.7**.



Scheme 4.7: Synthesis of compounds [Ln(4-^{t}Bu-PhO)I_2(dme)$_2$]·0.5dme (Ce **4.1**, Nd **4.2**, Lu **4.3**, Gd **4.4**, Ho **4.5**).

Satisfactory ^{1}H NMR spectra were obtained for the compounds **4.1**-**4.3** (**Fig. 4.1**-**4.3**). Due to paramagnetism ^{1}H NMR spectra for compounds **4.4** and **4.5** (**Fig. 4.4** and **4.5**) had broad features and unsatisfactory integrations. The ^{1}H NMR spectrum of compound **4.1** indicated the loss of 0.5 molecule dme of solvation, while compound **4.2** showed the loss of 1.5 molecules of dme (1 of crystallisation and 0.5 of solvation consistent with the elemental analyses. The ^{t}Bu resonances in the ^{1}H NMR were observed at 4.26 ppm for compound **4.1**, 3.25 ppm for compound **4.2** and 1.32 ppm for compound **4.3**. For compound **4.1** the methyl (CH_3) signals of dme appeared at -5.92 ppm, and the methylene (CH_2) signals at 10.02 ppm. In compound **4.2** the CH_2 signals of dme merged with ^{t}Bu at δ = 3.25 ppm and the CH_3 signals appeared at -11.21 ppm. In compound **4.3** the CH_3 signals of dme appeared at 3.13 ppm, and the CH_2 signals at 3.33 ppm. The aromatic CH signals from the phenyl (Ph) ring were observed at δ = 14.32 and 24.78 ppm in compound **4.1** and at 21.26 and 39.63 ppm in compound **4.2**. In compound **4.3** the CH signals of the Ph ring are found at 6.61, 7.10, 7.32 and 7.46 ppm. IR spectra showed the presence of the appropriate 4-^{t}Bu-PhO ligand. Additionally, micro and metal analyses validated their bulk purity; the latter being used when there were microanalysis difficulties. The melting points indicate significant thermal stability of the new phenolate compounds.

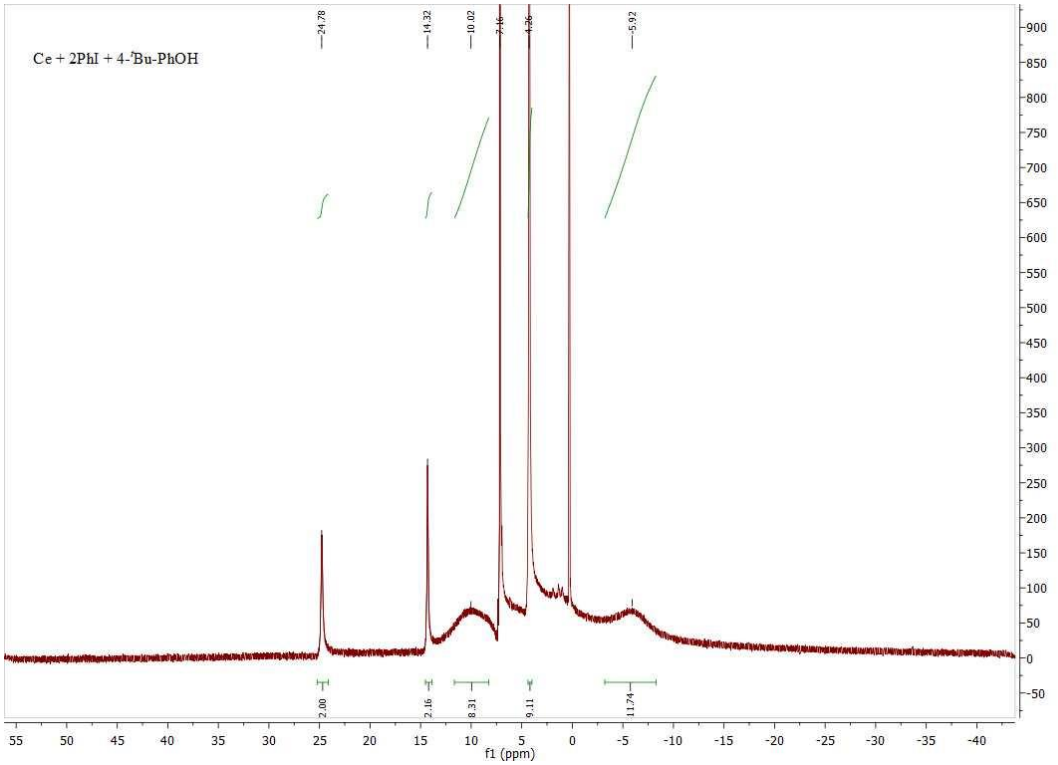


Figure 4.1: ^{1}H NMR spectrum of [**Ce(4-^{t}Bu-PhO)I$_2$(dme)$_2$]·0.5dme (4.1)** (loss of 0.5 molecule dme) in C_6D_6.

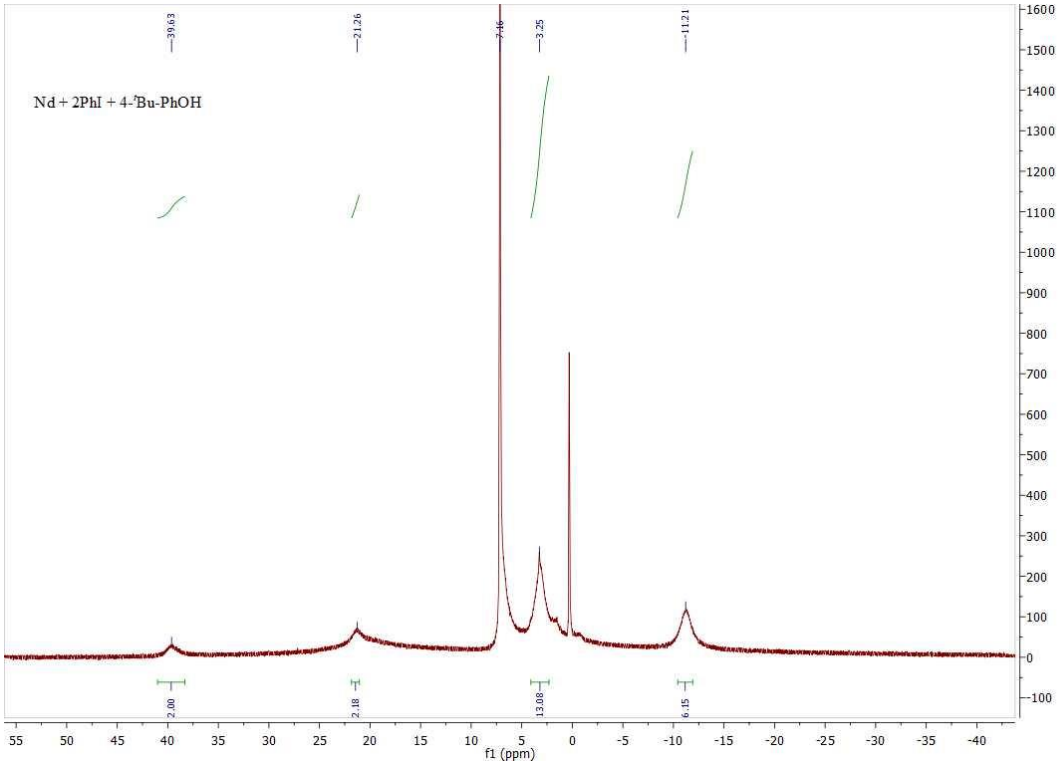


Figure 4.2: ^{1}H NMR spectrum of [**Nd(4-^{t}Bu-PhO)I$_2$(dme)$_2$]·0.5dme (4.2)** (loss of 1.5 molecules dme) in C_6D_6.

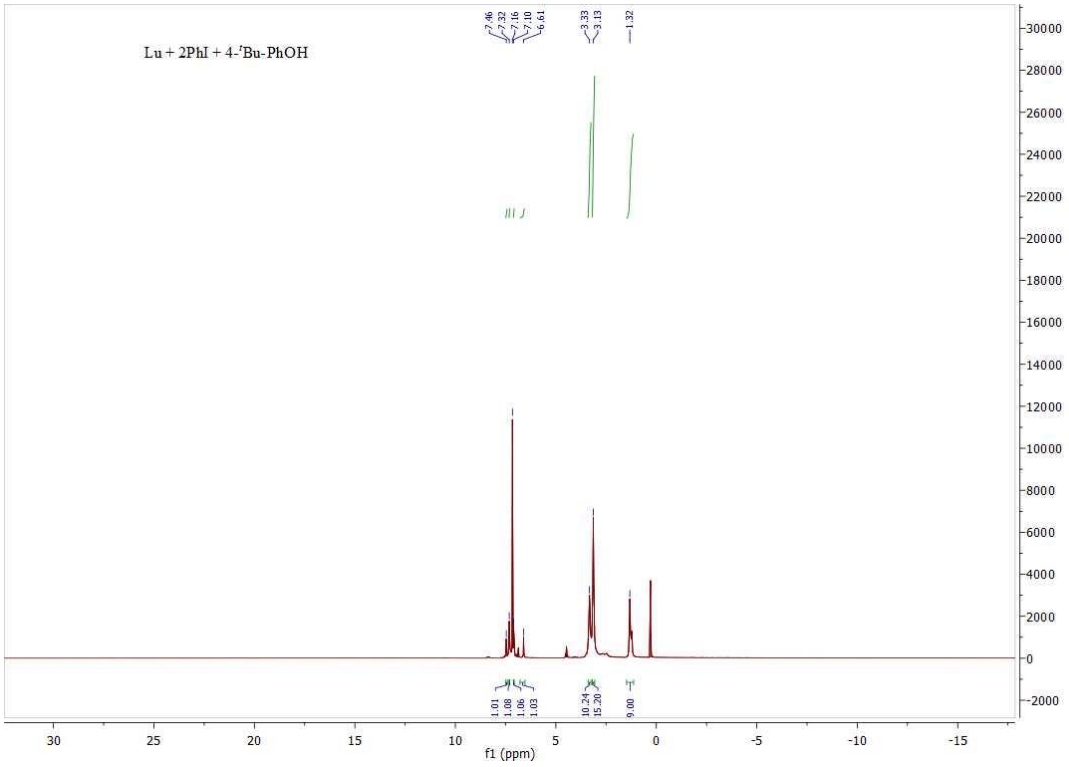


Figure 4.3: ^{1}H NMR spectrum of [**Lu(4-^{t}Bu-PhO)I_2(dme)$_2$]·0.5dme (4.3)** in C_6D_6.

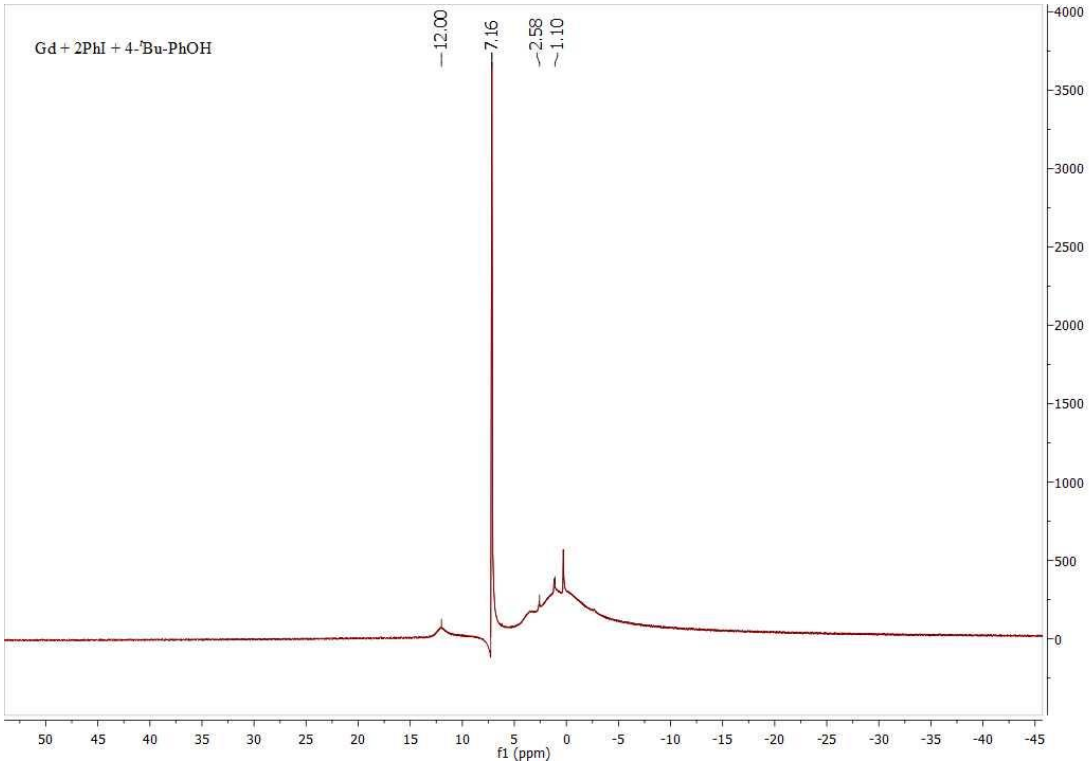


Figure 4.4: ^{1}H NMR spectrum of [**Gd(4-^{t}Bu-PhO)I_2(dme)$_2$]·0.5dme (4.4)** in C_6D_6.

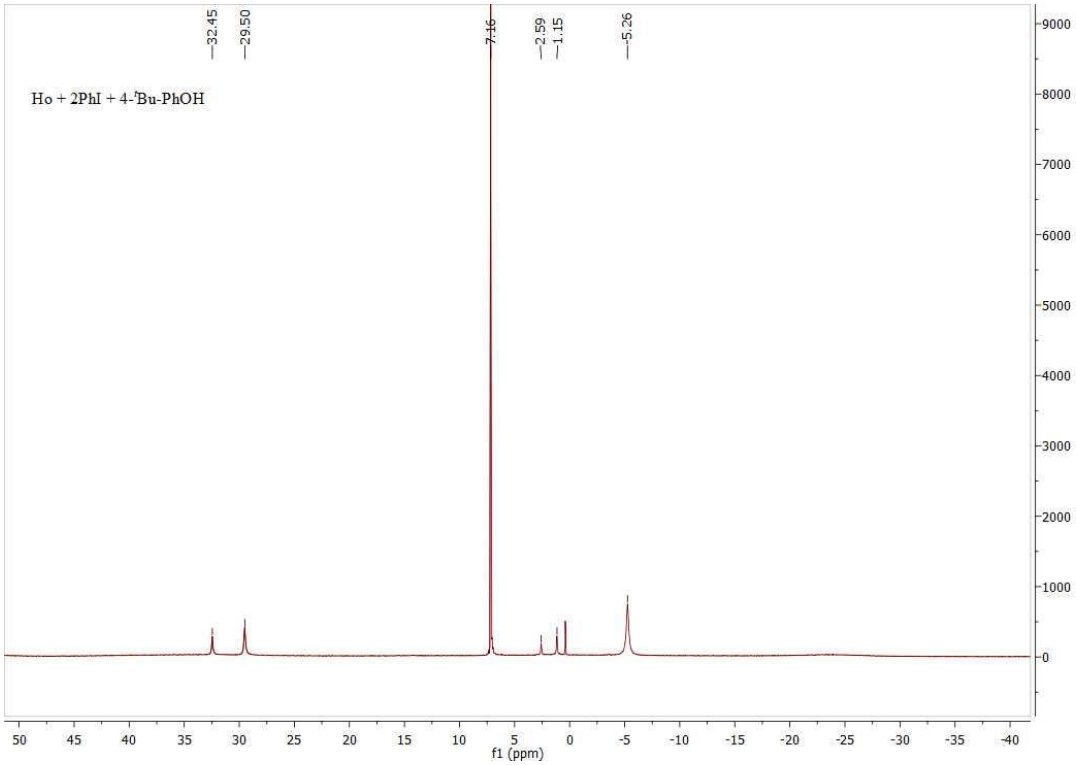
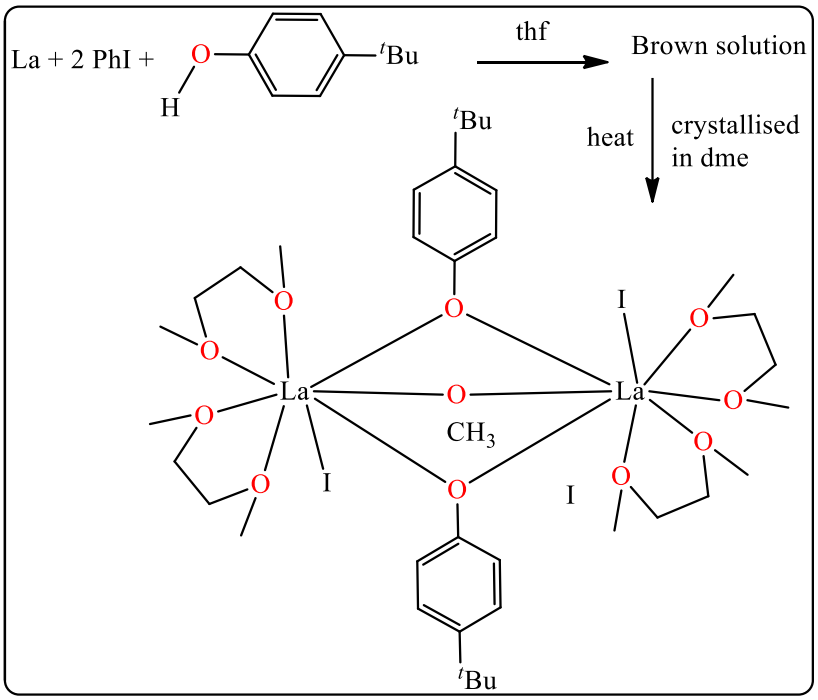


Figure 4.5: ^{1}H NMR spectrum of [**Ho(4-^{t}Bu-PhO)I_2(dme)$_2$]·0.5dme (4.5)** in C_6D_6.

By contrast, reaction for La metal, when dme, upon heating, yielded **[(La(4-^{t}Bu-PhO)I(dme)$_2$)$_2$(OCH$_3$)]I·2dme** (**4.6**) instead of the targeted **[La(4-^{t}Bu-PhO)I_2(dme)$_2$]·0.5dme** complex. The reaction and structural scheme of the complex (**4.6**) is illustrated in the **Scheme 4.8**.



Scheme 4.8: Synthesis of compound [(La(4-^{t}Bu-PhO)I(dme)$_2$)$_2$(OCH$_3$)]I·2dme (**4.6**).

Satisfactory ^{1}H NMR spectra were obtained for the compound **4.6** (**Fig. 4.6**). The ^{1}H NMR spectrum of compound **4.6** showed the loss of 3 dme (1 of crystallisation and 2 of solvation) consistent with the micro and metal analyses. The ^{t}Bu resonances in the ^{1}H NMR were observed at 1.29 ppm, where the CH_3 signals of dme appaired at 3.21 ppm, and the CH_2 signals at 3.11 ppm. The aromatic CH signals from the phenyl (Ph) ring were observed at 6.61, 6.86, 7.30 and 7.45 ppm, and the OCH_3 peak observed at 1.41 ppm. IR spectra showed the presence of the appropriate 4-^{t}Bu-PhO ligand. Additionally, metal analyses validated their bulk purity; its done due to the difficulties of microanalysis. The melting points indicate significant thermal stability of the new phenolate compounds.

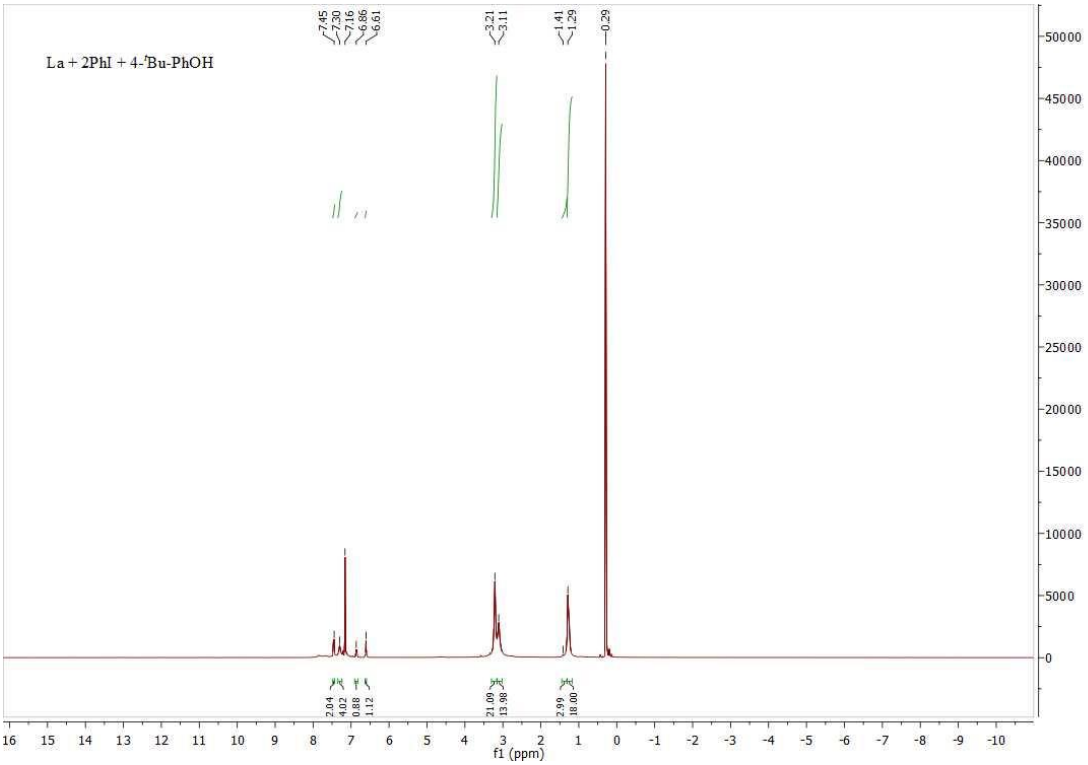


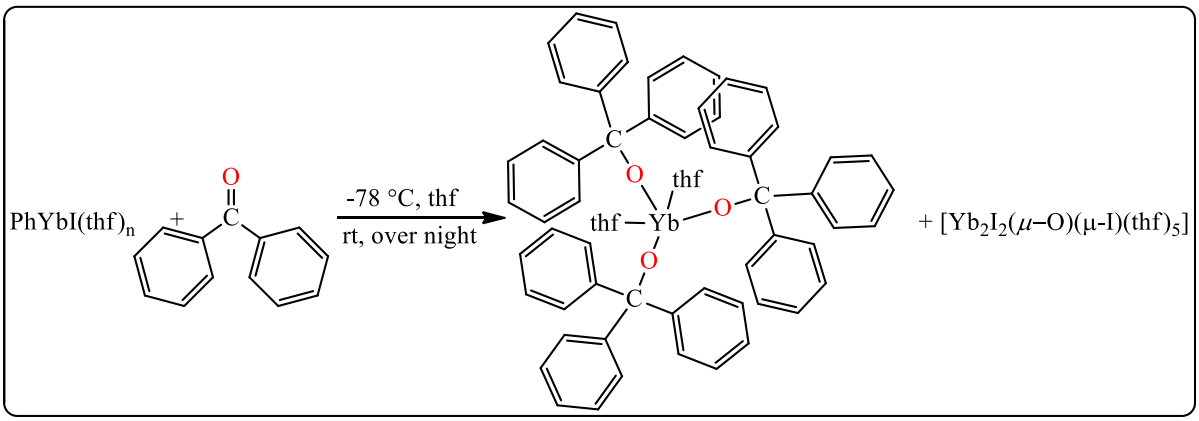
Figure 4.6: ^{1}H NMR spectrum of **[(La(4-^{t}Bu-PhO)I(dme)$_2$)$_2$(OCH$_3$)]I·2dme** (**4.6**) (loss of 3 molecules dme) in C_6D_6.

4.3.1.2 Reactivity of ytterbium pseudo-Grignard reagents with O/N-donor ligands

The ytterbium pseudo-Grignard reagent (PhYbI) was synthesised as described in chapter two. A 1:1 stoichiometric ratio of PhYbI and benzophenone (Ph_2CO) was mixed at -78 °C and stirred for 3 h, whereupon a dark orange solution was obtained after stirring overnight at room

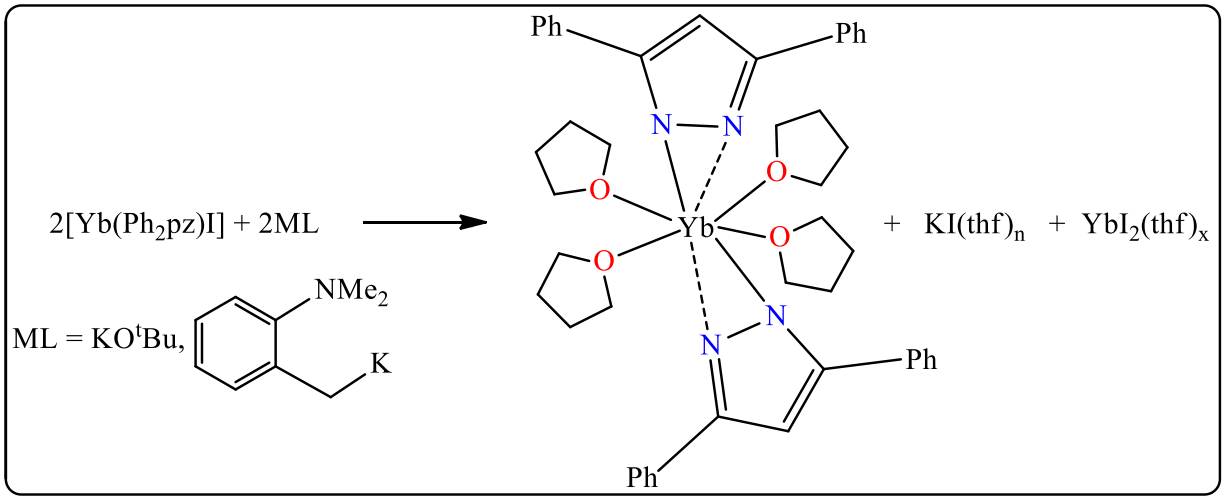
temperature. Crystallisation from the concentrated solution produced red crystals of **[Yb(OCPh$_3$)$_3$(thf)$_2$] (4.7a**), (expected to isolate [(Ph)$_2$Ċ-O-YbI], similar as when PhMgX treated with Ph$_2$C=O yielded [(Ph)$_2$Ċ-O-MgX]) [23] and as a Schlenk equilibrium product yellow crystals of the mixed valent **[Yb$_2$I$_2$(μ-O)(μ-I)(thf)$_5$]·thf (4.7b)** from the remaining solution. The reaction and structural scheme of these complexes **[Yb(OCPh$_3$)$_3$(thf)$_2$] (4.7a**) and **[Yb$_2$I$_2$(μ-O)(μ-I)(thf)$_5$]·thf (4.7b)** is presented in the **Scheme 4.9**.

Again, we tried the similar reaction of [PhYbI] with [CO{Ph(4-methoxy)}$_2$], obtained a red blood coloured solution after stirring overnight. From the concentrated solution yellow crystals of **[YbI$_2$(thf)$_5$]** were isolated, (a Schlenk equilibrium product), and we could not isolate the targeted product **[Yb(OC(Ph(OCH$_3$))$_3$)$_3$(thf)$_2$]** due to crystallisation difficulties.



Scheme 4.9: Synthesis of compounds [Yb(OCPh$_3$)$_3$(thf)$_2$] (4.7a) and [Yb$_2$I$_2$(μ-O)(μ-I)(thf)$_5$]·thf (4.7b).

To understand further reactivity of [Yb(Ph$_2$pz)I(thf)$_4$], we performed a reaction using a 1:1 stoichiometric ratio of [Yb(Ph$_2$pz)I(thf)$_4$] and KO^{t}Bu or (KMe)Ph(NMe$_2$) at room temperature, where dark brown solutions and colourless precipitates (probably KI salts) were obtained. From the concentrated solutions of both reactions was yielded [Yb(Ph$_2$pz)$_2$(thf)$_4$] as a Schlenk equilibrium rearrangement product. The possible reaction pathway of the complex **[Yb(Ph$_2$pz)$_2$(thf)$_4$]** (**4.8**) is presented in the **Scheme 4.10**.



Scheme 4.10: Possible reaction pathway of the compound $[Yb(Ph_2pz)_2(thf)_4]$ (4.8).

A satisfactory ^1H NMR spectrum was obtained for compound **4.8** (**Fig. 4.7**), indicated one extra molecule thf from solvation. The backbone (pz) resonance in the ^1H NMR spectrum merged with the Ph signal at 7.21 ppm, while the other two signals of the Ph ring were observed at 7.07 and 8.05 ppm. The CH_2 signals of thf were observed at δ = 1.31 and 3.67 ppm respectively. The IR spectrum showed the presence of the appropriate Ph_2pz ligand. Additionally, metal analysis validated its bulk purity. The melting point indicated significant thermal stability of the new compound.

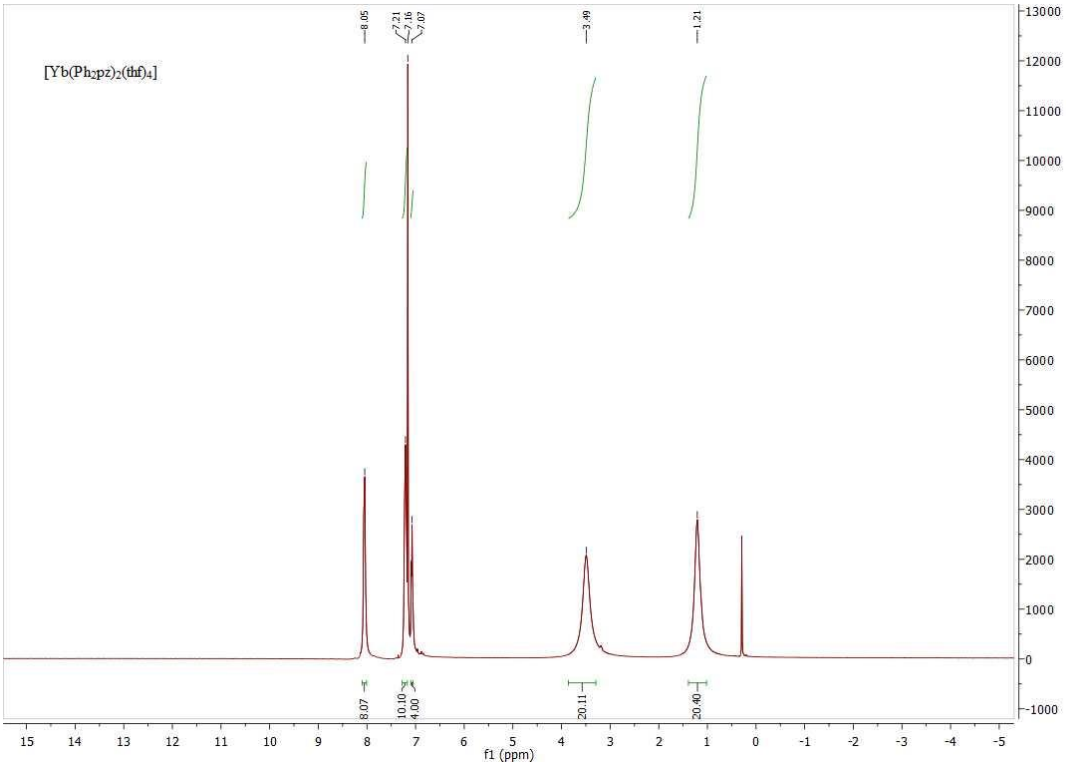


Figure 4.7: ^{1}H NMR spectrum of **[Yb(Ph$_2$pz)$_2$(thf)$_4$] (4.8)** (extra 1 molecule thf) in C_6D_6.

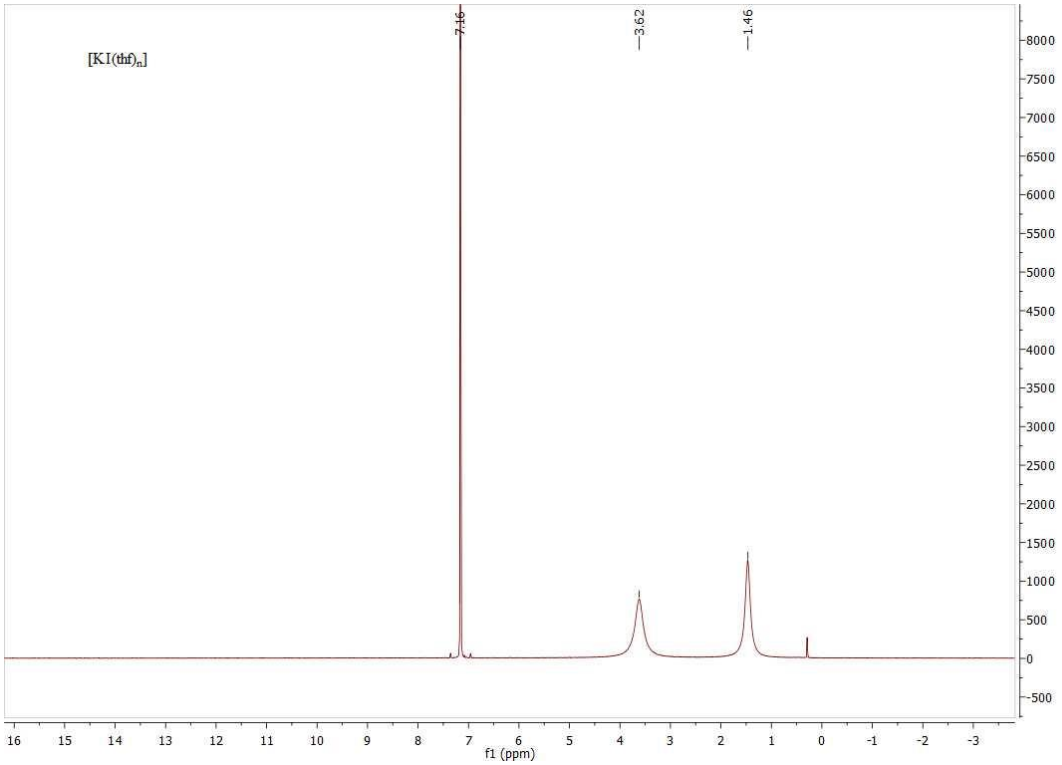


Figure 4.8: ^{1}H NMR spectrum of **[KI(thf)$_n$]** in C_6D_6.

4.3.2 X-ray Crystal Structures

4.3.2.1 **[Ln(4-^{t}Bu-PhO)I$_2$(dme)$_2$]·0.5dme** (**4.1** Ce, **4.2** Nd and **4.3** Lu)

Iso-structural compounds [Ln(4-^{t}Bu-PhO)I$_2$(dme)$_2$]·0.5dme (**4.1**-**4.3**) crystallised in the monoclinic space group *C*2/c. The coordination geometry of these monomeric complexes (**4.1**-**4.3**) is described as pentagonal bipyramidal, where the seven-coordinate metal centre is coordinated by one phenolate ligand, two bidentate dme ligands and two *transoid* iodide ligands (**Fig. 4.5**, **Ce** as a representative). The I(1)-Ln-I(2) bond angles are 169.76°, 169.89° and 169.92° for compounds **4.1**, **4.2** and **4.3** respectively. The iodide ligands are *cisoid* to the phenolate oxygen with bond angles (I(1)-Ce-O(1) at 87.70° and I(2)-Ce-O(1) at 99.80° in compound **4.1**, I(1)-Nd-O(1) at 87.30° and I(2)-Nd-O(1) at 100.28° in compound **4.2**, and I(1)-Lu-O(1) at 87.67° and I(2)-Lu-O(1) at 100.03° in compound **4.3**. The lanthanoid contraction is evident in the Ln-O(1) (phenolate oxygen) bond lengths, with Ce-O(1) at 2.16 Å, Nd-O(1) at 2.13 Å, and Lu-O(1) at 2.04 Å. These Ln-O bond lengths are shorter than observed (2.117(2) Å - 2.121(2) Å) in the five coordinate complex [Dy(OC$_6$H$_2$-2,4,6-^{t}Bu$_3$)Br(thf)$_2$].[24]

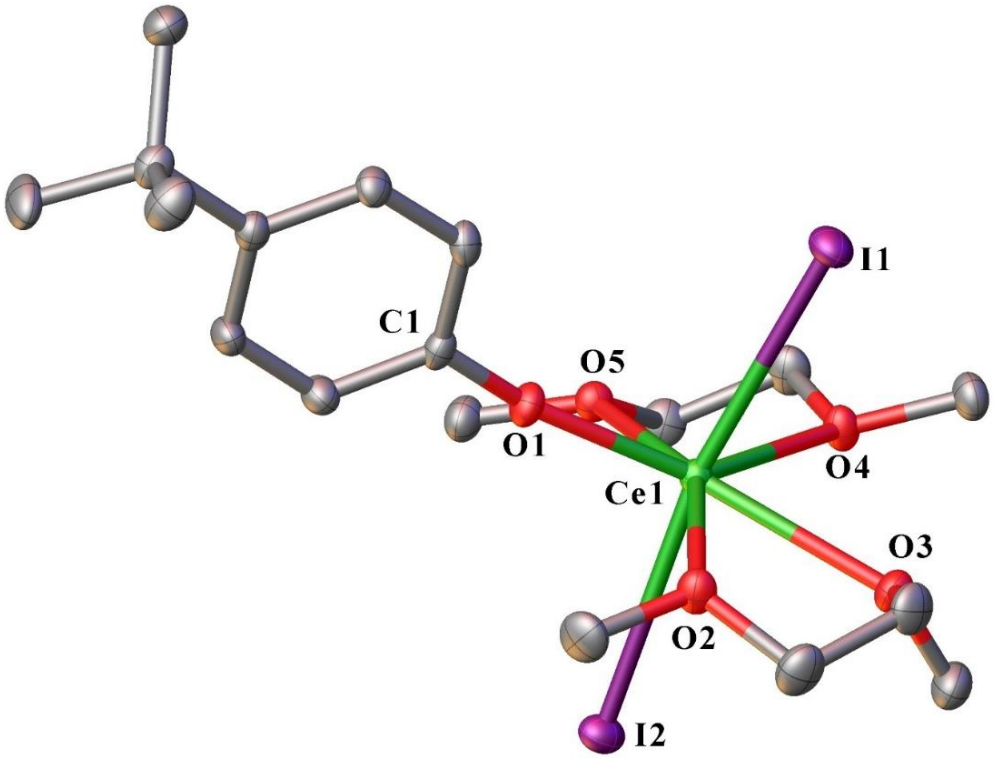


Figure 4.5: X-ray crystal structure of [Ce(4-^{t}Bu-PhO)I_2(dme)$_2$]·0.5dme (also representative of Nd **4.2** and Lu **4.3**). Thermal ellipsoids are set at the 50% probability level, hydrogen atoms and solvated dme are omitted for clarity. Selected bond lengths (Å): Ce(1)-I(1) 3.1375(4), Ce(1)-I(2) 3.1566(4), Ce(1)-O(1) 2.164(3), Ce(1)-O(2) 2.558(3), Ce(1)-O(3) 2.537(3), Ce(1)-O(4) 2.578(3) and Ce(1)-O(5) 2.552(3); Nd(1)-I(1) 3.104(6), Nd(1)-I(2) 3.1173(6), Nd(1)-O(1) 2.138(4), Nd(1)-O(2) 2.503(4), Nd(1)-O(3) 2.518(4), Nd(1)-O(4) 2.539(4) and Nd(1)-O(5) 2.507(4); Lu(1)-I(1) 2.9900(8), Lu(1)-I(2) 2.9799(7), Lu(1)-O(1) 2.044(5), Lu(1)-O(2) 2.396(5), Lu(1)-O(3) 2.370(5), Lu(1)-O(4) 2.420(5) and Lu(1)-O(5) 2.378(5). For more details, see the **Table 4.2**.

The average Ln-I bond length is 3.1470(4) Å in compound **4.1**, 3.1106(6) Å in compound **4.2** and 2.9849(7) Å in compound **4.3**, all longer than 2.9160(2) Å observed in the five coordinate complex [Yb(OC_6H_2-2,6-^{t}Bu_2-4-Me)I(thf)$_2$].[25] The average Ln-O bond lengths for the coordinated dme solvents is 2.556(3) Å in compound **4.1**, 2.519(4) Å in compound **4.2** and 2.391(5) Å in compound **4.3**.

Table 4.1: A comparison of the selected average bond lengths (Å) with similar compounds.

Complex	Ln-O$_{(ligand)}$	<Ln-O>$_{(solvents)}$	<Ln-X>	Ref.
[Ce(4-^{t}BuPhO)I_2(dme)$_2$]	2.164(3)	2.556(3)	3.1470(4)	Current work

[Nd(4-^{t}BuPhO)I_2(dme)$_2$]	2.138(4)	2.519(4)	3.1106(6)	Current work
[Lu(4-^{t}BuPhO)I_2(dme)$_2$]	2.044(5)	2.391(5)	2.9849(7)	Current work
[Yb(L^2)$_2$(OAr)]	2.068(2)			[26]
[Dy(OPh)Cl_2(thf)$_5$]	2.113(4)		2.5872(12)	[27]
[Sm(OPh)(C_5Me_5)(thf)]	2.1645(14)	2.4729(15)		[28]
[La($OPPh_3$)$_4I_2$]$^+$	2.367(5)		3.201(1)	[29]
[Ce($OPPh_3$)$_4I_2$]$^+$	2.344(3)		3.180(1)	[29]
[Nd($OPPh_3$)$_4I_2$]$^+$	2.314(4)		3.141(1)	[29]
[Dy(Cy_3PO)$_2I_3$(thf)]	2.188(4)	2.383(4)	2.9923(5)	[30]

Cy_3PO = tricyclohexylphosphine oxide

Table 4.2: Selected bond lengths and angles of compounds (**4.1**-**4.3**).

Bond lengths (Å)	**4.1**	**4.2**	**4.3**
Ln(1)-I(1)	3.1375(4)	3.1040(6)	2.9900(8)
Ln(1)-I(2)	3.1566(4)	3.1173(6)	2.9799(7)
Ln(1)-O(1)	2.164(3)	2.138(4)	2.044(5)
Ln(1)-O(2)	2.558(3)	2.503(4)	2.396(5)
Ln(1)-O(3)	2.537(3)	2.518(4)	2.370(5)
Ln(1)-O(4)	2.578(3)	2.507(4)	2.420(5)
Ln(1)-O(5)	2.552(3)	2.539(4)	2.378(5)
Bond angles (°)	**4.1**	**4.2**	**4.3**
I(1)-Ln(1)-I(2)	169.76(10)	169.897(15)	169.929(17)
O(1)-Ln(1)-I(1)	87.70(7)	87.31(13)	100.03(14)
O(1)-Ln(1)-I(2)	99.80(7)	100.28(13)	87.67(14)
O(1)-Ln(1)-O(2)	80.83(10)	145.02(15)	79.54(18)
O(1)-Ln(1)-O(3)	144.69(10)	80.74(15)	146.12(18)
O(1)-Ln(1)-O(4)	137.85(10)	80.32(15)	138.20(18)
O(1)-Ln(1)-O(5)	80.82(9)	137.76(15)	78.41(18)

4.3.2.2 **[(La(4-^{t}Bu-PhO)I(dme)$_2$)$_2$(OCH$_3$)I)]·2dme (4.6)**

Compound [(La(4-^{t}Bu-PhO)I(dme)$_2$)$_2$(OCH$_3$)I)]·2dme (**4.6**) crystallised in the triclinic space group *P*-1. The coordination geometry of the monomeric compound **4.6** is described as a distorted bicapped antiprism, where the eight-coordinate metal centre has two phenolate ligands, one methoxy ligand, two bidentate dme ligands and one iodide ligand (**Fig. 4.6**). The average La-I bond length in compound **4.6** is 3.2386(7) Å, same as 3.2358(4) Å in the seven coordinate compound [(dpp-Bian)LaI(dme)$_2$] (dpp-Bian = 1,2-bis[(2,6-diisopropylphenyl)imino]acenaphthene).[31]

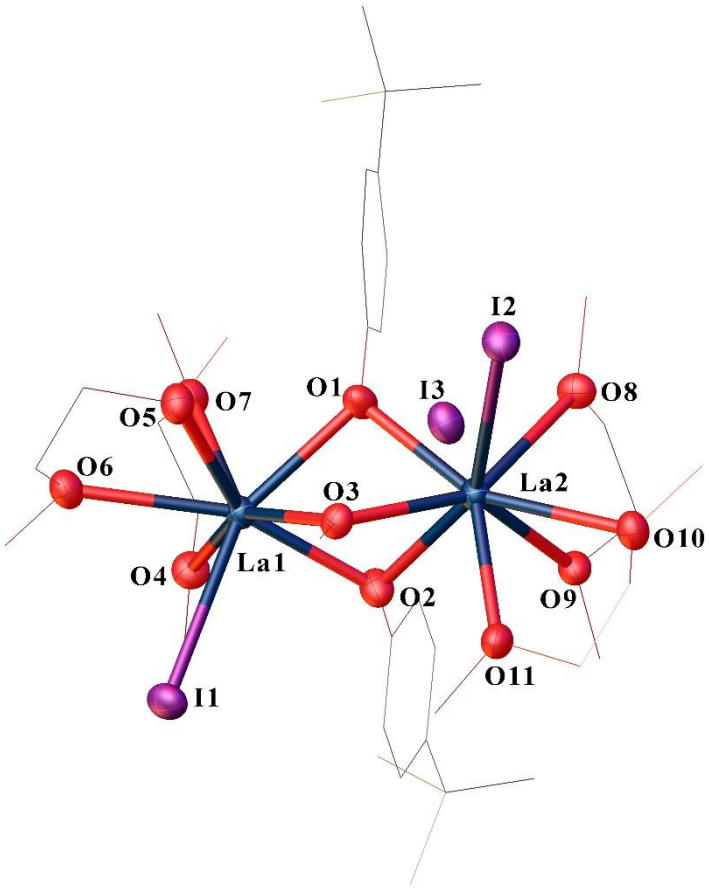


Figure 4.6: X-ray crystal structure of [(La(4-^{t}Bu-PhO)I(dme)$_2$)$_2$(OCH$_3$)I)·2dme (**4.6**). Thermal ellipsoids are set at the 50% probability level, hydrogen atoms and solvated dme are omitted, ^{t}BuPh, Me are made warfare for clarity. Selected bond lengths (Å): La(1)-I(1) 3.2398(7), La(1)-O(1) 2.468(5), La(1)-O(2) 2.429(5), La(1)-O(3) 2.379(5), La(1)-O(4) 2.642(5), La(1)-O(5) 2.596(5), La(1)-O(6) 2.656(5), La(1)-O(7) 2.590(5), La(2)-I(2) 3.2375(7), La(2)-O(1) 2.431(5), La(2)-O(2) 2.484(5), La(2)-O(3) 2.380(5), La(2)-O(8) 2.636(5), La(2)-O(9) 2.616(5), La(2)-O(10) 2.645(5), La(2)-O(11) 2.582(5). For more details including **La(2)**, see the **Table 4.3**.

The average La-O bond length of the phenolate is 2.453(5) Å, which is longer than 2.302(3) Å in the five coordinate [YbI(μ-OCPh$_3$)(η^2-dme)]$_2$.[32] The average La-O$_{(methoxy)}$ bond length is 2.379(5) Å which is longer than 2.185(4) Å in the five coordinate [YbI$_2$(μ-OMe)(η^2-dme)]$_2$.[32] Again the average La-O bond length of dme solvent is 2.627(5) Å, which is shorter than 2.692(7) Å in the seven coordinate compound [(dpp-Bian)LaI(dme)$_2$].[31] This phenomenon is attributed to the effect of ionic radius (eight coordinate La^{3+} 1.16 Å > seven coordinate La^{3+} 1.10 Å).[33]

Table 4.3: Selected bond lengths and angles of the compound (**4.6**).

Bond lengths (Å)	**4.6**	**Bond lengths (Å)**	**4.6**
La(1)-I(1)	3.2398(7)	La(2)-I(2)	3.2375(7)
La(1)-O(1)	2.468(5)	La(2)-O(1)	2.431(5)
La(1)-O(2)	2.429(5)	La(2)-O(2)	2.484(5)
La(1)-O(3)	2.379(5)	La(2)-O(3)	2.380(5)
La(1)-O(4)	2.642(5)	La(2)-O(8)	3.636(5)
La(1)-O(5)	2.596(5)	La(2)-O(9)	2.616(5)
La(1)-O(6)	2.656(5)	La(2)-O(10)	2.645(5)
La(1)-O(7)	2.590(5)	La(2)-O(11)	2.582(5)
Bond angles (°)	**4.6**	**Bond angles (°)**	**4.6**
La(1)-O(1)-La(2)	96.08(18)	O(1)-La(1)-O(2)	71.37(17)
La(1)-O(2)-La(2)	95.70(17)	O(1)-La(1)-O(3)	69.18(17)
La(1)-O(3)-La(2)	99.87(18)	I(2)-La(2)-O(1)	87.44(12)
I(1)-La(1)-O(1)	150.59(12)	I(2)-La(2)-O(2)	150.33(12)
I(1)-La(1)-O(2)	87.21(13)	I(2)-La(2)-O(3)	85.29(11)
I(1)-La(1)-O(3)	84.73(12)	O(1)-La(2)-O(2)	71.07(17)

4.3.2.3 $[Yb(OCPh_3)_3(thf)_2]$ (**4.7a**)

The compound **$[Yb(OCPh_3)_3(thf)_2]$** (**4.7a**) crystallised in the monoclinic space group $P2_1/n$. The coordination geometry of the monomeric complex **4.7a** is best described as trigonal bipyramidal, with the five-coordinate Yb centre bound to three $OCPh_3$ ligands and two thf ligands (**Fig. 4.7**). The average Yb-O bond length of the $OCPh_3$ ligands in **4.7a** is 2.046(2) Å, which is shorter than the 2.293(4) Å observed in the five coordinate complex $[Yb(\mu\text{-}OCPh_3)I(dme)]_2$.[34] The <Yb-O> bond length involving the thf ligands in **4.7a** is 2.332(2) Å, shorter than 2.416(4) Å in the five coordinate complex $[Yb(Dpp)I(thf)_3]$ (Dpp = 2,6-$Ph_2C_6H_3$).[35]

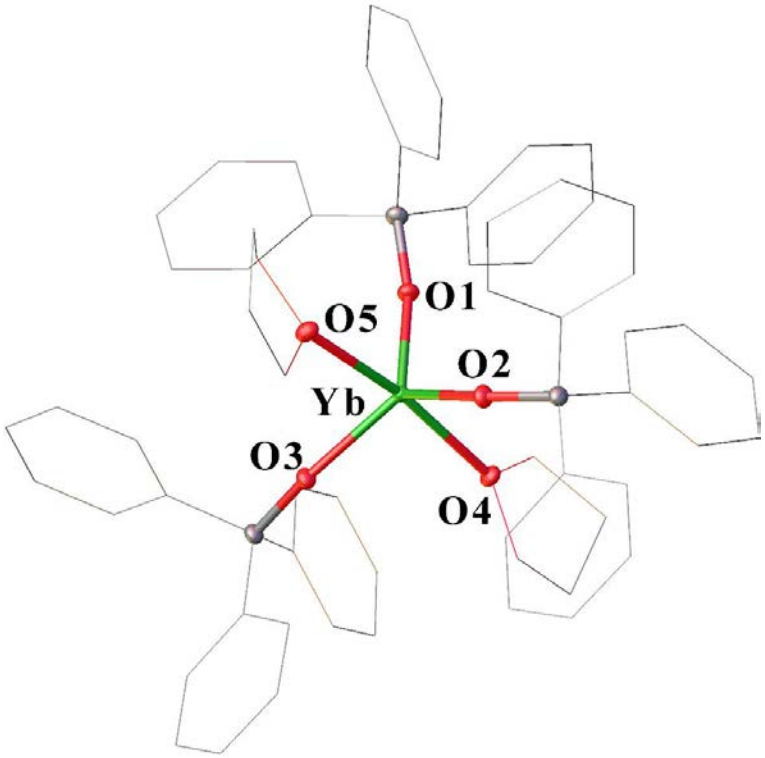


Figure 4.7: X-ray crystal structure of $[Yb(OCPh_3)_3(thf)_2]$ (**4.7a**). Thermal ellipsoids are set at the 50% probability level. Hydrogen atoms are omitted and coordinated thf molecules and Ph groups are drawn as wireframe for clarity. Selected bond lengths (Å): Yb(1)-O(1) 2.025(2), Yb(1)-O(2) 2.058(2), Yb(1)-O(3) 2.055(2), Yb(1)-O(4) 2.357(2) and Yb(1)-O(5) 2.308(2). For more details, see the **Table 4.4**.

Table 4.4: Selected bond lengths and angles of the compound (**4.7a**).

Bond lengths (Å)	**4.7a**	**Bond lengths (Å)**	**4.7a**
Yb-O(1)	2.025(2)	Yb-O(4)	2.357(2)
Yb-O(2)	2.058(2)	Yb-O(5)	2.308(2)
Yb-O(3)	2.055(2)		
Bond angles (°)		**Bond angles (°)**	
O(1)-Yb-O(2)	119.99(9)	O(2)-Yb-O(4)	83.26(8)
O(1)-Yb-O(3)	115.66(9)	O(2)-Yb-O(5)	91.02(8)
O(1)-Yb-O(4)	94.47(7)	O(3)-Yb-O(4)	86.03(7)
O(1)-Yb-O(5)	96.15(8)	O(3)-Yb-O(5)	89.78(7)
O(2)-Yb-O(3)	123.89(9)	O(4)-Yb-O(5)	89.78(7)

4.3.2.4 $[Yb_2I_2(\mu\text{-}O)(\mu\text{-}I)(thf)_5]\cdot thf$ (**4.7b**)

The compound **$[Yb_2I_2(\mu\text{-}O)(\mu\text{-}I)(thf)_5]\cdot thf$** (**4.7b**) crystallised in the monoclinic space group $P2_1/n$. The coordination geometry in compound **4.7b** is distinct for each ytterbium center: Yb(1) adopts a square pyramidal geometry, while Yb(2) has an octahedral coordination environment. The five-coordinate Yb(1) is bonded with two iodide ligands, two thf ligands and one oxygen ligand, whereas the six-coordinate Yb(2) is bonded with two iodide ligands, three thf ligands and one oxygen ligand (**Fig. 4.8**). The difference in Yb-I bond length (Yb(1)-I(2) (2.9976(6) Å> 3.1779(6) Å)> Yb(2)-I(2)) indicated that Yb(1) is trivalent and Yb(2) is divalent. The average Yb-I bond length in compound **4.7b** is 3.1281(6) Å, which is longer than 2.9320(1) Å observed in the six coordinate complex $[YbI_2(\mu\text{-}OMe)(dme)]_2$.[34] The <Yb-O($_{\mu\text{-}O}$)> bond length in **4.7b** is 2.186(5) Å, which is statistically equivalent with the<Yb-O($_{OMe}$)> 2.181(5) Å reported for the aforementioned $[YbI_2(\mu\text{-}OMe)(dme)]_2$.[34] Similarly, the <Yb-O($_{thf}$)> bond length in **4.7b** is 2.392(5) Å, which is longer than the 2.273(4) Å reported for the six coordinate complex $[YbI_3(thf)_3]$.[36] This difference can be attributed to the mixed oxidation states and varying coordination numbers present in compound **4.7b**.

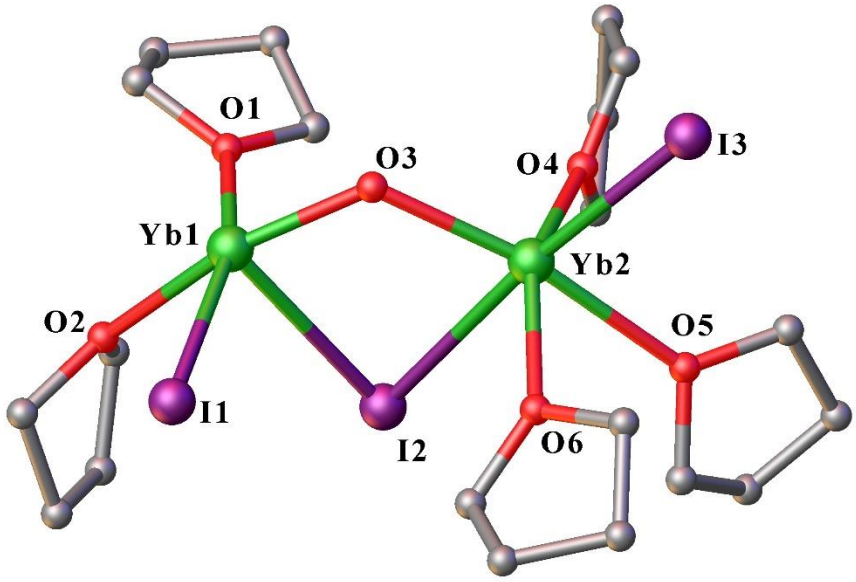


Figure 4.8: X-ray crystal structure of $[Yb_2I_2(\mu\text{-}O)(\mu\text{-}I)(thf)_5]\cdot thf$ (**4.7b**). Thermal ellipsoids are set at the 50% probability level. Hydrogen atoms are omitted for clarity. Selected bond lengths (Å): Yb(1)-I(1) 2.9976(6), Yb(1)-I(2) 3.1616(5), Yb(1)-O(1) 2.316(5), Yb(1)-O(2) 2.421(5), Yb(1)-O(3) 2.100(5), Yb(2)-I(2) 3.1779(6), Yb(2)-I(3) 3.0753(6), Yb(2)-O(3) 2.272(5), Yb(2)-O(4) 2.465(5), Yb(2)-O(5) 2.487(5) and Yb(2)-O(6) 2.455(5). For more details including **Yb(2)**, see the **Table 4.5**.

Table 4.5: Selected bond lengths and angles of the compound (**4.7b**).

Bond lengths (Å)	**4.7b**	**Bond angles (°)**	**4.7b**
Yb(1)-I(1)	2.9976(6)	Yb(1)-I(2)-Yb(2)	74.222
Yb(1)-I(2)	3.1616(5)	Yb(1)-O(3)-Yb(2)	122.031
Yb(1)-O(1)	2.316(5)	I(1)-Yb(1)-I(2)	94.797
Yb(1)-O(2)	2.421(5)	I(2)-Yb(2)-I(3)	175.180
Yb(1)-O(3)	2.100(5)	I(1)-Yb(1)-O(3)	100.778
Yb(2)-I(2)	3.1779(6)	I(2)-Yb(1)-O(3)	83.251
Yb(2)-I(3)	3.0753(6)	I(2)-Yb(2)-O(3)	80.364
Yb(2)-O(3)	2.272(5)	I(3)-Yb(2)-O(3)	103.993
Yb(2)-O(4)	2.465(5)	O(1)-Yb(1)-O(3)	96.707
Yb(2)-O(5)	2.487(5)	O(4)-Yb(2)-O(3)	101.821
Yb(2)-O(6)	2.455(5)	O(4)-Yb(2)-O(6)	101.654

4.3.2.5 $[Yb(Ph_2pz)_2(thf)_4]$ (**4.8**)

The compound $[Yb(Ph_2pz)_2(thf)_4]$ (**4.8**) crystallised in the monoclinic space group $P2_1/c$. The coordination geometry of the monomeric compound **4.8** is best described as square antiprismatic, where the eight-coordinate ytterbium centre is bonded to two η^2-Ph_2pz ligands and four thf ligands (**Fig. 4.9**). The average Yb-N bond length in compound **4.8** is 2.479(5) Å, which is slightly longer than the 2.424(7) Å observed in the eight coordinate complex $[Yb(Ph_2pz)_2(dme)_2]$.[37] This difference is likely due to the influence of the solvent; monodentate *vs* bidentate. The average Yb-O bond length is 2.514(4) Å in compound **4.8**, is greater than the 2.341(13) Å found in the eight coordinate compound $[Yb(Ph_2pz)_3(thf)_2]$, [38] a result that may be attributed to the steric effects of Ph_2pz ligand. The bite angles of compound **4.8** are (N(1)-Yb-N(2) 31.69°) and (N(3)-Yb-N(4) 31.83°), which are slightly smaller than the bite angle of 33.02° observed in the precursor complex $[Yb(Ph_2pz)I(thf)_4]$.[39] This phenomenon can be attributed to the ionic radius difference between eight coordinate Yb^{2+} (1.14 Å) and seven coordinate Yb^{2+} (1.08 Å).[33]

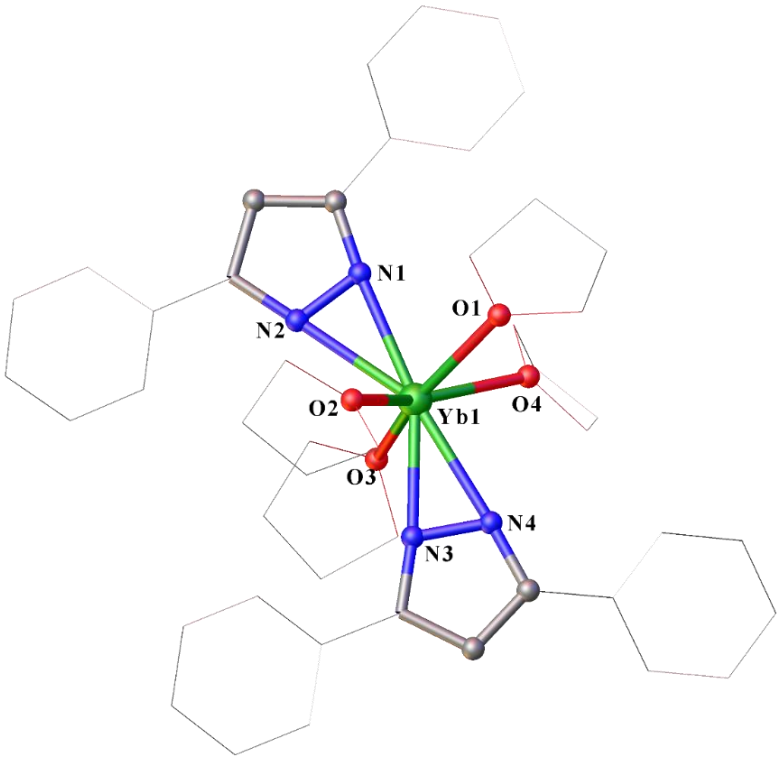


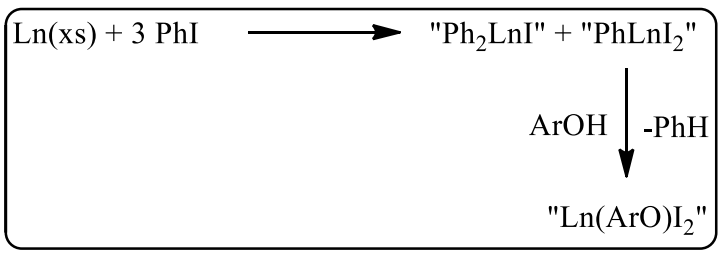
Figure 4.9: X-ray crystal structure of $[Yb(Ph_2pz)_2(thf)_4]$ (**4.8**). Thermal ellipsoids are set at the 50% probability level. Hydrogen atoms are omitted and coordinated thf molecules and Ph groups are drawn as wireframe for clarity. Selected bond lengths (Å): Yb(1)-N(1) 2.458(5), Yb(1)-N(2) 2.498(5), Yb(1)-N(3) 2.429(5), Yb(1)-N(4) 2.536(5), Yb(1)-O(1) 2.496(4), Yb(1)-O(2) 2.516(4), Yb(1)-O(3) 2.529(4), Yb(1)-O(4) 2.516(4). For more details, see the **Table 4.6**.

Table 4.6: Selected bond lengths and angles of the compound (**4.8**).

Bond lengths (Å)	4.8	Bond angles (°)	4.8
Ln-N(1)	2.458(5)	O(1)-Ln-O(2)	74.589
Ln-N(2)	2.498(5)	O(1)-Ln-O(3)	152.211
Ln-N(3)	2.429(5)	O(1)-Ln-O(4)	78.807
Ln-N(4)	2.536(5)	O(2)-Ln-O(3)	132.967
Ln-O(1)	2.496(4)	O(2)-Ln-O(4)	152.278
Ln-O(2)	2.516(4)	O(3)-Ln-O(4)	74.268
Ln-O(3)	2.529(4)	C(8)-Ln-O(1)	92.08
Ln-O(4)	2.516(4)	C(8)-Ln-O(2)	86.447
		C(8)-Ln-O(3)	87.076

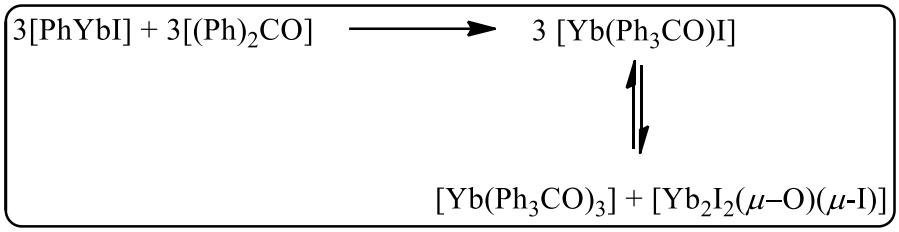
4.3.3 Discussion

The reaction between lanthanoid (III) metals (Ce, Nd, Gd, Ho and Lu) PhI and 4-^{t}Bu phenol, facilitated the isolation of Ln(III) pseudo-Grignard complexes, specifically [Ln(4-^{t}Bu-PhO)I_2(dme)$_2$]·0.5dme. The reaction with lanthanum metal yielded the dimeric complex [(La(4-^{t}Bu-PhO)I(dme)$_2$)$_2$(OCH_3)I]·2dme. All these findings are somewhat different what Bruin-Dickason obtained with the Ln(II) stable metals (Sm, Eu and Yb); [Yb(Odp)$_2$(thf)$_3$], [Ln(Odbmp)$_2$(thf)$_3$] (Ln = Eu, Yb), [Ln(Odip)$_3$(thf)$_2$] (Ln = Eu, Yb), [Yb(Odbmp)$_2$(μ-OH)(thf)]$_2$, and [Sm(Odbmp)(μ-I)(thf)$_3$]$_2$.[20] The possible reaction pathway for the complexes **4.1** to **4.5** is illustrated in **Scheme 4.11**. The formation of trivalent europium and ytterbium complexes for the less sterically bulky ligands, possible explanation is that the smaller phenolate ligands are unable to protect intermediate divalent aryloxide complexes from further oxidation.



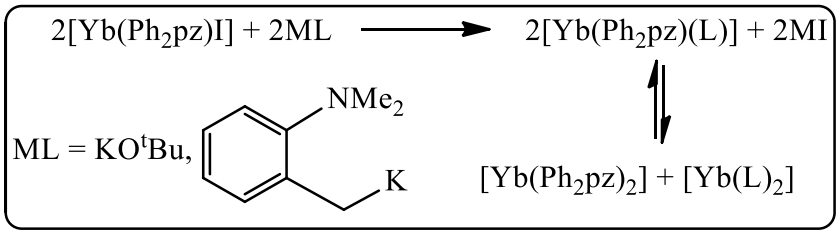
Scheme 4.11: Possible reaction pathway of the compounds (**4.1**-**4.5**) (ArOH = 4-^{t}Bu- phenol).

The reactivity of Yb pseudo-Grignard reagents with Ph_2CO yielded the Schlenk redistribution products, $[Yb(OCPh_3)_3(thf)_2]$ (**4.7a**) and $[Yb_2I_2(\mu\text{-}O)(\mu\text{-}I)(thf)_5]\cdot thf$ (**4.7b**), instead of the targeted product $[Yb(Ph_2CO)I(thf)_n]$. The possible reaction pathway of the complexes **4.7**(**a**, **b**) is illustrated in Scheme **4.12**, which satisfies the findings that Evans identified in 1971 and Ali *et al.* 2018.[40, 41] Evans stated the involvement of Ln(III) in the reaction mixtures and here we obtained trivalent compounds which are part of the complex Schlenk equilibrium for these metals where Ln(II) and Ln(III) are involved (see Scheme **4.9** earlier).



Scheme 4.11: Possible reaction mechanism of the compounds (**4.7((a, b)**).

To investigate the reactivity of $[Yb(Ph_2pz)I(thf)_4]$ with O-donor KO^{t}Bu and N-donor $K(Me)PhNMe_2$ ligands, unfortunately we were not able to isolate the desired $[Yb(Ph_2pz)(O^{t}Bu/Ph(Me)NMe_2)(thf)_x]$ complex, instead the equilibrium product $[Yb(Ph_2pz)_2(thf)_4]$ was isolated. The possible reaction pathway of the complex $[Yb(Ph_2pz)_2(thf)_4]$ is illustrated in Scheme **4.13**.



Scheme 4.11: The possible reaction pathway of the complex (**4.8**).

4.4 Conclusion and Future Outlook

The results obtained from this chapter demonstrate that the use of the Ph_nLnI_{3-n} (n = 1 or 2) Grignard reagents effectively trap O-donor ligand (4-^{t}Bu-phenol). The reaction of Ln^0 metals with PhI, followed by the addition of 4-^{t}Bu-phenol, allows for the synthesis of trivalent monomeric pseudo-Grignard complexes, $[Ln(4\text{-}^t\text{Bu-PhO})I_2(dme)_2]\cdot 0.5dme$ (Ln = Ce, Nd, Gd, Ho and Lu) and the dimeric complex $[(La(4\text{-}^t\text{Bu-PhO})I(dme)_2)_2(OCH_3)I]\cdot 2dme$ yielded comparative crystalline products. This finding obtained here are totally different from the analogous reaction for Ln(II) stable metals (Sm, Eu and Yb); $[Yb(Odp)_2(thf)_3]$, $[Ln(Odbmp)_2(thf)_3]$ (Ln = Eu, Yb), $[Ln(Odip)_3(thf)_2]$ (Ln = Eu, Yb), $[Yb(Odbmp)_2(\mu\text{-}OH)(thf)]_2$, and $[Sm(Odbmp)(\mu\text{-}I)(thf)_3]_2$.[20]

We further investigated the reactivity of PhYbI with benzophenone (Ph_2CO) and yielded $[Yb(OCPh_3)_3(thf)_2]$ and $[Yb_2I_2(\mu\text{-}O)(\mu\text{-}I)(thf)_5]\cdot thf$. Furthermore, we investigated the reactivity of $[Yb(Ph_2pz)I(thf)_4]$ Grignard complex with O-donor KO^{t}Bu and N-donor $K(Me)PhNMe_2$ reagents. However, in both cases, the Schlenk redistribution product $[Yb(Ph_2pz)_2(thf)_4]$ was isolated, instead of the anticipated products.

Lanthanoid phenolate complexes are widely used as single-molecule magnets (SMMs).[1, 2] Besides, phenolate ligand systems have been used to synthesise the main group and transition metal coordination complexes.[7-16] Bulk aryloxides are particularly effective in producing low coordinate lanthanoid complexes, which increase their further application.[4-6] Considering these potential applications, we can suggest that lanthanoid pseudo-Grignard phenolate complexes would be a good chemistry for investigation with different phenol derivatives such as 2,6-di-phenylphenol(dpOH), 2,6-di-tert-butyl-4-methylphenol (dbmpOH), 2,6-di-isopropylphenol (dipOH).

4.5 Experimental

4.5.1 General Aspects

For general aspects see the appendix 1.

4.5.1.1 Synthesis of lanthanoid (III) phenolate complexes

Excess amounts of lanthanoid (Ln^{III}) metal powder (1.5 mmol) were suspended in dry thf (15 ml) under N_2, and then stochiometric amount of phenyl iodide (PhI) with 1 drop mercury (Hg) were added at 25 °C. The mixture was sonicated for 10 min and stirred for 5-12 h at room

temperature, after the formation of Grignard reagent, solid phenol (4-^{t}Bu Phenol) (0.150 g, 1.0 mmol) were added at 0 °C and stirred for another 30-36 h. Crystals were obtained after the filtrates were evaporated and crystalised in dry dme at around 0~(-)25 °C. Yields were calculated based on the phenol (4-^{t}Bu Phenol) ligand.

[Ce(4-^{t}Bu-PhO)I_2(dme)$_2$]·0.5dme (4.1)

Cerium metal powder (0.210 g, 1.5 mmol) was suspended in dry thf (15 ml) under N_2, and then PhI (0.408 g, 2.0 mmol) with 1 drop Hg were added at 25 °C. The mixture was sonicated for 10 min and stirred for ~8 h at room temperature, when a light brown solution formed. Solid phenol (4-^{t}Bu Phenol) (0.15 g, 1.0 mmol) was added, and the mixture was stirred at 0 °C for 1 h, and a brown solution developed after stirring for 36 h at room temperature. The resulting mixture was filtered and crystalised in dme. The yellow crystals (0.376 g, 49%) were obtained in a week. M. P. 162-164 °C. Elemental analysis: Found: Ce 17.52, C 33.28, H 4.91; $C_{20}H_{38}CeI_2O_6$ (768.42 g/mol) requires: Ce 18.23, C 31. 26, H 4.94; extra 0.5 dme $C_{22}H_{43}CeI_2O_7$ (813.50 g/mol) requires: Ce 17.22, C 32. 48, H 5.33. IR (Nujol): 1597s, 1559w, 1281s, 1259w, 1192s, 1174m, 1159w, 1112s, 1038br-s, 973m, 871s, 845w, 724m, 789s cm^{-1}. ^{1}H NMR (400.13 MHz, C_6D_6): δ = -5.92 (12H, CH_3-dme), 4.26 (9H, ^{t}Bu), 10.02 (8H, CH_2-dme), 14.32 (2H, H(3,5)), and 24.78 ppm(2H, H(2,6)).

[Nd(4-^{t}Bu-PhO)I_2(dme)$_2$]·0.5dme (4.2)

Neodymium metal powder (0.216 g, 1.5 mmol) was suspended in dry thf (15 ml) under N_2, and then PhI (0.408 g, 2.0 mmol) with 1 drop Hg were added at 25 °C. The mixture was sonicated for 10 min and stirred for ~8 h at room temperature, when a light brown colour solution formed. Solid phenol (4-^{t}Bu Phenol) (0.15 g, 1.0 mmol) was added, and the mixture was stirred at 0 °C for 1 h, and a blue solution developed after stirring for 36 h at room temperature. The resulting mixture was filtered and crystalised in dme. The blue crystals (0.497 g, 64%) were obtained in a week. M. P. 154-156 °C. Elemental analysis: Found: Nd 20.86, C 28.28, H 4.68; $C_{20}H_{38}O_6I_2Nd$ (772.56 g/mol) requires: Nd 18.67, C 31.09, H 4.96; loss of 1 dme $C_{16}H_{28}O_4I_2Nd$ (682.44 g/mol) requires: Nd 21.14, C 28.16, H 4.14. IR (Nujol): 1597s, 1559w, 1391w, 1377s, 1362m, 1284s, 1265w, 1192s, 1174s, 1137m, 1102w, 1082w, 1039s, 1002w, 974s, 873s, 845w,

819m, 690s cm^{-1}. ^1H NMR (400.13 MHz, C_6D_6): δ = -11.21 (6H, dme), 3.25 (13H, ^{t}Bu, dme), 21.26 (2H, H(3,5)), and 39.63 ppm(2H, H(2,6)).

[Lu(4-^{t}Bu-PhO)I_2(dme)$_2$]·0.5dme (4.3)

Lutetium metal powder (0.263 g, 1.5 mmol) was suspended in dry thf (15 ml) under N_2, and then PhI (0.408 g, 2.0 mmol) with 1 drop Hg were added at 25 °C. The mixture was sonicated for 10 min and stirred for ~12 h at room temperature, when a light brown colour solution formed. Solid phenol (4-^{t}Bu Phenol) (0.15 g, 1.0 mmol) was added, and the mixture was stirred at 0 °C for 1 h, and a brown solution developed after stirring for 36 h at room temperature. The resulting mixture was filtered and crystalised in dme. The colourless crystals (0.296 g, 37%) were obtained in 10 d. M. P. 157-159 °C. Elemental analysis: found: C 31.13, H 4.98, Lu 21.16, $C_{20}H_{38}I_2LuO_6$ (803.29 g/mol) requires: C 29.90, H 4.77, Lu 21.78; extra 0.5 dme from crystallisation requires $C_{22}H_{43}I_2LuO_7$ (848.35 g/mol) requires: C 31.15, H 5.11, Lu 20.62. IR (Nujol): 1599s, 1557w, 1377m, 1308s, 1264w, 1191s, 1175s, 1160w, 1093s, 1031br-s, 977m, 878s, 844w, 719m, 792s cm^{-1}. ^1H NMR (400.13 MHz, C_6D_6): δ = 1.32 (9H, ^{t}Bu), 3.13 (15H, CH_3-dme), 3.33 (10H, CH_2-dme), 6.61, 7.10 (2H, H(3,5)), and 7.32, 7.46 ppm(2H, H(2,6)).

[Gd(4-^{t}Bu-PhO)I_2(dme)$_2$]·0.5dme (4.4)

Gadolinium metal powder (0.236 g, 1.5 mmol) was suspended in dry thf (15 ml) under N_2, and then PhI (0.408 g, 2.0 mmol) with 1 drop Hg were added at 25 °C. The mixture was sonicated for 10 min and stirred for ~10 h at room temperature, when a brownish yellow colour solution formed. Solid phenol (4-^{t}Bu Phenol) (0.15 g, 1.0 mmol) was added, and the mixture was stirred at 0 °C for 1 h, and a brown colour solution developed after stirring for 36 h at room temperature. The resulting mixture was filtered and crystalised in dme. The colourless powder (0.265 g, 36%) was obtained overnight. M. P. 123-125 °C. Metal analysis: Found: Gd 21.56; $C_{20}H_{38}O_6I_2Gd$ (785.57 g/mol) requires: Gd 20.02; loss of 0.5 dme $C_{18}H_{33}O_5I_2Gd$ (740.51 g/mol) requires: Gd 21.24. IR (Nujol): 1597s, 1558w, 1391w, 1376s, 1361m, 1283br-s, 1263w, 1246w, 1192s, 1173s, 1159w, 1136m, 1102w, 1082w, 1038br-s, 1001w, 973s, 873s, 845w, 819m, 735w, 723w, 689s cm^{-1}. ^1H NMR (400.13 MHz, C_6D_6): δ = got paramagnetic (Peaks are 12.00 ppm, 2.58 ppm, 1.10 ppm).

[Ho(4-^{t}Bu-PhO)I_2(dme)$_2$]·0.5dme (4.5)

Holmium metal powder (0.248 g, 1.5 mmol) was suspended in dry thf (15 ml) under N_2, and then PhI (0.408 g, 2.0 mmol) with 1 drop Hg were added at 25 °C. The mixture was sonicated for 10 min and stirred for ~12 h at room temperature, when a light brown colour solution formed. Solid phenol (4-^{t}Bu Phenol) (0.15 g, 1.0 mmol) was added, and the mixture was stirred at 0 °C for 1 h, and a brownish yellow colour solution developed after stirring for 36 h at room temperature. The resulting mixture was filtered and crystalised in dme. The colourless powder (0.212 g, 28%) was obtained in two days. M. P. 128-130 °C. Metal analysis: Found: Ho 22.78; $C_{20}H_{38}O_6I_2Ho$ (793.25 g/mol) requires: Ho 20.79; loss of 0.5 dme $C_{18}H_{33}O_5I_2Ho$ (748.19 g/mol) requires: Ho 22.04. IR (Nujol): 1596s, 1581m, 1392w, 1377m, 1362w, 1280br-s, 1262w, 1192s, 1174m, 1159w, 1136m, 1101w, 1038br-s, 973m, 871s, 844w, 736m, 689s cm^{-1}. ^{1}H NMR (400.13 MHz, C_6D_6): δ = got paramagnetic (Peaks are 32.45 ppm, 29.50 ppm, 2.59 ppm, 1.15 ppm, -5.26 ppm).

[(La(4-^{t}Bu-PhO)I(dme)$_2$)$_2$(OCH_3)]I·2dme (4.6)

Lanthanum metal powder (0.209 g, 1.5 mmol) was suspended in dry thf (15 ml) under N_2, and then PhI (0.408 g, 2.0 mmol) with 1 drop Hg were added at 25 °C. The mixture was sonicated for 10 min and stirred for ~5 h at room temperature, when a light brown solution formed. Solid phenol (4-^{t}Bu Phenol) (0.15 g, 1.0 mmol) was added, and the mixture was stirred at 0 °C for 1 h, and a brown solution developed after stirring for 30 h at room temperature. The resulting mixture was filtered and crystalised in dme (need to heat to dissolved in dme). The colourless crystals (0.123 g, 16%) were obtained for a month. M. P. 172-174 °C. Metal analysis: Found: La 22.46; $C_{45}H_{89}I_3La_2O_{15}$ (1528.68 g/mol) requires: La 18.17; loss of 3 dme molecules $C_{33}H_{59}I_3La_2O_9$ (1258.34 g/mol) requires: La 22.08. IR (Nujol): 1601s, 1571m, 1560w, 1392w, 1377m, 1363m, 1245br-s, 1177s, 1096br-s, 1042br-s, 910w, 856s, 823w, 731s, 702m, 686m cm^{-1}. ^{1}H NMR (400.13 MHz, C_6D_6): δ = 1.29 (18H, ^{t}Bu), 1.41 (3H, OCH_3), 3.11 (14H, CH_2-dme), 3.21 (21H, CH_3-dme), 6.61, 6.86 (2H, H(3)), 7.30 (4H, H(2,6)) and 7.45 ppm(2H, H(5)), indicate the loss of 2 dme molecules from solvation and 1 molecule dme of crystallisation.

4.5.1.2 Explored the reactivity of ytterbium pseudo-Grignard reagents

[Yb(OCPh$_3$)$_3$(thf)$_2$] (4.7a), [Yb$_2$I$_2$(μ-O)(μ-I)(thf)$_5$]·thf (4.7b)

Ytterbium metal powder (0.26 g, 1.5 mmol) was suspended in dry THF (15 ml) under N_2, and then PhI (0.205 g, 1.0 mmol) was added at -78 °C. The mixture was sonicated for 10 min when a brown/orange solution formed. After cooling to -78 °C, solid benzophenone (0.183 g, 1.0 mmol) was added, and the mixture was stirred at -78 °C for another 3 h. A dark-orange solution developed after further stirring for 24 h at room temperature. The resulting mixture was filtered and concentrated to 5 ml under vacuum. Red crystals (**4.7a**) (0.14 g, 36%) were obtained after cooling at -25 °C in 3 weeks. M. P. 156-158 °C. Metal analysis: found: Yb 15.56, $C_{69}H_{61}O_6Yb$ (1159.21 g/mol) requires: Yb 14.93. IR (Nujol): 1403w, 1378m, 1351s, 1295m, 1261s, 1168s, 1067w, 1031s, 967s, 919w, 874s, 803s, 775w, 751m, 700s cm^{-1}. Yellow crystals (**4.7b**) (0.507g, 46%) were obtained after cooling at -25 °C in 2 months. M. P. 172-174 °C. Metal analysis: found: Yb 32.04, $C_{24}H_{48}I_3O_7Yb_2$ (1175.40 g/mol) requires: Yb 29.44, loss of 1 mole thf from solvation $C_{20}H_{40}I_3O_6Yb_2$ (1103.32 g/mol) requires: Yb 31.37.

[Yb(Ph$_2$pz)$_2$(thf)$_4$] (4.8)

Ytterbium pseudo-Grignard compounds [Yb(Ph$_2$pz)I(thf)$_4$] (0.22 g, 0.27 mmol), KO^{t}Bu (0.03 g, 0.27 mmol) and dry THF (10 ml) were added in a Schlenk flask. A red orange solution and colourless precipitate (probably KI nothing shown in the ^{1}H NMR, Fig. **4.8**) was obtained after stirred the mixture for 24 h at room temperature. Orange solution filtrated from the precipitate and concentrated to ~2 ml under vacuum. Red crystals (0.09 g, 37%) were obtained after cooling at -25°C for over a couple of weeks. M. P. 138-140 °C. Metal analysis: Found: 18.62, $C_{46}H_{54}N_4O_4Yb$ (899.97 g mol^{-1}) requires: Yb 19.23; extra 1 mole thf from solvation $C_{50}H_{62}N_4O_5Yb$ (972.09 g mol^{-1}) requires: Yb 17.80. IR (Nujol): 1604s, 1512w, 1422m, 1406m, 1297w, 1261s, 1220m, 1154m, 1089w, 1071w, 1023s, 971s, 916s, 870s, 800s, 758s cm^{-1}. ^{1}H NMR (400.13 MHz, C_6D_6): δ = 1.21 (20H, thf), 3.49(20H, thf), 7.07 (4H, H(4)), 7.21 (10H, H(2,6, CH-pz)), 8.05 ppm(8H, H(3,5)), 1 extra thf from solvation.

4.6 X-ray crystal data

Single crystals coated with viscous hydrocarbon oil were mounted on glass fibres or loops. All complexes (**4.1**-**4.3** and **4.6**-**4.8**) were measured -173°C (100 K) at the Australian Synchrotron on the MX1 beamline, data integration was completed using Blue-ice [42] and XDS [43] software programs. Structural solutions were obtained by either direct methods [44] or charge flipping [45] methods and refined using full-matrix least-squares methods against F2 using SHELX2018, [46] in conjunction with the X-Seed [47] or Olex2 [45] graphical user interface. All hydrogen atoms were placed in calculated positions using the riding model. Multiscan were applied for absorption corrections. All CIF files were checked at https://checkcif.iucr.org.

[Ce(4-^{t}BuPhO)I_2(dme)$_2$]·0.5dme (4.1)

$C_{20}H_{38}CeI_2O_6$ (M =768.42 g/mol): monoclinic, space group $C2/c$ (no. 15), a = 25.805(2) Å, b = 10.0733(10) Å, c = 21.773(2) Å, β = 100.393(6)°, V = 5566.8(9) Å^3, Z = 8, T = 123.0 K, μ(MoKα) = 3.881 mm^{-1}, $Dcalc$ = 1.834 g/cm^3, 44865 reflections measured (4.35° ≤ 2Θ ≤ 56.578°), 6879 unique (R_{int} = 0.0673, R_{sigma} = 0.0449) which were used in all calculations. The final R_1 was 0.0338 (I > 2σ(I)) and wR_2 was 0.0749 (all data).

[Nd(4-^{t}BuPhO)I_2(dme)$_2$]·0.5dme (4.2)

$C_{20}H_{38}O_6I_2Nd$ (M =772.56 g/mol): monoclinic, space group $C2/c$ (no. 15), a = 25.675(2) Å, b = 10.0352(9) Å, c = 21.742(2) Å, β = 100.422(4)°, V = 5509.4(9) Å^3, Z = 8, T = 123.0 K, μ(MoKα) = 4.155 mm^{-1}, $Dcalc$ = 1.875 g/cm^3, 32734 reflections measured (4.368° ≤ 2Θ ≤ 56.622°), 6855 unique (R_{int} = 0.0995, R_{sigma} = 0.0846) which were used in all calculations. The final R_1 was 0.0473 (I > 2σ(I)) and wR_2 was 0.1183 (all data).

[Lu(4-^{t}BuPhO)I_2(dme)$_2$]·0.5dme (4.3)

$C_{20}H_{38}I_2LuO_6$ (M =803.27 g/mol): monoclinic, space group $C2/c$ (no. 15), a = 25.391(5) Å, b = 9.975(2) Å, c = 21.533(4) Å, β = 100.54(3)°, V = 5361.8(19) Å^3, Z = 8, T = 293(2) K, μ(MoKα) = 6.014 mm^{-1}, $Dcalc$ = 1.990 g/cm^3, 33161 reflections measured (3.264° ≤ 2Θ ≤ 57.422°), 5587 unique (R_{int} = 0.0470, R_{sigma} = 0.0307) which were used in all calculations. The final R_1 was 0.0465 (I > 2σ(I)) and wR_2 was 0.1173 (all data).

[(La(4-^{t}BuPhO)I(dme)$_2$)$_2$(OCH$_3$)]I·2dme (4.6)

$C_{45}H_{89}I_3La_2O_{15}$ (M =1528.68 g/mol): triclinic, space group P-1 (no. 2), a = 13.8002(7) Å, b = 14.2077(6) Å, c = 17.3406(9) Å, α = 87.203(2)°, β = 68.568(2)°, γ = 79.189(2)°, V = 3108.0(3) Å^3, Z = 2, T = 123.0 K, μ(MoKα) = 2.899 mm^{-1}, $Dcalc$ = 1.634 g/cm^3, 61152 reflections measured (3.818° ≤ 2Θ ≤ 55.058°), 14160 unique (R_{int} = 0.1051, R_{sigma} = 0.1150) which were used in all calculations. The final R_1 was 0.0581 (I > 2σ(I)) and wR_2 was 0.1400 (all data).

[Yb(OCPh$_3$)$_3$(thf)$_2$] (4.7a)

$C_{69}H_{61}O_6Yb$ (M =1159.21 g/mol): monoclinic, space group $P2_1/n$ (no. 14), a = 18.607(4) Å, b = 14.969(3) Å, c = 19.931(4) Å, β = 90.48(3)°, V = 5551.2(19) Å^3, Z = 4, T = 293(2) K, μ(MoKα) = 1.738 mm^{-1}, $Dcalc$ = 1.387 g/cm^3, 64368 reflections measured (2.982° ≤ 2Θ ≤ 50.048°), 9652 unique (R_{int} = 0.0344, R_{sigma} = 0.0188) which were used in all calculations. The final R_1 was 0.0320 (I > 2σ(I)) and wR_2 was 0.0857 (all data).

[Yb$_2$I$_2$(μ-O)(μ-I)(thf)$_5$]·thf (4.7b)

$C_{24}H_{48}I_3O_7Yb_2$ (M =1175.40 g/mol): monoclinic, space group $P2_1/n$ (no. 14), a = 12.9007(9) Å, b = 13.0116(10) Å, c = 20.5950(15) Å, β = 97.752(3)°, V = 3425.5(4) Å^3, Z = 4, T = 123.0 K, μ(MoKα) = 8.165 mm^{-1}, $Dcalc$ = 2.279 g/cm^3, 129483 reflections measured (3.982° ≤ 2Θ ≤ 56.744°), 8530 unique (R_{int} = 0.0950, R_{sigma} = 0.0420) which were used in all calculations. The final R_1 was 0.0406 (I > 2σ(I)) and wR_2 was 0.1011 (all data).

[Yb(Ph$_2$pz)$_2$(thf)$_4$] (4.8)

$C_{46}H_{54}N_4O_4Yb$, M_r =899.97 g/mol, monoclinic, space group $P2_1/c$ (no. 14), a = 24.560(3) Å, b = 9.0966(10) Å, c = 19.733(2) Å, β = 113.277(5)°, V = 4049.6(8) Å^3, Z = 4, T = 123.0 K, μ(MoKα) = 2.358 mm^{-1}, $Dcalc$ = 1.476 g/cm^3, 103122 reflections measured (4.128° ≤ 2Θ ≤ 56.668°), 10042 unique (R_{int} = 0.1819, R_{sigma} = 0.0992) which were used in all calculations. The final R_1 was 0.0523 (I > 2σ(I)) and wR_2 was 0.1261 (all data).

4.7 References

[1]. V. S. Parmar, F. Ortu, X. Ma, N. F. Chilton, R. Clerac, D. P. Mills and R. E. P. Winpenny, Chem. Eur. J., **2020**, 26, 7774-7778.

[2]. M. Brzozowska, G. Handzlik, K. Kurpiewska, M. Zychowicz and D. Pinkowicz, Inorg. Chem. Front., **2021**, 8, 2817-2828.

[3]. J. D. Rinehart and J. R. Long, Chem. Sci., **2011**, 2, 2078-2085.

[4]. D. C. Bradley, R. C. Mehrotra, I. P. Rothwell and A. Singh, Alkoxo and Aryloxo Derivatives of Metals, Academic Press, London, **2001**.

[5]. T. J. Boyle and L. A. M. Ottley, Chem. Rev., **2008**, 108, 1896-1917.

[6]. F. Ortu and D. P. Mills, Handbook on the Physics and Chemistry of Rare Earths, 55th edition, **2019**.

[7]. M. Gonza´lez-Maupoey, T. Cuenca, L. M. Frutos, O. Castano and E. Herdtweck, Organometallics, **2003**, 22, 2694-2704.

[8]. F. G. Sernetz, R. Mulhaupt, F. Amor, T. Eberle and J. Okuda, J. Polym. Sci., Part A: Polym. Chem., **1997**, 35, 1571-1578.

[9]. A. van der Linden, C. J. Schaverien, N. Meijboom, C. Ganter and A. G. Orpen, J. Am. Chem. Soc., **1995**, 117, 3008-3021.

[10]. D. Takeuchi, T. Nakamura and T. Aida, Macromolecules, **2000**, 33, 725-729.

[11]. W. Braune and J. Okuda, Angew. Chem., Int. Ed., **2003**, 42, 64-68.

[12]. H.-L. Chen, B.-T. Ko, B.-H. Huang and C.-C. Lin, Organometallics, **2001**, 20, 5076-5083.

[13]. Y.-C. Liu, B.-T. Ko and C.-C. Lin, Macromolecules, **2001**, 34, 6196-6201.

[14]. B.-T. Ko, C.-C. Wu and C.-C. Lin, Organometallics, **2000**, 19, 1864-1869.

[15]. A. Amgoune, C. M. Thomas and J. F. Carpentier, Pure Appl. Chem., **2007**, 79, 2013-2030.

[16]. X. Liu, X. Shang, T. Tang, N. Hu, F. Pei, D. Cui, X. Chen and X. Jing, Organometallics, **2007**, 26, 2747-2757.

[17]. D. M. Lyubov, A. O. Tolpygin and A. A. Trifonov, Coord. Chem. Rev., **2019**, 392, 83-145.

[18]. P. L. Arnold, R. W. F. Kerr, C. Weetman, S. R. Docherty, J. Rieb, F. L. Cruickshank, K. Wang, C. Jandl, M. W. McMullon, A.r Pothig, F. E. Kuhn and A. D. Smith, Chem. Sci., **2018**, 9, 8035-8045.

[19]. G. B. Deacon, G. Meyer and D. Stellfeldt, Eur. J. Inorg. Chem., **2000**, 1061-1071.

[20]. Caspar de Bruin-Dickason, undergraduate thesis: Lanthanoid pseudo-Grignard chemistry, School of Chemistry, Monash University, Australia, **2014**.

[21]. S. H. Ali, A. C. G. Shephard, J. Wang, Z. Guo, M. S. Davies, G. B. Deacon and P. C. Junk, Chem. Asian J., **2022**, 17, e202101328.

[22]. S. H. Ali, PhD thesis: Synthesis, structures, and reactivity of organolanthanoid complexes, College of Science and Engineering, James Cook University, Australia, **2017**.

[23]. T. Holm, J. Organomet. Chem., **1971**, 29, C45-C48.

[24]. V. S. Parmar, A. M. Thiel, M. S. Norre and J. Overgaard, Cryst. Growth Des., **2023**, 23, 6410-6417.

[25]. G. B. Deacon, G. Meyerb, D. Stellfeldta, G. Zelesnya, B. W. Skelton and A. H. White, Z. Anorg. Allg. Chem., **2001**, 627, 1652-1658.

[26]. G. B. Deacon, C. M. Forsyth and N. M. Scott, Dalton Trans., **2003**, 3216-3220.

[27]. Y.-S. Ding, T. Han, Y.-Q. Zhai, D. Reta, N. F. Chilton, R. E. P. Winpenny, and Y.-Z. Zheng, Chem. Eur. J., **2020**, 26, 5893-5902.

[28]. W. J. Evans, K. A. Miller and J. W. Ziller, Inorg. Chem., **2006**, 45, 424-429.

[29]. J.-C. Berthet, M. Nierlich and M. Ephritikhine, Polyhedron, **2003**, 22, 3475-3482.

[30]. H. Wu, B. Guo, X. Han, M. Li, B. Yin, Y. Chen, Y. Bian and H. Ke, S. Chen, Cryst. Growth Des., **2023**, 23, 309-319

[31]. I. L. Fedushkin, A. N. Lukoyanov and E. V. Baranov, Inorg. Chem., **2018**, 57, 8, 4301-4309.

[32]. D. J. Duncalf, P. B. Hitchcock and G. A. Lawless, Chem. Commun., **1996**, 269-271.

[33]. R. D. Shannon, Acta Crystallogr. Sect. A., **1976**, 32, 751-767.

[34]. D. J. Duncalf, P. B. Hitchcock and G, A. Lawless, Chem. Commun., **1996**, 269-271.

[35]. G. Heckmann and M. Niemeyer, J. Am. Chem. Soc., **2000**, 122, 4227-4228.

[36]. T. J. Emge, A. Kornienko and J. G. Brenna, Acta Cryst., **2009**, C65, m422-m425.

[37]. G. B. Deacon, E. E. Delbridge, B. W. Skelton, A. H. White, Eur. J. Inorg. Chem., **1998**, 543-545.

[38]. S. Beaini, G. B. Deacon, E. E. Delbridge, P. C. Junk, B. W. Skelton and A. H. White, Eur. J. Inorg. Chem., **2008**, 4586-4596.

[39]. M. Wiecko, G. B. Deacon and P. C. Junk, Chem. Commun., **2010**, 46, 5076-5078.

[40]. D. F. Evans, G. V. Fazakerley and R. F. Phillips, J. Chem. Soc. A., **1971**, 1931-1934.

[41]. S. H. Ali, G. B. Deacon, P. C. Junk, S. Hamidi, M. Wiecko and J. Wang, Chem. Eur. J., **2018**, 24, 230-242.

[42]. T. M. McPhillips, S. E. McPhillips, H. J. Chiu, A. E. Cohen, A. M. Deacon, P. J. Ellis, E. Garman, A. Gonzalez, N. K. Sauter, R. P. Phizackerley, S. M. Soltis and J. P. Kuhn, J. Synchrotron Radiat., **2002**, 9, 401-406.

[43]. W. Kabsch, J. Appl. Crystallogr., **1993**, 26, 795.

[44]. G. M. Sheldrick, Acta Crystallogr. Sect. A., **2008**, 64, 112-122.

[45]. O. V. Dolomanov, L. J. Bourhis, R. J. Gildea, J. A. K. Howard and H. Puschmann, J. Appl. Crystallogr., **2009**, 42, 339-341.

[46]. G. M. Sheldrick, Acta Cryst., **2015**, C71, 3-8.

[47]. L. J. Barbour, J. Supramol. Chem., **2001**, 1, 189-191.

Chapter 5

Alternative synthesis of pseudo-Grignard reagents from lanthanoid metal, I_2 and supporting ligands

Chapter 5

5.1 Introduction

Heteroleptic lanthanoid metal-organic halides, represented as R_2LnX or $RLnX_2$ (where Ln = lanthanoid metal, R is anionic ligand, and X = F, Cl, Br, or I), play a key role in synthesising functionalised heteroleptic compounds. These compounds, denoted as R_2LnX' or $RLnX'_2$, where X′ = hydride, amide, alkoxide, aryloxides or cyclopentadienyl, [1-8] are commonly prepared through a metathesis reaction. This process involves the reaction between lanthanoid halides (LnX_3) and alkali metal salts of the anionic ligands (MR where, M = alkali metal, R = anionic ligand) in a stoichiometric ratio, as shown in Equation **5.1**.[1-8]

$$\mathbf{LnX_3 + nMR \longrightarrow Ln(R)_nX_{3-n} + nMX}$$

Equation **5.1**: Synthesised of heteroleptic lanthanoid compounds from metathesis reaction (Ln = lanthanoid; X = F, Cl, Br, I; n = 1 or 2; M = Li, Na, K; R = anionic ligand).

A major issue with the metathesis reaction is the formation of alkali metal halide byproducts. [7-11] For dihalide complexes, various rearrangement reactions may also occur (**eqn. 5.2**).[8]

$$\mathbf{2\ R_2LnX \rightleftharpoons LnRX_2 + LnR_3}$$
$$\mathbf{\Updownarrow}$$
$$\mathbf{0.5\ LnX_3 + 0.5\ LnR_2X}$$

Equation **5.2**: Rearrangements that can occur in heteroleptic complexes.

Guo *et al.* (2021) synthesised a series of lanthanoidiodidoformamidinato (Ln^{III}) complexes through a direct one pot reaction involving the corresponding lanthanoid metals, formamidines and iodine. Using a 1:1 molar ratio of iodine to formamidine (FormH = DFFormH (*N*,*N*′-bis(2,6-difluorophenyl)formamidine)) or DippFormH (*N*,*N*′-bis(2,6-disopropylphenyl)formamidine)) resulted in the isolation of $[Ln(Form)I_2(thf)_3]$ (**eqn. 5.3 (i)**). In contrast, a 1:4 molar ratio of iodine to formamidine led to the isolation of $[Ln(Form)_2I(thf)_3]$ (**eqn. 5.3 (ii)**).[12]

$$\mathbf{Ln(xs) + I_2 + FormH \xrightarrow{thf} [Ln(Form)I_2(thf)_3] \quad (i)}$$
$$\mathbf{Ln(xs) + I_2 + 4FormH \xrightarrow{thf} [Ln(Form)_2I(thf)_3] \quad (ii)}$$

Equation **5.3**: Synthesis of trivalent pseudo-Grignard complexes from the direct synthesis method.[12]

The complexes obtained from this reaction are easy to isolate and typically have good yields. This synthetic process is broadly applicable to a wide range of weak acid pro-ligands. However, common disadvantages of this method include halide retention, the formation of ate complexes and low solubility of the resulting complexes.[12]

5.1.1 Preparation of pseudo-Grignard reagents using some alternative synthetic methods

Some common synthetic alternative methods for lanthanoid pseudo-Grignard compounds include redox transmetallation, redox transmetallation/protolysis (RTP), metathesis and C-X activation reactions.

Redox transmetallation reactions

The preparation of lanthanoid complexes from lanthanoid metals and metal-based ligands is known as redox transmetallation reaction (**eqn. 3.4**).[13]

$$\mathbf{mLn + nML_m \longrightarrow m[LnL_n] + nM}$$

L = anionic ligand

n = 2,3

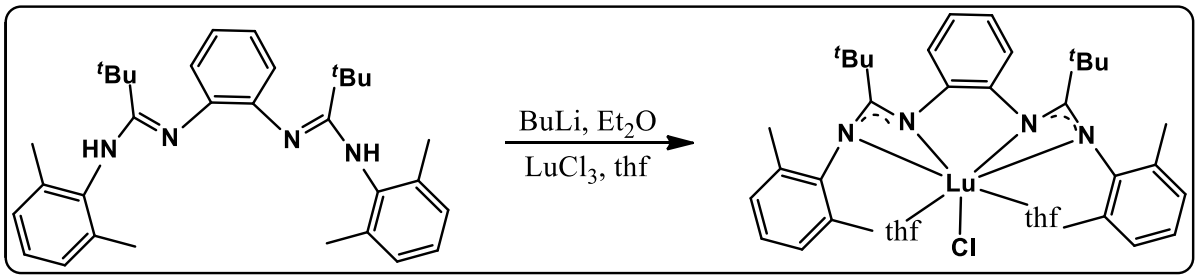
m = 1-4

M = Hg, Bi, Sn, $SnMe_3$

Equation 5.4: Redox transmetallation reactions in the synthesis of lanthanoid complexes.

An exchange reaction between potassium and lithium amidinate {2-$[Ph_2P(O)]C_6H_4NLiC(Bu^t)=N(2,6\text{-}Me_2C_6H_3)\}_2$ with $NdX_3(thf)_3$ (X = Cl, n = 0; X = I, n = 3.5) led to the isolation of dihalide amidinate complexes $[Nd\{2\text{-}[Ph_2P(O)]C_6H_4NC(Bu^t)N(2,6\text{-}Me_2C_6H_3)\}X_2(thf)_2]$.[14]

To synthesise the compound $[C_6H_4\text{-}1,2\text{-}\{NC(t\text{Bu})N(2,6\text{-}Me_2C_6H_3)\}_2]LuCl(thf)_2$, a mixture of $[C_6H_4\text{-}1,2\text{-}\{NC(t\text{Bu})NH(2,6\text{-}Me_2C_6H_3)\}_2]$ and *n*BuLi was stirred at 0°C for 1 h in Et_2O. After removing the solvent under vacuum, $LuCl_3$ was added in thf, and the reaction mixture was stirred at room temperature for 12 h (**Scheme 5.1**).[15]



Scheme 5.1: Synthesis of $[C_6H_4\text{-}1,2\text{-}\{NC(t\text{Bu})N(2,6\text{-}Me_2C_6H_3)\}_2]LuCl(thf)_2$ complex.[15]

Redox Transmetallation/Protolysis (RTP)

A well-established method for synthesising organometallic complexes is the redox transmetallation/protolysis (RTP) reaction. In this reaction, both transmetallation and protolysis occur consecutively. It is a very convenient synthesis of homoleptic compounds, but also lead to heteroleptic species.

$$\mathbf{2\ Ln + n\ M(C_6F_5)_p + 6\ LH \xrightarrow[rt]{thf} [2\ Ln(L)_3(thf)_q] + n\ M + 6\ C_6F_5H}$$

M = Hg, n = 3, p = 2; M = Bi, n = 2, p = 3; q = variable

LH = Protolytic ligand

rt = Room Temperature

Equation 5.6: Redox transmetallation/protolysis (RTP) reactions in the synthesis of lanthanoid complexes.[16-21]

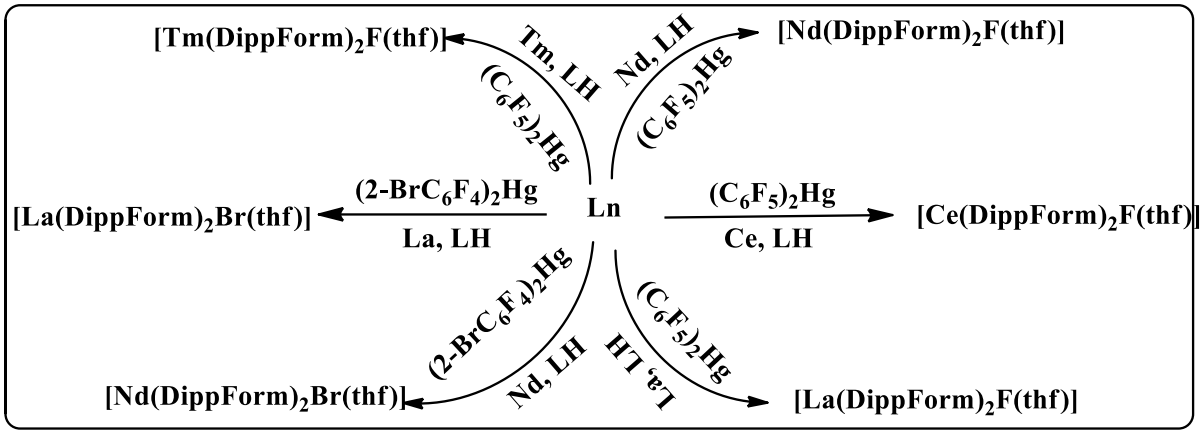
The reaction of lanthanum metal fillings and DippFormH (*N*,*N*′-bis(2,6-diisopropylphenyl) formamidine) with $Hg(C_6F_5)_2$ in thf led to the isolation of $[Ln(DippForm)_2F(thf)]$.[16] The resultant compound $[Ln(DippForm)_2F(thf)]$ is likely a C-F activated product of the intermediate $[Ln(DippForm)_2(C_6F_5)]$, where the six coordinate metal center is bonded to two *cisoid* DippForm ligands, one fluorine ligand and one thf ligand, forming a distorted tetrahedral geometry.[16] Another example of C-F activation was observed for the praseodymium (Pr) complex $[Pr(DippForm)_2F(thf)]$, where the bulk DippFormH underwent protolysis of $[Pr(DippForm)_2(C_6F_5)]$ to $[Pr(DippForm)_2F(thf)]$. The proposed reaction pathway is described in **Scheme 5.2**.

$$\mathbf{Pr_{(ex)} + Bi(C_6F_5)_3 + DippFormH \longrightarrow [Pr(DippForm)_2(C_6F_5)]}$$

$$\mathbf{[Pr(DippForm)_2(C_6F_5)] + DippFormH \longrightarrow [Pr(DippForm)_2F]}$$

Scheme 5.2: The reaction pathway for the formation of [Pr(DippForm)$_2$F(thf)] complex.[17]

When the same reaction was applied using bulkier formamidine (DippFormH), C-X (X = Br, F) activation products were obtained. The reaction of lanthanoid metals (Ln = La, Ce, Nd, and Tm) with either (2-BrC$_6$F$_4$)$_2$Hg or (C$_6$F$_5$)$_2$Hg in the presence of DippFormH produced [Ln(DippForm)$_2$X(thf)] (**Scheme 5.3**).[18-20]



Scheme 5.3: Synthesis of [Ln(DippForm)$_2$X(thf)] (Ln = La, Ce, Nd and Tm; X = F, Br; LH = DippFormH) complexes using the redox transmetallation/protolysis (RTP) reaction.[18-20]

Five bis(formamidinato)iodido lanthanoid complexes; [Gd(DFForm)$_2$I(py)$_2$]·PhMe, [Tb(DFForm)$_2$I(py)$_2$]·PhMe, [Er(DFForm)$_2$I(py)(thf)]·1.5thf, [Tm(DFForm)$_2$I(py)(thf)]·1.5thf, and [Lu(DFForm)$_2$I(py)(thf)] were synthesised from the reaction described in **equation 5.7**.[21]

$$\mathbf{Ln + DFFormH + [Ag(C_6F_5)(py)]} \xrightarrow[\mathbf{I_2}]{\mathbf{thf}} \mathbf{[Ln(DFForm)_2I]}$$

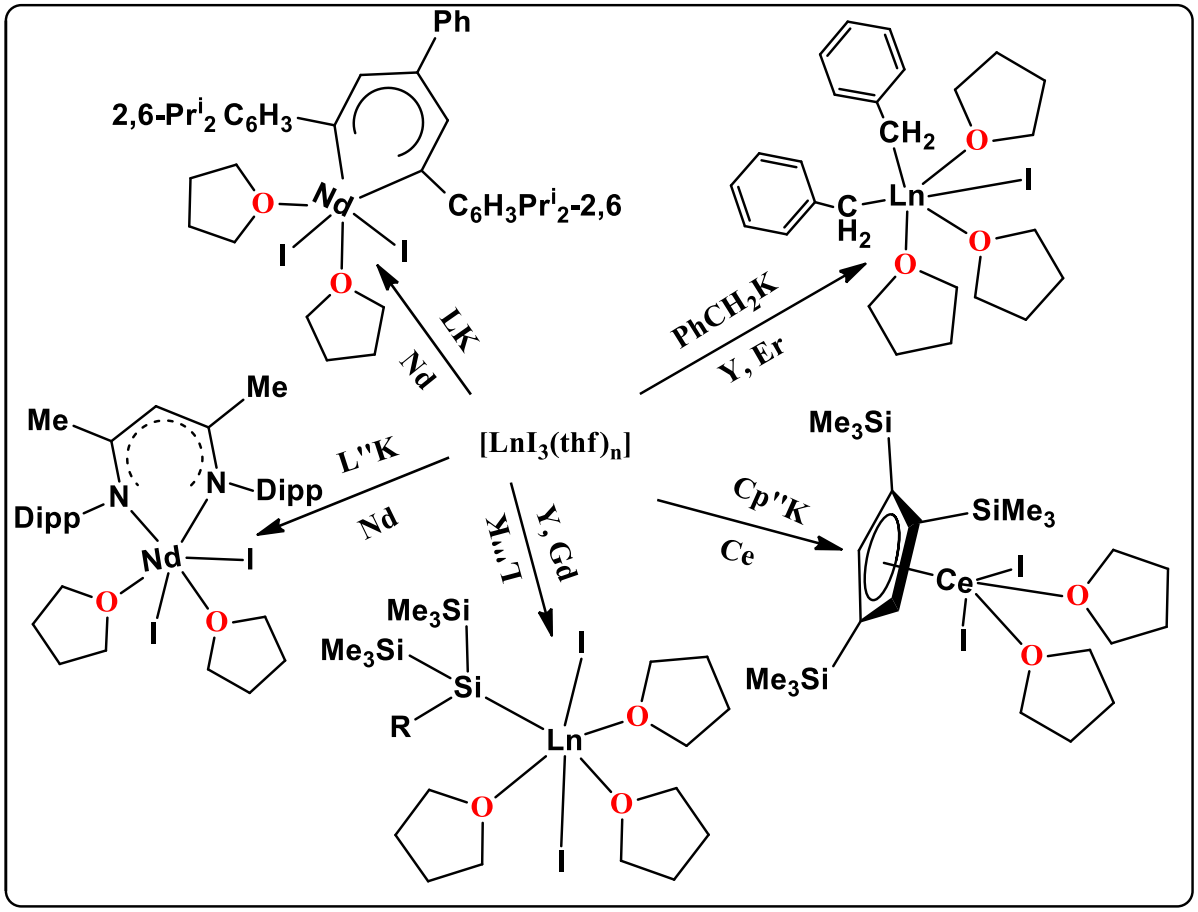
Equation 5.7: Preparation of [Ln(DFForm)$_2$I] (Ln = Gd, Tb, Er, Tm, and Lu) complex.[21]

Metathesis

The Ce(III) pseudo-Grignard complex [Ce(Piso)$_2$Cl] (Piso = [*t*BuC(NAr)$_2$]$^-$, Ar = C$_6$H$_2$*i*Pr$_2$-2,6) was isolated from the reaction of CeCl$_3$ with two equivalents of K(Piso) in thf over 72 h at room temperature. The compound [Ce(Piso)$_2$Cl] crystallised as monoclinic structure, where it is described as having a distorted trigonal bipyramidal geometry.[22]

Scheme **5.4** describes several pseudo-Grignard compounds synthesised *via* metathesis reactions. The complex [Nd({N(C$_6$H$_3$Pr$^i_2$-2,6)C(H)}$_2$CPh)I$_2$(thf)$_2$] was isolated from the

reaction between $\{N(C_6H_3Pr^i_2\text{-}2,6)C(H)\}_2CPhK$ and a stirred suspension of $[NdI_3(thf)_2]$ in thf at room temperature for 48 h.[23] The complex $[Nd\{(HC(C(NDipp)Me)_2\}I_2(thf)_2]$ was obtained from an equimolar reaction between $[NdI_3(thf)_{3.5}]$ and $(HC(C(NDipp)Me)_2K$ at room temperature for 3 h.[24] Complexes $[Ln\{R(Me_3Si)_2Si\}I_2(thf)_3]$ (Ln = Y, Gd) were isolated from the reaction between $[KSi(Me_3Si)_2R(thf)_2]$ (R = Me_3Si or Et) and $[GdI_3(thf)_{3.5}]$ in thf at room temperature.[25] The complex $[Ce(Cp''')I_2(thf)_2]$ was isolated from an equimolar reaction between $[CeI_3(thf)_4]$ and K(Cp‴) (Cp‴ = $\{C_5H_2(SiMe_3)_3\text{-}1,2,4\}$-) at -4 °C, and stirred the mixture for another 72 h at temperature.[26] The complexes $[Ln(PhCH_2)_2I(thf)_3]$ (Ln = Y, Er) were synthesised from the reaction between the corresponding $LnI_3(thf)_{3.5}$ and $PhCH_2K$ at 0°C for 4 h.[27]



Scheme 5.4: Synthesis of different pseudo-Grignard complexes using metathesis reactions (L = $\{N(C_6H_3Pr^i_2\text{-}2,6)C(H)\}_2CPh$, L″ = $(HC(C(NDipp)Me)_2$, L‴ = $\{R(Me_3Si)_2Si\}$(R = Me_3Si, Et)).[23-27]

Alternative synthetic methods have also been used to isolate trivalent pseudo-Grignard complexes. $CpLn(Me_2Pz)_2$ (Ln = Ho and Dy) complexes were synthesised by reacting Cp_3Ln with 2 equivalents of Me_2pzH at room temperature for 48 h. Using 1 equivalent of Cp_3Er and

Me_2pzH led to the isolation of the five coordinate monoclinic complex $Cp_2Er(Me_2Pz)(thf)$.[28] The protolysis reaction of $[Er(ArNC(Me)CHC(Me)NAr)(CH_2SiMe_3)_2]$ with 2 equivalents $[Et_3NH]I$ generates the erbium pseudo-Grignard complex $[Er(ArNC(Me)CHC(Me)NAr)I_2]$.[29] The complexes $[Ln\{(Me_3Si)_2C_5H_3\}_2I(thf)]$ (Ln = La, Er and Lu) were isolated from a one pot reaction mixture of 2 equivalents of $[Na\{(Me_3Si)_2C_5H_3\}]$ and NaI with the corresponding $LnCl_3$ salts.

$$\mathbf{2[Na\{(Me_3Si)_2C_5H_3\} + NaI + LnCl_3 \xrightarrow{thf} [Ln\{(Me_3Si)_2C_5H_3\}_2I(thf)]}$$

Equation 5.8: Preparation of $[Ln\{(Me_3Si)_2C_5H_3\}_2I(thf)]$ (Ln = La, Er and Lu) complexes.[30]

Additionally, a series of trivalent Cp (cyclopentadienide) and Cp* (pentamethyl-cyclopentadienide) lanthanoid complexes $[LnCpI_2(thf)_3]$ (Ln = Nd, Dy and Tm), $[TmCp_2I(thf)_2]$ and $[LnCp^*_2I(thf)_2]$ (Ln = Nd and Dy), were synthesised from the reaction of the corresponding LnI_2 with excess CpH or Cp*H. The reactions for Nd and Dy were performed at 0 °C, while the reaction for Tm was conducted at 60 °C.[31]

5.2 Current Study

This chapter aims to expand the study of trivalent organolanthanide iodide complexes, through the reactions between the lanthanoid metals (Ln^{III}), iodine (I_2) and pro-ligands (pyrazoles). This synthetic approach has previously been used to trap a wide range of $[Ln(L)I_2(solv)_n]$ and/or $[Ln(L)_2I(solv)_n]$ (L = formamidinato) complexes. This chapter investigates the same synthesis route for lanthanoid (Ln^{III}) complexes with $^tBu_2pzH$ and PhMepzH.

The direct reaction between lanthanoid metals (Ln = La, Ce, Nd, Er, and Lu), I_2 and $^tBu_2pzH$ produced several $Ln(^{III})$ compounds, including $[La(^tBu_2pz)I_2(thf)_4]$ (**5.1**), $[Ce(^tBu_2pz)I_2(thf)_4]$ (**5.2**), $[Nd(^tBu_2pz)I_2(thf)_4]$ (**5.3**), $[Er(^tBu_2pz)_2I(thf)_2]$ (**5.4**), and $[Lu(^tBu_2pz)_2I(thf)_2]$ (**5.5**).

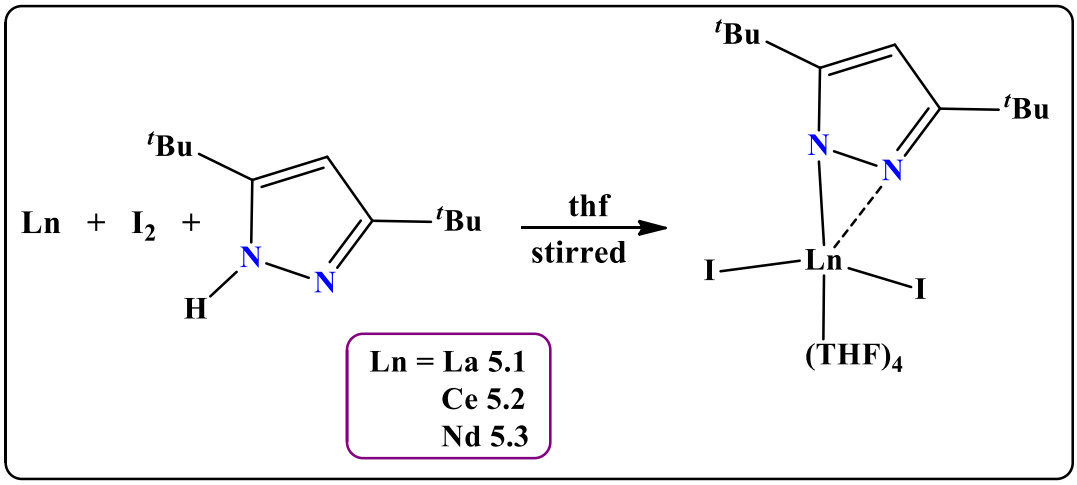
Additionally, this study involved reactions between lanthanoid metals (Ln = La, Ce, Nd, Tb and Lu), I_2 and PhMepzH, resulting in the formation of $Ln(^{III})$ compounds such as $[La(PhMepz)I_2(thf)_4]$ (**5.6**), $[Ce(PhMepz)I_2(thf)_4]$ (**5.7**), $[Nd(PhMepz)I_2(thf)_4]$ (**5.8**), $[Tb(PhMepz)I_2(thf)_3]\cdot thf$ (**5.9**) and $[Lu(PhMepz)I_2(thf)_3]$ (**5.10**).

5.3 Results and Discussion

5.3.1 Synthesis and spectroscopic characterisation

5.3.1.1 Synthesis of di-iodo lanthanoid pyrazolato complexes from corresponding metals, I_2 and ^{t}Bu$_2$pzH ligands.

The goal of this reaction is to isolate trivalent lanthanoid di-iodo, ^{t}Bu$_2$pz complexes. The reaction was conducted with a 1:1 stoichiometric ratio of I_2 and ^{t}Bu$_2$pzH with excess lanthanoid metals (La **5.1**, Ce **5.2** and Nd **5.3**) in thf at 0 °C. The mixture was sonicated for 10 min and then stirred for another 3-4 d at room temperature, resulting in solutions of the desired compounds (La light brown, Ce yellow and Nd blue). Crystallisation from the concentrated solutions yielded a colourless powder of **[La(^{t}Bu$_2$pz)I$_2$(thf)$_4$]** (**5.1**) colourless crystals of **[Ce(^{t}Bu$_2$pz)I$_2$(thf)$_4$]** (**5.2**) and blue crystals of **[Nd(^{t}Bu$_2$pz)I$_2$(thf)$_4$]** (**5.3**). Suitable X-ray quality crystals of **[La(^{t}Bu$_2$pz)I$_2$(thf)$_4$]** (**5.1**), could not be isolated and the structural data can be used only for connectivity puroses. The reaction and structural scheme of these compounds (**5.1** - **5.3**) are shown in Scheme (**5.5**).



Scheme 5.5: Synthesis of compounds [Ln(^{t}Bu$_2$pz)I$_2$(thf)$_4$] (La **5.1**, Ce **5.2** and Nd **5.3**).

Satisfactory ^{1}H NMR spectra were obtained for compounds **5.1** and **5.2** (which includes an extra solvated thf molecule) and compound **5.3** (**Fig. 5.1** to **Fig. 5.3**). The CH-pz resonances in the ^{1}H NMR spectra are significantly shifted to 6.49 ppm for compound **5.1** (**Fig. 5.1**), the CH_2 signals of thf appear at δ = 1.39 and 3.76 ppm respectively, while the CH_3 signals from

^{t}Bu appeared at δ = 1.62 ppm. The CH-pz resonances in the ^{1}H NMR spectra are significantly shifted with 15.15 ppm for compound **5.2** (**Fig. 5.2**) and 28.68 ppm for compound **5.3** (**Fig. 5.3**), compared with the proligand value of 6.00 ppm (**Fig. 5.4**). In compound **5.2**, the CH_2 signals of thf appear at δ = 1.82 and 3.79 ppm, while the CH_3 signals from ^{t}Bu appeared at δ = 3.33 ppm. In compound **5.3**, the CH_2 signals of thf are found at δ = 2.50 and 6.70 ppm, with CH_3 signals from ^{t}Bu appeared at δ = 1.66 ppm. IR spectra showed the presence of the appropriate ^{t}Bu$_2$pz ligand. The absence of (N-H) absorption (around 3300-3400 cm^{-1}) in the infrared spectra proved the complete deprotonation of the ligands. Additionally, metal analysis validated their bulk purity. The melting points indicate significant thermal stability of the new ^{t}Bu$_2$pz compounds.

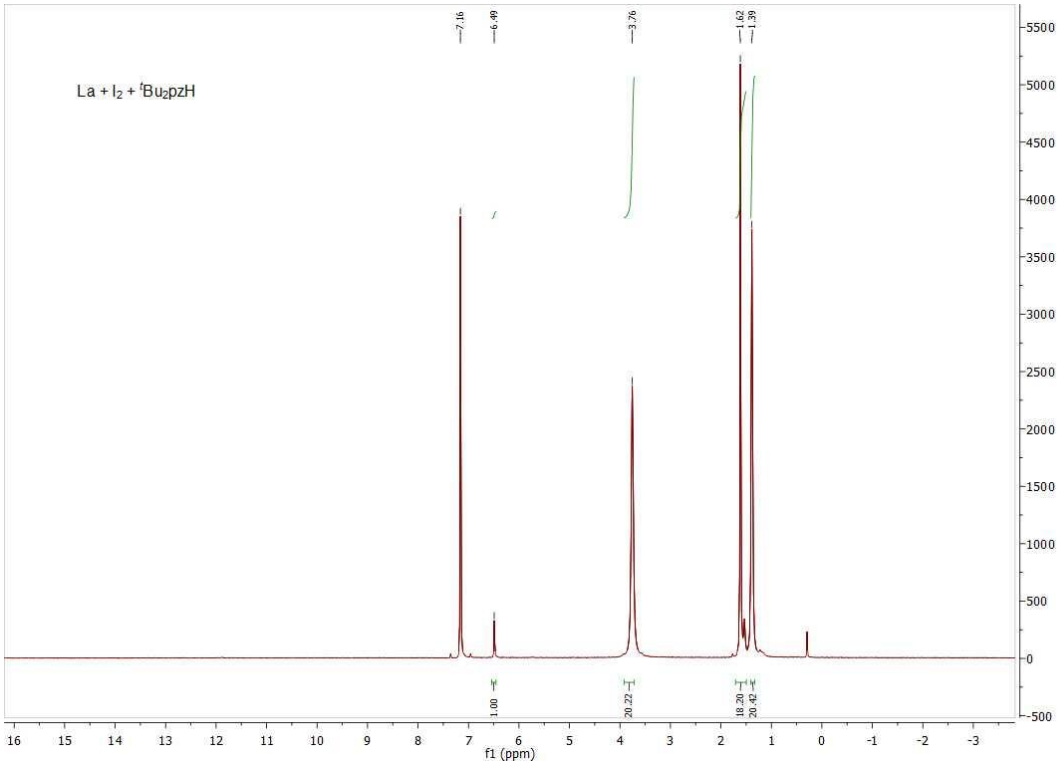


Figure 5.1. ^{1}H NMR spectrum of **[La(^{t}Bu$_2$pz)I$_2$(thf)$_4$]** (**5.1**) (extra 1 thf) in C_6D_6.

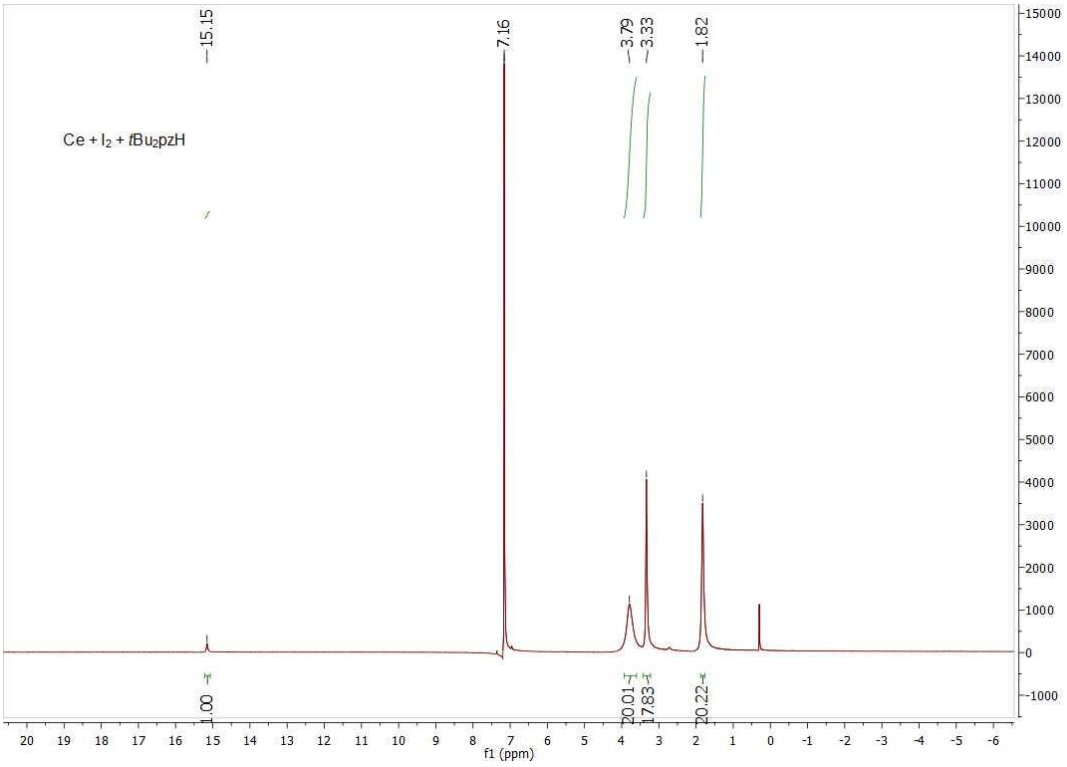


Figure 5.2. ^{1}H NMR spectrum of **[Ce(ᵗBu₂pz)I₂(thf)₄]** (**5.2**) (extra 1 thf) in C_6D_6.

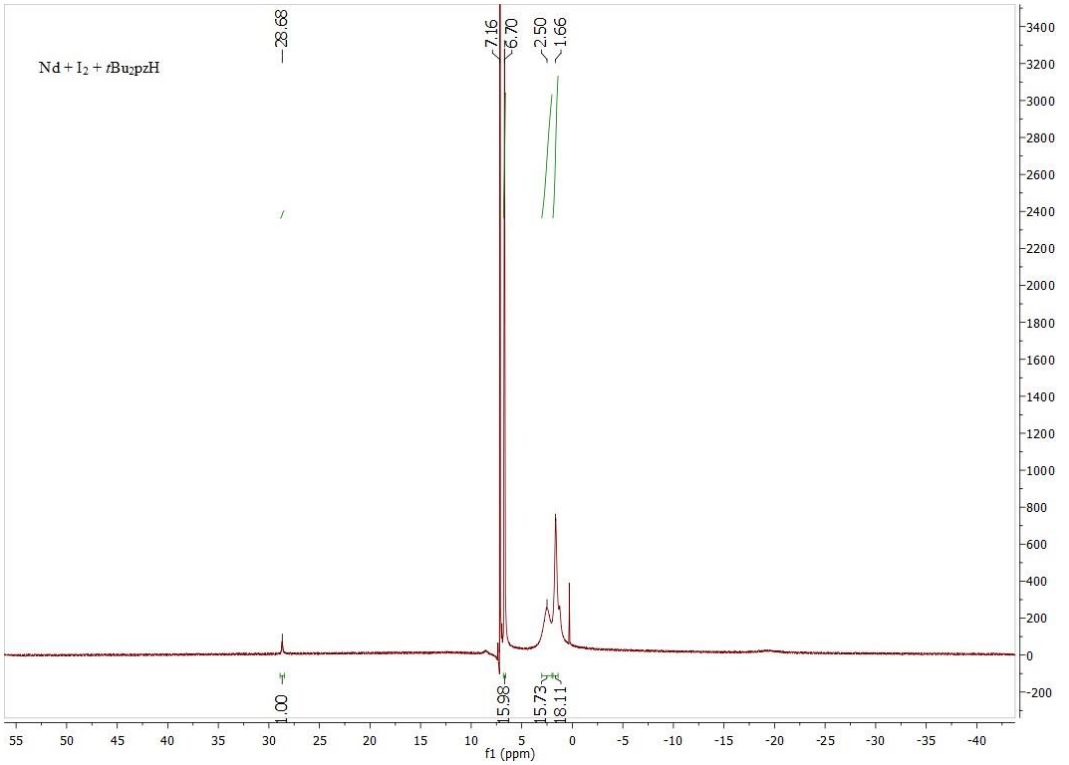


Figure 5.3. ^{1}H NMR spectrum of **[Nd(ᵗBu₂pz)I₂(thf)₄]** (**5.3**) in C_6D_6.

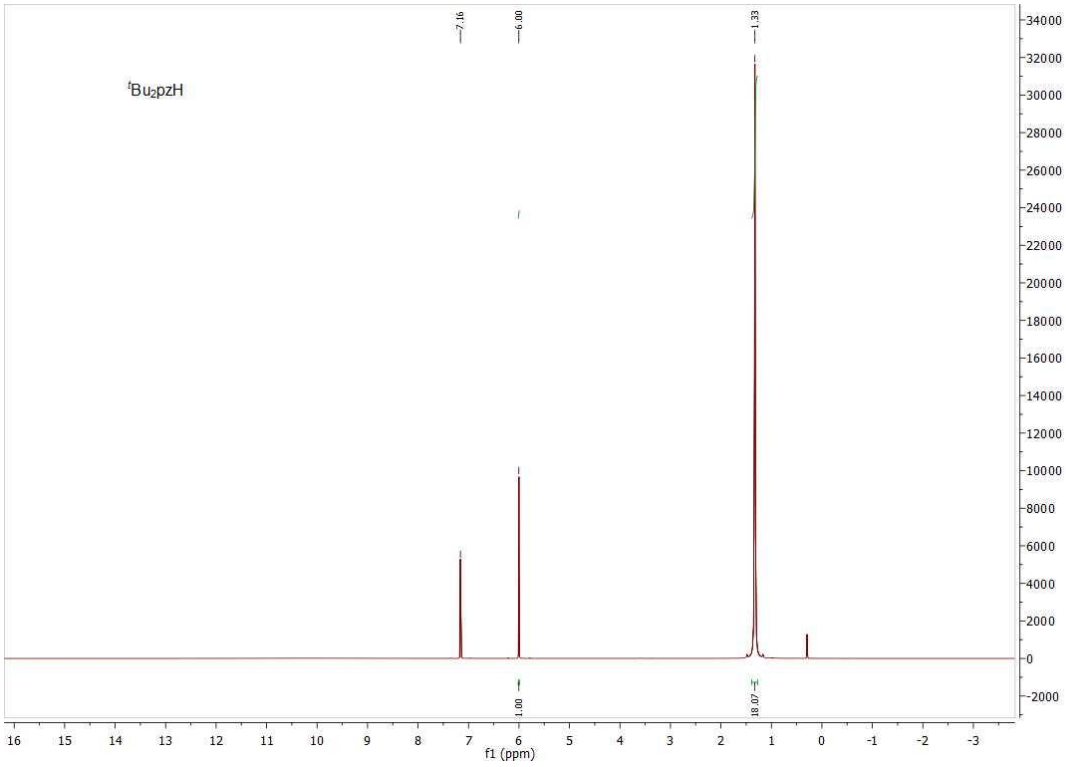


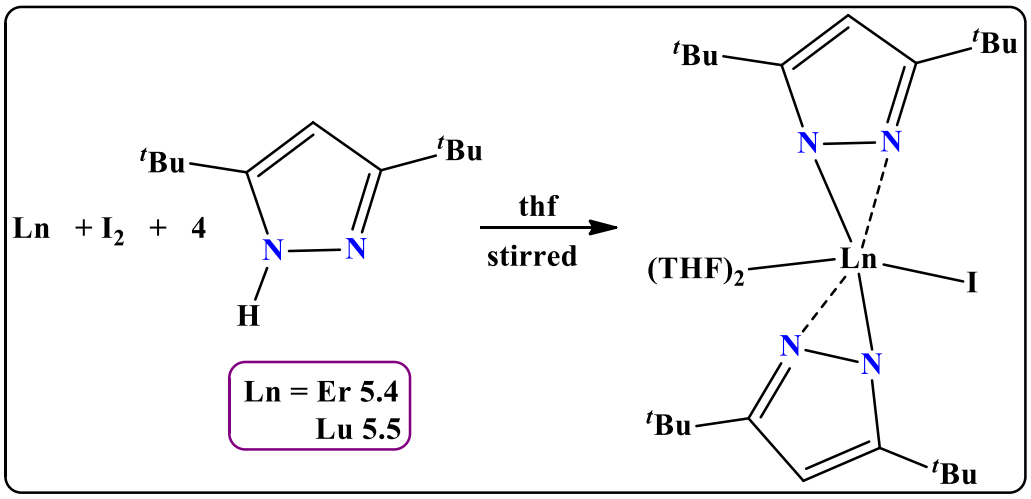
Figure 5.4. ^{1}H NMR spectrum of **[^{t}Bu$_2$pzH)]** in C_6D_6.

5.3.1.2 Synthesis of iodo lanthanoid di-pyrazolato complexes from corresponding metals, I_2 and ^{t}Bu$_2$pzH ligands.

The target products of this reaction were trivalent lanthanoid iodo, di-^{t}Bu$_2$pz complexes. The reaction was carried out using a 1:4 stoichiometric ratio of I_2 and ^{t}Bu$_2$pzH, with an excess of lanthanoid (Er **5.4** and Lu **5.5**) metals fillings in thf at 0 °C. The mixture was sonicated for 10 min and then stirred for 3-4 d at room temperature, yielding solutions of the desired compounds (Er pink, Lu light brown). Crystallisation from the concentrated solutions resulted in the formation of pink crystals of **[Er(^{t}Bu$_2$pz)$_2$I(thf)$_2$]** (**5.4**) and colourless crystals of **[Lu(^{t}Bu$_2$pz)$_2$I(thf)$_2$]** (**5.5**). Compounds (**5.4**) and (**5.5**) are isostructural. The reaction and structural scheme of the compounds (**5.4** and **5.5**) are provided in Scheme (**5.6**).

Satisfactory ^{1}H NMR spectra were obtained for compound **5.5** (**Fig. 5.6**), while compound **5.4** (**Fig. 5.5**) exhibited broad features with unsatisfactory integration due to paramagnetism (Er^{III}). In compound **5.5** (**Fig. 5.6**), the CH-pz resonances shifted to 6.53 ppm compared to the pro- ligand value (6.00 ppm **Fig. 5.4**). The CH_2 signals of thf were observed at δ = 1.06 and 3.37 ppm, while the CH_3 signals from ^{t}Bu appeared at δ = 1.63 ppm. IR spectra showed the presence of the appropriate ^{t}Bu$_2$pz ligand. The absence of an (N-H) absorption (around

3300-3400 cm^{-1}) in the infrared spectra proved the complete deprotonation of the ligands. Additionally, metal analysis validated their bulk purity. The melting points indicate significant thermal stability of the new $^{t}Bu_2pz$ compounds.



Scheme 5.6: Synthesis of compounds [Ln($^{t}Bu_2pz$)$_2$I(thf)$_2$] (Er **5.4**; Lu **5.5**).

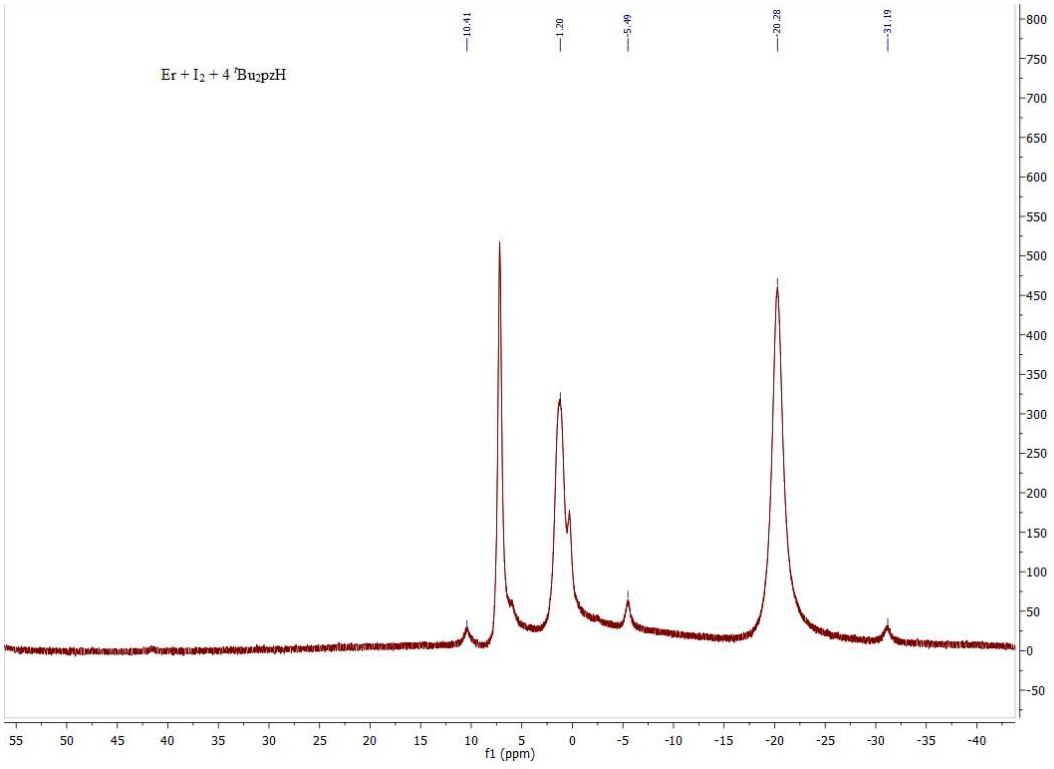


Figure 5.5. ^{1}H NMR spectrum of **[Er($^{t}Bu_2pz$)$_2$I(thf)$_2$] (5.4)** in C_6D_6.

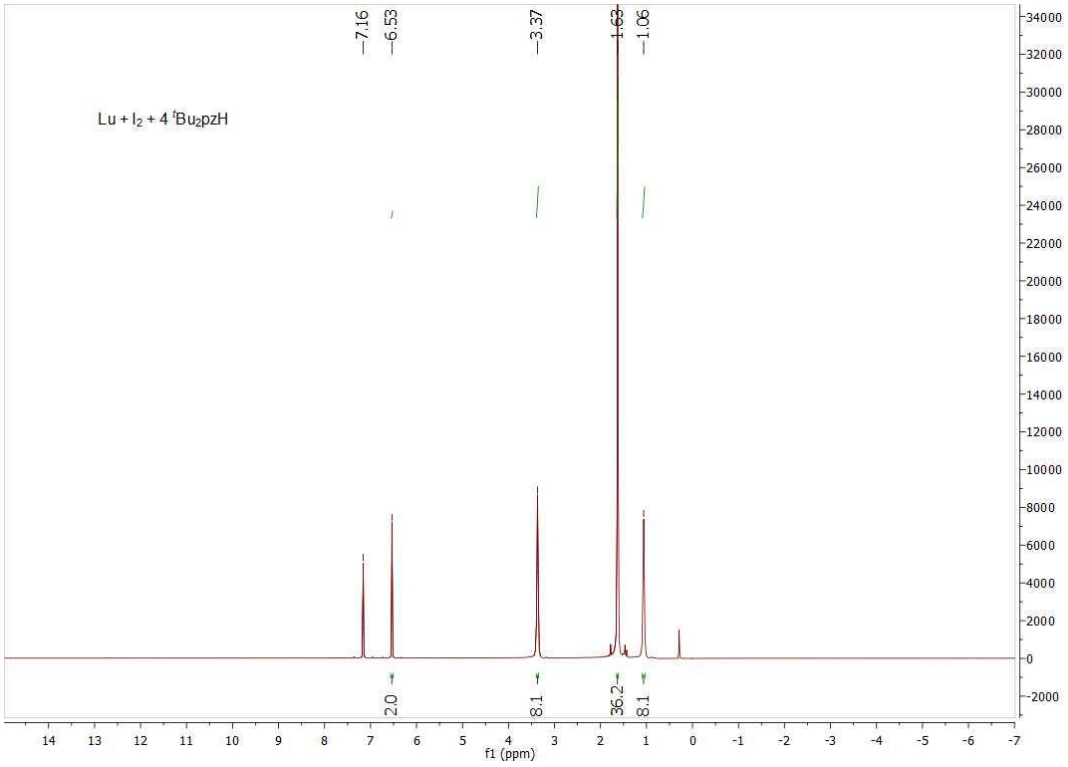
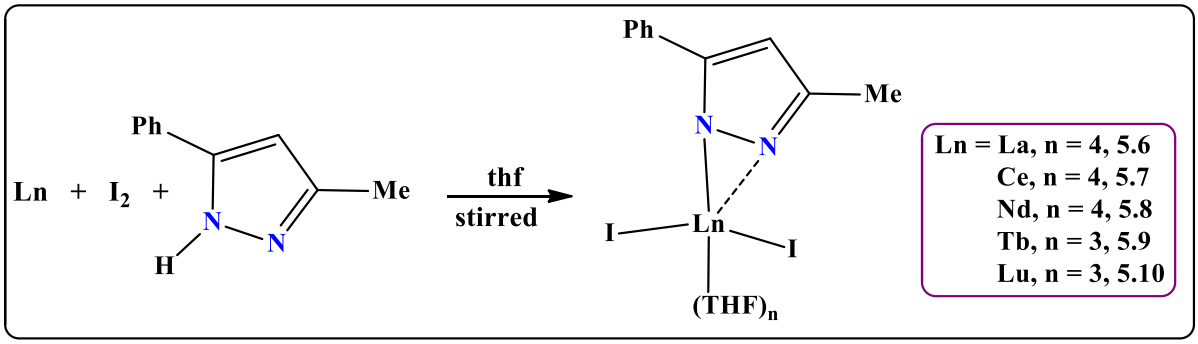


Figure 5.6. ^{1}H NMR spectrum of **[Lu(^{t}Bu$_2$pz)$_2$I(thf)$_2$] (5.5)** in C_6D_6.

5.3.1.3 Synthesis of lanthanoid di-iodo pyrazolato complexes from corresponding metals, I_2 and PhMepzH ligands.

The target products of this reaction were trivalent lanthanoid di-iodo, PhMepz complexes. The reactions were conducted using a 1:1 stoichiometric ratio of I_2 and PhMepzH with an excess of lanthanoid (La **5.6**, Ce **5.7**, Nd **5.8**, Tb **5.9**, and Lu **5.10**) metal filings in thf at 0 °C. The mixture was sonicated for 10 min and then stirred for 3-4 d at room temperature, yielding solutions of the target compounds (La brown, Ce yellow, Nd blue, Tb yellowish and Lu brown). Crystallisation from the concentrated solution resulted the formation of colourless crystals of **[La(PhMepz)I$_2$(thf)$_4$]** (**5.6**), **[Ce(PhMepz)I$_2$(thf)$_4$]** (**5.7**), **[Tb(PhMepz)I$_2$(thf)$_3$]·thf** (**5.9**) and **[Lu(PhMepz)I$_2$(thf)$_3$]** (**5.10**), and blue crystals of **[Nd(PhMepz)I$_2$(thf)$_4$]** (**5.8**). The crystallographic data of the compound **[Lu(PhMepz)I$_2$(thf)$_3$]** (**5.10**) showed one unit cell length is very long (73.932 Å), had poor diffraction, and the resulting structure can be used only for connectivity. The reaction and structural scheme of the compounds (**5.6 - 5.10**) is shown in Scheme (**5.7**).



Scheme 5.7: Synthesis of compounds [Ln(PhMepz)I_2(thf)$_4$] (La **5.6**, Ce **5.7**, Nd **5.8**, Tb **5.9**, and Lu **5.10**).

Satisfactory ^{1}H NMR spectra were obtained for all compounds **5.6 - 5.8** and **5.10** (**Fig. 5.7 - 5.9** and **5.11**). For compound **5.9** the ^{1}H NMR spectrum showed a broad feature which could not be integrated due to paramagnetism (**Fig. 5.10**). The CH-pz resonances in the ^{1}H NMR shifted to lower frequencies for compound **5.6** (**Fig. 5.7**) to δ = 6.62 ppm compared with the proligand value of δ = 12.01 ppm. The CH_2 signals of thf observed at δ = 1.31 and 3.85 ppm, while the CH signals from phenyl ring appeared at δ = 7.09, 7.32 and 8.26 ppm. The CH_3 signal of PhMepz ligand appaired at δ = 2.51 ppm. The NMR spectrum of compound **5.7** (**Fig. 5.8**) indicated the loss of 1 THF molecule of crystallisation, consistent with the metal analysis. The CH-pz resonances in the ^{1}H NMR shifted significantly for compound **5.7** to δ = 14.18 ppm compared with the pro- ligand value of δ = 12.01 ppm (**Fig. 5.12**). The CH_2 signals of thf observed at δ = 1.81 and 3.19 ppm, while the CH signals from phenyl ring appeared at δ = 7.31, 7.36 and 8.92 ppm. The CH_3 signal merge with the thf signals at δ = 1.81 ppm. For compound **5.8** (**Fig. 5.9**), the NMR spectrum indicated the loss of 2 THF molecules of crystallisation, consistent with the metal analysis. The CH-pz resonances for compound **5.8** shifted to δ = 26.41 ppm compared with the pro- ligand value of δ = 12.01 ppm (**Fig. 5.12**). The CH_2 signals of thf observed at δ = 0.72 and 1.05 ppm, while the CH signals from phenyl ring appeared at δ = 8.05-8.22, 11.70 and 12.67 ppm. The CH_3 signal merge with the thf signals at δ = 1.05 ppm. For compound **5.10** (**Fig. 5.11**) the CH-pz resonances in the ^{1}H NMR shifted to lower frequencies to δ = 6.66 ppm, while the CH_2 signals of thf observed at δ = 1.18 and 3.73 ppm. The CH signals from phenyl ring appeared at δ = 7.08, 7.28 and 8.17 ppm and the CH_3 signal of PhMepz ligand appeared at δ = 2.43 ppm. IR spectra showed the presence of the appropriate PhMepz ligand. The absence of (N-H) absorption (around 3300-3400 cm^{-1}) in the infrared spectra proved the complete

deprotonation of the ligands. Additionally, metal analysis validated their bulk purity. The melting points indicate significant thermal stability of the new PhMepz compounds.

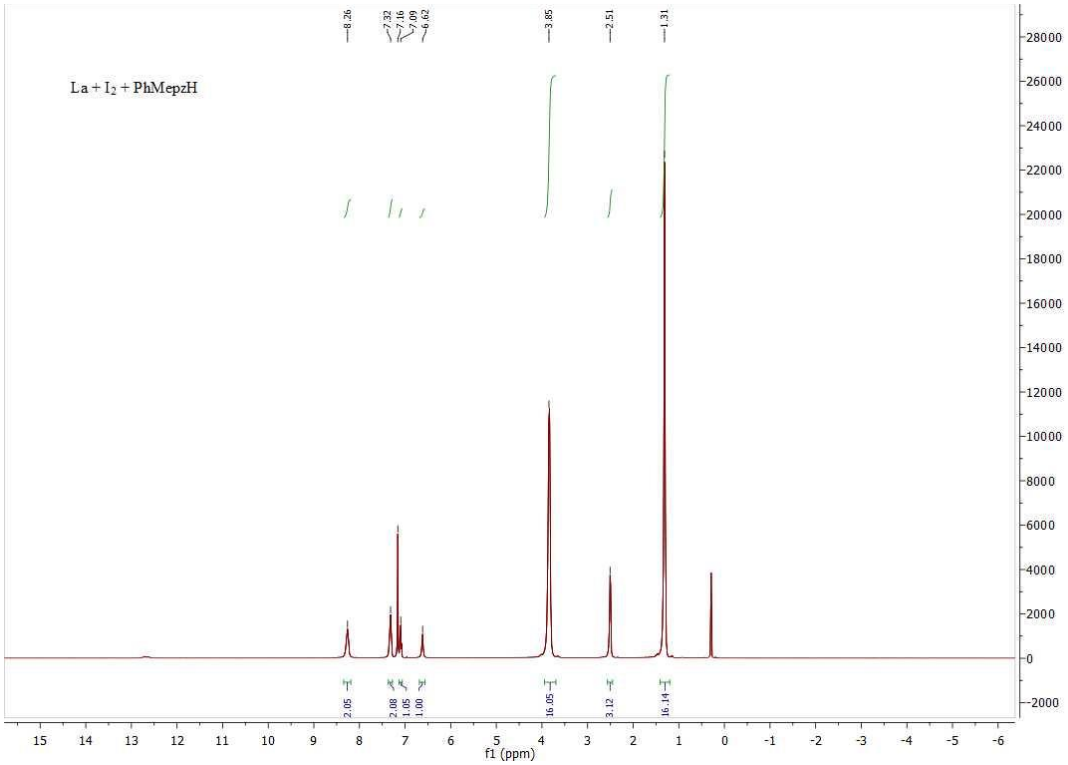


Figure 5.7. ^{1}H NMR spectrum of **[La(PhMepz)I$_2$(thf)$_4$]** (**5.6**) in C_6D_6.

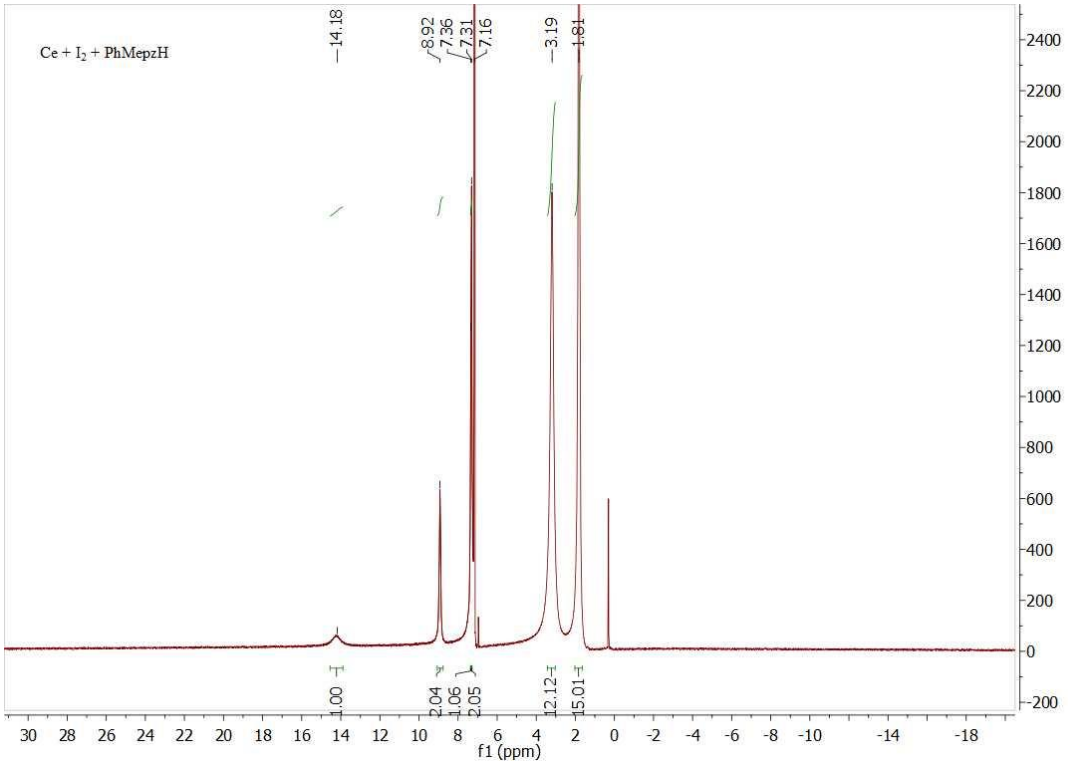


Figure 5.8. ^{1}H NMR spectrum of **[Ce(PhMepz)I_2(thf)$_4$]** (**5.7**) (loss 1 thf) in C_6D_6.

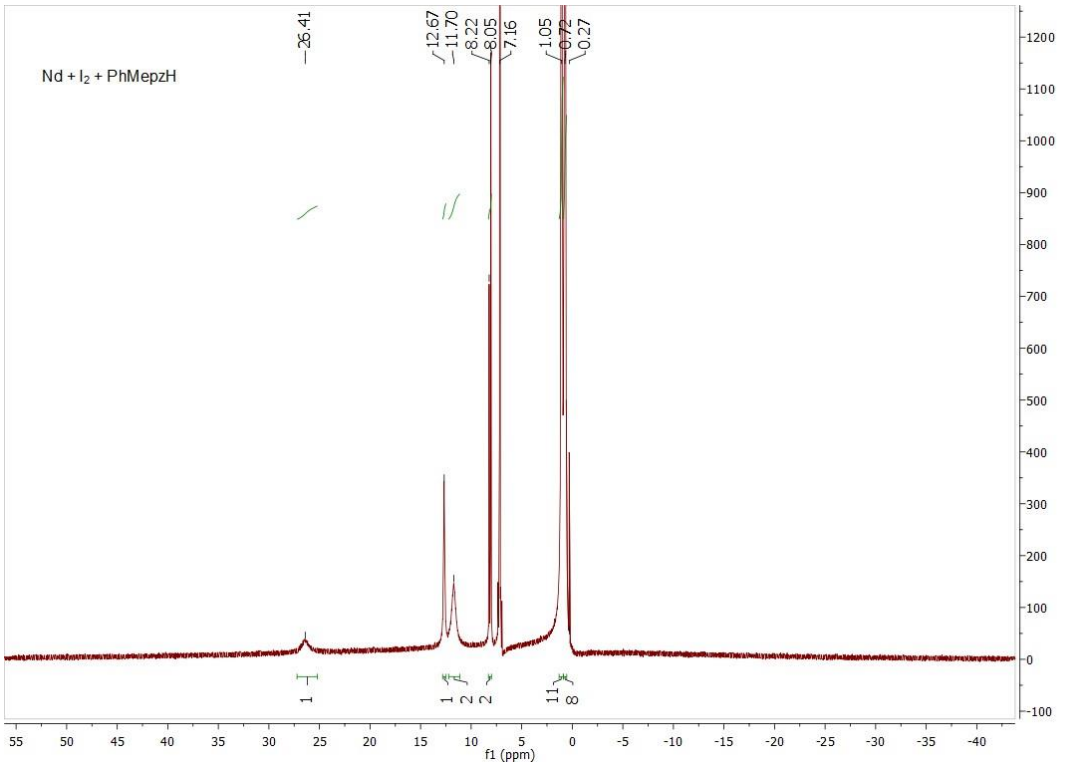


Figure 5.9. ^{1}H NMR spectrum of **[Nd(PhMepz)I_2(thf)$_4$]** (**5.8**) (loss 2 thf) in C_6D_6.

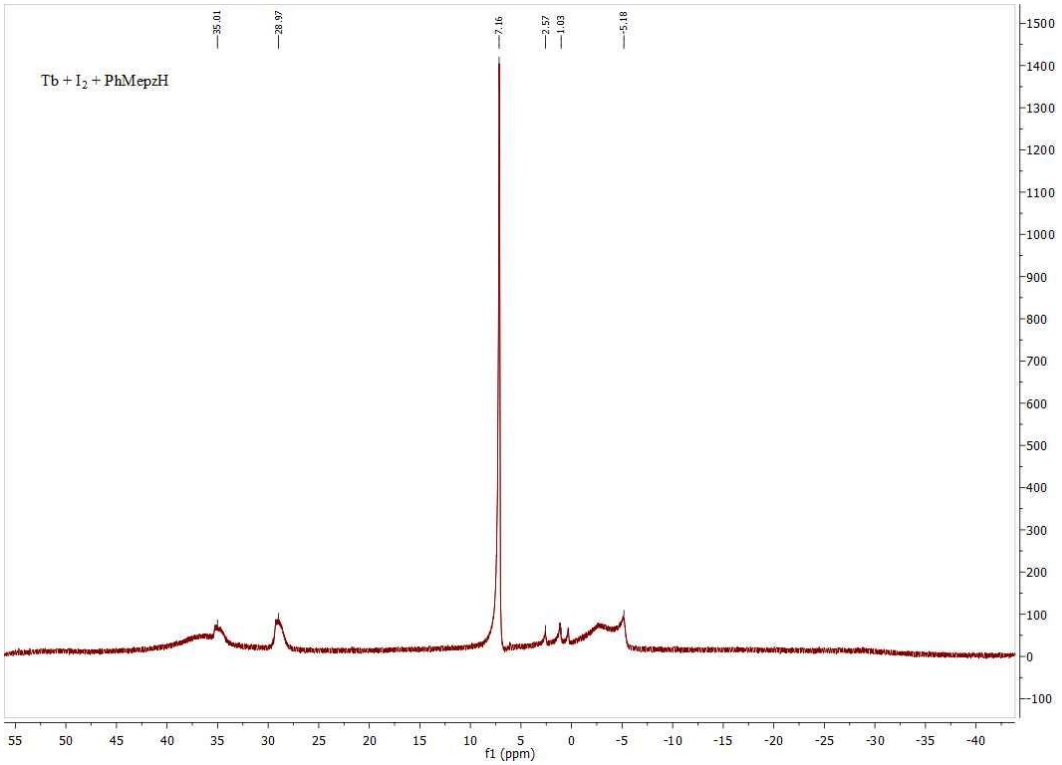


Figure 5.10. ^{1}H NMR spectrum of **[Tb(PhMepz)I$_2$(thf)$_3$]** (**5.9**) in C_6D_6.

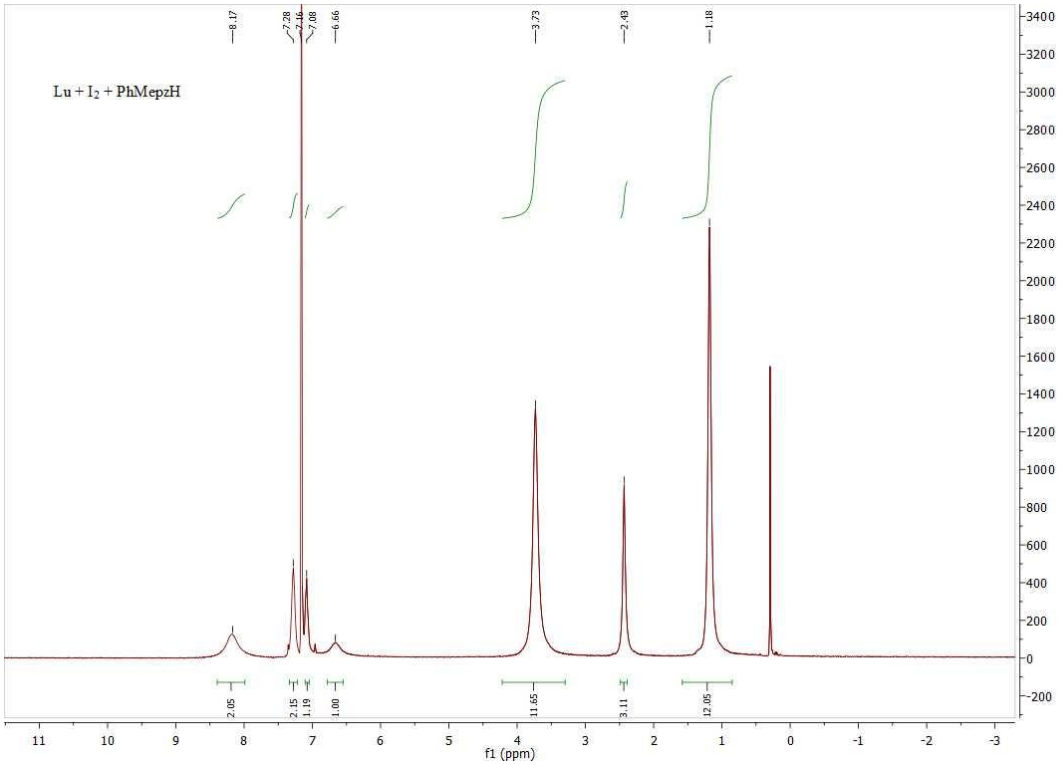


Figure 5.11. ^{1}H NMR spectrum of **[Lu(PhMepz)I$_2$(thf)$_3$]** (**5.10**) in C_6D_6.

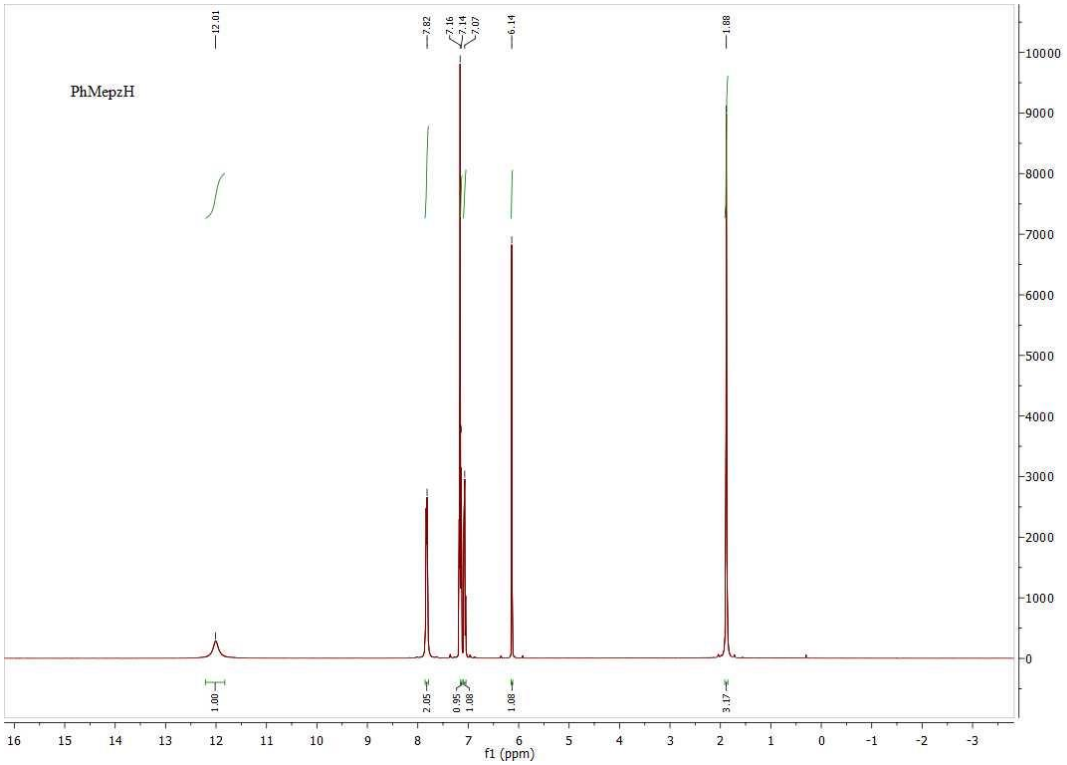


Figure 5.12. ^{1}H NMR spectrum of **[PhMepzH)]** in C_6D_6.

Table 5.1: Chemical shifts in ^{1}H-NMR spectra of complexes **5.1-5.10** in C_6D_6.

	Chemical shift (ppm)					
^{1}H-NMR	CH(pz)	CH_2(thf)	OCH_2(thf)	CH_3(^{t}Bu)	CH_3(Me)	Ph
5.1	6.49	1.39	3.76	1.62	-	-
5.2	15.15	1.82	3.79	3.33	-	-
5.3	28.68	2.50	6.70	1.66	-	-
5.5	6.53	1.06	3.37	1.63	-	-
5.6	6.62	1.31	3.85	-	2.51	7.09, 7.32, 8.26
5.7	14.18	1.81	3.19	-	1.81	7.31, 7.36, 8.92
5.8	26.41	0.72	1.05	-	1.05	8.05-8.22, 11.70, 12.67
5.10	6.66	1.18	3.73	-	2.43	7.08, 7.28, 8.17

5.3.2 X-ray Crystal Structures

5.3.2.1 [Ln(^{t}Bu$_2$pz)I$_2$(thf)$_4$] (La **5.1**, Ce **5.2** and Nd **5.3**)

Compounds [Ln(^{t}Bu$_2$pz)I$_2$(thf)$_4$] (La **5.1**, Ce **5.2** and Nd **5.3**) are eight coordinate monomers, where the metal center is coordinated to one chelating ^{t}Bu$_2$pz ligands, two *trans* iodine ligands and four thf ligands. The crystal system of these compounds is orthorhombic, with space group $P2_12_12_1$, and their geometry is described as octahedral. In compounds [Ln(^{t}Bu$_2$pz)I$_2$(thf)$_4$] (**5.1** to **5.3**) the iodine ligands are *cis* to the ^{t}Bu$_2$pz ligand {C(6)-La(1)-I(1) 100.011°, C(6)-La(1)-I(2) 98.725°, C(6)-Ce(1)-I(1) 99.973°, C(6)-Ce(1)-I(2) 98.722°, C(6)-Nd(1)-I(1) 108.087° and C(6)-Nd(1)-I(2) 98.495°} but *trans* to each other {I(1)-La(1)-I(2) 161.070(6)°, I(1)-Ce(1)-I(2) 161.150(4)° and I(1)-Nd(1)-I(2) 161.253(9)°}. The <Ln-N> bond length in compounds **5.1** -**5.3** varies from 2.420(3) Å to 2.477(16) Å, which is shorter than the <Ln-N> observed in the nine coordinate [Ln(Ph$_2$pz)$_3$(thf)$_3$] (Ln = La, Ce) compound [32] and close with 2.443(7) Å found in the eight coordinate compound [Nd(^{t}Bu$_2$pz)$_3$(thf)$_2$] [33] and 2.465(2) Å in the seven coordinate compound [Nd(EtForm)I$_2$(thf)$_3$].[34]

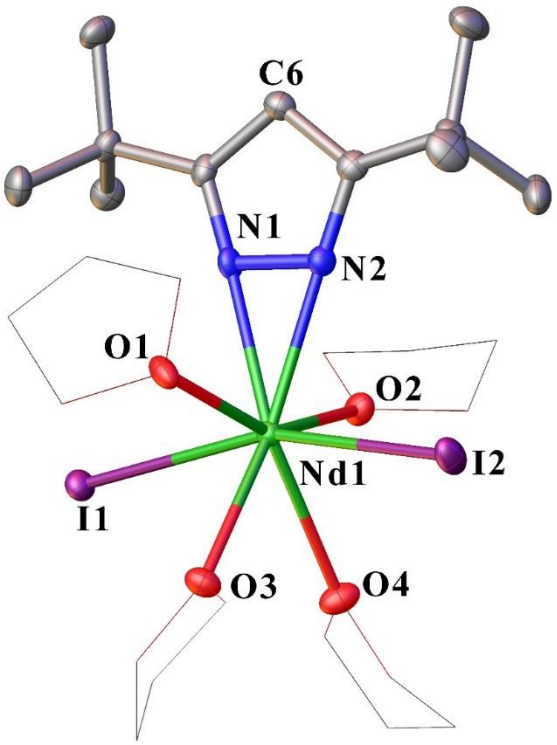


Figure 5.12. Molecular diagram of [Nd(^{t}Bu$_2$pz)I$_2$(thf)$_4$] (representative of La **5.1**, Ce **5.2**) in which relevant atoms are labelled. Thermal ellipsoids are set at the 50% probability level. Hydrogen atoms are omitted and coordinated thf molecules are drawn as wireframe for clarity. Selected bond lengths (Å): La(1)-N(1) 2.489(17), La(1)-N(2) 2.466(16), La(1)-I(1)

3.230(2), La(1)-I(2) 3.223(2); Ce(1)-N(1) 2.452(12), Ce(1)-N(2) 2.473(14), Ce(1)-I(1) 3.2137(13), Ce(1)-I(2) 3.2070(14); Nd(1)-N(1) 2.419(3), Nd(1)-N(2) 2.421(3), Nd(1)-I(1) 3.1787(6), Nd(1)-I(2) 3.1743(5). For more details, see the **Table 5.3**.

The <Ln-I> bond length in compound **5.1** is 3.231(2) Å, in **5.2** is 3.2103(13) Å and in **5.3** is 3.1765(5) Å longer than that found in the seven coordinate [Ln(DippForm)I_2(thf)$_3$] (Ln = La, Ce) compounds and 3.081(3) Å and 3.141(3) Å in compound [Nd(DFForm)I_2(thf)$_3$] and [Ce(XylForm)I_2(thf)$_3$] respectively, [12, 34] and is shorter than 3.455(9) Å found in the Nd complex [Nd(Ph_2pz)I_2(thf)$_4$].[35] The <Ln-O> bond length for compounds **5.1** to **5.3** changes from 2.581(16) Å to 2.563(3) Å, comparable with the nine coordinate compounds [La(fu_2pz)$_3$(thf)$_3$], [32] and [Ce(Ph_2pz)$_3$(thf)$_3$] [32] and statistically equivalent with 2.545(12) in the compound [La(Ph_2pz)I_2(thf)$_4$] [35] and shorter than 2.453(7) Å found in the compound [Nd(^{t}Bu$_2$pz)$_3$(thf)$_2$].[33]

Table 5.2: A comparison of selected bond lengths (Å) with similar complexes.

Compounds	<Ln-N>	<Ln-I>	<Ln-O>	Ref.
[La(^{t}Bu$_2$pz)I_2(thf)$_4$]	2.477(16)	3.2310(2)	2.581(16)	Current work
[La(Ph_2pz)$_3$(thf)$_3$]	2.531(4)		2.602(3)	[32]
[La(fu_2pz)$_3$(thf)$_3$]	2.520(2)		2.592(2)	[36]
[La(*ttf*pz)$_3$(thf)$_3$]	2.539(2)		2.696(18)	[37]
[La(DippForm)I_2(thf)$_3$]	2.519(3)	3.167(4)	2.555(3)	[34]
[Ce(^{t}Bu$_2$pz)I_2(thf)$_4$]	2.462(13)	3.2103(13)	2.583(10)	Current work
[Ce(DippForm)I_2(thf)$_3$]	2.495(10)	3.145(13)	2.521(9)	[34]
[Ce(XylForm)I_2(thf)$_3$]	2.489(3)	3.141(3)	2.516(2)	[34]
[Nd(^{t}Bu$_2$pz)I_2(thf)$_4$]	2.420(3)	3.1765(5)	2.563(3)	Current work
[Nd(^{t}Bu$_2$pz)$_3$(thf)$_2$]	2.443(7)	-	2.453(7)	[33]
[Nd(^{t}Bu$_2$pz)$_3$(dme)]	2.433(6)		2.552(5)	[38]
[Nd(Ph_2pz)$_3$(thf)$_3$]	2.459(9)		2.534(8)	[39]
[Eu(^{t}Bu$_2$pz)$_3$(Py)$_2$]	2.398(2)			[40]
[Yb(Ph_2pz)I_2(thf)$_3$]	2.249(14)	2.9916(13)	2.323(12)	[41]

Table 5.3: Selected bond lengths for complexes (**5.1** - **5.3**).

Bond lengths (Å)	**5.1**	**5.2**	**5.3**
Ln-N(1)	2.489(17)	2.452(12)	2.419(3)
Ln-N(2)	2.466(16)	2.473(14)	2.421(3)
Ln-I(1)	3.230(2)	3.2137(13)	3.178(6)
Ln-I(2)	3.223(2)	3.2070(14)	3.1743(5)
Ln-O(1)	2.620(2)	2.524(10)	2.501(3)
Ln-O(2)	2.529(16)	2.524(9)	2.492(3)
Ln-O(3)	2.537(17)	2.610(10)	2.575(3)
Ln-O(4)	2.636(19)	2.596(10)	2.585(3)

Table 5.4: Selected bond angles for complexes (**5.1** - **5.3**).

Bond angles (°)	**5.1**	**5.2**	**5.3**
O(1)-Ln-O(2)	68.0(6)	152.2(3)	152.46(8)
O(1)-Ln-O(3)	139.6(6)	139.6(4)	70.15(9)
O(1)-Ln-O(4)	69.5(5)	70.2(3)	139.56(10)
O(2)-Ln-O(3)	152.2(5)	68.0(3)	136.35(9)
O(2)-Ln-O(4)	136.7(6)	136.7(3)	67.74(9)
O(3)-Ln-O(4)	70.2(6)	69.6(3)	69.53(9)
C(8)-Ln-I(1)	100.011	99.973	100.087
C(8)-Ln-I(2)	98.725	98.722	98.495
I(1)-Ln-I(2)	161.07(6)	161.15(4)	161.253(9)

5.3.2.2 [Ln(^{t}Bu$_2$pz)$_2$I(thf)$_2$] (Er **5.4**, Lu **5.5**)

The seven coordinate compounds [Ln(^{t}Bu$_2$pz)$_2$I(thf)$_2$] (Ce **5.4**, Nd **5.5**) are isomorphous, where the metal center is coordinated to two chelating ^{t}Bu$_2$pz ligands, one iodine ligand and two thf ligands. These monomeric compounds crystallize in the orthorhombic system, space

group *P*bcn, with their geometry described as pentagonal bipyramid. In both compounds **5.4** and **5.5** the iodide ligand is *cis* to the ^{t}Bu$_2$pz ligand [{C(6)-Er(1)-I(1) 110.94°}, {C(6)-Lu(1)-I(1) 110.69°}]. The bond angles between the ^{t}Bu$_2$pz ligands and other coordination sites are as follows: C(6)-Er(1)-C(6*) is 138.117°, C(6)-Er(1)-O(1) is 79.591°, C(6)-Lu(1)-C(6*) is 138.614° and C(6)-Lu(1)-O(1) is 79.768°.

The <Er-N> bond length in compound **5.4** is 2.3079(15) Å, which is shorter than the 2.365(3) Å observed in the eight coordinate compound [Er(Ph$_2$pz)$_3$(py)$_2$].[32] The Er-I bond length is 2.9794(7) Å, nearly identical to the 2.9879(3) Å in the seven coordinate compound [Er(DFForm)$_2$I(thf)$_2$].[12] The average Er-O bond length is 2.3173(13) Å, slightly elongated with respect to 2.3010(17) Å observed in the same compound.[12] In compound **5.5** the <Lu-N> bond length is 2.2784(16) Å, shorter than the 2.337(3) Å observed in the eight coordinate compound [Lu(Ph$_2$pz)$_3$(py)$_2$].[32] The Lu-I bond length is 2.9515(7) Å, statistically equivalent to the 2.9754(7) Å in the seven coordinate compound [Lu(DFForm)$_2$I(thf)$_2$].[12] Again, the average Lu-O bond length is 2.2834(14) Å, slightly longer than 2.272(3) Å observed in the same compound.[12]

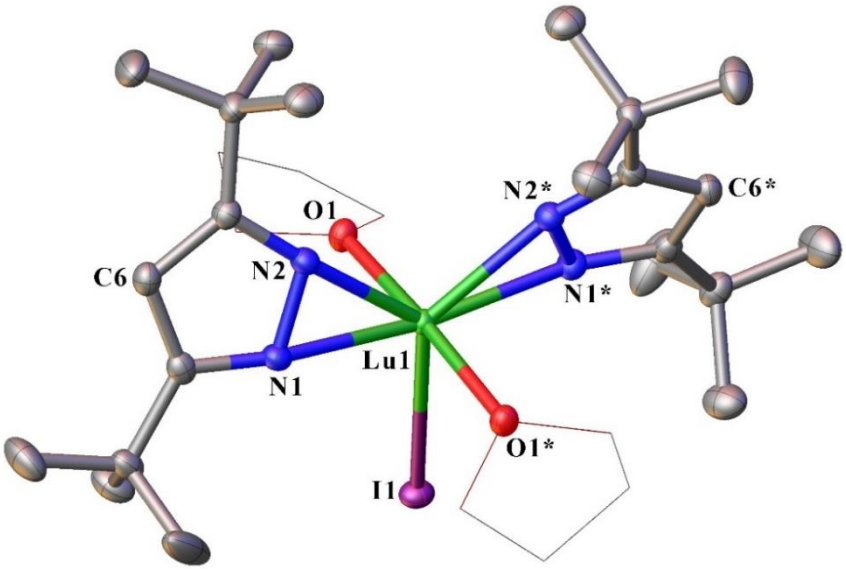


Figure 5.13. Molecular diagram of [Lu(^{t}Bu$_2$pz)$_2$I(thf)$_2$] (representative of Er **5.4**) in which relevant atoms are labelled. Thermal ellipsoids are set at the 50% probability level. Hydrogen atoms are omitted and coordinated thf molecules are drawn as wireframe for clarity. Selected bond lengths (Å): Er(1)-N(1) 2.2903(15), Er(1)-N(2) 2.3256(16), Er(1)-I(1) 2.9794(7); Lu(1)-N(1) 2.2975(17), Lu(1)-N(2) 2.2594(16), Lu(1)-I(1) 2.9515(7). For more details, see the **Table 5.6**.

Table 5.5: A comparison of selected bond lengths (Å) with similar complexes.

Compounds	<Ln-N>	Ln-I	<Ln-O>	Ref.
[Er(^{t}Bu$_2$pz)$_2$I(thf)$_2$]	2.3529(15)	2.9794(7)		Current work
[Er(^{t}Bu$_2$pz)$_3$(thf)$_2$]	2.351(8)		2.345(6)	[33]
[Er(^{t}Bu$_2$pz)$_3$(^{t}Bu$_2$pzH)$_2$]	2.396(4)			[42]
[Er(Ph$_2$pz)$_3$(dme)$_2$]	2.340(6)		2.481(9)	[38]
[Er(EtForm)I$_2$(thf)$_3$]·thf	2.380(2)	3.0018(2)	2.395(17)	[34]
[Er(DippForm)I$_2$(thf)$_3$]	2.381(2)	3.0078(2)	2.468(15)	[34]
[Lu(^{t}Bu$_2$pz)$_2$I(thf)$_2$]	2.2784(16)	2.9515(7)		Current work
[Lu(*ttf*pz)$_3$(thf)$_2$]	2.313(7)		2.301(7)	[37]
[Lu(^{t}Bu$_2$pz)$_3$(^{t}Bu$_2$pzH)$_2$]	2.316(4)			[42]
[Lu(EtForm)I$_2$(thf)$_3$]·thf	2.357(11)	2.9761(18)	2.369(17)	[34]
[Lu(XylForm)I$_2$(thf)$_3$]	2.351(9)	2.979(7)	2.374(7)	[34]

Table 5.6: Selected bond lengths and angles for complexes (**5.4** and **5.5**).

Bond lengths (Å)	5.4	5.5	Bond angles (°)	5.4	5.5
Ln-N(1)	2.2903(15)	2.2975(17)	O(1)-Ln-O(1^1)	174.42(6)	174.89(7)
Ln-N(2)	2.3256(16)	2.2594(16)	O(1)-Ln-I(1)	87.21(3)	87.44(3)
Ln-N(1^{1*})	2.2903(15)	2.2975(17)	N(1)-Ln-N(1^1)	101.50(7)	170.45(8)
Ln-N(2^{1*})	2.3256(16)	2.2594(16)	N(1)-Ln-N(2)	35.13(5)	35.64(5)
Ln-I(1)	2.9794(7)	2.9515(7)	C(6)-Ln-I(1)	110.942	110.693
Ln-O(1)	2.3173(13)	2.2834(14)	C(6)-Ln-O(1)	79.591	79.768
Ln-O(1^{1*})	2.3173(13)	2.2834(14)	C(6)-Ln-O(1^1)	102.443	102.072

5.3.2.3 [Ln(PhMepz)I$_2$(thf)$_4$] (La **5.6**, Ce **5.7**, Nd **5.8**)

Iso structural compounds [Ln(PhMepz)I$_2$(thf)$_4$] (La **5.6**, Ce **5.7**, Nd **5.8**) are eight coordinate monomers, where the metal center is coordinated to one chelating PhMepz ligand, two *trans* iodide ligands and four thf ligands. These compounds crystallized in the monoclinic system,

space group $P2_1/c$ with the geometry described as dodecahedral. For compounds [Ln(PhMepz)I_2(thf)$_4$] (**5.6** to **5.8**) the iodide ligands are *cis* to the PhMepz ligand [{C(8)-La(1)-I(1) 105.987°, C(8)-La(1)-I(2) 95.040°}, {C(8)-Ce(1)-I(1) 105.986°, C(8)-Ce(1)-I(2) 95.196°} and {C(8)-Nd(1)-I(1) 106.093°, C(8)-Nd(1)-I(2) 95.239°}] but *trans* to each other [{I(1)-La(1)-I(2) 158.961(12)°}, {I(1)-Ce(1)-I(2) 158.809(9)°}, {I(1)-Nd(1)-I(2) 158.664(9)°}].

In compound [La(PhMepz)I_2(thf)$_4$] **5.6** the average La-N bond length is 2.486(4) Å, shorter than the 2.531(4) Å observed in the nine coordinate [La(Ph$_2$pz)$_3$(thf)$_3$].[32] The <La-I> bond length is 3.2158(4) Å, is shorter than 3.455(9) Å found in the compound [Nd(Ph$_2$pz)I_2(thf)$_4$].[35] The <La-O> bond length is 2.581(3) Å, comparable to the 2.592(2) Å in the nine coordinate [La(fu$_2$pz)$_3$(thf)$_3$] compound and statistically equivalent with 2.545(12) in compound [La(Ph$_2$pz)I_2(thf)$_4$].[32, 35] The average Ce-N bond length in [Ce(PhMepz)I_2(thf)$_4$] **5.7** is 2.465(3) Å, shorter than the 2.507(3) Å observed in the nine coordinate [Ce(Ph$_2$pz)$_3$(thf)$_3$].[32] The <Ce-I> bond length is 3.1975(5) Å, longer than 3.1381(3) Å found in the seven coordinate [Ce(EtForm)I_2(thf)$_3$].[34] The <Ce-O> bond length is 2.563(10) Å, comparable to the 2.593(2) Å in the nine coordinate [Ce(Ph$_2$pz)$_3$(thf)$_3$].[32]

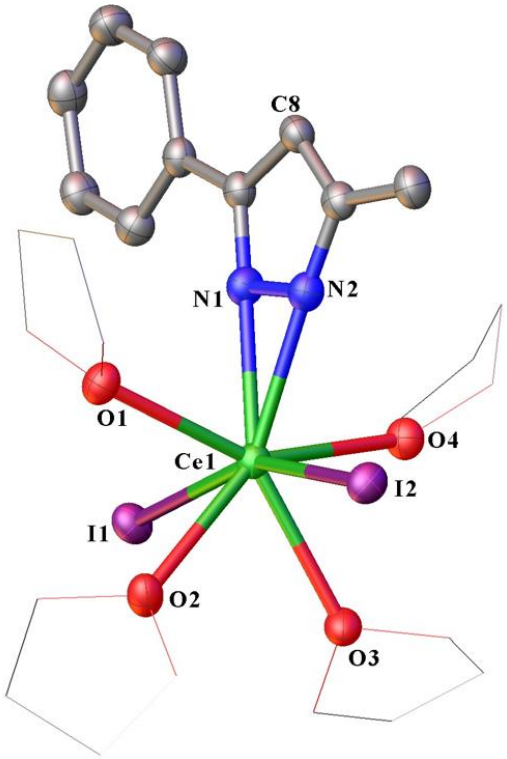


Figure 5.14. Molecular diagram of [Ce(PhMepz)I_2(thf)$_4$] (representative of La **5.6**, Nd **5.8**) in which relevant atoms are labelled. Thermal ellipsoids are set at the 50% probability level.

Hydrogen atoms are omitted and coordinated thf molecules are drawn as wireframe for clarity. Selected bond lengths (Å): La(1)-N(1) 2.437(4), La(1)-N(2) 2.535(4), La(1)-I(1) 3.2094(4), La(1)-I(2) 3.2222(4); Ce(1)-N(1) 2.417(3), Ce(1)-N(2) 2.513(3), Ce(1)-I(1) 3.2064(6), Ce(1)-I(2) 3.1886(5); Nd(1)-N(1) 2.480(3), Nd(1)-N(2) 2.379(2), Nd(1)-I(1) 3.1492(5), Nd(1)-I(2) 3.1703(5). For more details, see the **Table 5.9**.

The bite angle (N(1)-Nd-N(2)) of the compound (**5.8**) is 32.750(8)°, which is smaller than that of the seven coordinate trivalent ytterbium compound [Yb(Ph_2pz)I_2(thf)$_3$] (35.200(4)°).[38] The <Nd-N> bond length is 2.429(2) Å, similar to the 2.455(9) Å found in the eight coordinate compound [Nd(Ph_2pz)I_2(thf)$_4$].[35] The <Nd-I> bond length is 3.1597(5) Å, approximately same as 3.1670(12) Å in the previous compound [Nd(Ph_2pz)I_2(thf)$_3$].[35] The <Nd-O> bond length is 2.531(2) Å, longer than the 2.469(17) Å found in [Nd(DFForm)I_2(thf)$_3$].[12]

Table 5.7: A comparison of selected bond lengths (Å) with similar complexes.

Compounds	<Ln-N>	<Ln-I>	<Ln-O>	Ref.
[La(PhMepz)I_2(thf)$_4$]	2.486(4)	3.2158(4)	2.581(3)	Current work
[La(Ph_2pz)$_3$(thf)$_3$]	2.531(4)		2.602(3)	[32]
[La(fu_2pz)$_3$(thf)$_3$]	2.520(2)		2.592(2)	[36]
[La(*ttf*pz)$_3$(thf)$_3$]	2.539(2)		2.696(18)	[37]
[La(DippForm)I_2(thf)$_3$]	2.519(3)	3.167(4)	2.555(3)	[34]
[Ce(PhMepz)I_2(thf)$_4$]	2.465(3)	3.1975(5)	2.563(10)	Current work
[Ce(Ph_2pz)$_3$(thf)$_3$]	2.507(3)		2.593(2)	[32]
[Ce(EtForm)I_2(thf)$_3$]	2.497(3)	3.1381(3)	2.517(2)	[34]
[Ce(DippForm)I_2(thf)$_3$]	2.495(10)	3.145(13)	2.521(9)	[34]
[Nd(PhMepz)I_2(thf)$_4$]	2.429(2)	3.1597(5)	2.531(2)	Current work
[Nd(Ph_2pz)I_2(thf)$_4$]	2.455(9)	3.167(12)	2.524(8)	[35]
[Nd(Ph_2pz)$_3$(dme)$_2$]	2.458(3)		2.553(2)	[43]
[Nd(^{t}Bu$_2$pz)$_3$(thf)$_2$]	2.443(6)		2.453(7)	[33]

[Nd(DFForm)I_2(thf)$_3$]	2.488(2)	3.0833(3)	2.469(17)	[12]
[Yb(Ph$_2$pz)I_2(thf)$_3$]	2.249(14)	2.991(13)	2.323(12)	[41]
[Eu(PhMepz)$_2$(py)$_4$]	2.669(18)			[40]

5.3.2.4 [Tb(PhMepz)I_2(thf)$_3$]·thf (**5.9**)

[Tb(PhMepz)I_2(thf)$_3$]·thf (**5.9**) is a seven coordinate monomer, where the metal center is coordinated to one chelating PhMepz ligand, two *trans* iodine ligands and three thf ligands. The compound was crystallized in the triclinic space group *P*-1, with the geometry described as capped trigonal prism (if N-N is one bonding site geometry looks distorted octahedral). The iodine ligands in compound **5.9** are *cis* to the PhMepz ligand {C(8)-Tb(1)-I(1) 97.263°, C(8)-Tb(1)-I(2) 91.102°} but trans to each other {I(1)-Tb(1)-I(2) 171.116(8)°}. The average Tb-N bond length is 2.316(3) Å, longer than the 2.249(14) Å observed in the seven coordinate [Yb(Ph$_2$pz)I_2(thf)$_3$] compound.[41] The <Tb-I> bond length is 3.0425(3) Å, same as 3.0441(3) Å found in the seven coordinate compound [Tb(DippForm)I_2(thf)$_3$].[34] The <Tb-O> bond length is 2.384(2) Å, shorter than the 2.424(2) Å in the same compound [Tb(EtForm)I_2(thf)$_3$].[34]

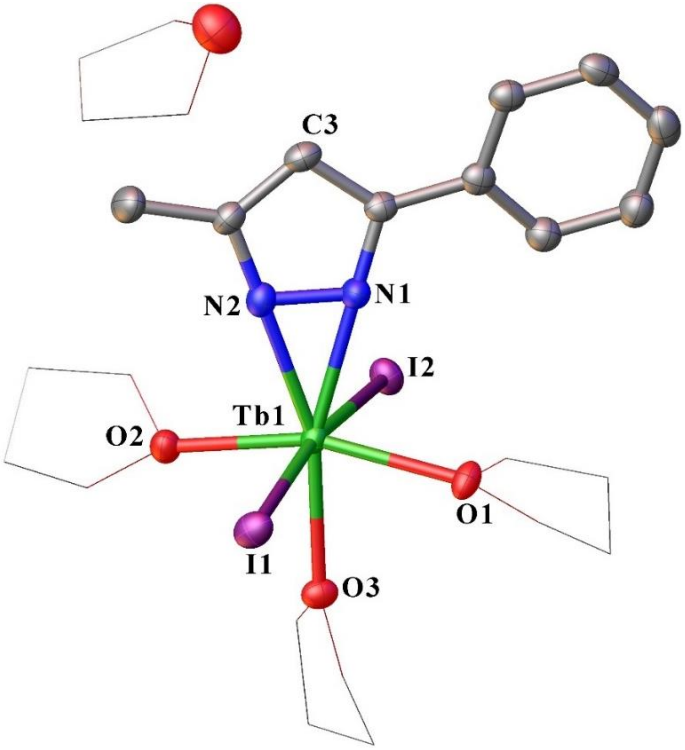


Figure 5.15. Molecular diagram of [Tb(PhMepz)I_2(thf)$_3$]·thf (**5.9**) in which relevant atoms are labelled. Thermal ellipsoids are set at the 50% probability level. Hydrogen atoms are omitted and coordinated thf molecules are drawn as wireframe for clarity. Selected bond lengths (Å): Tb(1)-N(1) 2.311(3), Tb(1)-N(2) 2.322(3), Tb(1)-I(1) 3.0386(3), Tb(1)-I(2) 3.0465(3). For more details, see the **Table 5.9**.

Table 5.8: A comparison of selected bond lengths (Å) with similar complexes.

Compounds	<Ln-N>	<Ln-I>	<Ln-O>	Ref.
[Tb(PhMepz)I_2(thf)$_3$]·thf	2.316(3)	3.0425(3)	2.384(2)	Current work
[Tb(*ttf*pz)$_3$(thf)$_3$]	2.469(7)		2.485(6)	[37]
[Yb(Ph_2pz)I_2(thf)$_3$]	2.249(14)	2.9916(13)	2.323(12)	[41]
[Tb(EtForm)I_2(thf)$_3$]	2.453(3)	3.0388(3)	2.424(2)	[34]
[Tb(DippForm)I_2(thf)$_3$]	2.454(3)	3.0441(3)	2.455(3)	[34]
[Er(Ph_2pz)(Ph)I(thf)$_3$]	2.313(3)	3.071(6)	2.386(3)	[35]

Table 5.9: Selected bond lengths for complexes (**5.6** - **5.9**).

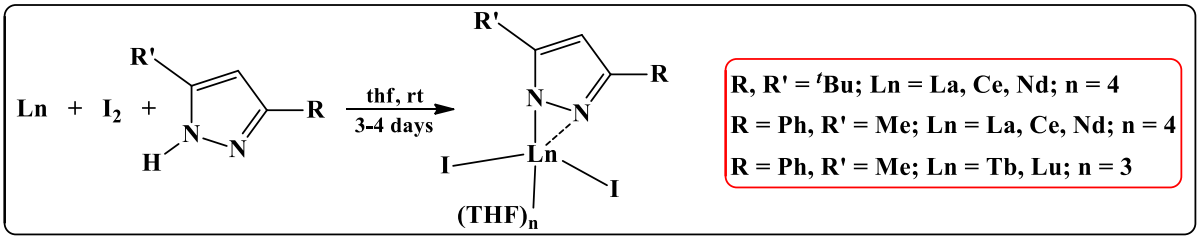
Bond lengths (Å)	5.6	5.7	5.8	5.9
Ln-N(1)	2.437(4)	2.513(3)	2.480(3)	2.311(3)
Ln-N(2)	2.535(4)	2.417(3)	2.379(2)	2.322(3)
Ln-I(1)	3.209(4)	3.188(5)	3.149(5)	3.038(3)
Ln-I(2)	3.222(4)	3.206(5)	3.170(5)	3.046(3)
Ln-O(1)	2.536(3)	2.516(2)	2.529(2)	2.366(2)
Ln-O(2)	2.604(3)	2.583(2)	2.488(2)	2.370(2)
Ln-O(3)	2.603(3)	2.579(2)	2.552(2)	2.416(2)
Ln-O(4)	2.580(3)	2.557(2)	2.554(2)	-

Table 5.10: Selected bond angles for complexes (**5.6** - **5.9**).

Bond angles (°)	5.6	5.7	5.8	5.9
O(1)-Ln-O(2)	69.85(10)	70.32(8)	147.03(7)	159.96(8)
O(1)-Ln-O(3)	143.03(10)	142.98(7)	69.71(7)	79.58(8)
O(1)-Ln-O(4)	147.39(10)	146.91(7)	141.80(7)	-
O(2)-Ln-O(3)	73.19(9)	72.65(7)	142.86(7)	80.60(8)
O(2)-Ln-O(4)	141.93(10)	141.78(7)	70.12(7)	-
O(3)-Ln-O(4)	69.12(9)	69.72(7)	72.74(7)	-
C(8)-Ln-I(1)	105.98	105.98	106.09	97.26
C(8)-Ln-I(2)	95.04	95.19	95.23	91.10
I(1)-Ln-I(2)	158.96(12)	158.81(9)	158.66(9)	171.12(8)

5.3.3 Discussion

Previously Guo *et al.* (**2021**) reported for the first time a direct reaction method for synthesising trivalent formamidinatoiodidolanthanoid ([Ln(Form)I_2(thf)$_3$, [Ln(Form)$_2$I(thf)$_2$] (FormH = DFForm, DippForm, XylForm and EtForm) complexes, through the reaction between lanthanoid metal, I_2 and the corresponding formamidine ligands (**Scheme 5.8** eqn. **i** and **ii**).[12, 34] Using the same reaction process, but replacing formamidine (DFFormH, DippFormH, EtFormH and XylFormH) ligands with pyrazole (^{t}Bu$_2$pzH and PhMepzH) ligands, we observed similar reactivity. A 1:1 molar ratio of ligand to I_2 led to the isolation of [Ln(^{t}Bu$_2$pz)I_2(thf)$_4$] (La **5.1**, Ce **5.2** and Nd **5.3**), [Ln(PhMepz)I_2(thf)$_4$] (La **5.6**, Ce **5.7**, Nd **5.8**), [Ln(PhMepz)I_2(thf)$_3$] (Ln = Tb **5.9**, Lu **5.10**) (**Scheme 5.8**) complexes.



Scheme 5.8: Alternative synthesis method for isolating pseudo-Grignard complexes.[12, 34]

The crystal system of the eight coordinate complexes [Ln(^{t}Bu$_2$pz)I$_2$(thf)$_4$] (La **5.1**, Ce **5.2**, Nd **5.3**) and [Ln(PhMepz)I$_2$(thf)$_4$] (La **5.6**, Ce **5.7**, Nd **5.8**) is orthorhombic, with both iodine atoms in *trans* position (angles varies from 158.664(9) to 161.253(9)°) and the ^{t}Bu$_2$pz ligand in a *cis* arrangement relative to the iodine ligands (angles varies from 95.040° to 108.087°). The metal center of these complexes is bonded with one chelating pyrazolato ligand, two iodine ligands and four thf ligands. Comparatively, smaller atomic radii molecules Tb yielded seven coordinated [Tb(PhMepz)I$_2$(thf)$_3$] with similar crystal rearrangement with the bulkier ligand based [Tb(EtForm)I$_2$(thf)$_3$] compound.[34]

In contrast, a 4:1 molar ratio of ligand to I$_2$ fascilated the isoltion of [Ln(^{t}Bu$_2$pz)$_2$I(thf)$_2$] (Er **5.4**, Lu **5.5**) complexes (**Fig. 5.16**). The pentagonal bipyramidal seven coordinated metal center is bonded with two chelating pyrazolato ligands, one iodine ligand and two thf ligands. Both thf molecules are approximately are in axial positions [O(1)-Ln-O(1*) 174.42(6), 174.89(7)], where the iodine atom is in *cis* position [I(1)-Ln-O(1) 87.21(3), 87.44(3)]. The bite angles of these complexes are 35.13(5) and 35.64(5) respectively.

Overall, we found that the comparatively smaller atomic radii lanthanoid centers; Tb, Er and Lu led to the isolation of lower (7) coordinate complexes (**5.4**, **5.5** and **5.9**), where larger atomic radii ions; La, Ce and Nd yielded eight coordinate complexes (**5.1**, **5.2**, **5.3**, **5.6**, **5.7**, and **5.8**). The lanthanoid contraction in average Ln-N bond distances is obvious for all the isolated complexes (La-N> Ce-N> Nd-N> Er-N> Lu-N (**5.1** - **5.5**); La-N> Ce-N> Nd-N> Tb-N (**5.6** - **5.9**)). The bite angles(°) (N(1)-Ln-N(2)) of these complexes increased with the decreasing the average Ln-N bond distances: 32.27(7) (**5.1**), 33.05(9) (**5.2**), 33.30(4) (**5.3**), 35.13(5) (**5.4**), 35.64(5) (**5.5**); 31.86(10) (**5.6**), 32.51(8) (**5.7**), 32.75(8) (**5.8**), 34.62(10) (**5.9**). These variations are attributed to the effect of ionic radius and different coordination numbers (eight coordinate La^{3+} 1.16 Å > eight coordinate Ce^{3+} 1.143 Å > eight coordinate Nd^{3+} 1.109 Å > seven coordinate Tb^{3+} 0.980 Å > seven coordinate Er^{3+} 0.945 Å).[44]

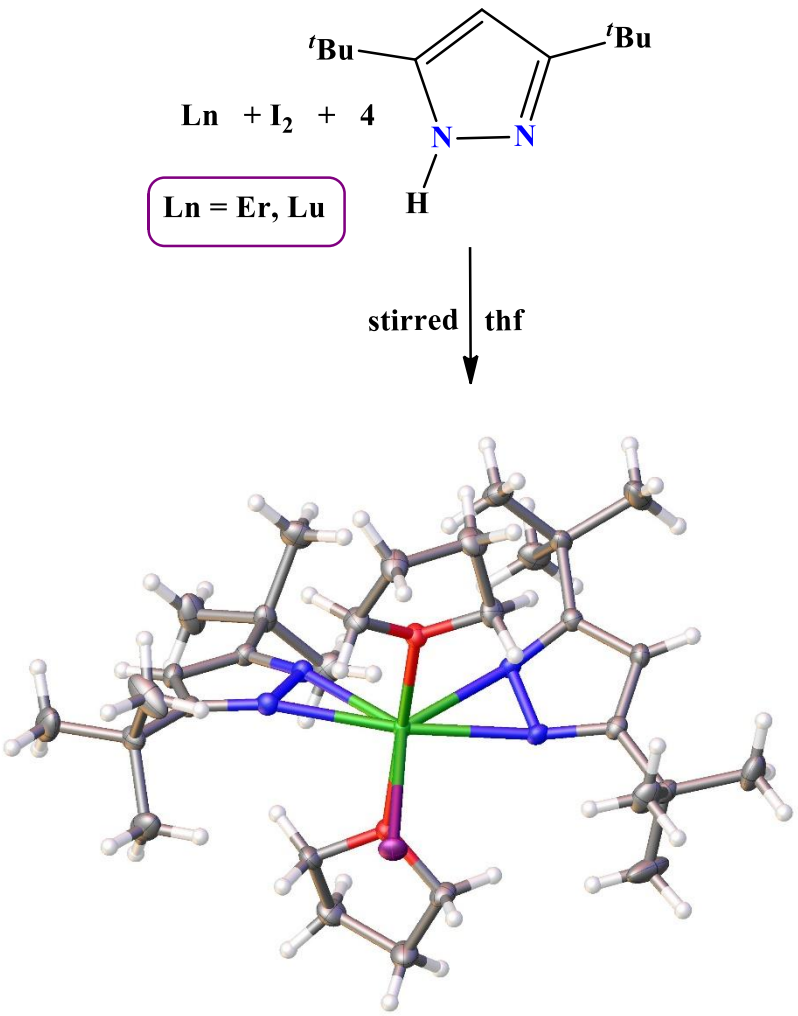


Figure 5.16. Molecular diagram of [Ln(^{t}Bu$_2$pz)$_2$I(thf)$_2$] (Ln = Er, Lu) complexes.

5.4 Conclusion and Future Outlook

The results presented in this chapter highlight that, the reported synthesis route, involving the direct reaction between Ln metals, I_2 and FormH ligands; FormH = DippFormH, EtFormH, XylFormH, DFFormH).[12, 34] can be readily applied to pyrazole ligands (^{t}Bu$_2$pzH, PhMepzH). The reaction of Ln^0 metals, I_2 and ^{t}Bu$_2$pzH facilitated the synthesis of trivalent monomeric pseudo-Grignard complexes, [Ln(^{t}Bu$_2$pz)I$_2$(thf)$_4$] (Ln = La **5.1**, Ce **5.2** and Nd **5.3**) and [Ln(^{t}Bu$_2$pz)$_2$I(thf)$_2$] (Ln = Er **5.4** and Lu **5.5**) with good crystalline yields (33% - 83%). A 1:1 molar ratio of ^{t}Bu$_2$pzH to I_2 produced eight coordinate diiodo complexes, while a 4:1 molar ratio resulted in seven coordinate monoiodo complexes.

Additionally, reactions between lanthanoid metals (Ln = La **5.6**, Ce **5.7**, Nd **5.8**, Tb **5.9** and Lu **5.10**), I_2 and PhMepzH in a 1:1 molar ratio led to the formation of Ln(^{III}) diiodo

complexes [Ln(PhMepz)I_2(thf)$_4$] (Ln = La, Ce, Nd), [Tb(PhMepz)I_2(thf)$_3$]·thf and [Lu(PhMepz)I_2(thf)$_3$]. Larger atomic radius metals (Ln = La, Ce, Nd) yielded eight coordinate complexes, while the smaller atomic radius metal Tb and Lu formed a seven-coordinate complex. The melting points of these complexes varies from 105 °C – 148 °C in a sealed glass tube under nitrogen. The melting points indicate significant thermal stability of the new pyrazolato complexes.

These findings suggest that the reported direct reaction method [12, 35] is well suited for use with pyrazoles (^{t}Bu$_2$pzH, PhMepzH) and holds promise for further studies with a broader range of N-donor ligands. But also these heteroleptic compounds are now well set up for further elaboration via metathesis reactions and will lead to a vast range of homoleptic lanthanoid complexes.

5.5 Experimental

5.5.1 General Aspects

For general aspects see the appendix 1.

5.5.2 Synthesis of pyrazolato lanthanoid complexes

Excess amounts of lanthanoid metal powder, a stoichiometric amount of iodine, pyrazole, and 10 ml of dry THF were placed in a Schlenk flask inside a nitrogen-filled dry box. The mixture was stirred for 3-4 days at room temperature. Crystals were obtained by evaporating the filtrate to half its volume under vacuum and then refrigerating it at approximately -25 °C. Yields were calculated based on the ligand (^{t}Bu$_2$pzH and PhMepzH).

[La(^{t}Bu$_2$pz)I_2(thf)$_4$] (5.1)

Lanthanum metal powder (0.139 g, 1.0 mmol), iodine (0.127 g, 0.5 mmol), ^{t}Bu$_2$pzH (0.09 g, 0.5 mmol) and dry THF (10 ml) were added in a Schlenk flask. A light brown colour solution was obtained in 4 days. The resulting mixture was filtered and concentrated to ~5 ml under vacuum. Colourless crystals (0.142 g, 33%) were obtained after cooling at -25 °C in 5 days. M.P. 122-124 °C. Metal analysis: Found: La 15.32; $C_{27}H_{51}LaI_2N_2O_4$ (860.42 gmol^{-1}) requires: La 16.14, extra 1 mole thf; $C_{27}H_{51}LaI_2N_2O_4$ (932.52 gmol^{-1}) requires: La 14.90. IR

(Nujol): 1593m, 1528m, 1505s, 1411m, 1377m, 1358s, 1308m, 1261s, 1227m, 1205w, 1096br, 1016s, 990m, 958w, 916s, 871s, 798s, 729m, 681m cm^{-1}. ^1H NMR (C_6D_6): δ = 1.39 (20H, CH_2-thf), 1.62 (18H, CH_3), 3.76 (20H, OCH_2, thf), 6.49 ppm (1H, CH-pz) indicating extra 1 mole thf from solvation.

[Ce(^{t}Bu$_2$pz)I$_2$(thf)$_4$] (5.2)

Cerium metal powder (0.14 g, 1.0 mmol), iodine (0.127 g, 0.5 mmol), *t*Bu$_2$pzH (0.09 g, 0.5 mmol) and dry THF (10 ml) were added in a Schlenk flask. A yellow colour solution was obtained in 4 days. The resulting mixture was filtered and concentrated to ~5 ml under vacuum. Colourless crystals (0.25 g, 58%), M.P. 138-140 °C, Metal analysis: Found: Ce 15.48; $C_{27}H_{51}CeI_2N_2O_4$ (861.61 $gmol^{-1}$) requires: Ce 16.26; 1 extra thf, $C_{31}H_{59}CeI_2N_2O_5$ (933.73 $gmol^{-1}$) requires: 15.01. IR (Nujol ν/cm): 1532s, 1506s, 1409s, 1357m, 1304s, 1295w, 1251s, 1227s, 1206w, 1178w, 1073m, 1020s, 994m, 953w, 921s, 865s, 803s, 726s, 667s, 627w, ^1H NMR (C_6D_6): δ = 1.82 (24H, CH_2-thf), 3.33 (18H, CH_3), 3.79 (24H, OCH_2-thf), 15.15 (1H, C-H, pz).

Alternative reaction done using cerium metal powder (0.14 g, 1.0 mmol), iodine (0.064 g, 0.25 mmol), *t*Bu$_2$pzH (0.180 g, 1 mmol) and dry THF (10 ml) were added in a Schlenk flask and stirred for 4 days. Colourless crystals of [Ce(*t*Bu$_2$pz)I$_2$(thf)$_4$] (**5.2**) was obtained from the yellow solutions confirmed from unit cell.

[Nd(^{t}Bu$_2$pz)I$_2$(thf)$_4$] (5.3)

Neodymium metal powder (0.144 g, 1.0 mmol), iodine (0.127 g, 0.5 mmol), *t*Bu$_2$pzH (0.09 g, 0.5 mmol) and dry THF (10 ml) were added in a Schlenk flask. A blue colour solution was obtained in 3 days. The resulting mixture was filtered and concentrated to ~5 ml under vacuum. Blue crystals (0.263 g, 61%) were obtained after cooling at -25 °C in overnight. M. P. 142-144 °C. Metal analysis: Found: Nd 17.18; $C_{27}H_{51}I_2N_2NdO_4$ (865.73 $gmol^{-1}$) requires: Nd 16.66. IR (Nujol): 1603w, 1530m, 1507s, 1409m, 1304w, 1295w, 1251s, 1227s, 1206w, 1174w-b, 1072w, 1020s-b, 994m, 953w, 921s, 865s-b, 803m, 726s, 667s cm^{-1}. ^1H NMR (C_6D_6): δ = 1.66 (18H, CH_3), 2.50 (16H, thf), 6.70 (16H, thf), 28.68 ppm (1H, CH-pz).

Alternative reaction done using neodymium metal powder (0.144 g, 1.0 mmol), iodine (0.064 g, 0.25 mmol), *t*Bu$_2$pzH (0.180 g, 1 mmol) and dry THF (10 ml) were added in a Schlenk

flask and stirred for 3 days. Blue crystals of [Nd(*t*Bu$_2$pz)I$_2$(thf)$_4$] (**5.3**) was obtained from the blue solutions confirmed from unit cell.

[Er(*t*Bu$_2$pz)$_2$I(thf)$_2$] (5.4)

Erbium metal powder (0.167g, 1.0 mmol), iodine (0.0625g, 0.25 mmol), *t*Bu$_2$pzH (0.18g, 1.0 mmol) and dry THF (10ml) were added in a Schlenk flask. A pink colour solution was obtained in 4 days. The resulting mixture was filtered and concentrated to ~5 ml under vacuum. Pink crystals (0.204g, 51%) were obtained after cooling at -25 °C in overnight. M.P. 146-148 °C. Metal analysis: Found: Er 23.24; $C_{30}H_{54}ErIN_4O_2$ (796.93 gmol^{-1}) requires: Er 20.99; loss of 1 thf of crystallisation, $C_{26}H_{46}ErIN_4O$ (724.83 gmol^{-1})) requires: Er 23.08. IR (Nujol): 1570s, 1520w, 1504w, 1414m, 1315s, 1285m, 1252s, 1226m, 1205m, 1137m, 1129w, 1101w, 1020w, 995w, 921s, 987s, 791w, 726s, 674m, 628m cm^{-1}. ^{1}H NMR (400 MHz, C_6D_6): Paramagnetic unable to integrate.

[Lu(*t*Bu$_2$pz)$_2$I(thf)$_2$] (5.5)

Lu metal powder (0.174 g, 1.0 mmol), iodine (0.0625 g, 0.25 mmol), *t*Bu$_2$pzH (0.18 g, 1.0 mmol) and dry THF (10 ml) were added in a Schlenk flask. A light brown colour solution was obtained in 4 days. The resulting mixture was filtered and concentrated to ~5 ml under vacuum. Colourless crystals (0.217 g, 54%) were obtained after cooling at -25 °C in 2 days. M.P. 143-145 °C. Metal analysis: Found: Lu 21.32; $C_{30}H_{54}ILuN_4O_2$ (804.64 gmol^{-1}) requires: Lu 20.96. IR (Nujol): 1593s, 1526m, 1504s, 1413m, 1376m, 1308s, 1247m, 1225m, 1206w, 1137m, 1111w, 1040m, 1016s, 989s, 957m, 919s, 872s, 797s, 728s, 686s, 627s cm^{-1}. ^{1}H NMR (C_6D_6): δ = 1.06 (8H, CH_2-thf), 1.63 (36H, CH_3), 3.37 (8H, OCH_2, thf), 6.53 ppm (2H, CH-pz).

[La(PhMepz)I$_2$(thf)$_4$] (5.6)

Lanthanum metal powder (0.139 g, 1.0 mmol), iodine (0.127 g, 0.5 mmol), PhMepzH (0.08 g, 0.5 mmol) and dry THF (10 ml) were added in a Schlenk flask. A brown colour solution was obtained in 4 days. The resulting mixture was filtered and concentrated to ~5 ml under vacuum. Colourless crystals (0.193 g, 46%) were obtained after cooling at -25 °C for 2 days.

M. P. 109-112 °C. Metal analysis: Found: La 16.89; $C_{26}H_{41}LaI_2N_2O_4$(838.32 $gmol^{-1}$) requires: La 16.57. IR (Nujol): 1602s, 1527m, 1411w, 1344w, 1294m, 1260s, 1200w, 1177m, 1151m, 1115s, 1079m, 1020s, 963s, 918s, 863s, 795w, 770s, 712s, 696s, 663s cm^{-1}. ^1H NMR (C_6D_6): δ = 1.31 (16H, thf), 2.51 (3H, CH_3), 3.85 (16H, thf), 6.62 (1H, CH-pz), 7.09 (1H, H(4)), 7.32 (2H, H(3,5)), 8.26 (2H, H(2,6)) ppm.

[Ce(PhMepz)I_2(thf)$_4$] (5.7)

Cerium metal powder (0.140 g, 1.0 mmol), iodine (0.127 g, 0.5 mmol), PhMepzH (0.08 g, 0.5 mmol) and dry THF (10 ml) were added in a Schlenk flask. A yellow colour solution was obtained in 4 days. The resulting mixture was filtered and concentrated to ~5 ml under vacuum. Colourless crystals (0.244 g, 58%) were obtained after cooling at -25 °C for 5 days. M. P. 107-109 °C. Metal analysis: Found: Ce 17.86; $C_{26}H_{41}CeI_2N_2O_4$(839.53 $gmol^{-1}$) requires: Ce 16.69; loss of 1 thf of crystallisation, $C_{22}H_{33}CeI_2N_2O_3$ (767.43 $gmol^{-1}$) requires: Ce 18.26. IR (Nujol): 1605s, 1530w, 1411m, 1344w, 1293m, 1196w, 1176m, 1152m, 1117m, 1079m, 1067w, 1019s, 962s, 919s, 864s, 795m, 770s, 710s, 696s, 661s cm^{-1}. ^1H NMR (C_6D_6): δ = 1.81(8H, thf, 3H, CH_3), 3.19 (8H, thf), 7.31-7.36 (3H, H(2,4,6)), 8.92 (2H, H(3,5)), 14.18 ppm (1H, CH-pz).

[Nd(PhMepz)I_2(thf)$_4$] (5.8)

Neodymium metal powder (0.144 g, 1.0 mmol), iodine (0.127 g, 0.5 mmol), PhMepzH (0.08 g, 0.5 mmol) and dry THF (10 ml) were added in a Schlenk flask. A blue colour solution was obtained in 3 days. The resulting mixture was filtered and concentrated to ~5 ml under vacuum. Blue crystals (0.35 g, 83%) were obtained after cooling at -25 °C in overnight. M. P. 105-107 °C. Metal analysis: Found: Nd 19.96; $C_{26}H_{41}I_2N_2NdO_4$ (843.65 $gmol^{-1}$) requires: Nd 17.10; loss of 2 thf of crystallisation, $C_{18}H_{25}NdI_2N_2O_2$ (699.45 $gmol^{-1}$) requires: Nd 20.62. IR (Nujol): 1601s, 1530m, 1411w, 1343w, 1294m, 1261m, 1202w, 1178m, 1150m, 1117s, 1079m, 1019s, 963s, 919s, 865s, 795m, 770s, 712s, 696s, 663s cm^{-1}. ^1H NMR (C_6D_6): δ = 0.72(8H, thf), 1.05 (8H, thf, 3H, CH_3), 8.05, 8.22 (2H, H(2,6)), 11.70 (2H, H(3,5)), 12.67 (H, H(4)), 26.41 ppm (1H, CH-pz).

[Tb(PhMepz)I_2(thf)$_3$]·thf (5.9)

Neodymium metal powder (0.159 g, 1.0 mmol), iodine (0.127 g, 0.5 mmol), PhMepzH (0.08 g, 0.5 mmol) and dry THF (10 ml) were added in a Schlenk flask. A yellowish colour solution was obtained in 4 days. The resulting mixture was filtered and concentrated to ~5 ml under vacuum. Colorless crystals (0.185 g, 42%) were obtained after cooling at 0 °C for 7 days. M. P. 112-114 °C. Metal analysis: Found: Tb 19.06; $C_{26}H_{41}I_2N_2TbO_4$ (858.33 gmol^{-1}) requires: Tb 18.52. IR (Nujol): 1603m, 1530m, 1343m, 1312w, 1297w, 1261s, 1172m, 1097w, 1071m, 1004s, 914s, 848s, 766m, 696m, 669s cm^{-1}. ^{1}H NMR (C_6D_6) spectra showed browed feature with unsatisfied integration due to paramagnetism (peaks observed: 35.01 ppm, 28.97 ppm, 2.57 ppm, 1.03 ppm and -5.18 ppm).

[Lu(PhMepz)I_2(thf)$_3$] (5.10)

Lutetium metal powder (0.174 g, 1.0 mmol), iodine (0.127 g, 0.5 mmol), PhMepzH (0.08 g, 0.5 mmol) and dry THF (10 ml) were added in a Schlenk flask. A yellowish-brown colour solution was obtained in 4 days. The resulting mixture was filtered and concentrated to ~5 ml under vacuum. Colourless crystals (0.193 g, 46%) were obtained after cooling at -25 °C for 5 days. M. P. 115-117 °C. Metal analysis: Found: Lu 21.28; $C_{26}H_{41}LuI_2N_2O_4$(802.28 gmol^{-1}) requires: Lu 21.81. IR (Nujol): 1602s, 1532m, 1342m, 1296m, 1261w, 1243w, 1206w, 1178m, 1115m, 1068m, 1015s, 965s, 851s, 803w, 770s, 713m, 697s cm^{-1}. ^{1}H NMR (C_6D_6): δ = 1.18 (12H, thf), 2.43 (3H, CH_3), 3.73 (12H, thf), 6.66 (1H, CH-pz), 7.08 (1H, H(4)), 7.28 (2H, H(3,5)), 8.17 (2H, H(2,6)) ppm. For compound **5.10** (orthorhombic) the unit cell is a = 9.004(5) Å, b = 73.932(14) Å, c = 12.166(5) Å, V = 8098.708(9) Å^3.

5.6 X-ray crystal data

Single crystals coated with viscous hydrocarbon oil were mounted on glass fibres or loops. The data integration was completed using Blue-ice [45] and XDS [46] software programs. Structural solutions were obtained by either direct methods [47] or charge flipping [48] methods and refined using full-matrix least-squares methods against F2 using SHELX2018, [49] in conjunction with the X-Seed [50] or Olex2 [48] graphical user interface. All hydrogen atoms were placed in calculated positions using the riding model. Multiscan were applied for absorption corrections. All CIF files were checked at https://checkcif.iucr.org.

Compounds **5.2-5.5**, **5.7-5.8** were identified by using the MX1 beamline Australian Synchrotron at 100(2) K having the wavelength (λ = 0.71073), where compounds **5.1**, **5.6** and **5.9** were identified by using the MX2 beamline at 123(10) K having the wavelength (λ = 0.71073).

[La(^{t}Bu$_2$pz)I$_2$(thf)$_4$] (5.1)

$C_{27}H_{51}I_2LaN_2O_4$, M =860.42 g/mol, orthorhombic, space group $P2_12_12_1$ (no. 19), a = 12.741(4) Å, b = 16.112(6) Å, c = 16.240(6) Å, V = 3334(2) Å^3, Z = 4, T = 123.0 K, μ(MoKα) = 3.160 mm^{-1}, *Dcalc* = 1.612 g/cm^3, 67337 reflections measured (4.064° ≤ 2Θ ≤ 55.154°), 7687 unique (R_{int} = 0.4039, R_{sigma} = 0.2911) which were used in all calculations. The final R_1 was 0.0715 (I > 2σ(I)) and wR_2 was 0.1815 (all data).

[Ce(^{t}Bu$_2$pz)I$_2$(thf)$_4$] (5.2)

$C_{27}H_{51}CeI_2N_2O_4$, M =861.61 g/mol, orthorhombic, space group $P2_12_12_1$ (no. 19), a = 12.7725(11) Å, b = 16.0992(12) Å, c = 16.2145(14) Å, V = 3334.1(5) Å^3, Z = 4, T = 123.0 K, μ(MoKα) = 3.248 mm^{-1}, *Dcalc* = 1.716 g/cm^3, 3964 reflections measured (4.06° ≤ 2Θ ≤ 49.998°), 3489 unique (R_{int} = 0.0457, R_{sigma} = 0.0771) which were used in all calculations. The final R_1 was 0.0513 (I > 2σ(I)) and wR_2 was 0.1341 (all data).

[Nd(^{t}Bu$_2$pz)I$_2$(thf)$_4$] (5.3)

$C_{27}H_{51}I_2N_2NdO_4$, Mr =865.73 g/mol, orthorhombic, space group $P2_12_12_1$ (no. 19), a = 12.726(3) Å, b = 16.039(3) Å, c = 16.151(3) Å, V = 3296.6(11) Å^3, Z = 4, T = 100(2) K, μ(Synchrotron) = 3.479 mm^{-1}, *Dcalc* = 1.744 g/cm^3, 42291 reflections measured (3.578° ≤ 2Θ ≤ 52.748°), 6691 unique (R_{int} = 0.0265, R_{sigma} = 0.0142) which were used in all calculations. The final R_1 was 0.0167 (I > 2σ(I)) and wR_2 was 0.0390 (all data).

[Er(^{t}Bu$_2$pz)$_2$I(thf)$_2$] (5.4)

$C_{30}H_{54}ErIN_4O_2$ (M =796.93 g/mol): orthorhombic, space group *P*bcn (no. 60), a = 17.658(4) Å, b = 18.348(4) Å, c = 10.548(2) Å, V = 3417.4(12) Å^3, Z = 4, T = 100(2) K, μ(MoKα) = 3.389 mm^{-1}, *Dcalc* = 1.549 g/cm^3, 35889 reflections measured (6.322° ≤ 2Θ ≤ 51.358°), 3141 unique (R_{int} = 0.0277, R_{sigma} = 0.0134) which were used in all calculations. The final R_1 was 0.0306 (I > 2σ(I)) and wR_2 was 0.0790 (all data).

[Lu(^{t}Bu$_2$pz)$_2$I(thf)$_2$] (5.5)

$C_{30}H_{54}ILuN_4O_2$ (M =804.64 g/mol): orthorhombic, space group Pbcn (no. 60), a = 17.671(4) Å, b = 18.276(4) Å, c = 10.510(2) Å, V = 3394.3(12) Å^3, Z = 4, T = 100(2) K, μ(Synchrotron) = 3.848 mm^{-1}, $Dcalc$ = 1.575 g/cm^3, 27684 reflections measured (5.908° ≤ 2Θ ≤ 50.054°), 2992 unique (R_{int} = 0.0963, R_{sigma} = 0.0449) which were used in all calculations. The final R_1 was 0.0464 (I > 2σ(I)) and wR_2 was 0.1019 (all data).

[La(PhMepz)I$_2$(thf)$_4$] (5. 6)

$C_{26}H_{41}I_2LaN_2O_4$ (M =838.32 g/mol): monoclinic, space group $P2_1/c$ (no. 14), a = 17.0879(18) Å, b = 8.9231(7) Å, c = 20.312(2) Å, β = 97.309(3)°, V = 3072.0(5) Å^3, Z = 4, T = 123.0 K, μ(MoKα) = 3.432 mm^{-1}, $Dcalc$ = 1.813 g/cm^3, 48880 reflections measured (4.044° ≤ 2Θ ≤ 55.018°), 7056 unique (R_{int} = 0.0794, R_{sigma} = 0.0569) which were used in all calculations. The final R_1 was 0.0379 (I > 2σ(I)) and wR_2 was 0.0704 (all data).

[Ce(PhMepz)I$_2$(thf)$_4$] (5. 7)

$C_{26}H_{41}CeI_2N_2O_4$, M_r =839.53 g/mol, monoclinic, space group $P2_1/c$ (no. 14), a = 17.109(3) Å, b = 8.9190(18) Å, c = 20.242(4) Å, β = 97.84(3)°, V = 3060.0(11) Å^3, Z = 4, T = 100(2) K, μ(Synchrotron) = 3.536 mm^{-1}, $Dcalc$ = 1.822 g/cm^3, 33379 reflections measured (2.402° ≤ 2Θ ≤ 50.062°), 5350 unique (R_{int} = 0.0315, R_{sigma} = 0.0174) which were used in all calculations. The final R_1 was 0.0250 (I > 2σ(I)) and wR_2 was 0.0675 (all data).

[Nd(PhMepz)I$_2$(thf)$_4$] (5.8)

$C_{26}H_{41}I_2N_2NdO_4$, M_r =843.65 g/mol, monoclinic, space group $P2_1/c$ (no. 14), a = 17.059(3) Å, b = 8.8960(18) Å, c = 20.128(4) Å, β = 98.06(3)°, V = 3024.4(11) Å^3, Z = 4, T = 100(2) K, μ(Synchrotron) = 3.790 mm^{-1}, $Dcalc$ = 1.853 g/cm^3, 32531 reflections measured (2.412° ≤ 2Θ ≤ 50.056°), 5281 unique (R_{int} = 0.0289, R_{sigma} = 0.0156) which were used in all calculations. The final R_1 was 0.0255 (I > 2σ(I)) and wR_2 was 0.0730 (all data).

[Tb(PhMepz)I$_2$(thf)$_3$]·thf (5.9)

$C_{26}H_{41}I_2N_2O_4Tb$, M_r =858.33 g/mol, triclinic, space group P-1 (no. 2), a = 9.5183(5) Å, b = 10.1225(6) Å, c = 17.7134(10) Å, α = 76.122(2)°, β = 88.522(2)°, γ = 67.628(2)°, V = 1528.06(15) Å^3, Z = 2, T = 123.0 K, μ(MoKα) = 4.366 mm^{-1}, $Dcalc$ = 1.865 g/cm^3, 99957

reflections measured ($4.492° \leq 2\Theta \leq 55.016°$), 7022 unique ($R_{int} = 0.0507$, $R_{sigma} = 0.0228$) which were used in all calculations. The final R_1 was 0.0247 ($I > 2\sigma(I)$) and wR_2 was 0.0603 (all data).

5.7 References

1. F. T. Edelmann, Comprehensive Organometallic Chemistry, 3rd edn, **2007**, vol. 4, ch. 4.
2. M. F. Lappert, A. V. Protchenko, P. P. Power and A. L. Seeber, Metal Amide Chemistry, Wiley, UK, **2009**.
3. D. C. Bradley, R. Mehrotra, I. Rothwell and A. Singh, Alkoxo and Aryloxo Derivatives of Metals, Academic Press, London, **2001**.
4. S. A. Cotton, Comprehensive Coordination Chemistry, 2nd edn, vol. 3, ch. 3, **2004**.
5. D. A. Atwood, The Rare Earth Elements, Fundamentals and Applications, John Wiley and Sons Ltd, West Sussex, **2012**.
6. H. C. Aspinall, Chemistry of the f-Block Chemistry, CRC Press, **2001**.
7. H. Schumann and J. A. Meese-Marktscheffel, Chem. Rev., **1995**, 95, 865.
8. F. T. Edelmann, D. M. M. Freckmann and H. Schumann, Chem. Rev., **2002**, 102, 1851.
9. M. Zimmermann and R. Anwander, Chem. Rev., **2010**, 110, 6194.
10. S. T. Liddle, Organometallic Chemistry Fundamental Principles, in The Rare Earth Elements, Fundamentals and Applications, ed. D. A. Atwood, John Wiley and Sons Ltd, West Sussex, **2012**.
11. F. T. Edelmann, J. Alloys Compd., **1994**, 182, 207-208.
12. Z. Guo, V. L. Blair, G. B. Deacon and P. C. Junk, Chem. Commun., **2021**, 57, 11513-11516.
13. M. N. Bochkarev, L. N. Zakharov and G. S. Kalinina, Organoderivatives of rare earth elements, Kluwer Academic Publishers Dordrecht, **1995**.
14. A. O. Tolpygin, O. A. Linnikova, T. A. Kovylina, A. V. Cherkasov, G. K. Fukin and A. A. Trifonova, Russ. Chem. Bull., Int. Ed., **2019**, 68, 32-39.
15. A. O. Tolpygin, A.S. Shavyrin, A. V. Cherkasov, G. K. Fukin and A. A. Trifonov, Organometallics, **2012**, 31, 5405-5413.
16. M. L. Cole, G. B. Deacon, P. C. Junk and K. Konstas, Chem. Commun., **2005**, 1581-1583.

17. Z. Guo, G. B. Deacon and P. C. Junk, Dalton Trans., **2023**, 52, 6619-6623.
18. M. L. Cole, G. B. Deacon, C. M. Forsyth, P. C. Junk, K. Konstas, J. Wang, H. Bittig and D. Werner, Chem. Eur. J., **2013**, 19, 1410-1420.
19. M. L. Cole, G. B. Deacon, C. M. Forsyth, P. C. Junk, K. Konstas and J. Wang, Chem. Eur. J., **2007**, 13, 8092-8110.
20. M. L. Cole, G. B. Deacon, P. C. Junk and K. Konstas, Chem. Commun., **2005**, 1581-1583.
21. Z. Guo, V. L. Blair, G. B. Deacon, and P. C. Junk, Dalton Trans., **2020**, 49, 13588-13600.
22. P. Dröse, C. G. Hrib, L. Hilpert, and F. T. Edelmann, Z. Anorg. Allg. Chem., **2011**, 637, 31-33.
23. Y. Cheng, P. B. Hitchcock, A. V. Khvostov and M. F. Lappert, Inorganica Chim. Acta, **2009**, 362, 4678-4684.
24. O. A. Mironova, T. S. Sukhikh, S. N. Konchenko and N. A. Pushkarevsky, Polyhedron, **2019**, 159, 337-344.
25. M. J. Sgro and W. E. Piers, Inorg. Chim. Acta, **2014**, 422, 243-250.
26. F. Ortu, J. M. Fowler, M. Burton, A. Formanuik and D. P. Mills, New J. Chem., **2015**, 39, 7633-7639.
27. D. P. Mills, A. J. Wooles, J. McMaster, W. Lewis, A. J. Blake and S. T. Liddle, Organometallics, **2009**, 28, 6771-6776.
28. X.-g. Zhou, Z.-e. Huang, R.-f. Cai, L.-b. Zhang and L.-x. Zhang, Organometallics, **1999**, 18, 4128-4133.
29. K. R. D. Johnson, A. P. Côté and P. G. Hayes, J. Organomet. Chem., **2010**, 695, 2747-2755.
30. Z. Xie, Z. Liu, F. Xue, Z. Zhang and T. C. W. Mak, J. Organomet. Chem., **1997**, 542, 285-289.
31. G. V. Khoroshen´kov, A. A. Fagin, M. N. Bochkarev, S. Dechert and H. Schumann, Russ. Chem. Bull., Int.Ed., **2003**, 52, 1627-1631.
32. Z. Guo, J. Luu, V. Blair, G. B. Deacon and P. C. Junk, Eur. J. Inorg. Chem., **2019**, 1018-1029.
33. J. E. Cosgrlff, G. B. Deacon, B. M. Gatehouse, H. Hemling and H. Schumann, Angew. Chem. Inf. Ed. EngI., **1993**, 32, 874-875.
34. Z. Guo, M. A. Halim, V. L. Blair, G. B. Deacon and P. C. Junk, Chem Asian J., **2023**, 18, e202300333.

35. M. A. Halim, Z. Guo, V. L. Blair, G. B. Deacon and P. C. Junk, Eur. J. Inorg. Chem., **2024**, e202400672.
36. G. B. Deacon, P. C. Junk and A. Urbatsch, Aust. J. Chem., **2012**, 65, 802-810.
37. G. B. Deacon, P. C. Junk and A. Urbatsch, Eur. J. Inorg. Chem., **2011**, 3592-3600.
38. J. E. Cosgriff, G. B. Deacon, G. D. Fallon, B. M. Gatehousea, H. Schumann and R. Weimann, Chem. Ber., **1996**,129, 953-958.
39. J. E. Cosgriff, G. B. Deacon and B. M. Gatehouse, Aust. J. Chem., **1993**, 46, 1881-1896.
40. Z. Guo, V. L. Blair, G. B. Deacon and P. C. Junk, Chem. Eur. J., **2022**, 28, e202103865.
41. S. H. Ali, G. B. Deacon, P. C. Junk, S. Hamidi, M. Wiecko and J. Wang, Chem. Eur. J., **2018**, 24, 230-242.
42. D. Pfeiffer, B. J. Ximba, L. M. Liable-Sands, A. L. Rheingold, M. J. Heeg, D. M. Coleman, H. B. Schlegel, T. F. Kuech and C. H. Winter, Inorg. Chem., **1999**, 38, 4539-4548.
43. S. Beaini, G. B. Deacon, M. Hilder, P. C. Junk and D. R. Turner, Eur. J. Inorg. Chem., **2006**, 3434-3441.
44. R. D. Shannon, Acta Crystallogr. Sect. A, **1976**, 32, 751-767.
45. T. M. McPhillips, S. E. McPhillips, H. J. Chiu, A. E. Cohen, A. M. Deacon, P. J. Ellis, E. Garman, A. Gonzalez, N. K. Sauter, R. P. Phizackerley, S. M. Soltis and J. P. Kuhn, J. Synchrotron Radiat., **2002**, 9, 401-406.
46. W. Kabsch, J. Appl. Crystallogr., **1993**, 26, 795.
47. G. M. Sheldrick, Acta Crystallogr. Sect. A., **2008**, 64, 112-122.
48. O. V. Dolomanov, L. J. Bourhis, R. J. Gildea, J. A. K. Howard and H. Puschmann, J. Appl. Crystallogr., **2009**, 42, 339-341.
49. G. M. Sheldrick, Acta Cryst., **2015**, C71, 3-8.
50. L. J. Barbour, J. Supramol. Chem., **2001**, 1, 189-191.

Chapter 6

Conclusions

This thesis mainly investigated the reactivity of lanthanoid pseudo-Grignard reagents (RLnX, R = Ph mainly, H_2N-Ph; X = I mainly, Br) with different N and O donor ligands. Furthermore, alternative synthesis method as, direct reaction between lanthanoid metal, I_2 and the corresponding ligands are also investigated.

Pseudo-Grignard reagents PhLnBr significantly alter the outcomes compared to the previous reactions involving PhLnI.[1, 2] Notably, the success observed with the samarium is particularly significant. The reaction of Ln^0 metals with PhBr, followed by the addition of DippFormH, facilitates the synthesis of the divalent dimeric pseudo-Grignard complexes, $[Ln(DippForm)Br(thf)_3]_2 \cdot 6thf$ (Ln = Sm, Eu) in moderate crystalline yields. The geometry of the seven coordinate compounds ($[Ln(DippForm)Br(thf)_3]_2 \cdot 6thf$) can be described as the distorted pentagonal bipyramidal. In contrast reaction, the pro-ligand Ph_2pzH, isolated the nine coordinate trivalent $[Sm(Ph_2pz)_3(thf)_3].3thf$, and $[Sm(Ph_2pz)_3(dme)_2] \cdot dme$ complexes, as well as the divalent compound $[Eu(Ph_2pz)_2(thf)_4]$ owing to the protonation of Schlenk redistribution products following oxidation in the case of Sm. However, the reaction of Yb with PhBr and Ph_2pzH did not yielded any crystals.

In the second phase for the reactivity of samarium (Sm) pseudo-Grignard reagent (PhSmI), where $Ln^{(III)}$ is more prevalent, yielded the trivalent Grignard products ($[Sm(L)I_2(thf)_3]$) (L = DippForm, Ph_2pz). The geometric structure of these seven-coordinate monomeric compound ($[Sm(L)I_2(thf)_3]$) is capped octahedral, where the metal centre is coordinated with one chelating DippForm or Ph_2pz ligand, three thf ligands and two *trans* iodide ligands. For further study, isolated some reported compounds; $[Eu(DippForm)I(thf)_4] \cdot thf$, $[Yb(DippForm)I(thf)_3] \cdot thf$ and $[Yb(Ph_2pz)I(thf)_4]$, derived from the reaction of $H_2NPhLnI(thf)_n$ (Ln = Eu, Yb) with pro-ligands (DippFormH and Ph_2pzH). One notable advantage of using H_2NPhI as oxidant, compared to the PhI, is the ability to conduct reactions at room temperature, making the process easier to manage.

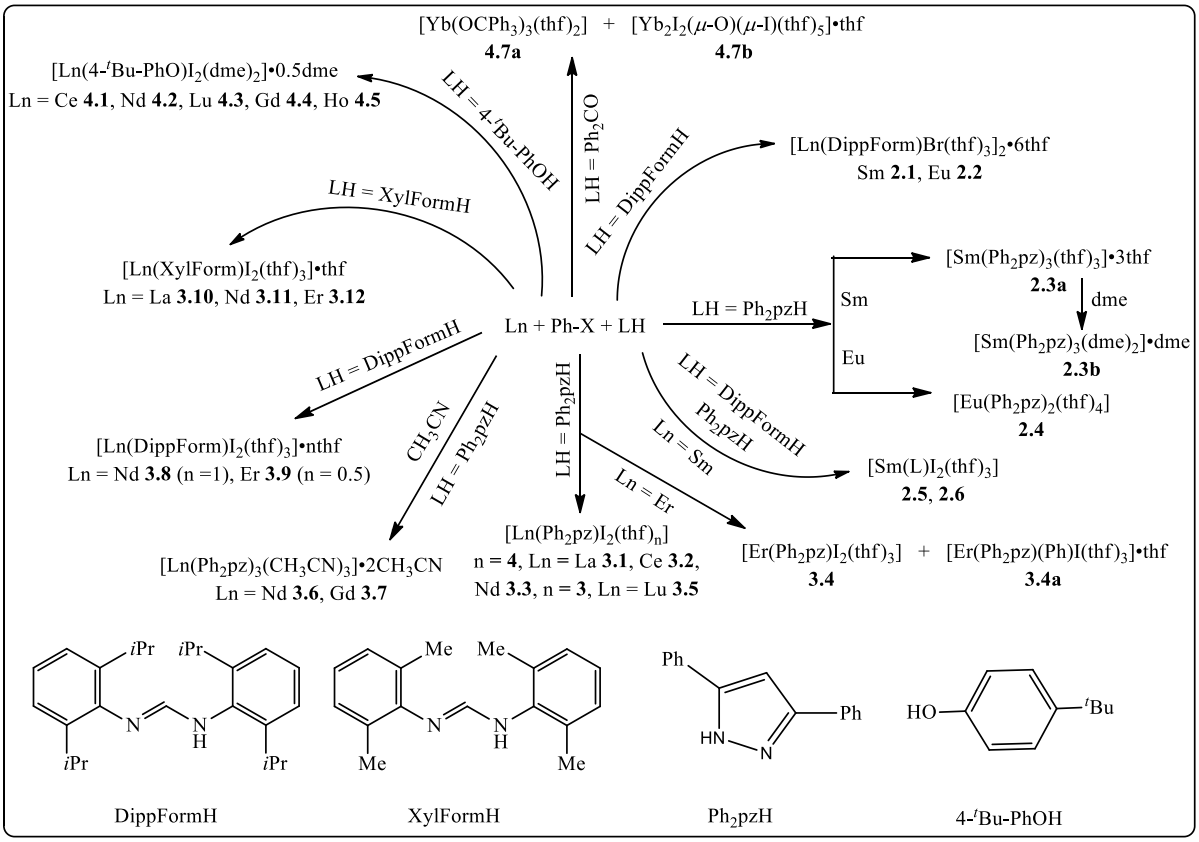
The trivalent lanthanoid pseudo-Grignard reagent (Ph_nLnI_{3-n} (n = 1 or 2)) effectively traps N-donor ligands such as Ph_2pzH, DippFormH, and XylFormH. The reaction of Ln^0 metals with PhI, followed by the addition of Ph_2pzH, allows for the synthesis of the trivalent monomeric pseudo-Grignard complexes, $[Ln(Ph_2pz)I_2(thf)_4]$ (Ln = La, Ce and Nd) and $[Ln(Ph_2pz)I_2(thf)_3]$ (Ln = Er and Lu). The geometry of the eight coordinate $[Ln(Ph_2pz)I_2(thf)_4]$ compounds is best described as anti-prism. Notably, for the reaction of Er, PhI and Ph_2pzH successfully isolated

the second product [Er(Ph_2pz)(Ph)I$(thf)_3$].thf alongside with the expected compound [Er(Ph_2pz)$I_2(thf)_3$]·thf. Both, Er compounds are seven coordinates, geometry is pentagonal bipyramid. By replacing the thf with acetonitrile, we obtained the nine coordinate Schlenk redistribution products, [Ln($Ph_2pz)_3(CH_3CN)_3$]·$2CH_3CN$ (Ln = Nd and Gd) instead of the targeted seven coordinate [Ln(Ph_2pz)$I_2(CH_3CN)_3$] complexes. As a further study the reaction pathway of Ph_nLnI_{3-n} (n = 1 or 2) with formamidine pro-ligands (DippFormH and XylFormH), and successfully isolated the seven coordinated Ln^{III} pseudo-Grignard compounds [Ln(DippForm)$I_2(thf)_3$]·nthf (Ln = Nd, n= 1; Er, n = 0.5) and [Ln(XylForm)$I_2(thf)_3$]·thf (Ln = La, Nd, Er). These findings align with those obtained from direct reactions involving iodine.[3, 4]

The trivalent lanthanoid pseudo-Grignard reagent (Ph_nLnI_{3-n} (n = 1 or 2)) also effectively works with 4-^{t}Bu Phenol, allows for the synthesis of the seven coordinate trivalent monomeric (monoclinic space group *C*2/c) pseudo-Grignard complexes, [Ln(4-^{t}Bu-PhO)$I_2(dme)_2$]·0.5dme (Ln = Ce, Nd and Lu), these findings are similar as we obtained from N-donor (formamidine and pyrazole) pro-ligands. Heat may alter the outcomes for lanthanum reaction, where the dimeric complex [(La(4-^{t}BuPhO)I$(dme)_2)_2(OCH_3)$I]·2dme were yielded. The reactivity of PhYbI with benzophenone (Ph_2CO) and yielded the Schlenk redistribution complexes [Yb$(OCPh_3)_3(thf)_2$] and [Yb_2I_2(μ-O)(μ-I)$(thf)_5$]·thf. Furthermore, the reactivity of the ytterbium Grignard complex, [Yb(Ph_2pz)I$(thf)_4$] with O-donor KO^{t}Bu and N-donor K(Me)PhNMe_2 ligands yielded, the Schlenk equilibria product [Yb$(Ph_2pz)_2(thf)_4$], instead of the anticipated products.

Alternative synthesis method; the direct reaction between lanthanoid metal, I_2 and pro-ligands (^{t}Bu_2pzH, PhMepzH) isolated lanthanoid pseudo-Grignard complexes. A 1:1 molar ratio of ligand to I_2 produced the eight coordinate mostly, seven coordinate for Tb only diiodo complexes [Ln(L)$I_2(thf)_n$] (Ln = La, Ce, Nd, Er, Tb and Lu; L = ^{t}Bu_2pz or PhMepz; n = 3 or 4), while a 4:1 molar ratio (^{t}Bu_2pzH:I_2) resulted the seven coordinated monoiodo complexes [Ln(^{t}$Bu_2pz)_2$I$(thf)_2$] (Ln = Er and Lu). These findings suggest that the reported direct reaction method [3, 4] is well suited for a broad range of N-donor pyrazoles. The crystal system of the eight coordinate compounds [Ln(L)$I_2(thf)_4$] (La, Ce, Nd) is orthorhombic, and their geometry is described as octahedral, where the seven coordinate compounds [Ln(^{t}$Bu_2pz)_2$I$(thf)_2$] (E, Lu) is pentagonal bipyramid. The geometry of the triclinic seven coordinate compound [Tb(PhMepz)$I_2(thf)_3$]·thf is best described as capped trigonal prism.

Overall, this thesis represents a significant contribution in the field of lanthanoid pseudo-Grignard chemistry. Chapters two and three describe the successful isolation of both the divalent and the trivalent complexes using formamidine and pyrazole pro-ligands. In chapter four, we investigate the reactivity of the trivalent pseudo-Grignard reagents with O-donor ligands, specially 4-^{t}Bu-Phenol. Finally, in the concluding chapter, we explore the extension of the iodine based direct reactions with pyrazoles.



Scheme 6.1: A summary of the major findings from the current work.

References

[1]. M. Wiecko, G. B. Deacon and P. C. Junk, Chem. Commun., **2010**, 46, 5076-5078.

[2]. S. H. Ali, G. B. Deacon, P. C. Junk, S. Hamidi, M. Wiecko and J. Wang, Chem. Eur. J., **2018**, 24, 230-242.

[3]. Z. Guo, V. L. Blair, G. B. Deacon and P. C. Junk, Chem. Commun., **2021**, 57, 11513-11516.

[4]. Z. Guo, M. A. Halim, V. L. Blair, G. B. Deacon and P. C. Junk, Chem. Asian J., **2023**, 18, e202300333.

Appendix 1

General Aspects

The lanthanoid compounds described here are highly air and moisture sensitive; therefore, hence were prepared and handled using vacuum-nitrogen line techniques and a glovebox under an atmosphere of purified nitrogen. Lanthanoid metals were collected from Santoku/Molycorp/Eutectix. Large chunks were filed in the drybox prior to use. Ligand compounds (formamidines; [1] DippFormH, EtFormH and pyrazoles; [2] Ph_2pzH, $^tBu_2pzH$) were synthesised according to the literature methods. All other reagents were purchased from Sigma and used without purification. Solvents (THF, DME, CH_3CN C_6D_6, toluene, n-hexane) were pre-dried by distillation over sodium or sodium benzophenone ketyl or calcium hydride before being stored under an atmosphere of nitrogen.

Infrared spectra were recorded as Nujol mulls between NaCl plates using a Perkin-Elmer/Nicolet-Nexus 1600 FTIR instrument, within the range of 4000**-** 650 cm^{-1}. ^1H NMR spectra were recorded with a Bruker 400MHz instrument using dry perdeuterobenzene as the solvent. Melting points were determined in sealed glass capillaries under nitrogen. Metal analyses were carried out by complexometric titration (Xylenol orange as indicator and hexamethylenetetramine as a buffer) after digestion with dilute hydrochloric acid.[3] Elemental analyses (C, H, N) were formed at the Microanalytical Laboratory, Science Centre, London Metropolitan University, England and Macquarie University, NSW, Australia. The samples were sent in sealed glass pipettes under nitrogen. Crystals were immersed in crystallography oil and were examined using the MX1 beamline at the Australian Synchrotron or the Rigaku SynergyS diffractometer.

References

1. R. M. Roberts, J. Org. Chem., **1949**, 14, 277-284.
2. J. Elguero, E. Gonzalez, R. Jacquier, Bull. Soc. Chim. Fr., **1968**, 707-713.
3. G. Dchwarzenbach, H. A. Flaschka, Complexometric Titrations, Methuen, Publishing Ltd, London, **1969**.

Appendix 2

List of publications

Serial	Title	Journal
01	Lanthanoid pseudo-Grignard reagents: A review.	Journal of Organometallic Chemistry
02	Bromobenzene Transforms Lanthanoid Pseudo-Grignard Chemistry	Chemistry–A European Journal
03	"Syntheses of Pyrazolato- and Formamidinato-lanthanoid(III) diiodides from *in situ* generated lanthanoid(III) pseudo-Grignard reagents"	European Journal of Inorganic Chemistry
04	Direct Reaction – One Step Route to Synthesize Lanthanoid-iodide Formamidinates	Chemistry–An Asian Journal

Journal of Organometallic Chemistry 1010 (2024) 123094



Contents lists available at ScienceDirect

Journal of Organometallic Chemistry

journal homepage: www.elsevier.com/locate/jorganchem





Lanthanoid pseudo-Grignard reagents: A review☆

Md. Abdul Halim [a], Zhifang Guo [a], Victoria L. Blair [b], Glen B. Deacon [b], Peter C. Junk [a,*]

[a] College of Science & Engineering, James Cook University, Townsville, QLD 4811, Australia
[b] School of Chemistry, Monash University, Clayton, VIC 3800, Australia

ARTICLE INFO

Keywords:
Lanthanoids
Rare earths
Grignard reagents
Synthesis
Structures

ABSTRACT

This review covers the progress of the chemistry of divalent lanthanoid pseudo-Grignard, compounds, with E-Ln-X bonding (E = C, N, O; *X* = I, Br, Cl, F), especially since the 2002 review of Petrov et al. (2002)[1]. Emphasis is on synthetic pathways and the structures of these compounds. Their use in oxidation and metathesis reactions is discussed together with a consideration of interactions with organic substrates. The compounds appear to have considerable untapped potential.

1. Introduction

In a major breakthrough, Dennis Evans first showed that ytterbium metal reacts with alkyl and aryl iodides to form "RYbI" species in a manner reminiscent of the formation of Grignard reagents [2]. This was followed up by similar studies with europium and samarium metal [3]. Magnetic susceptibility measurements by the Evans NMR method showed the products were a mixture of divalent and trivalent complexes. Divalent complexes were most prevalent for Ln = Eu and less so for Ln = Yb and considerably less for Ln = Sm {Eu^{2+} (99 %), Yb^{2+} (85 %) and Sm^{2+} (50 %)} [3]. In the case of ytterbium, the highest proportion of Yb^{II} was achieved with 2,6-dimethyliodobenzene [2]. Given the versatility and prevalence of Grignard reagents, it might have been expected that this discovery would have led to a burgeoning chemistry, but in fact, developments have been slow. From the 1980s, Russian workers have sought to examine the scope of their formation, and Japanese workers have developed some organic chemistry, and, from the 1990s, limited structures utilising bulky ligand stabilisation emerged. The reason for the lack of interest is not easily understood, but perhaps cost and accessibility of lanthanoid metals may be a factor. However, groups studying lanthanoid metal reactions have been able to overcome this problem. Bochkarev's book on lanthanoid organometallics [4] provided an initial detailed account of this area, and Petrov's 2002 review in this journal provided a further and later account [1]. It is therefore timely to examine the field with an emphasis on recent developments.

We use the term pseudo-Grignard to embrace *divalent* lanthanoid compounds of the form L-Ln-X(solv)$_n$ where L is a monoanionic ligand bound to Ln by C, N, or O; Ln = Sm, Eu, Yb; *X* = F, Cl, Br, I; solv = donor solvent. We have limited the review to the classic divalent lanthanoid elements Sm, Eu, and Yb, as products of reactions of other Ln metals with organic halides are predominantly trivalent species. Trivalent species of the type $LLnX_2$ would open an enormous Pandora's box. Compounds of this type are mentioned solely when they are products of oxidation of LLnX species.

2. Synthesis and characterization—compounds with C-Ln-X (*X* = I, Br, Cl, F) bonding

Lanthanoid pseudo-Grignard reagents are mainly prepared by the direct reaction [1,4].

$$Ln + RX \xrightarrow{solv} RLnX(solv)_n \quad (1)$$

solv = tetrahydrofuran (thf), 1,2-methoxyethane (dme), diethyl ether etc.

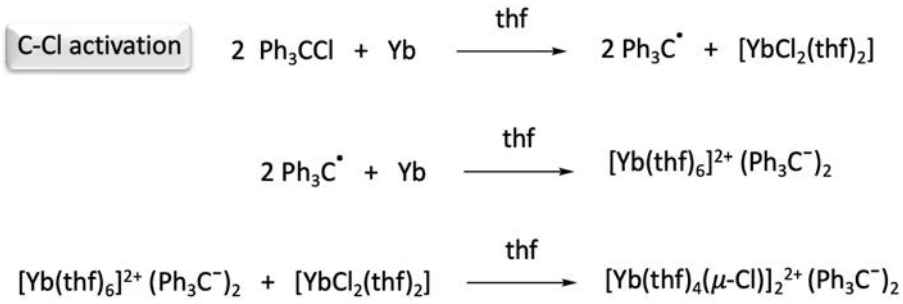
R = alkyl, aryl, heteroaryl.

In terms of prevalence, *I* > Br >> Cl >> F, an order which reflects the increasing C-X bond strength, *I* < Br < Cl<F. In addition, alkyl iodides often have a slight iodine impurity, which can activate Ln metals [5]. In the main Ln = Sm, Eu, Yb, the traditional Ln^{II} forming elements, but analogous reactions of Ce have been reported in some cases [6], though the oxidation state is uncertain. The prices of the three Ln elements (e.g. from Strem in USD), Sm (280/25 g) Eu (818/5 g) Yb (570/25 g) *cf.* Mg

☆ This paper is dedicated to Professor Evamarie Hey-Hawkins, a great friend and colleague on the occasion of her retirement from University of Leipzig. Eva has had an illustrious career and continues to produce outstanding contributions to chemistry.

* Corresponding author.
E-mail address: peter.junk@jcu.edu.au (P.C. Junk).

https://doi.org/10.1016/j.jorganchem.2024.123094
Received 4 February 2024; Received in revised form 12 March 2024; Accepted 12 March 2024
Available online 13 March 2024
0022-328X/© 2024 The Author(s). Published by Elsevier B.V. This is an open access article under the CC BY license (http://creativecommons.org/licenses/by/4.0/).



Scheme 1. Formation of an ionic pseudo-Grignard compound from Ph_3CCl and Yb metal.

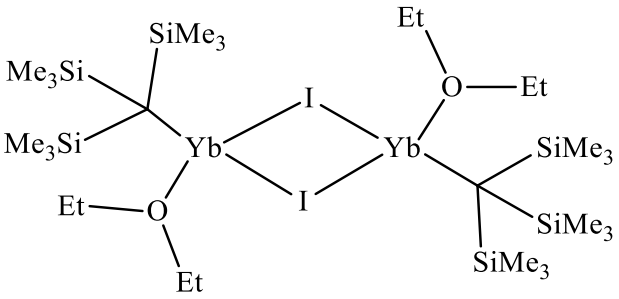


Fig. 2-1. Schematic of the X-ray structure of $[Yb\{C(SiMe_3)_3\}I(Et_2O)]_2$ (**1**) [10].

(<100/100 g) are a deterrent, but bulk Ln metals as a piece (ca. 100 g which can be filed in an inert atmosphere dry-box) are available at cheaper prices from Treibacher Industrie AG, Austria.

The innovative Russian work of the 1980s has been reviewed [1,4], but some features should be mentioned. The carboranyllanthanoid pseudo-Grignard iodides were mainly prepared by metathesis between lithiocarboranes, but Yb and Eu derivatives were also obtained by the direct method (1) from iodocarboranes. The products were identified by reactions with trimethylsilyl chloride and acyl chlorides giving trimethylsilylcarboranes or carboranylketones [7]. Success in the direct reaction was also achieved with $C_8H_{17}X$ for X = Cl, Br, I and with the best performance surprisingly with the bromide [8]. 2-Thienyl and pentafluorophenyl derivatives of Eu, Sm, Yb and Ce were also obtained by the direct method (1) from 2-iodothiophene and C_6F_5Br respectively, and were identified by reaction with triphenyltin chloride giving triphenyl(2-thienyl)tin and pentafluorophenyltriphenyltin respectively [6]. Of further interest, some were also prepared by an acidolysis reaction (Eq. (2)) with again organotin characterization.

$$PhLnI + C_6F_5H \rightarrow C_6F_5LnI + PhH \quad (2)$$

Three studies are of particular importance, as they have led to products characterized by X-ray crystallography. The first involves C—Cl activation of Ph_3CCl and appears to have led to the first structurally identified lanthanoid pseudo-Grignard reagent, albeit an ionic complex, *viz.* $\{[Yb(thf)_4(\mu\text{-}Cl)]_2\}^{2+}(Ph_3C^-)_2$ [9]. A complex reaction path was proposed (Scheme 1).

The reaction only proceeds if a trace of $[YbCl_2(thf)_2]$ is present, in which case $[Yb(thf)_6]^{2+}$ $(Ph_3C^-)_2$ is formed rapidly, but the final pseudo-Grignard reagent formed slowly, and was obtained in good yield from the reaction between Yb metal powders and triphenylmethyl chloride in thf at room temperature for 15 h. $\{[Yb(thf)_4(\mu\text{-}Cl)]_2\}^{2+}$ $(Ph_3C^-)_2$ was isolated as monoclinic crystals $P2_1/n$, where $[Yb_2(thf)_4(\mu\text{-}Cl)_2]^{2+}$ is a centrosymmetric dimer bonded with two symmetric μ-Cl bridges. The anion is symmetrical planar with a triangular array of phenyl groups rotated by 26–34° out of the plane containing the central C atom [9].

A very important series of dimeric pseudo-Grignard compounds

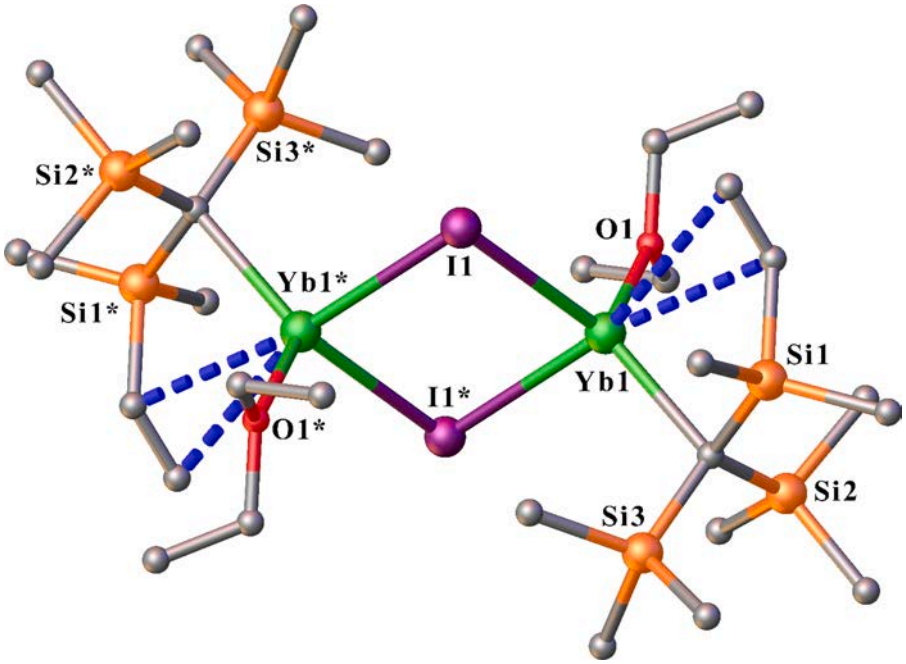


Fig. 2-2. X-ray structure of $[Yb\{C(SiMe_3)_2(SiMe_2(CH{=}CH_2))\}I(Et_2O)]_2$ (**2**), Hydrogen atoms are omitted for clarity [10].

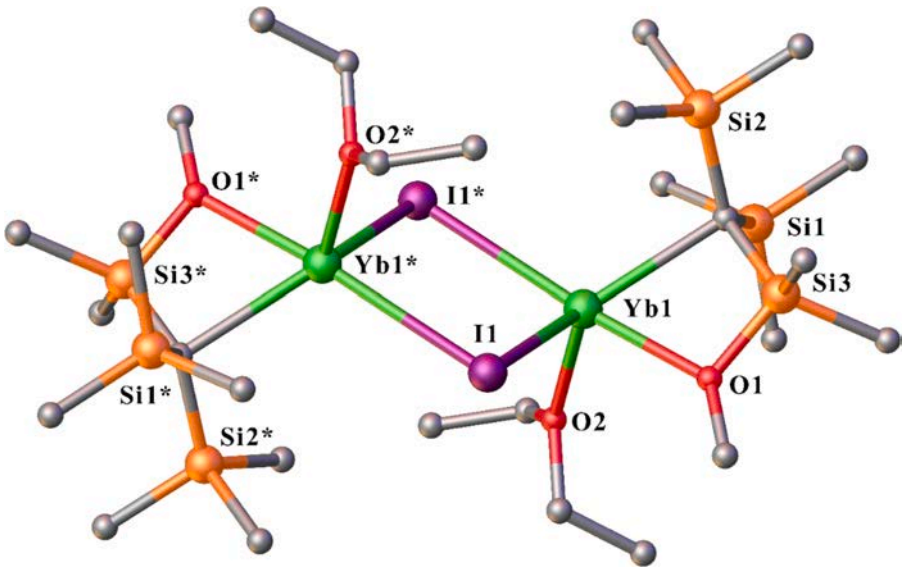


Fig. 2-3. X-ray structure of the of $[Yb\{C(SiMe_3)_2(SiMe_2(OMe))\}I(Et_2O)]_2$ (**3**), Hydrogen atoms are omitted for clarity [10].

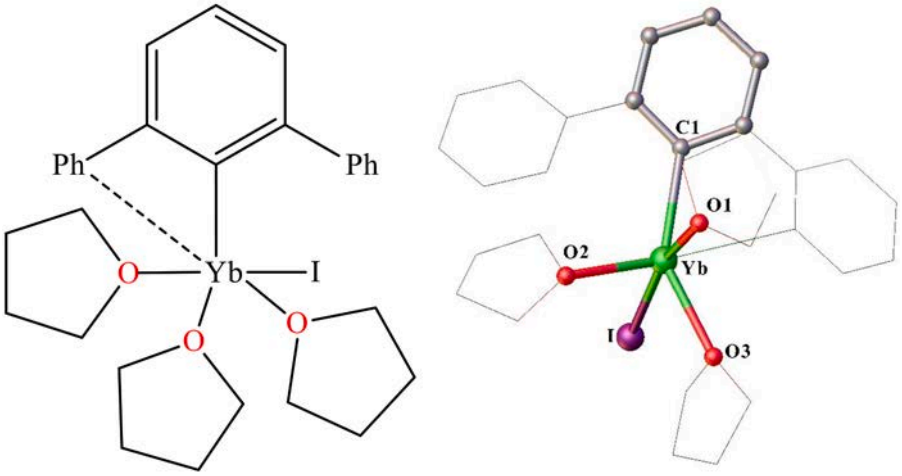
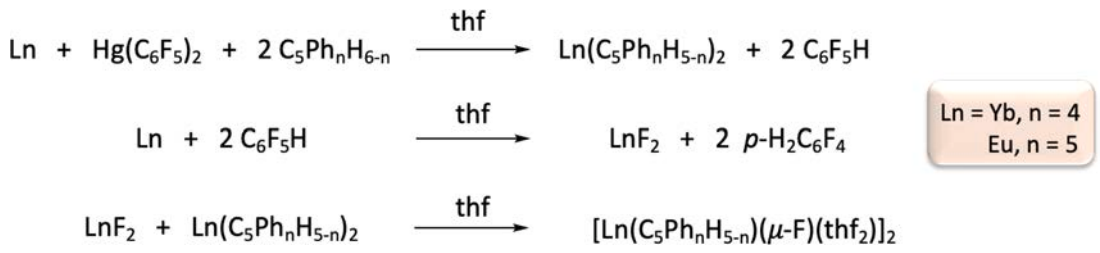


Fig. 2-4. Schematic and the X-ray structure of $[Yb\ (2,6\text{-}Ph_2C_6H_3)I(thf)_3]$ (**5**). Hydrogen atoms are omitted and thf molecules and Ph groups are drawn as wireframe for clarity [12].

namely $[Yb\{C(SiMe_3)_3\}I(Et_2O)]_2$ (**1**), $[Yb\{C(SiMe_3)_2(SiMe_2(CH{=}CH_2))\}I(Et_2O)]_2$ (**2**), $[Yb\{C(SiMe_3)_2(SiMe_2(OMe))\}I(Et_2O)]_2$ (**3**), $[Yb\{C(SiMe_3)_2(SiMe_2(Ph))\}I(Et_2O)]_2$ (**4**) have been prepared from the reaction between Yb metal with the corresponding $\{C(SiMe_3)_2(SiMe_2R)\}I$ (R = Me, CH=CH_2, MeO, Ph) oxidant in Et_2O at 25 °C [10], but (**1**) was initially obtained from the reaction of $[Yb(C(SiMe_3)_3)_2]$ with methyl iodide or methylene diiodide [11]. Compound (**1**) (Fig. 2-1) crystallized in orthorhombic space group *Pbca* [11], whereas both compounds (**2**) (Fig. 2-2) and (**3**) (Fig. 2-3) are described as distorted trigonal bipyramid with space group $P2_1/c$ and $P2_1/n$ respectively, [10]. In **2** and **3,** the structures are stabilised by intramolecular Yb·····(CH_2=CH^-) and Yb·····OMe bonding respectively.

The monomeric compound $[Yb(2,6\text{-}Ph_2C_6H_3)I(thf)_3]$ (**5**) was isolated from the reaction between Yb metal powder and $(2,6\text{-}Ph_2C_6H_3)I$ at room temperature in thf and was the first monomeric lanthanoid pseudo-Grignard reagent to be structurally identified [12]. The distorted tetragonal pyramidal compound $[Yb(2,6\text{-}Ph_2C_6H_3)I(thf)_3]$ (**5**) (Fig. 2-4) crystallized in space group $P2_1/n$. The Yb atom in compound (**5**) is



Scheme 2. Formation of cyclopentadiene based lanthanoid pseudo-Grignard fluorides.

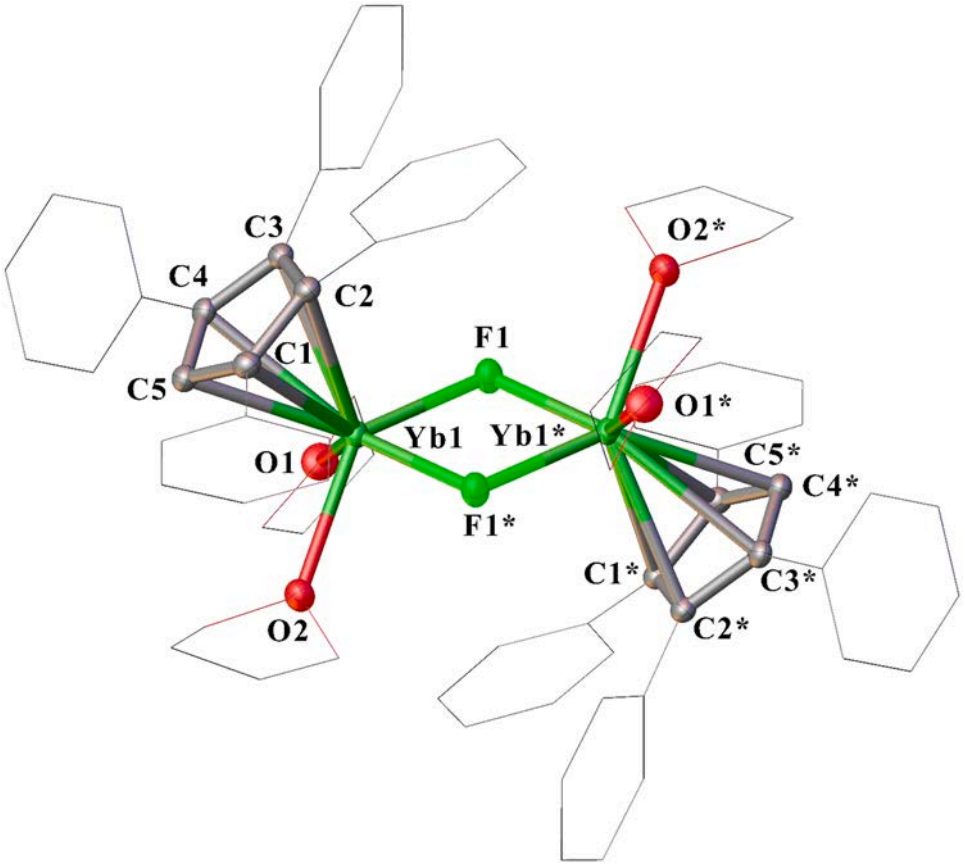


Fig. 2-5. X-ray structure of $[Yb(C_5Ph_4H)(\mu\text{-}F)(thf)_2]_2$(**7**). Hydrogen atoms are omitted, coordinated thf molecules, Ph groups are drawn as wireframe for clarity [13].

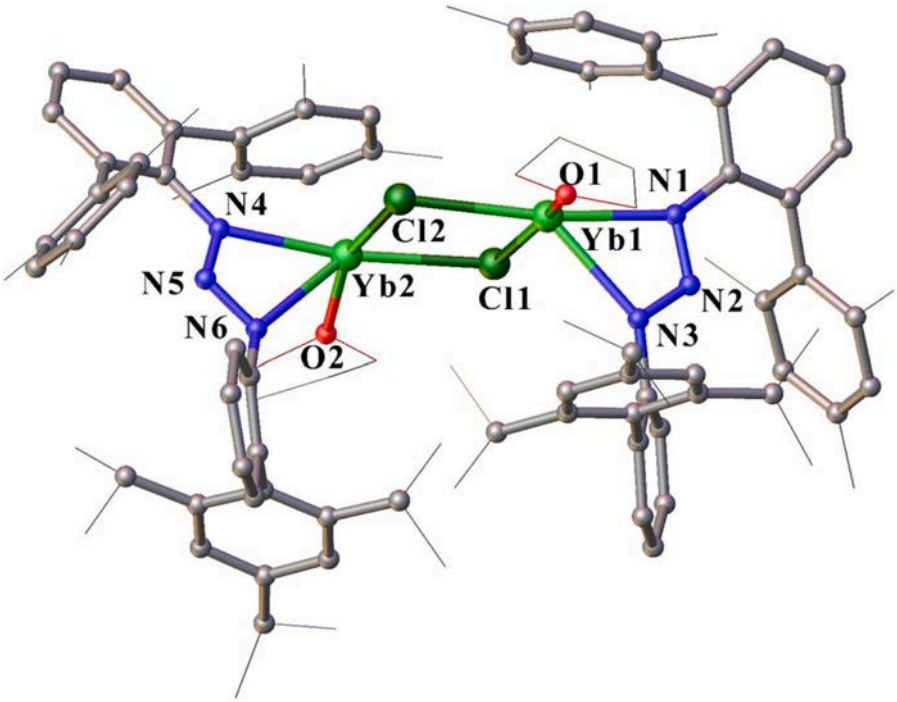


Fig. 2-6. X-ray structure of $[YbDmp(Tph)N_3Cl(thf)]_2$ (**8**) {Dmp = 2,6-$Mes_2C_6H_3$, Tph = 2′,4′,6′-triisopropylbiphenyl-2-yl}. Hydrogen atoms are omitted, coordinated thf molecules, *i*Pr and CH_3 groups are drawn as wireframe for clarity [16].

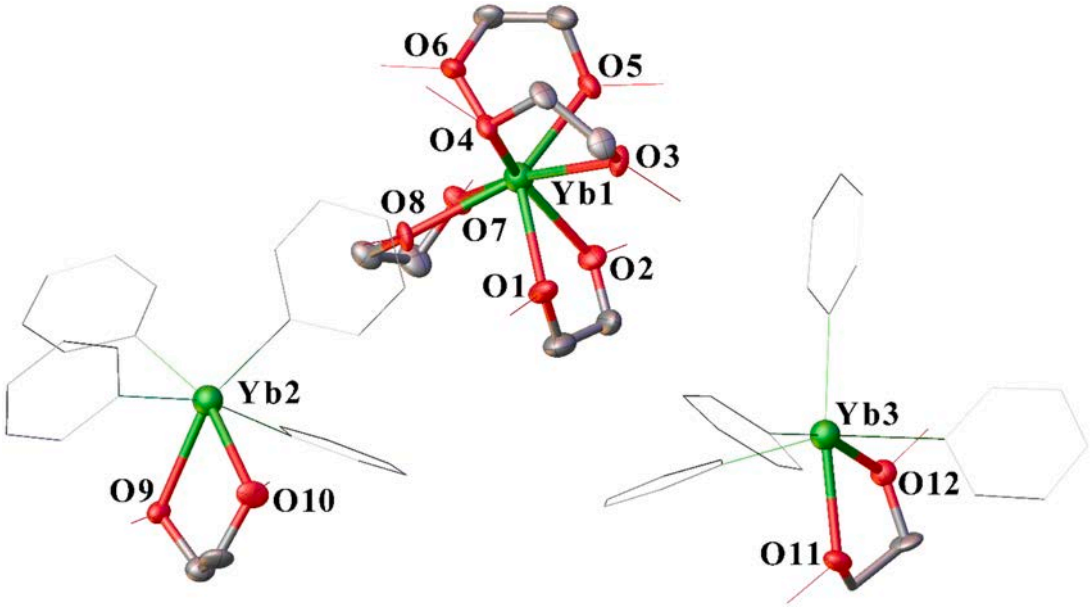
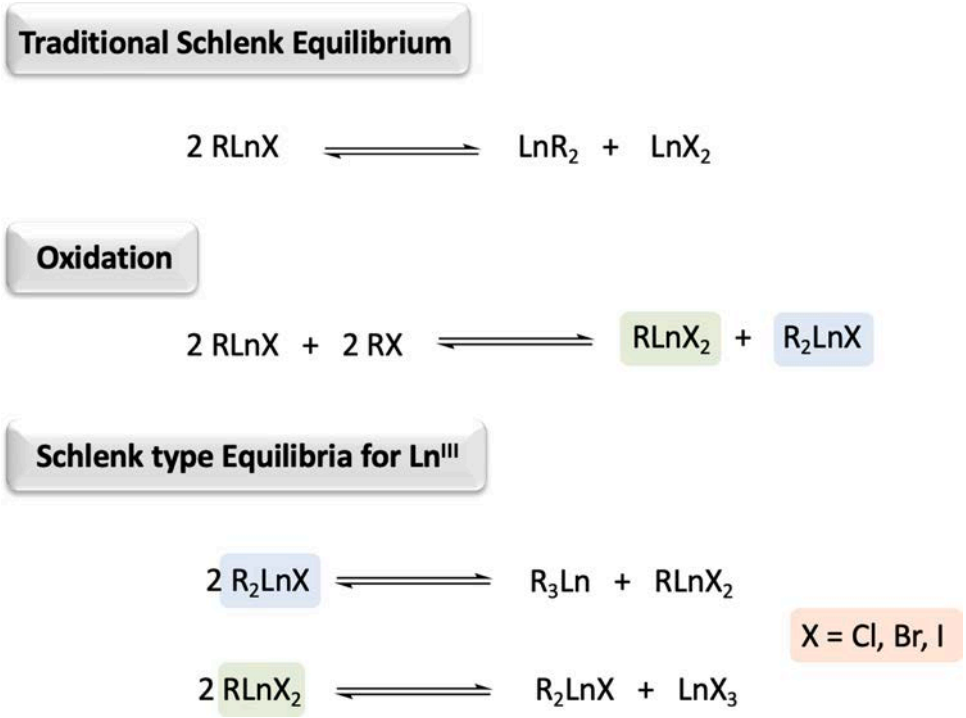


Fig. 2-7. X-ray structure of $[Yb^{II}(dme)_4][Yb^{III}Ph_4(dme)]_2$ (**9**). Hydrogen atoms are omitted, CH_3 and Ph groups are drawn as wireframe for clarity [18].

bound by the *ipso*-carbon of a phenyl group in addition to I, the phenyl C and three oxygens from thf ligands [12]. The ^{171}Yb NMR spectrum of **5** in D_8-thf showed not only a prominent resonance for **5** but also smaller equal intensity resonances attributable to YbI_2 and $[Yb(2,6\text{-}Ph_2C_6H_3)_2]$ formed through a Schlenk equilibrium (see below) [12].

Two lanthanoid pseudo-Grignard fluorides $[Eu(C_5Ph_5)(\mu\text{-}F)(thf)_2]_2$ and $[Yb(C_5Ph_4H)(\mu\text{-}F)(thf)_2]_2$ have been isolated from reaction of Eu or Yb metal with $Hg(C_6F_5)_2$, and pentaphenyl- or tetraphenyl-cyclopentadiene in thf [13,14]. The formation is explained by the path shown in Scheme 2.

In each case the last step has independently been effected between in situ generated $LnF_2(thf)_n$ and the appropriate bis (polyphenylcyclopentadienyl)lanthanoid complex [13,14]. An analogue of the last step has been used to prepare $[Sm(C_5Ph_4H)I(thf)_3]$ [15], and is related to the final step in the synthesis of the triphenylmethyl pseudo-Grignard reagent (Scheme 1) [9]. $[Eu(C_5Ph_5)(\mu\text{-}F)(thf)_2]_2$ (**6**) and $[Yb(C_5Ph_4H)(\mu\text{-}F)(thf)_2]_2$ (**7**) are fluoride bridged dimeric pseudo-Grignard compounds [13,14]]. Compound $[Eu(C_5Ph_5)(\mu\text{-}F)(thf)_2]_2$ (**6**) crystallized in the orthorhombic space group *Pbca*, where half of the dimer is generated by symmetry [13]. Compound $[Yb(C_5Ph_4H)(\mu\text{-}F)(thf)_2]_2$ (**7**) crystallized in the monoclinic space group $P2_1/n$ [14]. Both compounds (**6, 7**) have seven coordination, where the metal center is coordinated by one (η^5-C_5Ph_5 (**6**), C_5Ph_4H (**7**)) ring, two bridging fluorides and two thf molecules (Fig. 2-5) [13,14].



Scheme 3. Extended Schlenk equilibria and oxidation reactions accompanying lanthanoid pseudo-Grignard reagent formation.

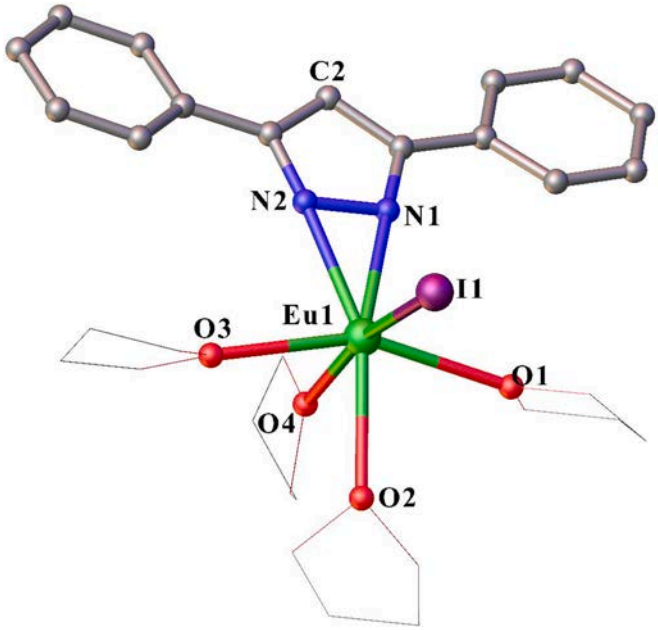


Fig. 3-1. X-ray structure of [Eu(Ph_2pz)I($thf)_4$] (**10**). Hydrogen atoms are omitted and coordinated thf molecules are drawn as wireframe for clarity. The ytterbium analogue is isomorphous [18].

In an innovative approach, Niemeyer used redox transmetallation reactions of bulky triazenidomercuric chlorides to generate a pseudo-Grignard triazenidoytterbium chloride (**8**) (Eq. (3)) [16] (Figs. 2-6 and 2-7).

$$2Yb + 2ArAr'N_3HgCl \rightarrow [Yb(ArAr'N_3)Cl(thf)_2 + 2Hg \quad (3)$$

The dimeric compound **(8)** crystallizes in the triclinic space group $P\bar{1}$ and has tetragonal pyramidal coordination, where the metal atom is bonded by two chelating nitrogens from the triazenide (κ^2-bonded), two bridging chloride ligands and one oxygen atom from THF [16].

In an amplification of this synthesis, redox transmetallation/ protolysis reactions between ytterbium (or calcium), PhHgBr, and tetraphenylcyclopentadiene gave [Yb(C_5Ph_4H)Br($thf)_2]_2$ (or the Ca analogue) (Eq. (4)) [17].

$$2Yb + 2PhHgBr + 2C_5Ph_4H_2 \rightarrow \left[Yb(C_5Ph_4H)Br(thf)_2\right]_2 + 2Hg + 2PhH \quad (4)$$

The unexpected isolation of a few crystals of the pseudo-Grignard reagent [Sm(C_5Ph_5)(μ-Br)($thf)_2]_2$·6thf from a preparation of [Sm($C_5Ph_5)_2$] has been attributed to a similar reaction arising from a PhHgBr impurity in a commercial sample of $HgPh_2$ [15].

The importance of using bulky ligands in isolation of crystalline stable divalent pseudo-Grignard reagents is well illustrated by attempts to crystallize PhYbI from thf and dme. In the former case, the products were [$YbPh_3(thf)_3$] and [$YbI_2(thf)_4$]. In the latter, after crystallization of [$YbI_2(dme)_3$], a low yield of the mixed valence species [$Yb^{II}(dme)_4$][$Yb^{III}Ph_4(dme)]_2$ (**9**) was obtained [18].

These outcomes reflect the intervention of oxidation to Ln^{III}, as mentioned in Evans' initial publications [2,3]. The oxidation leads to further species which can be involved in Schlenk-type equilibria analogous to that involving the initially formed RLnX pseudo-Grignard reagent. These reactions are summarized in Scheme 3.

In addition to the above complexity, there is the possibility of dimerisation of the above species as suggested by the structures of **2, 3**, and **7**.

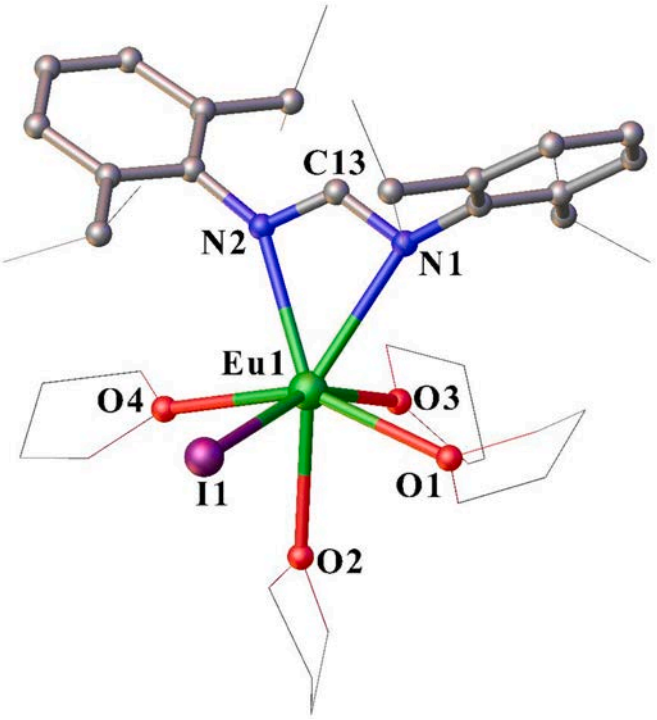


Fig. 3-2. X-ray structure of [Eu(DippForm)I($thf)_4$] (**12**). Hydrogen atoms and lattice thf molecules are omitted, coordinated thf molecules and *i*Pr groups are drawn as wireframe for clarity [20].

3. Synthesis and characterization—compounds with N-Ln-X (*X* = Cl, Br, I, F) bonding

Lanthanoid pseudo-Grignard compounds, C-Ln-X, can be converted into divalent N-Ln bonded pseudo-Grignard reagent derivatives by protolysis reactions. In optimum cases, this is achieved despite the complexity of the Schlenk equilibria featured in Scheme 3. Thus, [Ln(Ph_2pz)I($thf)_4$] (Ph_2pz = 3,5-diphenylpyrazolate, Ln = Eu **10**, (Fig. 3-1) Yb **11**) were obtained in high yield by reaction of PhLnI (Ln = Yb, Eu) with 3,5-diphenylpyrazole in thf at low temperature (Eq. (5)) [18].

$$PhLnI + Ph_2pzH \rightarrow Ln(Ph_2pz)I + PhH \quad (5)$$

The monomeric structures contrast the more common dimeric structures of the C-Ln-X pseudo-Grignard complexes apart from **5.** The *cisoid* N-Ln-I array however resembles the analogous C-Ln-I array of the carbon based compounds.

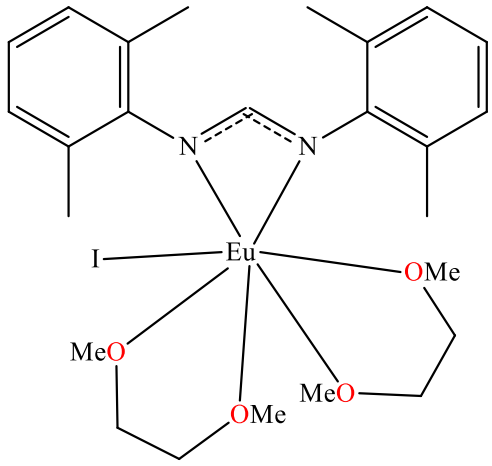


Fig. 3-3. Schematic of the X-ray structure of [Eu(XylForm)I($dme)_2$] (**13**) [20].

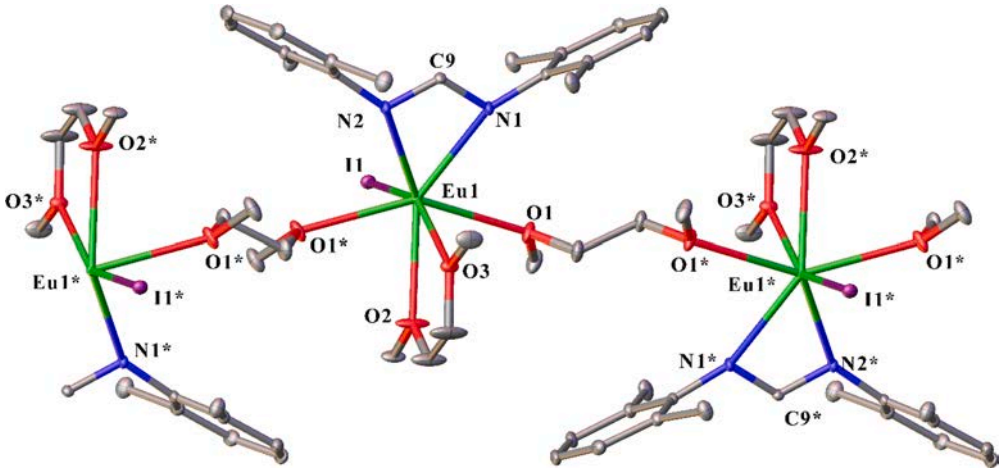


Fig. 3-4. X-ray structure of [Eu(XylForm)I(dme)(μ-dme)]$_n$ (**14**) [20].

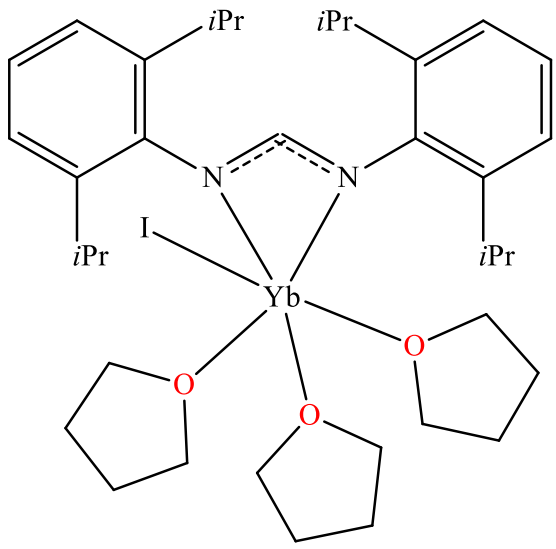


Fig. 3-5. Schematic of the X-ray structure of [Yb(DippForm)I(thf)$_3$] (**15**) [20].

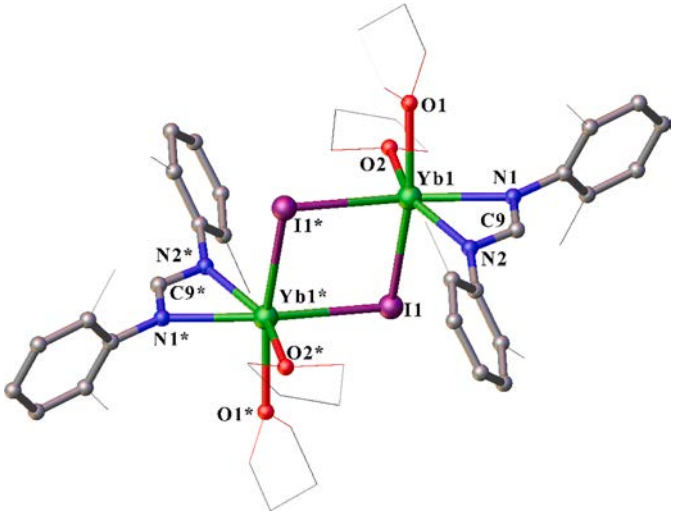


Fig. 3-6. X-ray structure of [{Yb(XylForm)I(thf)$_2$}$_2$] (**16**). Hydrogen atoms are omitted, coordinated thf molecules and CH_3 groups are drawn as wireframe for clarity [20].

When similar reactions were attempted with in situ generated PhLnBr, the outcomes were different. For Ln = Eu, the product was [Eu(Ph$_2$pz)$_2$(thf)$_4$], corresponding to protolysis of EuPh$_2$, a classic Schlenk equilibrium product (see Scheme 3, 1st step, *R* = Ph) (Eq. (6)) [19].

$$EuPh_2 + 2Ph_2pzH \rightarrow Eu(Ph_2pz)_2 + 2PhH \quad (6)$$

No crystalline product was obtained from the corresponding reaction of PhYbBr, whereas from PhSmBr, [Sm(Ph$_2$pz)$_3$(thf)$_3$] was crystallized, and also converted into [Sm(Ph$_2$pz)$_3$(dme)$_2$] by crystallization from dme. The formation of the former is attributed to protolysis of SmPh$_3$, an oxidation and redistribution product (Scheme 3 penultimate step), an outcome reflecting early conclusions about pseudo-Grignard reagent oxidation state behaviour (e.g., see Eq. (7)) [2,3].

$$SmPh_3 + 3Ph_2pzH \rightarrow Sm(Ph_2pz)_3 + 3PhH \quad (7)$$

When reactions of PhLnI (Ln = Eu, Yb) were extended to *N,N′*-diarylformamidines, the out- comes were more complex than the corresponding reactions with 3,5-diphenylpyrazole [20]. Six different divalent pseudo-Grignard compounds: [Eu(DippForm)I(thf)$_4$]·thf (DippForm = *N,N′*-bis(2,6-di-isopropylphenyl)formamidinate) (**12**) (Fig. 3-2), [Eu(XylForm)I(dme)$_2$]·0.5dme (XylForm = *N.N′*-bis(2,6-dimethylphenyl)formamidinate) (**13**) (Fig. 3-3), [Eu(XylForm)I(dme)(μ-dme)]$_n$ (**14**) (Fig. 3-4), [Yb(DippForm)I(thf)$_3$]·thf (**15**) (Fig. 3-5), [{Yb(XylForm)I(thf)$_2$}$_2$] (**16**) (Fig. 3-6) and [{Yb(MesForm)I(thf)$_2$}$_2$] (MesForm = *N,N'*-bis(2,4,6-trimethylphenyl)formamidinate) (**17**) were prepared by a similar procedure [20] and by changing solvent (using dme) for crystallizing (**13**) and (**14**) [20]. Pseudo-octahedral ([Eu(DippForm)I(thf)$_4$]·thf and [Eu(XylForm)I(dme)$_2$]·0.5dme are seven coordinate monomers having a chelating formamidinate ligand which is *cisoid* to the iodine ligand. In polymeric (**14**), two *transoid* oxygen atoms from bridging dme donors replace a chelating dme of (**13**), the compounds crystallizing as a mixture, though the microanalysis suggests (**13**) to be the dominant component [20], with iodine *cisoid* to the formamidinate in both. Not all Eu systems were satisfactory with MesFormH in dme yielding [EuI$_2$(dme)$_2$]$_2$ and XylFormH in thf [Eu(XylForm)I(thf)$_2$(OH)]$_2$ [20]. The ytterbium complexes are a six coordinate monomer (DippForm) (**15**) or iodide bridged dimers with the smaller XylForm (**16**) or MesForm (**17**). The steric bulk of iodide is less than that of thf [21]. However these reactions are far from simple with the DippFormH reaction also yielding the oxidation product [Yb(DippForm)I$_2$(thf)$_3$]·2thf, and with the XylFormH reaction giving the monomeric trivalent [Yb(XylForm)$_2$I(dme)]·dme after isolation of the Yb^{II} product (**16**), addition of dme, and further crystallization [20]. With the bulkier formamidines there is a reduction in coordination number from Eu to Yb in contrast to Ph$_2$pz. For the reaction of in situ generated PhYbI with DippFormH and with XylFormH, the reaction mixtures were

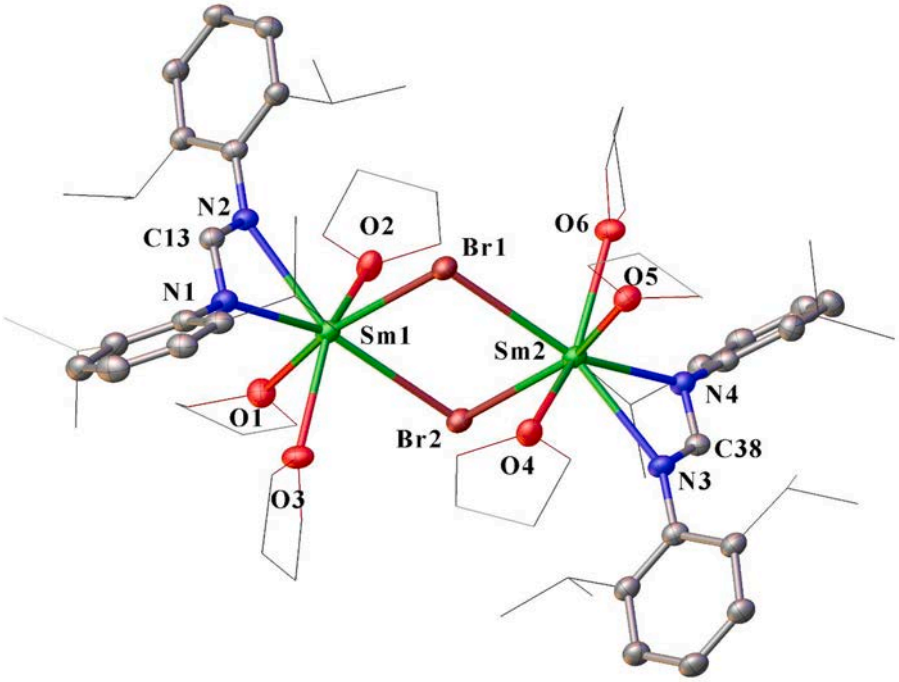


Fig. 3-7. X-ray structure of [Sm(DippForm)Br(thf)$_3$]$_2$·6thf (**18**). Hydrogen atoms and lattice thf molecules are omitted, coordinated thf molecules and *i*Pr groups are drawn as wireframe for clarity [19].

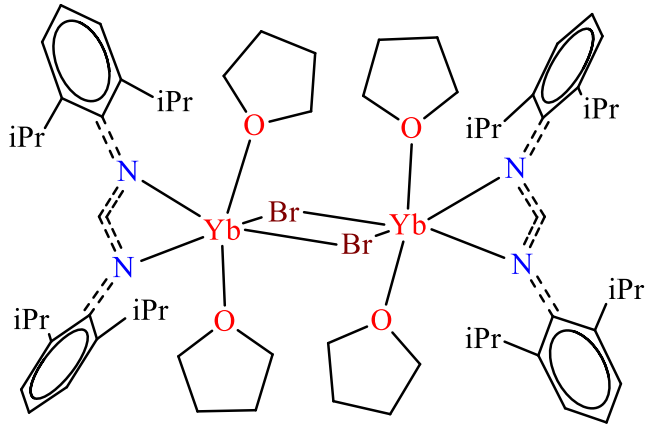


Fig. 3-8. Schematic of the X-ray structure of [Yb(DippForm)Br(thf)$_2$]$_2$·2thf (**20**) [19].

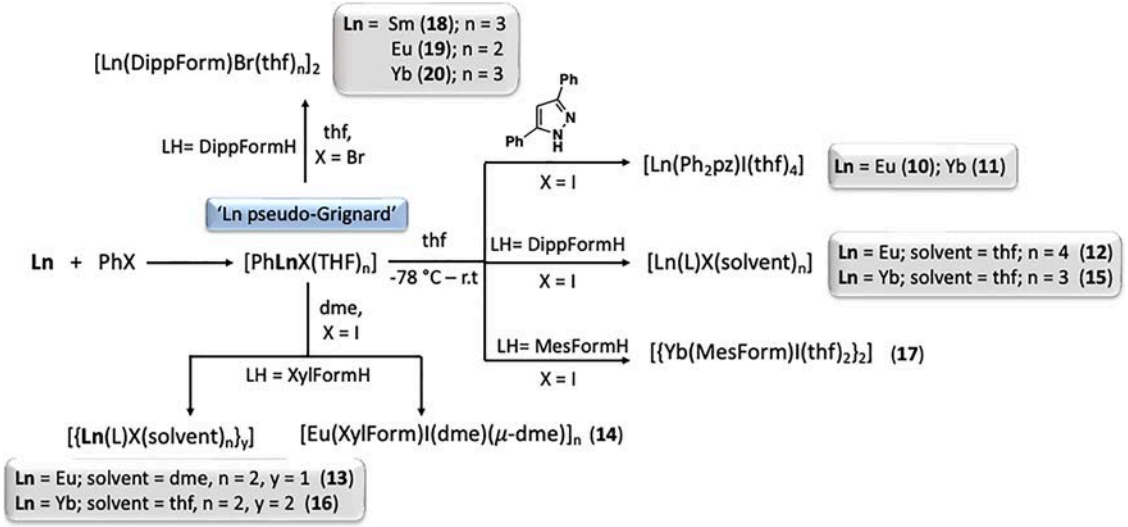
investigated by ^{171}Yb NMR spectroscopy. In the former case, both [Yb(DippForm)I(thf)$_3$I(thf)$_3$] (**15**) and YbI$_2$ were detected but not [Yb(DippForm)$_2$], the other component of the Schlenk equilibrium. Perhaps this had been oxidized to an NMR silent Yb^{III} (see e.g. Scheme 3, step 2). On the other hand, the XylFormH reaction mixture showed all three Schlenk equilibrium components, **16,** YbI$_2$, and [Yb(XylForm)$_2$] [20].

In view of Schlenk equilibria and oxidation state complexity in the reactions of PhLnBr with Ph$_2$pzH, and the formation of both divalent and trivalent formamidinatolanthanoid iodides in reactions of PhLnI with formamidines, the expectation would be that reactions of PhLnBr with formamidines would lead to both Ln^{II} and Ln^{III} products. To the contrary, three similar type lanthanoid(II) pseudo-Grignard compounds namely [Ln(DippForm)Br(thf)$_3$]$_2$·6thf (Ln = Sm **18** (Fig. 3-7) and Eu **19**) and [Yb(DippForm)Br(thf)$_2$]$_2$·2thf (**20**) (Fig. 3-8) were crystallized in 45–65 % yield from the reaction between the corresponding Grignard reagent (PhLnBr) and DippFormH [19]. The isolation of the Sm^{II} derivative is particularly noteworthy given the relative instability of this oxidation state and earlier data on the Sm^{II}:Sm^{III} ratio in solutions of "PhSmI" [2,3]. Compounds (**18** and **19**) have seven coordinate metal centers, and both are bromine-bridged dimers with one chelating DippForm ligand *cis* to Br1 and *trans* to Br2. Compound ([Yb(DippForm)Br(thf)$_2$]$_2$·2thf **20**) is a six coordinate centrosymmetric dimer where half is generated from the Yb(1)···Yb(1)* vector. Compounds (**18** and **19**) crystallize in the monoclinic $P2_1/c$ space group with distorted pentagonal bipyramidal stereochemistry and (**20**) in the triclinic *P*-1 space group (octahedral geometry). The lanthanoid contraction is very clear from the <Ln-N> values; Sm-N (2.64) ~ Eu-N (2.63)> Yb-N (2.46) [19]. A summary of reactions of PhLnX species with Ph$_2$pzH and with formamidines is given in Scheme 4.

A N—Yb—Cl pseudo-Grignard reagent (**8**) with a triazenide ligand has been prepared by redox transmetallation from the corresponding triazenidomercuric chloride (sections 2), and [Ln(Ap)I(thf)$_2$]$_2$ (Ln = Sm **21**, Yb **22**) were isolated from the reaction between KAp, and appropriate [LnI$_2$(thf)$_2$] ({ApH = (2,6-diisopropylphenyl)-[6-(2,4,6-triisopropylphenyl)pyridin-2-yl]amine}) compounds in THF and crystallised from toluene or hexane. [Sm(Ap)I(thf)$_2$]$_2$ (**21**) (Fig. 3-9) crystallizes in monoclinic space group $P2_1/c$ and [Yb(Ap)I(thf)$_2$]$_2$ (**22**) in triclinic space group $P\bar{1}$ [22]. Two isostructural divalent Eu compounds ([Eu(dpp-Bian)(μ-Cl)(dme)]$_2$ (**23**) and [Eu(dpp-Bian)(μ-Br)(dme)]$_2$ (**24**) (dpp-Bian = 1,2-bis[(2,6-diisopropylphenyl)imino]acenaphthene) were synthesized from the oxidation reaction between [Eu(dpp-Bian)(dme)$_2$] and [Sn(Ph)$_3$Cl] or [$C_2H_2Br_2(Ph)_2$]. The centrosymmetric distorted octahedral dimeric compounds ([Eu(dpp-Bian)(μ-X)(dme)]$_2$ (**23** and **24**) have triclinic crystal structures with space group $P\bar{1}$. The bite angle (N(1)-Eu(1)-N(2)) of these compounds is 66.60° and 66.92° respectively [23]. Divalent N-Ln-X pseudo-Grignard compounds are listed in Table 3.1.

4. Synthesis and characterization—compounds with O-Ln-X bonding

The divalent samarium pseudo-Grignard compound [Sm(ArO)(μ-I)(thf)$_3$]$_2$ (**25**) was synthesised in 91 % yield from the reaction of [Sm(OAr)$_2$(thf)$_3$] (Ar = $C_6H_2Bu^t_2$-2,6-Me-4) and SmI$_2$ (mole ratio 1:1) in



Scheme 4. Lanthanoid pseudo-Grignard compounds from the reactions of PhLnX species with Ph_2pzH and with formamidines.

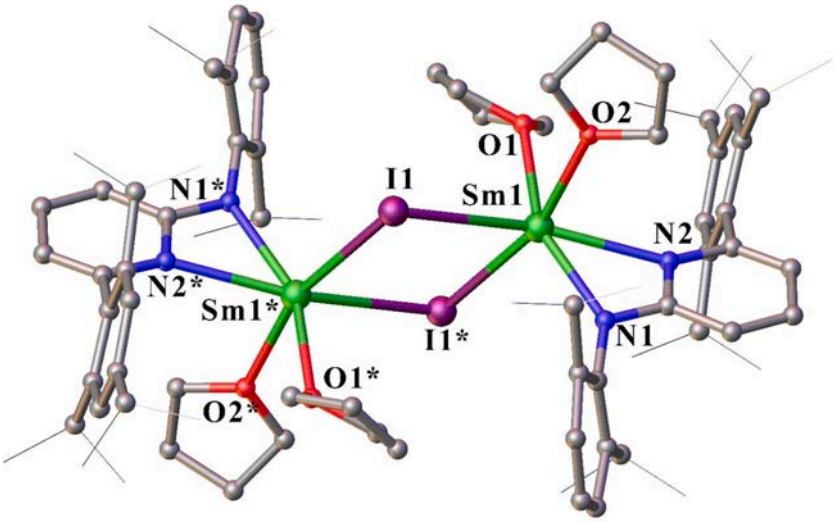


Fig. 3-9. X-ray structure of $[Sm(Ap)I(thf)_2]_2$(**21**). Hydrogen atoms are omitted and *i*Pr groups are drawn as wireframe for clarity [22].

THF. The six-coordinate distorted octahedral dimeric Sm^{II} complex (**25**) crystallized in monoclinic space group $P2_1/a$, with I(1)-Sm(1)-I(1*) 74.2 and Sm(1)-I(1)-Sm(1*) 105.8 [24] (Fig. 4-1).

5. Reactivity of divalent lanthanoid pseudo-Grignard compounds (N(O)-Ln-X) in oxidation and metathesis reactions

Oxidation and metathesis reactions of divalent lanthanoid pseudo-Grignard compounds expand their usefulness by providing access to new classes of complexes. Earlier reviews [1,4] have discussed use of protolysis reactions as well as metathesis reactions with trimethylsilyl chloride and triphenyltin chloride in characterization of divalent pseudo-Grignard reagents R-Ln-X and the metathesis reactions are mentioned in Section 2. The emphasis was on identification of the pseudo-Grignard reagents rather than on derived syntheses. Protolysis reactions of PhLnX are featured in Section 3 as a source of N-Ln-X pseudo-Grignard reagents.

Oxidation and metathesis reactions have led to new complexes (Scheme 5). Thus, $[Yb(Ph_2Pz)I_2(thf)_3]$ (**26**) was isolated from the oxidation reaction of $[Yb(Ph_2pz)I(thf)_4]$ with I_2 at 0 °C. The stereochemistry of compound (**26**) is a distorted pseudo-octahedron, with one η^2-Ph_2pz ligand, two *trans* iodine donors (I(1)-Yb(1)-I(2) 170.39°), and three thf molecules resulting in seven-coordination [20]. Both iodine atoms are *cisoid* to the pyrazolate (C(backbone)-Yb(1)-I(1) 95.42° and C (backbone)-Yb(1)-I(2) 94.03°). The structure of the product is derived simply by replacement of a thf ligand of the reactant by iodine. Compound $[Yb(C_5H_5)(Ph_2pz)(thf)]_n$ (**27**) (Fig. 5-1) was isolated from the metathesis reaction between $[Yb(Ph_2pz)I(thf)_4]$ and $Na(C_5H_5)$ at room temperature (Scheme 5). Compound (**27**) is a nine coordinate divalent metal coordination polymer, where the Yb atoms are bridged by μ-η^5:η^5-Cp (Cp = C_5H_5) ligands. The pyrazolate ligands are chelating and it is perhaps surprising they are not bridging rather than Cp given the prevalence of the μ-1κ(N):2κ(N') bridging mode in pyrazolate chemistry. Compound $[Sm(OAr)(C_5Me_5)(HMPA)_2]$ (**28**) was similarly prepared from the reaction of equimolar amounts of $[Sm(ArO)(\mu\text{-}I)(thf)_3]_2$ and C_5Me_5K in THF/HMPA (HMPA = hexamethylphosphoramide) (Scheme 5). Complex (**28**) crystallizes in the triclinic space group $P\bar{1}$ and is distorted tetrahedral, where the angle of O(Ar)-Sm-C_5Me_5 ring center is 116° [24], paralleling the *cisoid* C(N)-Ln-I array of pseudo-Grignard complexes. The reaction between [MeYbI] and $[KN(SiMe_3)_2]$ at −78 °C did not yield the targeted metathesis product $[MeYbN(SiMe_3)_2]$. Instead $[K(dme)_4][Yb\{N(SiMe_3)_2\}_3]$ (**29**) (Fig. 5-2) was crystallized

Table 3.1
Divalent lanthanoid N-Ln-X pseudo-Grignard compounds.

Compound	Oxidant	Proligand	Yield %	Ref.
[YbDmp(Tph)N_3Cl(thf)]$_2$(**8**)	HgDmp(Tph)N_3Cl		77	[16]
[Eu(Ph_2pz)I(thf)$_4$](**10**)	PhI	Ph_2pzH	76	[18]
[Yb(Ph_2pz)I(thf)$_4$](**11**)			87	[18]
[Eu(DippForm)I(thf)$_4$]·thf (**12**)		DippFormH	46	[20]
[Eu(XylForm)I(dme)$_2$]·0.5dme (**13**)		XylFormH		[20]
[Eu(XylForm)I(dme)(μ-dme)]$_n$ (**14**)				[20]
[Yb(DippForm)I(thf)$_3$]·thf (**15**)		DippFormH	16	[20]
[{Yb(XylForm)I(thf)$_2$}$_2$] (**16**)		XylFormH	5	[20]
[{Yb(MesForm)I(thf)$_2$}$_2$] (**17**)		MesForm	41	[20]
[Sm(DippForm)Br(thf)$_3$]$_2$·6thf(**18**)	PhBr	DippFormH	64	[19]
[Eu(DippForm)Br(thf)$_3$]$_2$·6thf(**19**)			48	[19]
[Yb(DippForm)Br(thf)$_2$]$_2$·2thf(**20**)			47	[19]
[Sm(Ap)I(thf)$_2$]$_2$(**21**)	–	ApH	26	[22]
[Yb(Ap)I(thf)$_2$]$_2$(**22**)	–		82	[22]
[Eu(dpp-Bian)(μ-Cl)(dme)]$_2$(**23**)	Ph_3SnCl		41	[23]
[Eu(dpp-Bian)(μ-Br)(dme)]$_2$(**24**)	Ph(Br)CHCH(Br)Ph		54	[23]

[20] (Scheme 5). It is unique in having an isolated triangular [Yb{N($SiMe_3$)$_2$}$_3$] complex anion (Yb(1)-N(1) 2.348(2), Yb(1)-N(2) 2.331(3), Yb(1)-N(3) 2.334(2)) in contrast to alkali metal analogues in which silylamide ligands bridge Yb and the alkali metal leading to distortion of the stereochemistry around Yb. The reaction of divalent [Sm(dpp-Bian)I(dme)]$_2$ with 0.5 equivalent [$(CH_3)_2NCS_2^-$]$_2$ gave the oxidation product [Sm(dpp-Bian)I($S_2CN(CH_3)_2$)(dme)] (**30**) (Scheme 5). The seven-coordinate compound (**30**) crystallizes in monoclinic space group *C*2/*c* [25] (Table 5.1).

6. Reactions of divalent pseudo-Grignard reagents with organic substrates

As part of the original characterization of PhYbI, Evans et al. treated the solutions with benzophenone and obtained triphenylmethanol after hydrolysis with hydrochloric acid [2,3]. Subsequently, a considerable effort has been put into reactions with organic substrates, particularly directed to finding differences from the corresponding reactions of classical Grignard reagents. These studies are mainly covered by three previous reviews [1,4,26]. More recently there has been a dearth of interest perhaps owing to the complexity uncovered and the shortage of distinctive clean outcomes. Particular interest has focused on differences from Grignard reagent reactivity, as for similar reactivity, magnesium is much cheaper. Some of the more interesting results are mentioned in an attempt to stimulate further developments. Reactions of a number of ketones and aldehydes with PhYbI formed the corresponding alcohols after hydrolysis, whilst nitriles gave low yields of ketones [27]. However, esters gave a mixture of ketones and alcohols with the former favoured at low temperature (but far from completely selective), though differentiating from classical Grignard reagent behaviour. A competitive reaction between methyl benzoate and acetophenone favoured the ketone over alcohol in the product by 2:1. Further investigation of the behaviour of methyl benzoate showed that addition of PhYbI to the ester improved selectivity of ketone formation, but still far from specific [28]. In reactions of benzoyl chloride with PhYbI, Ph_2CO and Ph_3COH were both obtained together with a low yield of Ph_3CH. The addition of PhYbI to PhCOCl improved ketone selectivity, and this was virtually specific in the presence of ferric chloride [28].

Three publications from the Fujiwara group [29–31] reveal the increasing complexity of the reactions of Ph(Me)Yb-I with *α, β*-unsaturated ketones. In the first, it is shown that a set of these mostly gives exclusive 1,2-addition compared with the lower selectivity of classical Grignard reagents, though two of three comparison Grignard cases favour 1,2-addition without the specificity of PhYbI [29]. Next in response to a report from Sigalov et al. [32] of propene formation in such reactions, the group reported that whilst chalcone gave 1,2-addition on reaction with an equimolar amount of PhYbI, use of an excess (mainly 3:1) of the pseudo-Grignard reagent gave *trans*-stilbene, 1,1,3- triphenylpropene, and diphenylethanol together with, in some cases, the 1,2-addition product, 1,1,3-triphenylprop-2-en-1-ol [30]. These observations were further elaborated in a full paper detailing reactions of Ph(Me)YbI with α,β-unsaturated ketones and -alcohols [31]. The complexity of the products with a RYbI:substrate ratio of 3:1 tends to obscure the clean 1,2-addition with a 1:1 ratio. The intervention of deoxygenation in these reactions has also been observed in reactions with ketones, where for example, anthraquinone with PhYbI on a 1:4 mole ratio yields 9-phenylanthracene [32]. In a detailed study of the deoxygenation of benzophenone and 9-fluorenone with PhYbX (*X* = Br, I), it was found that the ratio of phenylmethane to phenylcarbinol was not affected by the halide but was increased by increasing the PhYbX: substrate ratio from 1:1 to 2:1, and reached near 100 % on addition of

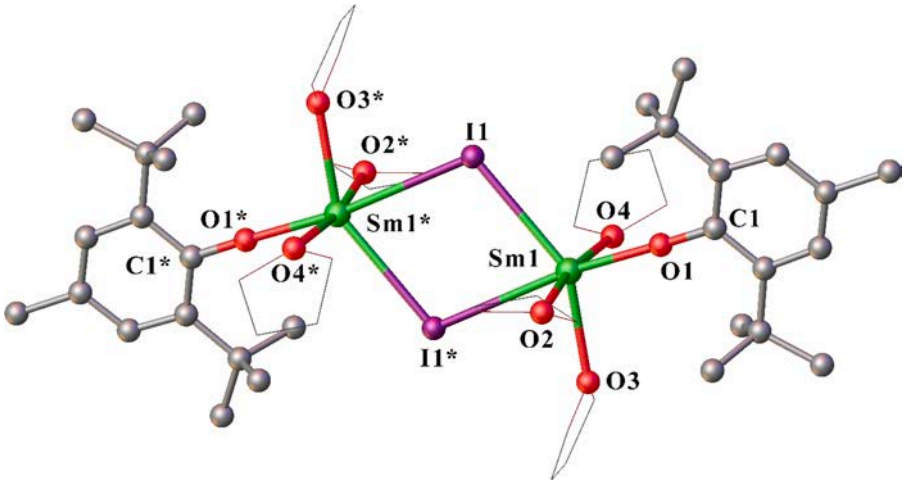
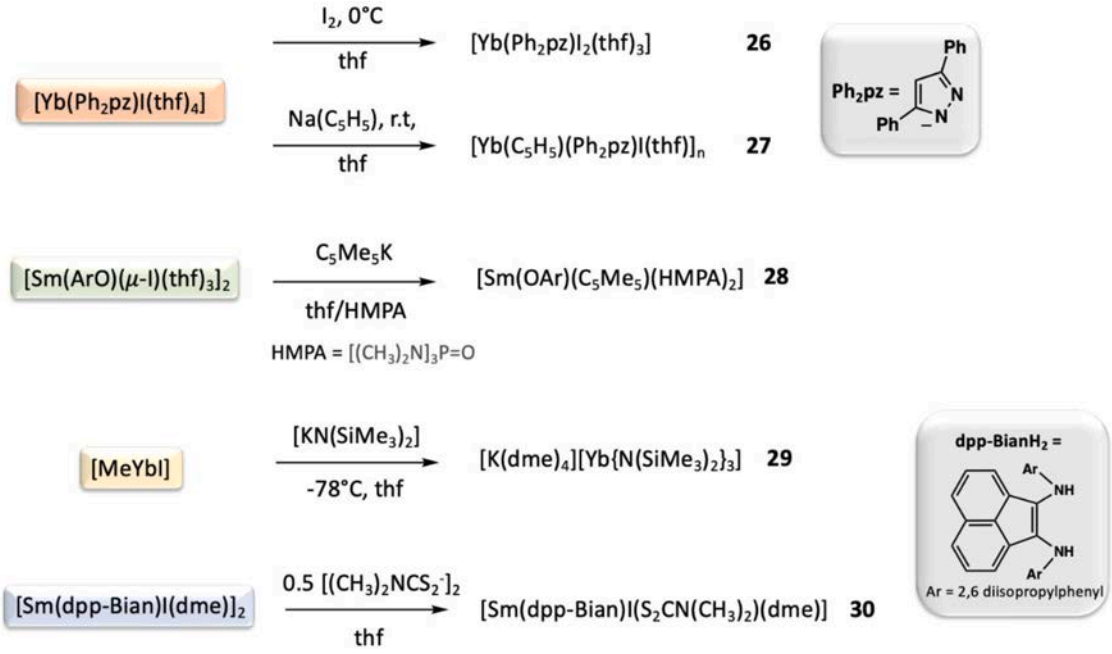


Fig. 4-1. X-ray structure of [Sm(ArO)(*μ*-I)(thf)$_3$]$_2$(**25**). Hydrogen atoms and lattice thf molecules are omitted, coordinated thf molecules are drawn as wireframe for clarity [24].



Scheme 5. Some reactions of N(O)-Ln-X divalent lanthanoid pseudo-Grignard reagents.

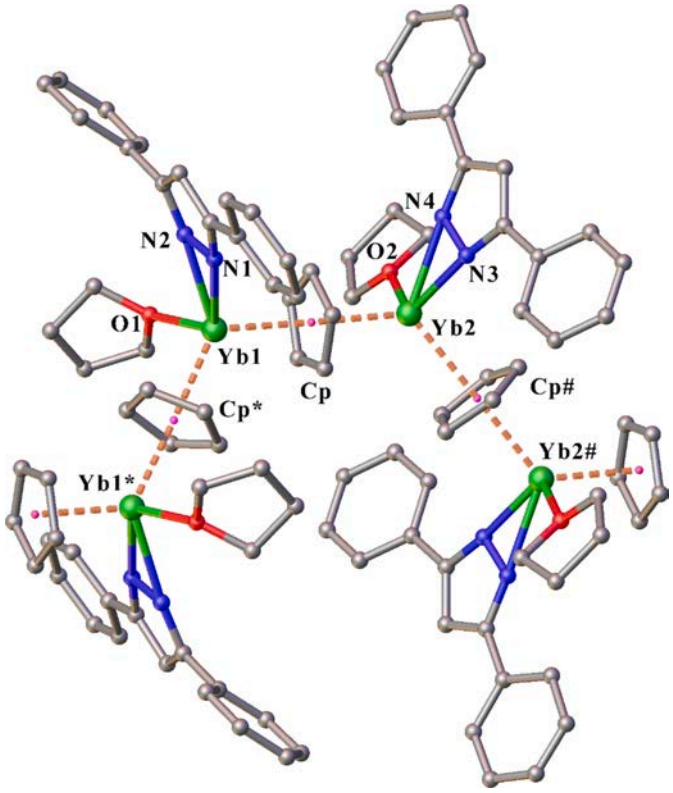


Fig. 5-1. X-ray structure of $[Yb(C_5H_5)(Ph_2pz)(thf)]_n$ (**27**). Hydrogen atoms and lattice thf molecule are omitted for clarity [20].

the co-reductant, biphenylyllithium [33]. On the other hand, the use of 2-thienyl- or 2-pyridyl-ytterbium iodide suppressed deoxygenation, and this was attributed to the stabilisation of the intermediate ytterbium carbinolate by intramolecular S(N)-Yb coordination.

Copper catalysed coupling of alkyl, benzyl, and styryl halides (RX) with PhYbI gave predominantly PhR rather than Ph_2, but coupling with BuLi was less specific [34]. In a different study, a range of arylytterbium iodides was found to arylate dihydrosilanes to give monohydrosilanes many in near quantitative yield (Eq. (8)) [35].

$$ArYbI + RPhSiH_2 \rightarrow ArRPhSiH + HYbI \quad (8)$$

Although a specialist use, this may be one of the most straightforward of applications in organic synthesis. The corresponding alkylations were attempted, and gave a more variable outcome, from near quantitative formation of RPhMeSiH derivative (e.g. R = Me, *i*Bu) to low yields (e.g. R = *i*Pr, *cyclo*-C_6H_{11}) [35].

Overall, lanthanoid pseudo-Grignard reagents still have find a major role in organic synthesis.

7. Conclusions

The pseudo-Grignard compounds of divalent lanthanoid metals have been reviewed. By varying the steric and electronic effects of the ligands, the coordination number, structures and reactivity of the resulting complexes are changed. The scope of divalent pseudo-Grignard derivatives E-Ln-X (E = C, N, O; X = halide) has been enhanced by isolable derivatives with pyrazolate, formamidinate, and aryloxide ligands to add to the limited examples of isolable complexes with C-Ln-X bonding. The potential of these compounds and the few isolated divalent cyclopentadienyllanthanoid halides in subsequent chemistry, such as metathesis and oxidation reactions or treatment with organic substrates is little explored so far. These well-defined complexes have advantages over in situ generated RLnX (R = aryl or alkyl) species where Schlenk equilibria, including ones involving Ln^{III} compounds, raise issues of reproducibility and may account in part for the complexity of some reactions with organic substrates. The current review considers the effects of Schlenk equilibria on the species isolated when attempting to prepare N-Ln-X compounds. Although a number of interesting and unique reactions with organic substrates have been observed for in situ generated C-Ln-X species, they have yet to find a major role in organic synthesis, but there appears to be significant scope for expansion. However, given the much greater cost of Ln metals than Mg (or Ca), it requires a distinctive role, as found for SmI_2 [36].

On the basis of $Ln^{3+} + e^- \rightarrow Ln^{2+}$ redox potentials, −1.55 (Sm), −1.15 (Yb), −0.35 (Eu) [37], the stability of the Ln pseudo-Grignards to

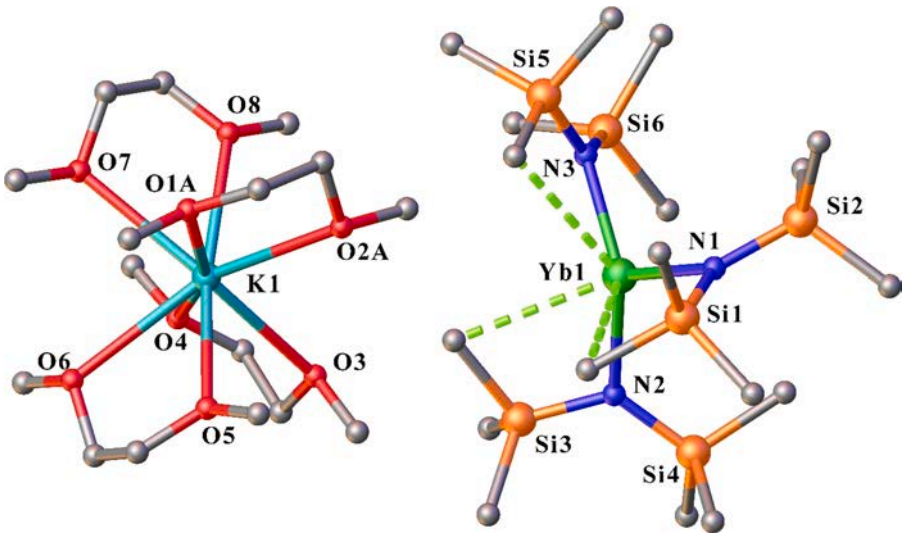


Fig. 5-2. X-ray structure of $[K(dme)_4][Yb\{N(SiMe_3)_2\}_3]$ (**29**). Disordered moieties and hydrogen atoms are omitted for clarity [20].

Table 5.1
Reactivity of divalent lanthanoid pseudo-Grignard compounds.

Reaction	Complex	Yield %	Ref.
$[Yb(Ph_2pz)I(thf)_4] + I_2$	$[Yb(Ph_2Pz)I_2(thf)_3]$ (**26**)	99	[20]
$[Yb(Ph_2pz)I(thf)_4] + NaC_5H_5$	$[Yb(C_5H_5)(Ph_2pz)(thf)]_n$(**27**)	53	[20]
$[Sm(ArO)(\mu\text{-}I)(thf)_3]_2 + C_5Me_5K$	$[Sm(OAr)(C_5Me_5)(HMPA)_2]$ (**28**)	11	[24]
$MeYbI + [KN(SiMe_3)_2]$	$[K(dme)_4][Yb\{N(SiMe_3)_2\}_3]$ (**29**)	<5	[20]
$[Sm(dpp\text{-}Bian)I(dme)]_2 + 0.5\ [(CH_3)_2NCS_2^-]_2$	[Sm(dpp-Bian)I($S_2CN(CH_3)_2$)(dme)](**30**)	69	[25]

oxidation should be Eu>Yb>Sm, but if the triscyclopentdienyls [38] are a guide to organometallic behaviour, all may be 0.7–1.0 V less stable. This sequence accords with Evans' earlier magnetic measurements [2, 3]. With only three elements forming divalent lanthanoid pseudo-Grignards of significant stability and two with approximately the same size [39], the scope for studying the effect of Lewis acidity (related to ion size), electronegativity etc. on behaviour is limited. Europium and ytterbium pseudo-Grignard reagents with 3,5-diphenylpyrazolate are both seven-coordinate, with reduction in ion size having no effect on the coordination number [18], whereas with the larger *N,N'*-bis(2,6-diisopropylphenyl)formamidinate, the coordination number falls from seven to six from the Eu to the Yb complex (Section 3) [19, 20]. On the other hand, exploration of trivalent $RLnX_2$ compounds may prove rewarding in terms of Ln effect on properties, though these species are not divalent pseudo-Grignards.

CRediT authorship contribution statement

Md. Abdul Halim: Writing – review & editing, Writing – original draft, Investigation. **Zhifang Guo:** Writing – review & editing, Writing – original draft, Methodology, Conceptualization. **Victoria L. Blair:** Writing – review & editing, Writing – original draft, Visualization, Conceptualization. **Glen B. Deacon:** Writing – review & editing, Writing – original draft, Methodology, Funding acquisition, Conceptualization. **Peter C. Junk:** Writing – review & editing, Writing – original draft, Methodology, Funding acquisition, Conceptualization.

Declaration of competing interest

The authors declare that they have no conflict of interest.

Data availability

Data will be made available on request.

Acknowledgements

PCJ, VLB and GBD gratefully acknowledge the Australian Research Council for funding (DP230100112). Md A. H. acknowledges James Cook University for a JCUPRS scholarship.

References

[1] E.S. Petrov, D.M. Roitershtein, L.F. Rybakova, J. Organomet. Chem. 647 (2002) 21–27.
[2] D.F. Evans, G.V. Fazakerley, R.F. Phillips, J. Chem. Soc. D (1970) 244.
[3] D.F. Evans, G.V. Fazakerley, R.F. Phillips, J. Chem. Soc. A (1971) 1931–1934.
[4] M.N. Bochkarev, L.N. Zakharov, G.S. Kalinina, Organoderivatives of Rare Earth Elements (1995) 364–423. Ch. 8.
[5] S. Hamidi, G.B. Deacon, P.C. Junk, P. Neumann, Dalton Trans. 41 (2012) 3541–3552.
[6] O.P. Syutkina, L.F. Rybakova, E.S. Petrov, I.P. Beletskaya, J. Organomet. Chem. 280 (1985) C67–C69.
[7] G.Z. Suleimanov, V.I. Bregadze, N.A. Kovalchuk, Kh.S. Khalilov, I.P. Beletskaya, J. Organomet. Chem. 255 (1983) C5–C7.
[8] T.A. Starostina, L.F. Rybakova, E.S. Petrov, Metalloorgan. Khim. (Russ.) 2 (1989) 915.
[9] L.N. Bochkarev, N.E. Molosnova, L.N. Zakharov, G.K. Fukin, A.I. Yanovsky, Y. T. Struchkov, J. Organomet. Chem. 485 (1995) 101–107.
[10] C. Eaborn, P.B. Hitchcock, K. Izod, Z.-R. Lu, J.D. Smith, Organometallics 15 (1996) 4783–4790.
[11] C. Eaborn, P.B. Hitchcock, K. Izod, J.D. Smith, J. Am. Chem. Soc. 116 (1994) 12071–12072.
[12] G. Heckmann, M. Niemeyer, J. Am. Chem. Soc. 122 (2000) 4227–4228.
[13] A.C.G. Shephard, A. Delon, R.P. Kelly, Z. Guo, S. Chevreux, G. Lemercier, G. B. Deacon, G.A. Dushenko, F. Jaroschik, P.C. Junk, Aust. J. Chem. 75 (2022) 746–753.
[14] G.B. Deacon, F. Jaroschik, P.C. Junk, R.P. Kelly, Chem. Commun. 50 (2014) 10655–10657.
[15] R.P. Kelly, T.D.M. Bell, R.P. Cox, D.P. Daniels, G.B. Deacon, F. Jaroschik, P.C. Junk, X.F.L. Goff, G. Lemercier, A. Martinez, J. Wang, D. Werner, Organometallics 34 (2015) 5624–5636.
[16] S.-O. Hauber, J. Woo Seo, M. Niemeyer, Z. Anorg. Allg. Chem. 636 (2010) 750–757.
[17] G.B. Deacon, F. Jaroschik, P.C. Junk, R.P. Kelly, Organometallics 34 (2015) 2369–2377.
[18] M. Wiecko, G.B. Deacon, P.C. Junk, Chem. Commun. 46 (2010) 5076–5078.
[19] M.A. Halim, Z. Guo, G.B. Deacon, P.C. Junk, Chem. Eur. J. 29 (2023) e202300956.
[20] S.H. Ali, G.B. Deacon, P.C. Junk, S. Hamidi, M. Wiecko, J. Wang, Chem. Eur. J. 24 (2018) 230–242.
[21] J. Marcalo, A.P.D. Matos, Polyhedron 8 (1989) 2431–2437.
[22] N.M. Scott, R. Kempe, Eur. J. Inorg. Chem. (2005) 1319–1324.

[23] I.L. Fedushkin, A.A. Skatova, D.S. Yambulatov, A.V. Cherkasov, S.V. Demeshkob, Russ. Chem. Bull. Int. Ed. 64 (2015) 38–43.
[24] Z. Hou, A. Fujita, T. Yoshimura, A. Jesorka, Y. Zhang, H. Yamazaki, Y. Wakatsuki, Inorg. Chem. 35 (1996) 7190–7195.
[25] I.L. Fedushkin, O.V. Maslova, M. Hummert, H. Schumann, Inorg. Chem. 49 (2010) 2901–2910.
[26] H.B. Kagan, J.L. Namy, Tetrahedron 42 (1986) 6573–6614.
[27] T. Fukagawa, Y. Fujiwara, K. Yokoo, H. Taniguchi, Chem. Lett. 10 (1981) 1771–1774.
[28] T. Fukagawa, Y. Fujiwara, H. Taniguchi, Chem. Lett. (1982) 601–602.
[29] K. Yokoo, Y. Yamanaka, T. Fukagawa, H. Taniguchi, Y. Fujiwara, Chem. Lett. (1983) 1301–1302.
[30] Z. Hou, N. Mine, Y. Fujiwara, H. Taniguchi, J. Chem. Soc., Chem. Commun. (1985) 1700–1701.
[31] Z. Hou, Y. Fujiwara, T. Jintoku, N. Mine, K. Yokoo, H. Taniguchi, J. Org. Chem. 52 (1987) 3524–3528.
[32] A.B. Sigalov, E.S. Petrov, L.F. Rybakova, I.P. Beletskaya, Izv. Akad. Nauk SSSR, Ser. Khim. (1983) 2615.
[33] A.V. Garbar, R.R. Shifrina, O.P. Syutkina, L.F. Rybakova, E.S. Petrov, Organomet. Chem. USSR 3 (1990) 651–653.
[34] K. Yokoo, T. Fukagawa, Y. Yamanaka, H. Taniguchi, Y. Fujiwara, J. Org. Chem. 49 (1984) 3237–3239.
[35] W.-S. Jin, Y. Makioka, T. Kitamura, Y. Fujiwara, Chem. Commun. (1999) 955–956.
[36] M. Szostak, N.J. Fazakerley, D. Parmar, D.J. Procter, Chem. Rev. 114 (2014) 5959–6039.
[37] W.J. Evans, Inorg. Chem. 46 (2007) 3435–3449.
[38] A.M. Bond, G.B. Deacon, R.H. Newnham, Organometallics 5 (1986) 2312–2316.
[39] R.D. Shannon, Acta Crystallogr. Sect. A 32 (1976) 751–767.

Check for updates

Chemistry–A European Journal
Research Article
doi.org/10.1002/chem.202300956
Chemistry Europe
European Chemical Societies Publishing
www.chemeurj.org

Bromobenzene Transforms Lanthanoid Pseudo-Grignard Chemistry

Special Collection

Md Abdul Halim,[a] Zhifang Guo,[a] Glen B. Deacon,[b] and Peter C. Junk*[a]

Abstract: Divalent lanthanoid pseudo-Grignard reagents PhLnBr (Ln = Sm, Eu and Yb) can be easily prepared by the oxidative addition of bromobenzene (PhBr) to lanthanoid metals in tetrahydrofuran (THF). PhLnBr reacts with bulky *N,N'*-bis(2,6-di-*iso*propylphenyl)formamidine (DippFormH) to generate Ln^{II} complexes, namely $[Ln(DippForm)Br(thf)_3]_2 \cdot 6thf$ (**1**; **Sm**, **2**; **Eu**), and $[Yb(DippForm)Br(thf)_2]_2 \cdot 2thf$ (**3**; **Yb**). Samarium and europium (in **1** and **2**) are seven coordinate, whereas ytterbium (in **3**) is six coordinate, and all are bromine-bridged dimers. When PhLnBr reacts with 3,5-diphenylpyrazole (Ph_2pzH), both divalent (**5**; $[Eu(Ph_2pz)_2(thf)_4]$) and trivalent (**4a**; $[Sm(Ph_2pz)_3(thf)_3] \cdot 3thf$, **4b**; $[Sm(Ph_2pz)_3(dme)_2] \cdot dme$) complexes are obtained. In the monomeric compounds **4**(**a**,**b**), samarium is nine coordinate but europium is eight coordinate in **5**. The use of PhLnBr in this work transforms the outcomes from earlier reactions of PhLnI.

Introduction

Pseudo-Grignard reagents of lanthanoid metals $[RLn(solv)_nX]$ (X = I mainly, Br) were discovered in the 1970s and were formed by the reaction between free metals (mainly Eu, Sm, Yb) and organic halides (Eq. (1)).[1,2]

$$Ln + RX \xrightarrow[-78 \text{ to } -50\ ^\circ C]{thf} \text{"}RLnX(thf)_n\text{"} \quad (1)$$

R = Me, Ph
Ln = Sm, Eu, Yb

Early characterization was largely based on reaction chemistry, for example towards acids and electrophiles and similarities to the behavior of classical Grignard reagents.[1–4] However, differences in reactivity with some organic substrates also attracted attention.[5,6] Thus, with α, β- unsaturated ketones, 1,2 addition occurred by contrast with 1,4-addition by Grignard reagents[5] and reactions with esters can give ketones unlike Grignard reagents.[6] Early magnetic measurements showed that the solution species were not exclusively Ln^{II} and that significant Ln^{III} derivatives were present, especially for Ln = Sm, Yb.[2] These are formed by an oxidation reaction, (Eq. (2))

$$2\ RLnX + RX = R_2LnX + RLnX_2 \quad (2)$$

Both the Ln^{II} and Ln^{III} complexes can undergo Schlenk-type equilibria further complicating the reaction chemistry. (Scheme 1 Equations (3–5)).

In addition, the low thermal stability of the Ln–C (σ-bond) produces another challenge for the isolation of these reagents.[7] Despite these problems, organolanthanoid(II) iodides have been isolated and structurally characterized by employing bulky alkyl,[8,9] for example $[Yb\{C(SiMe_3)_2(SiMe_2R)\}I(Et_2O)]_2$ (R = Me, MeO, CH=CH$_2$) and aryl groups,[10] for example 2,6-diphenylphenyl ligands. In addition, low yields of $[Sm(C_5Ph_5)(\mu\text{-}Br)(thf)_2]_2 \cdot 6thf$, and $[Yb(C_5Ph_4H)(mu\text{-}Br)(thf)_2]_2$ were obtained from redox transmetallation/protolysis reactions between Ln metal, PhHgBr, and C_5Ph_5H or $C_5Ph_4H_2$,[11,12] and $[Sm(C_5Ph_4H)_2I(thf)_3]$ from a redistribution reaction.[11] If the definition of lanthanoid pseudo-Grignard compounds is extended to $Ln^{II}L(X)$ where L = N or O donor, then more known complexes fall into this category. For example, pseudo-Grignard complexes, $[Sm(dpp\text{-}Bian)(dme)Br]_2$ {dpp-Bian = 1,2-bis[(2,6-diisopropylphenyl)imino]acenaphthene},[13] $[Eu(dpp\text{-}Bian)(dme)(\mu\text{-}X)]_2$ (X = Cl, Br),[14] $[Yb(dpp\text{-}Bian)(dme)(\mu\text{-}Br)]_2$,[15a] $[Yb(dpp\text{-}Bian)I(thf)_2]_2$,[15b] $[Sm(ArO)(\mu\text{-}I)(thf)_3]_2$,[16] (Ar=$C_6H_2Bu^t{}_2$-2,6-Me-4), $[Sm(Ap)I(thf)_2]_2$,[17] {ApH = (2,6-diisopropylphenyl)-[6-(2,4,6-triisopropylphenyl)pyridine-2-yl]amine}, $[Yb(Ap)I(thf)_2]_2$,[17] $[YbDmp(Tph)N_3Cl(thf)]_2$, {Dmp = 2,6-$Mes_2C_6H_3$, Tph = 2′,4′,6′-triisopropylbiphenyl-2-yl},[18] have been were synthesized previously by a variety of routes.

We have been interested in exploring the simple PhLnI species prepared in situ (Scheme 2, Equation (6)) as a source of other Ln(L)X complexes by trapping reactions with LH proligands. This enabled the preparation of $[Ln(Ph_2pz)I(thf)_4]$ (Ln = Eu or Yb) in high yield by reaction of PhYbI with 3,5-diphenylpyrazole (Scheme 2, Equation (7)).[19] However in reac-

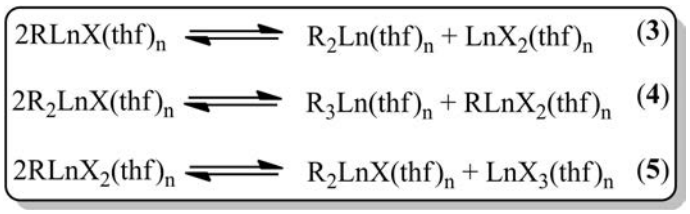
[a] M. A. Halim, Z. Guo, P. C. Junk
College of Science & Engineering
James Cook University
Townsville 4811, Qld (Australia)
E-mail: peter.junk@jcu.edu.au
[b] G. B. Deacon
School of Chemistry
Monash University
Clayton 3800 (Australia)

Supporting information for this article is available on the WWW under https://doi.org/10.1002/chem.202300956

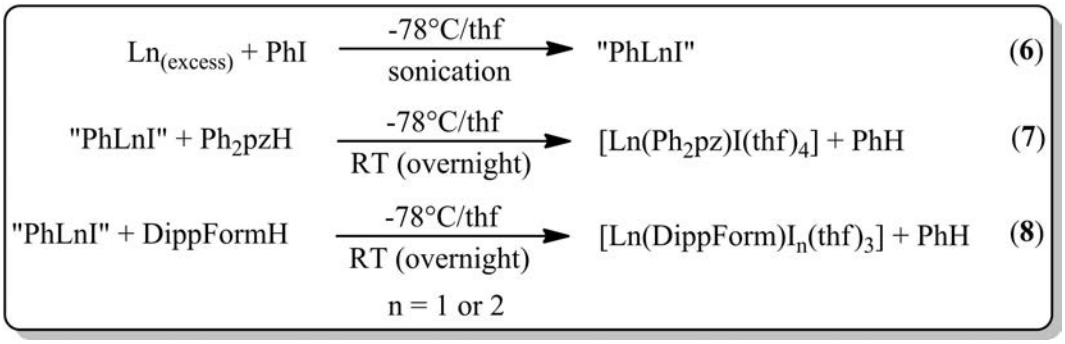
Part of a Special Collection on the p-block elements.

© 2023 The Authors. Chemistry - A European Journal published by Wiley-VCH GmbH. This is an open access article under the terms of the Creative Commons Attribution License, which permits use, distribution and reproduction in any medium, provided the original work is properly cited.

© 2023 The Authors. Chemistry - A European Journal published by Wiley-VCH GmbH



Scheme 1. Extended Schlenk equilibria for pseudo-Grignard reagents.



Scheme 2. Reported pseudo-Grignard reactions.

tions with formamidines, only PhEuI gave divalent complexes in some cases, whereas with ytterbium, both divalent and trivalent complexes were obtained, for example *N,N′*-bis(2,6-diisopropylphenyl)formamidine (DippFormH) gave a mixture of $[Yb^{II}(DippForm)I(thf)_3]$ and $[Yb^{III}(DippForm)I_2(thf)_3]$ (Scheme 2, Equation (8)).[20] Although the different oxidation state products could be separated by fractional crystallization, it took the gloss off the synthetic method and discouraged us from attempting to make Sm(Form)I by this approach as oxidation to Sm^{III} is even more likely. This led us to consider using the less investigated PhLnBr species, as, though the C–Br bond is stronger, perhaps inhibiting PhLnBr formation, greater stability of Ln–Br than Ln–I complexes might reign in oxidation. We now report that reactions of PhLnBr (Ln = Eu, Sm, Yb) with DippFormH have enabled the preparation of divalent pseudo-Grignard complexes in reasonable yields in all cases, the success with samarium being noteworthy. By contrast reactions with Ph_2pzH gave $Eu(Ph_2pz)_2$ and $Sm(Ph_2pz)_3$ species.

Results and Discussion

Synthesis and spectroscopic characterisation of divalent lanthanoid complexes from pseudo-Grignard reactions

Phenyllanthanoid bromides, PhLnBr (Ln = Sm, Eu, Yb) were generated in situ by reactions of an excess of Ln metal with bromobenzene in tetrahydrofuran on sonication and further stirring at room temperature for Ln = Sm. The products were treated with *N,N′*-bis(2,6-di-*iso*propylphenyl)formamidine (DippFormH) (mole ratio PhBr:DippFormH = 1:1) at 0 °C (Sm) or −78 °C (Ln = Eu, Yb) and then at room temperature to form the pseudo-Grignard complexes $[Ln^{II}(DippForm)Br(thf)_n]_2$ (n = 3, Ln = Sm **1**, Eu **2**; n = 2, Ln = Yb **3**) in 45–65% crystalline yield (Scheme 3). The result for samarium is of significance as solutions of PhSmI in thf are reported to have only 50% Sm^{II},[2] whilst the outcome for ytterbium contrasts the formation of $[YbI_2(thf)_4]$, $[Yb^{II}(DippForm)I(thf)_3]$ and $[Yb^{III}(DippForm)I_2(thf)_3]$, the last two in under 20% yield[5] from reaction of DippFormH with PhYbI.[20] The results for the DippFormH reactions are consistent with greater stability for PhLnBr than PhLnI. In addition the current complexes are isolated as bromide-bridged dimers, whereas the Yb^{II} and Yb^{III} DippForm iodides were obtained as monomers.[20] However iodide-bridged dimers were obtained with less bulky formamidines,[20] and [Yb(DippForm)I-$(thf)_2]_2$ was crystallized from THF/PhMe following a synthesis different from a pseudo-Grignard route.[21]

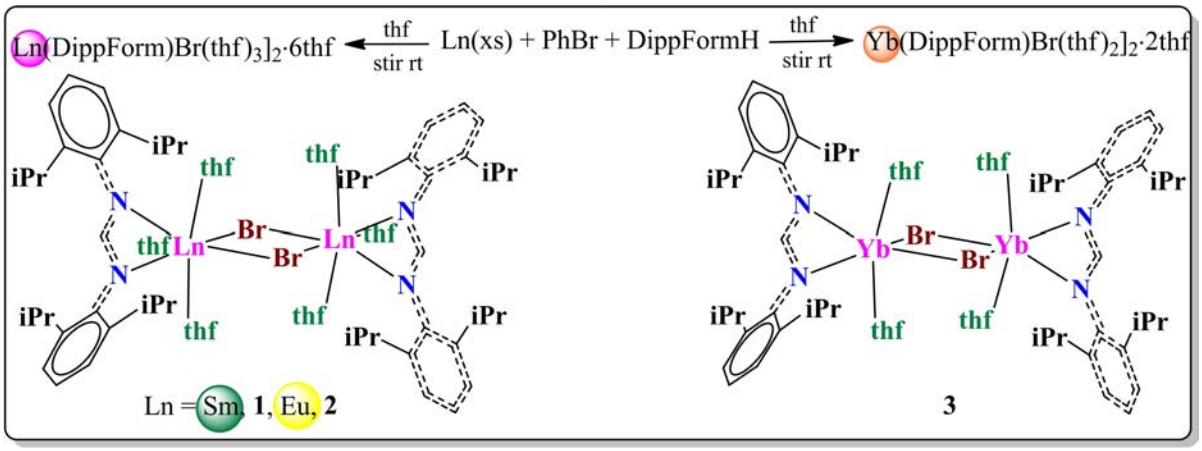
By contrast, for the Ph_2pzH pro-ligand, we obtained two reported compounds (Scheme 4), $[Sm(Ph_2pz)_3(thf)_3].3thf$ (**4a**)[22] and $[Eu(Ph_2pz)_2(thf)_4]$ (**5**)[23] in 60% yield. A new trivalent complex, $[Sm(Ph_2pz)_3(dme)_2]\cdot dme$ (**4b**) was synthesised by crystallizing **4a** from DME. No crystalline product could be obtained from the corresponding reaction of Yb. Products **5** and **4a** arise from protonation by Ph_2pzH of $EuPh_2$ and $SmPh_3$ respectively, which are Schlenk equilibrium products with additional oxidation for Sm (see Scheme 4).

These outcomes again contrast the behaviour of PhLnI (Ln = Eu, Yb), where the corresponding reactions yield the pseudo-Grignard reagents $[Ln(Ph_2Pz)I(thf)_4]$ in high yield.[5,19] A similar two step experimental method was used for reactions with both PhBr and PhI, hence the differences do not arise from the procedures.

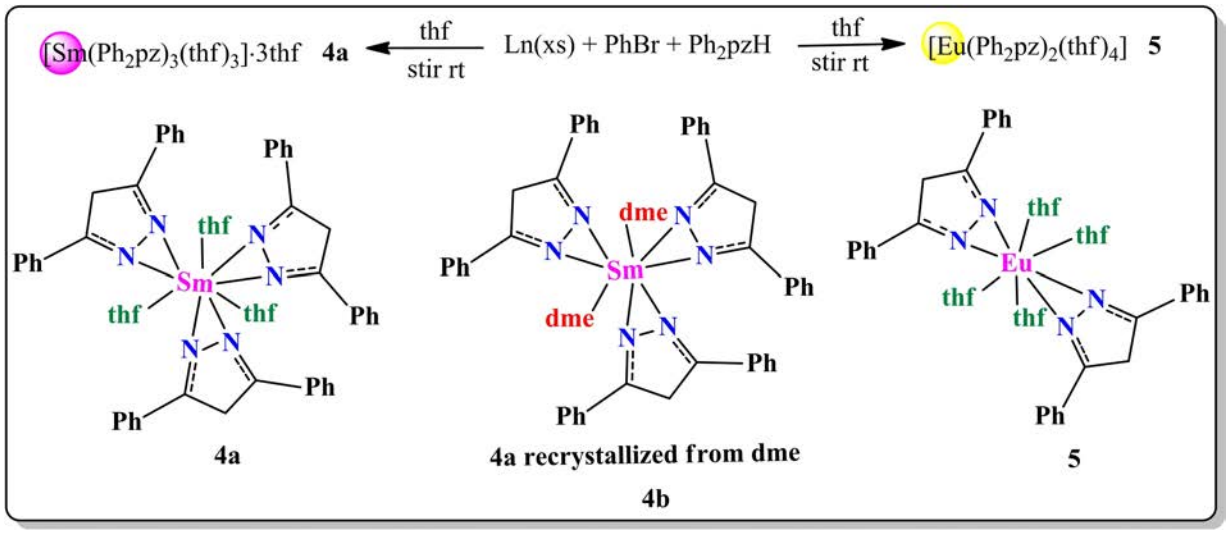
Compound **1** is green and compounds **2**, **3** and **5** are yellow, while both **4**(**a**, **b**) are colourless. The colour of **1** is

© 2023 The Authors. Chemistry - A European Journal published by Wiley-VCH GmbH

15213765, 2023, 36, Downloaded from https://chemistry-europe.onlinelibrary.wiley.com/doi/10.1002/chem.202300956 by Eddie Koiki Mahoo Library, Wiley Online Library on [05/09/2024]. See the Terms and Conditions (https://onlinelibrary.wiley.com/terms-and-conditions) on Wiley Online Library for rules of use; OA articles are governed by the applicable Creative Commons License



Scheme 3. Synthesis of complexes **1**–**3**.



Scheme 4. Synthesis of complexes **4a**, **4b** and **5**.

associated with a broad visible band at 588 nm in the UV/vis spectrum (Figure S8), which is attributable to an f^6 to f^5d^1 transition.[24]

IR spectra showed the presence of the appropriate DippForm or Ph_2pz ligand. For compounds **1**–**5**; the absence of (N–H) absorption (around 3300–3400 cm^{-1}) in the infrared spectrum proved the complete deprotonation of the ligands. Complexes **1**, **3** and **4**(**a**, **b**) gave satisfactory good ^{1}H NMR spectra in C_6H_6 (Figures S1,3,4,5), but **2** and **5** showed broad features with unsatisfactory integration owing to Eu^{II} paramagnetism (Figures S2, 6). Microanalyses or metal analysis established bulk purity, the latter being used when there were microanalysis difficulties. In some cases, analyses showed loss of solvent of crystallization from the analysis sample. The melting points indicate significant thermal stability of the new DippForm compounds. Complexes **1**, **3** and **4**(**a**, **b**) gave satisfactory ^{1}H NMR spectra in C_6H_6 (Figure S1, 3, 4, 5), but **2** and **5** showed broad features with unsatisfactory integration owing to Eu^{II} paramagnetism (Figure S2, 6). The NMR spectra of compound **1** indicated the loss of 3 THF of crystallization, consistent with the microanalysis, whereas **4**(**b**) had excess DME. The methine proton (NC*H*N) resonances in the ^{1}H NMR shifted significantly for compound **1** to lower frequencies (−10.70 ppm) comparable to paramagnetic [Sm(DippForm)$_2$(thf)$_2$] (−14.03 ppm),[25] whereas for the diamagnetic compound **3**, a higher (8.28 ppm) methine resonance than for DippFormH (δ = 7.50 ppm) was observed. For compound **4a** the CH-pz resonance shifted to 9.39 ppm and for **4b** it shifted to 8.75 ppm, compared with the pro- ligand value of 6.63 ppm.

Molecular structures

Compounds **1**–**5** were identified and authenticated by single crystal X-ray diffraction.

© 2023 The Authors. Chemistry - A European Journal published by Wiley-VCH GmbH

15213765, 2023, 36, Downloaded from https://chemistry-europe.onlinelibrary.wiley.com/doi/10.1002/chem.202300956 by Eddie Koiki Mahu Library, Wiley Online Library on [05/09/2024]. See the Terms and Conditions (https://onlinelibrary.wiley.com/terms-and-conditions) on Wiley Online Library for rules of use; OA articles are governed by the applicable Creative Commons License

Complexes [Ln(DippForm)Br(thf)$_3$]$_2$·6thf (**1**–**2**) are isostructural having similar crystallographic and molecular parameters, and crystallise in the monoclinic $P2_1/c$ space group. Compounds **1**–**3** (Figure 1a, b) were isolated as dimers, whereas **4a**, **4b** (Figure 2)) and **5** are monomeric. Selected bond lengths and angles of compounds **1**–**3**, **4**(**b**) are given with the figures and more details in the Supporting Information. The lanthanoid contraction is observed in the average Ln–N bond lengths of the complexes (**1**–**3**): Sm–N (2.64) > Eu–N (2.63) > Yb–N (2.46).

Compounds [Ln(DippForm)Br(thf)$_3$]$_2$·6thf (**1**, **2**) are seven coordinate Ln_2Br_2 bridged dimers with one chelating DippForm and three coordinated thf ligands bound to each Ln atom. The DippForm ligands are perpendicular to the LnBrBrLn plane, where one ligand is *cis* {C(13)-Sm(1)-Br(1) 95.06°, C(13)-Eu(1)-Br(1) 97.71°} to Br1 and *trans* {C(13)-Sm(1)-Br(2) 174.34°, C(13)-Eu(1)-Br(2) 176.92°} to Br2. The average bite angle in **1** is 51.7° and Br(1)-Sm-Br(2) is 79.48(18)° whereas in **2** the average bite angle is 0.01° larger and Br(1)-Ln-Br(2) is 0.26° smaller than in **1** (see the Supporting Information Table S1). The stereochemistry of the seven coordinate Sm^{2+} and Eu^{2+} (**1** and **2**) ions can be described as distorted pentagonal bipyramidal. The average Sm–N bond length in [Sm(DippForm)Br(thf)$_3$]$_2$ **1** is 2.64 Å, which is longer than the average Sm–N bond length 2.59 Å in six coordinate [Sm(DippForm)$_2$(thf)$_2$].[26] This is consistent with the change in coordination number.[27] The average Sm–Br bond length in seven coordinate **1** (3.09 Å), is very comparable to the average Sm–Br bond length is 3.03 Å in seven coordinate [Sm(C_5Ph_5)(μ-Br)(thf)$_2$]$_2$.[11] It is longer than the reported average Sm–Br bond length (2.84 Å) in seven coordinate [Sm(DippForm)Br$_2$(thf)$_3$],[28] because the latter has non-bridging Sm–Br bonds and a higher oxidation state for Sm. Again, the < Sm-$O_{(thf)}$ > bond length in **1** is 2.61 Å, which is very close to the < Sm-$O_{(thf)}$ > bond length (2.58 Å) in [Sm(C_5Ph_5)(μ-Br)(thf)$_2$]$_2$,[11] but longer than the < Sm-$O_{(thf)}$ > bond length (2.48 Å) in [Sm(DippForm)Br$_2$(thf)$_3$],[28] because of the oxidation state difference.[27] Comparisons of Eu–N, Eu-$O_{(thf)}$, and Eu–Br bond

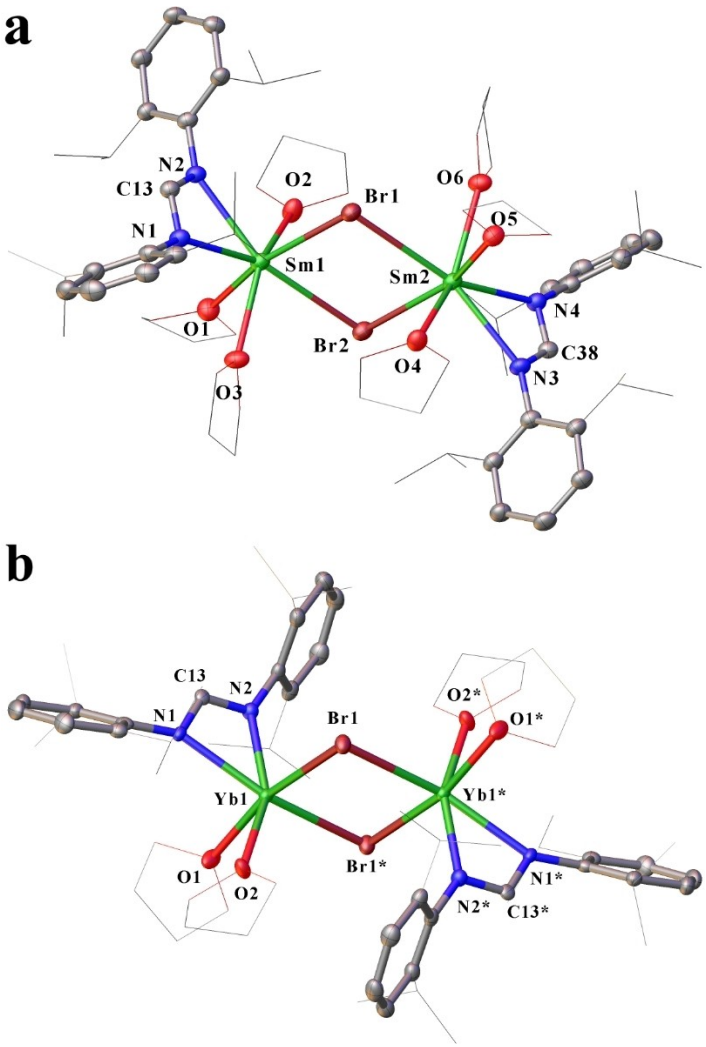


Figure 1. Molecular diagram of a) [Sm(DippForm)Br(thf)$_3$]$_2$·6thf (representative of Sm, **1**, Eu, **2**); b) [Yb(DippForm)Br(thf)$_2$]$_2$·2thf (**3**). Hydrogen atoms and lattice thf molecules are omitted and coordinated thf molecules and *i*Pr groups are drawn as wireframe for clarity and thermal ellipsoids are set to the 50% probability level. Selected bond lengths (Å): Sm(1)-N(1) 2.634(4), Sm(1)-N(2) 2.644(4), Sm(1)-Br(1) 3.0260(8); Eu(1)-N(1) 2.625(2), Eu(1)-N(2) 2.635(2), Eu(1)-Br(1) 3.1157(6); Yb(1)-N(1) 2.429(3), Yb(1)-N(2) 2.483(3), Yb(1)-Br(1) 2.892(7). More details are in the Supporting Information (Table S1).

© 2023 The Authors. Chemistry - A European Journal published by Wiley-VCH GmbH

15213765, 2023, 36, Downloaded from https://chemistry-europe.onlinelibrary.wiley.com/doi/10.1002/chem.202300956 by Eddie Koiki Mabo Library, Wiley Online Library on [05/09/2024]. See the Terms and Conditions (https://onlinelibrary.wiley.com/terms-and-conditions) on Wiley Online Library for rules of use; OA articles are governed by the applicable Creative Commons License

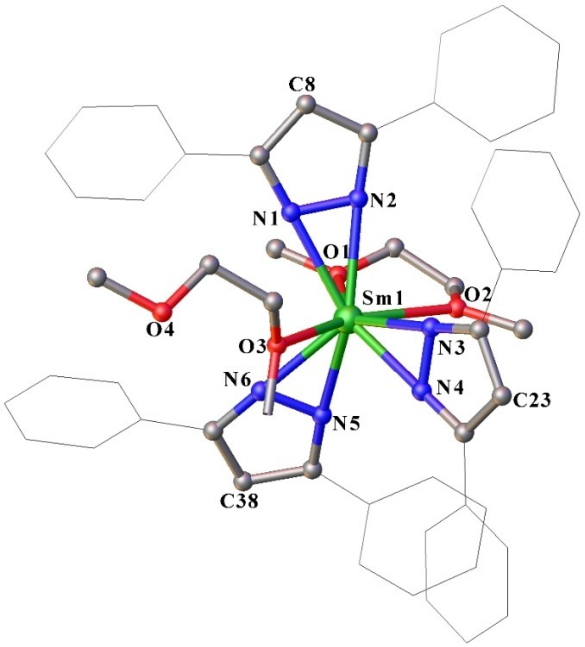


Figure 2. Molecular diagram of $[Sm(Ph_2pz)_3(dme)_2]\cdot dme$ (4b). Hydrogen atoms and lattice dme molecules are omitted, phenyl groups are drawn as wireframe for clarity and thermal ellipsoids are set to the 50% probability level. Selected bond lengths (Å): Sm(1)-N(1) 2.446(3), Sm(1)-N(2) 2.419(3), Sm(1)-N(3) 2.434(3), Sm(1)-N(4) 2.424(3), Sm(1)-N(5) 2.403(3), Sm(1)-N(6) 2.456(3). For more details, see the Supporting Information (Table S1 and associated text).

lengths of $[Eu(DippForm)Br(thf)_3]_2$ (**2**) with those of six coordinate $[Eu(DippForm)_2(thf)_2]$,[29] and $[(dpp\text{-}Bian)Eu(dme)(\mu\text{-}Br)]_2$,[14] show the expected relationships from the differences in coordination numbers.[27]

Compound $[Yb(DippForm)Br(thf)_2]_2$ (**3**) crystallises in the triclinic, space group *P*-1 and is a centrosymmetric dimer, where half is generated from symmetry at the midpoint of the Yb(1)···Yb(1)* vector. The six coordinate metal atom has an octahedral arrangement. The average Yb–N bond length in $[Yb(DippForm)Br(thf)_2]_2$ **3** is 2.45 Å, which is the same as the average Yb–N bond length (2.45 Å) of six coordinate $[Yb(DippForm)(\mu\text{-}I)(thf)_2]_2$[21] and nearly the same as the $<$Yb–N$>$ bond length 2.47 Å of six coordinate $[Yb(DippForm)_2(thf)_2]$.[29] The Yb–Br1 and Yb–Br1* bond lengths in **3** (2.8926(7) and 2.8979(11) Å) are comparable to the reported Yb–Br1 and Yb–Br1* bond lengths (2.8932(2) and 2.9216(3) Å) for seven coordinate $[Yb(C_5Ph_4H)(\mu\text{-}Br)(thf)_2]_2$[12] and six coordinate $[(dpp\text{-}Bian)Yb(dme)(\mu\text{-}Br)]_2$ (2.8673(9) Å and 2.9325(9) Å).[15a] The average Yb–$O_{(thf)}$ bond length in **3** is 2.42 Å, which is similar to the $<$Yb–$O_{(thf)}$$>$ bond length of 2.44 Å in $[Yb(C_5Ph_4H)(\mu\text{-}Br)(thf)_2]_2$,[12] 2.45 Å in $[Yb(DippForm)(\mu\text{-}I)(thf)_2]_2$,[21] and 2.46 Å in $[Yb(DippForm)_2(thf)_2]$.[29]

$[Sm(Ph_2pz)_3(dme)_2]$ (**4b**) crystallizes in the monoclinic space group $P2_1/c$ and has a nine coordinate trigonal prismatic structure. Three η^2-Ph_2pz (ligands), one chelating dme and one monodentate dme are attached to samarium. Complex (**4b**) is isostructural with $[Nd(Ph_2pz)_3(dme)_2]$.[22] The average Sm–N bond length in $[Sm(Ph_2pz)_3(dme)_2]$ (**4b**) is 2.44 Å, which is the same as the average Sm–N bond length 2.44 Å in nine coordinate $[Sm(Ph_2pz)_3(thf)_3]$,[22] and comparable to the $<$Nd–N$>$ bond length 2.46 Å in nine coordinate $[Nd(Ph_2pz)_3(dme)_2]$.[22] The ionic radii of nine coordinate Sm^{3+} (1.132 Å) and Nd^{3+} (1.163 Å)[27] are similar. The average Sm–$O_{(dme)}$ bond length in (**4b**) is 2.53 Å, which is close to the reported $<$Sm–$O_{(thf)}$$>$ bond length (2.54 Å) in $[Sm(Ph_2pz)_3(thf)_3]$,[22] and the $<$Nd–$O_{(dme)}$$>$ bond length (2.55 Å) in $[Nd(Ph_2pz)_3(dme)_2]$.[22]

Conclusions

The reaction of Ln^0 metals with PhBr followed by addition of DippFormH enables the synthesis of divalent dimeric pseudo-Grignard complexes, $[Ln(DippForm)Br(thf)_3]_2\cdot 6thf$ (Ln = Sm, Eu), and $[Yb(DippForm)Br(thf)_2]_2\cdot 2thf$ in good crystalline yields. These three compounds have a Ln_2Br_2 bridged dimer core and varying coordination numbers (Sm, Eu: 7; Yb: 6). The Ln···$C_{(backbone)}$ distances for **1**, **2** and **3** are 3.03 Å, 3.02 Å and 2.83 Å respectively. With the pro-ligand Ph_2pzH, we obtained nine coordinate trivalent $[Sm(Ph_2pz)_3(thf)_3].3thf$, and $[Sm(Ph_2pz)_3(dme)_2]\cdot dme$ complexes, and the divalent compound $[Eu(Ph_2pz)_2(thf)_4]$ owing to protonation of Schlenk equilibrium products with prior oxidation in the case of Sm. The outcomes differ completely from analogous reactions of PhLnI,[19,20] and the isolation of a Sm^{II} pseudo-Grignard reagent is noteworthy.

Experimental Section

General: The lanthanoid compounds described here are highly air and moisture sensitive, hence were prepared and handled using vacuum-nitrogen line techniques and a glovebox under an atmosphere of purified nitrogen. Lanthanoid metals were collected from Santoku/Molycorp/Eutectix. Large chunks were filed in the drybox before use. Ligands DippFormH[30] and Ph_2pzH[31] were synthesised according to the literature methods. All other chemicals were purchased from Sigma and used without purification. Solvents (THF, DME and C_6D_6) were pre-dried by distillation over sodium or sodium benzophenone ketyl before being stored under an atmosphere of nitrogen. Infrared spectra were recorded as Nujol mulls between NaCl plates using a Perkin-Elmer/Nicolet-Nexus 1600 FTIR instrument within the range 4000–650 cm^{-1}. ^1H NMR spectra were recorded with a Bruker 400 MHz instrument with dry perdeuterobenzene as the solvent. Satisfactory NMR spectra could not be obtained for Eu^{II} complexes due to paramagnetism. Melting points were determined in sealed glass capillaries under nitrogen. Metal analyses were carried out by complexometric titration (Xylenol orange as indicator and hexamethylenetetramine as buffer) after digesting with dilute hydrochloric acid.[32] Elemental analyses (C, H, N) were performed at the Microanalytical Laboratory, Science Centre, London Metropolitan University, England. The samples were sent in sealed glass pipettes under nitrogen. Crystals were immersed in crystallography oil and were examined using the MX1 beamline at the Australian Synchrotron. Crystal data and refinement details are given in Table S2 and associated text.

Deposition Number(s) 2248415 (**1**), 2248416 (**2**), 2248417 (**3**), 2248418 (for compound **4(b)**) contain(s) the supplementary crystallographic data for this paper. These data are provided free of

© 2023 The Authors. Chemistry - A European Journal published by Wiley-VCH GmbH

15213765, 2023, 36, Downloaded from https://chemistry-europe.onlinelibrary.wiley.com/doi/10.1002/chem.202300956 by Eddie Koiki Mahn Library, Wiley Online Library on [05/09/2024]. See the Terms and Conditions (https://onlinelibrary.wiley.com/terms-and-conditions) on Wiley Online Library for rules of use; OA articles are governed by the applicable Creative Commons License

charge by the joint Cambridge Crystallographic Data Centre and Fachinformationszentrum Karlsruhe Access Structures service.

[Sm(DippForm)Br(thf)$_3$]$_2$·6thf (1): Samarium metal powder (0.225 g, 1.5 mmol) was suspended in dry THF (15 ml) under N_2, and then PhBr (0.157 g, 1.0 mmol) was added at 0 °C. The mixture was sonicated for 10 min and stirred for 24 h at room temperature, when a light brown solution formed. Solid DippFormH (0.368 g, 1.0 mmol) was added and the mixture was stirred at 0 °C for 1 h, and a green solution developed after stirring for 24 h at room temperature. The resulting mixture was filtered and concentrated to 5 mL under vacuum. Green crystals (0.656 g, 64 %) were obtained after cooling at −25 °C for 3 days. M.P. 203–205 °C. Elemental analysis: Found: C 55.83, H 7.83, N 2.90; $C_{98}H_{166}Br_2N_4O_{12}Sm_2$ (2052.86 g mol^{-1}) requires: C 57.34, H 8.15, N 2.73; loss of 3 thf of crystallization, $C_{86}H_{142}Br_2N_4O_9Sm_2$ (1836.59 g mol^{-1}) requires: C 56.24, H 7.79, N 3.05. IR (Nujol): 2724w, 1671 s, 15991 m, 1529 m, 1340w, 1274 m, 1198w, 1103w, 1074 s, 1014 s, 948 m, 915 m, 857 m, 800 m, 774w, 755 m, 722 m, 666 w cm^{-1}. ^{1}H NMR (C_6D_6): δ =-10.70(s, 2H, NC(H)N), 1.20(m, 8H, CH), 1.78(d, 48H, CH_3), 3.23(s, br, 36H, thf), 4.55(d, 8H, H(3,5)), 4.99(s, 36H, thf), and 6.15 ppm(t, 4H, H(4)) corresponding to loss of 3 thf of crystallization. UV: broad peak at 588 nm.

[Eu(DippForm)Br(thf)$_3$]$_2$·6thf (2): Europium metal powder (0.23 g, 1.5 mmol) was suspended in dry THF (15 ml) under N_2, and then PhBr (0.157 g, 1.0 mmol) was added at −78 °C. The mixture was sonicated for 10 min when a brown solution formed. After cooling to −78 °C, solid DippFormH (0.368 g, 1.0 mmol) was added and the mixture was stirred at −78 °C for another 3 h. A brownish-yellow solution developed after further stirring for 24 h at room temperature. The resulting mixture was filtered and concentrated to 5 mL under vacuum. Yellow crystals (0.495 g, 48 %) were obtained after cooling at −25 °C for 3 days. M.P. 186–188 °C. Elemental analysis: Found: C 53.54, H 7.08, N 3.65, Eu 20.42; $C_{98}H_{166}Br_2Eu_2N_4O_{12}$ (2056.08 g mol^{-1}) requires: C 57.25, H 8.14, N, 2.72, Eu 14.78; loss of 6 thf of crystallisation and 2 coordinated. $C_{66}H_{102}Br_2Eu_2N_4O_4$ (1479.27 g mol^{-1}) requires: C 53.59, H 6.95, N 3.79, Eu 20.55. IR (Nujol): 2724w, 1668 s, 1589w, 1345w, 1312w, 1261 m, 1170 m, 1075 m, 1010 s, 923 m, 852w, 771w, 723 s, 665 w cm^{-1}.

[Yb(DippForm)Br(thf)$_2$]$_2$·2thf (3): Ytterbium metal powder (0.26 g, 1.5 mmol) was suspended in dry THF (15 ml) under N_2, and then PhBr (0.157 g, 1.0 mmol) was added at −78 °C. The mixture was sonicated for 10 min and a dark red-brown solution formed. After cooling to −78 °C, solid DippFormH (0.368 g, 1.0 mmol) was added and the mixture was stirred for another 3 h. A red-brown solution developed after stirring for 24 h at room temperature. The resulting mixture was filtered and concentrated to 5 mL under vacuum. Yellow crystals (0.365 g, 47 %) were obtained after cooling at −25 °C for 2 days. M.P. 176–178 °C. Elemental analysis: Found: C 51.96, H 6.23, N 3.37, Yb 22.98; $C_{74}H_{118}Br_2Yb_2N_4O_6$ (1665.62 g mol^{-1}) requires: C 53.36, H 7.14, N, 3.36, Yb 20.78; loss of 2 thf of crystallization, $C_{66}H_{102}Br_2Yb_2N_4O_4$ (1521.42 g mol^{-1}) requires; C 52.10, H 6.76, N 3.68, Yb 22.75. IR (Nujol): 2723w, 1567 s, 1587 m, 1518w, 1260 m, 1235w, 1187 m, 1074 s, 1016 m, 934w, 913 m, 864w, 801 s, 756 m, 723 m, 673 s, 607 w cm^{-1}. ^{1}H NMR (C_6D_6): δ = 8.28(s, 2H, NC(H)N), 7.18(8H, H(3,5)), 7.05(m, 4H, H(4)), 3.85(m, 8H, CH), 3.64(s, 24H, thf), 1.34-1.19 ppm(m, 72H: 24H, thf; 48H, CH_3). ^{13}C NMR (100 MHz, C_6D_6): δ = 22.74 ($CH(CH_3)_2$), 23.47 ($CH(CH_3)_2$), 24.05 (CH_2, thf), 24.40 ($CH(CH_3)_2$), 26.75 ($CH(CH_3)_2$), 27.17 ($CH(CH_3)_2$), 67.63 (CH_2, thf), 121.56 (Ar–*C*), 122.09 (Ar–*C*), 141.41 (Ar–*C*), 141.80 (Ar–*C*),147.28 (Ar–*C*), 165.80 ppm (N*C*N).

[Sm(Ph$_2$pz)$_3$(thf)$_3$]·3thf (4a): The synthesis procedure for **4(a)** was similar as described for **1**. Here, solid Ph_2pzH (0.22 g, 1.0 mmol) was added at 0 °C and a yellowish-brown solution was obtained. The resulting mixture was filtered and concentrated to 5 mL under vacuum. Colourless crystals (0.248 g, 60 %) were obtained after cooling at −25 °C for 4 days. M. P. 157–159 °C. Metal Analysis: Found: Sm 14.48 %; $C_{69}H_{81}N_6O_6Sm$ (1240.75 g mol^{-1}) requires: Sm 12.12 %; loss of 3 thf of crystallization, $C_{57}H_{57}N_6O_3Sm$ (1024.46 g mol^{-1}) requires: Sm,14.68 %. IR (Nujol): 1605 s, 1512w, 1340w, 1297 m, 1261w, 1229 m, 1178 m, 1156w, 1073 s, 1028 s, 971 s, 915 s, 868 s, 842w, 801 m, 762 s, 724w, 697 s, 684 m, 665 w cm^{-1}. ^{1}H NMR (400.13 MHz, C_6D_6): δ = 0.60 (s, 24H, thf), 2.17(s, 24H, thf), 7.28 (t, 6H, H(4)), 7.58 (t, 12H, H(3,5)), 7.77 (s, 3H, CH-pz), and 9.39 ppm(s, 12H, H(2,6)). For compound **4(a)** (triclinic, *P*-1space group) the unit cell is; a = 13.307(3)Å, b = 18.547(4)Å, c = 25.198(5)Å, α = 76.38(3)°, β = 84.83(3)°, γ = 87.37(3)°, V = 6018(2)Å^3, the reported unit cell is; a = 13.343(3), b = 18.579(4), c = 25.270(5) Å, α = 76.58(3), β = 85.19(3), γ = 87.35(3)°, V = 6070(2) Å^3.[22]

[Sm(Ph$_2$pz)$_3$(dme)$_2$]·dme (4b): Colorless crystals (0.19 g, 53 %) from a solution of **4(a)** in DME after cooling at −25 °C for 3 days. M. P. 161–163 °C. Elemental analysis: Found: C 63.59, H 5.93, N 7.46, Sm 14.07 %; $C_{57}H_{63}SmN_6O_6$ (1078.48 g mol^{-1}) requires: C 63.48, H 5.89, N 7.79, Sm 13.94 %. IR (Nujol): 2722 m, 1604 s, 1513 m, 1422w, 1338w, 1306 m, 1283 m, 1246 m, 1224w, 1193 s, 1114 m, 1027w, 970s, 913 s, 864 s, 802 m, 757 s, 695 s, 682 w cm^{-1}. ^{1}H NMR (400.13 MHz, C_6D_6): δ = 2.82 (s, 32H, dme), 2.95 (s, 48H, dme), 7.21 (t, 6H, H(4)), 7.40 (t, 12H, H(3,5)), 7.47 (s, 3H, CH-pz), 8.75 ppm(s, 12H, H(2,6)).

[Eu(Ph$_2$pz)$_2$(thf)$_4$] (5): The synthesis procedure for compound **5** was as described **2**. Here, solid Ph_2pzH (0.22 g, 1.0 mmol) was added at −78 °C, and a red brown solution formed. The resulting mixture was filtered and concentrated to 5 mL under vacuum. Yellow crystals (0.273 g, 62 %) were obtained after cooling at −25 °C for 5 days. M.P. 224–226 °C. Metal Analysis: Found Eu 17.64 %; $C_{46}H_{54}EuN_4O_4$ (878.89 gmol^{-1}) requires: Eu 17.29 %. IR (Nujol): 1602 s, 1524 m,1512w, 1421w, 1295w, 1259w, 1218 m, 1178w, 1042 s, 999w, 968 s, 903 s, 791w, 767 s, 753 s, 702 s, 681 s, 665 w cm^{-1}. ^{1}H NMR (400.13 MHz, C_6D_6): Paramagnetic. For compound **5** (triclinic, *P*-1space group) the unit cell is; a = 9.126(18)Å, b = 18.668(4)Å, c = 24.427(5)Å, α = 110.04(3)°, β = 91.64(3)°, γ = 90.22(3)°, V = 3907.5(16)Å^3, the reported unit cell is; a = 9.27(19)Å, b = 18.952(4)Å, c = 24.803(5)Å, α = 109.99(3)°, β = 91.78(3)°, γ = 90.52(3)°, V = 4092.1(16)Å^3.[23]

Acknowledgements

PCJ and GBD gratefully acknowledge the ARC for funding (DP230100112). Parts of this research were undertaken on the MX1 beamline at the Australian Synchrotron, part of ANSTO.[33] We thank Dr Safaa Ali for preliminary studies. Open Access publishing facilitated by James Cook University, as part of the Wiley - James Cook University agreement via the Council of Australian University Librarians.

Conflict of Interests

The authors declare no conflict of interest.

Data Availability Statement

The data that support the findings of this study are available from the corresponding author upon reasonable request.

© 2023 The Authors. Chemistry - A European Journal published by Wiley-VCH GmbH

15213765, 2023, 36, Downloaded from https://chemistry-europe.onlinelibrary.wiley.com/doi/10.1002/chem.202300956 by Eddie Koiki Mabo Library, Wiley Online Library on [05/09/2024]. See the Terms and Conditions (https://onlinelibrary.wiley.com/terms-and-conditions) on Wiley Online Library for rules of use; OA articles are governed by the applicable Creative Commons License

Keywords: bromine-bridge dimers · crystal structures · europium · lanthanoid(II) complexes · oxidative addition · Pseudo-Grignard reagents · samarium · ytterbium

[1] D. F. Evans, G. V. Fazakerley, R. F. Phillips, *J. Chem. Soc. D* **1970**, 244–244.
[2] D. F. Evans, G. V. Fazakerley, R. F. Phillips, *J. Chem. Soc. A* **1971**, 1931–1934.
[3] E. S. Petrov, D. M. Roitershtein, L. P. Rybakov, *J. Organomet. Chem.* **2002**, *647*, 21–27.
[4] O. P. Syutkina, L. F. Rybakova, E. S. Petrov, I. P. Beletskaya, *J. Organomet. Chem.* **1985**, *280*, C67-C69.
[5] Z. Hou, Y. Fujiwara, T. Jintoku, N. Mine, K. Yokoo, H. Taniguchi, *J. Org. Chem.* **1987**, *52*, 3524–3528.
[6] T. Fukagawa, Y. Fujiwara, K. Yokoo, H. Taniguchi, *Chem. Lett.* **1981**, *10*, 1771–1774.
[7] S. A. Cotton, *Coord. Chem. Rev.* **1997**, *160*, 93–127.
[8] C. Eaborn, P. B. Hitchcock, K. Izod, J. D. Smith, *J. Am. Chem. Soc.* **1994**, *116*, 12071–12072.
[9] C. Eaborn, P. B. Hitchcock, K. Izod, Z. Lu, J. D. Smith, *Organometallics* **1996**, *15*, 4783–4790.
[10] G. Heckmann, M. Niemeyer, *J. Am. Chem. Soc.* **2000**, *122*, 4227–4228.
[11] R. P. Kelly, T. D. M. Bell, R. P. Cox, D. P. Daniels, G. B. Deacon, F. Jaroschik, P. C. Junk, X. F. L. Goff, G. Lemercier, A. Martinez, J. Wang, D. Werner, *Organometallics* **2015**, *34*, 5624–5636.
[12] G. B. Deacon, F. Jaroschik, P. C. Junk, R. P. Kelly, *Organometallics* **2015**, *34*, 2369–2377.
[13] I. L. Fedushkin, O. V. Maslova, M. Hummert, H. Schumann, *Inorg. Chem.* **2010**, *49*, 2901–2910.
[14] I. L. Fedushkin, A. A. Skatova, D. S. Yambulatov, A. V. Cherkasov, S. V. Demeshkob, *Russ. Chem. Bull. Int. Ed.* **2015**, *64*, 38–43.
[15] a) I. L. Fedushkin, O. V. Maslova, E. V. Baranov, A. S. Shavyrin, *Inorg. Chem.* **2009**, *48*, 2355–2357; b) V. A. Dodonov, V. M. Makarov, M. N. Zemnyukova, D. A. Razborov, E. V. Baranov, A. S. Bogomyakov, V. I. Ovcharenko, I. L. Fedushkin, *Organometallics* **2023**, https://doi.org/10.1021/acs.organomet.2c00640.
[16] Z. Hou, A. Fujita, T. Yoshimura, A. Jesorka, Y. Zhang, H. Yamazaki, Y. Wakatsuki, *Inorg. Chem.* **1996**, *35*, 7190–7195.
[17] N. M. Scott, R. Kempe, *Eur. J. Inorg. Chem.* **2005**, 1319–1324.
[18] S.-O. Hauber, J. W. Seo, M. Niemeyer, *Z. Anorg. Allg. Chem.* **2010**, *636*, 750–757.
[19] M. Wiecko, G. B. Deacon, P. C. Junk, *Chem. Commun.* **2010**, *46*, 5076–5078.
[20] S. H. Ali, G. B. Deacon, P. C. Junk, S. Hamidi, M. Wiecko, J. Wang, *Chem. Eur. J.* **2018**, *24*, 230–242.
[21] D. Werner, G. B. Deacon, P. C. Junk, *Eur. J. Inorg. Chem.* **2018**, 2241–2246.
[22] S. Beaini, G. B. Deacon, M. Hilder, P. C. Junk, D. R. Turner, *Eur. J. Inorg. Chem.* **2006**, 3434–3441.
[23] Z. Guo, V. L. Blair, G. B. Deacon, P. C. Junk, *Chem. Eur. J.* **2022**, *28*, e202103865.
[24] M. Karbowiak, A. Urbanowicz, *Phys. Rev. B.* **2007**, *76*, 115125.
[25] M. L. Cole, G. B. Deacon, C. M. Forsyth, P. C. Junk, D. P. Ceron, J. Wang, *Dalton Trans.* **2010**, *39*, 6732–6738.
[26] M. L. Cole, P. C. Junk, *Chem. Commun.* **2005**, 2695–2697.
[27] R. D. Shannon, *Acta Crystallogr. Sect. A* **1976**, *32*, 751–767.
[28] M. L. Cole, G. B. Deacon, P. C. Junk, J. Wang, *Organometallics* **2013**, *32*, 1370–1378.
[29] M. L. Cole, G. B. Deacon, C. M. Forsyth, P. C. Junk, K. Konstas, J. Wang, H. Bittig, D. Werner, *Chem. Eur. J.* **2013**, *19*, 1410–1420.
[30] R. M. Roberts, *J. Org. Chem.* **1949**, *14*, 277–284.
[31] J. Elguero, E. Gonzalez, R. Jacquier, *Bull. Soc. Chim. Fr.* **1968**, 707–713.
[32] G. Dchwarzenbach, H. A. Flaschka, *Complexometric Titrations*, Methuen, Publishing Ltd, London, **1969**.
[33] N. P. Cowieson, D. Aragao, M. Clift, D. J. Ericsson, C. Gee, S. J. Harrop, N. Mudie, S. Panjikar, J. R. Price, A. RiboldiTunnicliffe, R. Williamson, T. Caradoc-Davies, *J. Synchrotron Radiat.* **2015**, *22*, 187.

Manuscript received: March 27, 2023
Accepted manuscript online: April 18, 2023
Version of record online: May 5, 2023

© 2023 The Authors. Chemistry - A European Journal published by Wiley-VCH GmbH

15213765, 2023, 36, Downloaded from https://chemistry-europe.onlinelibrary.wiley.com/doi/10.1002/chem.202300956 by Eddie Koiki Mahoo Library, Wiley Online Library on [05/09/2024]. See the Terms and Conditions (https://onlinelibrary.wiley.com/terms-and-conditions) on Wiley Online Library for rules of use; OA articles are governed by the applicable Creative Commons License

Check for updates

EurJIC
European Journal of Inorganic Chemistry

Research Article
doi.org/10.1002/ejic.202400672

Chemistry Europe
European Chemical Societies Publishing

www.eurjic.org

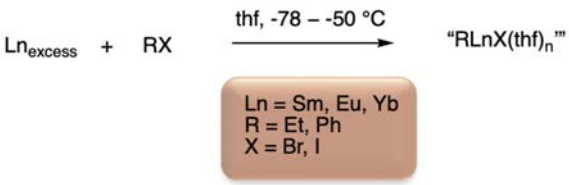
Syntheses of Pyrazolato- and Formamidinato-lanthanoid(III) Diiodides from *in Situ* Generated lanthanoid(III) Pseudo-Grignard Reagents

Md Abdul Halim,[a] Zhifang Guo,[a] Victoria L. Blair,[b] Glen B. Deacon,[b] and Peter C. Junk*[a]

Trivalent lanthanoid pseudo-Grignard reagents $Ph_pLn^{III}I_{(3-p)}$ (P = 1 or 2; Ln=La, Ce, Nd, Er and Lu) are readily prepared by the oxidation of lanthanoid metals with iodobenzene at 25 °C, following pre-activation of the metal with 1 drop Hg in tetrahydrofuran (thf) or acetonitrile (CH_3CN) and brief sonication. The protolysis of $Ph_pLn^{III}I_{(3-p)}$ with 3,5-diphenylpyrazole (Ph_2pzH) yields pyrazolato complexes $[Ln(Ph_2pz)I_2(thf)_n]$ (n = 4: Ln=La **1**, Ce **2**, Nd **3**; n = 3: Ln=Er **4**, Lu **5**). Interestingly, for Er, a competing complex $[ErPh(Ph_2pz)I(thf)_3]\cdot thf$ (**4a**) was obtained along with the expected $[Er(Ph_2pz)I_2(thf)_3]$ (**4**). In contrast, in CH_3CN, $[Ln(Ph_2pz)_3(CH_3CN)_3]\cdot 2CH_3CN$ (Ln=Nd **6**, Gd **7**) complexes were obtained through Schlenk equilibrium redistribution. Reactions with bulky *N,N′*-bis(2,6-di-*iso*propylphenyl)formamidine (DippFormH) and *N,N′* –bis(2,6-dimethylphenyl)formamidine (XylFormH) produced the $Ln^{(III)}$ complexes, $[Ln(DippForm)I_2(thf)_3]\cdot nthf$ (n = 1, Ln=Nd **8**; n = 0.5, Ln=Er **9**) and $[Ln(XylForm)I_2(thf)_3]\cdot thf$ (Ln=Nd **10**, Er **11**). All the complexes isolated in this study are monomeric; **4**–**5** and **8**–**11** are seven coordinate, complexes **1**–**3** are eight coordinate with one η^2-N-donor ligand and two *trans* iodine ligands, and complexes **6**–**7** are nine coordinate, featuring three η^2-Ph_2pz ligands, and three CH_3CN ligands.

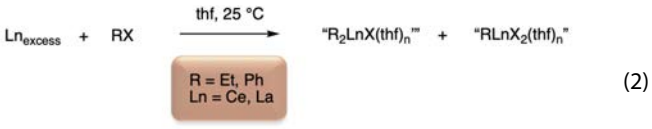
Introduction

Organolanthanoid(II) halides or pseudo-Grignard reagents, $RLnX(solv)_n$ (R = alkyl, aryl, heteroaryl etc, Ln=Sm, Eu, Yb; X=I, Br, Cl, F) are potentially attractive synthetic reagents, which can be used without isolation, owing to their ease of formation from lanthanoid metals and appropriate organic halides.[1–4]



(1)

However, problems arise from oxidation state ambiguities, with early magnetic measurements showing solutions contained increasing amounts of Ln^{III} species in the sequence (Ln=Eu < Yb < Sm).[5] With elements giving dominantly oxidation state +III compounds, some were found not to react, but products were obtained with Ce and La.[5]



(2)

Whilst oxidation state uncertainty is removed, species with different X/Ln ratios potentially complicate downstream chemistry, and additional Schlenk-type equilibria (giving LnR_3 and LnX_3) are possible. Subsequently, a wider range of trivalent metals (Ln=Pr, Nd, Gd and Ho) were shown to give triphenylmethyl derivatives $[(Ph_3C)_2LnCl]$ or $[(Ph_3C)LnCl_2]$.[6] Because of these complexities, most workers wishing to prepare and study $RLnX_2$ and R_2LnX complexes have chosen to obtain them by more defined routes, particularly metathesis.[4,7,8]

Despite their oxidation state ambiguity, *in situ* generated (Eq. (1)) PhLnX (Ln=Sm, Eu and Yb; X=I or Br) pseudo-Grignard reagents have proven to be successful synthons in protolysis reactions with N-donor LH pro-ligands, namely pyrazoles and formamidines. Thus, the 3,5-diphenylpyrazole (Ph_2pzH) proligand reacted with "PhLnI" to give $[Ln(Ph_2pz)I(thf)_4]$ (Ln=Eu or Yb) in high yield (Scheme 1 Eq. 3).[9] However, with formamidines, reactions of "PhYbI" resulted in the isolation of both Yb^{II} and Yb^{III} complexes. For example N,N′-bis(2,6-diisopropylphenyl)formamidine (DippFormH) gave $[Yb(DippForm)I(thf)_3]$ and $[Yb(DippForm)I_2(thf)_3]$. Where mixtures were obtained, fractional crystallization enabled separation though at some cost in yield.[10] On the other hand, *in situ* generated "PhLnBr" reacted with *N,N′*-bis(2,6-diisopropylphenyl)formamidine to afford divalent $[Ln(DippForm)Br(thf)_n]_2$ (Ln=Sm, Eu, Yb; n = 2 or 3) in good yields (Scheme 1 Eq. 4), whereas when Ph_2pzH was treated with PhLnBr (Ln = Sm or Eu), Schlenk rearrangements dominated

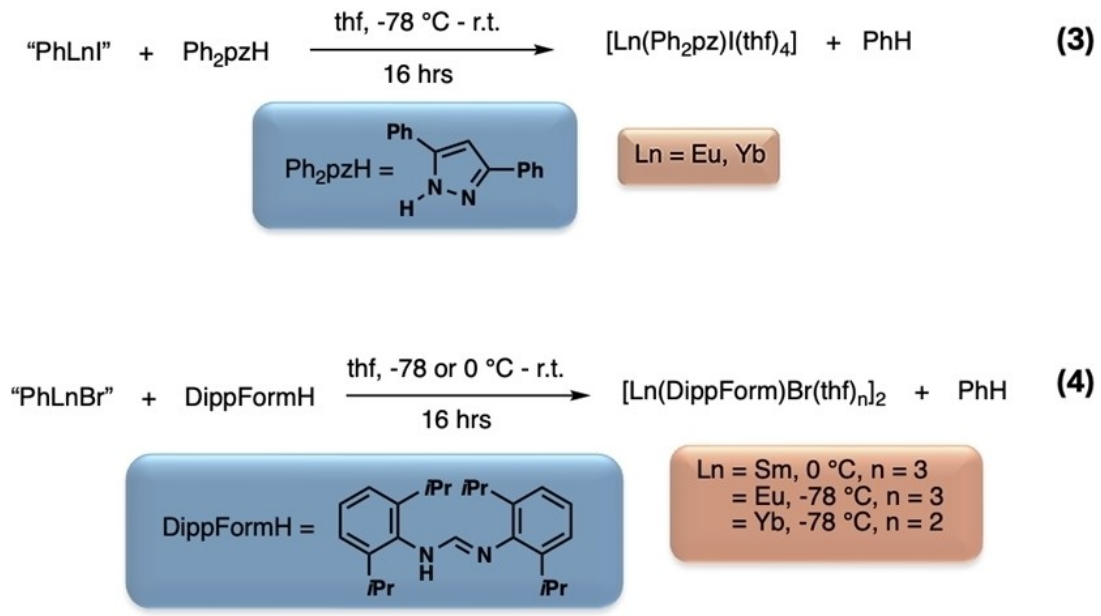
[a] *M. Abdul Halim, Z. Guo, P. C. Junk*
College of Science & Engineering, James Cook University, Townsville 4811, Qld, Australia
E-mail: peter.junk@jcu.edu.au

[b] *V. L. Blair, G. B. Deacon*
School of Chemistry, Monash University, Clayton 3800, Australia

Supporting information for this article is available on the WWW under https://doi.org/10.1002/ejic.202400672

© 2024 Wiley-VCH GmbH

Research Article
doi.org/10.1002/ejic.202400672



Scheme 1. Some reactions of reported pseudo-Grignard complexes.[9,11]

and $[Eu^{II}(Ph_2pz)_2]$ and the oxidation product $[Sm^{III}(Ph_2pz)_3]$ were isolated. Accordingly, with suitable choice of "PhLnI" or "PhLnBr", access to a range of divalent complexes could be achieved, despite the oxidation state uncertainty of the reagents. These successes have led us to examine reactions of the less explored trivalent $Ph_pLn^{III}I_{(3-p)}$ (p = 1 or 2) species with the N-donor LH pro-ligands.

We now report that the reactions of $Ph_pLn^{III}I_{(3-p)}$ (Ln=La, Ce, Nd, Er and Lu) with Ph_2pzH have successfully yielded trivalent complexes $[Ln(Ph_2pz)I_2(thf)_n]$ (n = 4, La, Ce and Nd; n = 3, Er and Lu) in reasonable yields. In the reaction with Er, we were also able to isolate the organometallic product $[Er(Ph_2pz)(Ph)I(thf)_3]\cdot thf$. Similarly, reactions with DippFormH or XylFormH ligands resulted in the formation of diiodo complexes ($[Ln(ligand)I_2(thf)_3]$). Collectively, these syntheses illustrate the preparative potential of *in situ* generated $Ph_pLn^{III}I_{(3-p)}$ species. In contrast, reactions with Ph_2pzH in acetonitrile solvent gave Schlenk rearrangement products $[Ln(Ph_2pz)_3(CH_3CN)_3]\cdot 2CH_3CN$ (Ln=Nd, Gd) indicating that outcomes are solvent dependent.

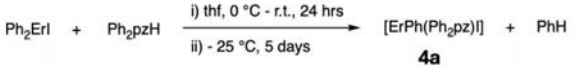
Results and Discussion

Synthesis and Spectroscopic Characterisation of Trivalent Lanthanoid (Ph_2pz/DippForm/XylForm) Complexes from *in Situ* Generated Pseudo-Grignard Reactants

Phenyllanthanoid halides, $Ph_pLnI_{3-p}(solv)_n$ (p = 1 or 2; Ln=La, Ce, Nd, Gd, Er and Lu) were generated *in situ* by reactions of an excess of Ln metal activated with Hg metal with iodobenzene (PhI) in an appropriate solvent (tetrahydrofuran or acetonitrile) on sonication and further stirring at room temperature. Experiments without Hg activation were also carried out, observing that La reacts with PhI overnight (~ 15 h), while Nd requires approximately 36 h to achieve the desired reaction. To increase the yield, the reaction rate and reduce the initiation time, we introduced Hg metal to activate the lanthanoid metals.

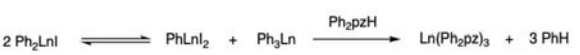
The products were treated with the proligand 3,5-diphenylpyrazole (Ph_2pzH) (mole ratio PhX: Ph_2pzH = 2:1) at 0 °C for 1 h and then at room temperature. $[Ln(Ph_2pz)I_2(thf)_n]$ (n = 4, Ln=La **1**, Ce **2**, Nd **3**; n = 3, Ln=Er **4**, Lu **5**) complexes were isolated in 44–62% crystalline yield (Scheme 2). The reaction with Er also yielded $[ErPh(Ph_2pz)I(thf)_3]\cdot thf$ (**4a**) along with **4**. The complexes $[Ln(Ph_2pz)_3(CH_3CN)_3]\cdot 2CH_3CN$ (Ln = Nd **6**, Gd **7**) were isolated in 26–62% crystalline yield (Scheme 3) from reactions in acetonitrile. Reaction with *N,N′*-bis(2,6-di-*iso*propylphenyl)formamidine (DippFormH) and bis(2,6-dimethylphenyl)formamidine (XylFormH) yielded $[Ln(DippForm)I_2(thf)_3]\cdot nthf$ (Nd **8**, n = 1; Er **9**, n = 0.5) and $[Ln(XylForm)I_2(thf)_3]\cdot thf$ (Ln=Nd **10**, Er **11**) (Scheme 4).

The formation of (**4a**) can be attributed to protolysis of Ph_2ErI, the only case where the second product of reaction (2) gave rise to an isolable compound. Thus, formation of both **4** and **4a** from the reaction with Er metal supports the formation of both products of Eq. 2



(5)

Complexes **6** and **7** result from protolysis of Ph_3Ln, formed by Schlenk redistribution in MeCN.

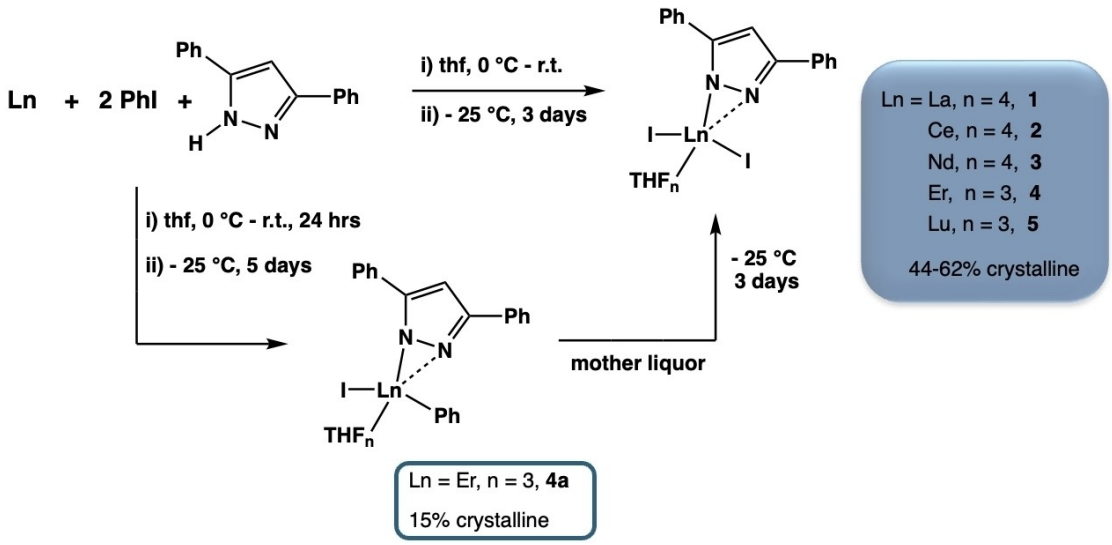


(6)

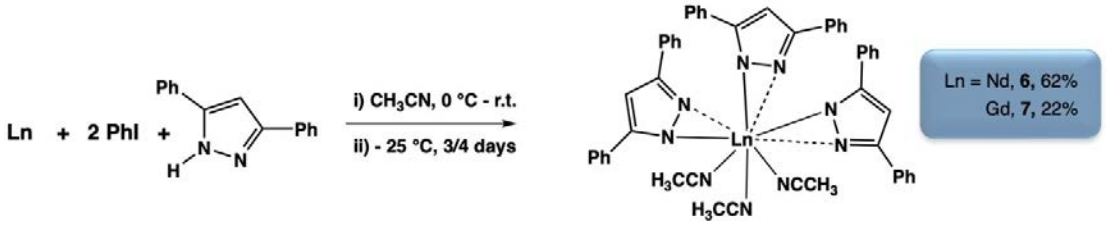
© 2024 Wiley-VCH GmbH

10990682c, 0 Downloaded from https://chemistry-europe.onlinelibrary.wiley.com/doi/10.1002/ejic.202400672 by James Cook University, Wiley Online Library on [09/01/2025]. See the Terms and Conditions (https://onlinelibrary.wiley.com/terms-and-conditions) on Wiley Online Library for rules of use; OA articles are governed by the applicable Creative Commons License

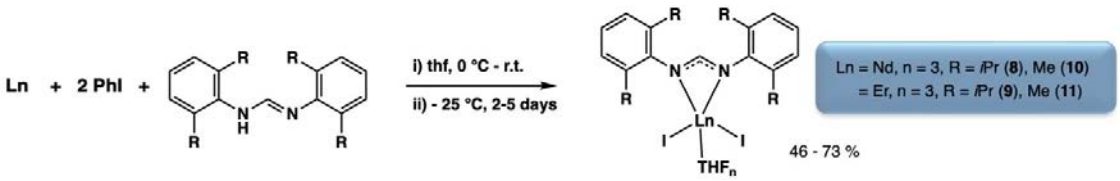
Research Article
doi.org/10.1002/ejic.202400672



Scheme 2. Synthesis of complexes 1–5 (products derived from precursors shown in Eq 2).



Scheme 3. Synthesis of complexes 6–7.



Scheme 4. Synthesis of complexes 8–11.

Ln(Form)I_2 complexes have previously been prepared by reaction of Ln metals with iodine and FormH proligands,[13,14] but the synthesis has not been examined with Ph_2pzH or other pyrazoles.

IR spectra showed the presence of the appropriate Ph_2pz, XylForm or DippForm ligand. For compounds **1–11**; the absence of (N–H) absorption (around 3300–3400 cm^{-1}) in the infrared spectra proved the complete deprotonation of the ligands. Complexes **1–3, 5–6, 8–10** gave satisfactory ^{1}H NMR spectra in C_6H_6 (Figure S1,2,3,5,6,8,9,10), but **4**, **7** and **11** showed broad features with unsatisfactory integration owing to Ln^{III} paramagnetism (Figure S4,7,11). Micro or metal analysis established bulk purity; the latter being used when there were microanalysis difficulties. In some cases, analyses showed loss of solvent of crystallization from the analysis sample. The melting points indicate significant thermal stability of the new Ph_2pz/DippForm compounds. The NMR spectra of compound **3**, **6**, **8**, **10** indicated the loss of (0.5 or 1) solvent of crystallization, consistent with the elemental analysis. For compound **3** the CH-pz resonance in the ^{1}H NMR spectrum is shifted significantly to 26.17 ppm and for **2** it is shifted to 13.52 ppm due to paramagnetism, whereas for both diamagnetic **1** and **5**, the resonance is shifted to 7.28 ppm and 7.50 ppm respectively, compared with the proligand value of 6.63 ppm, as is usual on coordination and consistent with reported results.[12] In compound **6**, the CH-pz resonance is shifted to 16.77 ppm, again owing to paramagnetism. The methine proton (NC*H*N) resonance of the Nd complex [Nd(DippForm)I_2(thf)$_3$]·thf **8** is shifted significantly to higher frequencies (30.10 ppm), which is in agreement with the reported resonance (30.04 ppm) for the compound prepared by the direct reaction between Nd, iodine and DippFormH,[13] and it is shifted to 25.24 ppm for complex [Er(DippForm)I_2(thf)$_3$]·0.5thf **9**. The NC*H*N resonance of [Nd-

© 2024 Wiley-VCH GmbH

10990682c, 0 Downloaded from https://chemistry-europe.onlinelibrary.wiley.com/doi/10.1002/ejic.202400672 by James Cook University, Wiley Online Library on [09/01/2025]. See the Terms and Conditions (https://onlinelibrary.wiley.com/terms-and-conditions) on Wiley Online Library for rules of use; OA articles are governed by the applicable Creative Commons License

Research Article
doi.org/10.1002/ejic.202400672

(XylForm)I_2(thf)$_3$]·thf **10** is shifted to 30.60 ppm, while it is at 25.93 ppm in the reported [Ce(XylForm)I_2(thf)$_3$]·1.5thf.[14]

Molecular Structures

Compounds **1**–**11** were identified, and structures determined by single crystal X-ray diffraction. The crystallographic data of the complexes [Ln(Ph_2pz)I_2(thf)$_4$] (La **1**, Ce **2**) and [Er(Ph_2pz)I_2(thf)$_3$] (**4**) showed poor diffraction, and can be used only for connectivity.

Isomorphous compounds [Ln(Ph_2pz)I_2(thf)$_4$] (**1**–**3**) were isolated in the triclinic space group *P*-1, where two molecules are present in one unit cell. The coordination geometric environment of these monomeric compounds (**1**–**3**) is described as square antiprismatic, where the eight-coordinate metal centre has one η^2-Ph_2pz ligand, four thf ligands and two *transoid* iodine ligands (Figure 1). As the crystal data for **1** and **2** were of connectivity quality only, the structure of the isomorphous Nd complex **3** is discussed as representative. The I(1)-Nd–I(2) bond angle is *transoid* (156.28(3)°) for **3**. The iodide ligands are *cis* (I(1)-Nd–C(8) 100.209° and I(2)-Nd–C(8) 102.894°) to the Ph_2pz ligand.

The bite angle (N(1)-NdC-N(2)) in compound (**3**) is 32.400(3)°, is smaller than that of the seven coordinate trivalent ytterbium compound [Yb(Ph_2pz)I_2(thf)$_3$] (35.200(4)°).[10] The <Nd–N> bond length (2.455(9) Å) is 0.04 Å smaller than that of the seven coordinate compound [{2-[Ph_2P(O)]C_6H_4NC(Bu^t)N(2,6-$Me_2C_6H_3$)}NdI_2(thf)$_2$], where the ligand is bulkier.[15] The <Nd–I> bond length in compound **3** is 3.167(12) Å and is larger than 3.115(4) Å in seven coordinate compound [Nd(DippForm)I_2(thf)$_3$],[13] consistent with the change in coordination number.[16]

Compound [ErPh(Ph_2pz)I(thf)$_3$] (**4a**) crystallized in the monoclinic space group $P2_1/c$. The coordination geometric environment of the monomeric compound (**4a**) is pentagonal bipyramidal, where the seven-coordinate metal atom has one η^2-Ph_2pz ligand, one phenyl (Ph), one iodine and three thf ligands (Figure 2). The phenyl (Ph) ring is *cis* to both Ph_2pz (C(21)-Er–C(8) 96.861°) and iodine (C(21)-Er–I(1) 98.309(11)°) ligands. The iodine ligand is *transoid* to the Ph_2pz ligand (I(1)-Er–C(8) bond angle is 164.783°). The bond angles between iodine and thf molecules vary from 79.420(7) to 88.760(7)°. The <Er–N> bond length is 2.313(3) Å is smaller than for the seven coordinate compound [Er(DFForm)$_2$I(thf)$_2$],[13] attributable to the bulkier Form ligand. The Er–I bond length in compound **4a** is 3.071(6) Å is very close to 3.082(3) Å in six coordinate compound [Er($CH_2C_6H_5$)$_2$I(thf)$_3$].[17] The <Er–O> bond length (2.386(3) Å) of compound **4a** is also comparable with the average Er–O bond length 2.358(2) Å in that compound.[17]

Compounds [Ln(Ph_2pz)I_2(thf)$_3$] (Ln=Er **4**, **Lu 5**) crystallize in the monoclinic space group *C*2/c. As the data for **4** were of connectivity quality, **5** is discussed as representative. The lutetium atoms in compound **5** are seven coordinate with an η^2-Ph_2pz ligand, two iodine atoms and three molecules of thf (Figure 3). The geometry is distorted pentagonal bipyramidal. The two iodine atoms are in a *trans* arrangement (I(1)-Lu–I(2) 173.750(3)°) but both are *cis* to the Ph_2pz (I(1)-Lu–C(8) 92.157° and I(2)-Lu–C(8) 93.815°). The Ph_2pz ligand and thf O(2) are almost linear (C(8)-Lu–O(2) 177.843°), but the O(1)–Lu–O(3) angle (159.600(3)°) deviates significantly from 180°.

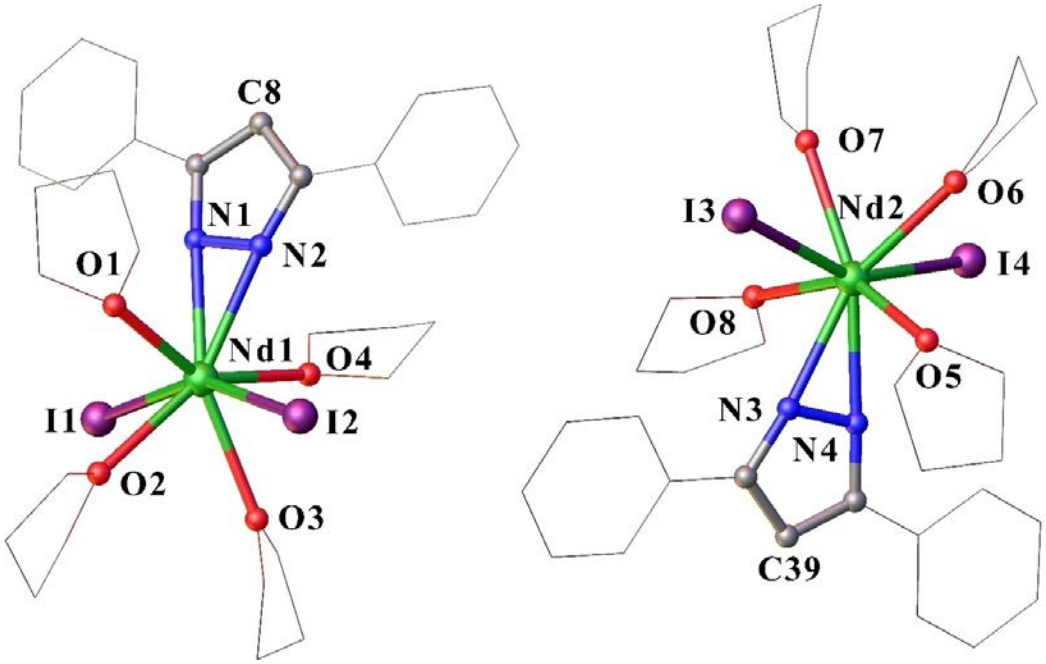


Figure 1. Molecular diagram of [Nd(Ph_2pz)I_2(thf)$_4$] (3). Hydrogen atoms are omitted and coordinated thf molecules and Ph groups are drawn as wireframe for clarity and thermal ellipsoids are set at the 50% probability level. Selected bond lengths (Å): Nd(1)-N(1) 2.458(9), Nd(1)-N(2) 2.451(9), Nd(1)-N(3) 2.449(10), Nd(1)-N(4) 2.467(10), Nd(1)-I(1) 3.161(13), Nd(1)-I(2) 3.169(12), Nd(1)-I(3) 3.149(15), Nd(1)-I(4) 3.165(15). More details including parameters for Ln(2) are in the supporting information (Table S1).

© 2024 Wiley-VCH GmbH

10990682c, 0 Downloaded from https://chemistry-europe.onlinelibrary.wiley.com/doi/10.1002/ejic.202400672 by James Cook University, Wiley Online Library on [09/01/2025]. See the Terms and Conditions (https://onlinelibrary.wiley.com/terms-and-conditions) on Wiley Online Library for rules of use; OA articles are governed by the applicable Creative Commons License

Research Article
doi.org/10.1002/ejic.202400672

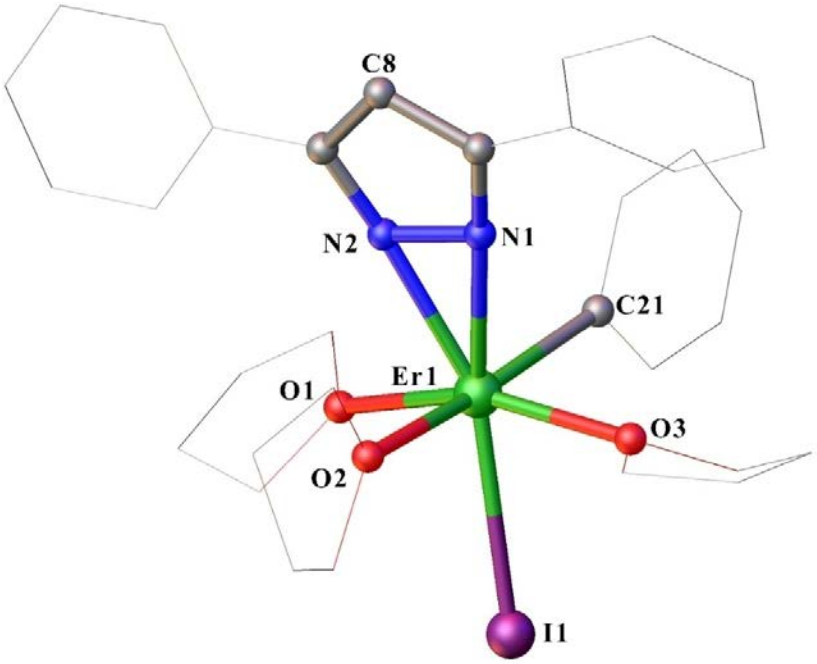


Figure 2. Molecular diagram of [ErPh(Ph$_2$pz)I(thf)$_3$]·thf (4a). Hydrogen atoms and lattice thf molecules are omitted and coordinated thf molecules and Ph groups are drawn as wireframe for clarity and thermal ellipsoids are set at the 50% probability level. Selected bond lengths (Å): Er(1)-N(1) 2.309(3), Er(1)-N(2) 2.318(3), Er(1)-C(21) 2.396(4), Er(1)-I(1) 3.0709(6). For more details, see the Supporting Information (Table S1).

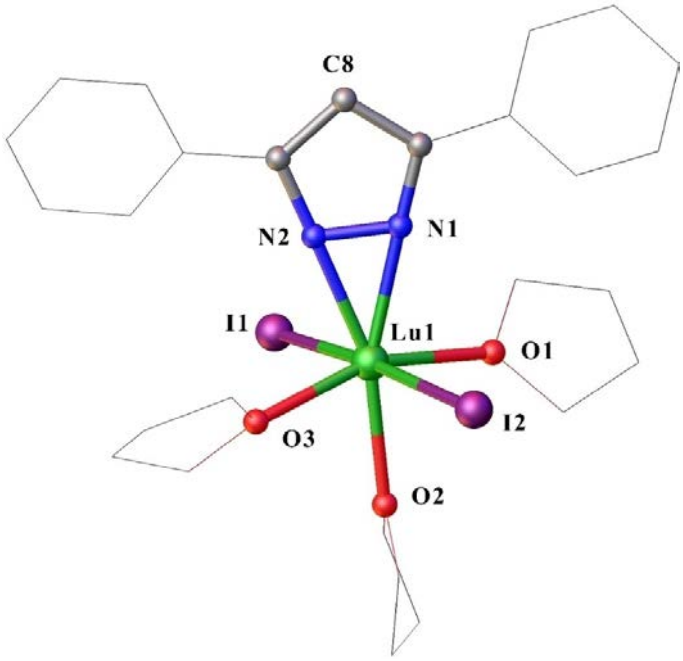


Figure 3. Molecular diagram of [Lu(Ph$_2$pz)I$_2$(thf)$_3$] (also representative of Er 4). Hydrogen atoms are omitted and coordinated thf molecules and Ph groups are drawn as wireframe for clarity and thermal ellipsoids are set at the 50% probability level. Selected bond lengths (Å): Lu(1)-N(1) 2.269(10), Lu(1)-N(2) 2.252(11), Lu(1)-I(1) 2.9637(14), Lu(1)-I(2) 3.0123(14). For more details, see the Supporting Information (Table S1).

The <Lu–N> bond length in **5** is 2.259(10) Å is slightly smaller than that (2.301(5) Å) of the six coordinate compound [Lu(Ap)Cl$_2$(thf)$_2$] {ApH = (2,6-diisopropylphenyl)-[6-(2,4,6-triisopropylphenyl)pyridin-2-yl]amine}),[18] with a bulkier bidentate ligand. The <Lu–O> bond length (2.315(9) Å) of compound **5** is close to the average Lu–O bond length 2.349(2) Å in compound [Lu(ImN^{Dipp})Cl$_2$(thf)$_3$] { ImN^{Dipp}H = 1,3-bis(2,6-diisopropylphenyl)imidazolin-2-imine}.[19]

Compounds [Ln(Ph$_2$pz)$_3$(CH$_3$CN)$_3$] (**6**, **7**) are isomorphous having similar crystallographic and molecular parameters, and crystallize in the monoclinic $P2_1/c$ space group and are monomeric (Figure 4). The nine coordinate Ln (Nd **6**, Gd **7**) metal atom is coordinated by three η^2-Ph$_2$pz ligands, and three CH$_3$CN ligands. The stereochemistry of these compounds is tricapped trigonal prismatic. The lanthanoid contraction is observed in the average Ln–N bond lengths < Nd–N > (2.52) > < Gd–N > (2.47).

Using [Nd(Ph$_2$pz)$_3$(CH$_3$CN)$_3$] (**6**) as a representative compound, all Ph$_2$pz ligands are unsymmetrically η^2-bonded to neodymium as the Nd–N lengths differ significantly 0.019 Å [N(1)-N(2)] through 0.029 Å [N(5)-N(6)] to the more substantial 0.076 Å [N(3)-N(4)]. All Ph$_2$pz ligands are *cis* to each other (C(8)-Nd–C(23) 95.529°, C(8)-Nd–C(38) 95.994° and C(23)-Nd–C(38) 98.496°), as are the MeCN ligands. Each CH$_3$CN is *transoid* to a Ph$_2$pz ligand (C(8)-Nd–N(8) 162.947°, C(23)-Nd–N(9) 161.916°, C(38)-Nd–N(7) 161.316°). The <Nd–N> bond length for Ph$_2$pz in **6** is 2.464(3) Å and is the same (2.467(9) Å) as in nine coordinate [Nd(Ph$_2$pz)$_3$(thf)$_3$].[20] The stereochemical arrangement in **6** is similar to that recently observed in [Sm{(Ph$_2$P(O))$_2$N}$_3$(CH$_3$CN)$_3$].[21]

Compound [Er(DippForm)I$_2$(thf)$_3$]·0.5thf crystallized in the orthorhombic space group *P*bca and is isomorphous with [Ln(DippForm)I$_2$(thf)$_3$]·0.5thf (Ln=La, Ce, Nd, Sm, Gd, Dy, Tb, Ho, Tm), but the reported [Er(DippForm)I$_2$(thf)$_3$]·2thf crystal-

© 2024 Wiley-VCH GmbH

10990682c, 0 Downloaded from https://chemistry-europe.onlinelibrary.wiley.com/doi/10.1002/ejic.202400672 by James Cook University, Wiley Online Library on [09/01/2025]. See the Terms and Conditions (https://onlinelibrary.wiley.com/terms-and-conditions) on Wiley Online Library for rules of use; OA articles are governed by the applicable Creative Commons License

Research Article
doi.org/10.1002/ejic.202400672

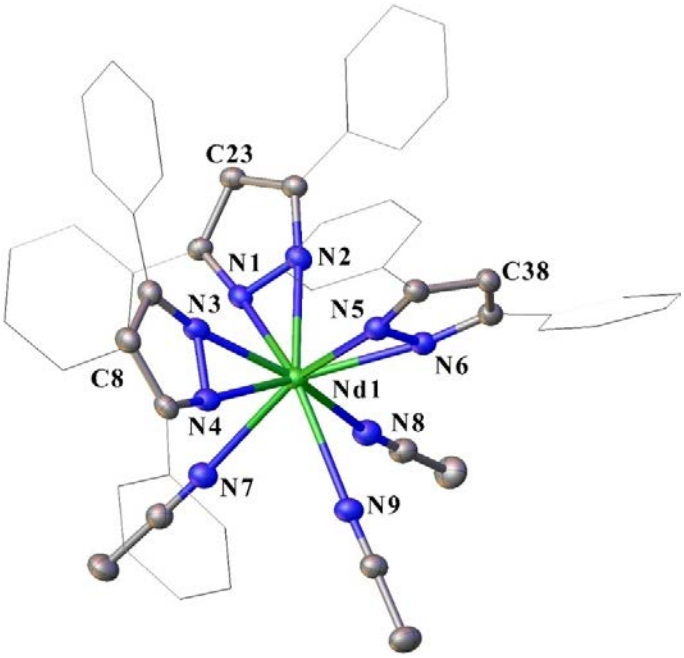


Figure 4. Molecular diagram of $[Nd(Ph_2pz)_3(CH_3CN)_3]\cdot 2CH_3CN$ (representative Nd 6, Gd 7). Hydrogen atoms and lattice CH_3CN are omitted, and Ph groups are drawn as wireframe for clarity and thermal ellipsoids are set at the 50% probability level. Selected bond lengths (Å): Nd(1)-N(1) 2.469(3), Nd(1)-N(2) 2.450(3), Nd(1)-N(3) 2.430(3), Nd(1)-N(4) 2.506(3), Nd(1)-N(5) 2.447(3), Nd(1)-N(6) 2.476(3), Nd(1)-N(7) 2.636(3), Nd(1)-N(8) 2.657(4), Nd(1)-N(9) 2.650(3); Gd(1)-N(1) 2.425(2), Gd(1)-N(2) 2.402(2), Gd(1)-N(3) 2.436(2), Gd(1)-N(4) 2.396(2), Gd(1)-N(5) 2.379(2), Gd(1)-N(6) 2.461(2), Gd(1)-N(7) 2.573(2), Gd(1)-N(8) 2.579(2), Gd(1)-N(9) 2.579(2). For more details, see the Supporting Information (Table S2).

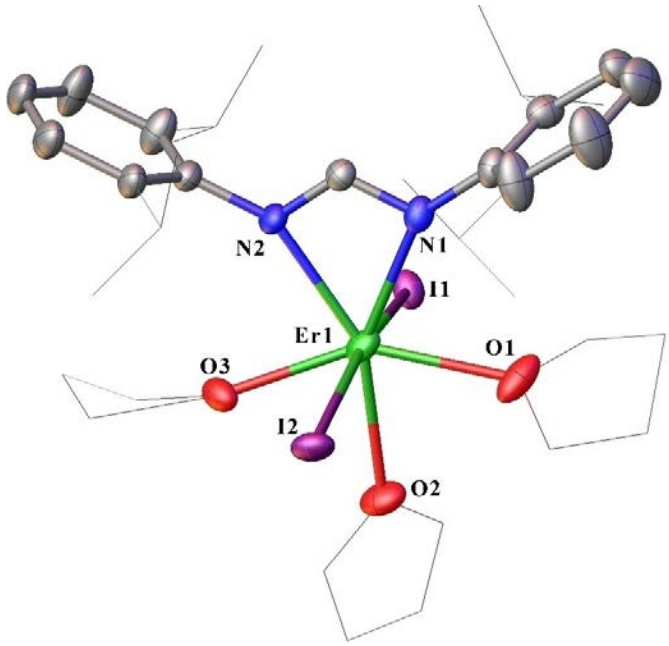


Figure 5. Molecular diagram of $[Er(DippForm)I_2(thf)_3]\cdot 0.5thf$ (9). Hydrogen atoms and lattice thf molecules are omitted and coordinated thf molecules and *i*Pr groups are drawn as wireframe for clarity and thermal ellipsoids are set to the 50% probability level. Selected bond lengths (Å): Er(1)-N(1) 2.384(5), Er(1)-N(2) 2.378(4), Er(1)-I(1) 3.012(7), Er(1)-I(2) 3.044(12). For more details, see the Supporting Information (Table S3).

lized in the triclinic space group with more solvent of crystallization.[14] The compound is monomeric and the geometry of the seven coordinate Er metal is pentagonal bipyramidal, with one chelating DippForm ligand, two *trans* iodide ligands (I(1)-Er–I(2) 165.17(3)°), and three thf ligands (Figure 5). The iodide ligands are *cisoid* to the DippForm ligand [I(1)-Er–C(13) is 96.045° and I(2)-Er–C(13) is 97.466°].

Compound $[Er(XylForm)I_2(thf)_3]\cdot thf$ (**11**) crystallized in the monoclinic space group *C*2/c. The monomeric Er^{III} compound **11** is seven coordinate, with one chelating XylForm ligand, two *transoid* iodide ligands (I(1)-Er–I(2) 170.100(2) and three thf ligands (Figure 6). The geometry of compound **11** is a distorted pentagonal bipyramid, which is similar to the reported $[Ln(ArForm)I_2(thf)_3]$ (ArForm = DFForm or DippForm).[13] The geometric parameters are consistent with those of other lanthanoid $[Ln(XylForm)_2I(thf)_2]$ (Ln=Nd, Gd, Tm, Lu) complexes.[14]

Conclusions

A significant number of $[La(Ph_2pz)I_2(thf)_n]$ (n = 3 or 4) complexes were synthesised through the oxidation of Hg -activated Ln^0 metals with PhI, followed by the addition of Ph_2pzH, in good crystalline yields. The coordination number of these monomeric complexes decreased from 8 in the case of lanthanoids with the larger atomic radii (La, Ce, Nd) to 7 for those with smaller atomic radii (Er, Lu). When CH_3CN was used as the solvent, nine coordinate $[Ln(Ph_2pz)_3(CH_3CN)_3]\cdot 2CH_3CN$ (Ln=Nd, Gd) complexes were obtained owing to protolysis of Schlenk equilibrium redistribution products. Thus the outcomes of protolysis of *in situ* generated lanthanoid(III) pseudo-Grignard reagents are dependent on the solvent. Further investigation into the reactivity of $Ph_pLn^{III}I_{(3-p)}$ with FormH (DippFormH or XylFormH) ligands led to the isolation of $[Ln(ArForm)I_2(thf)_3]\cdot nthf$ (n = 0.5 or 1) complexes. For $LnFormI_2$ derivatives, this synthesis is an alternative to reaction of Ln metals with iodine and formamidines,[13,14] but the pseudo-Grignard reagent method though simple, has the disadvantage of requiring activation of Ln metals by Hg. For $Ln(Ph_2pz)I_2$ complexes, the pseudo-Grignard reagent route holds sway as the Ln metal/I_2 method remains to be tested.

Experimental

General

The lanthanoid compounds described here are highly air and moisture sensitive, hence were prepared and handled using vacuum-nitrogen line techniques and a glovebox under an atmosphere of purified nitrogen. Lanthanoid metals were collected from Santoku/Molycorp/Eutectix. Large chunks were filed in the drybox before use. Ligands Ph_2pzH,[22] XylFormH and DippFormH[23] were synthesised according to the literature

© 2024 Wiley-VCH GmbH

10990682c, 0 Downloaded from https://chemistry-europe.onlinelibrary.wiley.com/doi/10.1002/ejic.202400672 by James Cook University, Wiley Online Library on [09/01/2025]. See the Terms and Conditions (https://onlinelibrary.wiley.com/terms-and-conditions) on Wiley Online Library for rules of use; OA articles are governed by the applicable Creative Commons License

Research Article
doi.org/10.1002/ejic.202400672

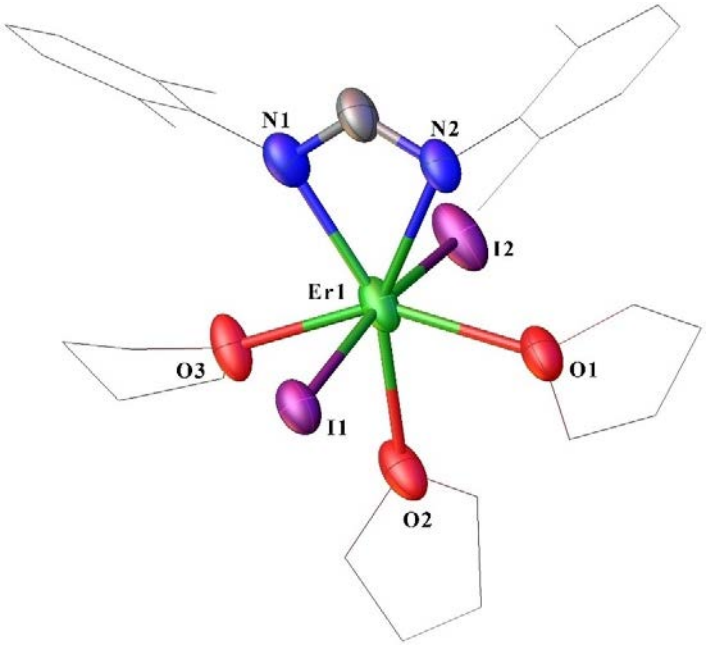


Figure 6. Molecular diagram of [Er(XylForm)I_2(thf)$_3$]·thf (11). Hydrogen atoms and lattice thf molecules are omitted and coordinated thf molecules and Ph, Xyl groups are drawn as wireframe for clarity and thermal ellipsoids are set to the 50% probability level. Selected bond lengths (Å): Er(1)-N(1) 2.354(9), Er(1)-N(2) 2.381(6), Er(1)-I(1) 3.008(8), Er(1)-I(2) 2.996(8). For more details, see the Supporting Information (Table S3).

methods. All other reagents were purchased from Sigma and used without purification. Solvents (THF, Acetonitrile and C_6D_6) were pre-dried by distillation over sodium or sodium benzophenone ketyl or calcium hydride before being stored under an atmosphere of nitrogen. Infrared spectra were recorded as Nujol mulls between NaCl plates using a Perkin-Elmer/Nicolet-Nexus 1600 FTIR instrument within the range 4000–650 cm^{-1}. ^{1}H NMR spectra were recorded with a Bruker 400 MHz instrument with dry perdeuterobenzene as the solvent. Satisfactory NMR spectra could not be obtained for Er^{III} complexes due to paramagnetism, except for 9. Melting points were determined in sealed glass capillaries under nitrogen. Metal analyses were carried out by complexometric titration (Xylenol orange as indicator and hexamethylenetetramine as buffer) after digesting with dilute hydrochloric acid.[24] Elemental analyses (C, H, N) were performed at the Microanalytical Laboratory, Science Centre, London Metropolitan University, England. The samples were sent in sealed glass pipettes under nitrogen. Crystals were immersed in crystallography oil and were examined using the MX1 beamline at the Australian Synchrotron. Crystal data and refinement details are given in Table S3 and associated text, and comments on crystal quality affecting R1 values and effects of twinning are there. CCDC 2384571 for compound **3**, 2384572 for compound **4a**, 2384573–2384575 for compounds **5–7**, 2384576 for compound **9**, 2384577 for compound **11**, contains the supplementary crystallographic data for this paper. These data can be obtained free of charge from The Cambridge Crystallographic Data Centre via www.ccdc.cam.ac.uk/data_request/cif.

Synthesis of Complexes 1–7

Ln metal powder (1.5 mmol) was suspended in dry THF/acetonitrile (15 ml) under N_2, and then PhI (2.0 mmol) and 1 drop Hg were added at room temperature. The mixture was sonicated for 10 min and stirred for 5 (La), 8 (Ce, Nd), 10 (Er) and 12 h (Lu) at room temperature, when a light brown colour solution formed. Ph_2pzH (1.0 mmol) was added, and the mixture was stirred at 0 °C for 1 h, and a coloured solution developed after stirring for 24 h at room temperature. The resulting mixture was filtered and concentrated to 5 ml under vacuum.

[La(Ph$_2$pz)I$_2$(thf)$_4$] 1

Colourless crystals (0.396 g, 44%) were obtained after cooling at −25 °C for 5 days. M. P. 128–130 °C. Elemental analysis: Found: C 41.32, H 4.46, N 2.75, La 15.62; $C_{31}H_{43}I_2LaN_2O_4$ (900.38 g/mol) requires: C 41.35, H 4.81, N 3.11, La 15.43. IR (Nujol): 1603 s, 1420 w, 1400 w, 1342 w, 1295 m, 1261 s, 1227 w, 1179 m, 1152 m, 1093 w, 1021 s, 969 s, 962 w, 919 s, 861 s-br, 808 m, 766 s, 698 s cm^{-1}. ^{1}H NMR (400.13 MHz, C_6D_6): δ = 1.27 (m, 16H, thf), 3.83(m, 16H, thf), 7.15 (t, 2H, H(4)), 7.29 (s, 1H, CH-pz), 7.37 (d, 4H, H(2,6)), 8.34 ppm(t, 4H, H(3,5)). For compound **1** (triclinic, ***P*-1** space group) the unit cell is: a = 8.986(7) Å, b = 18.420(2) Å, c = 20.510(2) Å, α = 99.09(4)°, β = 90.07(3)°, γ = 97.52(3)°, V = 3323(6) Å^3.

[Ce(Ph$_2$pz)I$_2$(thf)$_4$] 2

Colourless crystals (0.416 g, 46%) were obtained after cooling at −25 °C for 3 days. M. P. 135–137 °C. Elemental analysis: Found: C 40.87, H 4.53, N 2.91, Ce,15.82; $C_{31}H_{43}I_2N_2CeO_4$ (901.61 g/mole) requires: C 41.30, H 4.81, N 3.11, Ce 15.54. IR (Nujol): 1603 s, 1508 m, 1421 w, 1341 w, 1295 m, 1260 s, 1229 m, 1179 w, 1153 m, 1064 w, 1022 s, 970 s, 915 s, 866 s, 801 w, 762 s, 696 m, 684 m cm^{-1}. ^{1}H NMR (400.13 MHz, C_6D_6): δ = 0.61 (m, 16H, thf), 1.54(m, 16H, thf), 7.65 (t, 2H, H(4)), 7.79 (t, 4H, H(3,5)), 10.58 (d, 4H, H(2,6)), 13.52 ppm(s, 1H, CH-pz). For compound **2** (triclinic, ***P*-1** space group) the unit cell is: a = 8.983(2) Å, b = 18.355(4) Å, c = 20.473(4) Å, α = 98.62(3)°, β = 90.04(3)°, γ = 97.53(3)°, V = 3304.6(12) Å^3.

© 2024 Wiley-VCH GmbH

10990682c, 0 Downloaded from https://chemistry-europe.onlinelibrary.wiley.com/doi/10.1002/ejic.202400672 by James Cook University, Wiley Online Library on [09/01/2025]. See the Terms and Conditions (https://onlinelibrary.wiley.com/terms-and-conditions) on Wiley Online Library for rules of use; OA articles are governed by the applicable Creative Commons License

Research Article
doi.org/10.1002/ejic.202400672

10990682c, 0 Downloaded from https://chemistry-europe.onlinelibrary.wiley.com/doi/10.1002/ejic.202400672 by James Cook University, Wiley Online Library on [09/01/2025]. See the Terms and Conditions (https://onlinelibrary.wiley.com/terms-and-conditions) on Wiley Online Library for rules of use; OA articles are governed by the applicable Creative Commons License

[Nd(Ph$_2$pz)I$_2$(thf)$_4$] 3

Purple crystals (0.562 g, 62%) were obtained after cooling at −25 °C for 3 days. M. P. 123–125 °C. Elemental analysis: Found: C 40.03, H 4.42, N 3.23, Nd,16.42; $C_{31}H_{43}I_2N_2NdO_4$ (905.71 g/mol) requires: C 41.11, H 4.79, N 3.09, Nd, 15.93; loss of 0.5 thf of crystallization $C_{29}H_{39}I_2NdN_2O_{3.5}$ (869.71 g/mol) requires: C 40.04, H 4.51, N 3.22, Nd 16.58. IR (Nujol): 1603 s, 1510 m, 1419 w, 1341 m, 1294 m, 1261 s, 1228 w, 1179 m, 1153 m, 1073 w,1023 w, 969 s, 912 s, 807 w, 771 w, 698 s, 686w, 666w cm^{-1}. ^{1}H NMR (400.13 MHz, C_6D_6): δ = 1.26 (m, 16H, thf), 1.74 (m, 16H, thf), 8.45 (m, 6H, H(3,4,5)), 13.88 (d, 4H, H(2,6)), 26.17 (s, 1H, CH-pz).

[Er(Ph$_2$pz)I$_2$(thf)$_3$] 4 and [Er(Ph$_2$pz)(Ph)I(thf)$_3$].thf 4 a

Pink crystals of **4 a** (0.132 g, 15%) were obtained after standing at −25 °C for 5 days. M. P. 137–139 °C. Pink crystals of **4** (0.427 g, 46%) were obtained after another 3 days from the mother liquor. M. P. 125–127 °C. Elemental analysis **4**: Found: C 35.12, H 3.99, N 3.62, Er 21.42; $C_{27}H_{35}ErI_2N_2O_3$ (856.65 g/mol) requires: C 37.86, H 4.12, N 3.27, Er 19.52; loss of one thf of crystallisation $C_{23}H_{27}ErI_2N_2O_2$ (784.54 g/mol) requires: C 35.21, H 3.47, N 3.57, Er 21.32. IR (Nujol): 1603 s, 1508 w, 1421 m, 1408 m, 1342 m, 1293 w, 1281 w, 1261 s, 1227 m, 1174 s, 1093 w, 1073 w, 1055 m, 1012 s, 913 w, 857 s, 822 m, 774 w, 763 m, 703w cm^{-1}. The unit cell of **4** is: a = 15.367(3) Å, b = 12.038(2) Å, c = 31.263(6) Å, α = 90°, β = 97.88(3)°, γ = 90°, V = 5729(2) Å^3.

[Lu(Ph$_2$pz)I$_2$(thf)$_3$] 5

Colourless crystals (0.41 g, 47%) were obtained for 3 days. M. P. 118–120 °C. Elemental analysis: Found: C 38.97, H 4.07, N 3.10, Lu 20.04; $C_{27}H_{35}I_2LuN_2O_3$ (864.34 g/mol) requires: C 37.52, H 4.08, N 3.24, Lu, 20.24; extra 0.5 thf from solvation $C_{29}H_{39}I_2LuN_2O_{3.5}$ (890.4 g/mol) requires: C 39.40, H 4.44, N 3.16, Lu, 19.65. IR (Nujol): 1604 s, 1508 w, 1422 m, 1410 m, 1343 m, 1297 m, 1281 w, 1261 w, 1227 s, 1189 w, 1177 w, 1152 w, 1095 w, 1068 w, 1053 m, 1022 w, 971 s, 916 s, 857 s-br, 769 s, 722 s cm^{-1}. ^{1}H NMR (400.13 MHz, C_6D_6): δ = 1.10 (m, 16H, thf), 3.75(m, 16H, thf), 7.29 (d, 4H, H(2,6)), 7.34 (t, 2H, H(4)), 7.52 (s, 1H, CH-pz), 8.34 ppm(t, 4H, H(3,5)), 1 extra thf from solvation.

[Nd(Ph$_2$pz)$_3$(CH$_3$CN)$_3$]·2CH$_3$CN 6

The yellow needle crystals (0.56 g, 62%) were obtained after cooling at −25 °C for 3 days. M. P. 195–197 °C (decomposed). Metal analysis: Found: Nd 15.48; $C_{55}H_{48}N_{11}Nd$ (1007.28 g/mol) requires: 14.32; loss of 1 CH_3CN of crystallization requires $C_{53}H_{45}N_{10}Nd$ (966.23 g/mol): Nd 14.93. IR (Nujol): 2297 m, 2270 m, 2250 w, 1603 s, 1511 w, 1421 w, 1364 w, 1281 w, 1222 m, 1159 m, 1073 w, 1058 s, 1027 m, 999 w, 970 s, 929 w, 917 m, 758 s cm^{-1}. ^{1}H NMR (400.13 MHz, C_6D_6): δ = −1.65 (s, 12H, CH_3CN), 7.79 (t, 18H, H(3,4,5)), 10.91 (d, 12H, H(2,6)), 16.77 (s, 3H, CH-pz) corresponding to loss of 1 CH_3CN.

[Gd(Ph$_2$pz)$_3$(CH$_3$CN)$_3$]·2CH$_3$CN 7

Colourless crystals (0.228 g, 22%) were obtained after cooling at −25 °C for 4 days. M. P. 148–150 °C. Metal analysis: Found Gd 16.42; $C_{55}H_{48}N_{11}Gd$ (1020.29 g/mol) requires: Gd, 15.41; loss of 1 CH_3CN of crystallization, $C_{53}H_{45}N_{10}Gd$ (979.24 g/mol) requires: Gd, 16.06. IR (Nujol): 2299 m, 2272 m, 2250 w, 1603 s, 1512 w, 1422 w, 1367 w, 1281 w, 1270 w, 1222 m, 1156 m, 1084 w, 1073 w, 1060 s, 1027 m, 1000 m, 970 s, 929 w, 917 m, 758 s cm^{-1}. ^{1}H NMR (400.13 MHz, C_6D_6): δ = Very broad paramagnetic peak.

Synthesis of Complexes 8–11

The syntheses were carried out as for **1–7**, except that DippFormH/XylFormH (0.5 mmol) was added with other reagents scaled in proportion.

[Nd(DippForm)I$_2$(thf)$_3$]·thf 8

Purple crystals (0.386 g, 73.5%) were obtained after cooling at −25 °C for 2 days. M.P. 221–223 °C, reported M. P. 226–228 °C.[13] Metal Analysis: Found: Nd 14.88, $C_{41}H_{67}I_2N_2O_4Nd$ (1050.6 g/mol) requires: Nd 13.74; loss of 1 thf of crystallization, $C_{37}H_{59}I_2N_2O_3Nd$ (977.92 g/mol) requires: Nd 14.75. IR and ^{1}H NMR consistent with the reported.[13] For compound **8** (orthorhombic, *P*bca space group) the unit cell is: a = 19.66 Å, b = 18.90 Å, c = 24.05 Å, V = 8872.6(3) Å^3, the reported unit cell is: a = 19.6958(3) Å, b = 18.9803(3) Å, c = 24.0171(5) Å, V = 8978.4(3) Å^3.[13]

[Er(DippForm)I$_2$(thf)$_3$]·0.5 thf 9

Pink crystals (0.238 g, 46%) were obtained after cooling at −25 °C for 5 days. M.P. 248–250 °C. Elemental analysis: Found: C 45.41, H 6.31, N 2.55, Er 16.34; $C_{39}H_{63}ErI_2N_2O_{3.5}$ (1036.99 g/mol) requires: C 45.17, H 6.12, N 2.70, Er 16.13. IR (Nujol): 1664 m, 1593 m, 1559 w, 1379 s, 1360 m, 1334 w, 1275 s, 1195 s, 1100 m, 1067 m, 1018 s, 914 m, 870 s, 805 s, 773 s, 762 m cm^{-1}. ^{1}H NMR (C_6D_6): δ = −6.66 (m, 14H, thf), −3.51 (m, 4H, CH), 1.21 (t, 2H, H(4)), 3.42 (s, 1H, NC(H)N), 5.69 (m, 14H, thf), 5.80 (d, 24H, CH_3), and 25.24 ppm (d, 4H, H(3,5)).

[Nd(XylForm)I$_2$(thf)$_3$]·thf 10

Light blue crystals (0.299 g, 69%) were obtained after cooling at −25 °C for 2 days. M.P. 201–203 °C, reported M. P. 202–205 °C.[14]. Metal analysis: Nd 17.58, $C_{33}H_{51}I_2N_2NdO_4$ (937.79 g/mol) requires: Nd 16.38; loss of 1.5 thf $C_{27}H_{39}I_2N_2NdO_{2.5}$ (829.69 g/mol) requires: Nd 17.37. IR consistent with the reported.[14] ^{1}H NMR (400.13 MHz, C_6D_6): δ = 2.08 (m, 12H, thf), 4.79 (m, 24H, thf, CH_3), 8.34 (t, 2H, H(4)), 10.10 (d, 4H, H(3,5)), 30.60 ppm (s, 1H, NCHN). For compound **10** (orthorhombic, *P*bca space group) the unit cell is a = 19.66(2) Å, b = 18.932(3) Å, c = 24.052(6) Å, V = 8912.2(3) Å^3, the reported unit cell is a = 19.6958(3) Å, b = 18.9803(3) Å, c = 24.0171(5) Å, V = 8978.4(3) Å^3.[14]

[Er(XylForm)I$_2$(thf)$_3$]·thf 11

Pink crystals (0.0.296 g, 62%) were obtained after cooling at −25 °C for 4 days. M.P. 182–184 °C. Found: C 41.53, H 5.31, N 2.75, Er 17.98; $C_{33}H_{51}ErI_2N_2O_4$ (960.81 g/mol) requires: C 41.25, H 5.35, N 2.75, Er 17.41. IR (Nujol): 1656 m, 1594 m, 1532 s, 1279 s, 1210 s, 1068 s, 1015 s, 945 m, 917 s, 858 s, 773 s, 734w cm^{-1}.

Without Activation with Hg

Ln metal powder (Ln=La, Nd) was suspended in dry THF (15 ml) under N_2, and then PhI was added at room temperature. The mixture was sonicated for 10 mins and stirred at room temperature. A brown coloured solution formed after 15 h for La and 36 h for Nd, (slower than the same reactions activated by one drop of Hg). From La metal colourless crystals (0.272 g, 30%), M. P. 130–132 °C. IR and ^{1}H NMR spectra agreed with those of structurally characterised compound **1**.

© 2024 Wiley-VCH GmbH

Research Article
doi.org/10.1002/ejic.202400672

10990682c, 0 Downloaded from https://chemistry-europe.onlinelibrary.wiley.com/doi/10.1002/ejic.202400672 by James Cook University, Wiley Online Library on [09/01/2025]. See the Terms and Conditions (https://onlinelibrary.wiley.com/terms-and-conditions) on Wiley Online Library for rules of use; OA articles are governed by the applicable Creative Commons License

Acknowledgements

PCJ, VLB and GBD gratefully acknowledge the ARC for funding (DP230100112). Parts of this research were undertaken on the MX1 beamline at the Australian Synchrotron, part of ANSTO.[25]

Conflict of Interests

The authors declare no conflict of interest.

Data Availability Statement

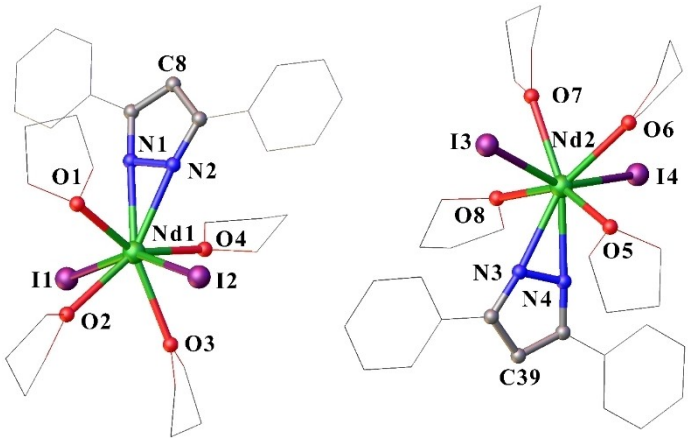
The data that support the findings of this study are available from the corresponding author upon reasonable request.

Keywords: Pseudo-Grignard reagents · Lanthanum · Cerium · Neodymium · Erbium · Lutetium · Oxidative addition · Lanthanoid(III) complexes · Crystal structures

[1] E. S. Petrov, D. M. Roitershtein, L. F. Rybakova, *J. Organomet. Chem.* **2002**, *647*, 21–27.
[2] M. N. Bochkarev, L. N. Zakharov, G. S. Kalinina, *Organoderivatives of Rare Earth Elements*, **1995**, Springer Science, Dordrecht, Ch. *8*, 364–423.
[3] M. A. Halim, Z. Guo, V. L. Blair, G. B. Deacon, P. C. Junk, *J. Organomet. Chem.* **2024**, *1010*, 123094.
[4] A. Mortis, R. Anwander, *Eur. J. Inorg. Chem.* **2024**, *27*, e202400127.
[5] D. F. Evans, G. V. Fazakerley, R. F. Phillips, *J. Chem. Soc. A.* **1971**, 1931–1934.
[6] B. A. Dolgoplosk, E. I. Tinyakova, I. N. Markevich, T. V. Soboleva, G. M. Chernenko, O. K. Sharaev, V. A. Yakovlev, *J. Organomet. Chem.* **1983**, *255*, 71–79.
[7] F. T. Edelmann, D. M. M. Freckmann, H. Schumann, *Chem. Rev.* **2002**, *102*, 1851–1896.
[8] F. Ortu, *Chem. Rev.* **2022**, *122*, 6040–6116.
[9] M. Wiecko, G. B. Deacon, P. C. Junk, *ChemComm.* **2010**, *46*, 5076–5078.
[10] S. H. Ali, G. B. Deacon, P. C. Junk, S. Hamidi, M. Wiecko, J. Wang, *Chem. Eur. J.* **2018**, *24*, 230–242.
[11] M. A. Halim, Z. Guo, G. B. Deacon, P. C. Junk, *Chem. Eur. J.* **2023**, *29*, e20230095.
[12] Z. Guo, J. Luu, V. Blair, G. B. Deacon, P. C. Junk, *Eur. J. Inorg. Chem.* **2019**, 1018–1029.
[13] Z. Guo, V. L. Blair, G. B. Deacon, P. C. Junk, *ChemComm.* **2021**, *57*, 11513–11516.
[14] Z. Guo, M. A. Halim, V. L. Blair, G. B. Deacon, P. C. Junk, *Chem Asian J.* **2023**, *18*, e202300333.
[15] A. O. Tolpygin, O. A. Linnikova, T. A. Kovylina, A. V. Cherkasov, G. K. Fukin, A. A. Trifonov, *Russ. Chem. Bull., Int. Ed.* **2019**, *68*, 32–39.
[16] R. D. Shannon, *Acta Crystallogr. Sect. A.* **1976**, *32*, 751–767.
[17] D. P. Mills, A. J. Wooles, J. McMaster, W. Lewis, A. J. Blake, S. T. Liddle, *Organometallics.* **2009**, *28*, 6771–6776.
[18] S. M. Guillaume, M. Schappacher, N. M. Scott, R. Kempe, *J. Polym. Sci., Part A: Polym. Chem.* **2007**, *45*, 3611–3619.
[19] T. K. Panda, S. Randoll, C. G. Hrib, P. G. Jones, T. Bannenberg, M. Tamm, *Chem. Commun.* **2007**, 5007–5009.
[20] J. E. Cosgriff, G. B. Deacon, B. M. Gatehouse, *Aust. J. Chem.* **1993**, *46*, 1881–1896.
[21] S. Rangarajan, O. Beaumont, M. S. Balakrishna, G. B. Deacon, V. L. Blair, *Inorganica Chim. Acta.* **2025**, *574*, 122385.
[22] J. Elguero, E. Gonzalez, R. Jacquier, *Bull. Soc. Chim. Fr.* **1968**, 707–713.
[23] R. M. Roberts, *J. Org. Chem.* **1949**, *14*, 277–284.
[24] G. Dchwarzenbach, H. A. Flaschka, Complexometric Titrations, Methuen, Publishing Ltd, London, **1969**.
[25] T. J. Boyle, L. A. M. Ottley, T. M. Alam, M. A. Rodriguez, P. Yang, S. K. Mcintyre, *Polyhedron* **2010**, *29*, 1784–1795.

Manuscript received: October 9, 2024
Revised manuscript received: November 5, 2024
Accepted manuscript online: November 5, 2024
Version of record online: ■■, ■■

© 2024 Wiley-VCH GmbH



*M. Abdul Halim, Z. Guo, V. L. Blair, G. B. Deacon, P. C. Junk**

1 – 10

Syntheses of Pyrazolato- and Formamidinato-lanthanoid(III) Diiodides from *in Situ* Generated lanthanoid(III) Pseudo-Grignard Reagents

Trivalent lanthanoid pseudo-Grignard reagents $Ph_pLn^{III}I_{(3-p)}$ (p = 1 or 2; Ln = La, Ce, Nd, Er and Lu) are readily prepared by the oxidation of lanthanoid metal with iodobenzene at 25 °C, following pre-activation of the metal with 1 drop Hg in tetrahydrofuran (thf) or acetonitrile (CH_3CN) and brief sonication. The protolysis of $Ph_pLn^{III}I_{(3-p)}$ with 3,5-diphenylpyrazole (Ph_2pzH) yields pyrazolato complexes [Ln-(Ph_2pz)I_2(thf)$_n$].

10990682c, 0, Downloaded from https://chemistry-europe.onlinelibrary.wiley.com/doi/10.1002/ejic.202400672 by James Cook University, Wiley Online Library on [09/01/2025]. See the Terms and Conditions (https://onlinelibrary.wiley.com/terms-and-conditions) on Wiley Online Library for rules of use; OA articles are governed by the applicable Creative Commons License

Check for updates

ACES Asian Chemical Editorial Society

doi.org/10.1002/asia.202300333

CHEMISTRY AN ASIAN JOURNAL Research Article

www.chemasianj.org

VIP

Direct Reaction – One Step Route to Synthesize Lanthanoid-iodide Formamidinates**

Zhifang Guo,[a, b] Md Abdul. Halim,[b] Victoria L. Blair,[a] Glen B. Deacon,[a] and Peter C. Junk*[b]

Abstract: This paper describes a novel and simple method – direct reaction of lanthanoid metals with equimolar amounts of iodine and a formamidine under ultrasonication as an effective, metal-based route to lanthanoid(III) diiodide formamidinates, namely **I**. *N,N′*-Bis(2,6-diisopropylphenyl)formamidinatodiiodidolanthanoid(III) complexes [Ln(DippForm)I_2(thf)$_3$] (Ln = La, **1**, Ce, **2**, Tb, **3**, Ho, **4**, Er, **5**, Tm, **6**); **II**. *N,N′*-Bis(2,6-diethylphenyl)formamidinatodiiodidolanthanoid(III) complexes [Ln(EtForm)I_2(thf)$_3$] (Ln = Ce, **7**, Nd, **8**, Gd, **9**, Tb, **10**, Dy, **11**, Ho, **12**, Er, **13**, Lu, **14**). **III**. *N,N′*-bis(2,6-dimethylphenyl)formamidinatodiiodidolanthanoid(III) complexes [Ln(XylForm)I_2(thf)$_3$] (Ln = Ce, **15**, Nd, **16**, Gd, **17**, Tm, **18**, Lu **19**); **IV**. *N,N′*-bis(phenyl)formamidinatodiiodidolanthanoid complexes [Ln(PhForm)I_2(thf)$_3$] (Ln = Nd, **20**, Gd, **21**, Er, **22**). Compound [Ce(XylForm)$_2$I(thf)$_2$] (**23**) was also synthesized by the same method except the ratio of I_2 to XylFormH was 1 : 4. Divalent *N,N′*-bis(2,6-diisopropylphenyl)formamidinato-iodido-lanthanoid(II) complexes [Eu(DippForm)I(thf)$_4$]·thf (**24**), [Yb(DippForm)I(thf)$_3$]·2DippFormH (**25**), [Sm(DippForm)I(thf)$_4$]·thf (**26**) have also been synthesized by direct reactions of the free metals, iodine and DippFormH. Interestingly, [Sm(DippForm)I_2(thf)$_3$] (**27**) was obtained by the oxidation of [Sm(DippForm)I(thf)$_4$]·thf (**26**) on exposure to air. *N,N′*-Bis(2,6-dimethylphenyl)formamidinatoiodidosamarium(II) [Sm(XylForm)I(thf)$_3$]$_n$ (**28**) was also prepared by direct reaction of Sm, iodine and XylFormH (mole ratio of I_2: XylFormH = 1 : 2). All products have been identified by X-ray crystallography and all the trivalent complexes [Ln(Form)$_n$I$_{3-n}$] (n = 1 or 2) are stable to rearrangement.

Introduction

Reactive heteroleptic lanthanoid(III) complexes, including hydrides, amides, alkoxides, aryloxides, and cyclopentadienyls have usually been synthesized from $LnLX_2$ or LnL_2X (L = anionic ligand, X = halide) complexes by metathesis reactions (Scheme 1).[1–6] The reactants [Ln(L)$_n$X$_{3-n}$] (X = Cl, Br, I) have usually been prepared by metathesis reactions with stoichiometric modification (Scheme 2, eq. (1)).[7–8] However, metathesis syntheses of [Ln(L)$_n$X$_{3-n}$] (n = 1 or 2) compounds have potential rearrangement outcomes (Scheme 2, eq. (2)). Rearrangement reactions between LnL_3 and LnX_3 complexes provide another general approach but are subject to similar rearrangement issues (Scheme 2, eq. (3)) with the low solubility of $LnCl_3$ species inhibiting successful outcomes.[6b] The Dolgoplosk group and co-workers have successfully synthesised trivalent lanthanoid complexes [(Ph$_3$C)$_2$LnCl], [(Ph$_3$C)LnCl$_2$], and the sesquichloride complex [(Ph$_3$C)$_3$Ln$_2$Cl$_3$] (Ln = Pr^{3+}, Nd^{3+}, Gd^{3+} and Ho^{3+}) employing lanthanoid metals and triphenylmethyl chloride, but the products underwent rearrangement and no crystal structures were reported.[9]

To prepare divalent heteroleptic lanthanoid complexes [LnL(L′)], pseudo-Grignard reagents "RLnI" are a potential starting point and can be prepared by the reaction of organic iodides with lanthanoid metals.[10] However most attention has been given to their unique reducing properties and their alkylation/arylation capacity.[11–14] Limited crystallographic characterization of such species has been performed by utilising bulky ligands.[14] Divalent lanthanoid-iodide pyrazolates [LnPh$_2$pzI(thf)$_4$] (Ln = Eu, Yb),[15] and lanthanoid-iodide formamidinates [Ln(Form)$_n$I$_{3-n}$] (n = 1 or 2) (Ln = Eu, Yb) (FormH = XylFormH, MesFormH and DippFormH (ArNCHNAr; Ar = 2,6-Me$_2$C$_6$H$_3$, 2,4,6-Me$_3$C$_6$H$_2$, and 2,6-iPr$_2$C$_6$H$_3$)[16] have been prepared by the sonication of lanthanoid metal with iodobenzene, followed by the addition of a trapping proligand (pzH or FormH), but all the reported complexes were limited to those of the divalent favouring lanthanoids Eu/Yb, and the lanthanoid formamidinates were obtained in low yields owing to Schlenk equilibrium and (for Yb) oxidation to Ln^{III}.

Lanthanoid complexes have been successfully prepared by direct reaction of rare earth metals and protic agents (for example 3,5-disubstituted pyrazoles, pyrazolones, 2,6-di*iso*propylphenol and other phenols) with small amount of iodine as an activation catalyst (Scheme 3, eq. (1)).[17] This method provides encouragement to extend the applicability of iodine activated Ln metals in synthesis. Initially, the aim of this work was to synthesize lanthanoid formamidinates [Ln(ArForm)$_3$] by direct reaction of iodine activated Ln metals and formamidines, but [Ln(ArForm)$_2$I] complexes were also obtained with low

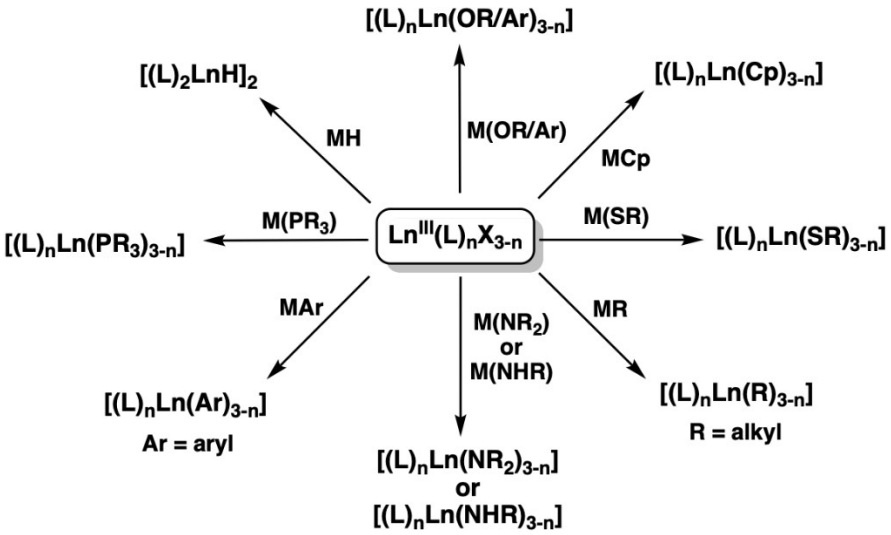
[a] Dr. Z. Guo, Dr. V. L. Blair, Prof. Dr. G. B. Deacon
School of Chemistry, Monash University, Clayton, VIC, 3800 (Australia)
[b] Dr. Z. Guo, M. A. Halim, Prof. Dr. P. C. Junk
College of Science & Engineering, James Cook University, Townsville, QLD, 4811 (Australia)
E-mail: peter.junk@jcu.edu.au

[**] We dedicate this paper to Professor Frank T. Edelmann of Otto-von-Guericke-Universität Magdeburg in recognition of his major contribution to rare earth chemistry and for his valuable help to other workers in the field with his annual reviews of progress in the area.

Supporting information for this article is available on the WWW under https://doi.org/10.1002/asia.202300333

© 2023 The Authors. Chemistry - An Asian Journal published by Wiley-VCH GmbH. This is an open access article under the terms of the Creative Commons Attribution Non-Commercial NoDerivs License, which permits use and distribution in any medium, provided the original work is properly cited, the use is non-commercial and no modifications or adaptations are made.

© 2023 The Authors. Chemistry - An Asian Journal published by Wiley-VCH GmbH



Scheme 1. Heteroleptic lanthanoid metal-organic compounds synthesized from $[Ln^{III}(L)_nX_{3-n}]$.

$$LnX_3 + n\,ML \longrightarrow [Ln(L)_nX_{3-n}] + n\,MX \quad (X = Cl, Br, I;\ M = Li, Na, K) \qquad (1)$$

$$2\,[X_2LnL] \rightleftharpoons LnX_3 + [LnL_2X] \rightleftharpoons 1/2\,LnL_3 + 1/2\,[X_2LnL] \qquad (2)$$

$$n\,LnL_3 + (3\text{-}n)\,LnX_3 \longrightarrow 3\,[LnL_nX_{3-n}] \qquad (3)$$

Scheme 2. Metathesis syntheses and potential rearrangement of $[Ln(L)_nX_{3-n}]$.

$$Ln + n\,LH \xrightarrow[I_2\text{ as catalyst};\ n = 2 \text{ or } 3]{thf} Ln(L)_n + n/2\,H_2 \qquad (1)$$

$$2Ln + (3\text{-}n)\,I_2 + 2n\,LH \xrightarrow[n = 1 \text{ or } 2]{} 2\,Ln(L)_n(I)_{3-n} + n\,H_2 \qquad (2)$$

Scheme 3. Synthesis of lanthanoid complexes with I_2.

yields in addition to $[Ln(ArForm)_3]$.[18] Hence, it appeared possible to exploit this observation and synthesize $[Ln(ArForm)_nI_{3-n}]$ complexes on a preparative scale (Scheme 3, eq. (2)). These are potentially valuable synthons for a wide range of heteroleptic complexes, such as hydrides, organometallics, cyclopentadienyls, organoamides, and organo-oxides, etc. (Scheme 1, X = I)

Recently we presented a preliminary report that this simple method gave a number of trivalent lanthanoid formamidinates $[Ln(ArForm)_nI_{3-n}]$ (ArForm = *N,N*′-bis(2,6-difluorophenyl)formamidinate (DFForm), or *N,N*′-bis(2,6-diisopropylphenyl)formamidinate (DippForm)) in reasonable yields.[19] For the less bulky DFFormH, the stoichiometry n = 1 or 2 can be controlled by employing different ratios of iodine and DFFormH, but the bulkier DippFormH gave only diiodides. For Eu and Yb, the heteroleptic [Ln(DFForm)I] was obtained together with the Schlenk equilibrium products, $[Ln(DFForm)_2]$, and $[LnI_2]$. This paper examines the generality of the direct reaction of Ln, I_2 and different formamidines to afford new $[Ln(ArForm)I_2]$ (ArForm = DippForm, EtForm, XylForm, PhForm Scheme 4) complexes in good yields.

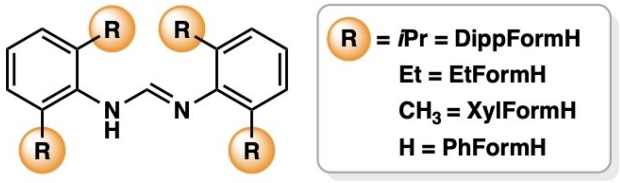
Results and discussion

Synthesis of formamidinatoiodidolanthanoid(III) complexes

The *N,N*′-bis(2,6-diisopropylphenyl)formamidinatodiiodidolanthanoid(III) complexes, $[La(DippForm)I_2(thf)_3]\cdot 0.5thf$ **1**, [Ce-

© 2023 The Authors. Chemistry - An Asian Journal published by Wiley-VCH GmbH

1861471x, 2023, 14, Downloaded from https://aces.onlinelibrary.wiley.com/doi/10.1002/asia.202300333 by Eddie Koiki Mabo Library, Wiley Online Library on [01/09/2024]. See the Terms and Conditions (https://onlinelibrary.wiley.com/terms-and-conditions) on Wiley Online Library for rules of use; OA articles are governed by the applicable Creative Commons License



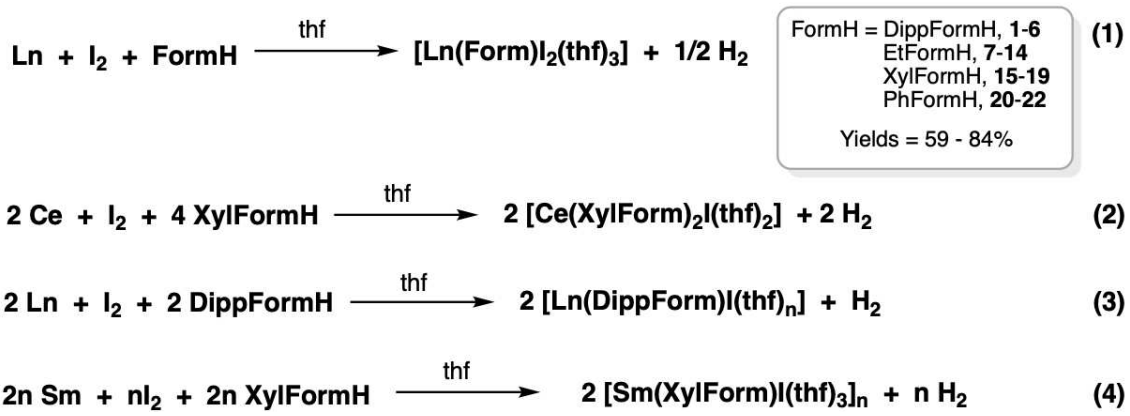
Scheme 4. N,N′-Bis(aryl)formamidine (ArFormH) proligands used in this paper.

$(DippForm)I_2(thf)_3]\cdot 0.5thf$ **2**, $[Tb(DippForm)I_2(thf)_3]\cdot 0.5thf$ **3**, $[Ho(DippForm)I_2(thf)_3]\cdot 0.5thf$ **4**, $[Er(DippForm)I_2(thf)_3]\cdot 2thf$ **5** and $[Tm(DippForm)I_2(thf)_3]\cdot 0.5thf$ **6**, *N,N′*-bis(2,6-diethylphenyl)formamidinatodiiodidolanthanoid complexes $[Ln(EtForm)I_2(thf)_3]\cdot thf$ (Ln = Ce, **7**, Nd, **8**, Gd, **9**, Tb, **10**, Dy, **11**, Ho, **12**, Er, **13**, Lu, **14**), *N,N′*-bis(2,6-dimethylphenyl)formamidinatodiiodidolanthanoid complexes, $[Ce(XylForm)I_2(thf)_3]\cdot 1.5thf$ **15**, $[Nd(XylForm)I_2(thf)_3]\cdot thf$ **16**, $[Gd(XylForm)I_2(thf)_3]\cdot thf$ **17**, $[Tm(XylForm)I_2(thf)_3]\cdot thf$ **18**, and $[Lu(XylForm)I_2(thf)_3]\cdot thf$ **19**, and *N,N′*-bis(diphenyl)formamidinatodiiodidolanthanoid complexes $[Ln(PhForm)I_2(thf)_3]$ (Ln = Nd, **20**, Gd, **21**, Er, **22**) were prepared by direct reactions between an excess of lanthanoid metal, iodine and the corresponding pro-ligand FormH (DippFormH, EtFormH, XylFormH, and PhFormH) (mole ratio of I_2: FormH = 1 : 1) in thf on ultrasonication (Scheme 5, eq. (1)). This greatly extends the scope of the synthetic method from the examples $[Ln(DippForm)I_2(thf)_3]$ (Ln = Nd, Gd, Dy, Lu) of our preliminary report.[19] For the bulky ligand DippFormH, the reaction was complete in one week, while all other subjected ligands required only three days. Compound $[Ce(XylForm)_2I(thf)_2]\cdot 2.25thf$ **23** was also synthesized by the same method except the ratio of I_2 to XylFormH was 1 : 4 (Scheme 5, eq. (2)). As **15** and **23** were prepared successfully, both reactions (Scheme 5, eq. (1) and (2)) can work with the same metal. However, the synthesis of $[Ln(XylForm)_2I]$ failed for the smaller metals Gd and Tm with $[Ln(XylForm)I_2]$ isolated instead. Likewise an attempt to prepare $[Ce(EtForm)_2I]$ for the bulkier Form ligand furnished $[Ce(EtForm)I_2]\cdot 2thf$, a different solvate from complex **7**. So far $[Ln(Form)_2I]$ complexes are only generally accessible for the smaller DFForm.[19] Single crystals of the trivalent complexes $[Ln(DippForm)I_2(thf)_3]$ (**1**–**4**, and **6**) have the same composition as the reported $[Ln(DippForm)I_2(thf)_3]$ (Ln = Nd, Gd, Dy, Lu), previously characterized as mono(thf) solvates.[19]

Good yields (based on the FormH ligands) of crystalline products were obtained from the concentrated filtrates. Complexes **1**–**23** were characterized by single crystal X-ray diffraction and the bulk samples by metal analysis after problems with some microanalyses. These were close to the values expected for the compositions found by X-ray crystallography or to values corresponding to loss of lattice/coordinated thf solvent (see below). Appropriate ^1H NMR spectra were obtained for diamagnetic **1**, **14**, and **19** (Figure S1, S4, S6) and paramagnetic **7**, **8**, **15**, and **12** (Figure S2, S3, S5), but again with loss of thf in some cases. Infrared spectra (see experimental section) showed features expected for the Form ligands together with ring stretching C–O bands of coordinated thf[20] at *ca.* 1010 and 870–850 cm^{-1}.

Synthesis of formamidinatoiodidolanthanoid(II) complexes

N,N′-Bis(2,6-diisopropylphenyl)formamidinatoiodidolanthanoid(II) complexes $[Eu(DippForm)I(thf)_4]\cdot thf$ **24**, $[Yb(DippForm)I(thf)_3]\cdot 2DippFormH$ **25** and $[Sm(DippForm)I(thf)_4]\cdot thf$ **26** were also prepared by direct reactions of the free metals, iodine and DippFormH (mole ratio of I_2: DippFormH = 1 : 2) on ultrasonication for three days (Scheme 5 eq. (3)). Crystalline products were obtained by evaporation of the filtrates under vacuum. For Sm, the trivalent compound $[Sm(DippForm)I_2(thf)_3]\cdot 0.5thf$ **27** was obtained by the oxidation of divalent $[Sm(DippForm)I(thf)_4]$ **26** on brief exposure to air. A co-product must be formed, e.g. Sm(DippForm)O, but only single crystals of **27** were identified. The extreme sensitivity to oxygen of **26** is shown by an attempted visible/near infrared spectrum obtained under inert atmosphere conditions, since this showed features of Sm^{II} (**26**)[21a] and Sm^{III} (**27**)[21b–e] (Experimental section), despite the



Scheme 5. Synthesis of formamidinatoiodidolanthanoids.

© 2023 The Authors. Chemistry - An Asian Journal published by Wiley-VCH GmbH

1861471x, 2023, 14, Downloaded from https://aces.onlinelibrary.wiley.com/doi/10.1002/asia.202300333 by Eddie Koiki Mabo Library, Wiley Online Library on [01/09/2024]. See the Terms and Conditions (https://onlinelibrary.wiley.com/terms-and-conditions) on Wiley Online Library for rules of use; OA articles are governed by the applicable Creative Commons License

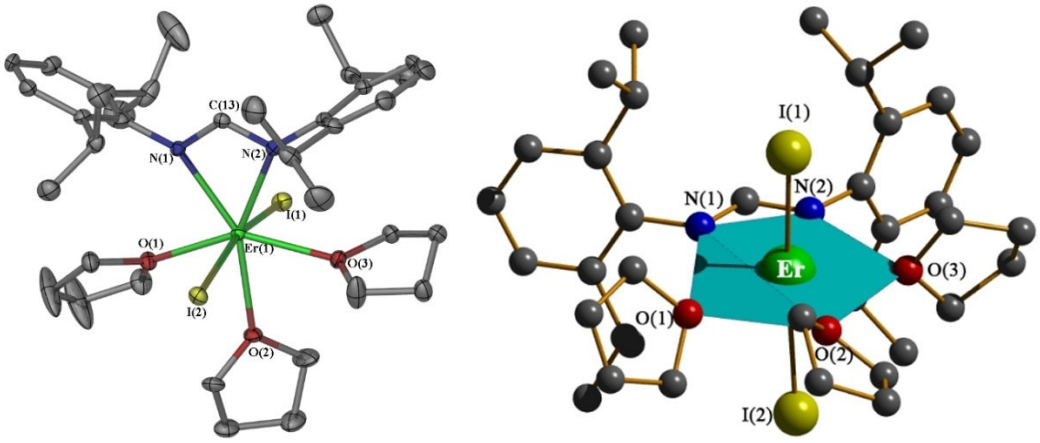


Figure 1. Molecular structure of [Er(DippForm)I_2(thf)$_3$] (representative of La, **1**, Ce, **2**, Tb, **3**, Ho, **4**, Er, **5**, Tm, **6**, Sm, **27**) with non-hydrogen atoms represented by 50% thermal ellipsoids. The lattice thf molecules and hydrogen atoms have been omitted for clarity. Selected bond lengths (Å) and angles (°) for **5** Er–N(1) 2.395(2), Er–N(2) 2.366(2), Er–O(1) 2.3905(19), Er–O(2) 2.4458(19), Er–O(3) 2.384(2), Er–I(1) 3.0107(2), Er–I(2) 3.0044(2), O(1)–Er–O(2) 74.00(7), O(1)–Er–O(3) 147.25(7), O(2)–Er–O(3) 73.40(7), I(1)–Er–I(2) 165.565(7), C(13)–Er–I(1) 99.99(6), C(13)–Er–I(2) 94.44(6).

solution having the deep blue colour characteristic of **26** (see picture in Figure S7). The multiple bands in the near infrared region are as expected for Sm^{III}.[21b–e] Complex [Yb(DippForm)I(thf)$_3$]·2DippFormH **25**, previously obtained as a mono(tetrahydrofuran) solvate [Yb(DippForm)I(thf)$_3$]·thf,[16] has now been obtained with free pro-ligand of crystallization. Complex [Eu(DippForm)I(thf)$_4$]·thf **24** has been previously observed and reported.[16] The *N,N'*-bis(2,6-dimethylphenyl)formamidinatoiodidolanthanoid(II) complex [Sm(XylForm)I(thf)$_3$]$_n$ **28** was also prepared by direct reaction of Sm metal, iodine and XylFormH (mole ratio of I_2: XylFormH = 1 : 2) (Scheme 5, eq. (4)).

Molecular structures

Representative structures of **1**–**28** are shown in Figures 1–6, which also list selected bond angles (°) and lengths (Å). Additional structural metrics are available in the SI.

Complexes [Ln(DippForm)I_2(thf)$_3$] (1-6 and 27)

All [Ln(DippForm)I_2(thf)$_3$] (Ln = La, **1**, Ce, **2**, Tb, **3**, Ho, **4**, Er, **5**, Tm, **6**, Sm, **27**) complexes, **1**–**4**, **6** and **27** crystallize in the orthorhombic space group *Pbca*, and are isomorphs of [Ln(DippForm)I_2(thf)$_3$].thf (Ln = Nd, Gd, Dy)[19] despite lattice solvent differences. Only complex **5** crystallized in the triclinic space group *P*-1, and is an isomorph of [Lu(DippForm)I_2(thf)$_3$]·2thf.[19] The complexes are monomeric and the Ln atoms are found to be seven coordinate at the centre of a pentagonal bipyramid, with one chelating DippForm ligand, two *transoid* iodide ligands, and three thf ligands (Figure 1). The I(1)–Ln–I(2) angles are from 165.565(7)–167.58(2)°, displaying a near linear coordination of the negatively charged donor atoms. Three O atoms (from thf) in a *mer* array and two N atoms are in the equatorial plane with Ln^{III} (Figure 1 RHS). The iodide ligands are *cisoid* to

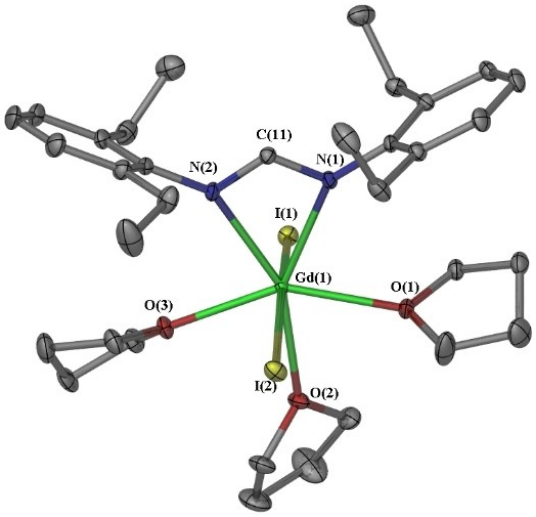


Figure 2. Molecular structure of [Gd(EtForm)I_2(thf)$_3$] (representative of Ce, **7**, Nd, **8**, Gd, **9**, Tb, **10**, Dy, **11**, Ho, **12**, Er, **13**, Lu, **14**) with non-hydrogen atoms represented by 50% thermal ellipsoids. Selected bond lengths (Å) and angles (°) **9** Gd–N(1) 2.4216(16), Gd–N(2) 2.4244(16), Gd–O(1) 2.4353(14), Gd–O(2) 2.4627(14), Gd–O(3) 2.4231(14), Gd–I(1) 3.04992(17), Gd–I(2) 3.04930(17), O(1)–Gd–O(2) 73.38(5), O(1)–Gd–O(3) 149.11(5), O(2)–Gd–O(3) 75.92(5), I(1)–Gd–I(2) 166.490(5), C(11)–Gd–I(1) 97.234, C(11)–Gd–I(2) 96.215.

the DippForm ligand (I(1)–Ln–C(13) and I(2)–Ln–C(13) are 94–100°). The average Ln–N bond lengths for **1**–**6**, and **27** are 2.52 (2.524(3) and 2.514(3)), 2.50 (2.493(10) and 2.498(11)), 2.41(2.407(3) and 2.412(3)), 2.39 (2.391(7) and 2.392(8)), 2.38 (2.395(2) and 2.366(2)), 2.37 (2.371(4) and 2.364(4)) and 2.44 (2.438(6) and 2.435(6)) Å respectively, and the average Ln–I bond lengths for **1**–**6**, and **27** are 3.17 (3.1676(4) and 3.1684(4)), 3.15 (3.1451(13) and 3.1462(13)), 3.04 (3.0369(4) and 3.0514(3)), 3.03 (2.991(10) and 3.059(3)), 3.01 (3.0107(2) and 3.0044(2)), 3.00 (3.0081(5) and 2.9935(5)) and 3.10 (3.0877(7) and 3.110(4)) Å respectively, with the sequential decreases being consistent with the lanthanoid contraction.

© 2023 The Authors. Chemistry - An Asian Journal published by Wiley-VCH GmbH

1861471x, 2023, 14, Downloaded from https://aces.onlinelibrary.wiley.com/doi/10.1002/asia.202300333 by Eddie Koiki Mabo Library, Wiley Online Library on [01/09/2024]. See the Terms and Conditions (https://onlinelibrary.wiley.com/terms-and-conditions) on Wiley Online Library for rules of use; OA articles are governed by the applicable Creative Commons License

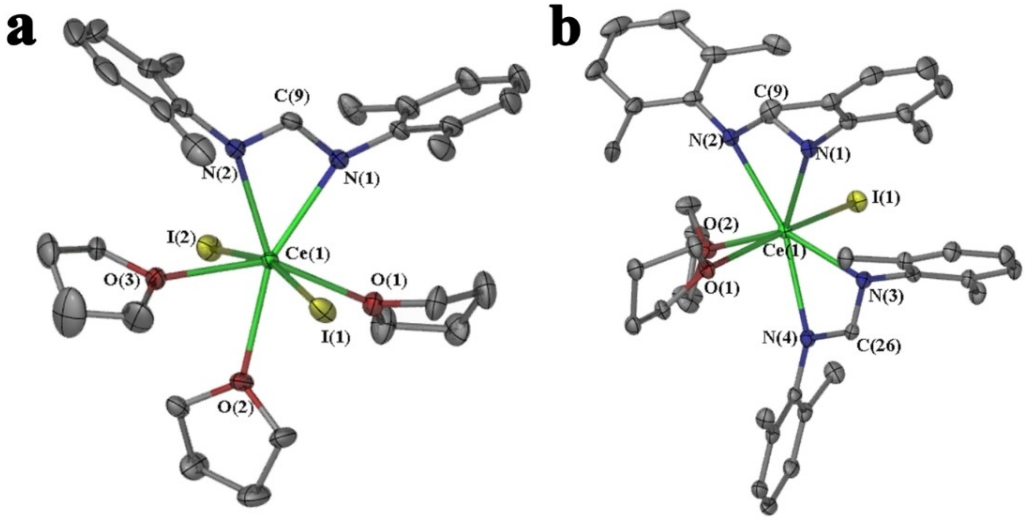


Figure 3. Molecular structure of (**a**) [Ce(XylForm)I_2(thf)$_3$] (representative of Ce, **15**, Nd, **16**, Gd, **17**, Tm, **18**, Lu, **19**) and (**b**) [Ce(XylForm)$_2$I(thf)$_2$] **23** with non-hydrogen atoms represented by 50% thermal ellipsoids. Selected bond lengths (Å) and angles (°) **15** Ce–N(1) 2.493(3), Ce–N(2) 2.486(3), Ce–O(1) 2.496(2), Ce–O(2) 2.570(2), Ce–O(3) 2.496(2), Ce–I(1) 3.1359(3), Ce–I(2) 3.1449(3), O(1)–Ce–O(2) 77.33(8), O(1)–Ce–O(3) 150.18(8), O(2)–Ce–O(3) 72.89(8), I(1)–Ce–I(2) 165.53(3), C(9)–Ce–I(1) 98.59(7), C(9)–Ce–I(2) 95.88(7); **23** Ce–N(1) 2.538(2), Ce–N(2) 2.543(2), Ce–N(3) 2.478(2), Ce–N(4) 2.575(2), Ce–O(1) 2.532(2), Ce–O(2) 2.574(2), Ce–I(1) 3.1379(6), O(1)–Ce–I(1) 162.09(5), O(2)–Ce–I(1) 82.71(5), O(1)–Ce–O(2) 80.18(7), C(9)–Ce–C(26) 136.79(8).

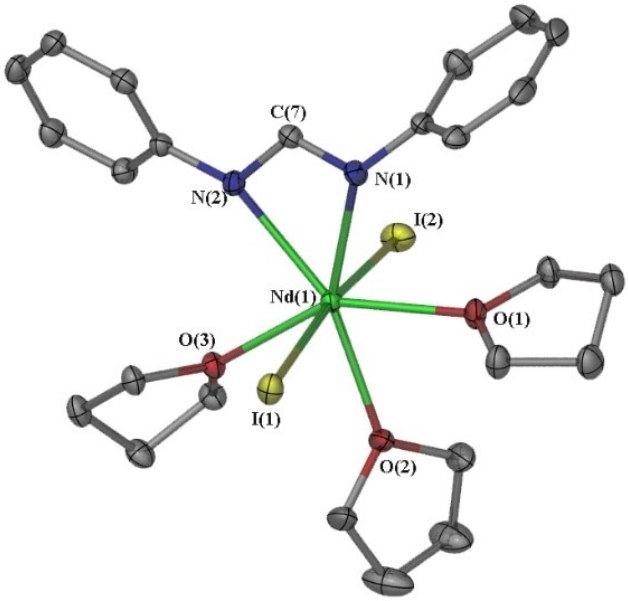


Figure 4. Molecular structure of [Nd(PhForm)I_2(thf)$_3$] (representative of Nd, **20**, Gd, **21**, Er, **22**) with non-hydrogen atoms represented by 50% thermal ellipsoids. Selected bond lengths (Å) and angles (°) **20** Nd–N(1) 2.440(3), Nd–N(2) 2.492(3), Nd–O(1) 2.483(3), Nd–O(2) 2.505(3), Nd–O(3) 2.456(2), Nd–I(1) 3.0929(6), Nd–I(2) 3.1061(6), O(1)–Nd–O(2) 72.55(10), O(1)–Nd–O(3) 147.91(9), O(2)–Nd–O(3) 75.37(9), I(1)–Nd–I(2) 171.982(9), C(7)–Nd–I(1) 99.01(8), C(7)–Nd–I(2) 88.99(8).

Complexes [Ln(EtForm)I_2(thf)$_3$] (7–14)

All [Ln(EtForm)I_2(thf)$_3$]·thf complexes (**7**–**14**) crystallize in the triclinic space group *P*-1. The Ln^{3+} ion is monomeric and seven coordinate, with one chelating EtForm ligand, two *transoid* iodide ligands (e.g. I(1)–Gd–I(2) 166.490(5)°; range 166.024(10) to167.054(6)°), and three *mer* thf ligands (Figure 2). The Ln^{3+} ion possesses a distorted pentagonal bipyramidal coordination with three O atoms and two N atoms in the equatorial plane. The average Ln–N, Ln–O, and Ln–I bond lengths for **7**–**14** (see SI section 1.2) are consistent with the lanthanoid contraction.

Complexes [Ln(XylForm)I_2(thf)$_3$] (15–19 and 23)

All [Ln(XylForm)I_2(thf)$_3$] complexes (**15-19**) crystallize in the monoclinic space group *C*2/*c*. The Ln^{3+} ion in **15**–**19** is monomeric and seven coordinate, with one chelating XylForm ligand, two *transoid* iodide ligands (I(1)–Ln–I(2) 164.12(14) to 172.90(8)°), and three thf ligands (Figure 3a). The Ln^{3+} ion possesses a distorted pentagonal bipyramidal coordination sphere, which is similar to complexes **1**–**14** and the reported [Ln(ArForm)I_2(thf)$_3$] (ArForm = DFForm or DippForm).[19] The I-(1)–Ln–I(2) bond angles are close to linear. The average Ln–N, Ln–O, and Ln–I bond lengths for **15**–**19** are consistent with the lanthanoid contraction. The X-ray crystal structure of [Ce-(XylForm)$_2$I(thf)$_2$] **23** reveals a monomeric and seven coordinate complex, comprising two chelating XylForm ligands (C9–Ln–C26 136.79(8)°), one terminal iodide ligand, and two *cis* thf ligands (O1–Ce–O2 80.18(7)°) (Figure 3b), which is different from [Ln(DFForm)$_2$I(thf)$_2$] which has two *trans* thf ligands (O1–Ln–O1# from 170 to 172 °).[19]

Complexes [Ln(PhForm)I_2(thf)$_3$] (20–22)

[Ln(PhForm)I_2(thf)$_3$] (Ln = Nd, **20**, Gd, **21**, Er, **22**) crystallize in the monoclinic space group $P2_1/c$ (**20**) and $P2_1/n$ (**21**, **22**). The complexes are monomeric and seven coordinate, with one chelating PhForm ligand, two *transoid* iodide ligands, and three

© 2023 The Authors. Chemistry - An Asian Journal published by Wiley-VCH GmbH

1861471x, 2023, 14, Downloaded from https://aces.onlinelibrary.wiley.com/doi/10.1002/asia.202300333 by Eddie Koiki Mabo Library, Wiley Online Library on [01/09/2024]. See the Terms and Conditions (https://onlinelibrary.wiley.com/terms-and-conditions) on Wiley Online Library for rules of use; OA articles are governed by the applicable Creative Commons License

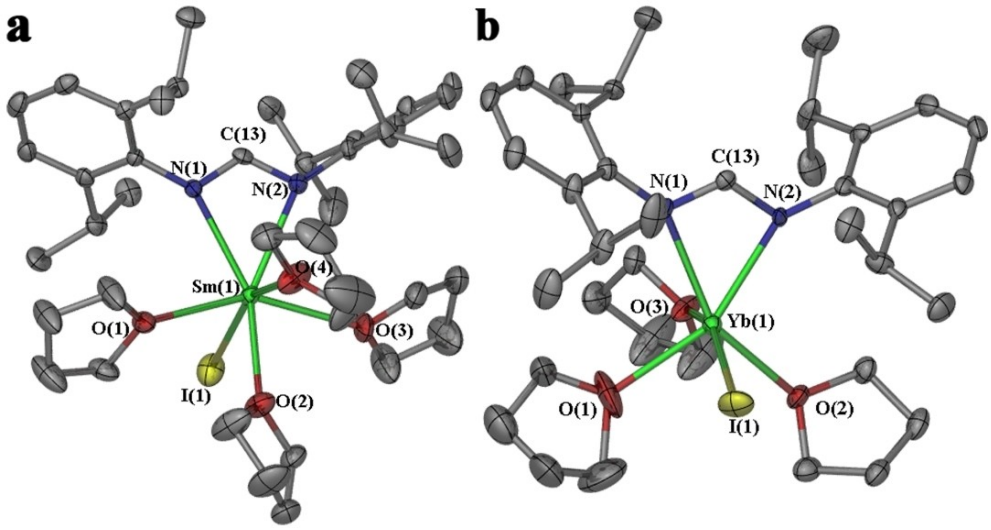


Figure 5. Molecular structure of **(a)** [Sm(DippForm)I(thf)$_4$]·thf (representative of Eu, **24**, Sm, **26**) **(b)** [Yb(DippForm)I(thf)$_3$]·2DippFormH (**25**) with non-hydrogen atoms represented by 50% thermal ellipsoids. The lattice thf molecules, DippFormH and hydrogen atoms have been omitted for clarity. Selected bond lengths (Å) and angles (°) **25** Yb–N(1) 2.466(5), Yb–N(2) 2.463(4), Yb–O(1) 2.443(5), Yb–O(2) 2.416(4), Yb–O(3) 2.449(4), Yb–I(1) 3.1241(4), C(13)–Yb–I(1) 109.93(11), O(1)–Yb–O(2) 101.82(19), O(1)–Yb–O(3) 78.50(19), O(2)–Yb–O(3) 78.76(15), I(1)–Yb–O(1) 86.17(16), I(1)–Yb–O(2) 88.49(10), I(1)–Yb–O(3) 157.49(10), C(13)–Yb–O(1) 129.8(2), C(13)–Yb–O(2) 124.93(15), C(13)–Yb–O(3) 92.57(15); **26** Sm–N(1) 2.598(6), Sm–N(2) 2.642(6), Sm–O(1) 2.570(6), Sm–O(2) 2.612(6), Sm–O(3) 2.632(6), Sm–O(4) 2.600(6), Sm–I(1) 3.2752(10), C(13)–Sm–I(1) 111.44(14), O(1)–Sm–O(2) 72.4(2), O(1)–Sm–O(3) 150.2(8), O(1)–Sm–O(4) 89.1(2), O(2)–Sm–O(3) 78.7(2), O(2)–Sm–O(4) 72.5(2), O(3)–Sm–O(4) 86.3(2), I(1)–Sm–O(1) 90.00(14), I(1)–Sm–O(2) 86.92(15), I(1)–Sm–O(3) 84.09(17), I(1)–Sm–O(4) 158.62(16), C(13)–Sm–O(1) 103.07(19), C(13)–Sm–O(2) 161.3(2), C(13)–Sm–O(3) 105.8(2), C(13)–Sm–O(4) 89.5(2).

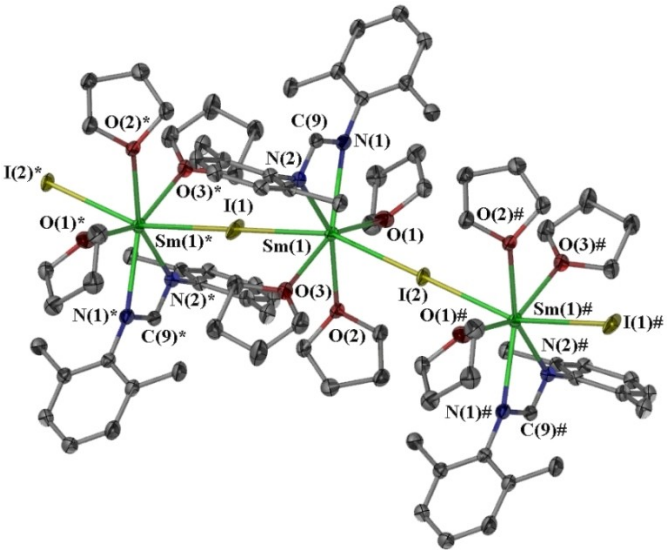


Figure 6. Molecular structure of [Sm(XylForm)I(thf)$_3$]$_n$ **28** with non-hydrogen atoms represented by 50% thermal ellipsoids. Selected bond lengths (Å) and angles (°) **28** Sm–N(1) 2.637(4), Sm–N(2) 2.565(4), Sm–O(1) 2.583(4), Sm–O(2) 2.641(4), Sm–O(3) 2.621(4), Sm–I(1) 3.2824(8), Sm–I(2) 3.2873(7), O(1)–Sm–O(2) 70.01(12), O(1)–Sm–O(3) 150.64(12), O(2)–Sm–O(3) 83.19(8), I(1)–Sm–I(2) 160.017(11), C(9)–Sm–I(1) 94.59(8), C(9)–Sm–I(2) 104.05(8). Symmetry operators: *1-x, 1-y, 1-z; #1-x, 1-y, 2-z.

thf ligands (Figure 4), and are otherwise similar to the preceding complexes **1**–**19**.

Overall, the structures of complexes **1**–**22** have a striking structural similarity to those of [LnCpI$_2$(thf)$_3$] (Ln = Sm, Tm),[22] where a Cp is interchanged for a Form ligand. The average Sm–I and Sm–O bond lengths of [Sm(DippForm)I$_2$(thf)$_3$]·0.5thf **27** are 3.10 and 2.47 Å, similar to [SmCpI$_2$(thf)$_3$] <Sm-I 3.16 Å> and <Sm-O> 2.46 Å.[22a] The average <Tm-I> bond lengths are 3.00 and 2.99 Å for complexes [Tm(DippForm)I$_2$(thf)$_3$]·0.5thf **6** and [Tm(XylForm)I$_2$(thf)$_3$]·thf **18**, and average <Tm-O> bond lengths are 2.41 and 2.38 Å respectively, which are comparable to [TmCpI$_2$(thf)$_3$] <Tm-I> 3.09 Å>; <Tm-O> 2.36 Å>.[22b] The longer <Ln-I> values for the Cp complexes are as expected for the higher formal cordination number (8) compared with 7 for the Form complexes. However the same relationship is not seen for the <Ln-O&gt bond lengths which are either similar for Ln = Sm, or longer in the Form complexes for Ln = Tm. Despite the formal coordination number difference, the similarities in the structures support the view that formamidinates can be regarded as N donor alternatives to cyclopentadienyls.

Complexes [Ln(DippForm)I(thf)$_n$] (24–26)

Single crystals of [Ln(DippForm)I(thf)$_4$]·thf (Ln = Eu, **24**, Sm, **26**) are isomorphous, and **24** has unit cell parameters in agreement with the reported X-ray data for [Eu(DippForm)I(thf)$_4$]·thf.[16] Compounds **24** and **26**, which crystallize in the monoclinic space group $P2_1/c$, are seven coordinate pseudo-octahedral, with one chelating DippForm ligand, one iodide ligand and four molecules of thf (Figure 5a). [Yb(DippForm)I(thf)$_3$]·2DippFormH (**25**), solvated with two proligands of crystallization, crystallizes in the monoclinic space group *Pc* (Figure 5b). The complex is monomeric and the Yb^{2+} ion is six coordinate distorted-octahedral, with one chelating DippForm ligand, one iodide ligand and three thf donors. The structure is similar to that of the reported [Yb(DippForm)I(thf)$_3$]·thf. The reduced coordina-

© 2023 The Authors. Chemistry - An Asian Journal published by Wiley-VCH GmbH

1861471x, 2023, 14, Downloaded from https://aces.onlinelibrary.wiley.com/doi/10.1002/asia.202300333 by Eddie Koiki Mabo Library, Wiley Online Library on [01/09/2024]. See the Terms and Conditions (https://onlinelibrary.wiley.com/terms-and-conditions) on Wiley Online Library for rules of use; OA articles are governed by the applicable Creative Commons License

tion number compared to those of the seven-coordinate Eu (**24**) and Sm (**26**) complexes is consistent with the smaller ionic radius of Yb^{2+}.[23] For complexes **24**–**26**, the DippForm ligand and iodide ligand are arranged in a *cisoid* fashion [C(13)–Yb–I(1) 109.93(11)°, C(13)–Sm–I(1) 111.44(14)°]. The average Ln–N bond lengths are 2.47 Å (2.466(5) and 2.463(4)) for Yb **25** [2.43 Å in [Yb(DippForm)I(thf)$_3$]·thf], and 2.62 Å (2.598(6) and 2.642(6)) for Sm **26**, and 2.60 Å for the reported [Eu(DippForm)I-(thf)$_4$]·thf.[16] The Ln–I bond length is 3.1241(4) Å for Yb [3.05 Å in [Yb(DippForm)I(thf)$_3$]·thf], 3.2752(10) Å for Sm, and 3.26 Å for reported [Eu(DippForm)I(thf)$_4$]·thf,[16] respectively, which are consistent with the lanthanoid ion radii differences.

Complex [Sm(XylForm)I(thf)$_3$]$_n$ 28

The polymeric compound [Sm(XylForm)I(thf)$_3$]$_n$ **28** crystallizes in the triclinic space group *P*-1, and has seven coordinate pseudo-octahedral stereochemistry for the Sm^{2+} ions, with one chelating XylForm ligand, two *transoid* iodide ligands (I-(1)–Sm–I(2) 160.017(11)°), and three thf donors (Figure 6). The XylForm ligand and the iodide ligands are arranged in a *cisoid* fashion [C(9)–Sm–I(1) 94.59(8), C(9)–Sm–I(2) 104.05(8)]. The [Sm(XylForm)I(thf)$_3$] units are bridged by the I1 and I2 atoms, and each unit is inverted by the symmetry code: *1-x,1-y,1-z and #1-x,1-y,2-z. Compared to the divalent [Sm(DippForm)I-(thf)$_4$] with a terminal I atom, the less bulky XylForm forms a polymer with one more coordinated I, but one less thf molecule. This change reduces steric crowding.[24]

Conclusions

A simple reaction between free lanthanoid metals, iodine, and formamidines (FormH) provides a convenient high yield synthesis of multiple [Ln(Form)I$_2$(thf)$_3$] (Form = DippForm, EtForm, XylForm, PhForm) complexes **1**–**23**, thereby establishing the generality of the method. The products are stable to rearrangement, hence are potential reagents to access a wide variety of heteroleptic lanthanoid formamidinates [Ln(Form)X$_2$] (e.g. X = R, OAr, Cp, NR$_2$ etc). All are seven coordinate monomers with *transoid* iodides with a structural similarity to the corresponding cyclopentadienyls, supporting the potential of formamidinates as N-donor alternatives to Cps. Attempts to obtain [Ln(Form)$_2$I-(thf)$_n$] by stoichiometric modification of the synthesis were much less successful implying a steric block in the synthesis. The method was also adapted to give Ln^{II}(Form)I (Ln = Sm, Eu, Yb) **24-26** complexes but the samarium(II) derivatives were exceptionally air sensitive. [Sm^{II}(XylForm)I(thf)$_3$]$_n$ is a novel iodide bridged polymer contrasting the monomeric structure for similarly crystallised [Sm(DippForm)I(thf)$_4$].

Experimental

General

The lanthanoid compounds described here are highly air- and moisture- sensitive, hence they were prepared and handled using vacuum-nitrogen line techniques and a dry box under an atmosphere of purified nitrogen. All formamidines were prepared by reported literature methods.[25] Lanthanoid metals were purchased from Santoku/Molycorp/Eutectix. Large chunks of the representative Ln metals were filed in the drybox before use. All other reagents were purchased from Sigma and used without purification. Solvents (thf, toluene and C_6D_6) were pre-dried by distillation over sodium or sodium benzophenone ketyl before being stored under an atmosphere of nitrogen over 3 Å molecular sieves. IR spectra were recorded as Nujol mulls between NaCl plates using an Agilent Technologies Cary 630 FTIR or a Perkin Elmer 1600 Series FTIR instrument within the range 4000–700 cm^{-1}. UV-Vis-NIR spectra were collected as solution in a J. Young valve quartz cell (1 mm) on a Cary 5G UV-Vis-NIR Spectrophotometer. ^{1}H NMR spectra were recorded with a Bruker 400 MHz spectrometer. Microanalyses were determined by the Elemental Analysis Service, London Metropolitan University, with all samples sealed in tubes under nitrogen. The metal analyses were carried out after decomposition of the sample with dilute HCl, buffering and complexometric titration with Na_2H_2(edta) and Xylenol Orange indicator. Melting points were determined in sealed glass capillaries under nitrogen and are uncalibrated. Crystals were measured on a Rigaku SynergyS diffractometer or at the Australian Synchrotron on the MX1 macromolecular beamlines. Crystal data and refinement details are given in Table S1. CCDC 2255902–2255924 for compounds **1**–**23**, 2255925–2255928 for compounds **25**–**28**, contain the supplementary crystallographic data for this paper. These data can be obtained free of charge from The Cambridge Crystallographic Data Centre (CCDC) via www.ccdc.cam.ac.uk/data_request/cif.

Synthesis of formamidinatoiodidolanthanoid(III) complexes

General procedure for 1–22

Lanthanoid metal powder (1.0 mmol), iodine (0.25 mmol), DippFormH/ EtFormH/XylFormH/PhFormH (0.25 mmol) and dry THF (10 ml) were placed in a Schlenk flask in a nitrogen-filled dry box. The mixture was ultrasonicated for one week. The reaction mixture was filtered. Crystals were obtained after the filtrate was evaporated to half volume under vacuum.

[La(DippForm)I$_2$(thf)$_3$]·0.5 thf 1

Colourless crystals (0.164 g, 63%), M.p. > 300 °C. (Found: La, 14.36%; $C_{39}H_{63}I_2LaN_2O_{3.5}$ (1008.62) requires La, 13.77%, loss of 0.5 thf of crystallisation, $C_{37}H_{59}I_2LaN_2O_3$ (972.59) requires La, 14.28%). IR (crystal oil): 1666 m, 1589 m, 1528 s, 1325 s, 1276 s, 1181 s, 1106 s, 1062 s, 1018vs, 936 s, 911 s, 885 s, 801 s, 770s, 753 m 716 m cm^{-1}. ^{1}H NMR (400 MHz, C_6D_6, ppm): 8.51 (s, 1H, NCHN), 7.19-7.05 (m, 6H, H(3,4,5)), 4.27 (m, 4H, CH), 3.83 (m, 14H, thf), 1.52–1.32 (m, 24H, CH_3), 1.24 (m, 14H, thf).

[Ce(DippForm)I$_2$(thf)$_3$]·0.5 thf 2

Colourless crystals (0.148 g, 59%), decomposed 200 °C. (Found: Ce, 14.42%; $C_{39}H_{63}CeI_2N_2O_{3.5}$ (1009.83) requires Ce, 13.87%, loss of 0.5 thf of crystallisation, $C_{37}H_{59}CeI_2N_2O_3$ (973.80) requires Ce, 14.39%). IR

© 2023 The Authors. Chemistry - An Asian Journal published by Wiley-VCH GmbH

1861471x, 2023, 14, Downloaded from https://aces.onlinelibrary.wiley.com/doi/10.1002/asia.202300333 by Eddie Koiki Mabo Library, Wiley Online Library on [01/09/2024]. See the Terms and Conditions (https://onlinelibrary.wiley.com/terms-and-conditions) on Wiley Online Library for rules of use; OA articles are governed by the applicable Creative Commons License

(crystal oil): 1665 m, 1592 m, 1521 s, 1319 s, 1270s, 1191 s, 1100 s, 1066 s, 1017vs, 944 m, 914 m, 863 s, 804 s, 760s, 724 m cm^{-1}.

[Tb(DippForm)I$_2$(thf)$_3$]·0.5 thf 3

Colourless crystals (0.179 g, 70%), M.p. 234–236 °C. (Found: Tb, 16.28%; $C_{39}H_{63}I_2N_2O_{3.5}Tb$ (1028.63) requires Tb, 15.45%, loss of 0.5 thf of crystallisation, $C_{37}H_{59}I_2N_2O_3Tb$ (992.61) requires Tb, 16.01%). IR (crystal oil): 1666 m, 1592 m, 1525 s, 1320s, 1272 s, 1192 s, 1102 s, 1067 s, 1019vs, 948 m, 916 m, 864 s, 805 s, 762 s, 724 m cm^{-1}.

[Ho(DippForm)I$_2$(thf)$_3$]·0.5 thf 4

Pink crystals (0.164 g, 66%), M.p. 242–244 °C. (Found: Ho, 16.36%; $C_{39}H_{63}HoI_2N_2O_{3.5}$ (1034.64) requires Ho, 15.94%, loss of 0.5 thf of crystallisation, $C_{37}H_{59}HoI_2N_2O_3$ (998.61) requires Ho, 16.52%). IR (Nujol): 1666 m, 1593 m, 1524 s, 1320 m, 1272 m, 1192 s, 1101 m, 1069 s, 1017vs, 935 m, 916 m, 863 s, 804 s, 774 s, 760s, 723 m cm^{-1}.

[Er(DippForm)I$_2$(thf)$_3$]·2 thf 5

Pink crystals (0.232 g, 81%), M.p. 246–248 °C, (Found: C, 38.35; H, 5.40; N, 3.51; $C_{45}H_{75}ErI_2N_2O_5$ (1145.13), loss of five thf, $C_{25}H_{35}ErI_2N_2$ (784.63) requires C, 38.27; H, 4.50; N, 3.57%). IR (Nujol): 1669 m, 1587 w, 1525 m, 1334 w, 1297 m, 1272 m, 1235 w, 1189 s, 1159 w, 1097 m, 1075 s, 1030vs, 935 m, 919 w, 863 m, 824 m, 799 s, 756 s, 722 s cm^{-1}.

[Tm(DippForm)I$_2$(thf)$_3$]·0.5 thf 6

Colourless crystals (0.205 g, 79%), M.p. 260–262 °C. (Found: Tm, 17.00%; $C_{39}H_{63}I_2N_2O_{3.5}Tm$ (1038.64) requires Tm, 16.26%, loss of 0.5 thf of crystallisation, $C_{37}H_{59}I_2N_2O_3Tm$ (1002.62) requires Tm, 16.85%). IR (crystal oil): 1667 m, 1593 m, 1523 s, 1321 s, 1273 s, 1193 s, 1101 s, 1068 s, 1018vs, 944 m, 916 m, 865 s, 805 s, 761 s, 723 m cm^{-1}.

[Ce(EtForm)I$_2$(thf)$_3$]·thf 7

Yellow crystals (0.186 g, 75%), M.p. 206–208 °C. (Found: Ce, 14.28%; $C_{37}H_{59}CeI_2N_2O_4$ (989.78) requires Ce, 14.16%). IR (Nujol): 1667 s, 1592 w, 1302 w, 1277 w, 1170 w, 1077 m, 1010 w, 968 w, 917 w, 892 w, 852 w, 774 w, 723 s cm^{-1}. ^{1}H NMR (400 MHz, C_6D_6, ppm): δ = 26.05 ppm (1H; NC(H)N), 8.23 (4H; CH, Ar), 7.76 (2H; CH, Ar), 2.61 (8H; CH_2), 1.50 (12H; CH_3).

[Nd(EtForm)I$_2$(thf)$_3$]·thf 8

Purple crystals (0.196 g, 79%), M.p. 205–208 °C. (Found: Nd, 14.70%; $C_{37}H_{59}I_2N_2NdO_4$ (993.90) requires Nd, 14.51%). IR (Nujol): 1666 s, 1589 m, 1525 s, 1336 w, 1279 m, 1260 w, 1195 m, 1099 m, 1074 s, 1010 s, 945 w, 914 m, 854 s, 800 w, 755 s, 723 m, 668 m cm^{-1}. ^{1}H NMR (400 MHz, C_6D_6, ppm): δ = 31.19 ppm (1H; NC(H)N), 10.10 (4H; CH, Ar), 8.41 (2H; CH, Ar), 4.79 (8H; CH_2), 2.61 (4H; OCH_2, thf), 1.41 (4H; CH_2, thf), 1.11(12H; CH_3). Crystals dried before the spectrum was recorded hence loss of thf.

[Gd(EtForm)I$_2$(thf)$_3$]·thf 9

Colourless crystals (0.210 g, 83%), M.p. 177–179 °C. (Found: Gd, 15.83%; $C_{37}H_{59}GdI_2N_2O_4$ (1006.91) requires Gd, 15.62%); IR (Nujol): 1672 s, 1590 w, 1528 w, 1341 w, 1275 w, 1178 w, 1074 m, 1017 w, 915 w, 868 w, 800 m, 754w, 722 m cm^{-1}. IR suggests some loss of thf from the sample

[Tb(EtForm)I$_2$(thf)$_3$]·thf 10

Colourless crystals (0.207 g, 82%), M.p. 222–224 °C. (Found: Tb, 15.89%; $C_{37}H_{59}I_2N_2O_4Tb$ (1008.58) requires Tb, 15.76%). IR (Nujol): 1664 m, 1593 m, 1528 s, 1342 w, 1275 s, 1239 w, 1198 m, 1103 m, 1073 s, 1012 s, 949 m, 915 m, 856 s, 797w, 775 m, 752 s, 724 w cm^{-1}.

[Dy(EtForm)I$_2$(thf)$_3$]·thf 11

Colourless crystals (0.184 g, 73%), M.p. 254–256 °C. (Found: Dy, 16.45%; $C_{37}H_{59}DyI_2N_2O_4$ (1012.16) requires Dy, 16.05%, loss of 0.5 thf of crystallisation, $C_{35}H_{55}DyI_2N_2O_{3.5}$ (976.13) requires Dy, 16.65%). IR (Nujol): 1676 m, 1592 m, 1534 m, 1333 w, 1276 s, 1200s, 1104 m, 1070 m, 10122 s, 949 m, 915 s, 866 s, 802 m, 759 s, 734 m cm^{-1}.

[Ho(EtForm)I$_2$(thf)$_3$]·thf 12

Colorless crystals (0.193 g, 76%), M.p. 238–240 °C. (Found: Ho, 16.41%; $C_{37}H_{59}HoI_2N_2O_4$ (1014.59) requires Ho, 16.26%), IR (Nujol): 1663 m, 1592 s, 1530 s, 1334 w, 1274 s, 1199 m, 1104 s, 1074 s, 1012 m, 948 m, 914 m, 857 w, 800 m, 775 m, 755 m, 733 m, 666 s cm^{-1}. IR suggests some loss of thf from sample.

[Er(EtForm)I$_2$(thf)$_3$]·thf 13

Pink crystals (0.186 g, 73%), M.p. 156–158 °C. (Found: Er, 16.75%; $C_{37}H_{59}ErI_2N_2O_4$ (1016.92) requires Er, 16.45%). IR (Nujol): 1652 m, 1592 m, 1529 s, 1337 w, 1273 s, 1200s, 1104 m, 1073 m, 1012 s, 949 m, 915 s, 858 s, 801 m, 756 s, 722 m cm^{-1}.

[Lu(EtForm)I$_2$(thf)$_3$]·thf 14

Colourless crystals (0.203 g, 79%), M.p. 150–152 °C. (Found: Lu, 17.21%; $C_{37}H_{59}I_2LuN_2O_4$ (1024.63) requires Lu, 17.08%). IR (Nujol): 1666 m, 1593 m, 1535 s, 1342w, 1274 s, 1200 m, 1103 m, 1074 m, 1008 s, 948 w, 915 w, 894 w, 851 s, 799 w, 774 w, 755 m, 723 m, 666 m cm^{-1}. ^{1}H NMR (400 MHz, C_6D_6, ppm): δ = 8.05 ppm (1H; NC(H)N), 7.11 (4H; CH, Ar), 7.07 (2H; CH, Ar), 3.70 (16H; OCH_2, thf), 3.25 (8H; CH_2), 1.37 (12H; CH_3), 1.25 (16H; CH_2, thf).

[Ce(XylForm)I$_2$(thf)$_3$]·1.5 thf 15

Yellow crystals (0.189 g, 78%), M.p. 232–234 °C. (Found: Ce, 16.18%; $C_{35}H_{55}CeI_2N_2O_{4.5}$ (969.73) requires Ce 14.45%, loss of 1.5 thf of crystallisation, $C_{29}H_{43}CeI_2N_2O_3$ (861.59) requires Ce 16.26%). IR (Nujol): 1676 m, 1592 m, 1522 s, 1287 s, 1206 s, 1092 s, 1015 s, 942 m, 918 s, 858 s, 772 s, 723 w cm^{-1}. The solution was dried under vacuum, and the powder was used for ^{1}H NMR, ^{1}H NMR (400 MHz, C_6D_6, ppm): δ = 25.83 ppm (1H; NC(H)N), 8.16-7.66 (6H; CH, Ar), 2.37 (12H; CH_3).

[Nd(XylForm)I$_2$(thf)$_3$]·thf 16

Purple crystals (0.164 g, 70%), M.p. 202–204 °C. (Found: Nd, 17.02%; $C_{33}H_{51}I_2N_2NdO_4$ (937.79) requires Nd, 15.38%, loss of one thf of crystallisation, $C_{29}H_{43}I_2N_2NdO_3$ (865.71) requires Nd, 16.66%). IR (Nujol): 1675 m, 1592 m, 1521 s, 1282 s, 1205 s, 1071 s, 1018 s, 942 m, 915 s, 861 s, 772 s, 726 w cm^{-1}.

© 2023 The Authors. Chemistry - An Asian Journal published by Wiley-VCH GmbH

1861471x, 2023, 14, Downloaded from https://aces.onlinelibrary.wiley.com/doi/10.1002/asia.202300333 by Eddie Koiki Mabo Library, Wiley Online Library on [01/09/2024]. See the Terms and Conditions (https://onlinelibrary.wiley.com/terms-and-conditions) on Wiley Online Library for rules of use; OA articles are governed by the applicable Creative Commons License

1861471x, 2023, 14, Downloaded from https://aces.onlinelibrary.wiley.com/doi/10.1002/asia.202300333 by Eddie Koiki Mabo Library, Wiley Online Library on [01/09/2024]. See the Terms and Conditions (https://onlinelibrary.wiley.com/terms-and-conditions) on Wiley Online Library for rules of use; OA articles are governed by the applicable Creative Commons License

[Gd(XylForm)I$_2$(thf)$_3$]·thf 17

Colourless crystals (0.200 g, 84%), M.p. 196–198 °C. (Found: Gd, 18.21%; $C_{33}H_{51}GdI_2N_2O_4$ (950.80) requires Gd, 16.54%, loss of one thf of crystallisation, $C_{29}H_{43}GdI_2N_2O_3$ (878.72) requires Gd, 17.90%). IR (Nujol): 1669 m, 1593 m, 1526 s, 1283 s, 1208 s, 1073 s, 1019 s, 945 m, 916 s, 859 s, 774 s, 725 w cm^{-1}.

[Tm(XylForm)I$_2$(thf)$_3$]·thf 18

Colourless crystals (0.196 g, 81%), M.p. 162–164 °C. (Found: Tm, 18.24%; $C_{33}H_{51}I_2N_2O_4Tm$ (962.48) requires Tm, 17.55%, loss of 0.5 thf of crystallisation, $C_{31}H_{47}I_2N_2O_{3.5}Tm$ (926.46) requires Tm, 18.23%,). IR (Nujol): 1670 m, 1593 m, 1528 s, 1281 s, 1209 s, 1071 s, 1018 s, 946 m, 915 s, 860s, 770s, 728 w cm^{-1}.

[Lu(XylForm)I$_2$(thf)$_3$]·thf 19

Colourless crystals (0.172 g, 71%), M.p. 260–262 °C. (Found: Lu, 19.86%; $C_{33}H_{51}I_2LuN_2O_4$ (968.53) requires Lu, 18.07%, loss of one thf of crystallisation, $C_{29}H_{43}I_2LuN_2O_3$ (896.44) requires Lu, 19.52%). IR (Nujol): 1676 s, 1594 m, 1527 m, 1263 s, 1209 m, 1075 s, 1022 s, 956 m, 917 m, 866 m, 790s, 722 m cm^{-1}. ^{1}H NMR (400 MHz, C_6D_6, ppm): δ = 7.66 ppm (1H; NC(H)N), 6.95–7.03 (6H; CH, Ar), 3.77 (16H; OCH_2, thf), 2.71 (12H; CH_3), 1.25 (16H; CH_2, thf).

[Nd(PhForm)I$_2$(thf)$_3$] 20

Purple crystals (0.138 g, 68%), M.p. 214–216 °C. (Found: Nd, 17.56; $C_{25}H_{35}I_2N_2NdO_3$ (809.59) requires Nd, 17.82%). IR (Nujol): 1686 m, 1595 m, 1527 m, 1262 s, 1217 w, 1074 s, 1018 vs, 945 m, 918 m, 862 m, 802 vs, 756 m cm^{-1}.

[Gd(PhForm)I$_2$(thf)$_3$] 21

Colourless crystals (0.168 g, 82%), M.p. 172–174 °C. (Found: Gd, 19.45; $C_{25}H_{35}GdI_2N_2O_3$ (822.60) requires Gd, 19.12%). IR (Nujol): 1685 m, 1594 m, 1527 m, 1261 s, 1224 w, 1093 s, 1019 vs, 946 m, 917 m, 862 m, 800 vs, 758 m cm^{-1}.

[Er(PhForm)I$_2$(thf)$_3$] 22

Pink crystals (0.162 g, 78%), M.p. 158–160 °C. (Found: Er, 19.87; $C_{25}H_{35}ErI_2N_2O_3$ (832.61) requires Er, 20.09%). IR (Nujol): 1667 m, 1587 m, 1533 m, 1261 s, 1227 m, 1074 s, 1017vs, 947 m, 918 m, 854 m, 805 vs, 766 m cm^{-1}.

[Ce(XylForm)$_2$I(thf)$_2$]·2.25 thf 23

Cerium metal powder (2.0 mmol), iodine (0.5 mmol), XylFormH (2.0 mmol) and dry THF (10 ml) were placed in a Schlenk flask in a nitrogen-filled dry box. The mixture was ultrasonicated for three days, and the reaction mixture was filtered. Yellow crystals (0.426 g, 79%), M.p. 180–182 °C. (Found: Ce, 15.78; $C_{51}H_{72}CeIN_4O_{4.25}$ (1076.14) requires Ce, 13.07%, loss of 2.25 thf of crystallisation, $C_{42}H_{54}CeIN_4O_2$ (913.92) requires Ce 15.33%). IR (Nujol): 1667 m, 1593 m, 1532 s, 1278 s, 1210s, 1193 m, 1094 m, 1074 s, 1012 s, 946 m, 916 m, 854 m, 771 m, 733 w cm^{-1}.

General procedure for 24–27

Lanthanoid metal powder (1.0 mmol), iodine (0.5 mmol), DippFormH (1.0 mmol) and dry THF (10 ml) were placed in a Schlenk flask in a nitrogen-filled dry box. The mixture was ultrasonicated for three days. The reaction mixture was filtered and crystals were obtained after the filtrate was evaporated to half volume under vacuum.

[Eu(DippForm)I(thf)$_4$]·thf 24

Green crystals (0.562 g, 56%), M.p. 270–272 °C. **7** crystallized in the monoclinic space group $P2_1/c$, a = 16.359(3) Å, b = 16.776(3) Å, c = 17.082(3) Å, β = 91.64(3)°, V = 4686.0(16) Å^3, which is similar to that reported,[17f] monoclinic space group $P2_1/c$, a = 16.326(3) Å, b = 16.752(3) Å, c = 17.069(3) Å, β = 91.62(3)°, V = 4666.4(16) Å^3. IR (Nujol): 1665 m, 1593 m, 1518 m, 1320 m, 1295 s, 1254 m, 1234 m, 1187 s, 1100 m, 1074 s, 1035 s, 993 m, 916 s, 884 s, 801 s, 756 s, 723 m cm^{-1}. The IR was consistent with the reported one.[17f]

[Yb(DippForm)I(thf)$_3$]·2DippFormH 25

Orange crystals (0.501 g, 62%), decompose 188 °C. IR (Nujol): 1669 s, 1589 m, 1525 s, 1338 w, 1317 w, 1289 s, 1261 s, 1237 w, 1188 m, 1098 m, 1075 s, 1030 vs, 952 w, 916 m, 874 s, 801 s, 757 s, 723 s cm^{-1}.

[Sm(DippForm)I(thf)$_4$]·thf 26 and [Sm(DippForm)I$_2$(thf)$_3$]·0.5 thf 27

26 blue crystals (M.p. 280 °C), Vis/NIR: Sm^{II} 424, 576, 624, Sm^{III} 921, 1207, 1381, 1717 nm, very sensitive to the air (colour change from blue to yellow within seconds), and [Sm(DippForm)I$_2$(thf)$_3$]·0.5thf **27** was obtained, yellow crystals (0.423 g, 83%), M.p. 238–240 °C. IR (Nujol): 1665 m, 1587 m, 1332 m, 1286 s, 1261 s, 1234 m, 1180s, 1097 s, 1020 s, 936 m, 800s, 753 m, 721 m cm^{-1}. Vis/NIR: 921, 1207, 1381, 1717 nm. **27** has some limited stability in air.

[Sm(XylForm)I(thf)$_3$]$_n$ 28

Samarium metal powder (2.0 mmol), iodine (0.5 mmol), XylFormH (1.0 mmol) and dry THF (10 ml) were placed in a Schlenk flask in a nitrogen-filled dry box. The mixture was ultrasonicated for three days, and the reaction mixture was filtered. Blue crystals, M.p. 198 °C decomposed. IR (Nujol): 1648 m, 1588 m, 1560 m, 1342 m, 1297 m, 1260 m, 1201 m, 1179 m, 1074 m, 1030 vs, 953 w, 918 s, 870 vs, 758 m, 722 m cm^{-1}.

Acknowledgements

PCJ, GBD and VLB gratefully acknowledge the ARC for funding (DP230100112). Parts of this research were undertaken on the MX1 beamline at the Australian Synchrotron, part of ANSTO.[26] Open Access publishing facilitated by James Cook University, as part of the Wiley - James Cook University agreement via the Council of Australian University Librarians.

Conflict of Interests

There are no conflicts of interest to declare.

© 2023 The Authors. Chemistry - An Asian Journal published by Wiley-VCH GmbH

Data Availability Statement

The data that support the findings of this study are available from the corresponding author upon reasonable request.

Keywords: Lanthanoids · Rare earths · synthesis · structures · heteroleptic compounds

[1] a) R. Duchateau, C. T. van Wee, A. Meetsma, J. H. Teuben, *J. Am. Chem. Soc.* **1993**, *115*, 4931–4932; b) F. T. Edelmann, *J. Alloys Compd.* **1994**, *207/208*, 182; c) F. T. Edelmann, *Coord. Chem. Rev.* **1994**, *137*, 403–481; d) R. Duchateau, C. T. van Wee, A. Meetsma, P. T. van Duijnen, J. H. Teuben, *Organometallics* **1996**, *15*, 2279–2290; e) J. R. Hagadorn, J. Arnold, *Organometallics* **1996**, *15*, 984–991; f) T. Dubé, S. Conoci, S. Gambarotta, G. P. A. Yap, G. Vasapollo, *Angew. Chem. Int. Ed.* **1999**, *111*, 3890–3892; *Angew. Chem. Int. Ed.* **1999**, *38*, 3657–3659; g) V. K. Belsky, A. B. Erofeev, B. M. Bulychev, G. L. Soloveichik, *J. Organomet. Chem.* **1984**, *265*, 123–133; h) W. J. Evans, M. S. Sollberger, S. I. Khan, R. Bau, *J. Am. Chem. Soc.* **1988**, *110*, 439–446; i) W. J. Evans, J. H. Meadows, A. L. Wayda, W. E. Hunter, *J. Am. Chem. Soc.* **1982**, *104*, 2008–2014; j) A. Z. Voskoboynikov, I. N. Parshina, A. K. Shestakova, K. P. Butin, I. P. Beletaskaya, L. G. Kuz′mina, J. A. K. Howard, *Organometallics* **1997**, *16*, 4041–4055; k) Z. Hou, Y. Zhang, O. Tardif, Y. Wakatsuki, *J. Am. Chem. Soc.* **2001**, *123*, 9216–9217.

[2] a) T. D. Tilley, R. A. Andersen, *Inorg. Chem.* **1981**, *20*, 3267–3270; b) J. W. Evans, R. A. Keyer, J. W. Ziller, *Organometallics* **1993**, *12*, 2618–2633.

[3] a) P. B. Hitchcock, S. A. Holmes, M. F. Lappert, S. Tian, *Chem. Commun.* **1994**, 2691–2692; b) F. T. Edelmann, A. Steiner, D. Stalke, J. W. Gilje, S. Jagner, M. Håkansson, *Polyhedron* **1994**, *13*, 539–546.

[4] W. J. Evans, R. N. R. Broomhall-Dillard, J. W. Ziller, *Organometallics* **1996**, *15*, 1351; *J. Organomet. Chem.* **1998**, *569*, 89–97.

[5] a) A. A. Trifonov, E. N. Kirillov, A. Fischer, F. T. Edelmann, M. N. Bochkarev, *Chem. Commun.* **1999**, 2203–2204; b) A. A. Trifonov, E. N. Kirillov, A. Fischer, F. T. Edelmann, M. N. Bochkarev, *J. Organomet. Chem.* **2002**, *647*, 94–99; c) G. E. Herberich, U. Englert, A. Fischer, J. Ni, A. Schmitz, *Organometallics* **1999**, *18*, 5496–5501; d) J. Stehr, R. D. Fischer, *J. Organomet. Chem.* **1992**, *430*, C1–C4.

[6] a) H. Schumann, J. A. Meese-Marktscheffel, L. Esser, *Chem. Rev.* **1995**, *95*, 865–986; b) F. T. Edelmann, D. M. M. Freckmann, H. Schumann, *Chem. Rev.* **2002**, *102*,1851–1896; c) S. A. Cotton, *Coord. Chem. Rev.* **1997**, *160*, 93–127.

[7] a) C. J. Schaverien, *Adv. Organomet. Chem.* **1994**, *36*, 283–363; b) F, T. Edelmann, In *Comprehensive Organometallic Chemistry II* (Eds.: F. G. A. Stone, G. Wilkinson, E. W. Abel), Pergamon Press, Oxford, U. K., **1995**, Vol. 4, Chapter 2; c) F. T. Edelmann, *Angew. Chem. Int. Ed.* **1995**, *107*, 2647–2669; *Angew. Chem. Int. Ed. Engl.* **1995**, *34*, 2466–2488; d) K. Jacob, W. Kretschmer, K. H. Thiele, H. Gornitzka, F. T. Edelmann, I. Pavlik, A. Lycka, J. Holecek, *J. Organomet. Chem.* **1992**, *436*, 231–240; e) T. Dubé, S. Gambarotta, G. Yap, *Organometallics* **2000**, *19*, 121–126; f) J. L. Atwood, J. H. Bums, P. G. Laubereau, *J. Am. Chem. Soc.* **1973**, *95*, 1830–1833; g) M. Tsutsui, L. B. Chen, D. E. Bergbreiter, T. K. Miyamoto, *J. Am. Chem. Soc.* **1982**, *104*, 855–856.

[8] a) D. A. Atwood, *The Rare Earth Elements, Fundamentals and Applications*, John Wiley and Sons Ltd., West Sussex, **2012**; b) M. L. Cole, G. B. Deacon, C. M. Forsyth, P. C. Junk, K. Konstas, J. Wang, *Chem. Eur. J.* **2007**, *13*, 8092–8110; c) M. L. Cole, P. C. Junk, *Chem. Commun.* **2005**, 2695–2697.

[9] B. A. Dolgoplosk, E. I. Tinyakova, I. N. Markevich, T. V. Soboleva, G. M. Chernenko, O. K. Sharaev, V. A. Yakovlev, *J. Organomet. Chem.* **1983**, *255*, 71–79.

[10] a) D. F. Evans, G. V. Fazakerley, R. F. Phillips, *J. Chem. Soc. D.* **1970**, 244; b) D. F. Evans, G. V. Fazakerley, R. F. Phillips, *J. Chem. Soc. A.* **1971**, 1931–1934.

[11] M. N. Bochkarev, L. N. Zakharov, G. S. Kalinina, *OrganoderiVatiVes of Rare Earth Elements*, Kluwer Academic, Dordrecht **1995**.

[12] a) C. Eaborn, P. B. Hitchcock, K. Izod, J. D. Smith, *J. Am. Chem. Soc.* **1994**, *116*, 12071–12072; b) C. Eaborn, P. B. Hitchcock, K. Izod, Z. R. Lu, J. D. Smith, *Organometallics* **1996**, *15*, 4783–4790.

[13] D. J. Duncalf, P. B. Hitchcock, G. A. Lawless, *Chem. Commun.* **1996**, 269–271.

[14] a) G. Heckmann, M. Niemeyer, *J. Am. Chem. Soc.* **2000**, *122*, 4227–4228; b) M. Niemeyer, *Z. Anorg. Allg. Chem.* **2000**, *626*, 1027–1029; c) M. Niemeyer, *Eur. J. Inorg. Chem.* **2001**, 1969; d) C. Eaborn, P. B. Hitchcock, K. Izod, Z. R. Lu, J. D. Smith, *Organometallics*, **1996**, *15*, 4783-4790.

[15] M. Wiecko, G. B. Deacon, P. C. Junk, *Chem. Commun.* **2010**, *46*, 5076–5078.

[16] S. H. Ali, G. B. Deacon, P. C. Junk, S. Hamidi, M. Wiecko, J. Wang, *Chem. Eur. J.* **2018**, *24*, 230–242.

[17] a) A. V. Safronova, L. N. Bochkarev, I. P. Malysheva, E. V. Baranov, *Inorg. Chim. Acta.* **2012**, *392*, 454–458; b) D. M. Kuzyaev, D. L. Vorozhtsov, N. O. Druzhkov, M. A. Lopatin, E. V. Baranov, A. V. Cherkasov, G. K. Fukin, G. A. Abakumov, M. N. Bochkarev, *J. Organomet. Chem.* **2012**, *698*, 35–41; c) K. Mashima, H. Fukumoto, Y. Nakayama, K. Tani, A. Nakamura, *Polyhedron* **1998**, *17*, 1065–1071; d) G. B. Deacon, S. Hamidi, P. C. Junk, R. P. Kelly, J. Wang, *Eur. J. Inorg. Chem.* **2014**, 460–468; e) G. B. Deacon, P. C. Junk, A. Urbatsch, *Eur. J. Inorg. Chem.* **2011**, 3592–3600; f) G. B. Deacon, P. C. Junk, A. Urbatsch, *Aust. J. Chem.* **2012**, *65*, 802–810; g) S. Hamidi, G. B. Deacon, P. C. Junk, P. Neumann, *Dalton Trans.* **2012**, *41*, 3541–3552.

[18] Z. Guo, V. Blair, G. B. Deacon, P. C. Junk, *Dalton Trans.* **2020**, *49*, 13588–13600.

[19] Z. Guo, V. Blair, G. B. Deacon, P. C. Junk, *Chem. Commun.* **2021**, *57*, 11513–11516.

[20] J. Lewis, J. R. Miller, R. L. Richards, A. Thompson, *J. Chem. Soc.* **1965**, 5850–5860.

[21] a) M. Karbowiak, A. Urbanowicz, *Phys. Rev. B.* **2007**, *76*, 115125 (1–9); b) G. B. Deacon, A. J. Koplick, W. D. Raverty, D. G. Vince, *J. Organomet. Chem.* **1979**, *182*, 121–141; c) G. B. Deacon, A. J. Koplick, T. D. Tuong, *Aust. J. Chem.* **1984**, *37*, 517–525; d) G. B. Deacon, S. Nickel, P. MacKinnon, E. R. T. Tiekink, *Aust. J. Chem.* **1990**, *43*, 1245–1257; e) J. E. Cosgriff, G. B. Deacon, B. M. Gatehouse, H. Hemling, H. Schumann, *Aust. J. Chem.* **1994**, *47*, 1223–1235.

[22] a) D. D. Stellfeldt, G. Meyer, G. B. Deacon, *Z. Anorg. Allg. Chem.* **1999**, *625*, 1252–1254; b) G. V. Khoroshen′kov, A. A. Fagin, M. N. Bochkarev, S. Dechert, H. Schmann, *Russ. Chem. Bull.* **2003**, *52*, 1715–1719.

[23] R. D. Shannon, *Acta Crystallogr. Sect. A* **1976**, *32*, 751–767.

[24] J. Marcalo, A. Pires de Matos, *Polyhedron* **1989**, *8*, 2431–2437.

[25] R. M. Roberts, *J. Org. Chem.* **1949**, *14*, 277.

[26] N. P. Cowieson, D. Aragao, M. Clift, D. J. Ericsson, C. Gee, S. J. Harrop, N. Mudie, S. Panjikar, J. R. Price, A. Riboldi-Tunnicliffe, R. Williamson, T. Caradoc-Davies, *J. Synchrotron Radiat.* **2015**, *22*, 187–190.

Manuscript received: April 17, 2023
Revised manuscript received: May 15, 2023
Accepted manuscript online: May 19, 2023
Version of record online: May 26, 2023

© 2023 The Authors. Chemistry - An Asian Journal published by Wiley-VCH GmbH

1861471x, 2023, 14, Downloaded from https://aces.onlinelibrary.wiley.com/doi/10.1002/asia.202300333 by Eddie Koiki Mabo Library, Wiley Online Library on [01/09/2024]. See the Terms and Conditions (https://onlinelibrary.wiley.com/terms-and-conditions) on Wiley Online Library for rules of use; OA articles are governed by the applicable Creative Commons License